

Attachment - 2



**UNITED STATES
NUCLEAR REGULATORY COMMISSION**

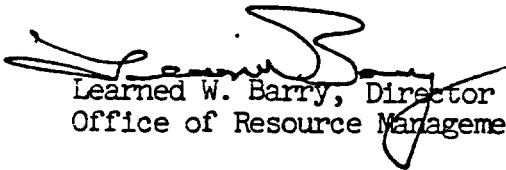
ANNOUNCEMENT NO. 1

DATE: January 2, 1985

TO: All NRC Employees

SUBJECT: NRC STRUCTURAL ORGANIZATION CHART

Attached is a revised structural organization chart for NRC, dated January 1, 1985. Extra copies of this chart, printed on white paper, are available from Distribution Services, Ext. 492-7333.


Learned W. Barry, Director
Office of Resource Management

Attached:
NRC Structural Organization Chart

B502270070 B50206
PDR WMRES EXIORNL
B-0287 PDR

NUREG/CR-3091
BNL-NUREG-51630
Vol. 6

Attachment-3

REVIEW OF WASTE PACKAGE VERIFICATION TESTS
BIANNUAL REPORT

C. Anderson
C. Brewster
M. S. Davis
E. P. Gause
H. Jain
C. Pescatore
C. Sastre
P. Soo
T. Sullivan

DECEMBER 1984

NUCLEAR WASTE MANAGEMENT DIVISION
DEPARTMENT OF NUCLEAR ENERGY, BROOKHAVEN NATIONAL LABORATORY
UPTON, NEW YORK 11973



Prepared for the U.S. Nuclear Regulatory Commission
Office of Nuclear Materials Safety and Safeguards
Contract No. DE-AC02-76CH00016

REVIEW OF WASTE PACKAGE VERIFICATION TESTS
BIANNUAL REPORT

C. Anderson
C. Brewster
M. S. Davis
E. P. Gause
H. Jain
C. Pescatore
C. Sastre
P. Soo
T. Sullivan

December 1984

Prepared by the Nuclear Waste Management Division
D. G. Schweitzer, Head
Department of Nuclear Energy, Brookhaven National Laboratory
Associated Universities, Inc.
Upton, New York 11973

Prepared for the U. S. Nuclear Regulatory Commission
Office of Nuclear Materials Safety and Safeguards
Contract No. DE-AC02-76CH00016
FIN No. A-3167

ABSTRACT

The potential of WAPPA, a second-generation waste package system code, to meet the needs of the regulatory community are analyzed. The analysis is based on the contents of the code manual, a letter-form update of the code and, to a lesser extent, on the source program. The analysis includes an in-depth review of WAPPA's individual process models and a review of WAPPA's operation. The analysis lists and discusses potential problems in the use of WAPPA. It is concluded that the code is of limited use to the NRC in the present form. Recommendations for future improvement, usage, and implementation of the code are also given.

This report also describes the results of a testing program undertaken to determine the chemical environment that will be present near a high level waste package emplaced in a basalt repository. For this purpose, low carbon 1020 steel (a current BWIP reference container material), synthetic basaltic groundwater and a mixture of bentonite and basalt were exposed, in an autoclave, to expected conditions some period after repository sealing (150°C, ≈ 10.4 MPa). The experimental program consisted of three phases. The Phase I test involved a two-month gamma irradiation test in an inert argon environment. The Phase II test involved an irradiation test in a methane-containing environment also for a period of two months. These two experiments were followed by a Phase III study which was conducted in the absence of radiation in a methane environment. Parameters measured include changes in gas pressure with time and gas composition, variation in dissolved oxygen (DO), pH and certain ionic concentrations of water in the packing material across an imposed thermal gradient, mineralogic alteration of the basalt/bentonite mixture, and carbon steel corrosion behavior.

A second testing program was initiated to check the likelihood of stress corrosion cracking of austenitic stainless steels and Incoloy 825 which are being considered for use as waste container materials in the tuff repository program. The issue arose because data in the literature showed that one of the candidate steels (Type 304L) cracked in boiling water containing air and low chloride levels in the presence of gamma irradiation. Preliminary data from three-month tests are given.

CONTENTS

ABSTRACT	iii
FIGURES	x
TABLES	xv
ACKNOWLEDGMENTS	xvii
EXECUTIVE SUMMARY	
1. INTRODUCTION (M. S. Davis, P. Soo)	5
2. REVIEW OF WAPPA (C. Pescatore, T. Sullivan, C. Sastre)	11
2.1 Introduction	11
2.1.1 Background Information	11
2.1.2 The Code WAPPA	12
2.1.3 Objectives and Organization of this Report	12
2.2 Review of WAPPA's Process Models	14
2.2.1 WAPPA's Radiation Model (RMODEL)	14
2.2.1.1 Review of Modeling Approach	14
2.2.1.1.1 Source Term Submodel	14
2.2.1.1.2 Attenuation Submodel	15
2.2.1.1.3 Radiolysis Submodel	15
2.2.1.1.4 Damage Submodel	15
2.2.1.2 Discussion	15
2.2.1.2.1 Source Term Submodel	16
2.2.1.2.2 Attenuation Submodel	16
2.2.1.2.3 Radiolysis Submodel	18
2.2.1.2.4 Damage Submodel	19
2.2.1.3 Conclusions	19
2.2.2 WAPPA's Thermal Model (TMODEL)	20
2.2.2.1 Review of Modeling Approach	20
2.2.2.2 Discussion	21
2.2.2.3 Conclusions	22
2.2.3 WAPPA's Mechanical Model (FMODEL)	22
2.2.3.1 Review of Modeling Approach	23

CONTENTS (Continued)

2.2.3.1.1	Canister Fracture Submodel	23
2.2.3.1.2	Waste Form Fracture Submodel	23
2.2.3.1.3	Stress Analysis Submodel	23
2.2.3.2	Discussion	24
2.2.3.2.1	Limitations of the Modeling Approach	24
2.2.3.2.2	Adequacy of the Modeling Approach	25
2.2.3.3	Conclusions	25
2.2.4	WAPPA's Corrosion Model (CMODEL)	25
2.2.4.1	Review of Modeling Approach	27
2.2.4.1.1	Dry Corrosion	27
2.2.4.1.2	Wet Corrosion	27
2.2.4.2	Discussion	27
2.2.4.3	Conclusions	30
2.2.5	WAPPA's Leach-and-Transport Model (WMODEL)	30
2.2.5.1	Review of Modeling Approach	30
2.2.5.1.1	Leach Submodel	30
2.2.5.1.2	Transport Submodel	32
2.2.5.2	Discussion	33
2.2.5.2.1	Leach Submodel	33
2.2.5.2.2	Transport Submodel	36
2.2.5.3	Conclusions	38
2.2.6	Conclusions	38
2.3	Review of WAPPA's Operation	40
2.3.1	Initial Specifications	40
2.3.1.1	Geometrical Configuration and Materials Specification	40
2.3.1.2	Calculation Times and Error Control	42

CONTENTS (Continued)

2.3.1.3	Nuclides Requested	43
2.3.1.4	Repository Boundary Conditions	43
2.3.1.5	Data Base	44
2.3.1.6	Radionuclide, Gamma Alpha, and Thermal Power Source Terms	44
2.3.2	Output Specifications	45
2.3.3	Conclusions	45
2.4	Conclusions and Recommendations	45
2.4.1	Conclusions	45
2.4.2	Recommendations	47
2.5	References	49
3.	DETERMINATION OF LOCAL CORROSION CONDITIONS APPROPRIATE FOR A HIGH LEVEL CONTAINER IN A BASALT REPOSITORY (E. Gause, C. Brewster, P. Soo)	51
3.1	Introduction	51
3.2	Materials	52
3.3	Autoclave System Design	56
3.4	Experimental Procedures	58
3.4.1	Slurry Preparation	58
3.4.2	Autoclave Pressurization	60
3.4.3	Irradiation Procedure	61
3.4.4	Post-Test Procedures	61
3.5	Results and Discussion	62
3.5.1	Pressure Measurements	62
3.5.2	Pressure Changes Due to Radiolysis	63
3.5.2.1	Radiolysis of Water in a Closed System	63
3.5.2.2	Radiolysis of Methane in Aqueous Solution and in the Gaseous Phase	65
3.5.3	Gas Analyses Results	70
3.5.3.1	Phase I Test Gas Analysis Results	70
3.5.3.2	Phase II Test Gas Analysis Results	70
3.5.3.3	Phase III Test Gas Analysis Results	71
3.5.3.4	Comparison of Gas Analyses Results	71
3.5.4	Measurement of pH and DO and Calculation of Eh	72

CONTENTS (Continued)

3.5.4.1	Measurement of pH and Dissolved Oxygen of Unreacted Packing Material Slurry	72
3.5.4.2	Measurement of pH and Dissolved Oxygen of Reacted Packing Material Slurry	73
3.5.4.2.1	Measurement of Phase I Test pH and Dissolved Oxygen and Calculation of Eh	73
3.5.4.2.2	Measurement of Phase II Test pH and Dissolved Oxygen and Calculation of Eh	74
3.5.4.2.3	Measurement of Phase III Test pH and Dissolved Oxygen and Calculation of Eh	75
3.5.4.3	Comparison of pH and DO Measurements and Eh Calculations for All Tests	75
3.5.5	Measurement of Ionic Concentrations in Slurry Water	76
3.5.5.1	Measurement of Ionic Concentrations in Phase I Test	78
3.5.5.2	Measurement of Ionic Concentrations in Phase II Test	78
3.5.5.3	Measurement of Ionic Concentrations in Phase III Test	78
3.5.5.4	Comparison of Measured Ionic Concentrations For All Tests	79
3.5.6	SEM-EDX Analysis of Colloidal Material	80
3.5.6.1	SEM-EDX Analysis of Colloidal Material Removed From Phase I Test Solution	80
3.5.6.2	SEM-EDX Analysis of Colloidal Material Removed From Phase II Test Solution	81
3.5.6.3	SEM-EDX Analysis of Colloidal Material Removed From Phase III Test Solution	81
3.5.6.4	Comparison of SEM-EDX Analyses of Colloidal Materials	81
3.5.7	Analysis of Unreacted Bentonite and Reacted Bentonite Portion of Slurry	89
3.5.7.1	Analysis of Bentonite	89
3.5.7.2	Analysis of Montmorillonite Portion of Bentonite	89

CONTENTS (Continued)

3.5.7.2.1	Montmorillonite XRD Phase I Test	89
3.5.7.2.2	Montmorillonite XRD Phase II Test	98
3.5.7.2.3	Montmorillonite XRD Phase III Test	100
3.5.7.2.4	Comparison of Montmorillonite XRD Studies For All Tests	101
3.5.8	Analysis of Reacted Basalt	102
3.5.8.1	Comparison of XRD Patterns of Pulverized Basalt	102
3.5.8.2	Comparison of Micrographs of Polished Basalt Thin Sections	105
3.5.9	Metallography of Carbon Steel Sleeve and Identification of Surface Products	105
3.5.9.1	Metallography of Phase I Test Sleeve	108
3.5.9.2	Metallography of Phase II Test Sleeve	112
3.5.9.3	Metallography of Phase III Test Sleeve	117
3.5.9.4	Comparison of Pitting Corrosion For All Tests	119
3.6	Summary	119
3.7	Recommendations for Future Work	123
3.8	References	123
4.	TESTING FOR STRESS CORROSION CRACKING OF HIGH LEVEL WASTE CONTAINER MATERIALS IN TUFF REPOSITORY ENVIRONMENTS (H. Jain, C. Brewster, C. Anderson, P. Soo)	127
4.1	Introduction	127
4.2	Survey of Stress-Corrosion Behavior of Austenitic Stainless Steels in Relatively Pure Steam/Water/Air Environments	127
4.3	Test Plan	133
4.4	Materials and Specimens	134
4.5	Apparatus	139
4.6	Test Procedure	140
4.7	Results to Date	144
4.8	References	152

FIGURES

2.1.	Schematic representation of how WAPPA operates within each time step	13
2.2.	Geometrical representation of the waste form as a line source surrounded by the engineered barriers of the waste package	17
2.3.	Typical waste form and canister design	26
2.4.	Schematic representation of oxide thickness versus time. WAPPA considers thickness as a function of temperature and time	29
2.5.	Improved oxide thickness calculation considers thickness as a function of temperature and previous history	29
2.6.	Geometry of waste package	31
2.7.	Initial configuration of the waste package in WAPPA's complex verification test case.	
3.1.	Generalized stratigraphy of the Columbia River Basalt Group, Yakima Basalt Subgroup, and intercalated and suprabasalt sediments within the Pasco Basin	53
3.2.	Autoclave system being leak checked	57
3.3.	Cross section through autoclave	58
3.4.	Lengthwise section through autoclave	59
3.5.	Pressure changes with time and temperature in the autoclave system for the three phases of the experiment: Phase I (absence of methane and presence of radiation), Phase II (presence of methane and radiation), Phase III (presence of methane and absence of radiation.)	64
3.6.	Effect of dose rate on H ₂ equilibrium pressures for concrete (neat), concrete containing Fe ₂ O ₃ , and concrete containing MnO ₂	66
3.7.	Solubility of methane in water at high temperatures and pressures .	67
3.8.	Solubilities of O ₂ , N ₂ , and H ₂ in water as a function of temperature	72
3.9.	Micrograph of colloidal material recovered from the Phase I test (800X)	82
3.10.	EDX analysis of colloidal material recovered from the Phase I test	82

FIGURES (Continued).

3.11.	EDX analysis of rod in colloidal material recovered from the Phase I test	83
3.12.	EDX analysis of crystal in colloidal material recovered from the Phase I test	83
3.13.	Micrograph of protuberances appearing in colloidal material recovered from the Phase I test after bombardment with 17-kV electrons (1000X)	84
3.14.	Micrograph of colloidal material recovered from the Phase II test heater region (1000X)	84
3.15.	Micrograph of colloidal material recovered from the Phase II test wall region (1000X)	85
3.16.	Micrograph of colloidal material recovered from the Phase II test heater region (300X)	85
3.17.	Micrograph of the colloidal material recovered from the Phase III test heater region (100X)	86
3.18.	Micrograph of the colloidal material recovered from the Phase III test wall region (100X)	86
3.19.	EDX analysis of colloidal material recovered from the Phase III test heater region	87
3.20.	EDX analysis of colloidal material recovered from the Phase III test wall region	87
3.21.	EDX(TEM) analysis of colloidal material recovered from the Phase III test wall region	88
3.22.	Micrograph of unreacted bentonite clay (100X)	88
3.23.	Comparison of X-ray diffraction patterns of reacted and unreacted bentonite present in the Phase I test centrifuged packing material slurry samples prepared as oriented clay mounts by evaporation of slurry on glass slides. [Range of scan: $2\theta = 3-37^\circ$ ($d = 2.43-29.4$ A).]	90
3.24.	Comparison of X-ray diffraction patterns of reacted and unreacted bentonite present in the Phase II test centrifuged packing material slurry samples prepared as oriented clay mounts by evaporation of slurry on glass slides. [Range of scan: $2\theta = 3-37^\circ$ ($d = 2.43-2.94$ A)]	43

FIGURES (Continued)

3.25. Comparison of X-ray diffraction patterns of reacted and unreacted bentonite present in the Phase III test centrifuged packing material slurry samples prepared as oriented clay mounts by evaporation of slurry on glass slides. [Range of scan: $2\theta = 3-37^\circ$ ($d = 2.43-29.4 \text{ \AA}$)] 44

3.26. Appearance of Phase I centrifuged packing material slurries before and after reaction 45

3.27. Comparison of X-ray diffraction patterns of Phase I test reacted and unreacted montmorillonite present in the centrifuged packing material slurry samples prepared as oriented clay mounts by evaporation of slurry on glass slides; treatment by glycolation, followed by heating to 300°C for one hour. [Range of scan: $2\theta = 3-9.5^\circ$ ($d = 9.30-29.4 \text{ \AA}$)] 48

3.28. Comparison of X-ray diffraction patterns of Phase II test reacted and unreacted montmorillonite present in the centrifuged packing material slurry samples prepared as oriented clay mounts by evaporation of slurry on glass slides; heat-treated at 300°C for 18 hours, followed by glycolation at 60°C . [Range of scan: $2\theta = 3-9.5^\circ$ ($d = 9.30-29.4 \text{ \AA}$)] 97

3.29. Comparison of X-ray diffraction patterns of Phase III test reacted and unreacted montmorillonite present in the centrifuged packing material slurry samples prepared as oriented clay mounts by evaporation of slurry on glass slides; heat-treated at 150°C , followed by glycolation at 60°C , followed by heat-treatment at 300°C , followed by glycolation at 60°C . [Range of scan: $2\theta = 3-9.5^\circ$ ($d = 9.30-29.4 \text{ \AA}$)] 99

3.30. Comparison of X-ray diffraction patterns for reacted and unreacted basalt, prepared as unoriented mounts of pulverized basalt. [Range of scan: $2\theta = 3-65^\circ$ ($d = 1.43-29.4 \text{ \AA}$)] 103

3.31. Minerals in unreacted basalt as determined with a polarizing microscope under crossed polars (100X) 106

3.32. Minerals in Phase I test reacted basalt sampled from the heater region as determined with a polarizing microscope under crossed polars (100X) 106

3.33. Minerals in Phase I test reacted basalt sampled from the wall region as determined with a polarizing microscope under crossed polars (100X) 107

3.34. Minerals in the Phase III test reacted basalt sampled from the wall region as determined with a polarizing microscope under crossed polars (100X) 107

FIGURES (Continued)

3.35.	Appearance of carbon steel sleeve prior to reaction (left) and subsequent to Phase I test reaction (right)	109
3.36.	Micrograph of outside diameter of carbon steel sleeve subsequent to Phase I test reaction showing metal oxide and thin clay deposition layer (marked by arrow) (250X)	110
3.37.	Micrograph of outside diameter of carbon steel sleeve subsequent to Phase I test reaction showing metal oxide and thick clay deposition layer between arrows (250X)	110
3.38.	SEM-EDX micrograph of iron-rich layered material in Phase I test carbon steel surface product (1000X)	111
3.39.	Micrograph of outside diameter of carbon steel sleeve prior to Phase I test reaction (250X)	111
3.40.	Micrograph of weld metal in carbon steel sleeve subsequent to Phase I test reaction (250X)	113
3.41.	Micrograph of outside diameter of carbon steel sleeve subsequent to Phase II test reaction showing metal oxide and thin clay deposition layer (marked by arrows) (250X)	113
3.42.	Micrograph (SEM) of orange-brown sleeve surface product from Phase II test (100X)	114
3.43.	Micrograph (SEM) of magnetic green-yellow sleeve surface product from Phase II test (100X)	114
3.44.	Point plot of EELS spectrum of orangish-brown sleeve surface product from the Phase II test showing well-defined crystalline material containing iron and oxygen	115
3.45.	Debye-Scherrer powder pattern for orange-brown sleeve surface product from Phase III test	116
3.46.	Debye-Scherrer powder pattern for green-yellow sleeve surface product from Phase II test	116
3.47.	Micrograph of outside diameter of carbon steel sleeve subsequent to Phase III test showing pitting, and a thin detached oxide layer (250X)	118
3.48.	Micrograph of Phase III test green carbon steel surface product (100X)	120
3.49.	EDX of Phase III test green carbon steel surface product	120

FIGURES (Continued)

3.50.	Micrograph of Phase III test orange-brown carbon steel surface product (100X)	121
3.51.	EDX of Phase III test orange-brown carbon steel surface product . .	121
4.1.	Proposed relationship between chloride and oxygen content of alkaline phosphate treated boiler water and susceptibility to stress corrosion cracking of austenitic stainless steel exposed to the steam phase with intermittent wetting	128
4.2.	The relationship between original strain in bent-beam specimen and time-to-crack for (a) Type 321 stainless steel at 300°C and (b) Type 304 stainless steel at 200°C	129
4.3.	Effect of chloride added as NaCl on cracking of Type 304 stainless steel at 100°C. Solution transported by porous material to specimen	130
4.4.	(a) Schematic diagram of double U-bend type specimen. (b) Schematic diagram of γ -ray irradiation	131
4.5.	C-ring specimen design	135
4.6.	C-ring stress corrosion cracking test apparatus	140
4.7.	Load vs deflection of Type 304L stainless steel sensitized C-ring test specimen under compression	141
4.8.	Schematic of the specimen arrangement in a test vessel	143
4.9.	Load vs in situ strain at the apex of a Type 316L stainless steel C-ring specimen	145
4.10.	Microstructure of Type 304L stainless steel. (a) As-received, etched in glycerregia. (b) Sensitized at 600°C for 100 hours, etched in oxalic acid	146
4.11.	pH of the six test solutions at 101°C as a function of time. Each symbol represents the solution in one test vessel	147
4.12.	C-ring specimens of Type 321 sensitized stainless steel after three-month test in "synthetic J-13 water"	149

TABLES

1.1.	List of estimated spent fuel waste package conditions for a salt repository	7
1.2.	List of estimated spent fuel waste package conditions for a basalt repository	8
1.3.	List of estimated spent fuel waste package conditions for a tuff repository	9
2.1.	Significant limitations of WAPPA's modeling	39
3.1.	Compositions of Middle Sentinel Bluffs Flow basalt and reference Wyoming bentonite	54
3.2.	Petrographic characteristics of primary and secondary phases reported as present in Grande Ronde basalt.	55
3.3.	Composition of synthetic Grande Ronde groundwaters	56
3.4.	Comparison of composition of gases sampled after reaction as determined by mass spectrometry	69
3.5.	pH and DO as measured for packing material slurry and Eh as calculated for all tests	76
3.6.	Comparison of ionic concentrations of reacted Grande Ronde GR-3 groundwater	77
3.7.	Comparison of (00 $\bar{1}$) d-spacings based on X-ray diffractometer studies of reacted and unreacted bentonite portions of centrifuged packing material slurries prepared as oriented clay mounts by evaporation of centrifuged slurry on glass slides. [Intensities not specified. Range of scan: $2\theta = 3-37^\circ$ ($d = 2.43-29.4$ A).]	94
3.8.	Comparison of (00 $\bar{1}$) d-spacings based on X-ray diffractometer studies of Phase I test reacted and unreacted montmorillonite, prepared as oriented clay mounts by evaporation of centrifuged packing material slurry on glass slides; treatment by glycolation at 60°C, followed by heating to 300°C for one hour. [Intensities not specified. Range of scan: $2\theta = 3-9.5^\circ$ ($d = 9.30-29.4$ A).]	95
3.9.	Comparison of (00 $\bar{1}$) d-spacings based on X-ray diffractometer studies of Phase II reacted and unreacted montmorillonite, prepared as oriented clay mounts by evaporation of centrifuged packing material slurry on glass slides; treatment by heating to 300°C for 18 hours, followed by glycolation at 60°C. [Intensities not specified. Range of scan: $2\theta = 3-9.5^\circ$ ($d = 9.30-29.4$ A).]	98

TABLES (Continued)

3.10.	Comparison of (00 l) d-spacings based on X-ray diffractometer studies of Phase III reacted and unreacted montmorillonite, prepared as oriented clay mounts by evaporation of centrifuged packing material slurry on glass slides; heat-treatment at 150°C, followed by glycolation at 60°C, followed by heat-treatment at 300°C, followed by glycolation at 60°C. [Intensities not specified. Range of scan: $2\theta = 3-9.5^\circ$ ($d = 9.30-29.4 \text{ \AA}$).]	101
3.11.	Comparison of (hkl) d-spacings based on X-ray diffractometer studies of reacted and unreacted basalt, prepared as unoriented mounts of pulverized basalt. [Intensities not specified. Range of scan: $2\theta = 3-65^\circ$ ($d = 1.43-29.4 \text{ \AA}$).]	104
3.12.	Calculated d-spacings of Phase II test sleeve surface product based on measured Debye-Scherrer electron diffraction powder patterns . .	117
4.1.	SCC test in boiling deionized water	132
4.2.	Test matrix for stress corrosion of candidate stainless steels and Incoloy-825	133
4.3.	Vendor supplied chemical analysis of test alloys (weight percent) .	134
4.4.	Mechanical properties of as-received test alloys (vendor supplied data)	134
4.5.	Geochemical analysis of Topopah Spring tuff	137
4.6.	Reference groundwater composition for tuff repositories (based on composition of Jackass Flats Well J-13 at the Nevada Test Site) . .	138
4.7.	Amount of chemical compounds used in preparing 20 liters of synthetic J-13 water	139
4.8.	Stress-strain properties of eight alloys as obtained from Instron machine tests on smooth C-ring specimens	142
4.9.	pH of test solutions at the end of the three-month tests	148
4.10.	Chemical composition of test solutions obtained at the end of three-month tests	150
4.11.	Room temperature chemical composition of filtered solutions obtained from the reaction of distilled water with crushed tuff. Composition of reference J-13 groundwater is included for the purpose of comparison	151

ACKNOWLEDGMENTS

In the testing program the authors would especially like to thank Dr. Ramesh Dayal for his review of the manuscript. They are also grateful to Dr. Harpal Arora for his helpful discussions regarding the use of the X-ray diffractometer and mineralogical identification. Appreciation is also extended to Robert Sabatini and Johan Tafto for performing the SEM-EDX analyses and for their efforts in attempting to identify the composition of the carbon steel surface products. They would also like to thank Eugene Ferreri, Mary Kinsley, Andrew Cendrowski, Sue Oakley, Robert Wilson and John Warren for ion chromatography results, atomic absorption results, metallographic results, silica content determinations, gas analyses and SEM-EDX analysis of the colloidal material, respectively. The authors would also like to express their gratitude to Ms. Grace Searles for her patience and skill in the typing and preparation of this report.

EXECUTIVE SUMMARY

This Biannual Report describes two aspects of an ongoing program concerned with high level waste package evaluation. The first deals with a review of selected codes and models being developed by DOE to predict package performance, and the second is to perform verification tests to provide information on critical issues related to package behavior. Specifically, the potential of the WAPPA code (Waste Package Performance Assessment Code) to meet the needs as a licensing tool have been analyzed. This analysis is based on the contents of the code manual, an update of the code and the source program. The latter part of this report describes testing programs conducted by BNL to determine the chemical environment of a high level waste package in a basalt repository and to assess the potential of stainless steel containers to fail by stress corrosion cracking in a tuff repository system.

The WAPPA code in its present form is of limited use to the NRC. This code implements a modeling approach that is mostly empirical in nature. In practice, it operates as a data base manager that simply selects which correlation and which data are applicable to each particular situation. Because of the large amount of data the user has to supply for the empirical models and the number of situations for which they may have to be specified, data gathering, interpretation, and validation will require a significant effort by personnel who are thoroughly familiar with the assumptions that went into the code. The difficulty of preparing the data files will be compounded by the scarcity of adequate data in the literature and by ambiguities the required data may entail, e.g., data are needed which require a priori estimate of future waste package performance; and data are needed for correlations which factor in only a few of the several variables on which a particular process may depend. Furthermore, since most of the models are empirical, their applicability must be proven. This will require a suite of auxiliary codes representing state-of-the-art modeling of the actual processes considered.

While the use of WAPPA as a licensing tool requires extensive data and model validation, one may relax these requirements for use as a site screening tool or as a tool for preliminary design analysis. It will be necessary, however, to remove first some of the major inconsistencies identified in the modeling, e.g., the leach-and-transport model needs to be modified to conserve mass, etc. WAPPA is hardly amenable to probabilistic reliability analysis because of the large number of parameters to be sampled and the need to re-run the code a number of times to insure convergence. The last difficulty may be hard to remove even if sensitivity analysis is performed first.

The objective of the first testing program was to determine the chemical environment that will be present within high level nuclear waste packages emplaced in a basalt repository. For this purpose, low carbon 1020 steel (a current BWIP reference container material), synthetic basaltic groundwater and a mixture of bentonite and basalt were exposed in an autoclave to expected repository conditions shortly after repository sealing (150°C, 10.4 MPa). The experimental program consisted of three phases. Phase I involved a two-month irradiation test $(3.8 \pm 0.5) \times 10^4$ rad/h in an argon environment. The Phase II

test was similar but was conducted in a methane environment. These two tests were followed by a Phase III control test which was similar to the Phase II study but it was performed in the absence of radiation.

All of these studies concentrated on changes in gas pressure and composition; on the differences in pH, dissolved oxygen (DO), calculated Eh and the concentration of those ions, which have been implicated in the corrosion of carbon steel, as sampled across a thermal gradient; on alterations of the packing material as determined by X-ray diffraction (XRD); and on the determination of localized and uniform corrosion of the carbon steel sleeve.

Trends in gas pressure were similar in each of the three tests. Over the two-month test periods, the gas pressure in the autoclave ranged from 9.3-9.7 MPa (1357 psi to 1404 psi) in the Phase I test, from 11.1-13.2 MPa (1612 psi to 1919 psi) in the Phase II test and from 9.8-11.7 MPa (1416 psi to 1702 psi) in the Phase III test. There was an early trend to decreasing pressures followed by a trend to pressures approaching or slightly exceeding the initial values. This indicates that pressure in a sealed repository environment may initially decrease and be followed by a slow increase. Overall, in all three tests, hydrogen was produced and oxygen was consumed, as determined by gas analyses and dissolved oxygen measurements. More hydrogen was produced in the Phase II test than in the Phase I and III tests due to the radiolysis of methane. Similar amounts of hydrogen were produced in the irradiated Phase I test and in the non-irradiated Phase III test. These results indicate that, in a repository, hydrogen will be produced and oxygen will be consumed but that some residual oxygen may be present, at least in the short term. Carbon-containing gases were produced in the Phase I test (CO_2 and CH_4) and in the Phase II test (CO_2 and C_2H_6) and possibly in the Phase III test.

There were different thermal gradients established across the packing material in each test. For Phase I, II, and III tests, these were, respectively, 1.0, 0.6, and $2^\circ\text{C}/\text{mm}$. After cooling the autoclave over a period of 25 minutes, the pH of the water in the basalt/bentonite packing material measured at room temperature was nearly neutral. There did not appear to be a significant change in pH across the thermal gradient in the packing material in any of the three tests. There did not appear to be a significant change in DO across the thermal gradient of the packing material in any of the tests. The calculated Eh values indicate that an oxidizing environment existed after quenching the contents of the autoclave. Reducing environments were not achieved under the current test conditions.

The concentrations of Cl^- and SO_4^{2-} measured at room temperature were greater near the cooler end of the thermal gradient in the tests. Changes in ionic concentrations occur across the thermal gradients but bulk changes in ionic concentrations, relative to the groundwater composition, may be more significant in terms of corrosive environments. The bulk of the Fe and Si content of the liquid system is present as colloidal material that is filterable. Colloids are formed in the absence of radiation but their production seems to be enhanced if radiation is present.

Hydrothermal conditions cause some change in the bentonite component of the packing material as determined by X-ray diffraction (XRD). The

expandability of the bentonite portion of the wet packing material may be affected by periods of heating and simultaneous dehydration. Radiation may enhance expandability. Optical and XRD studies indicate that some changes occur in the mineralogical content of basalt during hydrothermal testing. The alteration of the pyroxenes in the basalt is one mineralogical change that was observed. Other alteration also occurs in the presence or absence of radiation as evidenced by changes in XRD patterns.

Adherent surface products removed from the carbon steel sleeve in the Phase I test contained mainly montmorillonite clay. Scanning electron microscope (SEM-EDX) analysis indicated the presence of other materials containing more Fe than that found in montmorillonite. Surface products removed from the carbon steel sleeve in the Phase II test were analyzed by SEM-EDX and electron diffraction but were not readily identifiable. (An orange-brown product contained large amounts of Si, Fe, and Al, while the green-yellow product was largely composed of Fe and Si.) Identification was also not possible for the Phase III surface products, which were analyzed by SEM-EDX and XRD. (Both Phase III surface products contained large amounts of Si and Fe, with the green phase also containing a large amount of Ca.)

There was no pitting on the carbon steel sleeve or the steel weldment in the Phase I test. There were hemispherically-shaped pits approximately 12 microns in depth in the Phase II test, and shallower (approximately 8 microns in depth) and more closely-spaced pits were formed in Phase III. Under the conditions of these tests, the maximum predicted pit depth in 300 years is estimated to be <2.2 cm.

A literature survey of the pertinent stress corrosion data on stainless steels suggested that this mode of failure can occur in some of the materials under consideration by the tuff repository program for HLW containers. Therefore, a testing program was initiated to evaluate the stress corrosion cracking (SCC) susceptibility of the candidate alloys viz. Types 304L, 316L and 321 stainless steels, and Incoloy 825 in a simulated tuff repository environment. The notched C-ring test method has been adopted in which each specimen is stressed to 90% of the elastic limit calculated for the unnotched condition. Stressed specimens are being exposed at $\approx 100^{\circ}\text{C}$ to the liquid as well as the steam phase over synthetic J-13 groundwater and ten-times concentrated J-13 groundwater both in equilibrium with crushed Topopah Spring tuff for a duration of 3, 6 and 12 months. The use of concentrated water simulates the situation when salts precipitated after initial evaporation of groundwater are redissolved in water subsequently percolating towards the repository horizon.

The three-month tests have been completed recently. Preliminary examination of the specimens shows that macroscopic stress corrosion cracks are absent. Examinations to detect microcracks are in progress. Chemical analysis shows that the concentrations of several ionic species increases during testing. This increase in concentration presumably results from the dissolution of salts in the crushed tuff. More results will be obtained upon completion of the six- and 12-month tests.

BLANK PAGE

1. INTRODUCTION

The NRC Rule for the Disposal of High Level Waste in Geologic Repositories (10 CFR 60) dated June 1983, specifies two main performance objectives for the engineered barrier system:

Containment of HLW within the waste packages will be substantially complete for a period to be determined by the Commission taking into account the factors specified in subsection 60.113(b) (of 10 CFR 60) provided, that such period shall be not less than 300 years nor more than 1,000 years after permanent closure of the geologic repository; and

The release rate of any radionuclide from the engineered barrier system following the containment period shall not exceed one part in 100,000 per year of the inventory of that radionuclide calculated to be present at 1,000 years following permanent closure, or such other fraction of the inventory as may be approved or specified by the Commission; provided, that this requirement does not apply to any radionuclide which is released at a rate less than 0.1% of the calculated total release rate limit. The calculated total release rate limit shall be taken to be one part in 100,000 per year of the inventory of radioactive waste, originally emplaced in the underground facility, that remains after 1,000 years of radioactive decay.

In order to show compliance with these performance objectives the license applicant will need to provide a data base and analyses to quantify anticipated behavior of the waste package/repository system after permanent closure. This will necessarily involve research and testing programs to evaluate the likely modes by which engineered system components will degrade or fail by chemical or mechanical means. Knowledge of the ways in which the engineered barriers fail will permit estimates to be made regarding the containment capability of the waste package and the radionuclide release rate from the engineered system. A sequence of events leading to loss of containment and the release of radionuclides would include:

- a. Groundwater entering the engineered barrier system
- b. Groundwater penetrating the geologic packing material
- c. Groundwater penetrating the container/overpack system
- d. Groundwater leaching radionuclides from the waste form
- e. Radionuclides transported through the failed container/overpack system, packing material and disturbed host rock to the near field environment.

For these scenarios, in which the individual engineered barriers are breached, probable chemical (corrosion) failure/degradation modes and mechanical failure/degradation modes need to be identified and quantified. These will depend on the specific design of the engineered system including selection of materials, local temperatures, local repository water conditions, radiation effects, water flow rates, and lithostatic/hydrostatic pressures, etc.

Estimates are given in Tables 1.1 through 1.3 of the potential range of conditions around a waste package in salt, basalt and tuff (NUREG/CR-2482, Vol. 7, 1984). These will of course be strongly dependent on final package geometries, designs and material selection. It is the interaction of the package with its environment that must be evaluated in order to predict with reasonable assurance that applicable regulatory criteria are met. The licensee will need to supply an appropriate data base and analysis, based on adequate test methods to support the projected performance of engineered barrier systems under anticipated repository conditions.

This report details two aspects of Brookhaven's program of reviewing DOE activities in the area of waste package performance verification testing. The first part of this report is a review of the Waste Package Performance Assessment Code (WAPPA). This code was designed as a tool to aid in waste package design, repository design, site selection and characterization and system assessment. The objective of this evaluation is to examine the adequacy of the modeling in WAPPA and to determine its potential use as a licensing tool.

The remainder of this report describes two test programs conducted by BNL. One was to determine the local corrosion conditions pertinent to a high level waste container in a basalt repository and the other was to check the possibility of stress corrosion cracking effects in stainless steel containers being considered for use in a tuff repository.

In the first test, low carbon steel (a current Basalt Waste Isolation Project, BWIP, reference container material), a basalt/bentonite packing material, and synthetic Grande Ronde basaltic water were reacted in an autoclave at 150°C and 10.4 MPa (1500 psi) pressure. The tests lasted for two-month periods and the gamma irradiation flux, when used, was $(3.8 \pm 0.5) \times 10^4$ rad/h. The Phase I irradiation test used an inert argon environment and Phase II involved a similar set of experimental conditions but used a methane cover gas. This was performed because high methane concentrations have been detected in basaltic water samples taken from Borehole RRL-2 in the Grande Ronde formation. The Phase III control test was also conducted in a methane environment, but in the absence of irradiation.

Measurements on the packing material slurry at the conclusion of the tests included pH and dissolved oxygen (DO) determination. The concentrations of Cl^- , total Fe (measured as Fe^{2+}), and SO_4^{2-} ions in the filtrate were also measured, since these ions are associated with the corrosion of carbon steel. Gases generated during the irradiation period may include H_2 , O_2 , N_2 and CO_2 . Since several of these gases could have a deleterious effect on the waste container, gas analyses were made at the conclusion of the test period. The carbon steel sleeves were metallurgically evaluated for uniform and pitting corrosion. Hydrothermal alteration of the rock and clay constituents of the packing material was also investigated.

The stress corrosion cracking program was initiated because of concern that some reference container materials being considered for a tuff repository (Type 304L, 316L, 321 stainless steels and Incoloy-825) were susceptible to stress corrosion cracking. The issue arose because of data in the literature that show that stressed C-ring samples of Type 304L cracked in boiling water

containing small quantities of air and chloride ion in the presence of gamma radiation. The tests carried out in the current program involved the testing of stressed, V-notched C-rings in boiling water in the presence of crushed tuff.

References

Code of Federal Regulations, "Final Rule for the Disposal of High Level Waste In Geologic Repositories," 10 CFR Part 60, June 1983.

NUREG/CR-2482, Vol. 7, BNL-NUREG-51494, "Review of DOE Waste Package Program - Subtask 1.1 National Waste Package Program, Biannual Report," E. Gause and P. Soo, Brookhaven National Laboratory, September 1984.

Table 1.1. List of estimated spent fuel waste package conditions for a salt repository.

Parameter	Estimated Value			
	Operations Period	Thermal Period (0-300 yr)	Transition Period (300-1000 yr)	Geologic Control (>1000 yr)
Temperature at Centerline (Thermal Loading 12.4 W/m ²)		375°C max.	Approximately 150-110°C	<110°C
Total Gamma Dose (rad)		10 ⁹ -10 ¹⁰	Little additional irradiation.	Little additional irradiation.
Brine Flow Rate		Total of about 7 liters per borehole for 24.7 W/m ² thermal loading.	Little additional brine inflow	Little additional brine inflow
Brine Chemistry	Brine A or Brine B chemistries depending on repository location.	Brine A or Brine B with significant NaOH levels.	Brine A or Brine B with NaOH present.	
pH (measured at 25°C)	Steam/air plus small amounts of HCl/SO ₂ /CO ₂ /H ₂ S.	Initially acidic brine (pH =3.5) due to dissolution of acid gases. Changing to alkaline brine because of dissolution of colloidal sodium by brine inclusions. pH could rise to 9.5 based on experiments with irradiated salt and deionized water.	Probably alkaline.	Probably alkaline.
pH (at high temperature)		Lower than values measured at 25°C but no reliable values can be specified because of complex hydrothermal reactions and irradiation effects.		
Redox Conditions	Oxic	Probably oxic due to brine radiolysis.	Approaching Anoxic	Probably anoxic.
Stress (MPa)	0.1	Initially 0.1 MPa, rising to lithostatic stress of 16.2 MPa as host rock settles.		

Table 1.2. List of estimated spent fuel waste package conditions for a basalt repository.

Parameter	Estimated Value			
	Operations Period	Thermal Period (0-300 yr)	Transition Period (300-1000 yr)	Geologic Control (>1000 yr)
Temperature at Centerline (Thermal Loading 13.0 W/m ²)	230°C	265°C max. after ≈35 yr.	140-125°C	<125°C
Total Gamma Dose (rad)		10 ⁷ -10 ⁸	Little additional irradiation.	No additional irradiation.
Vertical Hydraulic Conductivity (m/sec.)		Unknown, but likely to be much greater than that for horizontal flow because of buoyancy effects.		
Water Chemistry	Steam/air.	Significant increases in K ⁺ , Ca ²⁺ , Fe, Si, and SO ₄ ⁻² in the packing material water at higher temperatures. F ⁻ is reduced in concentration.		Not known, but there should be a tendency to return to original Grand Ronde water chemistry.
pH (measured at 25°C)		Initially 6.0 in packing material water, decreasing to 6.3-7.3.	Increasing to approximately 9.0.	
pH (at high temperatures)		Lower than values measured at 25°C but no reliable values can be specified because of complex hydrothermal reactions and irradiation effects.		
Redox Conditions	Oxic.	Probably oxic due to water radiolysis.	Approaching anoxic.	Probably anoxic.
Stress (MPa)	0.1	Initially 0.1 MPa, rising to a value between hydrostatic and lithostatic stresses (11 to 33 MPa).		

Table 1.3. List of estimated spent fuel waste package conditions for a tuff repository.

Parameter	Estimated Value			
	Operations Period	Thermal Period (0-300 yr)	Transition Period (300-1000 yr)	Geologic Control (>1000 yr)
Temperature at Centerline* (Thermal Loading 12.4 W/m ²)		330°C max. to 100°C	100-60°C	<60°C
Total Gamma Dose (rad)		≈10 ¹⁰	Little additional irradiation.	No additional irradiation.
Water Flow Rate	Steam/air conditions.	Steam/air for first several hundred years followed by liquid water flowing at about 8 mm/yr.	About 8 mm/yr.	About 8 mm/yr.
Water Chemistry	Steam/air conditions.	Probably similar to J-13 well water after steam conditions subside. May be more concentrated than J-13 water if precipitated salts redissolve.	Probably similar to J-13 well water but could be more concentrated if precipitated salts redissolve.	
pH (Measured at 25°C)		7.1 for J-13 well water. May be acidic because of radiolysis of N ₂ /O ₂ /H ₂ O mixtures.	≈7.1	≈7.1
Redox Conditions	Oxic	Oxic	Oxic	Oxic
Stress (MPa)	0.1	Initially 0.1 MPa, rising to the lithostatic stress of 8.6 MPa as host rock settles.		

*Calculations were made for waste package without packing material.

2. REVIEW OF WAPPA

2.1 Introduction

2.1.1 Background Information

The Code of Federal Regulations 10 CFR Part 60, §60.113 (June 1983) requires that the applicant for a license to operate a nuclear waste repository demonstrate compliance of the proposed design with the following performance criteria of individual barriers after permanent closure:

1. Containment of HLW within the waste packages should be substantially complete for a period to be determined by the Nuclear Regulatory Commission. Such a period shall be not less than 300 years nor more than 1000 years after permanent closure of the repository.
2. The release rate of any radionuclide from the engineered barrier system following the containment period should not exceed one part in 100,000 per year of the inventory of that radionuclide calculated to be present at 1,000 years. Exception to this rule is allowed for radionuclides whose release rate is less than 0.1% of the calculated total release rate limit, which is taken to be 1 part in 100,000 per year of the (total) inventory of radioactive waste that remains after 1,000 years of radioactive decay.
3. Pre-waste-emplacment groundwater travel time along the fastest path of likely radionuclide travel from the disturbed zone to the accessible environment should be at least 1,000 years or such other travel time as may be approved or specified by the Nuclear Regulatory Commission.

Although the controlled release requirement is on the engineered barrier system (the waste package and the underground facility), it is expected that the applicant will rely primarily on the waste package. Thus, waste package performance is the direct concern of two out of three NRC individual-barrier performance criteria.

Two waste-package system performance codes have been developed: BARIER and WAPPA. Both codes were developed for the salt program (ONWI-302, 1981; ONWI-452, 1982), but were kept general enough to be applied to hard rock repositories. At present, development of the code BARIER has been discontinued, and WAPPA is the only code used by the salt and tuff programs for integrated waste package performance. In particular, the tuff program is modifying WAPPA to allow its use for nonsaturated conditions. The basalt program does not have a waste-package system code.

This document presents a review of the code WAPPA as it is presented in the code manual ONWI-452 of April 1983 and in a subsequent, letter-form update of December 1983 by the code custodian¹. For clarity, the code WAPPA is briefly introduced in Section 2.1.2. This document's objectives and organization are presented in Section 2.1.3.

¹Private communication from Leslie A. Scott to Claudio Pescatore, December 14, 1983.

2.1.2 The Code WAPPA

The Waste Package Performance Assessment Code WAPPA was constructed for general applicability to all candidate geologic media, to any waste type, and to conventional waste package designs and geometries. The code was designed to serve as a tool in all of the following major areas: waste package design, repository design, site selection and characterization, and system assessment.

WAPPA consists of about 13,000 source program statements representing five physical process models and a system drive model. With reference to Figure 2.1, the five process models include a radiation model, a thermal model, a mechanical model, a corrosion model, and a leach-and-transport model. These models are sequentially activated in the above order within each time step by the system drive model. Each process model applies to all waste package barriers at the same time. For instance the radiation model would determine the radiation field throughout the waste package as well as corrosion and leaching enhancement factors for wetted barriers. Thus, the implemented approach is termed "barrier-integrated and process-sequential." The code uses one-dimensional, radial axisymmetric geometry with correction factors for finite length effects.

The modeling approach implemented in WAPPA is more empirical than mechanistic. Thus a most significant but little emphasized task in the operation of WAPPA is the preparation of a data base encompassing all empirical parameters for the problem at hand. The task can be overwhelming due to the recognized lack of pertinent data in the literature and to the large variation of problems one may have to solve.

2.1.3 Objectives and Organization of this Report

The present review of WAPPA has been prompted by the importance of this code within the DOE community which regards it as the preferred code for integrated waste package analysis.

The objective of this report is to examine the code's level of modeling in order to determine its potential uses for the regulatory community, i.e., whether the code could be used for licensing, reliability analysis, screening of various waste package designs, etc. Furthermore, we have also examined the possibility of adapting parts of WAPPA into existing codes at BNL.

Chronologically, we have first run the code at BNL and examined the Complex Verification Test Case provided by the code developer. This indicated some potential problems in the code modeling and its structure. We then examined each process model following the code manual and, to some extent, the source program. This effort also resulted in re-writing part of the Leach-and-Transport model. Our findings were documented in a series of memos-to-file which were made available to the NRC and its contractors (BNL, MF 125, 126, 127, 132, 135, 141, 142, 149, 151, 1983 through 1984).

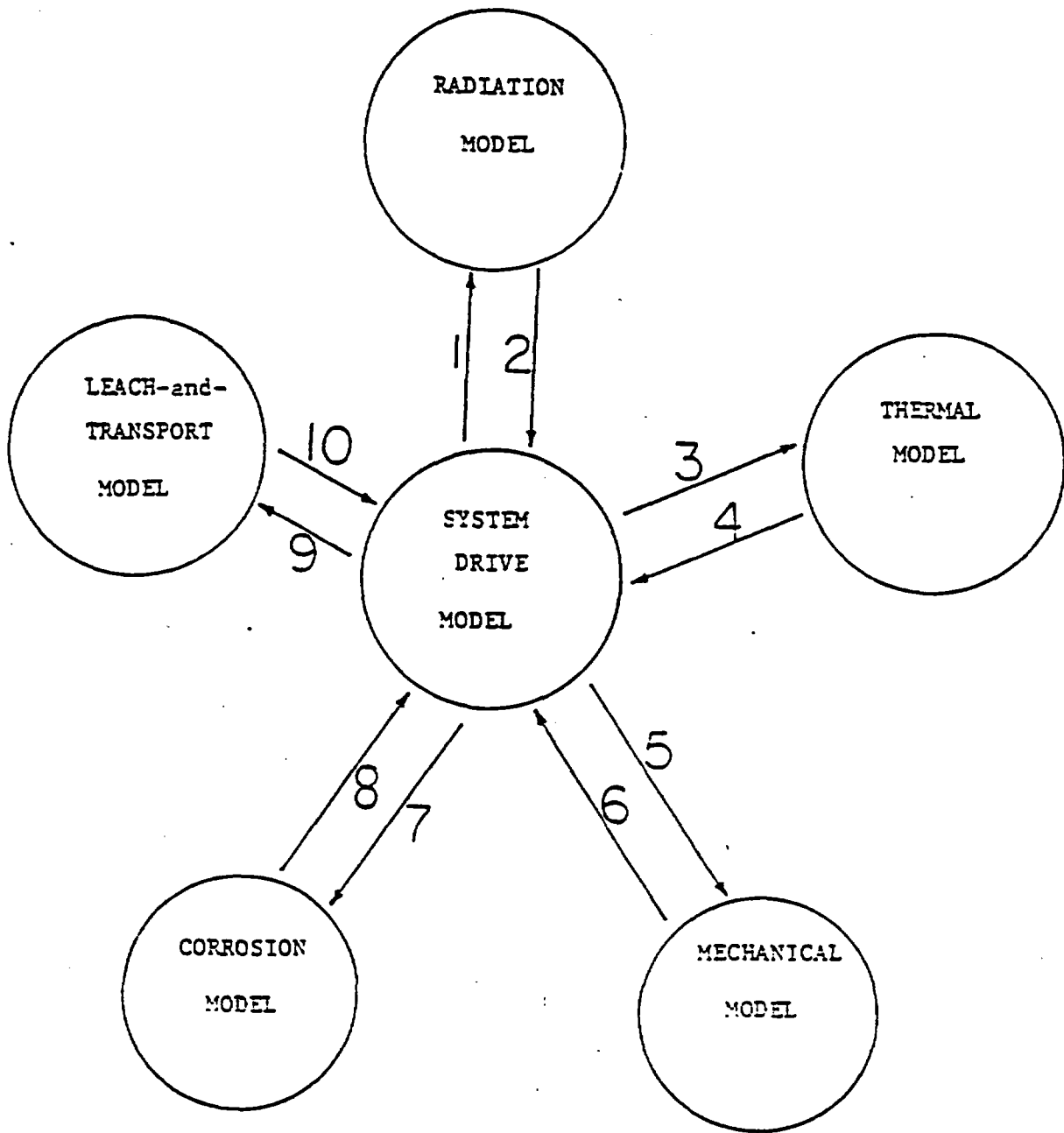


Figure 2.1 Schematic representation of how WAPPA operates within each time step.

The present report draws on the material of our original memoranda. With minor changes they constitute Section 2.2 and 2.3 of the document, and deal with each process model and WAPPA's operation, respectively. Conclusions are drawn in Section 2.4, which also gives our final recommendations.

2.2 Review of WAPPA's Process Models

As indicated earlier, the code WAPPA was constructed for general applicability to all candidate geologic media, to any waste type, and to conventional waste package designs.

The code uses one-dimensional, radial axisymmetric geometry with correction factors for finite length effects, where applicable. System performance is determined through sequential use of five main process models a radiation model, thermal model, mechanical model, corrosion model, and leach-and-transport model. With reference to Figure 2.1, sequential coupling in the above order is operated by a system drive model. Thus, within each time step, results from the Radiation Model can be used in the four remaining process models, results from the Thermal Model can be used in the three remaining models, and so on. Each model is reviewed separately in Sections 2.2.1 through 2.2.5. General conclusions about WAPPA's level of modeling are drawn in Section 2.2.6.

2.2.1 WAPPA's Radiation Model (RMODEL)

The primary function of the radiation model is to calculate radiation induced effects that are required as input to other WAPPA process models. Thus, the radiation model obtains the decay heat rate which is used by the thermal model, the alpha damage to the waste form to be used in the mechanical model, and corrosion and leaching enhancement factors due to radiolysis to be used in the corrosion and leach-and-transport models, respectively. These quantities are calculated through four distinct submodels: (a) Source Term, (b) Attenuation, (c) Radiolysis, and (d) Damage. These are reviewed in the following section.

2.2.1.1 Review of Modeling Approach

2.2.1.1.1 Source Term Submodel

The first function of this submodel is to obtain the decay heat rate, gamma ray and alpha particle emission rate, and radionuclide mass inventory within the waste form at any given time. The basis of the calculation is a logarithmic interpolation procedure using a user supplied time-dependent data base. Presently, this data base is prepared by using the isotope buildup and decay code ORIGEN2 (ORNL-5621).

The second function of this submodel is to calculate the gamma dose and the alpha particle displacement dose at the waste form periphery. The alpha particle displacement dose is used by the Damage submodel to calculate degradation of waste form properties. The gamma dose is used by the Radiolysis

submodel to calculate enhancement of corrosion and leaching caused by gamma radiolysis. It should be emphasized that this gamma dose is at the periphery of the waste form and not in the groundwater where the radiolysis occurs.

2.2.1.1.2 Attenuation Submodel

This submodel calculates the attenuation of gamma rays as they travel from the waste form to the repository. This is accomplished by calculating the gamma flux as a product of the source in the waste form, a buildup factor, and an attenuation factor. The empirical buildup factor simulates the effect of scattered radiation. The attenuation factor is a function of the thickness and type of barriers in the waste package.

2.2.1.1.3 Radiolysis Submodel

WAPPA assumes that the influence of gamma radiolysis on corrosion and leaching can be modeled through empirically determined enhancement factors. These are multiplicative factors defined so that multiplication of the leach or corrosion rate by the enhancement factor gives the enhanced rate due to radiolysis. The radiolysis submodel determines these enhancement factors, as function of the gamma flux, dose rate and cumulative dose at the edge of the waste form, through a logarithmic interpolation of user supplied data.

2.2.1.1.4 Damage Submodel

This submodel calculates changes in the thermal conductivity, fracture strength, thermal expansion coefficient and density of the waste form due to alpha-induced damage. These properties remain unchanged until the alpha displacement dose reaches a user defined critical value. After reaching this value, the material property under consideration is degraded according to a saturating exponential which depends on the cumulative dose and empirically determined coefficients.

2.2.1.2 Discussion

The primary method used in WAPPA's radiation submodels for calculating a desired quantity involves reading a data base. This causes two problems. First, the input required for the data base may not be readily available. If this is the situation, the required information could be obtained through ad hoc experiments or through use of more advanced computer simulations. For example, assuming that the buildup factor in basalt is unknown, a detailed photon transport calculation could be performed and the buildup factor chosen such that the flux as calculated by the transport code matched the flux calculated by WAPPA's attenuation submodel. The second problem is that each user must construct his own data base. WAPPA does not supply the data. It does not even supply a list of references where the appropriate data can be found. This makes the calculation subject to the user's ability to obtain the proper data. Because of the paucity of present data, and the uncertainty in some of the data, it is unlikely that any two users will create the same data base.

2.2.1.2.1 Source Term Submodel

The Source Term submodel's major function involves reading waste-form inventory information from a data base. The modeling it implements does have two conservative approximations: (1) it does not account for redistribution of nuclides due to leaching; therefore it overpredicts the radiation source within the waste form; and (2) it uses the gamma flux and total dose at the waste form periphery for determining enhancement of leaching and corrosion, which overpredicts the effects of radiolysis. Indeed, during the containment period the flux at the waste form periphery will be much greater than in the groundwater. Thus, the calculated total dose to the groundwater will exceed the actual dose. Since the enhancement is a function of both dose and flux, radiolysis effects are overpredicted.

2.2.1.2.2 Attenuation Submodel

The attenuation submodel serves no obvious purpose. Currently, the only use for the gamma flux is to determine the amount of radiolysis that occurs in the groundwater. However, since WAPPA uses the gamma flux at the waste form boundary, as determined by the Source Term submodel, calculations of the flux in the remainder of the waste package are superfluous.

Assuming that future revisions of the code do use the gamma flux within the waste package, the following comments become relevant.

The documentation for this submodel lacks detail and justifies this shortcoming on the claim that the model uses standard expressions from the Reactor Shielding Design Manual (Rockwell, T.; 1956). However, the equations are applied incorrectly in WAPPA. The error involves improper definition of the buildup factors. Before explaining this error, a description of buildup factors and their properties is presented.

Buildup Factors

WAPPA assumes that the effects of scattered radiation can be accounted for through a buildup factor. This prevents the need for a detailed transport calculation. However, it requires the use of an empirically determined buildup factor, defined as the ratio of the total flux to the uncollided flux. As the distance travelled by the gamma rays increases, the proportion of scattered flux to the total flux increases. Therefore, the buildup factor increases with distance. This does not imply the total flux increases with distance, in fact it decreases with distance as the total flux is the product of a buildup factor and an attenuation factor which decreases faster than the buildup factor increases.

Error in the Buildup Factor

Viewing Figure 2.2, and noting that WAPPA approximates the gamma radiation from the cylindrical waste form as originating from an infinite line source, the error made in WAPPA can be explained. For a gamma ray originating within the line segment dl , it must travel a distance R to reach point P .

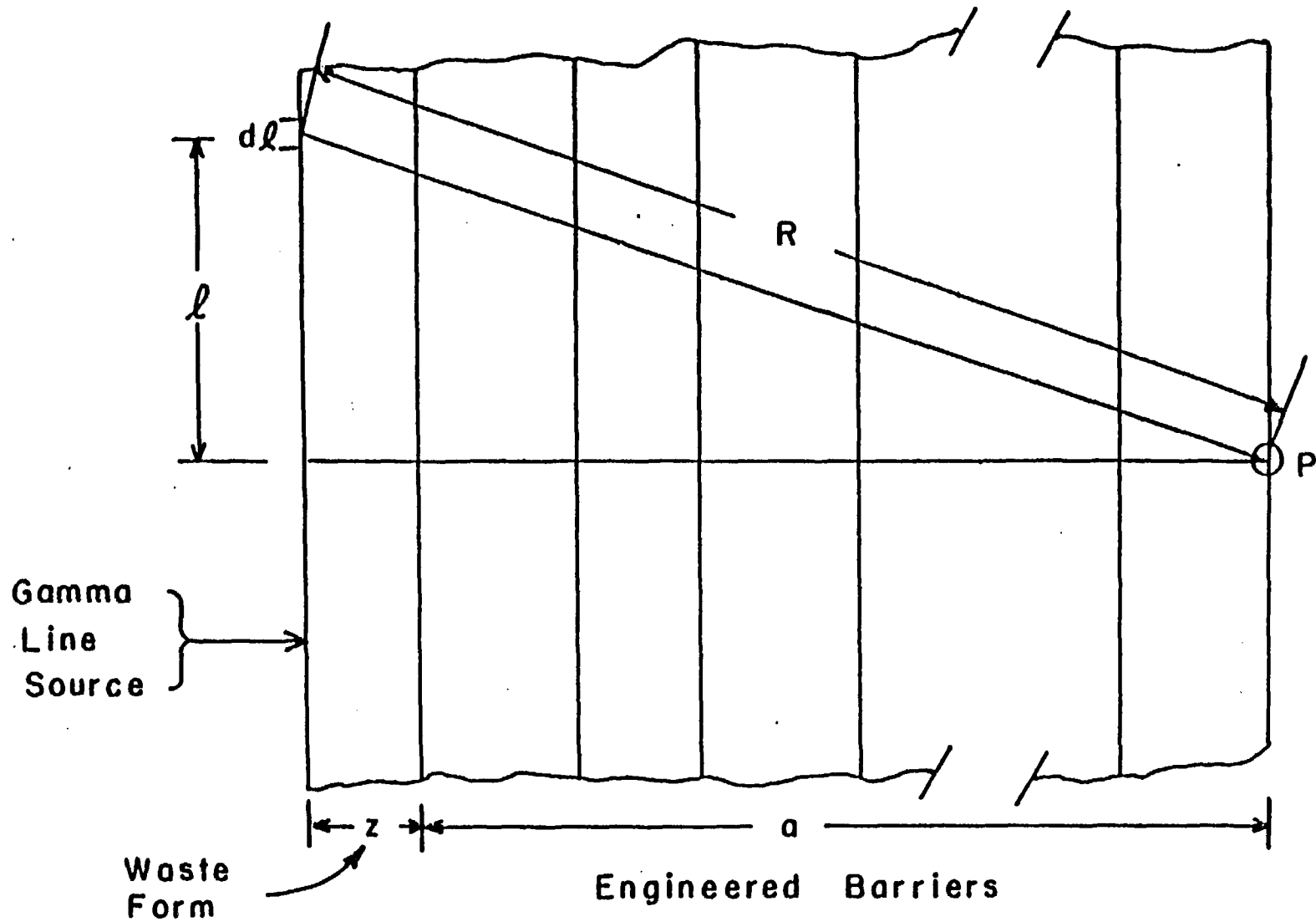


Figure 2.2 Geometrical representation of the waste form as a line source surrounded by the engineered barriers of the waste package.

However, WAPPA calculates the buildup factor based on the normal distance between the line source and point P, the distance $a+z$ in Figure 2.2. Because $(a+z) < R$ and the buildup factors increase with distance, this assumption is non-conservative. Heuristic arguments (Sullivan, T., MF-142, 1984), indicate that the calculated flux will be within a factor of 10 of the flux obtained using the distance R in calculating the buildup factor. Considering the uncertainties in the entire calculation and the fact that corrosion or leaching are expected to be enhanced by less than 20 percent for an order of magnitude increase in gamma dose, this error may not be significant, but it should be addressed in the code manual.

Empirical Coefficients in Buildup Factor Expression

Although WAPPA claims to use standard formulae, the expression for the buildup factor uses slightly different definitions for the empirical coefficients when compared to the definitions found in the Reactor Shielding Design Manual (Rockwell, T., 1956), the reference for buildup factors cited by WAPPA.

WAPPA defines the buildup factor B_1 for material "i" as:

$$B_1 = A_{1i} e^{-\alpha_{1i} t_i} + A_{2i} e^{-\alpha_{2i} t_i} \quad (2.1)$$

where A_{1i} , A_{2i} , α_{1i} , and α_{2i} are material dependent empirical coefficients and t_i is the thickness of material "i" normal to the line source. In contrast, the Reactor Shielding Design Manual defines the buildup factor as:

$$B_1 = A_{1i} e^{-k_{1i} \mu_i T_i} + A_{2i} e^{-k_{2i} \mu_i T_i} \quad (2.2)$$

where A_{1i} , A_{2i} , k_{1i} , and k_{2i} are material dependent empirical coefficients and μ_i is the adsorption coefficient of the medium, and T_i is the thickness of medium that the gamma ray passes through.

From these two expressions it is clear that

$$a_{ji} = k_{ji} \mu_i \quad j = 1,2 \quad (2.3)$$

and the equations are similar. However, this discrepancy is not pointed out in the manual.

2.2.1.2.3 Radiolysis Submodel

WAPPA calculates only one leach enhancement factor. This assumes that radiolysis has the same effect on all waste form constituents. However, radiolysis changes the number and types of molecular and radical species present in the groundwater. This in turn influences the solubilities of the different species in the groundwater and alters the leach rates from the waste form. Each species will react differently to these radiation induced changes.

WAPPA does not model alpha radiolysis nor does it attempt to account for the gamma flux in the groundwater that arises from particles leached from the waste form. Once leaching begins, alpha and gamma emitting species enter the groundwater. Alpha particles do not interact with the groundwater in the same manner as gamma rays (PNL-4452, 1983). Therefore, the water chemistry is different and leaching from the waste form will respond accordingly. This effect may be negligible because the amount of alpha and gamma emitting nuclides in the groundwater should be small.

The WAPPA manual does not mention the possibility of chemical changes due to gamma irradiation in salt repositories (BNL-NUREG-33658, 1983). In principle, this could be handled through leach and corrosion enhancement factors as currently done in WAPPA.

Lack of a detailed water chemistry model in WAPPA limits any attempt at modeling radiolysis effects to be heuristic and prone to be at most qualitatively correct. The accuracy of the radiolysis model is totally dependent on external justification.

2.2.1.2.4 Damage Submodel

Although the idea that alpha damage can be represented as a saturating exponential function of the total dose is not new, the data base to support this is limited. This may be a particular problem for glass. The reference cited in WAPPA (Weber, W. J., 1980) that proposes the saturating exponential correlation bases its model on experimental results on radiation effects in crystalline ceramic materials. The other radiation damage reference (Weber, W. J., 1979) does consider glass, however the data reported is for one glass composition and does not provide data for all of the radiation-induced property changes used in WAPPA.

The damage submodel does not attempt to calculate a leach enhancement factor due to alpha damage of the waste form. Apparently this was considered at one time by the developers of WAPPA because the empirical coefficients for the saturating exponential correlation are requested as input. However, these coefficients are unused. The manual does not justify neglecting this effect.

2.2.1.3 Conclusions

All of the submodels used to evaluate radiation-induced phenomena are structured to rely heavily on a user supplied data base. Assuming the data are available, the radiation model might provide a conservative estimate of the processes it models. Use of a data base approach allows the models to be simple and the computational times short. However, it also places a large burden on the user. Furthermore, because of the large quantity of data requested, coupled with the uncertainty in some data, it is unlikely any two users will develop the same data base.

2.2.2 WAPPA's Thermal Model (TMODEL)

WAPPA's Thermal Model computes the temperature profile within the waste package and feeds it to the System Drive Model for updating temperature dependent parameters in the Mechanical, Corrosion, and Leach-and-Transport models. Following a description of the modeling approach in Section 2.2.2.1, Section 2.2.2.2 discusses the limitations of the implemented submodels. Conclusions are drawn in Section 2.2.2.3.

2.2.2.1 Review of Modeling Approach

WAPPA's thermal modeling approach rests on the assumption that the heat capacity of waste package barriers is negligible and that the temperature distribution is a function only of radial distance from the waste form centerline. In the waste form it is assumed that the heat source is uniform. Solution of the resulting steady-state heat conduction equation yields a parabolic temperature distribution (Perry, R. H. and C. H. Chilton; 1973). In the cylindrical annulus representing the various waste package barriers it is assumed that there is no generation of heat. Solution of the heat conduction equation in this region without a source results then in a logarithmic profile (Perry, R. H. and C. H. Chilton; 1973). In terms of the temperatures at the waste form centerline and at the interfaces between adjoining barriers, the waste package temperature profile is expressed as follows:

$$T_0 = T_1 + \frac{q'(t)r_1^2}{4k_0(T_1)} \quad (2.4)$$

$$T_i = T_{i+1} + \frac{Q_i(t)}{2\pi H k_i(T_{i+1})} \ln(r_{i+1}/r_i), \quad i=1,2,\dots,N \quad (2.5)$$

where T_0 is the centerline temperature; T_1 is the temperature at the waste form periphery; r_i is the distance of the i -th interface from the waste form centerline; $T_i = T(r_i, t)$; $q'(t)$ is the volumetric heat generation rate in the waste form; H is the height of the waste package; $k_0(T_1)$ is the effective thermal conductivity of the waste form; $k_i(T_{i+1})$ is the effective thermal conductivity of the i -th barrier based on the temperature at the outer edge of the barrier; $Q_i(t)$ is the effective, total conductive heat flux out of the i -th interface.

Heat transfer by convection is considered important in liquid or gas filled annuli when the Grashof number exceeds 20,000. The Grashof number is a dimensionless parameter defined as:

$$N_{GR} = \frac{X^3 \rho^2 g \beta_f \Delta T}{\mu^2} \quad (2.6)$$

where X is the gap width; ρ is the density of the fluid; g is the acceleration due to gravity; β_f is the volumetric expansion coefficient; ΔT is the

temperature difference across the gap; and μ is the fluid viscosity. When convection is important, the parameter k_1 in Equation (2.5) is the familiar thermal conductivity corrected through an equivalent conduction enhancement factor which is a function of the Grashof number.

Heat transfer by radiation is considered for gas filled annuli and is modeled through modification of the conductive heat flux. Thus, for gas gaps, the quantity $Q_1(t)$ used in Equation (2.5) is the total heat flux minus the total radiative heat flux, $q_1(t)$, which is defined as follows:

$$q_1 = A_i F_{i,i+1} \sigma (T_i^4 - T_{i+1}^4), \quad (2.7)$$

where:

- A_i - area of i -th interface
- $F_{i,i+1}$ - view factor from i -th to $(i+1)$ -th interface
- σ - Stefan-Boltzmann constant.

Radiation heat transport will be most important during the first few years after burial when the heat source and temperature gradients through the waste package are largest.

Equations (2.4) and (2.5) can be solved sequentially once either the temperature at the waste form centerline or the temperature at the waste package-host rock interface is specified as function of time. The Thermal Model adopts the second one as the reference temperature. The waste package-host rock interface temperature is provided in the code as a user supplied table of temperature data versus time.

The above formulation is abandoned when the total heat generation rate becomes less than 1 watt. At that time, a few hundred years, all temperatures within the waste package are set equal to the user-provided, reference repository temperature.

2.2.2.2 Discussion

WAPPA's assumed parabolic-logarithmic temperature profile within the waste package is the profile that would exist in the system if this had had infinite time to equilibrate thermally with its surroundings while the heat generation rates were kept constant. As such, it would certainly yield a conservative estimate of waste package temperatures if, at any time t , the user-supplied boundary temperature were the thermally equilibrated value. Engineering judgement, however, suggests that, after the first few months during which heat storage effects in the waste package are important, Equations (2.4) and (2.5) closely represent the shape of the waste package temperature profile. Therefore, the accuracy of WAPPA's temperature estimates within the waste package after the first few months rests on the accuracy of

the user supplied boundary temperature data. If these data are in error by X degrees, the calculated temperature profile is displaced by the same number of degrees in the waste package.

Since the waste package-repository boundary temperature depends on waste package dimensions and heat generation rates as well as on repository properties, such as rock thermal properties, waste package arrangement, area thermal load, etc., the present Thermal Model logic would call for a large data base of boundary temperature values versus time. In analogous situations, other researchers have preferred to couple the waste package thermal model, Equations (2.4) and (2.5), with a thermal code for the repository. Both options would require substantial improvement of WAPPA.

WAPPA is inadequate for reliable temperature prediction during the first few months after burial as the Thermal Model formulation breaks down in the limit when heat storage effects in the the waste package are important. However, the model would still provide reasonable estimates of internal waste package temperatures provided an "appropriate" set of boundary temperature data is supplied by the user.

2.2.2.3 Conclusions

The usefulness of WAPPA's thermal model usefulness for short-term temperature prediction, i.e., during the first few months after burial, is limited to providing conservative estimates of waste package temperatures by selecting "appropriate" values for the user-supplied boundary temperature. Reliable, short-term temperature prediction would require adding a temperature submodel to the code which includes heat storage effects.

WAPPA's thermal model may provide reliable estimates of waste package temperatures a few months after burial provided the user-supplied data base of boundary temperatures is shown to be accurate. This may require a separate run of a repository thermal code which takes into account waste package heat generation rates and dimensions as well as waste package arrangement, rock thermal properties, etc.

2.2.3 WAPPA's Mechanical Model (FMODEL)

In WAPPA's modeling approach three types of stress-assisted breaching of waste package barriers can occur: 1. stress corrosion cracking of metallic barriers, 2. fracture of metallic barriers at pre-existing cracks, and 3. brittle fracture of the waste form.

The purpose of FMODEL is to predict the magnitude of local stresses (stress intensity factors) at pre-existing flaws on metal surfaces, and to determine the extent to which the waste form fractures due to the applied stress. These tasks are accomplished by coupling a Canister Fracture (CF) Submodel and a Waste Form fracture (WF) Submodel to a Stress Analysis (SA) Submodel. These submodels are introduced next. A discussion follows in Section 2.2.3.2. Conclusions are drawn in Section 2.2.3.3.

2.2.3.1 Review of Modeling Approach

2.2.3.1.1 Canister Fracture Submodel

Given the calculated stress level from the SA submodel and the user-specified length of pre-existing cracks on metallic barriers, the CF submodel computes empirical, elastic stress intensity factors.

If the metal has not yielded plastically, the stress intensity factor is compared with the metal's critical value of fracture toughness. Breaching occurs when the stress intensity factor exceeds the fracture toughness.

If the metal has already yielded plastically, a new effective crack length is calculated. The stress intensity factor is then recomputed and compared with the fracture toughness of the material.

The equations used in this submodel are empirical in nature. Therefore one must make sure they apply to the materials, loading pattern, and geometry at hand. To that effect, the CF submodel write-up does not give useful references, therefore these equations must be accepted with reservations.

2.2.3.1.2 Waste Form Fracture Submodel

From the various components of the stress as calculated by the SA submodel, the WF submodel checks for regions where tensile stresses exceed the fracture strength of the material. Since the problem is regarded as axisymmetric, this defines an outer annulus where the waste form is fractured. The volume of the fractured region is then multiplied by an empirical coefficient to determine an equivalent surface-area increase to be used later by the Leach-and-Transport Model.

2.2.3.1.3 Stress Analysis Submodel

While the CF and WF submodels are empirical in nature, the SA submodel is based on classical theories of materials strength and stress analysis.

For a strength analysis, the FMODEL considers five types of materials whose properties are modeled as follows:

1. The waste form is modeled as an elastic/brittle material which undergoes fracture in the region where tensile stresses exceed the waste form fracture strength.
2. Metallic barriers are modeled as elastic/plastic materials. These materials yield plastically in regions where the TRESCA criterion is satisfied. Namely, when

$$\text{Max} (|\sigma_r - \sigma_\theta|, |\sigma_\theta - \sigma_z|, |\sigma_r - \sigma_z|) \geq \sigma_{\text{yield}}$$

3. Packing materials are modeled as compressible elastic elements. They yield, i.e., they are extruded, when the Von Mises maximum stress exceeds the yield stress. That is when:

$$\sigma_{\max} = \frac{3}{2} \sqrt{(\sigma_r - \sigma_H)^2 + (\sigma_\theta - \sigma_H)^2 + (\sigma_z - \sigma_H)^2} > \sigma_{\text{yield}},$$

σ_H - the hydrostatic pressure.

4. Gas gaps are modeled as having zero pressure and no stress transfer capability.
5. Liquid gaps are modeled as incompressible elements. Also, all "failed" portions of the barriers, i.e., the fractured waste form region, the plastically yielded portion of metallic barriers, and all corrosion layers are treated as incompressible elements.

From a stress analysis point of view, the modeling approach regards the waste package as a series of concentric cylindrical annuli encircling a solid core. The length of the waste package is infinite and loading compressive in both the horizontal and vertical directions. Horizontal loading is due to the repository confining horizontal pressure, to thermal expansion, and to initial residual stresses at the canister/waste form interface. Vertical loading is due to the repository vertical confining pressure. No shear, torsion, or bending is accounted for, nor are gravity loading and friction between components. As a result, all deformations take place horizontally in the radial direction. Stress enhancement due to the finite length of the waste package is handled through an empirical factor which multiplies the calculated stress.

2.2.3.2 Discussion

2.2.3.2.1 Limitations of the Modeling Approach

Any model appearing in a general purpose code like WAPPA can only be expected to handle a few important effects and failure modes. In the case of the FMODEL, the modelers have identified brittle fracture of the waste form and cracking of the metal barriers at pre-existing flaws as the main mechanical failure modes of the waste package. To that end they disregard bending, torsion, gravity loading, friction effects, creep, buckling, etc., which is likely to be an acceptable approach but it is not justified in the document. Also, the expressions used for calculating empirical stress intensity factors at pre-existing cracks are not properly referenced and justified.

The implemented modeling approach does present some desirable features, i.e., it accounts for degradation of mechanical properties due to radiation (empirical factors and data have to be used) and for the influence of temperature on the stress. The model also accounts for initial, residual processing stresses.

The most important limitations are that materials strength, as measured by yield stress and tensile strength, is not modeled as a function of temperature, and that the volumetric expansion of the corrosion products is not addressed. Corrosion products are known to exert very large pressures in constricted regions, e.g., the phenomenon of denting in nuclear steam generators and the wedging action of corrosion products (Pickering, H. W.; 1962).

2.2.3.2 Adequacy of the Modeling Approach

Two relevant waste package failure modes are not given sufficient attention in the implemented modeling approach. These are, 1.) failure of the waste package ends and, 2.) buckling of metal barriers beyond their elastic stability region.

With reference to Figure 2.3, which reports a typical waste package design for high-level waste (AESD-TME-3131, 1982), it appears that a weak area in the canister structure is the neck area. In that area the metal is not supported by the waste form and the neck shape favors concentration of stresses. Thus, crushing of the air gap appears to be an important failure mode which ought to be addressed. Stresses may also concentrate at the bottom of the canister at the welds between the base and the rest of the metal, thus causing the base to detach. This failure mode should also be addressed.

Furthermore, it should be noted that as the unfailed part of metal barriers becomes progressively thinner due to corrosion and plastic yielding, it may be subject, at one point, to elastic instability, i.e., under sufficiently high stress the cylindrical metal annulus may buckle into an "eight" shape. This may be an important failure mode for waste package performance.

FMODEL uses a number of empirical correlations to represent mechanical behavior of the waste package. For this reason, the ability of FMODEL to provide a conservative estimate of waste form fracture and canister failure can not be guaranteed unless the data used by the correlations can be shown to be conservative.

2.2.3.3 Conclusions

The FMODEL cannot be used by itself in a predictive mode. It relies heavily on user-supplied data which may not be obtained from the literature and for which the user may have to make ad hoc experiments. This is the case for important quantities related to failure mode analysis, such as (a) the empirical coefficient to convert waste form fractured volume to an increase in waste form surface area, (b) the empirical formulae used to calculate stress intensity factors, and (c) the empirical coefficient to deal with end effects. The FMODEL does not factor in the volumetric expansion of corrosion products which, depending on the degree of fracturing of the host rock, may result in additional confining pressures. Furthermore, the model does not take into account failure of both canister ends nor does it account for the elastic stability of the metal barriers.

2.2.4 WAPPA's Corrosion Model (CMODEL)

The corrosion model calculates the degradation of each metallic barrier in the waste package due to the following processes:

- (1) Dry oxidation;
- (2) General corrosion;
- (3) Galvanic corrosion;
- (4) Localized corrosion, including pitting and crevice corrosion; and
- (5) Stress corrosion cracking, including hydrogen embrittlement and active path stress corrosion cracking.

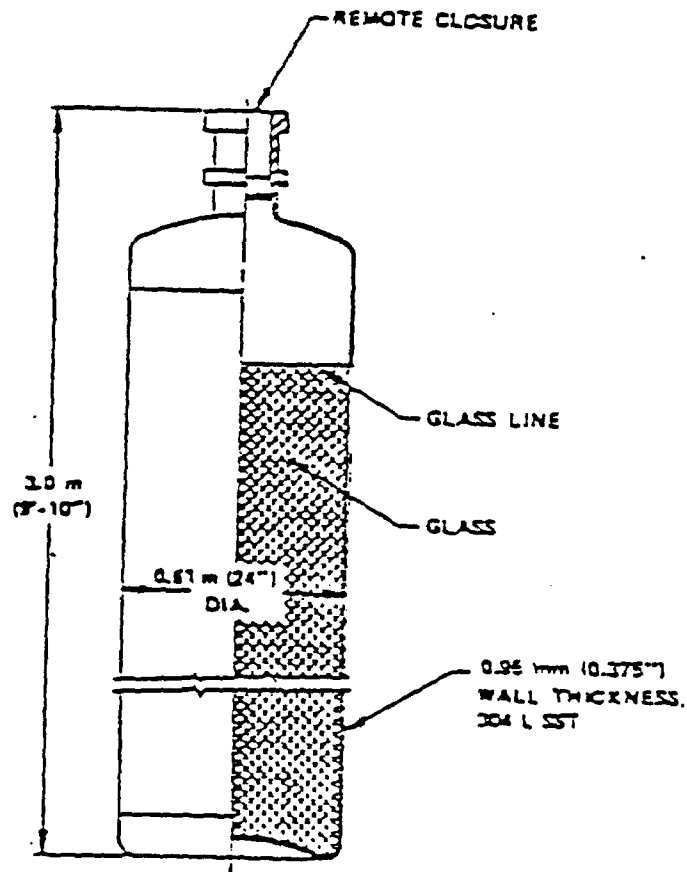


Figure 2.3 Typical waste form and canister design (adapted from AESD-TME-3131, 1982).

Along with barrier degradation, CMODEL tracks the penetration of water into the waste package as the barriers fail. Following a description of the submodels, Section 2.2.4.2 discusses the limitations of CMODEL and conclusions are drawn in Section 2.2.4.3.

2.2.4.1 Review of Modeling Approach

2.2.4.1.1 Dry Corrosion

Before a barrier is contacted by water, CMODEL considers the spatially uniform one-dimensional thinning of barriers due to oxidation. Oxide growth is calculated by one of three empirical growth laws: logarithmic, parabolic, or a power relation in time. The coefficients required in these laws are defined as a function of temperature through user supplied input tables.

2.2.4.1.2 Wet Corrosion

Upon wetting of a barrier, wet corrosion models are activated. A distinction is made between mechanisms that cause a uniform degradation of the entire barrier versus mechanisms that cause local barrier degradation. Uniform corrosion submodels consider galvanic and general corrosion. Local corrosion includes stress corrosion cracking, pitting, and crevice corrosion.

The submodel for galvanic corrosion determines whether water (an electrolyte) is in contact with two adjacent barriers thereby allowing a galvanic cell to form. (This situation can only occur if local corrosion has caused a breach in an outer barrier.) Based on input data, the barrier that acts as the anode is determined and the thickness of this barrier is reduced linearly with time. The rate of degradation is a function of temperature and is increased through the effects of radiolysis. The model does not give credit for cathodic protection.

The model for general corrosion provides a spatially uniform thinning of the barrier. The rate of degradation is determined from an input table, for each barrier, of corrosion rate versus temperature. The effects of radiolysis are incorporated by multiplying the corrosion rate by an enhancement factor which is a function of the gamma dose and flux. The net rate of corrosion is a linear function of time.

Local corrosion events are considered "catastrophic". That is, if the conditions required to initiate one of these processes arise, the barrier is considered breached instantaneously at the beginning of the current time step. Given user supplied empirical data for pitting/crevice/crack size and density, the total "breached" area is calculated. Simultaneous with the breach of the barrier, groundwater flows to contact the next barrier.

2.2.4.2 Discussion

WAPPA's corrosion model was developed with the intention of providing a calculation of the maximum rate of barrier degradation, i.e., a conservative estimate. However, before conservatism can be assured, the following points concerning the data and numerical modeling must be considered.

First, and most important, it is emphasized that all of the corrosion submodels are empirical and extremely data intensive. Corrosion is a complex phenomena that is not understood well from a quantitative, fundamental viewpoint. For this reason, CMODEL uses empirical correlations to supply all the information on corrosion rates for each of the various models and for each barrier. The coefficients used in each correlation are supplied by the code user as a function of temperature. No attempt is made at modeling the influence of solution chemistry on corrosion rate. The effect of solution chemistry is assumed to be incorporated in the empirical input supplied by the user. Before CMODEL can be considered conservative, the data used in the empirical correlations must be shown to be conservative over the entire range of potential repository conditions.

Second, the numerical strategy used in CMODEL contains two flaws. The first error involves solution for the amount of dry oxidation, general and/or galvanic corrosion. The solution strategy in WAPPA is process sequential, that is, WAPPA looks at radiation, thermal, mechanical, corrosion, and leaching processes as occurring sequentially in a given time step. In particular, the temperature distribution is calculated before CMODEL calculates the temperature dependent corrosion rate. If the temperature is decreasing with time, this is the expected condition after the first few hundred years, the corrosion rate is calculated based on a lower temperature and therefore the calculation is non-conservative. This could be corrected through use of the temperature at the previous time step to calculate the amount of corrosion when the temperature is decreasing.

The other error involves solution of the dry oxidation corrosion model. The empirical laws used in calculating oxide thickness are, in general, developed from non-linear, integral-type relationships based on isothermal experimental data. For this non-isothermal system, care must be taken to account for the influence of temperature variations on oxide growth.

The method of solution used in WAPPA for calculating oxide thickness is most easily understood while viewing Figure 2.4, a plot of oxide thickness versus time for two temperatures. For the initial time step, time zero to time t_1 , the system is at temperature T_1 and the oxide grows to a depth, d_1 . In the subsequent time step, time t_1 to time t_2 , the system temperature has been updated and is T_2 . WAPPA calculates the incremental oxide growth, Δd_2 , as the amount of growth that would have occurred over the time interval t_2-t_1 provided the system had been held at temperature T_2 for the entire calculation time. This growth is represented by the curve through points b and c on the graph. The total oxide thickness is obtained by summation of d_1 , the oxide thickness and Δd_2 , the incremental growth. Viewing each time step as a new initial value problem, it is seen that the WAPPA code changes the "initial condition" for oxide thickness at each time step. Since growth rate is a function of thickness, this procedure is incorrect.

A better solution procedure is schematically represented in Figure 2.5. Here, after the oxide has grown to a depth d_1 at temperature T_1 , time is advanced to the next time step and the temperature is updated and is T_2 . In this case, growth of the oxide is calculated starting from a depth d_1 on the isothermal curve for temperature T_2 . This is point b in Figure 2.5. Growth

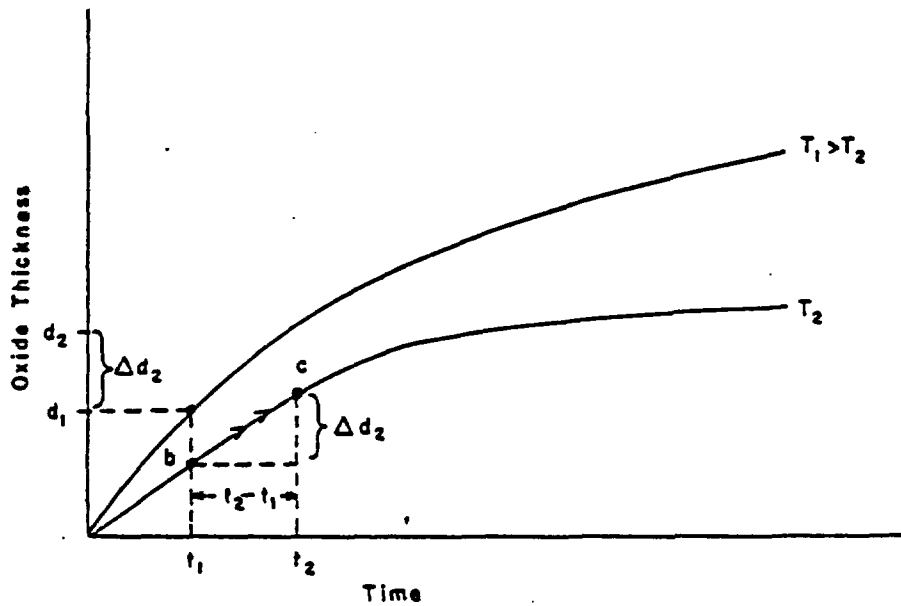


Figure 2.4 Schematic representation of oxide thickness versus time. WAPPA considers thickness as a function of temperature and time.

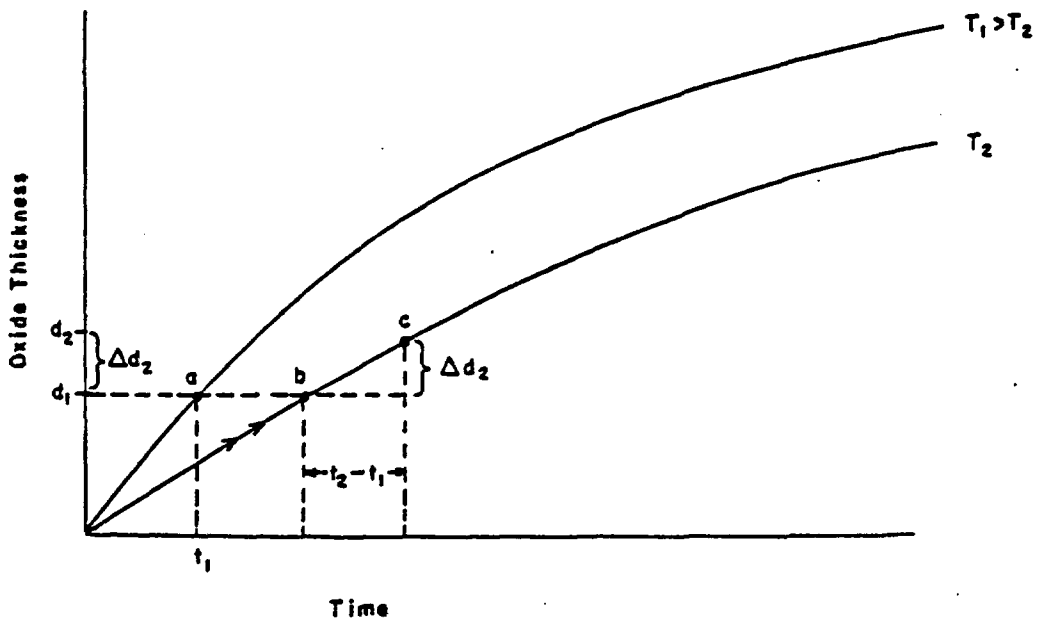


Figure 2.5 Improved oxide thickness calculation considers thickness as a function of temperature and previous history.

progresses along this isothermal curve for a time period corresponding to the length of the time step, $t_2 - t_1$. This is represented by the path between points b and c. The new oxide thickness is the sum of d_1 , the initial thickness, and Δd_2 , the incremental growth. This model takes the viewpoint that corrosion rate is a function of temperature and oxide thickness whereas the WAPPA model views the corrosion rate as a function of temperature and time.

Provided the temperature is monotonically decreasing with time and neglecting the "improper" use of the temperature at the end of the time step to calculate oxide growth as previously mentioned, the solution procedure currently used by WAPPA for dry oxidation will overpredict the amount of corrosion. Although this approach is inconsistent from a physical viewpoint, it will be conservative.

2.2.4.3 Conclusions

The corrosion models used in WAPPA are intended to provide a conservative framework for estimating the degradation of the metallic barriers in the waste package. The modeling approach relies exclusively on user supplied empirical corrosion rates for each type of corrosion process. These corrosion rates are generally supplied as a function of temperature only. The influence of other environmental parameters such as solution composition are not accounted for explicitly. Assurance that WAPPA's corrosion models are conservative requires that the input data can be shown to be conservative under any conditions expected in the repository during the containment period and the numerical solution procedure improved to calculate corrosion based on the maximum temperature during the time step.

2.2.5 WAPPA's Leach-and-Transport Model (WMODEL)

With reference to Figure 2.6, the Leach-and-Transport Model is activated when all barriers have failed through one or more degradation mechanisms and the waste form is exposed to direct attack from the fluid flooding the breached barriers.

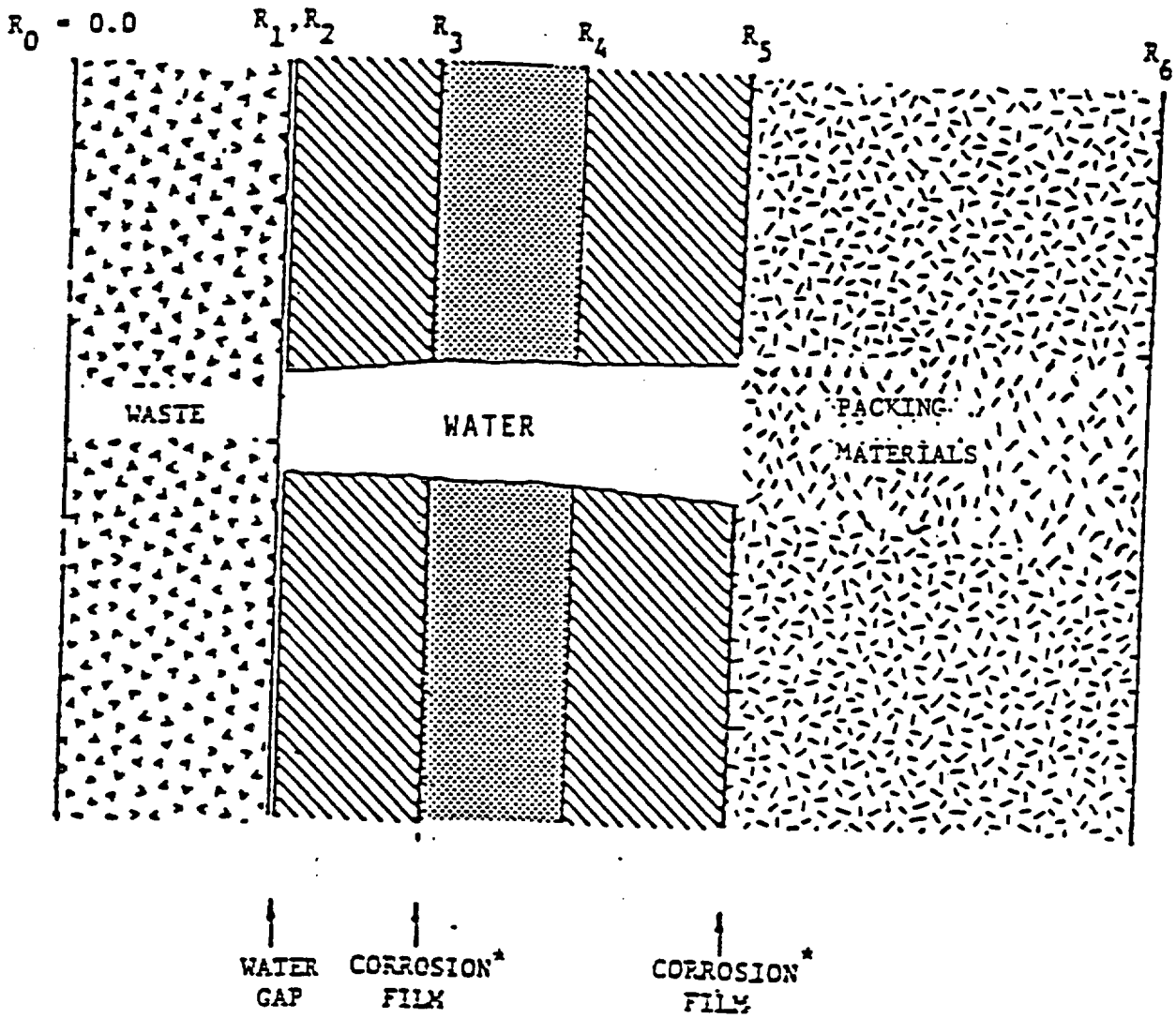
The purpose of WMODEL is to calculate the release of radionuclides from the waste form, their transport out of the waste package, and the accumulated mass of each radionuclide delivered to the host rock. To that effect, the WMODEL relies on a leach submodel and on a transport submodel.

A description of the modeling approach is provided in Section 2.2.5.1. A discussion follows in Section 2.2.5.2 and conclusions are drawn in Section 2.2.5.3.

2.2.5.1 Review of Modeling Approach

2.2.5.1.1 Leach Submodel

The leaching submodel is a leach rate expression which includes both dissolution and diffusion from the waste form and is modified by empirical correlations to account for the effects of temperature, radiation, solution saturation, and waste form fracturing. The implemented expression is:



* Corrosion layer placed on the outer radius of the metal

Figure 2.6 Geometry of waste package (adapted from ONWI-452, 1982).

$$Q_L = \left(\frac{1}{2} k_{dif} t^{-1/2} + k_{dis} \right) \cdot A_{FW} \cdot LEF \cdot SDENSF \left(1 - \frac{C_{WM}}{C_{sat}} \right) \exp \frac{E(T-T_o)}{RTT_o} \quad (2.8)$$

where:

Q_L	= mass leach rate from waste form to solution (g/s);
k_{dif}	= leach rate coefficient for diffusion ($g/m^2-s^{1/2}$);
k_{dis}	= leach rate coefficient for dissolution (g/m^2-s);
A_{FW}	= total surface area of the waste form, including geometric and fractured areas (m^2);
LEF	= combined leach enhancement factor, the product of leach enhancement factors for alpha damage and γ -radiolysis as obtained in RMODEL (dimensionless);
$SDENSF$	= density degradation factor due to alpha damage as obtained in RMODEL (dimensionless);
C_{WM}	= concentration of the solute in the fluid at the waste form/canister boundary (g/m^3);
C_{sat}	= saturation concentration of the solute (g/m^3);
T_o	= reference temperature for k_{dif} and k_{dis} ($^{\circ}K$);
E	= activation energy (kcal/g-mole);
R	= gas constant (kcal/g-mole- $^{\circ}K$);
T	= temperature of the waste form ($^{\circ}K$).

The release rate depends on which species is being modeled as the two leach rate coefficients and the saturation concentration vary for each nuclide under consideration.

2.2.5.1.2 Transport Submodel

For modeling purposes and with reference to Figure 2.6, the WMODEL subdivides the cylindrical layered medium representing the waste package into three distinct regions: the waste form plus the fluid filled region extending to the first metal barrier, the flooded barriers, and the packing materials. The model further assumes that each species under consideration behaves independently from other species. Thus, given a particular species, one is left in general with solving a system of three coupled equations in terms of the concentration of the given species in the leachant next to the waste form, in the leachant within the flooded barriers, and in the pore fluid of the packing materials. In practice, however, the WMODEL solves a system of four equations which could be shown to reduce to one nonlinear ordinary differential equation. Proceeding from the waste form radially outwards, the reference equations of the WMODEL are as follows:

- (a) The first equation describes the rate at which any selected species is transferred from the waste form to the contacting aqueous solution. This is Equation (2.8). It is the same for all species and it is the classical, diffusion and network-dissolution expression for the leach rate modified by a concentration-dependent, solubility limited factor and by further leach enhancement factors due to

cracking of the waste form surface, α -damage to the waste form structure, and γ -radiolysis of the water. The dependence on temperature is handled through an Arrhenius expression. In particular, the concentration profile within the water gap between the waste form and the canister is assumed to be uniform and to be controlled by diffusion processes taking place within the flooded barriers.

- (b) The second equation couples the concentration of any given species in the water gap next to the waste form to the concentration of the same species at the interface between the flooded barriers and the packing materials. The concentration profile in this region is assumed to respond instantly to concentration variations at its boundaries and corresponds to a steady-state diffusion profile. Taking into account the layered, cylindrical geometry of the system, solution of the diffusion equation yields a concentration profile which drops logarithmically across the flooded barriers.
- (c) The third equation computes a time-dependent, space-averaged concentration of a given species within the packing materials. This is accomplished by treating the packing materials as a mixing cell, i.e., the entering fluid is instantaneously mixed in the volume of the packing materials, and the concentration varies as function of time only. Any directionality of the flow field is lost in this approach, and convection in and out of the packing materials is handled through a leachant renewal frequency term. Diffusion in and out of the packing materials is difficult to justify in this approach. Nevertheless, a diffusion term, which has some directional information, appears in the equation. In particular, diffusion out of the system is assumed to take place through a concentration gradient operating from the location of the log mean radius of the packing materials to their boundary with the host rock where the concentration of all species is assumed to be zero. Sorption on the packing materials is modeled through a constant retardation coefficient which slows transport out of the region.
- (d) By continuity, the above space-averaged concentration of any species in the packing materials could be set equal to the concentration at the interface with the outer metal. This is not deemed, or recognized to be acceptable. Thus the fourth equation in the WMODEL relates the two concentrations through a proportionality constant defined as the ratio between the thickness from the log mean radius to the outer radius of the packing materials and the total thickness of the packing materials.

2.2.5.2 Discussion

2.2.5.2.1 Leach Submodel

Three major limitations have been found in the leach submodel. They are:

- (1) The leach rate expression is not coupled with the radionuclide inventory in the waste form.
- (2) The leach rate expression does not account for increasing radionuclide inventory under certain conditions.
- (3) There is an inconsistency in the calculated mass released to the repository when the waste form is depleted.

Limitation(1)

The first limitation can be found through examination of the leach rate expression, Equation (2.8), which states that the rate of mass transfer from the waste form into solution is independent of the concentration in the waste form. According to this expression, the leach rate depends heavily on the diffusion and dissolution coefficients, k_{dif} and k_{dis} , which are to be determined empirically from experimental results and are specified in the code as input parameters that are constant with time. However, it can be shown theoretically (Pescatore, C., 1983) that both k_{dif} and k_{dis} are the product of the nuclide concentration in the waste form times a physical parameter that is process specific. For example, the leach rate dissolution coefficient is the product of surface concentration, $C(t)$, times the waste form dissolution velocity, $u(t)$:

$$k_{dis} = u \cdot C(t). \quad (2.9)$$

Since the waste form concentration is a function of time due to leaching and radioactive decay, k_{dis} , as expressed in Equation 2.9, is also a function of time even if the dissolution velocity were constant.

To make the release rate a function of waste form concentration, k_{dis} and k_{dif} would have to be expressed as explicit functions of waste form concentration. However, WAPPA does not make any attempt to calculate waste form concentration. Thus, if the WAPPA model is to be retained, k_{dis} would have to be input as a time dependent function which reflects the changes in waste form concentration. This implies that the user would need to estimate the waste form concentration as a function of time before performing the calculation. Similar remarks apply to k_{dif} .

The release rates of Cm-244 and Cm-245, as obtained from WAPPA's complex verification test case (Pescatore, C. and Sullivan, T., MF-127, 1983; Sullivan, T., MF-135, 1984) provide an example of the problems that can arise by not coupling the leach rate to the mass inventory in the waste form. Since Cm-244 and Cm-245 are isotopes of the same element, they were given identical leach rate coefficients in the test problem. Therefore both nuclides were calculated to be released from the waste form at the same rate, despite a 14-orders-of-magnitude mismatch in their initial inventories. In fact, WAPPA predicted all of the Cm-244 to be released from the waste form within the first second of leaching.

Furthermore, the nuclide concentration within the breached engineered barriers and the packing materials is a function of the nuclide release rate from the waste form. Thus, a consequence of unreasonably high leach rates is that calculated concentrations throughout the waste package are much too large and mass is not conserved.

For example, at 5600 years, which is the end of the first computational time step since the beginning of leaching, WAPPA calculates the average Cm-244 concentration as $5 \times 10^{-3} \text{ g/m}^3$. However, the total inventory supplied by the data base is $6 \times 10^{-16} \text{ g}$. WAPPA does check whether the total mass released to the repository exceeds the current inventory in the waste form and it does prevent spurious mass from entering the repository. Nevertheless, it is wrong and misleading to calculate the concentration within the waste package as being so large that mass is not conserved.

Limitation (2)

The second situation in which WAPPA does not conserve mass occurs when the inventory of a given nuclide is increasing in time due to decay of other nuclides in the waste form. WAPPA calculates the release of each species until the mass released at a given time step equals the total mass found in the waste package. After this time, WAPPA assumes this species is completely and permanently removed from the waste form. WAPPA neglects to check for production of the species due to decay of other nuclides after the nuclide under study has been removed from the waste form. This approach is non-conservative and can underpredict the release of a nuclide to the repository. To clarify this point, the complex verification test case was run and the results for Th-229 (which does have an inventory that increases in time) mass release to the repository was examined (Sullivan, T., MF-135, 1984). WAPPA predicted that $2.6 \times 10^{-3} \text{ g}$ of the Th-229 was released to the repository over the first time step since the onset of leaching. At this time, this was the entire Th-229 inventory. Therefore, WAPPA stopped calculating release of Th-229 and $2.6 \times 10^{-3} \text{ g}$ remained as the total release to the repository. However, the inventory of Th-229 continued to increase reaching a value of 2.1g at the end of the calculation. Thus, there is a non-conservative discrepancy between the amount of mass in the system and the amount of mass in the repository.

Limitation (3)

The third problem occurs because WAPPA takes an inconsistent approach to mass conservation within the repository. In most cases, radioactive decay within the repository is not taken into account. The output data for Tc-99 provides an example: after 10^6 years WAPPA predicts there are 435 grams of Tc-99 in the repository. However, part of the data base required to run WAPPA is the mass inventory that would exist if the waste form had been left undisturbed. In this test problem, the mass inventory supplied from the ORIGEN2 computer code for Tc-99 at 10^6 years is only 16.8 grams. The cause of this discrepancy is that WAPPA does not account for radioactive decay once a nuclide has left the waste form. Thus, the Tc-99 which leaves the waste form when the inventory is high enters the repository and remains there. Neglecting radioactive decay provides a conservative estimate of the mass in the repository.

However, there is one exception when radioactive decay in the repository is taken into account. This occurs when the waste form concentration is depleted by leaching during a time step. In this case, WAPPA sets the amount of mass in the repository to the total available for leaching. This approach has the effect of accounting for radioactive decay in the repository and can lead to a decrease in the amount of mass in the repository. Pu-239 exhibits the results of this logic. After 10^5 years, the calculated release to the repository is 34.4 grams. At 2×10^5 years, the end of the next computational time step, the ORIGEN2 inventory of Pu-239 is 8.6 grams and it is all released to the repository. Instead of adding the 8.6 grams to the amount in the repository and thereby neglecting decay, the mass in the repository is set to the ORIGEN2 inventory of 8.6 grams. Provided the mass inventory is decreasing, accounting for decay in this manner will still be conservative. However, it is inconsistent.

In addition to the logic flaw identified above, the expression for the leach rate itself appears to be unrealistic, or very conservative, for species which exhibit large solubility in water, e.g., the alkalis. Indeed, the model predicts for these species an initial inverse-square-root-of-time law for the release rate followed by a constant release rate at longer times, which is contrary to experience at low flow rates. This however does not constitute a serious error unless alkali leach rates are used in the future for helping predict the groundwater chemistry.

Another error in the leach submodel occurs when there are isotopes of a chemical element. In this case, saturation of the solution with respect to the element should be calculated based on all of the isotopes. This would require the saturation limiting term in the leach rate, Eqn (2.8), be changed from:

$$\begin{aligned} & 1 - C_{WM}/C_{sat}; \\ \text{to:} & 1 - \sum C_{WM,i}/C_{sat}; \end{aligned}$$

where the summation on i represents the addition of all isotopes. This change would also require a new concentration boundary condition as the current model assumes that saturation exists at the waste form boundary for all species.

2.2.5.2.2 Transport Submodel

Despite claims to the contrary, the WMODEL does not give "realistic" credit to partially breached barriers for retardation of radionuclide transport. Indeed, as soon as the breach occurs, the waste form is assumed to become totally wetted and to release directly into the packing materials. The only attenuation of the leach rate comes from adjusting its concentration dependent term to reflect a logarithmic concentration profile across the flooded barriers. Since this correction is very small, the barriers do not play any meaningful retarding role. Thus, under the logic of the WMODEL, a marked decrease in leach rates occurs only when solution saturation limits, with a value typical of waste form/canister interface fluid, are approached in the packing materials. This conservativeness is probably unnecessary.

The treatment of radionuclide transport in the packing materials is also unrealistic. The mixing-cell approach applies best to situations where flow is not laminar, and it breaks down when diffusion becomes the predominant transport mechanism. Since the case has often been made for the packing materials to reduce convection and to make diffusion dominant mode of transport, a space- and time-dependent equation for the concentration of any given species in the packing materials would be more adequate. This would also eliminate the problem of extrapolating a space-dependent concentration from a space-averaged one, as is presently being done. Nevertheless, the approach implemented in the WMODEL is conservative providing accurate parameters are fed into the model.

Another potential problem with the transport submodel involves retardation of solute transport in the packing materials which is handled by a constant retardation coefficient. As the groundwater percolates through the packing materials some of the nuclides become sorbed on the solid thereby slowing their transport. In dilute solutions, experiments indicate the distribution between the solid and liquid phases is constant and therefore retardation is constant. However, as the solution concentration increases this is often no longer true (RHO-BWI-LD-48, 1981) and retardation decreases. Therefore, since the solution will be near the solubility limits around the waste package, a constant retardation coefficient may not be justified everywhere in the packing materials.

Furthermore, the retardation coefficient is expressed in terms of an experimentally determined distribution coefficients K_d and before the retardation coefficient can be useful for WAPPA it must be shown that the K_d 's used are relevant to the situation. In particular, current K_d measurements are obtained from single component tests. For example, the distribution of plutonium between the solid and liquid phases is measured in an experiment which has only plutonium in solution. In general, sorption is a complex phenomenon which depends strongly on solution chemistry. Therefore, single component tests may not be applicable to repository conditions which will contain all of the nuclides released from the waste form. A more detailed examination of the potential problems with using a constant K_d (and therefore constant retardation coefficient) coefficient have been enumerated (Sullivan, T., MF-150, 1984).

The numerical strategy implemented in the WMODEL appears to be too crude and error prone. In practice, the WMODEL solves a non-linear differential equation of the type:

$$\frac{dC_B}{dt} = f(t, C_B) \quad (2.10)$$

in terms of the space-averaged concentration of radionuclides in the packing materials, $C_B(t)$, during a time step (t_i, t_{i+1}) , where $f(t, C_B)$ is a nonlinear function of time. The quantity $C_B(t)$ is related to the concentration at the outer surface of the metal, C_u , through a practically constant factor, b , comprised between 1 and 2 (Section 2.2.5.1.2):

$$C_n(t) = b C_B(t) \quad (2.11)$$

The concentration at the waste form-metal barriers interface, C_1 , is related to C_B through the following relationship:

$$\begin{aligned} C_1(t) &= C_n(t) + d \cdot (k_1 t^{-1/2} + k_2) \left(1 - \frac{C_1}{C_{sat}}\right) \\ &= b \cdot C_B(t) + d \cdot (k_1 t^{-1/2} + k_2) \left(1 - \frac{C_1}{C_{sat}}\right) \end{aligned} \quad (2.12)$$

where d is nearly constant, and k_1 , k_2 and C_{sat} are constants. The WMODEL solves the above problem by taking t in the RHS of Equation (2.9) and $t^{-1/2}$ in Equation (2.11) as constant over the time step, which is obviously a poor approximation if the time step is large. Thus, even if, with adequate data, the logic of the WMODEL would insure conservatism, one can not guarantee it until a numerical error analysis is made.

2.2.5.3 Conclusions

WAPPA's Leach-and-Transport Model is inadequate in that it does not conserve mass, does not couple the leach rate of a nuclide to the concentration within the waste form, does not even calculate the waste form concentration, and at times is inconsistent with its own assumptions. To properly repair the WAPPA model would require expansion of the current scheme of calculating four primary variables: leach rate, and concentrations in the packing materials, at the edge of the packing materials, and in solution at the surface of the waste form; to include a fifth variable: concentration within the waste form. Also, a global mass balance should be performed to insure that mass is conserved and that the total mass in the waste package/repository system is equal to the mass inventory supplied as input. To accomplish this would require that a substantial part of WAPPA's leach-and-transport model be rewritten.

As currently implemented in WAPPA, the Leach-and-Transport model will provide a conservative estimate of the release of any species from the waste package through the engineered barriers to the repository only if the mass inventory of a given species decreases with time and the accuracy or conservativeness of the input parameters and numerical solution can be assured. This cannot be done easily.

2.2.6 Conclusions

A common aspect to all of WAPPA's process models is that they involve an empirical approach to modeling the physico-chemical behavior of the waste package under expected repository conditions. A list of specific limitations of the modeling work in general and of the individual process models in particular is presented in Table 2.1.

Table 2.1 Significant limitations of WAPPA's modeling.

<u>Model</u>	<u>Limitations</u>
General	<ol style="list-style-type: none"> 1) Most models are empirical and extremely data intensive. 2) No explicit groundwater chemistry model. 3) Groundwater flow treated as a boundary condition. 4) No internal time step selection and error control.
Radiation	<ol style="list-style-type: none"> 1) Data requested for radiation damage models may be unavailable. 2) Radiolysis effects are independent of temperature, groundwater chemistry, and nuclide under consideration.
Thermal	<ol style="list-style-type: none"> 1) Temperature at the waste package/repository boundary is required as input.
Mechanical	<ol style="list-style-type: none"> 1) Materials strength is independent of temperature. 2) Expansion of corrosion products is neglected. 3) Failure of the waste package ends is neglected. 4) Data for empirical formulae may not be available.
Corrosion	<ol style="list-style-type: none"> 1) All corrosion processes depend only on temperature. 2) Data for pitting, crevice, and/or crack size and density may not be available.
Leach-and-Transport	<ol style="list-style-type: none"> 1) No global mass balance. 2) Leach rate independent of mass in the waste form. 3) Leach rate does not consider radionuclide inventory increasing due to decay of other nuclides. 4) Inconsistent approach in calculating mass released to the repository. 5) Leaching and transport retardation are independent of solution chemistry. 6) Data may be unavailable or difficult to obtain.

The main shortcoming of this modeling approach is that the process models are not self-standing, i.e., they imply a large number of assumptions and rely heavily on user-supplied inputs. For practical applications and acceptability of the results, it will behoove any potential user of WAPPA to make sure that all assumptions that went into the modeling are indeed warranted and that the data used are indeed relevant for each problem. Both tasks are significant as they may require comparison with more detailed analyses and initial information that is difficult to obtain from or may not even exist in the literature. In particular, because of the recognized lack of pertinent data in the literature and the uncertainty associated with some of the data, it is unlikely that any two users will create the same data base.

An additional complication of the implemented modeling approach is that it requires a priori knowledge of the coupling between repository and waste package performance as temperature, pressure, and groundwater flow rate at the waste package-host rock interface as a function of time do depend on waste package feedback effects. At present it is not clear how this inconsistency can be solved.

A major omission in WAPPA's modeling approach is a groundwater chemistry model. The influence of groundwater chemistry on corrosion, leaching, and nuclide transport is assumed to be incorporated into the user supplied input. There is no provision for modeling the coupling between these processes and changes in groundwater chemistry. This places on the user the extra burden of showing that the selected data is indeed conservative under all expected groundwater compositions.

2.3 Review of WAPPA's Operation

WAPPA's modeling approach is more empirical than mechanistic, which places the task of preparing extensive data files to run the code for each problem at hand on the user.

In order to make clearer how the code operates, user's input specifications to WAPPA are reviewed in Section 2.3.1. Output specifications are briefly touched upon in Section 2.3.2. Conclusions are drawn in Section 2.3.3.

The analysis presented is based on the code manual and the complex verification test case which accompanies the code. The test case will be referred to as "the test listing".

2.3.1 Initial Specifications

2.3.1.1 Geometrical Configuration and Materials Specification

With reference to Figure 2.7 which shows the initial configuration of the waste package in WAPPA's Complex Verification Test Case, the waste package is always approximated by a cylindrical, axisymmetric set of concentric barriers. This permits a one-dimensional radial formulation with empirical corrections for end effects.

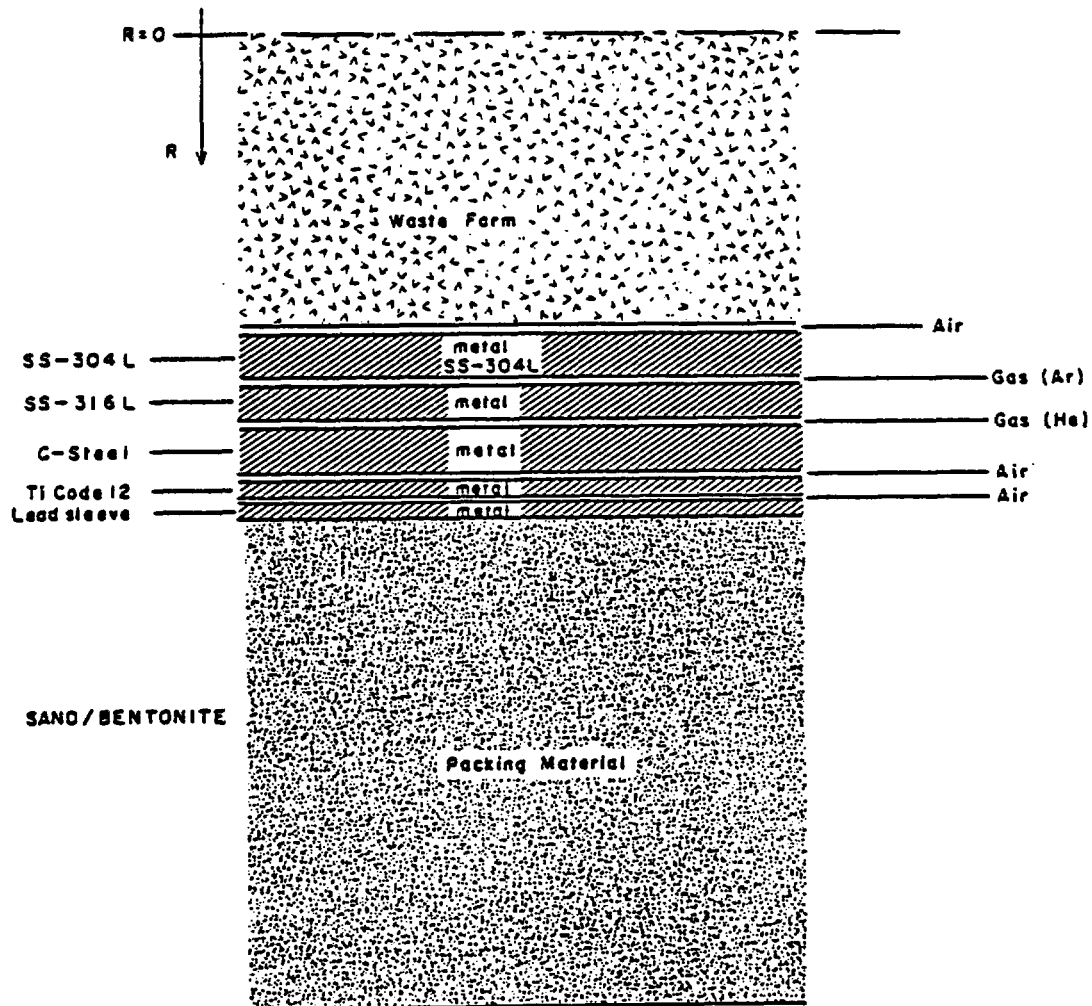


Figure 2.7 Initial configuration of the waste package in WAPPA's complex verification test case.

Proceeding from the inside of the waste package outwards, materials specifications are indicated by entering the material identifier and its outer radius. Materials identifiers are 3-digit numbers. They are used to locate the material properties in the data base for each barrier material.

Allowable barriers are waste forms, metals, corrosion films, gases and packing materials. There can be 17 barriers at most; one waste form, one packing material, and five each of the other barrier materials. The materials reported in Figure 2.1 were inferred from Chapter 2 in the code manual. As a general comment, the test listing does not provide a key to the identification of each particular material constituting the waste package barriers. For instance the listing leaves one uncertain as to whether the waste form is glass or spent fuel.

Initially there will be no corrosion layer. Thus, WAPPA automatically assigns a zero thickness corrosion layer on the outside of each metal barrier. As a minor point, however, since WAPPA accounts for dry oxidation of metals, it would seem more consistent if, when applicable, corrosion layers were placed on both sides of metal barriers.

The above information is complemented by inputting the waste package length, the volume fraction of the waste form which is waste, the density of the waste form matrix without the waste, the density of the waste, and the mass ratio of reprocessed waste-to-original fuel fed in the reactor. In particular, the listing does not mention the age of the waste. That has to be inferred by examining the power source decay rate.

2.3.1.2 Calculation Times and Error Control

In the preparation of the input to the code, the user must define the time span to be investigated along with a set of up to 400 time steps into which the analysis should be subdivided. A restart option also exists which allows restarting the program at any specified time point and continuing the analysis with a newly defined time-step vector.

In any numerical simulation of a time-dependent problem, the solution accuracy can be enhanced, while retaining efficiency, by selecting a time step that is small when changes are most rapid and increasing the time step when the rate of change decreases. In modeling waste package performance, the time when changes are going to be most rapid are initially when the heat source decreases most rapidly due to the decay of short-lived radionuclides, and, at later times, when breaching of a barrier occurs allowing the groundwater to contact the next barrier. Since the user specifies the time step through an input table containing all of the time steps, WAPPA does not determine the time step consistent with the physical processes that occur. This can lead to large, although conservative, errors in the calculated times of breaching and onset of leaching. For example, if the calculation showed the barrier adjacent to the waste form will breach between the requested computational times of 1000 and 1500 years, leaching would be assumed to begin at 1000 years.

To define the temporal location of barrier failures more precisely, the calculation must be repeated with a finer subdivision of computational times. WAPPA can facilitate this process through the restart option. Using the previous example, to determine the onset of leaching within a 50 year period, the calculation could be restarted at 1,000 years requesting a computation every 50 years between 1,000 and 1,500 years. This procedure is a cumbersome burden to the user which could have been avoided by incorporating some time step selection logic into the computer code.

Furthermore, the lack of error control during the calculation prompts the question of how accurate is the solution. The only method the user has to determine if the solution has converged is to rerun the code several times using a finer time step for each new run and comparing the results. Again, this is a burden to the user which could be resolved by proper checks within the computer code.

2.3.1.3 Nuclides Requested

The user is required to specify as input the radionuclides to be tracked during a particular computation. Each radionuclide is identified by a five digit number representing the radionuclide's atomic number and its atomic mass. Thus, 43099 is Tc-99 and 93237 is Np-237. As an added feature each nuclide is also reported in the test listing using the element symbol and its atomic mass.

2.3.1.4 Repository Boundary Conditions

In order to account for waste package interaction with the near field of the repository the user must supply WAPPA with the temperature, fluid flux, vertical stress, and radial stress at the waste package-host rock interface as function of time. The user must also specify packing materials resaturation time.

Singling out the waste package-host rock temperature, one must reason that it depends, as a function of time, both on repository properties such as rock thermal properties, area thermal load, waste package arrangement, etc. and on intrinsic waste package properties such as waste package dimensions and heat generation rates. Thus, in order to specify the problem, it would seem that one needs to have solved it before hand. The same is true for packing materials resaturation time, fluid flux, and, to a lesser extent, for the repository confining pressures.

Boundary conditions specification is one of the most limiting problems in the use of WAPPA, as the above quantities do depend on waste package feedback effects. The problem might be solved by attempting to develop simplified near- and far-field models and interface them with WAPPA.

2.3.1.5 Data Base

WAPPA's basic modeling approach is empirical in nature and therefore extremely data intensive.

Data needed in order to operate the code include radiation decay properties, radiation shielding properties, empirical data for radiation damage, thermal properties, mechanical properties, empirical data for end effects on stress analysis, empirical data for corrosion, empirical data for leaching. Some of these data need to be supplied as a function of waste package system variables like temperature, pH, etc.

The task of assembling such a large data base can be overwhelming for several reasons. First, the user must be thoroughly acquainted with the limitations and the range of applicability of the models. He should also be able to judge whether the data exist in the literature. If the data are not available, ad hoc experiments and/or extensive calculations are needed. Because of the paucity of the data and uncertainty in some of the data, it is unlikely that any two users will create the same data base. The second problem is that the range of experimental data to be inserted in the data base should cover the entire history of the waste package under expected repository conditions. The waste package environment and physical barriers can vary so extensively during the time span of a repository that it is hardly conceivable that an adequate data base where all synergistic effects are accounted for can be produced. For instance, the Corrosion Model uses empirical correlations to supply all information regarding corrosion rates for each of the various models and barriers. The coefficients used in each correlation are supplied by the code user as a function of temperature alone. One would expect corrosion to depend also on pH, Eh, salts content of the groundwater, etc. which readily increases the complexity of the problem of obtaining adequate experimental data. It is foreseeable that the user of WAPPA shall not model all synergisms and will refer to single or few-component test data. In that case, the user will have to show that these data are conservative.

2.3.1.6 Radionuclide, Gamma, Alpha, and Thermal Power Source Terms

At each new time step WAPPA updates the radionuclide inventory and the thermal-power, gamma-photon, and alpha-particle densities in the waste form through use of user-provided input tables. These tables are prepared by first running an isotope inventory code like ORIGEN2.

The task of preparing the above inputs is not onerous to the user as it requests that only the age and type of waste be known. Barring numerical errors due to WAPPA's lack of internal time step and numerical errors controls, this approach is conservative, as the source term code would not account for radionuclide depletion with time from the waste form due to leaching and transport.

2.3.2 Output Specifications

WAPPA allows many options to control the amount of data to be printed. Options exist for echo prints of the input as well as the output of results generated during execution. Always provided are the total radial heat flow leaving the waste package, the cumulative γ -radiation dose, nuclide fluxes at the waste package boundary, total nuclide mass outflow through the waste package boundary, radial nuclide concentration, profiles of the waste package, barrier wetting times, and barrier failure times.

The output of the code reads well. It requires however some familiarity with the code structure and how it operates. As a general comment we would suggest that the output be improved to show 1) The name of each material being considered rather than only a numerical identifier, 2) The mode by which a barrier may have failed, and 3) Whether mass is conserved or not in the system. Additional minor points are the following: 1) the leach rate diffusion and dissolution coefficient are given wrong dimensions; 2) dimensions are missing from the oxidation rate constants A through G; and 3) on restart runs the radionuclide mass inventory, alpha flux, and gamma flux are given wrong dimensions.

2.3.3 Conclusions

The operation of WAPPA involves the preparation of extensive input and support data files. These should be prepared by qualified personnel who are thoroughly acquainted with the assumptions which went into the formulation of each process model.

The task of preparing input and support data files can be overwhelming for two main reasons. First, some of the input data require a pre-knowledge of how the waste package would perform. Second, the amount and quality of the needed data contrasts with the recognized paucity of pertinent data in the literature and their associated uncertainty. To that effect, it should be mentioned that WAPPA users will probably be limited to data which factor in only a few of the system variables on which they depend. Thus, it will be necessary for any WAPPA user to show that these data are conservative.

WAPPA's implemented numerical strategy lacks internal control of time step and of numerical errors. This may lead to unnecessary conservatism and place on the user the extra burden of redefining the time step vector and re-running the code several times in order to make sure that convergence is achieved. This feature, along with the large number of data whose uncertainty needs to be known, limits WAPPA's applicability for Monte-Carlo-type reliability analysis, which requires short computational time for each case run.

2.4 Conclusions and Recommendations

2.4.1 Conclusions

WAPPA is a modular code implementing radiation, thermal, mechanical, corrosion, and leach-and-transport modeling to determine system performance of

WAPPA was not designed to be a self-standing code. It implements a mostly empirical approach requiring model justification, and extensive data gathering, interpretation and validation. These tasks constitute the major limitations of the code and will require a significant effort to resolve by personnel who are thoroughly familiar with the modeling.

In practice, WAPPA operates as a data base manager that simply selects which correlation and which data are applicable for each particular situation. Construction of the data base will be troublesome as the implemented correlations may be defined in terms of only a few variables, whereas the actual processes may depend on more system variables; the required data are likely to be unavailable in many cases or they may be difficult to adapt from the literature; or they may imply a pre-knowledge of future package performance, as is the case for temperatures, pressure, and groundwater flow rate at the waste package/host rock interface. Furthermore, as reported in Table 2.1, a few limitations have been identified in the process models.

The number of parameters which will have to be supplied and the number of different situations for which they may have to be specified will result in very large data files. After formation of these files, the user must make sure that the adopted data base is realistic or conservative for the problem under study. The code user will also have to prove that all assumptions that went into modeling are warranted. This will involve a detailed comparison of predictions from each process model with experimental results or with the predictions of state-of-the-art individual codes for each of the processes considered. In particular, since individual validation of each process model neglects the synergistic effects that may couple various processes, simultaneous validation of several models should be done whenever possible.

After validation of the data and models, the code user still must insure that the numerical solution procedure provides reliable calculations. At present, time step selection is determined from a user supplied input table which does not necessarily reflect the physical processes that occur, such as the breach of a barrier. Therefore, to insure the calculation is converged, the user must first run the code and determine the approximate times of major system changes. Then, the code must be rerun with a finer time step near the times of major system changes. This procedure must be repeated until the desired level of convergence has been achieved.

While adherence to the above procedures for code usage will be necessary for a license application, their rigor may be relaxed for work in site screening, preliminary design analysis, and in estimating acceptable ranges of parameters through sensitivity analysis. In this case, it may turn out to be profitable to use WAPPA once a few improvements have been made, e.g., mass conservation should be fixed in the leach-and-transport model, the temperature boundary condition could be given through a simplified far-field model, etc. All together these improvements may require a significant effort.

WAPPA cannot be used in its present form for straightforward reliability analysis, e.g., Monte Carlo simulation through Latin Hypercube sampling. There would be too many parameters to be sampled and probability distributions for all of them would not be available. Sensitivity analysis may alleviate the task by reducing the number of parameters to be sampled. However, the need to rerun to code a number of times to insure convergence may still prove a stumbling block for the reliability analysis both in terms of computer time and trouble to the user.

2.4.2 Recommendations

1. The WAPPA code is receiving considerable attention from the DOE's Salt and Tuff programs (DOE/RW-0005, 1984). For this reason, the NRC should keep the code readily operable in its most recent form.
2. If the DOE decides to use WAPPA to obtain relevant licensing information, the NRC should request the code custodian to prepare an extensive data preparation manual which includes: a list of all the data required; a description of how the data is used; a description of model limitations; a list of appropriate references for obtaining the data; and a detailed example of how to construct the data base.
3. Any application of WAPPA should be complemented with an extensive justification of the data. Data should be prepared in accordance with the "Draft Technical Position on Waste Package Reliability" (NUREG/CR-0997n, 1983). That is, an estimate of the experimental errors in the data should be presented along with a description of experimental procedures and a citation to the original reference.
4. Further work by the NRC using WAPPA does not seem to be justified unless the DOE indicates it will use the code to obtain relevant licensing information. In that case, an effort should be made to improve upon the present modeling approach of specifying the waste package/repository boundary conditions as a user-supplied function of time. For example, WAPPA could be coupled with a temperature field analysis which calculates the required boundary temperature as the calculation proceeds. Also, the various process models should be improved to remove their internal limitations. In general, model validation will be of primary importance.
5. If the NRC desires to have the capability to independently check-waste package performance calculations, it will need, in addition to a general systems code like WAPPA, a suite of state-of-the-art analysis codes that model the various individual processes that are relevant. Examples of these processes include: groundwater flow, groundwater chemistry, heat transport, structural analysis, leaching, nuclide migration, and corrosion.

6. In the future, code manuals which provide a description of the mathematical and computational models should be prepared in accordance with the "Draft Technical Position on Documentation of Models" (NUREG-0856, 1981). In particular, the WAPPA manual, in many cases, did not provide adequate justification of the models, did not discuss the range of validity of the models, and did not address the problem of numerical stability and accuracy.
7. In the future, it would greatly assist the NRC if, in the code manual, the DOE provided a list or diagram of failure modes addressed by the code. Indeed, the preparation of a system code like WAPPA should be preceded by a failure mode and effects analysis (FMEA), in order to insure that all relevant failures are incorporated in the code. If available, this FMEA should at least be referred to in the code manual.
8. Although the modular structure of WAPPA would allow retrieval and re-adaptation of each process model to another code with a modular structure, this does not appear to be advantageous at present in view of the several shortcomings identified within each of WAPPA's process models.

2.5 References

AESD-TME-3131, 1982, Westinghouse Electric Corporation, Engineered Waste Package Conceptual Design in Salt, Sept. 1982.

Brookhaven National Laboratory, MF-125, Preliminary Review of the Leach-and-Transport Model in WAPPA, Pescatore, C., (December 1983).

Brookhaven National Laboratory, MF-126, Preliminary Review of the Metal Barriers Corrosion Models in WAPPA, Sullivan, T., (December 1983).

Brookhaven National Laboratory, MF-127, Review of WAPPA's Complex Corrosion Verification Test Case, Pescatore, C. and Sullivan, T., (February 1984).

Brookhaven National Laboratory, MF-132, Review of WAPPA's Thermal Model, Pescatore, C., (February 1984).

Brookhaven National Laboratory, MF-135, Mass Conservation in WAPPA's Leach-and-Transport Model, Sullivan, T., (February 1984).

Brookhaven National Laboratory, MF-141, Preliminary Review of the Radiation Model in WAPPA, Sullivan, T., (April 1984).

Brookhaven National Laboratory, MF-142, Derivation of the Attenuation Model Used in WAPPA, Sullivan, T., (April 1984).

Brookhaven National Laboratory, MF-149, Review of WAPPA's Mechanical Model, Pescatore, C., (June 1984).

Brookhaven National Laboratory, MF-150, Potential Problems with Using the Constant Kd Approach in Radionuclide Transport Calculations in the Near Field of a Nuclear Waste Repository, Sullivan, T., (June 1984).

Brookhaven National Laboratory, MF-151, Review of the Solution Strategy Used in WAPPA, Sullivan, T., (June 1984).

BNL-NUREG-33658, "An Evaluation of Chemical Conditions Caused by Gamma Irradiation of Natural Rock Salt, Panno, S. V. and Soo, P., 1983.

DOE/RW-0005, Mission Plan for the Civilian Radioactive Waste Management Program, Vol. II, Draft, 1984.

NUREG-0856, Draft Technical Position on Documentation of Models, Silling, S. A., 1981.

NUREG-0997R, Brookhaven National Laboratory, Draft Technical Position on Waste Package Reliability, Sastre, C., and Pescatore, C., 1983.

ONWI-302, Battelle Memorial Institute, Columbus, OH., Waste Package Performance Evaluation, Lester, D. H. et al., 1983. (Content of this report was effective as of December 1981).

ONWI-452, Battelle Memorial Institute, Columbus, OH., WAPPA: A Waste Package Performance Assessment Code, INTERA Environmental Consultants, Inc., 1983. (Content of this report was effective as of October 1982).

ORNL-5621, ORIGEN2- A Revised and Updated Version of the Oak Ridge Isotope Generation and Depletion Code, Croff, N.G., 1980.

Perry, R. H. and C. H. Chilton, 1973, Chemical Engineers Handbook, Fifth Edition, McGraw Hill Book Company, New York, N.Y., p. 10-6.

Pescatore, C., 1983. "Mechanistic Modeling of Nuclear Waste Form Leaching by Aqueous Solutions," PhD. Thesis, University of Illinois.

Pickering, H. W., et al., "Wedging Action of Solid Corrosion Product During Stress Corrosion of Austenitic Stainless Steels." Corrosion, Vol. 18, p. 230 (June 1962).

PNL-4452, Nuclear Waste Package Materials Testing Report: Basaltic and Tuffaceous Environments, p. 82., Bradley, D. J., Coles, D. G., Hodges, F. N., McVay, G. L., and Westermen, R. E., 1983.

RHO-BWI-LD-48, Rockwell Hanford Operations, Richland, WA., The Sorption Behavior of Selected Radionuclides on Columbia River Basalts, Salter, P. F., Ames, L. L., and McGarrah, J. E., 1981.

Rockwell, T., ed., 1956. Reactor Shielding Design Manual, Van Nostrand, Princeton, N. J.

Weber, W. J., Turcotte, R. P., Bunnell, L. R., Roberts, F. P., and Westsik, J. M., 1979. CONF-790420, "Radiation Effects in Vitreous and Devitrified Simulated Waste Glass," Ceramics in Nuclear Waste Management, p. 294.

Weber, W. J., Wald, J. W., and Gray, W. J., 1980. "Radiation Effects in Crystalline High-Level Nuclear Waste Solids." Proc. 3rd Symp. Scientific Basis for Nuclear Waste Management, p. 441.

3. DETERMINATION OF LOCAL CORROSION CONDITIONS APPROPRIATE FOR A HIGH LEVEL CONTAINER IN A BASALT REPOSITORY

3.1 Introduction

The objective of this program is to determine the chemical environment that will be present in high level nuclear waste packages emplaced in a basalt repository. For this purpose, low carbon steel (a current Basalt Waste Isolation Project, BWIP, reference container material), a basalt/bentonite packing material, and synthetic Grande Ronde basaltic water were reacted in an autoclave at 150°C and ≈10.4 MPa (1500 psi) pressure. The tests lasted for two-month periods and the gamma irradiation flux, when used, was $(3.8 \pm 0.5) \times 10^4$ rad/h. The Phase I irradiation test used an inert argon environment and Phase II involved a similar set of experimental conditions but used a methane cover gas. This was performed because high methane concentrations have been detected in basaltic water samples taken from Borehole RRL-2 in the Grande Ronde formation. The Phase III control test was also conducted in a methane environment, but in the absence of irradiation.

Measurements on the packing material slurry at the conclusion of the tests included pH and dissolved oxygen (DO) determinations. The Eh could have also been measured but, according to available information (NUREG/CR-3389, 1984), its observed value may not be very meaningful¹. The concentrations of Cl⁻, total Fe (measured as Fe²⁺), and SO₄²⁻ ions in the filtrate were also measured, since these ions are associated with the corrosion of carbon steel². Gases generated during the irradiation period may include H₂, O₂, N₂ and CO₂. Since several of these gases could have a deleterious effect on the waste container, gas analyses were made at the conclusion of the test period. The carbon steel sleeves were metallurgically evaluated for uniform and pitting corrosion. Hydrothermal alteration of the rock and clay constituents of the packing material was also investigated.

¹There is no reason to believe that the potential of a platinum (or other noble metal) electrode immersed in a solution is a thermodynamic potential or even a reasonably reproducible potential. Most likely, such a measured potential is a mixed potential dependent on the kinetics of the various redox processes occurring in the system. In the absence of significant concentrations of oxygen and other possible redox active species, the potential may depend on the corrosion rate, however small, of the indicator electrode (NUREG/CR-3389, 1984).

²Basaltic groundwater contains F⁻ ion but this has not been associated with the corrosion of carbon steel (Hall, E., 1982). Qualitative tests for H₂S and S⁻² were to be performed in the current study to determine if quantitative tests were needed.

3.2 Materials

Basalt from the Cohasset Flow of the Sentinel Bluffs Sequence of the Grande Ronde Formation (see Figure 3.1) and bentonite clay from Wyoming³, saturated with simulated Grande Ronde groundwater, were used to prepare the packing material slurry. The major-element oxide compositions for the Middle Sentinel Bluffs Flow (assumed to be representative of other flows in the Sentinel Bluffs Sequence, including the reference Cohasset Flow) and the reference Wyoming bentonite (coded SWy-1 by the Clay Minerals Society) are given in Table 3.1. Analyses for S and F contents were not reported for the basalt but were reported as 0.05% S and 0.11% F for the bentonite. Some information is also available on the carbonate content of the bentonite. Upon ignition to 1000°C, the bentonite lost 6.43% of its weight [assumed to be due to the loss of adsorbed and structural water (5.1%) and CO₂] (Van Olphen, H., 1979). An infrared spectrum of the bentonite confirmed the trace carbonate content and a moderate content of iron in the lattice in the ferric state (Van Olphen, H., 1979). The availability of information, e.g., the infrared spectrum, and the characterization of the standard clay, SWy-1, was a primary reason for its use in the experiment. As a reference clay, it is reported to have a surface area of 31.82 ± 0.22 m²/g (Van Olphen, H., 1979), as determined at 77K using the BET gas (N₂) adsorption method designed by S. Brunauer, P. H. Emmett and E. Teller (1938). However, it should be noted that surface areas determined by gas adsorption techniques on SWy-1 clay do not necessarily correspond to the the reactive surface areas in solution (Lerman, A., 1979). The surface that reacts with the solution may be smaller than the total measured. It is not expected that the use of an argon or methane overpressure will block reactive sites of the clay in solution, based on results of Stoessel and Byrne (1982). They showed that methane solubilities in water at 25°C and at pressures of methane up to 5 MPa were not significantly affected by the presence of clay and that there was no detectable sorption of methane onto SWy-1 clay, under these conditions. It is assumed that argon will behave similarly to methane because of its inertness. It is also assumed, without evidence to the contrary, that at higher pressures and temperatures, there is no blocking of reactive sites by argon or methane.

³Reference basalt and clay as specified by BWIP Rockwell-Hanford personnel. The density of the basalt rock that was crushed to pellet size was measured to be 2.8 g/cc. These basalt pieces are not uniform in size but are chips ranging in size from 0.187 to 0.250 inches in diameter.

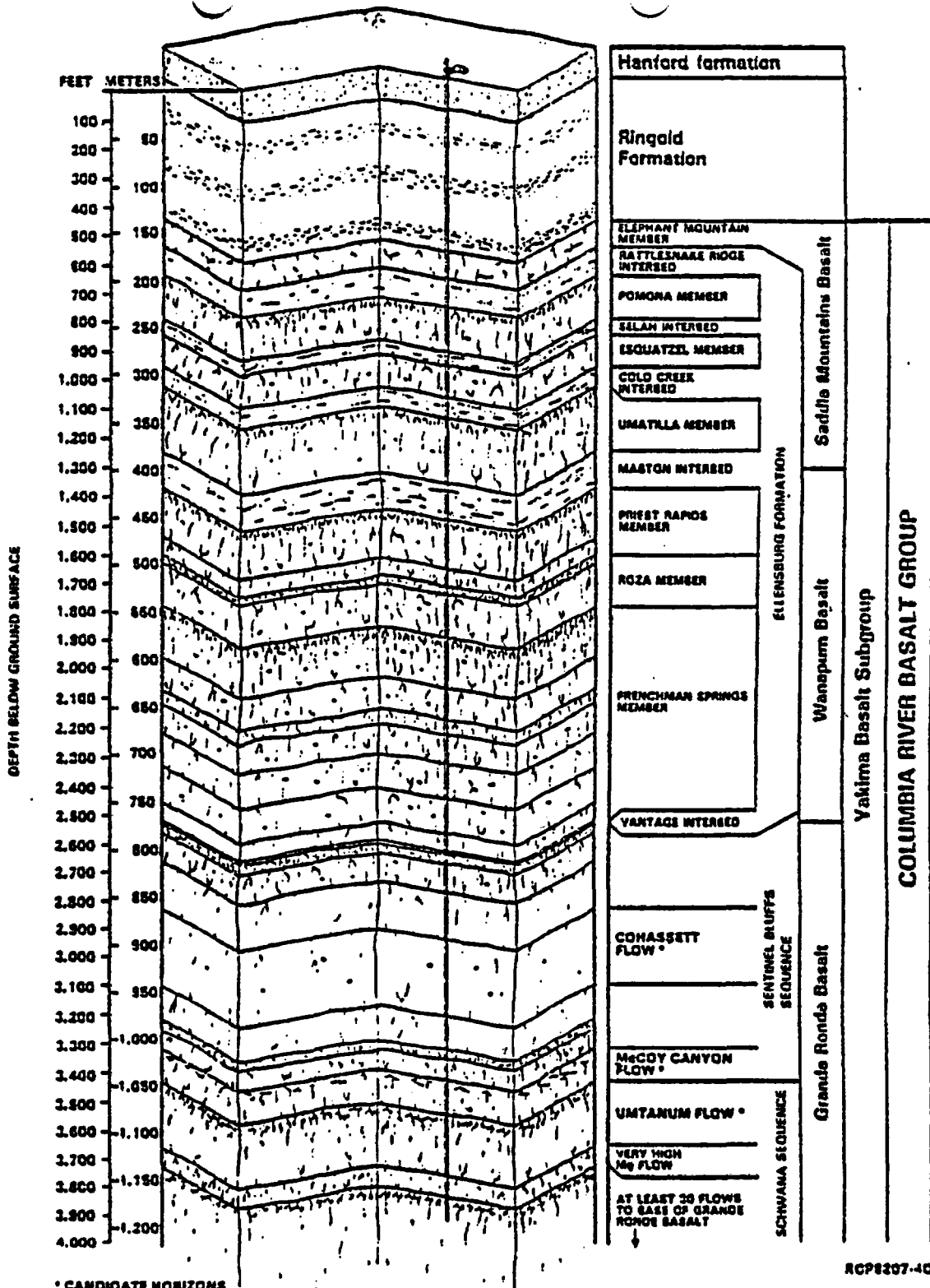


Figure 3.1. Generalized stratigraphy of the Columbia River Basalt Group, Yakima Basalt Subgroup, and intercalated and suprabasalt sediments within the Pasco Basin (RHO-BW-SA-303P, 1983). (Details of the stratigraphy are not discussed in this report.)

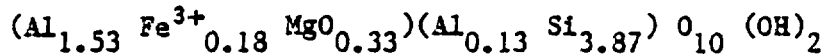
Table 3.1. Compositions of Middle Sentinel Bluffs Flow basalt and reference Wyoming bentonite.

Oxide Component	Basalt (Weight Percent) (DOE/RL 82-3, Vol. II, 1982)	Bentonite (Weight Percent) (Van Olphen, H, 1979)
SiO ₂	53.4	62.9
TiO ₂	1.79	0.09
Al ₂ O ₃	15.0	19.6
FeO	11.7	0.32
Fe ₂ O ₃	—	3.35
MnO	0.21	0.006
MgO	4.99	3.05
CaO	8.86	1.68
Na ₂ O	2.48	1.53
K ₂ O	1.03	0.53
P ₂ O ₅	0.29	0.049

Mineralogically, bentonite is montmorillonite clay with some quartz present (Van Olphen, H., 1979)⁴. Steindler and others (ANL 83-19, 1983) reported the mineralogical composition of SWy-1 clay to consist of montmorillonite, quartz, calcite, and K-feldspars. No gypsum was detected.

The Grande Ronde basalt flows of the Columbia Plateau are continental flood basalts. Mineralogically, these basalts contain the principal minerals pyroxene, plagioclase, titaniferous magnetite, olivine and interstitial glass

⁴Montmorillonite is a mineral which is essentially a hydrated aluminosilicate with some substitution within the lattice. A "typical" packet of montmorillonite is formed by the bonding of a layer of alumina octahedra with two layers of silica tetrahedra. In general, Wyoming bentonite contains a mineral of the montmorillonite type as the principal component with the structural formula:



(Grimshaw, R. W., 1971). (This notation indicates that Al, Fe, and Mg are present in dioctahedral coordination and that Al and Si are present in tetrahedral coordination. There are also ten divalent oxygen and two hydroxyl anions per packet, as shown by the formula.) The presence of adsorbed cations (i.e. the exchangeable cations such as Ca²⁺, Na⁺, Mg²⁺, K⁺ and H⁺) and other minerals (e.g. quartz) present in the Wyoming bentonite are not indicated by this formula.

of variable composition (DOE/RL 82-3, Vol. II, 1982). The secondary minerals are predominantly smectite clays and zeolite (clinoptilolite), with lesser amounts of SiO₂. Textures vary considerably, with typical textures dominated by a lath-shaped plagioclase and pyroxene grains locked together by an interstitial glassy matrix. Primary and secondary phases in Grande Ronde basalt are listed in Table 3.2.

Table 3.2. Petrographic characteristics of primary and secondary phases reported as present in Grande Ronde basalt (DOE/RL 82-3, Vol. II, 1982).

Characteristic Primary Phase	Abundance Volume %	Chemical Formula
Plagioclase (anorthite)	25-50	CaAl ₂ Si ₂ O ₈
Pyroxene		
Augite	20-45	(Ca)(Mg,Fe ²⁺ ,Fe ³⁺ ,Al,Ti)(Si,Al) ₂ O ₆
Pigeonite	0-10	(Mg,Fe ²⁺ ,Ca,Mn)(Mg,Fe ²⁺ ,Mn)[Si,Al] ₂ O ₆
Orthopyroxene	0-trace	(Ca,Mg,Fe ²⁺)(SiO ₃)
Glassy Mesostasis	15-70	SiO ₂ = 60 to 74% (by weight)
Titaniferous Magnetite	0-7	FeO·(Fe ₂ O ₃ ,TiO ₂)
Apatite	0-2	Ca ₅ (PO ₄) ₃ F, occurs as acicular crystals in the mesostasis.
Olivine	0-3	(Mg,Fe ²⁺) ₂ SiO ₄
Alteration Products (secondary phases)	1-9	Includes smectites, zeolites, SiO ₂

The nominal composition of the synthetic Grande Ronde water identified as GR-3 is given in Table 3.3. Its pH at 25°C is 9.74 (RHO-RE-SR-5, 1982). In addition to the components listed, GR water has been found to contain the following gases: 25 ppm N₂, 10 ppm Ar, and up to 700 ppm CH₄ at 25°C (RHO-BW-SA-315P, 1983). The results of an analysis of the synthetic groundwater used in this experiment are also given in Table 3.3. The recipe for the synthetic groundwater is based on analyses of water samples collected from the DC-6 well in the test horizon just below the Umtanum basalt flow (990-1075 m). (The composition of GR-4 synthetic groundwater is given in Table 3 for comparison and is based on analysis of a Cohasset flow bottom sample from Borehole RRL-2 in the reference repository location. It should be noted that GR-4 water has much less sulfate content than the GR-3 water which was used in the present experiment.)

Table 3.3. Composition of synthetic Grande Ronde groundwaters.

Chemical Species	GR-3 Nominal Composition (ppm) (RHO-RE-SR-5, 1982)	GR-3 Experimental Composition (ppm)	GR-4 Nominal Composition (ppm) (SD-BWI-TP-022, 1984)
Na ⁺	358	363	334
Cl ⁻	312	312	405
SO ₄ ²⁻	173	165	40
Si as SiO ₂ *	76.2	79.3	96.4
Inorganic C as HCO ₃ ⁻	54.6	—	92.0
F ⁻	33.4	29.9	19.9
K ⁺	3.43	3.63	13.8
Ca ²⁺	2.78	2.10	2.20
Mg ²⁺	0.032	0.030	—

*Total dissolved silica content is not partitioned in its speciated forms, H₃SiO₄⁻ and H₄SiO₄.

3.3 Autoclave System Design

The hydrothermal conditions in the current tests were achieved by use of a stainless steel autoclave, which was pressurized with Ar and/or CH₄ to approximately 6.9 MPa (1000 psi) at room temperature to obtain the expected hydrostatic pressure at temperature. (The contribution to the pressure due to water vapor at 150°C is 0.52 MPa, 75 psi.) Figure 3.2 shows the exterior of the autoclave. The placement of internal components is shown in Figures 3.3 and 3.4. The autoclave weighs approximately 20.4 kg and is approximately 15.9 cm in depth and has an internal diameter of 6.3 cm. A rod-shaped resistance heater was placed vertically near the wall of the autoclave to ensure the development of a thermal gradient across the packing material. A low carbon 1020 steel sleeve was placed over the heater to simulate actual waste container/packing material conditions. It has a welded-on cap and is 25.5 mm in diameter, 143 mm in length and 2 mm in thickness. The sleeve was heated to 150°C and a temperature differential was established across the 38-mm thickness of the packing material. The temperatures at the heater (T₂) and at the wall (T₁) were monitored by Type 316 stainless steel thermocouples which were 3 mm in diameter and were inserted to a depth of approximately 75 mm and bent to contact the heater and wall. It is assumed that thermocouples maintain contact during test. During the tests, packing material was extruded into the space between the heater and the inner surface of the steel sleeve. This would act as an insulating medium which, together with the excellent thermal conductivity of the sleeve, would greatly minimize local hot spots on the latter. In the

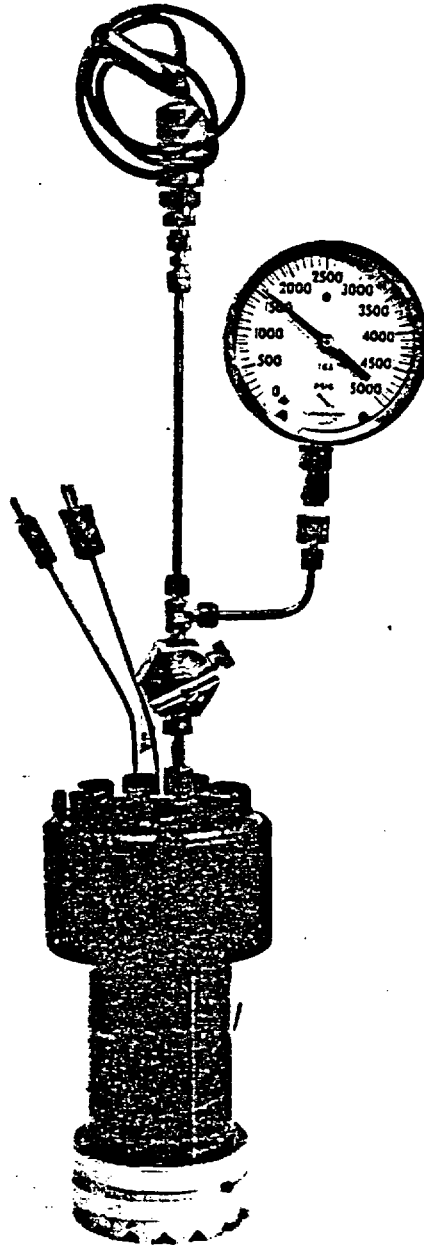


Figure 3.2. Autoclave system being leak checked. (Pressure gauge was removed prior to placement in gamma pool.) Magnification is 0.2X.

Phase I test an attempt was made to obtain water samples for analysis by incorporating two Type 304 stainless steel sampling tubes in the packing material. These were 7 mm in diameter and 150 mm in length, and each contained 23 small drilled holes to allow water ingress while retarding passage of the slurry. Since the tubes displace a volume of only 20 mL compared to a slurry volume of 440 mL, no significant changes in thermal conductivity or temperatures in the packing were expected. Sampling tubes were not used in the Phase II and III tests since the volumes of water collected by their use were minimal.

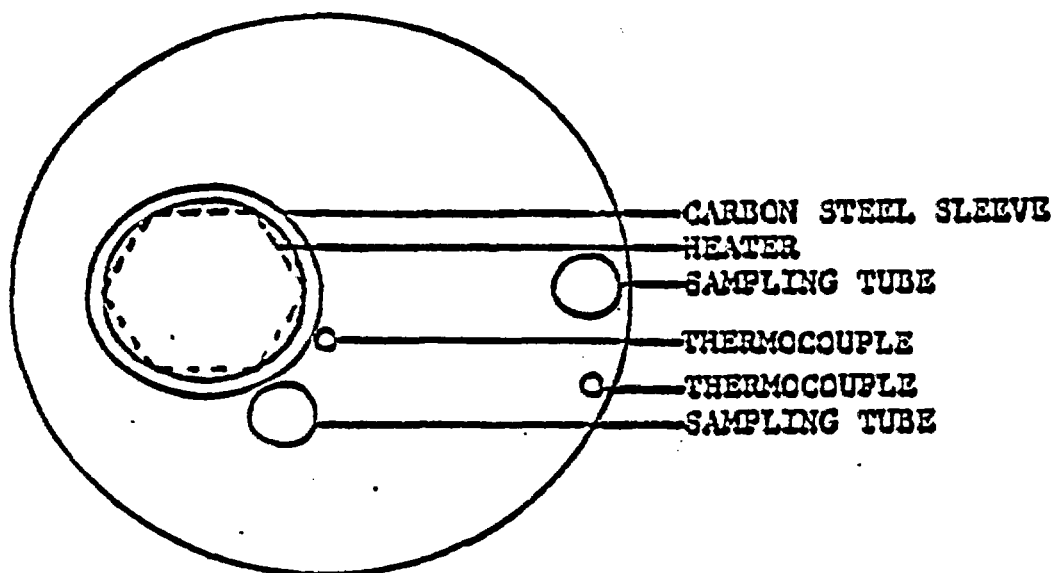


Figure 3.3. Cross section through autoclave (drawn to scale).

3.4 Experimental Procedures

3.4.1 Slurry Preparation

The bentonite was used in the as-received condition (-400 mesh, with a density of 0.78 g/cc). The basalt was crushed to pellets ranging in size from 0.187 to 0.250 inch in diameter. An excess amount of slurry was first prepared by mixing 33.5 g of bentonite with 478 mL of freshly-made synthetic groundwater which was prepared using details given in the literature (RHO-RE-SR-5, 1982). The ratio of 7:100 (by weight) of bentonite to water was selected on the basis of BWIP work which showed this composition to be optimal for restricting water flow in basalt repositories (RHO-BWI-C-66, 1980). To minimize the presence of air and voids, the slurry was prepared so that water replaced the air present in the packing material. This mixture was allowed to gel overnight in the presence of air. Pellets of basalt including fines (209 g occupying a volume of \approx 129 mL) were then added to the bentonite slurry. This packing material was also allowed to equilibrate overnight in the presence of air. This procedure yielded a 3:1 (by volume) mixture of basalt:bentonite and a solution:solid

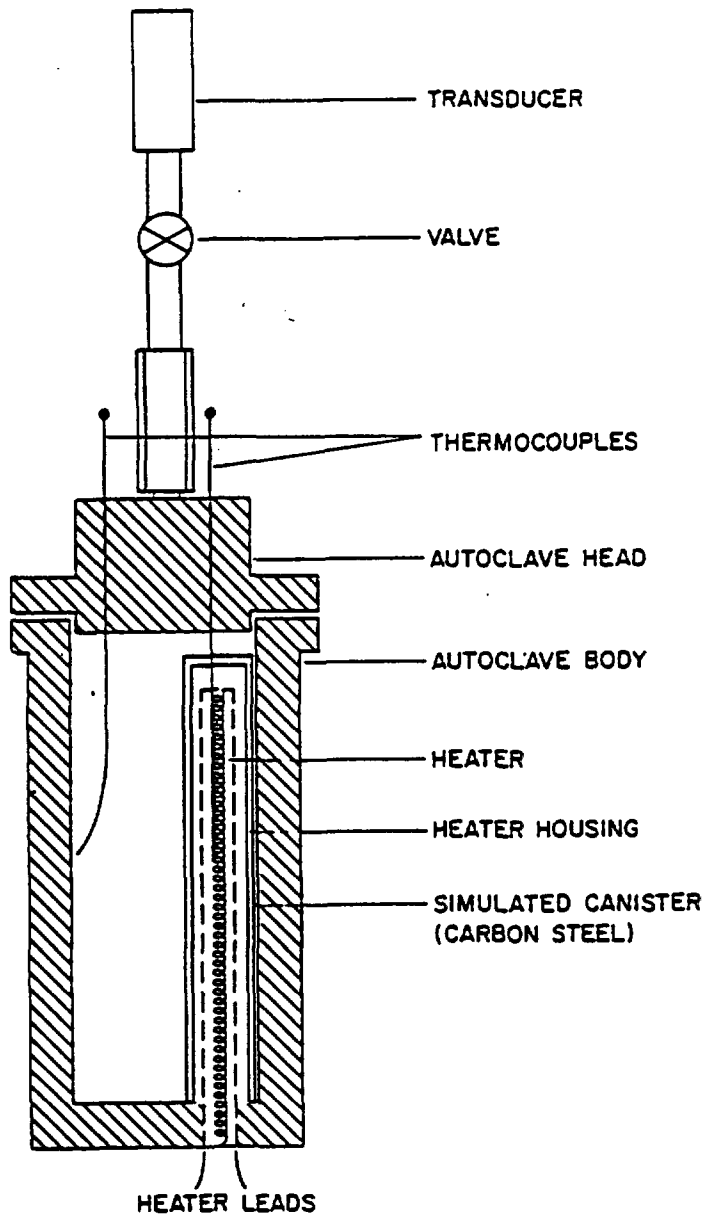


Figure 3.4. Lengthwise section through autoclave. Magnification is 0.35X.

ratio (by weight) of about 2. Most of the packing material slurry was placed in the autoclave, giving a void space below the autoclave head of approximately 20 mL. (The use of the sampling tubes gave a total void of ≈ 30 mL.)

3.4.2 Autoclave Pressurization

In the Phase I test, the slurry was placed in the autoclave leaving a void space of ≈ 30 mL. The autoclave was flushed with argon and pressurized to 6.9 MPa (1000 psi) with argon at 24°C. After lowering the autoclave and monitoring/control attachments into the gamma pool, the temperature was slowly raised to 150°C \pm 2°C over a period of 24 hours. A mean temperature differential of ≈ 37 °C across the packing material test section was achieved and maintained. The temperature at the autoclave wall and pressure transducer readings were recorded hourly by use of an automated data logger. The transducer readings in volts had previously been calibrated to pressure.

In the Phase II test, slurry was placed in the autoclave, with a void space of ≈ 20 mL remaining. (The sampling tubes were not used in the Phase II and Phase III tests.) Because of the ≈ 50 mL drop in slurry level discovered at the conclusion of the Phase I test, a different pressurization technique was followed in Phase II. The autoclave was pressurized to 10.4 MPa (1500 psi) at room temperature with argon and maintained overnight. The autoclave was opened and there was again found to be a noticeable drop in the slurry level. Additional slurry was added to keep an estimated void space of ≈ 20 mL. The autoclave was again pressurized to 10.4 MPa with argon at room temperature to check for leakage. The argon was then bled off and methane (99.93% pure, ethane 0.07%) was added to attain a pressure of 6.2 MPa (900 psi) at 18°C. It was predicted that the system would approach a pressure of ≈ 9.7 MPa at the test temperature, including a water vapor pressure contribution. However, the pressure attained when the system was at 150°C was in excess of 13.1 MPa (1900 psi). After lowering the autoclave and monitoring/control attachments into the gamma pool⁵, the temperature at the heater was slowly raised to 150°C \pm 4°C over a period of 52 hours. A temperature differential across the packing of ≈ 22 °C \pm 4°C was achieved at the end of that time. After 157 hours of irradiation, a malfunction developed in the heater regulator, causing the temperature to drop to 108°C at the heater (T₂) by morning. After the regulator was replaced, the temperature was increased to normal over a period of 11 hours. The pressure reading at 176 hours (11.9 MPa) was ≈ 1.0 MPa lower than the pressure reading at 159 hours. It is not known whether this reduction in pressure would have occurred if the regulator had not failed; nor is the cause of the reduction clear. A mean temperature differential of ≈ 22 °C was maintained throughout the Phase II test.

In the Phase III test, a procedure similar to that described for the Phase II test was used to check for leakage. The argon was again bled off and

⁵A methane monitor was emplaced over the tube containing the autoclave in the gamma pool. Continuous purging over the entry of the tube with argon was carried out.

methane added to attain a pressure of 7.4 Mpa (1074 psi) at 18.4°C. It was predicted that the system would approach a pressure of ≈10.4 MPa, with the addition of the water vapor pressure contribution. The actual pressure attained was ≈10.6 MPa. An air blower and/or cooling coils were used in this non-irradiation test in an attempt to obtain a thermal gradient in the packing similar to those obtained for the Phase I and Phase II tests which were placed in the gamma pool. Their use across the body of the autoclave increased the thermal gradient. However, an air stream across the top of the autoclave was used because its use decreased the thermal gradient. Because of the blower tests, there was some fluctuation in autoclave pressure during the first 195 hours of testing.

The initial pressurization value was kept the same for all three phases of the experiment. The fact that the pressure in the Phase II experiment exceeded that predicted may be due to the generation of a radiolytically-produced gas. Differences in pressure developing in the autoclave seem to also be inversely proportional to the size of the thermal differential across the packing material. The effect of this pressure difference between the Phase II and Phase III tests on the results is not known.

3.4.3 Irradiation Procedure

The ambient air temperature in the gamma pool test hole was 22°C. A dosimetry measurement, which was performed on the empty autoclave, indicated that a dose rate of $(3.8 \pm 0.5) \times 10^4$ rad/h was delivered to the interior of the vessel by the ^{60}Co source. The dose rate was measured by use of radiochromic film which is calibrated to a National Bureau of Standards (NBS) standard by comparing optical densities. No measurement of distribution of the gamma energies from the ^{60}Co source is available. In the Phase I test, the autoclave was irradiated for 1486 h, to a dose of $(5.6 \pm 0.7) \times 10^7$ rad. In the Phase II test, the autoclave was irradiated for 1727 h, to a dose of $(6.6 \pm 0.9) \times 10^7$ rad. The Phase III test did not incorporate any irradiation.

3.4.4 Post-Test Procedures

Procedures for analyses on the gas, the packing material, water and carbon steel sleeve were initiated after the autoclave had been cooled to room temperature (at a rate of approximately 5°C/min). As many as six gas samples were taken, and analyses carried out by a mass spectrometric technique. Gas remaining in the autoclave was vented to the air and the autoclave was opened in a glove bag filled with argon. Measurements of pH and DO were made at several depths in the slurry both near the heater and near the autoclave wall. The pH electrode had previously been calibrated with buffers having standardized pH values of 2, 7, and 10. Readings are accurate to ±0.05 units. The DO electrode had been calibrated against the DO content of water at 25°C, which is 8.4 ppm. Dissolved oxygen (DO) readings have an estimated accuracy of ±0.5 ppm.

The appearance of the material in the autoclave was changed after reaction in all three tests. There were portions of the slurry which were white and/or orange in comparison to the unreacted slurry color (beige). No caking or odor were detected. Some orange coloration was also evident on the slurry adhering to the steel sleeve.

Two-core samples (each ≈5 mL) were taken from both the heater and autoclave wall regions (these are designated by the letters H and W, respectively, in subsequent discussions). Test tubes containing the slurry were centrifuged for one hour and the liquid portion was removed. Approximately 3 mL of solution were collected from the sample taken from the region near the autoclave wall and approximately 2 mL from the sample taken from the heater region. The liquid was cloudy and was passed through a membrane filter having a pore size of 0.025 μm. The filtrates were analyzed for Fe, Si, Cl⁻, and SO₄²⁻ content⁶. After the cores were removed, an additional sample (i.e. samples designated R) was obtained by combining portions of the slurry that were randomly selected. The test tube containing this "combination" sample was also centrifuged, but the supernate was analyzed in the unfiltered form.

Basalt pellets were removed from the corings near the heater and the autoclave wall and prepared as thin-section specimens for microscopic analysis. Unreacted basalt thin sections were also made for comparison. Pulverized basalt and glass slides coated with reacted centrifuged slurry were also prepared for mineralogical studies using a Philips XRG 3100 X-ray diffractometer. Colloidal matter obtained from R samples, by filtration through a 0.025-micron membrane filter, was analyzed by SEM-EDX procedures.

The slurry was removed from the carbon steel sleeve by washing in water. The slurry adhering to the sleeve was isolated for SEM-EDX studies. The carbon steel sleeve was placed in a desiccator and kept for metallographic analysis.

3.5 Results and Discussion

3.5.1 Pressure Measurements

After the test temperature was attained, the pressure within the autoclave was recorded. The following ranges of pressure were found for the three tests over the two-month test periods:

- 9.3-9.7 MPa (1357-1404 psi) — Phase I
- 11.1-13.2 MPa (1612-1919 psi) — Phase II, and
- 9.8-11.7 MPa (1416-1702 psi) — Phase III.

Note that the initial large pressure fluctuations in the Phase III test caused by attempts to achieve a specific thermal gradient in the packing are not included.

⁶The Fe content was determined by atomic absorption (AA). The Si content was determined by an automated standard colorimetric method using ammonium molybdate reagent. The Cl⁻ and SO₄²⁻ contents were measured by ion chromatography (IC). This analytical technique gives quantification of ionic species in the sub ppb to ppm range and allows for the analysis of small volumes (≈1 mL) of sample. Precision is normally ±5%, but due to the large amount present in our samples, it was approximately ±2%.

A plot of P/T_1 values versus time should be an indicator of change in the number of moles of gas present in the system and/or the volume that the gas occupies, since $P/T_1 = nR/V$, where R is the gas constant. It is assumed that T_1 , the temperature at the autoclave wall, is representative of the average temperature experienced by the gases contained in the autoclave. Figure 3.5 gives P/T_1 values for the three tests conducted. Fluctuations in the P/T_1 values from the mean are less than ± 1 percent and may be due to instrumentation characteristics or small fluctuations in volume. There is a basic trend in the pressure changes during each test involving an initial decrease in pressure over the first 500 h followed by an increase for the remainder of each test. For the Phase I test, this trend is more clearly detected by a magnified P/T_1 scale. Although the pressure at the end of each test never exceeded the initial pressure, it is possible that very long term reaction could lead to monotonic pressure increases.

Reasons for the initial decrease in pressure include consumption of gases such as oxygen and an increase in the void space in the autoclave during a test. Pressure decreases in the Phase I, II and III tests are 0.14, 0.83, and 0.48 MPa (20, 120 and 70 psi), respectively. This would represent a decrease in gaseous oxygen (sorbed or dissolved oxygen will not cause a pressure decrease after reaction) of 100-200 mg. This explanation is not likely since this relatively large amount of free oxygen (i.e. not sorbed or dissolved) would not be present in the test system. A more plausible explanation of the initial pressure decrease is a change in the volume above the packing material. Volumetric increases of only 1%, 7%, and 4% would be needed to account for the observed pressure decrease in the Phase I, II and III tests, respectively. This could be caused by shrinkage of the bentonite during hydrothermal interaction. The increases in pressure observed in the later stages of a test are likely to be partly associated with radiolytic gas generation and/or hydrogen generation by basalt/water interaction (see below).

3.5.2 Pressure Changes Due to Radiolysis

Any radiolytic effects which result in the production or consumption of gas and associated pressure changes are assumed to occur on (1) the slurry water in the Phase I and II tests, (2) methane as dissolved gas in the water in the Phase II test and (3) methane in the void space in the Phase II test. No radiation-induced structural damage to the bentonite silicate lattice is expected (Krumhansl, J. L., 1982).

3.5.2.1 Radiolysis of Water in a Closed System

Since we are concerned with the radiolytic products of water in a closed system (constant volume) in the Phase I and II tests, pressure buildup studies at Savannah River Laboratory (SRL) on the irradiation of concrete waste forms in sealed containers have yielded specific conclusions (DP-1464, 1978), which may enable an interpretation of our data to be made on the basis of radiolytic effects on the amount of gas present in the system. In the SRL tests, 500-mL glass bottles containing set cement (with voids in different samples ranging from 125 to 223 mL depending on the amount of cement and water that was added to the bottle) were irradiated at 40-50°C. Both high and low dose rate tests established that the initial production rate of H_2 from the radiolysis of water

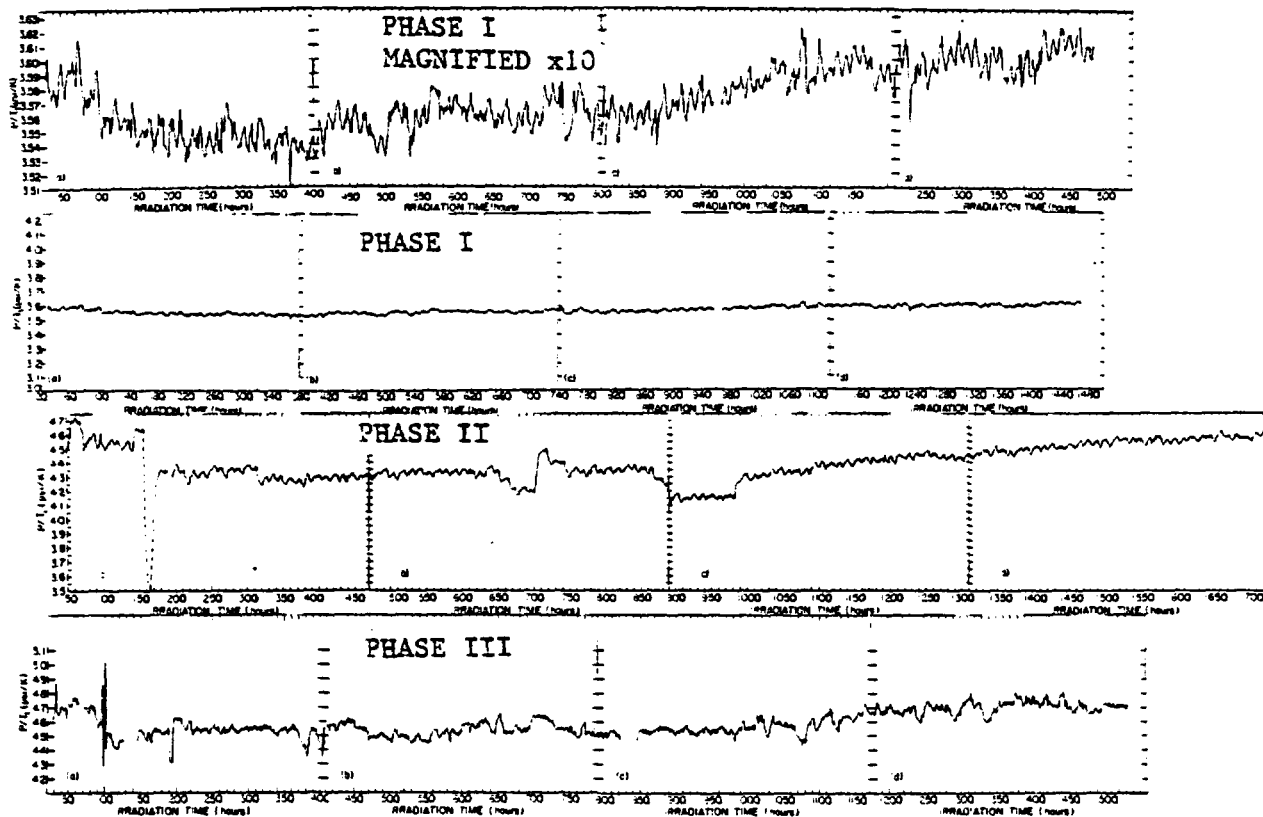


Figure 3.5. Pressure changes with time and temperature in the autoclave system for the three phases of the experiment: Phase I (absence of methane and presence of radiation), Phase II (presence of methane and radiation), Phase III (presence of methane and absence of radiation.)

was dependent upon the dose rate; but as the H₂ pressure increased, a reaction removing H₂ was initiated and the pressure reached a steady state. This equilibrium pressure was also directly dependent upon the dose rate. The gas volume and the water-to-cement ratio did not affect the pressure attained. Gas composition at the end of the test showed that O₂ content from the air sealed within the concrete was 95% consumed and N₂ content was unchanged. In water containing oxygen, the oxidizing power of the dissolved oxygen is made available by reactions of e⁻(aq) and H[•] to give O₂⁻, which is a powerful oxidizing species. Presumably the consumed oxygen was incorporated in oxidation products. This depletion of oxygen resulted in a 0.014 MPa (≈2 psi) decrease in pressure over a period of 100 days at a constant dose rate (DP-MS-16-51, 1976). See Figure 3.6 for data on dose rate versus the steady state H₂ pressure.

It is also known that if the radiolysis occurs at a higher temperature, the increase in temperature will lead to an increase in the primary species [i.e. the hydrated electron e⁻(aq), the hydrogen atom and the hydroxyl radical OH] and a decrease in the number of molecules (H₂ or H₂O₂) (Draganic, I. G., 1971). It has also been determined that there is no effect of pressure on the yields of primary reducing species, hydrogen atoms, and H₂ (Draganic, I. G., 1971). Thus, we assume that the dose rate is the determinant of the final H₂ pressure from the radiolysis of water. If we chose the largest pressure at the radiation dose of $(3.8 \pm 0.5) \times 10^4$ rad/h, which is what the packing slurry receives in this experiment, this value is less than 0.17 MPa (25 psi) (assuming linear extrapolation) under ambient conditions. For a temperature of 150°C, this would correspond to a pressure of less than 0.24 MPa (35 psi). From the use of the baseline data indicated in Figure 3.5, it is clear that any increase in pressure due to H₂ production on the order of 0.24 MPa, and any decrease in pressure due to O₂ consumption, will fall within the baseline scatter and will not be observable.

3.5.2.2 Radiolysis of Methane in Aqueous Solution and in the Gaseous Phase

Gas production and consumption are also affected by the presence of methane in the Phase II test. Methane is the predominant gaseous constituent in the Saddle Mountains and Wanapum basaltic groundwaters, comprising 60 to 98 percent of the total dissolved gas. Methane comprises from <0.01 to 1.6 percent of the total dissolved gas in the groundwater of the Grande Ronde in Boreholes DB-6 and DC-14, but comprises 98 percent of the total dissolved gas in the Grande Ronde groundwater in Borehole RRL-2 (on the order of 10² to 10³ ppm) (NUREG-0960, Vol. 2, 1983).

Methane (99.93%) was used to attain a pressure of 7.4 MPa (1074 psi) at 18.4°C in the Phase II test. The solubility of methane in water at 25°C at 1 atm of methane over-pressure is approximately 21 ppm (Dean, J. A., 1979). The Henry's Law coefficient for methane at this temperature is $\approx 4 \times 10^4$ atm/mole fraction (Himmelblau, D. M., 1960). A calculation using this coefficient gives a concentration of ≈1600 ppm of methane in water at 7.4 MPa pressure. Solubilities at high temperature and high pressure conditions are graphically represented in Figure 3.7. At 150°C and 10.4 MPa (1500 psi) (see arrows in Figure 3.7), the solubility is approximately 1500 ppm.

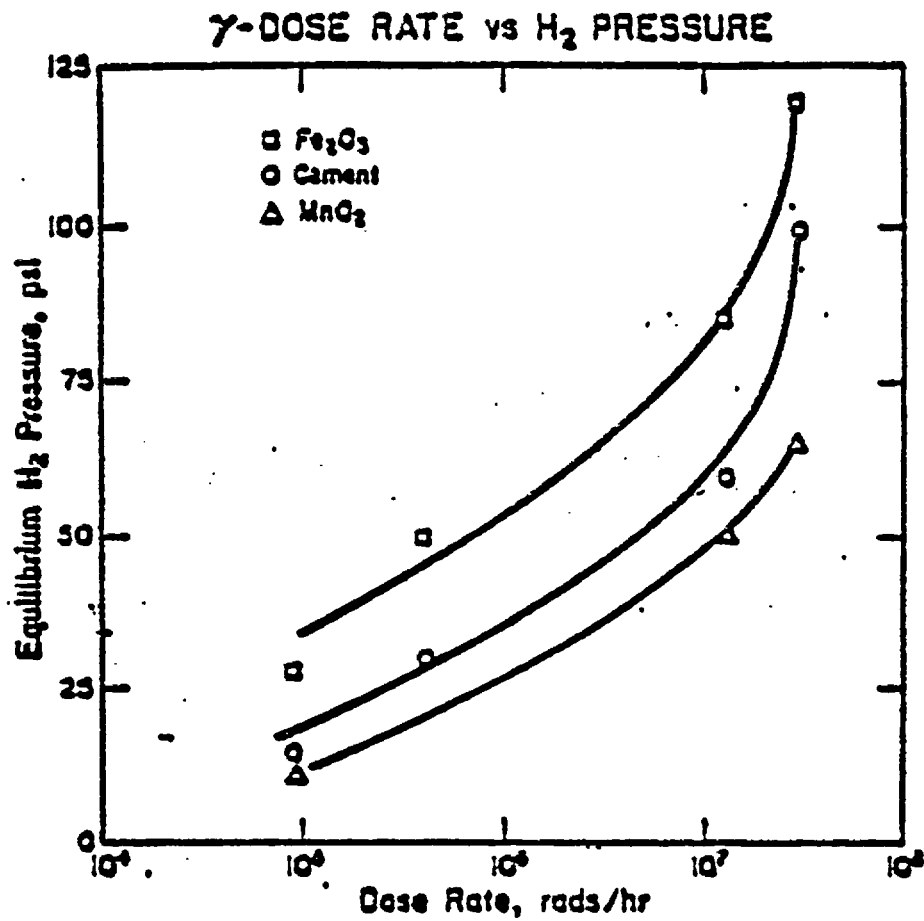


Figure 3.6. Effect of dose rate on H₂ equilibrium pressures for concrete (neat), concrete containing Fe₂O₃, and concrete containing MnO₂ (DP-MS-76-51, 1976).

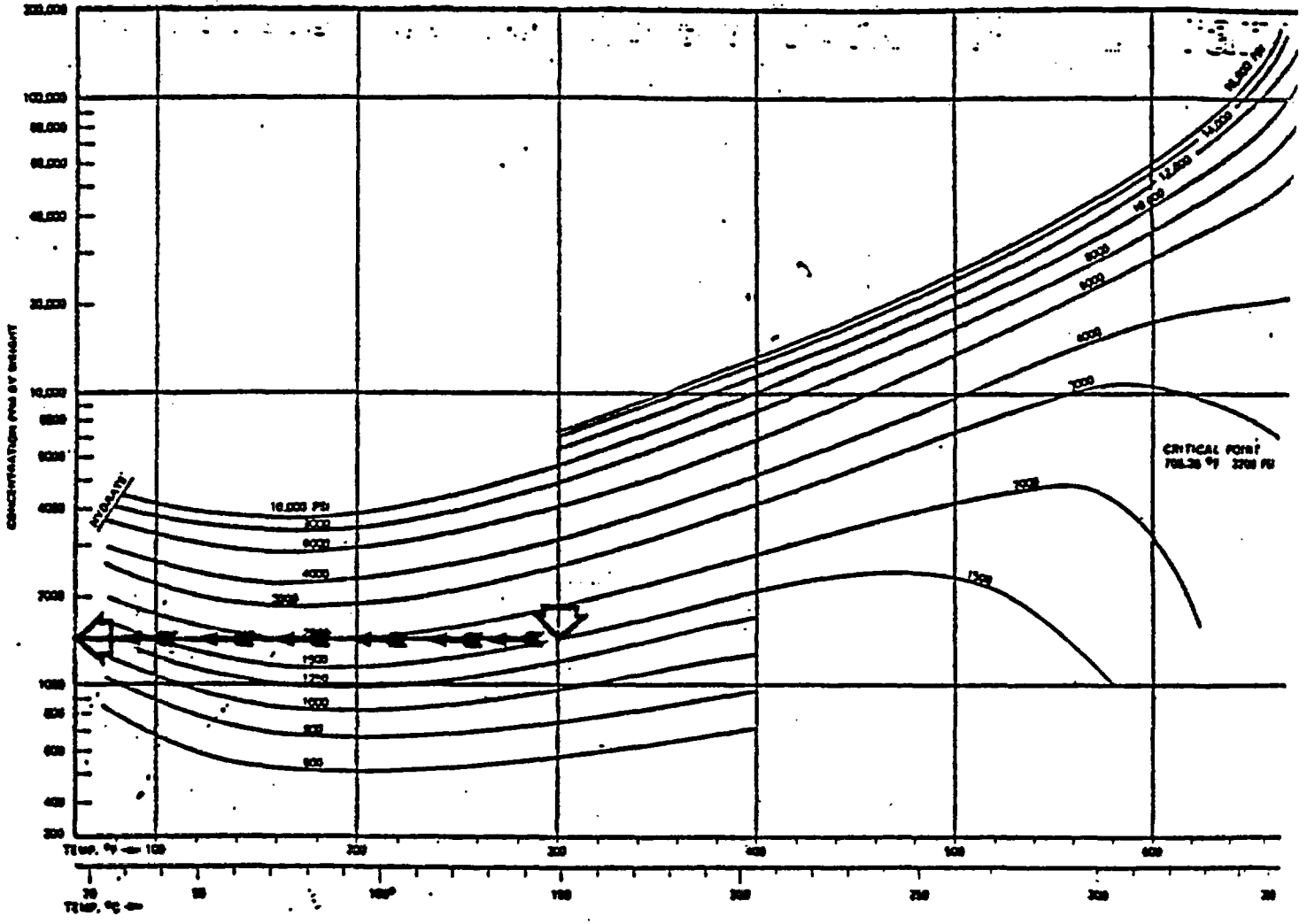


Figure 3.7. Solubility of methane in water at high temperatures and pressures (Bonham, L. C., 1978).

Results of a study on the gamma radiolysis of aqueous methane solutions (Stevens, G. C., 1972) have indicated that only the OH free radical (from the water radiolysis) reacts with methane to any appreciable extent. Methyl radical is the product of this reaction. Methyl radical then reacts with the radiolysis products of water to yield methane, hydroxyl ion and methanol. It also reacts with another methyl radical to produce ethane. Ethane reacts with the various radicals present in the system to produce ethyl radical, methane and hydrogen. This process could continue as higher alkanes are formed which themselves interact with radicals present in the system to produce hydrogen, ethylene, propane, n-butane, i-butane, n-pentane, i-pentane, neopentane, acetylene, propylene, l-butene and polymeric type molecules (Arai, H., 1981).

In the BNL tests, gas samples were taken from the autoclave after cooling to room temperature. Detailed data are given in Table 3.4.

The largest $G(H_2)$ value from the radiolysis of methane in the gas phase and subsequent reactions is 13.26 molecules/100 eV of absorbed radiation (Arai, H., 1981). No $G(H_2)$ value for the aqueous methane solution was reported in the Stevens (1972) study. Although this $G(H_2)$ value is much larger than that obtained for water (0.45), it should be noted that the methane content (≈ 0.1 mol) in our system is approximately 250 times less than the content of water. Thus, we could estimate that more hydrogen would be produced from the radiolysis of water than the radiolysis of methane. However, as shown in Table 3.4, more hydrogen was produced in the Phase II test than in the Phase I test.

A valid estimation of the amount of hydrogen produced by the radiolysis of methane is not possible due to the combination of major experimental factors that will affect gas production rates, viz. temperature, pressure, and increased surface area of adsorbent. The presence of other gases initially present in the system and those possibly generated by chemical reactions will also affect the dominant mechanisms in the radiolysis of methane. However, some specific effects from other studies which varied single parameters are summarized as follows:

- The G values for all products are affected by an increase in temperature (Arai, H., 1981). The G values for the formation of n-butane and acetylene decrease with increasing temperature. The G values for the formation of other significant products increase with temperature.
- An increase in pressure causes a decrease in $G(H_2)$ and $G(C_2H_6)$ (Maurin, J., 1962).
- The influence of the basalt/bentonite mixture, due to chemical composition and increased surface area available for reaction, on the production of gases, in combination with the other variables that are present, is not known. Synergistic and/or catalytic effects may be operative. Results from Norfolk (1977) on the gamma radiolysis of methane gas adsorbed on gamma-alumina suggest that methane at the temperature under consideration will react only with radiolytic intermediates derived from surface hydration and that direct energy transfer to the adsorbed methane from the alumina did not occur.

Table 3.4. Comparison of composition of gases sampled after reaction as determined by mass spectrometry. (Gas composition is given as mole percent.)

Gas	Molecular Weight	Phase I ^a	Phase II ^b	Phase III ^c
H ₂	2	3.71	17.6	4.21
CH ₄	16	0.019	78.3 ^d	91.5 ^d
NH ₃	17	ND ^e	ND	ND
H ₂ O	18	0.020	0.028	0.063
CO	28	ND	f	ND
C ₂ H ₄	28	ND	ND	0.03
N ₂	28	1.00	0.18 ^f	0.28
C ₂ H ₆	30	ND	0.43 ^d	ND ^d
NO	30	ND	ND	ND
O ₂	32	0.027	ND ^g	0.020 ^h
H ₂ S	34	ND	ND	ND
Ar	39.9 ⁱ	95.1	3.04	3.84
CO ₂	44	0.12 ^j	0.17 ^j	0.04 ^j
NO ₂	46	ND	ND	ND

^aThese values represent compositions averaged from the last two of the three gas samples taken.

^bThese values represent compositions averaged from the fourth and fifth samples of the six gas samples taken.

^cThese values represent compositions averaged from a total of five gas samples taken.

^dThe methane was analyzed and was found to contain 0.07% ethane. On this basis, we would predict that the Phase II test and Phase III test gas analyses would show a maximum ethane content of 0.07%.

^eND is an abbreviation for not detected.

^fCarbon monoxide and nitrogen concentrations are not distinguishable at these low levels.

^gMinimum detection limit was stated to be 0.017%.

^hOxygen was detected in the first two samples out of a total of five samples.

ⁱThe argon used contains <0.001% oxygen.

^jDry air contains by mole percent: 78% N₂, 20.9% O₂, 0.9% Ar, 0.03% CO₂, and 0.2% other gases.

- The presence of other gases initially present in the system and those generated by chemical reactions will also affect the radiolysis of methane. A G value for the depletion of hydrocarbon, G(-hydrocarbon), in a system containing carbon dioxide, carbon monoxide, methane, water and hydrogen has been estimated to be ≈ 16 (Norfolk, D. J., 1983).

3.5.3 Gas Analyses Results

3.5.3.1 Phase I Test Gas Analysis Results

In the Phase I argon-overpressure test, hydrogen, carbon dioxide, and methane were produced and radiolytic and/or adsorbed oxygen was consumed. The source of the nitrogen is assumed to be air remaining after slurry preparation. Some carbon dioxide is also present in the starting slurry, but a source of carbon must be available to account for the presence of methane and additional carbon dioxide. It is known that calcite is present in the bentonite and that the groundwater contains carbonate species. There may also be some organic surface contamination of the basalt that could act as a source of carbon.

3.5.3.2 Phase II Test Gas Analysis Results

The Phase II test system was pressurized with methane. During the course of irradiation and reaction, hydrogen, ethane, and carbon dioxide are produced and oxygen was consumed overall. A small amount of carbon monoxide may have been produced. There is some residual argon in the system from leak testing and the nitrogen is assumed to be from residual air present in the system.

Work related to the Phase II test has been conducted by PNL (RHO-BW-SA-315P, 1983) on the irradiation of synthetic Grande Ronde (GR-3) basaltic groundwater saturated with methane in the absence of basalt and bentonite at 150°C for 72-hour periods at dose rates ranging from $1.1-5.3 \times 10^6$ rad/h. The initial methane content of the pressurizing gas used was at least 95%, and the final methane content of the vented gas ranged from 70-85%. This decrease is due to the radiolysis of methane. Hydrogen was produced and its content in the vented gas ranged from 9.9 to 24%. In the Phase II test, the methane content was decreased to $\approx 78\%$ and $\approx 18\%$ H₂ was formed. However, different gases and filterable material were produced in the Phase II test than were produced in the PNL work. Carbon dioxide and ethane, and perhaps carbon monoxide, were the only carbon-containing gases found in the Phase II test. In the PNL study, carbon dioxide and higher alkanes, e.g. derivatives of propane and butane, were formed.

The filterable colloidal material in the Phase II test was mainly inorganic and contained 1.8% C, 0.3% H, and <0.03% N. The polymeric solids formed in the PNL work were mainly organic and contained $\approx 86\%$ C, $\approx 12\%$ H, and $\approx 1\%$ O. The extent of polymerization as evidenced by weight-average molecular weights is directly dependent on the dose rate. In the PNL work, the dose rate was three to four orders of magnitude greater and there was no packing material present.

3.5.3.3 Phase III Test Gas Analysis

During the course of this non-irradiation control test, hydrogen was produced and oxygen was consumed. Small amounts of carbon dioxide may also have been produced. In work performed by Siskind (NUREG/CR-3091, Vol. 3, 1983), gas analyses performed after hydrothermal reaction of packing material at 250°C (in argon and in the absence of irradiation) showed that carbon dioxide, hydrogen, and methane were produced. However, it is not possible to state whether any methane was produced during the Phase III test since this would be masked by the large volume of this gas used for pressurization.

3.5.3.4 Comparison of Gas Analyses Results

A comparison of the gas compositions from the Phase I, II, and III tests, given in Table 3.4, results in the following conclusions:

- Hydrogen is produced in all three tests, i.e. in the presence and in the absence of radiation. More hydrogen appears to be produced in the Phase II test, probably as a result of methane radiolysis. Hydrogen in the Phase I and II tests probably forms by basalt/water reactions.
- Since no methane is known to be present in the initial gas composition of the Phase I test, its detection indicates formation during this test. Because methane was used to pressurize the Phase II and Phase III test systems, it is difficult to determine whether any methane was produced. However, there is less methane remaining at the end of the Phase II test when compared to Phase III. This difference may be attributable to the radiolysis of methane which would explain the relatively large volume of hydrogen in Phase II.
- There is more nitrogen present in the gas at the end of the Phase I test than for the other two tests. This difference is indicative of the change in pressurization techniques after the Phase I test (see above).
- Oxygen was detected in the Phase I and III gas samples. The concentrations of 0.027 and 0.020 percent, respectively, correspond to partial pressures (at 6.9 MPa, 1000 psi) of 0.018 atm (0.27 psi) and 0.014 atm (0.20 psi). Using a Henry's Law coefficient of 5×10^4 atm/mole fraction from Figure 8, these oxygen partial pressures give the following DO levels: 0.6 ppm (Phase I) and 0.5 ppm (Phase III). See Section 3.5.4 for measured values.
- Carbon dioxide in amounts exceeding that in dry air (i.e. 0.03%) was found in all three tests.

3.5.4 Measurement of pH and DO and Calculation of Eh

3.5.4.1 Measurement of pH and Dissolved Oxygen of Unreacted Packing Material Slurry

The pH electrode was calibrated with buffer solutions having pH values of 2, 7, and 10. The accuracy of the pH measurement is ± 0.05 units. Prior to testing, the pH in the bentonite/basalt packing material was determined to be 8.14 at mid-depth and 7.84 at the bottom of the beaker containing the mixture.

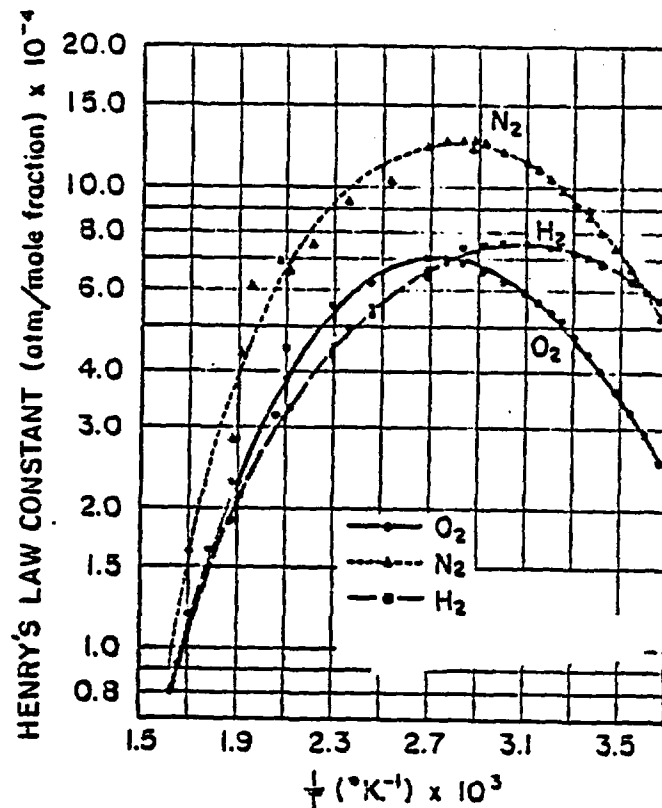


Figure 3.8. Solubilities of O_2 , N_2 , and H_2 in water as a function of temperature (Himmelblau, D. M., 1960). Note that the solubility of O_2 goes through a minimum near $100^{\circ}C$.

The DO electrode was calibrated against the DO content of water at $25^{\circ}C$, which is 8.4 ppm. The DO of the starting bentonite slurry without basalt was found to be 8.3 ± 0.5 ppm. It was concluded on the basis of obtaining this 8.3 ppm value that readings are not affected by the presence of a solid phase. After the addition of basalt to the slurry, DO was measured near the surface and at mid-depth, at three locations. Results for the near-surface measurements ranged from 4.1 ppm to 6.5 ppm, with an average value of 5.4 ppm. Results for the mid-depth measurement ranged from 2.8 ppm to 3.7 ppm, with an average value of 3.2. It is clear that the DO content of the bentonite/basalt

slurry is reduced by basalt/water interaction. The wide range of results obtained in the DO values led to uncertainty in the accuracy of the measurements. Accuracy is taken to be ± 0.5 ppm based on DO measurements on a solution prepared to contain zero dissolved oxygen (Method 421F, A. Greenberg, 1980).

3.5.4.2 Measurement of pH and Dissolved Oxygen of Reacted Packing Material Slurry

The following general procedure was used for each of the three tests: The autoclave was opened and kept in a glove bag filled with argon. The pH and DO measurements were made, almost immediately, at several depths in the slurry near the heater and near the autoclave wall. It was felt that these in situ measurements would be most representative of the conditions achieved during a test. It should be noted, however, that autoclave depressurization forces gases such as carbon dioxide and oxygen out of solution and causes the pH reading to be higher and DO to be lower than those under the pressurized condition. The use of these measurements after decompression in the calculation of the Eh would, therefore, result in a more reducing value.

3.5.4.2.1 Measurement of Phase I Test pH and Dissolved Oxygen and Calculation of Eh

In the irradiated Phase I test, pH values near the heater increased from 6.84 to 6.92 as the depth of measurement increased. The three pH values obtained averaged 6.88. Near the autoclave wall, the pH was found to be 7.16 near the surface of the slurry, 6.73 in the middle and 6.88 near the bottom. These pH values averaged 6.92. If the average pH value at the heater is compared to the average pH value at the wall, there does not appear to be a significant difference across the thermal gradient. The average pH of the Phase I test irradiated system was, therefore, taken to be 6.90 in the Eh calculations described below.

Dissolved oxygen measurements taken near the heater gave values of 0.64 ppm near the surface, and 0.56 ppm at a depth of approximately 5 cm. For measurements near the autoclave wall, the DO was found to be 0.70 ppm near the surface and 0.52 ppm at a depth of approximately 5 cm. These values may be compared to the average of 3.2 ppm for a system containing only bentonite, basalt, and synthetic groundwater and open to the air. There is significantly less DO in the reacted system which is probably due to reaction with various system components, i.e. packing and carbon steel, during irradiation to form corrosion products and colloids. However, there does not seem to be a significant difference between the DO content across the thermal gradient. The average DO content of the Phase I irradiated system was taken to be 0.6 ppm for the Eh calculation given below.

It has been speculated by BWIP that the environment in a basalt repository will be sufficiently reducing to inhibit corrosion of the carbon steel. Reducing conditions, however, were not achieved in the Phase I test based on the following calculation of Eh. The Eh was calculated using the experimental DO

and pH results from the following equation (DOE/RL 82-3, Vol. II, 1982)⁷ for a temperature of 24°C (297.2°K) to compare with BWIP estimates:

$$Eh (V) = 1.23 + 0.0147 \log fO_2 - 0.0590 pH + 0.000136.$$

If we assume that the pressure exerted by the dissolved oxygen on the system is equivalent to the fugacity of oxygen needed as input to the equation and that the use of this oxygen pressure rather than the oxygen overpressure (1670 Pa)⁸ leads to a smaller value for fO_2 , then the fugacity is calculated to be 46.3 Pa by use of the Ideal Gas Law, based on a DO content of 0.6 ppm (1.875×10^{-8} mol/mL)⁹. Accordingly, the Eh is +0.85 V, indicating that an oxidizing environment existed in the Phase I test after quenching the autoclave.

3.5.4.2.2 Measurement of Phase II Test pH and Dissolved Oxygen and Calculation of Eh

Measurements for the Phase II test were similar to those for Phase I. Adjacent to the heater, the pH was 6.62 near the surface of the slurry, 6.52 in the middle, and 6.68 near the bottom, with an average value of 6.61. Adjacent to the wall, the pH was 6.53 near the surface of the slurry, 6.49 in the middle, and 6.70 near the bottom, with an average value of 6.57. Although

⁷The total range of Eh values for the Middle Sentinel Bluffs and Umtanum flows from 51°C to 300°C was estimated to be -0.54 to -0.37 V (DOE/RL 82-3, Vol. II, 1982). The equation used to calculate Eh should be applicable at a temperature of 24°C, because the equations for pH and fO_2 used in the derivation are valid at this temperature (Equations 11-6 and 11-16, DOE/RL 82-3, Vol. II, 1982).

⁸By use of the Henry's Law coefficient for oxygen at 25°C ($\approx 5 \times 10^4$ atm/mole fraction), it was calculated that an overpressure of 0.0165 atm of oxygen is needed to sustain an oxygen solubility in water of 0.6 ppm (The mole fraction of oxygen was calculated to be 3.3×10^{-7} .) The amount of oxygen overpressure expressed as a volume per cent of the mixture of gases at 1000 psi (68 atm) is 0.024%, which is very close to the measured oxygen content of the gas vented after quenching. It should be noted that an oxygen content of 0.2 ppm in water at 25°C would require an overpressure of 0.0055 atm of oxygen, which would constitute 0.008% of a gas mixture at 68 atm, and which would be below the mass spectrometric detection limit for oxygen of 0.017%.

⁹The compressibility factor of oxygen at 1 atm of oxygen and 300 K is 0.9994, indicating that oxygen behaves as an ideal gas under the conditions for which fugacity is calculated (Braker, W., 1980). It is interesting to also note that the compressibility factors (Z) for 100 atm of methane and 100 atm of argon at 300 K are 0.8493 and 0.9553, respectively. At higher temperatures, the values for Z increase and approach 1.0000, indicating more ideal behavior of methane and argon.

does not seem to be a significant change in pH across the thermal gradient, there does appear to be a significant change in pH with depth. The pH of the Phase II test for the purpose of Eh calculations will be taken as 6.60.

Near the heater, the DO was 0.21 ppm near the surface of the slurry and 0.22 ppm at a depth of approximately 5 cm. The DO near the autoclave wall was 0.16 ppm at similar depths. There does not appear to be a significant change in DO across the thermal gradient. The value of DO for Eh calculations will be taken as 0.2 ppm.

The Eh was calculated to be 0.86 V using the values for pH and fugacity of oxygen of 15.4 Pa (based on a DO of 0.2 ppm).

3.5.4.2.3 Measurement of Phase III Test pH and Dissolved Oxygen and Calculation of Eh

Adjacent to the heater, the pH was 7.10 near the surface of the slurry, 7.05 in the middle, and 7.28 near the bottom, with an average value of 7.14. Adjacent to the wall, the corresponding pH values were 7.03, 7.02 and 7.06, respectively, with an average value of 7.03. There does not appear to be a significant difference in pH as measured across the thermal gradient. The pH measured at 24°C is taken to be 7.10.

Near the heater, the DO was 0.6 ppm near the surface of the slurry and 0.5 ppm at a depth of approximately 5 cm. The DO near the autoclave wall was 0.4 ppm at similar depths. The DO content does not vary significantly across the thermal gradient. The average DO content in the test is taken to be 0.5 ppm.

Using the equation cited above, the Eh (after quenching) was calculated to be 0.83 V.

3.5.4.3 Comparison of pH and DO Measurements and Eh Calculations for All Tests

The pH and DO data for the three tests along with the calculated Eh values after quenching are summarized in Table 3.5.

The unreacted slurry components are basic in contrast to the reacted slurries. The latter are either slightly basic (the non-irradiated Phase III test) or slightly acidic (the irradiated Phase I and Phase II tests). Comparison of the DO data for the reacted (closed system) and unreacted (open system) shows that there is approximately an order of magnitude difference in the DO levels. The addition of basalt in an open system reduced the DO content and it was further reduced in the irradiated and non-irradiated tests. Within the accuracy of the measurements, there is no obvious difference in DO content among the three tests. The calculated Eh values show a more oxidizing environment in the closed reacted systems than in the open unreacted systems, due to lower pH values in the closed reacted system. It would appear that radiation does not significantly affect the Eh of the system under consideration.

Table 3.5. pH and DO as measured for packing material slurry and Eh as calculated for all tests.

	pH ^a	DO (ppm) ^b	Eh (V) ^c
Phase I test slurry	6.9 ± 0.05	0.6 ± 0.5	0.85 ± 0.01
Phase II test slurry	6.6 ± 0.05	0.2 ± 0.5	0.86 ± 0.01
Phase III test slurry	7.1 ± 0.05	0.5 ± 0.5	0.83 ± 0.01
Unreacted bentonite slurry	8.7 ± 0.05	8.3(mean) ± 0.6(2σ)	0.76
Unreacted bentonite + basalt slurry	8.0(mean)	4.3(mean) ± 3(2σ)	0.79
Unreacted groundwater	9.7 ± 0.05	8.4	0.70

^aThese reported pH values represent the average of six readings made with a pH electrode which was calibrated with buffer solutions having pH values of 2, 7, and 10. The accuracy of the pH measurement is 0.05 units.

^bThe reported DO values represent the average of four or more readings. Accuracy is taken to be 0.5 ppm. The DO electrode was calibrated with the oxygen content of water at 25°C, which is 8.4 ppm.

^cThese Eh values are calculated based on the pH and DO measurements of the slurry at 24°C.

3.5.5 Measurement of Ionic Concentrations in Slurry Water

It was considered important to measure the concentrations of ions particularly associated with the corrosion of carbon steel and to determine whether significant differences occurred across a thermal gradient. Therefore, the concentrations of Cl⁻, Fe(total), and SO₄²⁻ in W samples (filtered) and H samples (filtered) were measured as detailed in the experimental section. These concentrations in R samples (unfiltered) were also measured to determine differences in content between filtered and unfiltered samples. The concentration of Si, reported as SiO₂, was also determined but only for the Phase I test samples. Results of these analyses are summarized in Table 3.6 and uncertainties are given wherever they are known. However, it must be emphasized that these are the results of one analysis on single samples after quenching has

occurred¹⁰. Any conclusions derived from these data would have to be supported by valid experiments that have eliminated any effects due to quenching. Therefore, these results should be regarded only as indications of possible differences in ionic concentration across a thermal gradient.

Table 3.6. Comparison of ionic concentrations of reacted Grande Ronde GR-3 groundwater (in ppm).

Sample	Cl ⁻	SO ₄ ²⁻	Fe(Total)	SiO ₂
GR-3 (initial composition)	312	165	0	79
Sample H-I (filtered) ^a	305±6	260±5	ND(<2)	29
Sample W-I (filtered) ^b	321±6	300±6	ND(<2)	39
Sample R-I (unfiltered) ^c	357±7	330±7	500±100	116
Sample H-II (filtered) ^d	263±5	220±4	1.4	---
Sample W-II (filtered) ^b	328±7	272±5	0.9	---
Sample R-II (unfiltered) ^c	--- ^d	330±7	700±140	---
Sample R-II (filtered) ^c	177±3	145±3	2.4	---
Sample H-III (filtered) ^a	388±8	204±4	0	---
Sample W-III (filtered) ^b	429±9	258±5	1.0	---
Sample R-III (unfiltered) ^c	--- ^d	345±7	500±100	---
Sample R-III (filtered) ^c	368±7	200±4	2.5	---

^aSample H is the designation for the supernate of the centrifuged slurry removed from the heater region in the autoclave. Experimental phases are designated by Roman numeral I, II or III.

^bSample W is the designation for the supernate of the centrifuged slurry, removed from the wall region in the autoclave.

^cSample R is the designation for the supernate of the centrifuged slurry removed from random locations in the autoclave.

^dInsufficient sample remained for this analysis to be performed.

¹⁰Evidence exists (RHO-BWI-C-105, 1981) that the state of leachates under hydrothermal conditions is not completely preserved in quench rates of ≈25°C/min. Experiments conducted on the interaction of seawater and basalt (Seyfried, W. E., 1979) at 150°C showed that significant retrograde changes occurred in ionic concentrations and pH measurements after a quenching period of 45 minutes. Approximate cooling time for all tests in the current study was 25 minutes.

3.5.5.1 Measurement of Ionic Concentrations in Phase I Test

The concentrations of Cl^- , SO_4^{2-} and Si were greater near the cooler end (the wall) of the thermal gradient which was at approximately 113°C . The change in concentration of Cl^- across a thermal gradient may be significant. However, the difference in concentration of SO_4^{2-} across the gradient does seem significant, based on these single measurements. It is not known whether the Si concentrations are significant, since the precision is not known and they are an order of magnitude smaller than the Cl^- and SO_4^{2-} concentrations. Comparison of these ionic concentrations with those measured in the synthetic groundwater (see Table 3.6) reveals a decrease of Si and an increase of SO_4^{2-} in the filtrates. If any Fe was present in the filtrates, it was in amounts < 2 ppm, the detection limit of the analysis. Total iron in Sample R-I was determined quantitatively after acidification of the unfiltered liquid with HF. It was also determined that a significant portion of the total Fe was in the ferrous state (Fe^{2+})¹¹.

It appears that the bulk of the Fe and Si content of the unfiltered water is present in the colloidal state. This is also reflected by relatively low concentrations of Si and below detection for Fe in filtered samples. The filterable material appears to be acting as a sink for iron, the source of which can be the basalt, bentonite, or carbon steel.

3.5.5.2 Measurement of Ionic Concentrations in Phase II Test

The only measurements that appeared to change significantly across the temperature differential of $\approx 22^\circ\text{C}$ were the concentrations of SO_4^{2-} and Cl^- . Concentrations were lower at the hotter end of the gradient, i.e. near the heated carbon steel sleeve.

From the results of these single determinations, it appears that less Cl^- and more SO_4^{2-} than are present in the starting groundwater would be found near the carbon steel sleeve. It is clear that, for the Phase I test results, the bulk of the Fe content of the unfiltered supernate is present in the colloidal form. However, very small amounts of iron remain in the filtered supernates.

3.5.5.3 Measurement of Ionic Concentrations in Phase III Test

As was the case in the previous tests, concentrations of Cl^- and SO_4^{2-} were significantly lower at the hotter end of the gradient. Again, the bulk of the iron is present in colloidal material.

¹¹The Fe^{2+} content was estimated using the phenanthroline standard method. Three molecules of 1,10-phenanthroline chelate each atom of ferrous ion to form an orange-red complex. The intensity of the color is dependent on the amount of ferrous ion present. A visual comparison with color standards was made to determine content of ferrous ion. Another portion of Sample R was treated to convert any ferric ion to ferrous and another phenanthroline complexation determination was made. The color of the reduced solution was very similar to that of the first determination, indicating that most of the iron was in the ferrous state in the original sample.

3.5.5.4 Comparison of Measured Ionic Concentrations For All Tests

The results of the water analyses for Fe(total), Cl^- , and SO_4^{2-} from the three tests were summarized in Table 3.6. There were different thermal differentials established across the packing materials in each test. For Phases I, II and III, these were, respectively, 1.0, 0.6 and $2^\circ\text{C}/\text{mm}$. Results from the three tests, therefore, cannot be quantitatively compared. However, qualitative differences among ionic concentrations are noted for the three tests. It must be emphasized that these results are from the analyses of single specimens from individual tests. Therefore, in the absence of statistical information, a difference is deemed significant if one measured value differs from another by a quantity that exceeds the experimental error. Experimental precision is indicated in the table where it is known. The results for the chloride and sulfate concentrations are based on IC measurements and are estimated to vary by $\pm 2\%$. On this basis the following conclusions can be drawn by comparing and contrasting the ionic concentrations measured in the three tests after quenching:

- Compared to unreacted groundwater, the chloride content of filtered reacted water is usually decreased in hotter regions of the packing material and increased in cooler regions. The exception occurred in the Phase III control test where increases in chloride level were evident for both the hotter and cooler regions. Nevertheless, there was still the same general behavior in terms of higher chloride in the cooler regions.
- Compared to unreacted groundwater, the sulfate content of filtered reacted water is always increased. The increase is larger in the cooler regions of the packing material.
- For unfiltered reacted groundwater the concentrations of chloride, sulfate, and especially SiO_2 and total iron, are significantly increased. This shows that the colloidal particles present in the groundwater contain relatively high concentrations of these three constituents.
- In terms of the effect of thermal gradients on the concentration differences across the packing it was found that chloride and sulfate differences were largest for the Phase II test, which had the smallest thermal gradient. These concentration trends were very similar for Phase I and Phase III even though the temperature differentials across the packing were quite different (viz. 37 and 73°C , respectively). It is, therefore, unclear what factors controlled the changes in concentration along the thermal gradient.

Similar increases in chloride concentrations were reported by Wood (RHO-BW-SA-219P, 1983), who studied changes in ionic concentrations with time for closed non-irradiated systems containing Umtanum basalt (free of fines) or Baroid National Western¹² bentonite and GR-3 synthetic groundwater at 300°C

¹²The Baroid bentonite contained 85% montmorillonite, 5% quartz, 5% feldspar, 2% illite, and 1% calcite and gypsum.

and 29.9 MPa for one month. However, in Wood's work, the sulfate concentration was lower in the reacted bentonite/groundwater system and was unchanged in the reacted basalt/groundwater system. This would seem to indicate that for these particular systems basalt and bentonite are sources of chloride and that the bentonite can act as a sink for sulfate. An additional experiment containing bentonite/basalt/groundwater reacted under the same hydrothermal conditions for three months showed that sulfate concentration was slightly increased at 28 days and was significantly decreased at the 56-day sampling. In the same test, chloride concentration increased and reached a maximum between 28 and 56 days.

Also, in Wood's study it was found that the iron concentrations in reacted groundwater were highest in the bentonite/water system (up to 0.14 ppm) and similar for basalt/water and basalt/bentonite/water systems (up to 0.08 ppm). This indicates that bentonite is a prime source of iron in the water. In another study, carried out at a 200°C test temperature, a basalt/water system gave a reacted water containing 35.4 ppm of iron after 718 hours (RHO-BW-ST-21P, 1982). The trend to higher total iron concentrations, as the test temperature is decreased from 300 to 200°C, is evident from Wood's work. In the BNL study, however, much of the iron originated from the carbon steel present in the system and iron was present in colloidal form which was not reported as present in Wood's work.

3.5.6 SEM-EDX Analysis of Colloidal Material

A part of R sample from each of the tests was passed through a 0.025- μ m membrane filter to collect colloidal material for analysis. The latter was removed as a film from the filter when it dried. They were mounted with epoxy on a graphite holder and examined by SEM-EDX (17-kV electrons). It should be noted that comparatively less colloidal material was extracted from the Phase III (non-irradiated) test.

3.5.6.1 SEM-EDX Analysis of Colloidal Material Removed From Phase I Test Solution

A micrograph of the dried colloidal material film from the Phase I test is given in Figure 3.9. A rod-shaped phase and a small rectangular particle are seen to be embedded in the colloidal material. SEM-EDX analyses given in Figures 3.10 through 3.12 show that the colloidal material is rich in Si, Fe, Ca and Al with smaller quantities of Mg and K. The rod-shaped phase also contains Si with significant amounts of Mg, Ca, Ba, Zn K and Al present. In the case of the small particle, the dominant element detected is Ca with a minor proportion of Si. The colloidal material substrate in Figure 3.9 has an elemental composition consistent with that for clay particles, as expected (Table 3.1). The small calcium-rich phase is possibly calcite which has been found in bentonite by other workers (ANL-83-19, 1983). At the present time, the identification of the rod-shaped phase is unknown. Zinc has been observed in small crystals found in bentonite (ANL-83-19, 1983) but this phase could have also originated from the basalt component of the packing material. More work is needed to characterize the colloidal material obtained from the current studies.

An interesting effect was observed as the colloidal material was bombarded with 17-kV electrons in the SEM as shown in Figure 3.13. Small protuberances developed in the sample film which could have been caused by vaporization of residual moisture.

3.5.6.2 SEM-EDX Analysis of Colloidal Material Removed From Phase II Test Solution

Micrographs of the dried colloidal material recovered from the Phase II test heater and wall regions are shown in Figures 3.14 and 3.15. Both of these samples were analyzed by EDX and were found to be high in Si and Al along with some Fe and Ca. This is similar to the composition determined by EDX for the Phase I test material, except that no K or Mg was detected (see Figure 3.10).

However, several differences are evident upon comparison of the two micrographs taken at the same magnification. The material from the heater region is much coarser in texture. This may be due to different thicknesses of material deposited on the filter. Additionally, there is a dendritic structure lying on the substrate in the material taken from the wall region (see Figure 3.15). The structure was analyzed by EDX and found to contain large amounts of Ca and S. See Figure 3.16 for a micrograph taken at a lower magnification (300X) of the material recovered from the heater region in the Phase II test. Analysis by EDX of the nodule present shows a high content of Ca, S and Si along with some Al.

3.5.6.3 SEM-EDX Analysis of Colloidal Material Recovered from the Phase III Test Solution

Micrographs of the colloidal material recovered from the heater and wall regions of the Phase III control test are shown in Figures 3.17 and 3.18. Corresponding EDX analyses for these materials are given in Figures 3.19 and 3.20. Both have essentially the same composition: high Si and Al content with moderate Fe and Ca amounts along with some trace elements. No differences in composition were noted for localized variations in substrate texture. Additionally, the presence of oxygen was confirmed in the sample taken from the wall region by use of transmission electron microscopy (TEM)-EDX (see Figure 3.21). The dried sample taken from the heater region was too thick to permit an analysis by TEM-EDX.

3.5.6.4 Comparison of SEM-EDX Analyses of Colloidal Materials

A comparison of the information gained by use of SEM-EDX techniques in the three test systems yields the following conclusions:

- The bulk composition of all colloidal materials, from both the wall and heater regions, is essentially the same. There is a high Si and Al content, some Ca and Al, along with trace elements. Oxygen is believed to be present in all samples but was only confirmed by TEM-EDX in the colloidal material taken from the wall region of the Phase III test.



Figure 3.9. Micrograph of colloidal material recovered from the Phase I test (800X).

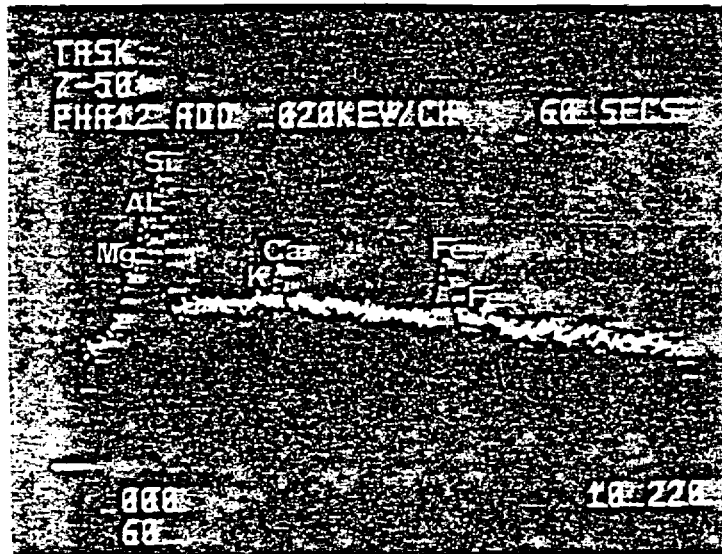


Figure 3.10. EDX analysis of colloidal material recovered from the Phase I test.

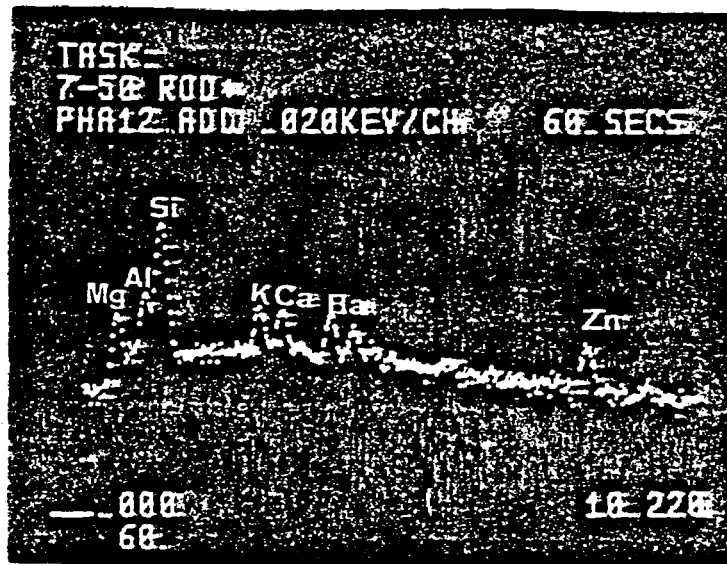


Figure 3.11. EDX analysis of rod in colloidal material recovered from the Phase I test.

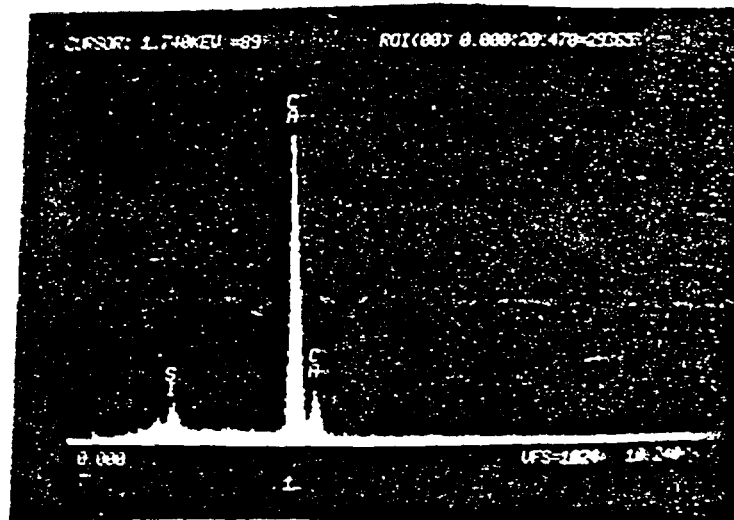


Figure 3.12. EDX analysis of crystal in colloidal material recovered from the Phase I test.



Figure 3.13. Micrograph of protuberances appearing in colloidal material recovered from the Phase I test after bombardment with 17-kV electrons (1000X).

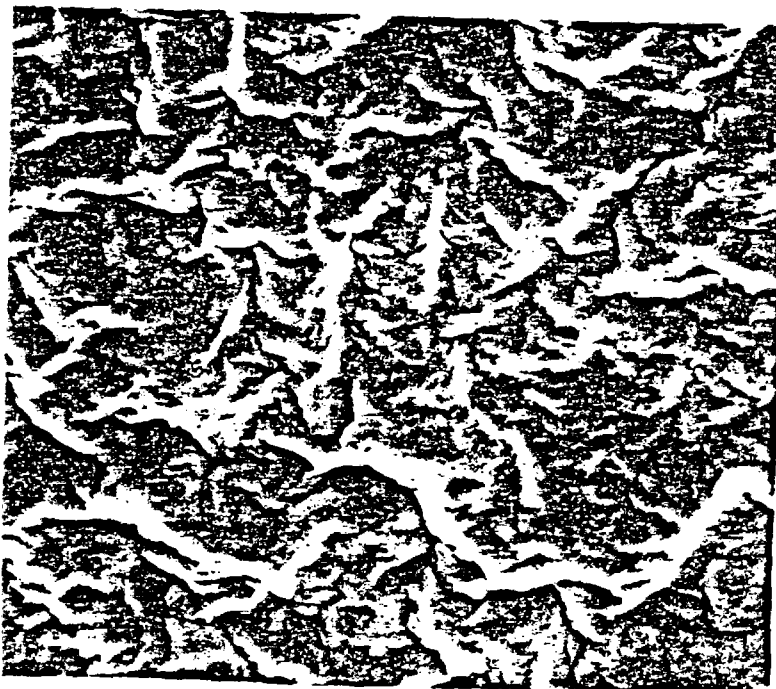


Figure 3.14. Micrograph of colloidal material recovered from the Phase II test heater region (1000X).

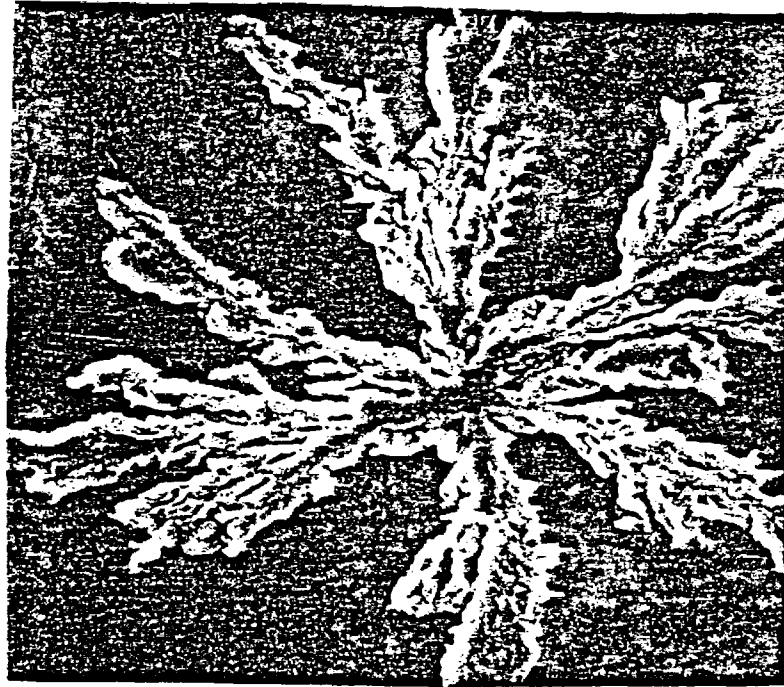


Figure 3.15. Micrograph of colloidal material recovered from the Phase II test wall region (1000X).

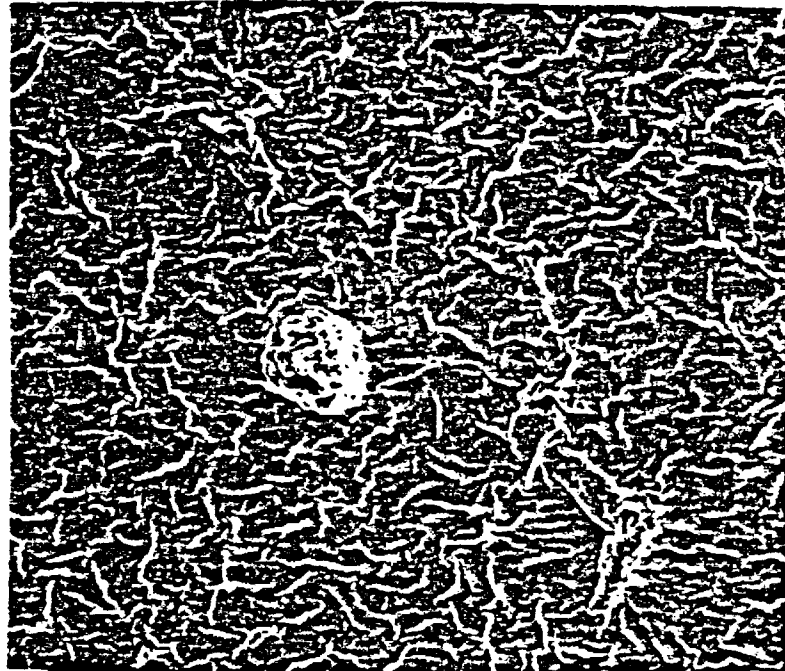


Figure 3.16. Micrograph of colloidal material recovered from the Phase II test heater region (300X).

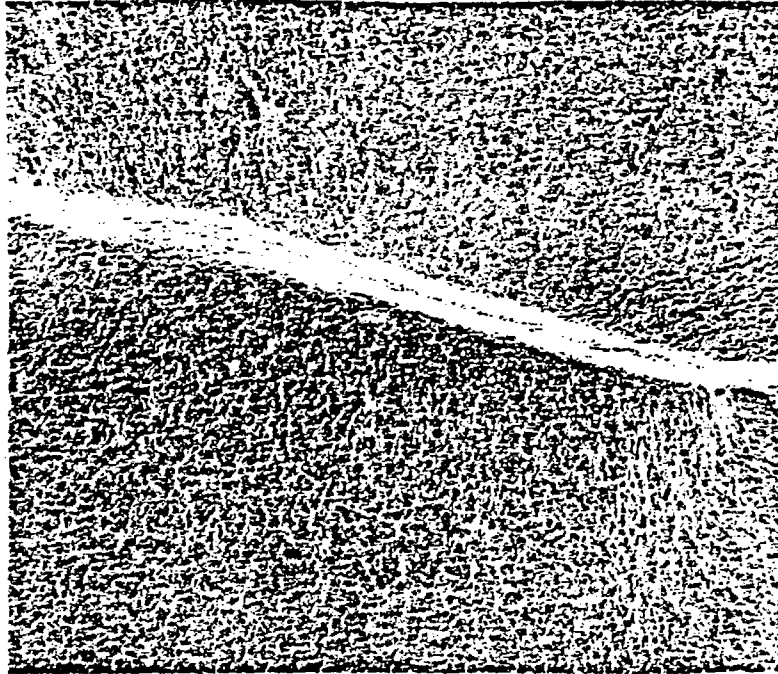


Figure 3.17. Micrograph of the colloidal material recovered from the Phase III test heater region (100X).

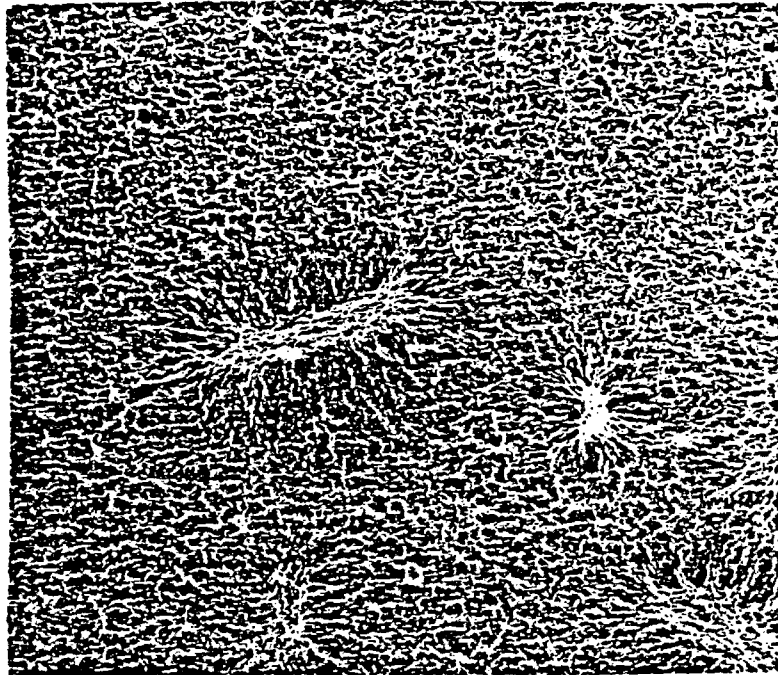


Figure 3.18. Micrograph of the colloidal material recovered from the Phase III test wall region (100X).

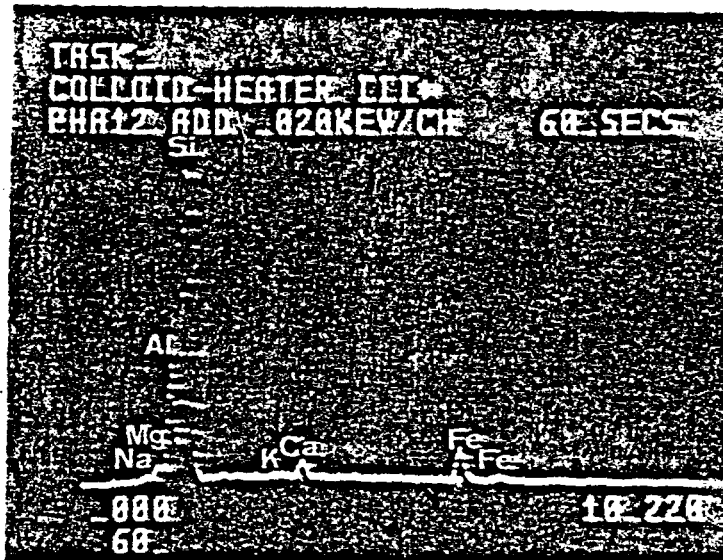


Figure 3.19. EDX analysis of colloidal material recovered from the Phase III test heater region.

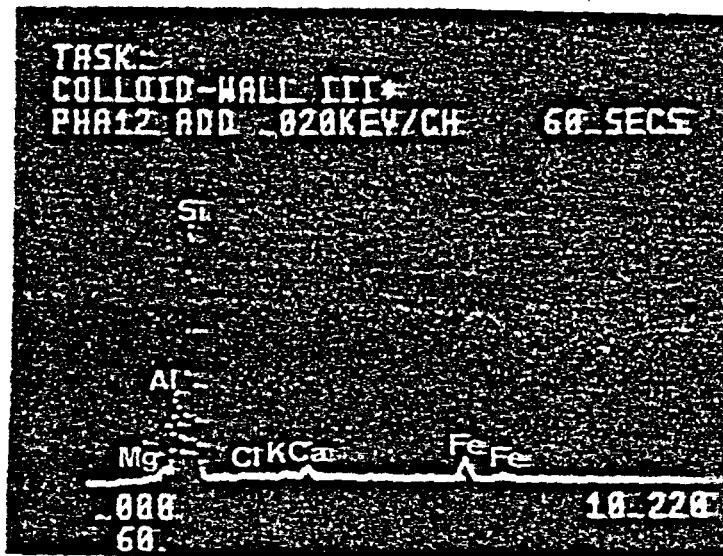


Figure 3.20. EDX analysis of colloidal material recovered from the Phase III test wall region. The presence of oxygen was confirmed by EDX, see Figure 21.

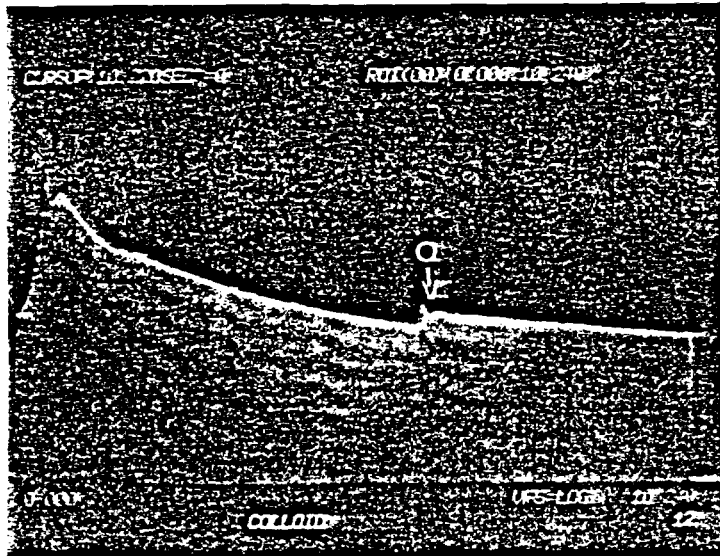


Figure 3.21. EDX(TEM) analysis of colloidal material recovered from the Phase III test wall region.



Figure 3.22. Micrograph of unreacted bentonite clay (100X).

- A variety of embedded and deposited phases that differ in shape and composition can be seen in the micrographs of the colloidal material recovered from the Phase I and Phase II tests. None of these was seen in the colloidal material recovered from the Phase III test. This indicates that radiation plays some role in the formation of these phases.

3.5.7 Analysis of Unreacted Bentonite and Reacted Bentonite Portion of Slurry

3.5.7.1 Analysis of Bentonite

A micrograph of unreacted SWy-1 bentonite is given in Figure 3.22. The semi-quantitative EDX analysis shows that the following elements were present at two locations in the sample: Si ($\approx 75\%$), Al ($\approx 15\%$), Fe ($\approx 6\%$), 4% (Mg, K, Ca, V, Na, Cu, Zn, Ti).

Reacted bentonite portions of the packing material were centrifuged, and the solid placed on a glass slide and allowed to dry. There were no basalt pellets in any of these specimens. They were examined with an X-ray diffractometer in the range $2\theta = 3-37^\circ$ using Cu K_α radiation and the resulting patterns are shown in Figures 3.23, 3.24, 3.25. The 2θ values were converted into d-spacings using standard tables (Rose, A. J., 1957). A comparison is given in Table 3.7. It is clear that differences exist in the d-spacings of the Phase I, Phase II and Phase III test samples. For illustrative purposes, the materials remaining after centrifugation and removal of the supernatant liquid in the Phase I test are shown in Figure 3.26. This appearance is similar to those for materials from the Phase II and Phase III tests. Samples from near the heater (Tubes A and D in Figure 3.26) were a combination of orange, white and tan in color. Material samples near the wall (Tubes B and E in Figure 3.26) was mostly tan and white in color. A tube of unreacted slurry (Tube C in Figure 3.26) was centrifuged for comparison purposes and was tan in color. See Section 3.5.8.1 for the results of solids analysis performed in the study by Wood (RHO-BW-SA-219P, 1983).

3.5.7.2 Analysis of Montmorillonite Portion of Bentonite

The major peaks attributable to the montmorillonite in the control samples appear in the range $2\theta = 7.1$ ($d = 12.4 \text{ \AA}$) to $2\theta = 7.8$ ($d = 11.3 \text{ \AA}$). These single peaks are shown for Phase I, Phase II and Phase III test samples in Figures 3.27b to 3.29b, respectively. These peaks shift in the reacted, glycolated, and heat-treated slurry samples.

3.5.7.2.1 Montmorillonite XRD Phase I Test

The two reacted samples in the Phase I test gave very similar results but the strongest peak obtained was significantly shifted compared to the equivalent peak for the control, which may indicate that the incorporation of a large cation in the interlayer sites occurred and that the distance between successive layers of the smectite (i.e. basal spacing) increased due to swelling. There is some illite present in the samples before and after reaction, as evidenced by the peak at $\approx 2\theta = 9^\circ$ ($d = 9.9 \text{ \AA}$). See the last three columns of Table 3.8 for a tabulation of these data.

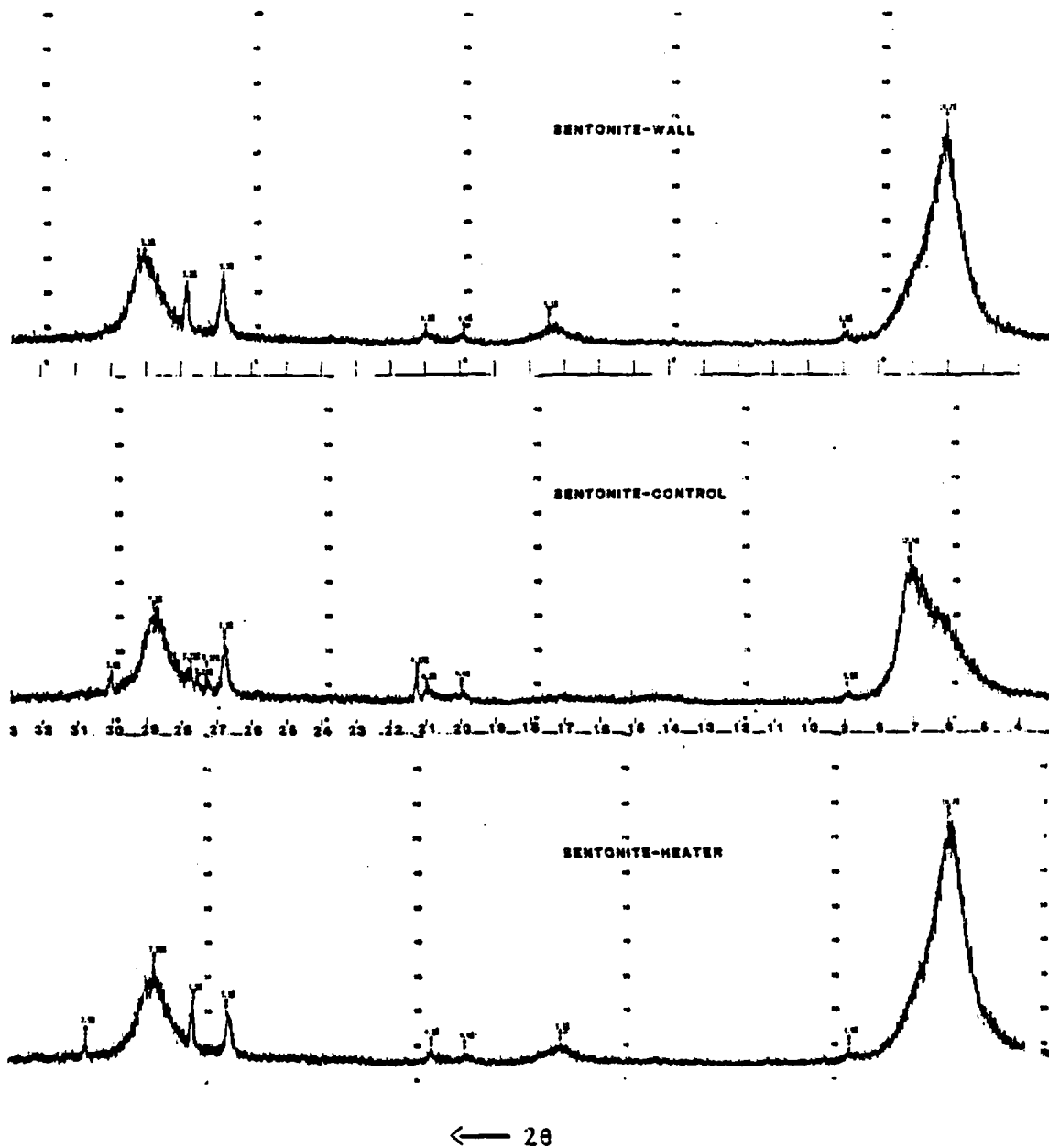
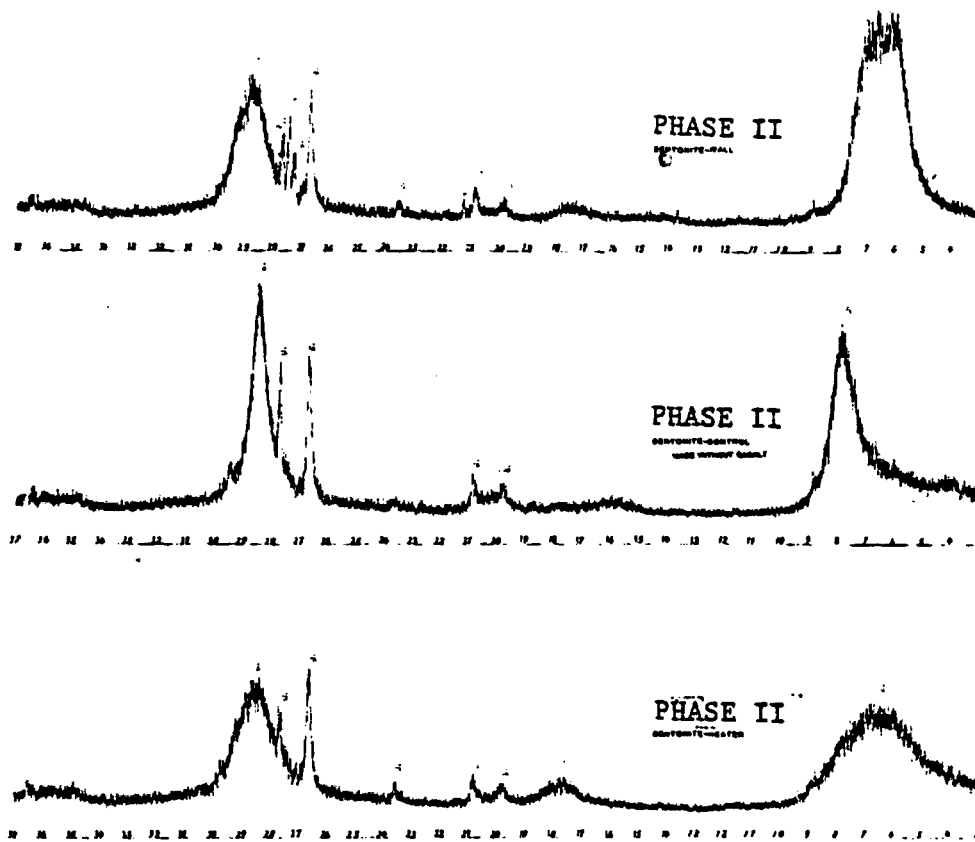
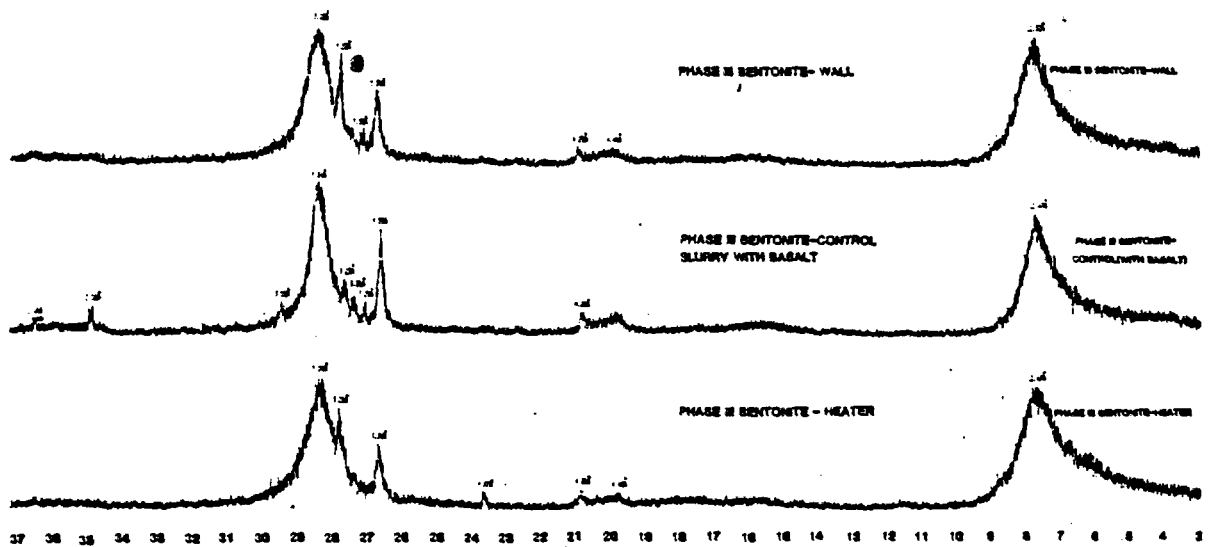


Figure 3.23. Comparison of X-ray diffraction patterns of reacted and unreacted bentonite present in the Phase I centrifuged packing material slurry samples prepared as oriented clay mounts by evaporation of slurry on glass slides. [Range of scan: $2\theta = 3-37^\circ$ ($d = 2.43-29.4 \text{ \AA}$).] (Control sample consisted of a slurry of bentonite and basalt with synthetic groundwater.)



← 2θ

Figure 3.24. Comparison of X-ray diffraction patterns of reacted and unreacted bentonite present in the Phase II test centrifuged packing material slurry samples prepared as oriented clay mounts by evaporation of slurry on glass slides. [Range of scan: $2\theta = 3-37^\circ$ ($d = 2.43-2.94 \text{ \AA}$)]. (Control sample consisted of a slurry of bentonite with synthetic groundwater.)



← 2θ

Figure 3.25. Comparison of X-ray diffraction patterns of reacted and unreacted bentonite present in the Phase III test centrifuged packing material slurry samples prepared as oriented clay mounts by evaporation of slurry on glass slides. [Range of scan: $2\theta = 3-37^\circ$ ($d = 2.43-29.4 \text{ \AA}$)]. (Control sample consisted of a slurry of bentonite and basalt with synthetic groundwater.)

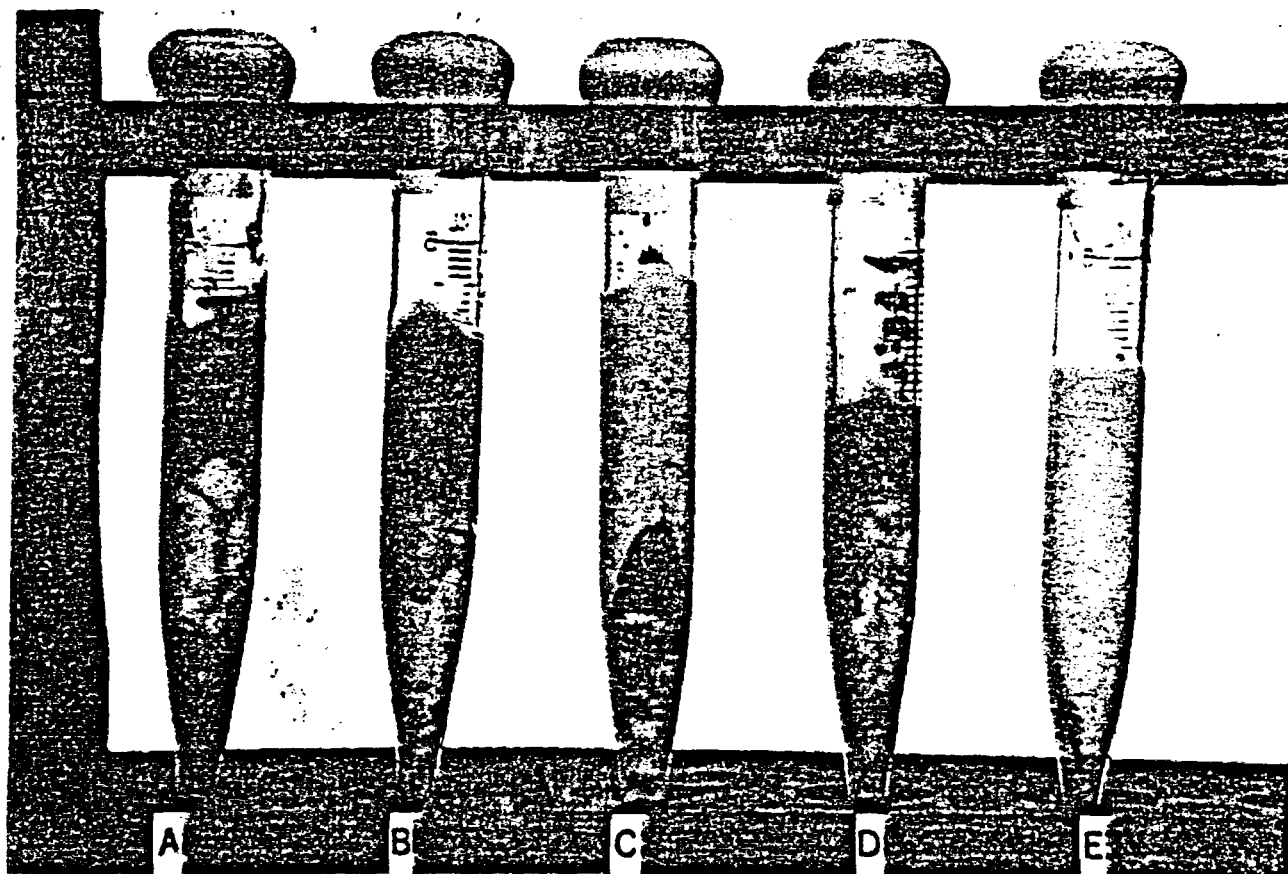


Figure 3.26. Appearance of Phase I centrifuged packing material slurries before and after reaction. (Tubes are shown full-scale. Black material in bottom of tubes is basalt fines.)
(A) Sampled near heater
(B) Sampled near autoclave wall
(C) Control unreacted
(D) Sampled near heater
(E) Sampled near autoclave wall.

Table 3.7. Comparison of (00 l) d-spacings based on X-ray diffractometer studies of reacted and unreacted bentonite portions of centrifuged packing material slurries prepared as oriented clay mounts by evaporation of centrifuged slurry on glass slides. [Intensities not specified. Range of scan: $2\theta = 3-37^\circ$ ($d = 2.43-29.4 \text{ \AA}$).]

d (Å) Wall Sample	d (Å) Heater Sample	d (Å) Control Sample ^a
<u>Phase I Test</u>		
14.7	14.7	12.4
—	9.9	9.9
5.1	5.1	—
4.4	4.4	4.4
4.2	4.2	4.2
—	—	4.17
3.3	3.3	3.3
—	—	3.26
—	—	3.23
3.2	3.2	3.22
3.1	3.09	3.1
—	—	3.0
<u>Phase II Test</u>		
13.6	13.4	11.3
6.50	—	—
—	—	5.53
5.09	5.01	—
4.47	4.48	4.49
4.27	4.27	4.25
3.77	3.77	3.77
3.34	3.35	3.34
3.28	—	—
3.25	—	—
3.23	3.22	3.22
3.11	3.13	3.14
<u>Phase III Test</u>		
11.3	11.5	11.5
4.44	4.48	4.49
4.25	4.26	4.28
—	3.77	—
3.34	3.34	3.35
3.30	—	3.29
—	—	3.26
3.22	3.21	3.23
3.15	3.14	3.14
—	—	3.03
—	—	2.58
—	—	2.46

^aControl samples for each test were prepared separately and contained bentonite/basalt in Phase I and III tests but contained only bentonite/groundwater for the Phase II test.

Table 3.8. Comparison of (001) d-spacings based on X-ray diffractometer studies of Phase I test reacted and unreacted montmorillonite, prepared as oriented clay mounts by evaporation of centrifuged packing material slurry on glass slides; treatment by glycolation at 60°C, followed by heating to 300°C for one hour. [Intensities not specified. Range of scan: $2\theta = 3-9.5^\circ$ ($d = 9.30-29.4 \text{ \AA}$).]

d (Å)								
Heater	Wall	Control	Heater	Wall	Control	Heater	Wall	Control
Samples Glycolated			Samples Glycolated and Heat Treated			Samples Untreated		
17.0	16.0	16.6	15.2*	15.2*	15.5*	14.7	14.7	12.4
9.9	9.7	9.9	—	9.9	—	9.9	9.8	9.9

*Peak intensity is drastically reduced when compared to the peak intensities in the diffraction patterns of the untreated and glycolated samples. This decrease in intensity is due to the collapse of the smectite structure.

The slides, coated with centrifuged reacted and unreacted (control) packing material slurries, were subsequently given standard glycolation¹³ and heat treatments to study the changes in the (001) reflections of the montmorillonite clay (Carroll, D., 1970). The first treatment consists of glycolation. See the first three columns of Table 3.8 for tabulation of the data on the glycolated samples and Figures 3.27d, e, and f for the diffraction patterns of the glycolated samples. An expandable clay such as montmorillonite will characteristically swell upon glycolation due to the increase in basal spacing between layers because of the incorporation of organic molecules in the interlayer sites and this will be evidenced by a shift in the d-spacing at $\approx 12-15 \text{ \AA}$ to $\approx 16-18 \text{ \AA}$. Compare Figures 3.27a and d; Figures 3.27b and e; Figures 3.27c and f. The sample taken from the heater region had the largest d-spacing value, followed by that for the control sample, followed by that for the sample taken from the wall region.

¹³Samples are glycolated by placing the coated slides in a desiccator, which contains ethylene glycol in the well normally filled with desiccant, and by heating in an oven at 60°C for at least an hour.

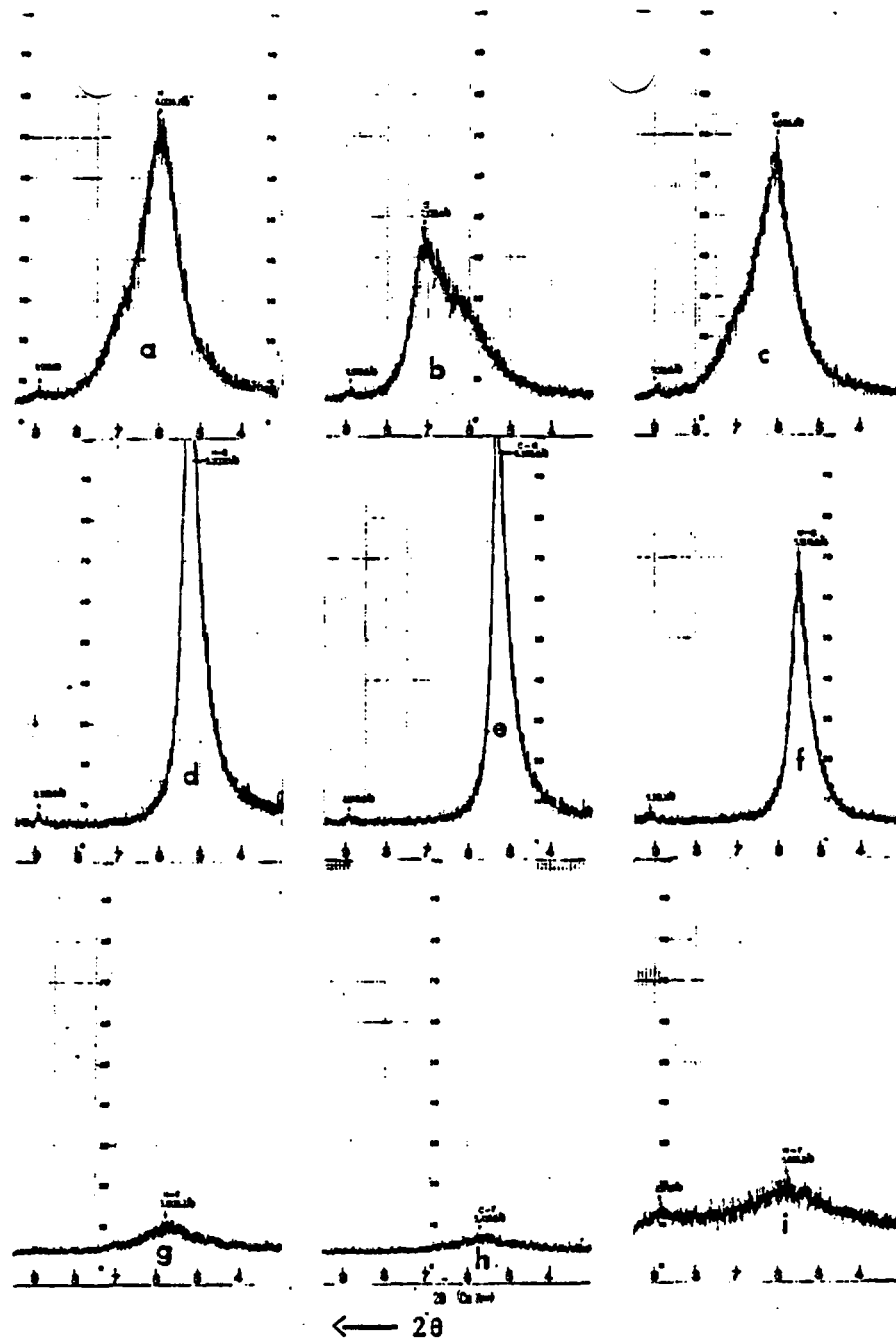
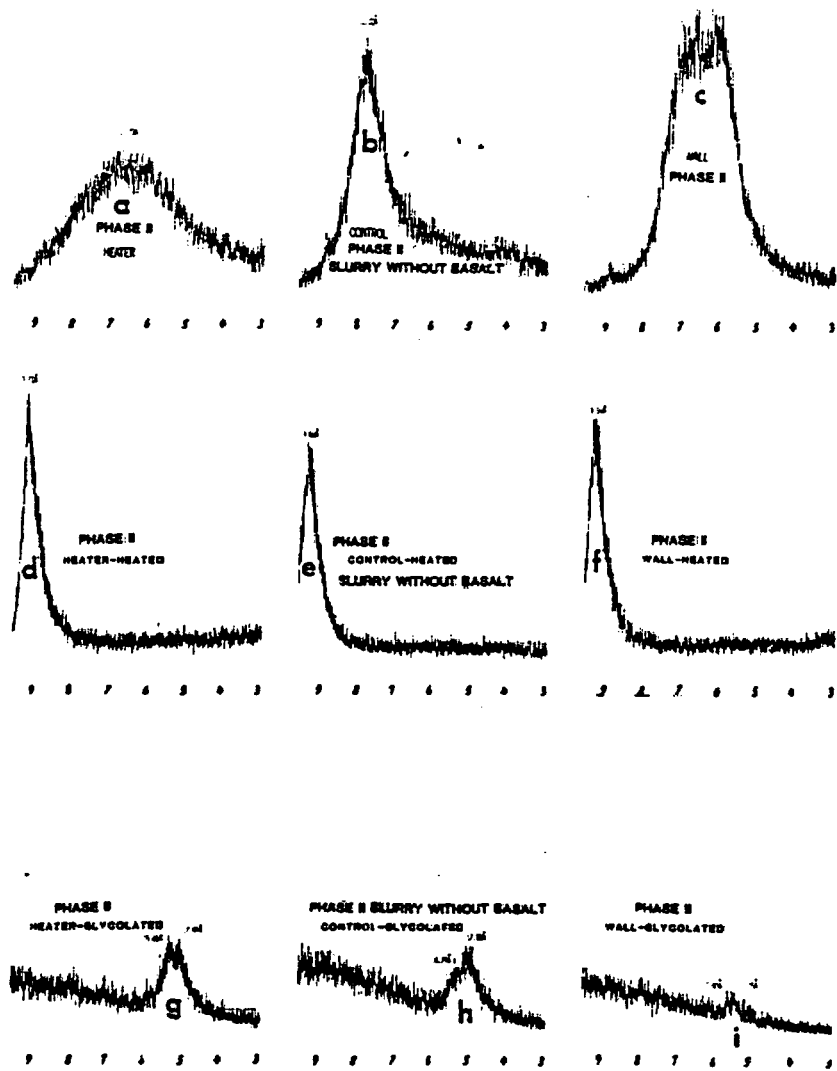


Figure 3.27. Comparison of X-ray diffraction patterns of Phase I test reacted and unreacted montmorillonite present in the centrifuged packing material slurry samples prepared as oriented clay mounts by evaporation of slurry on glass slides; treatment by glycolation, followed by heating to 300°C for one hour. [Range of scan: $2\theta = 3.9-5^\circ$ ($d = 9.30-29.4 \text{ \AA}$)].

- (a) Untreated slurry sampled from heater region
- (b) Untreated slurry (control)
- (c) Untreated slurry sampled from wall region
- (d) Glycolated (60°C) slurry sampled from heater region
- (e) Glycolated (60°C) slurry (control)
- (f) Glycolated (60°C) slurry sampled from wall region
- (g) Heat-treated (300°C) slurry sampled from heater region
- (h) Heat-treated (300°C) slurry (control)
- (i) Heat-treated (300°C) slurry sampled from wall region.



← 2θ

Figure 3.28. Comparison of X-ray diffraction patterns of Phase II test reacted and unreacted montmorillonite present in the centrifuged packing material slurry samples prepared as oriented clay mounts by evaporation of slurry on glass slides; heat-treated at 300°C for 18 hours, followed by glycolation at 60°C. [Range of scan: $2\theta = 3-9.5^\circ$ ($d = 9.30-29.4 \text{ \AA}$)].

- (a) Untreated slurry sampled from heater region
- (b) Untreated slurry (control)
- (c) Untreated slurry sampled from wall region
- (d) Heat-treated (300°C at 18 h) slurry sampled from heater region
- (e) Heat-treated (300°C at 18 h) slurry (control)
- (f) Heat-treated (300°C at 18 h) slurry sampled from wall region
- (g) Glycolated (60°C) slurry sampled from heater region
- (h) Glycolated (60°C) slurry (control)
- (i) Glycolated (60°C) slurry sampled from wall region.

The second standard treatment for a smectite consists of heating the glycolated samples to 300°C for at least one hour. The interlayer water is removed by this procedure and, characteristically the original (001) reflection collapses and is replaced by one in the ≈9-10 Å region. This is evident upon comparison of Figures 3.27a and g; Figures 3.27b and h; and Figures 3.27c and i. See Columns four through six of Table 3.8. Although these heat-treated samples were not rehydrated to see if the (001) reflection due to swelling would reappear, it is obvious that after heating to 300°C, the expandability has been drastically reduced. The reflection at ≈9-10 Å attributable to the formation of a non-expandable clay was not observed. Additional heating at 300°C may be needed to see this effect. With the loss of interlayer water, montmorillonite may be transformed into hydromica (illite) if sufficient potassium is available, or into chlorite, if sufficient magnesium is present. The main effect of pressure and temperature on a hydrous mineral will be dehydration. Reviews of the literature concerning the hydrothermal stability of the packing material can be found in NUREG/CR-2482, Vols. 3 and 5 (1983) and NUREG/CR-3091, Vols. 1 and 2 (1983).

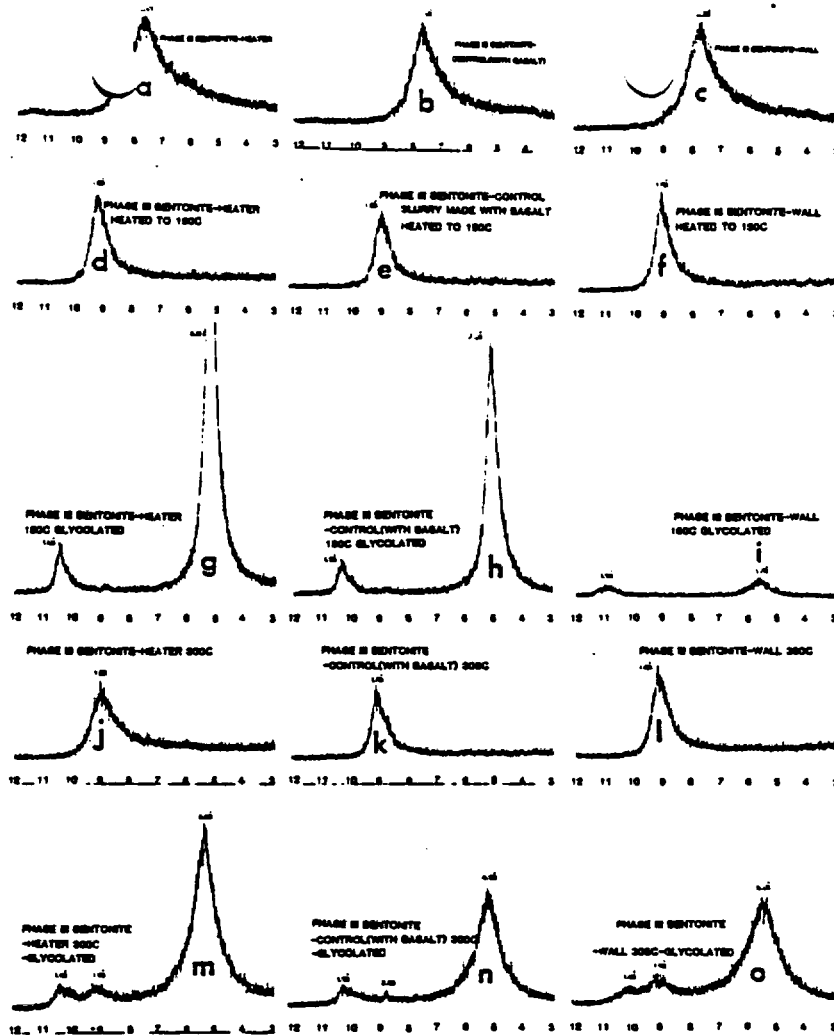
3.5.7.2.2 Montmorillonite XRD Phase II Test

Similar treatments were given to the Phase II test samples, except that the order of glycolation and heating was reversed. This was done in order to see to what extent swelling would occur after heating. See Figures 3.28a to i. The shifts in d-spacings evident in the diffraction patterns after these treatments are summarized in Table 3.9.

Table 3.9. Comparison of (001) d-spacings based on X-ray diffractometer studies of Phase II reacted and unreacted montmorillonite, prepared as oriented clay mounts by evaporation of centrifuged packing material slurry on glass slides; treatment by heating to 300°C for 18 hours, followed by glycolation at 60°C. [Intensities not specified. Range of scan: $2\theta = 3-9.5^\circ$ ($d = 9.30-29.4 \text{ \AA}$).]

d (Å)								
Heater	Wall	Control	Heater	Wall	Control	Heater	Wall	Control
Samples Heat-Treated			Samples Heat-Treated and Glycolated			Samples Untreated		
9.7	9.5	9.60	17.7*	16.0*	17.8*	13.8	13.6	11.3
			16.7*	15.6*	16.8*			

*Peak intensity is drastically reduced when compared to the peak intensities in the diffraction patterns for the untreated and heated samples.



← 20

Figure 3.29. Comparison of X-ray diffraction patterns of Phase III test reacted and unreacted montmorillonite present in the centrifuged packing material slurry samples prepared as oriented clay mounts by evaporation of slurry on glass slides; heat-treated at 150°C, followed by glycolation at 60°C, followed by heat-treatment at 300°C, followed by glycolation at 60°C. [Range of scan: $2\theta = 3-9.5^\circ$ ($d = 9.30-29.4 \text{ \AA}$)].

- (a) Untreated slurry sampled from heater region
- (b) Untreated slurry (control)
- (c) Untreated slurry sampled from wall region
- (d) Heat-treated (150°C) slurry sampled from heater region
- (e) Heat-treated (150°C) slurry (control)
- (f) Heat-treated (150°C) slurry sampled from wall region
- (g) Glycolated (60°C) slurry sampled from heater region after heating to 150°C
- (h) Glycolated (60°C) slurry (control) after heating to 150°C
- (i) Glycolated (60°C) slurry sampled from wall region after heating to 150°C
- (j) Heat-treated (300°C) slurry sampled from heater region
- (k) Heat-treated (300°C) slurry (control)
- (l) Heat-treated (300°C) slurry sampled from wall region
- (m) Glycolated (60°C) slurry sampled from heater region after heating to 300°C
- (n) Glycolated (60°C) slurry (control) after heating to 300°C
- (o) Glycolated (60°C) slurry sampled from wall region after heating to 300°C

Swelling of the montmorillonite occurred in the Phase II test as evidenced by the shift in d-spacing from 11.3 Å to 13.8 Å (in the sample taken from the heater region) and to 13.6 Å (in the sample taken from the wall region). This is shown in Figures 3.28a to c. Upon heating of the samples to 300°C, the d-spacings of the major montmorillonite peak shifted to a range of 9.5-9.7 Å, indicative of dehydration and collapse of the smectite structure. See Figures 3.28d to f for the XRD patterns of the heated samples. These samples were subsequently glycolated and some swelling did occur as can be seen in Figures 3.28g to i by the shift in the d-spacings to a range of 15.6-17.8 Å. However, the intensity of the peaks is drastically reduced when compared to the intensity of the peaks of the hydrated montmorillonite (Figures 3.28a to c). This seems to indicate that dehydration may not be reversible.

3.5.7.2.3 Montmorillonite XRD Phase III Test

The X-ray diffraction patterns of the samples from the Phase III unirradiated test are shown in Figures 3.29a to c. Various treatments were applied and X-ray diffraction studies subsequently made to determine the effects of the treatments on the expandability of the montmorillonite. The d-spacings for each of the patterns are given in Table 3.10. There was a slight increase in the basal spacing of the untreated reacted samples when compared to the untreated unreacted sample. See Figures 3.29a to c. After heating the samples to 150°C for 12 hours, dehydration with the accompanying decrease in basal spacing occurred, as shown in Figures 3.29d to f. Up to this point, all XRD patterns for the Phase III test samples were very similar to each other. The samples were subsequently glycolated at 60°C to determine differences in expandability. The XRD patterns of the glycolated Phase III test control sample and the Phase III test sample taken from the heater region shown in Figures 3.29g and h show a large increase in the montmorillonite basal spacing, along with the appearance of a new peak. Intensities of these two peaks are similar and are much greater than the corresponding intensities in the XRD patterns of the untreated samples. The XRD pattern of the glycolated heat treated sample taken from the wall region of the Phase III test system shows less expandability of the montmorillonite and decreased intensities of the montmorillonite major peak and of the newly formed one. These samples were then heated to 300°C for several hours and XRD patterns were obtained. Significant and similar decreases in basal spacings are evident in all three samples, as shown in Figures 3.29j to l. Samples were then subjected to glycolation at 60°C. Similar expansion of the basal spacing occurred in all samples, indicating that swelling of the montmorillonite was still occurring and that dehydration was apparently reversible in the case of these samples and their successive treatments.

Table 3.10. Comparison of (001) d-spacings based on X-ray diffractometer studies of Phase III reacted and unreacted montmorillonite, prepared as oriented clay mounts by evaporation of centrifuged packing material slurry on glass slides; heat-treatment at 150°C, followed by glycolation at 60°C, followed by heat-treatment at 300°C, followed by glycolation at 60°C. [Intensities not specified. Range of scan: $2\theta = 3-9.5^\circ$ ($d = 9.30-29.4 \text{ \AA}$).]

	d(Å)		
	Heater	Wall	Control
Untreated	11.5	11.3	11.5
Heat-treated (150°C)	9.6	9.7	9.8
Glycolated (60°C)	17.0	15.8*	17.1
	8.6	8.0	8.6
Heat-treated (300°C)	9.8	9.7	9.7
Glycolated (60°C)	16.5	16.2	17.0
	9.5	9.7	10.1
	8.5	8.7	8.6

*Peak intensity is drastically reduced when compared to the peak intensities in the diffraction pattern of the untreated sample.

3.5.7.2.4 Comparison of Montmorillonite XRD Studies For All Tests

A comparison of the d-spacings obtained for untreated and treated montmorillonite samples from the three tests yielded the following conclusions:

- The basal spacings in the samples taken from the wall and heater regions of the irradiated systems are increased in comparison to an unreacted control sample. This suggests that irradiation may enhance expandability.
- The shape and intensity of the major montmorillonite peak in the Phase II test samples differs significantly for the heater sample and the wall sample. This is not true for the corresponding samples of the Phase I and Phase II tests.

- Expandability may be affected by heat treatments. After heating the samples from the Phase II tests for 18 hours at 300°C, and subsequent glycolation, it was apparent that the major montmorillonite peak had almost disappeared. This did not occur in the case of the Phase III test samples after heating at 300°C for several hours. But it should also be noted that other peaks appeared in the Phase III test XRD patterns, indicating that other minerals had been produced. This is also supported by the XRD patterns obtained over the entire range. Qualitatively it can be seen by comparison of the overall patterns that differences exist between the reacted and unreacted clays in each test and in the three different test systems.

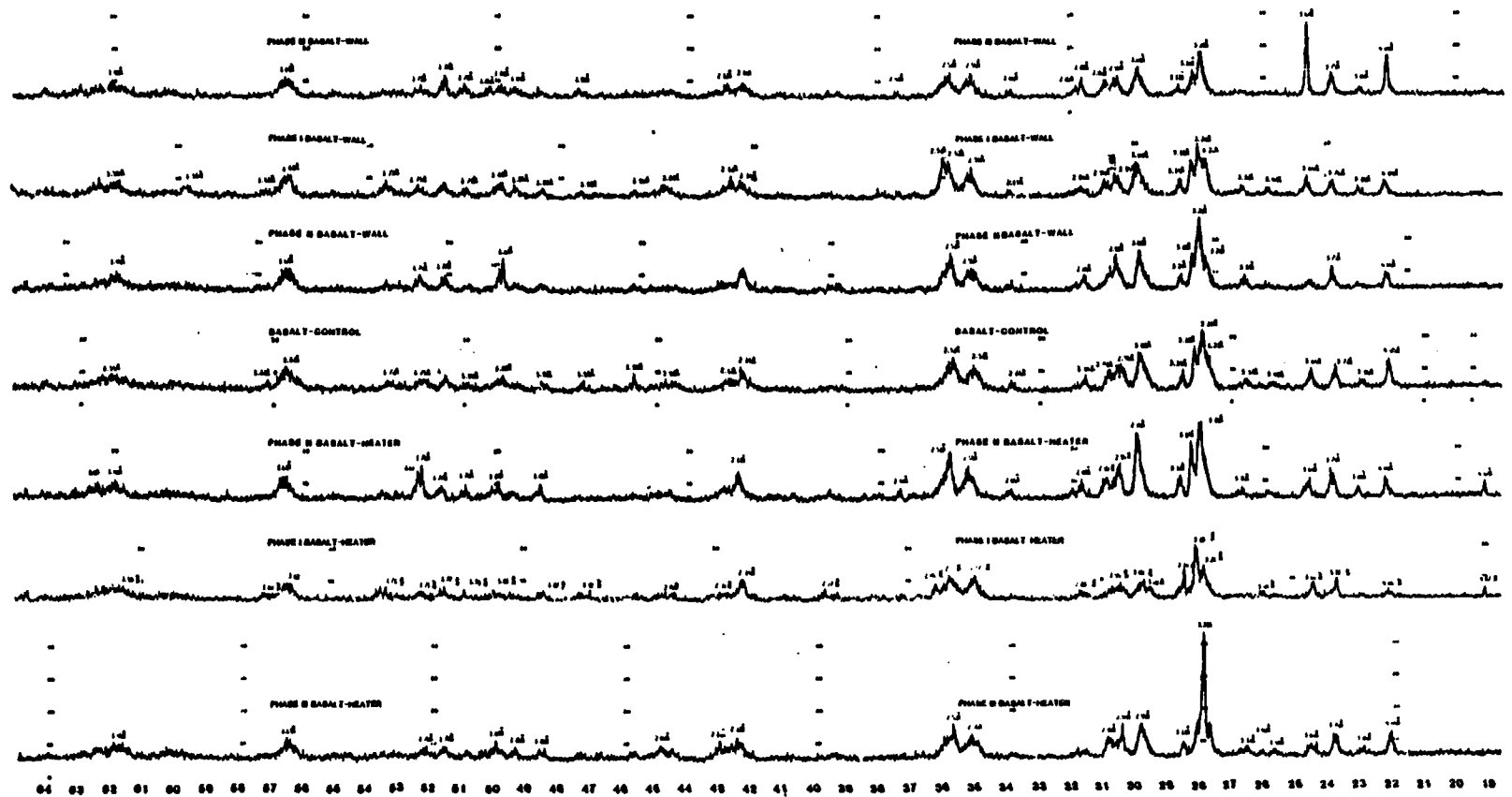
3.5.8 Analysis of Reacted Basalt

3.5.8.1 Comparison of XRD Patterns of Pulverized Basalt

The basalt pellets removed from regions near the heater and near the wall in each of the three phases and an unreacted control sample were pulverized and analyzed by XRD to detect any differences due to reaction. Interpretation of the complex diffraction patterns to identify specific changes in mineralogical composition would require a significant effort and is beyond the scope of this work. Polished thin section basalt samples were also prepared and examined with a polarizing microscope to help detect changes in basalt mineralogy.

The XRD patterns for all basalt samples are reproduced in Figure 3.30. The data for the observed (hkl) reflections are summarized in Table 3.11. If a comparison of the patterns shown in Figure 3.30 is made, it is obvious that there are differences among the patterns, showing that changes occur in the mineralogical composition of the basalt upon reaction. For example, there is a d-spacing of 4.67 Å for samples taken from the heater region in the irradiated systems which is not present in the samples taken from the wall or heater regions in the unirradiated system. More detailed and comprehensive studies are needed to characterize the changes that occur and to determine the effects of these changes in composition on the repository environment.

A preliminary solids analysis and solution analysis performed in the Wood hydrothermal bentonite/basalt/groundwater non-irradiated experiment (RHO-BW-SA-219P, 1983) at 300°C and 28.9 MPa suggests that the primary reaction in the basalt-bearing system is the dissolution of basalt glass followed by the precipitation of a pure silica phase (that is, cristobalite and/or quartz) and smectite, illite, and mordenite (zeolite). It was thought that some alteration of the bentonite to illite may have occurred but this was not seen when a bentonite/groundwater system was tested in a similar manner.



← 2θ

Figure 3.30. Comparison of X-ray diffraction patterns for reacted and unreacted basalt, prepared as unoriented mounts of pulverized basalt. [Range of scan: $2\theta = 3-65^\circ$ ($d = 1.43-29.4$ A)].

Table 3.11. Comparison of (hkl) d-spacings based on X-ray diffractometer studies of reacted and unreacted basalt, prepared as unoriented mounts of pulverized basalt. [Intensities not specified. Range of scan: $2\theta = 3-65^\circ$ ($d = 1.43-29.4 \text{ \AA}$).]

d (Å)						
Wall Sample Phase I Test	Wall Sample Phase II Test	Wall Sample Phase III Test	Heater Sample Phase I Test	Heater Sample Phase II Test	Heater Sample Phase III Test	Control Sample
4.04	4.04	4.04	4.67	4.67	4.04	4.05
3.89	3.88	3.89	4.04	4.03	3.89	3.90
3.76	3.75	3.75	3.77	3.74	3.74	3.77
3.64	3.64	3.67	3.64	3.64	3.64	3.64
3.47	3.47	3.47	3.46	3.46	3.48	3.48
3.37	3.45	3.45	3.44	3.44	3.42	3.42
3.22	3.37	3.37	3.35	3.35	3.37	3.37
3.20	3.23	3.23	3.21	3.21	3.23	3.23
3.18	3.21	3.21	3.19	3.19	3.21	3.21
3.14	3.18	3.18	3.18	3.17	3.18	3.18
3.00	3.14	3.13	3.14	3.13	3.13	3.14
2.94	3.01	3.01	3.02	3.02	3.00	3.00
2.93	2.94	2.94	2.94	2.94	2.99	2.95
2.90	2.93	2.93	2.90	2.90	2.94	2.94
2.84	2.92	2.92	2.83	2.83	2.90	2.91
2.65	2.84	2.83	2.83	2.83	2.84	2.85
2.56	2.82	2.82	2.80	2.80	2.81	2.81
2.52	2.65	2.66	2.65	2.65	2.65	2.65
2.51	2.56	2.56	2.57	2.55	2.56	2.57
2.41	2.52	2.52	2.51	2.51	2.52	2.52
2.14	2.51	2.51	2.48	2.48	2.51	2.51
2.12	2.41	2.41	2.27	2.27	2.41	2.41
2.03	2.14	2.14	2.27	2.27	2.41	2.41
1.99	2.11	2.12	2.14	2.13	2.13	2.14
1.92	2.11	2.12	2.10	2.11	2.11	2.12
1.88	2.03	2.03	2.02	2.02	2.02	2.03
1.85	1.99	1.99	1.99	1.99	1.99	1.99
1.83	1.92	1.92	1.92	1.92	1.95	1.95
1.79	1.87	1.88	1.87	1.88	1.93	1.93
1.77	1.85	1.84	1.85	1.85	1.88	1.87
1.75	1.83	1.83	1.83	1.83	1.85	1.85
1.72	1.83	1.83	1.83	1.83	1.83	1.83
1.63	1.79	1.79	1.79	1.79	1.79	1.80
1.61	1.77	1.77	1.77	1.77	1.77	1.77
1.55	1.75	1.75	1.75	1.75	1.76	1.75
1.50	1.72	1.72	1.71	1.71	1.71	1.72
1.49	1.63	1.63	1.62	1.63	1.63	1.63
1.49	1.61	1.61	1.60	1.60	1.60	1.61
1.49	1.49	1.49	1.50	1.50	1.49	1.50

3.5.8.2 Comparison of Micrographs of Polished Basalt Thin Sections

Examination of polished basalt thin sections under a polarizing microscope revealed the presence of at least three mineralogical phases: plagioclase, pyroxene, and olivine. These were identified by their respective characteristic shapes and optical properties (Kraus, E. H., 1959; Deer, W. A., 1966). The three phases are shown in Figure 3.31. Examination of reacted basalt samples taken from the heater region for each test under the polarizing microscope indicates that plagioclase and olivine appear to be relatively unchanged. However, the pyroxene appears to have been altered, as evident from the alteration features observed on pyroxene grains from a Phase I test sample shown in Figure 3.32. Additionally, there are red-brown areas in the reacted basalt that are not present in the unreacted basalt in samples from the three tests. See Figure 3.33. There do not seem to be gross differences in the irradiated and non-irradiated basalt thin sections under the polarizing microscope. It was observed that there were very few red-brown areas in the Phase III specimen. In the Phase III specimen, they were mainly yellow-brown in color. Compare Figures 3.33 and 3.34. An additional observation is that these areas not present in the unreacted basalt specimen appear to be more numerous in the samples taken from the wall region than in the samples taken from the heater region in all three tests.

Work has been done at BWIP on identifying alteration products resulting from the reaction under hydrothermal conditions at 150°C for 120 days of basalt/bentonite/groundwater (BWIP/NRC Geochemistry Workshop, 1984). It was observed that (1) partial dissolution of basalt mesostasis and clay occurred, (2) smectite structure was preserved, and (3) iron and potassium were substituted in the smectite structure. The reaction product was identified as Fe-smectite. In the present work, XRD analysis of the powdered basalt samples did not reveal any basal spacings $\geq 9.6 \text{ \AA}$, which is the minimum basal spacing a smectite can display and corresponds to the fully collapsed state (Deer, W. A., 1966)¹⁴.

Much work needs to be conducted to identify the specific mineralogical changes that are occurring in the basalt after reaction. In particular, the effects of the repository conditions on the basaltic glassy phases need to be determined. Also, correlations need to be made between the changes seen microscopically and the changes seen in the XRD patterns.

3.5.9 Metallography of Carbon Steel Sleeve and Identification of Surface Products

In the three phases of the test program, individual 1020 carbon steel sleeves were used to simulate the waste container. End caps were welded on to isolate the internal heater. The sleeves (25.4-mm diameter, 155-mm length and

¹⁴The observable range of d-spacings was 1.43-29.4 Å. Any d-spacings greater than 29.4 Å would not have been seen.



Figure 3.31. Minerals in unreacted basalt as determined with a polarizing microscope under crossed polars (100X). (Key: Pl = plagioclase, P_y = pyroxene and O = olivine.)



Figure 3.32. Minerals in Phase I test reacted basalt sampled from the heater region as determined with a polarizing microscope under crossed polars (100X). (Key: Pl = plagioclase, P_y = pyroxene and O = olivine.)

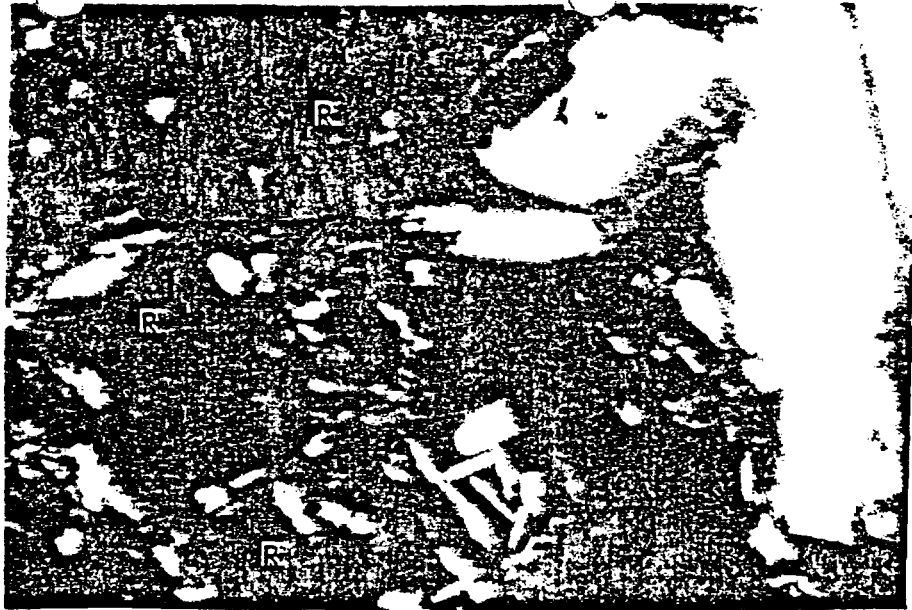


Figure 3.33. Minerals in Phase I test reacted basalt sampled from the wall region as determined with a polarizing microscope under crossed polars (100X). (Red-brown areas are indicated by R in photo.)



Figure 3.34. Minerals in the Phase III test reacted basalt sampled from the wall region as determined with a polarizing microscope under crossed polars (100X). (Yellow-brown areas are indicated by y in photo.)

2-mm thick) were removed from the stainless steel autoclave after the packing material slurries had been examined after the 60-day test periods. Figure 3.35 shows the reacted sleeve after the Phase I test and compares it to one which was not tested. It should be noted that the sleeve for the Phase I test was in the as-received condition whereas the Phase II and Phase III test sleeves were polished through 600-grit silicon carbide paper, in an attempt to remove the decarburized surface layer which was introduced by tube manufacturing processes.

3.5.9.1 Metallography of Phase I Test Sleeve

Figure 3.36 shows a metallographic section perpendicular to the axis of the Phase I steel sleeve. The steel consists primarily of white ferritic grains interspersed with dark pearlitic regions. A thin gray oxide layer is observed on the outer surface, which was in contact with the packing material. The oxide is adherent but in certain locations is found to be fractured. Within the two-month testing period at 150°C, no obvious surface pitting or intergranular corrosion was observed. Small indentations which were present originated in the starting material. Immediately above the oxide, a slightly thicker black layer (indicated by arrow) is just discernible between the oxide and plastic compound used to mount the sample for metallographic preparation. Figure 3.37 is a micrograph taken at a different location and shows a thicker dark layer (between the arrows). This represents an adherent orange-red clay layer which remained after most of the basalt/bentonite mixture contacting it was removed. Samples of this layer were mechanically removed and subjected to X-ray diffraction. It seems from a comparison of Figures 3.36 and 3.37 that the metal oxide layer is thinner in regions where the orange-red layer is thick. This indicates that this adherent layer minimized uniform corrosion.

Analysis by SEM-EDX of the sleeve surface product revealed the presence of a material similar in composition to a sample of bentonite that was examined separately. However, there were some compositional differences at various locations on the sleeve, as the semi-quantitative elemental analyses revealed. The elemental analysis of bentonite clay by SEM-EDX shows that Si is the most abundant element ($\approx 75\%$), with some Al ($\approx 15\%$) and Fe ($\approx 6\%$), and minor amounts of other elements ($\approx 4\%$). At some sites on the sleeve, the surface products that were probed showed more Fe relative to the amount indicated in bentonite. For some sites, the Fe and Si peaks were similar in intensity but in others the Fe peaks were much stronger than those for Si. One surface product sample, shown in Figure 3.38, is a layered material whose elemental composition was mainly Fe with some Si and a small amount of Mg. There was not sufficient material, however, to pursue more quantitative experiments.

As noted above, the Phase I test sleeve, which was used in the as-received condition, was decarburized to a depth of approximately 50 microns (Figures 3.36 and 3.37). Figure 3.39, showing a section through a non-reacted steel tube, proves that decarburization was a result of standard manufacturing processes rather than from hydrothermal testing.

During the Phase I test, the slurry level inside the autoclave had fallen to a level below the top of the carbon steel sleeve. Above this waterline,

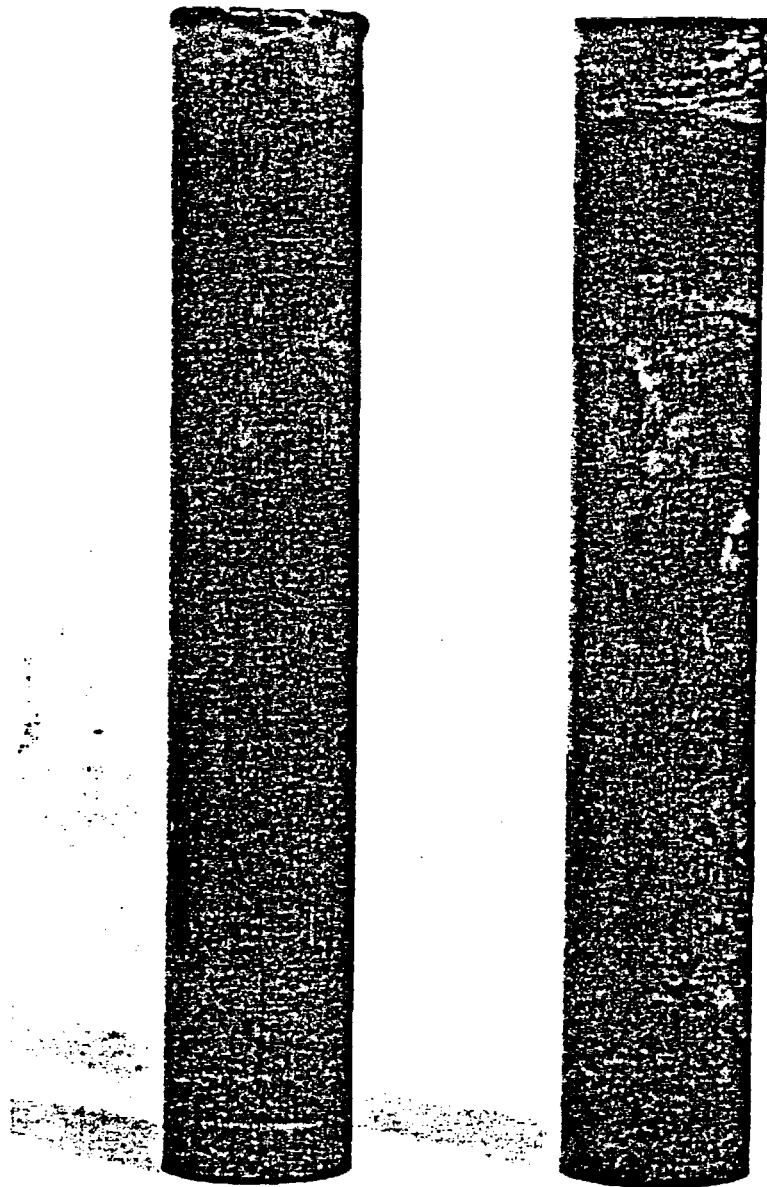


Figure 3.35. Appearance of carbon steel sleeve prior to reaction (left) and subsequent to Phase I test reaction (right). (Sleeves are shown full-scale.)



Figure 3.36. Micrograph of outside diameter of carbon steel sleeve subsequent to Phase I test reaction showing metal oxide and thin clay deposition layer (marked by arrow) (250X).

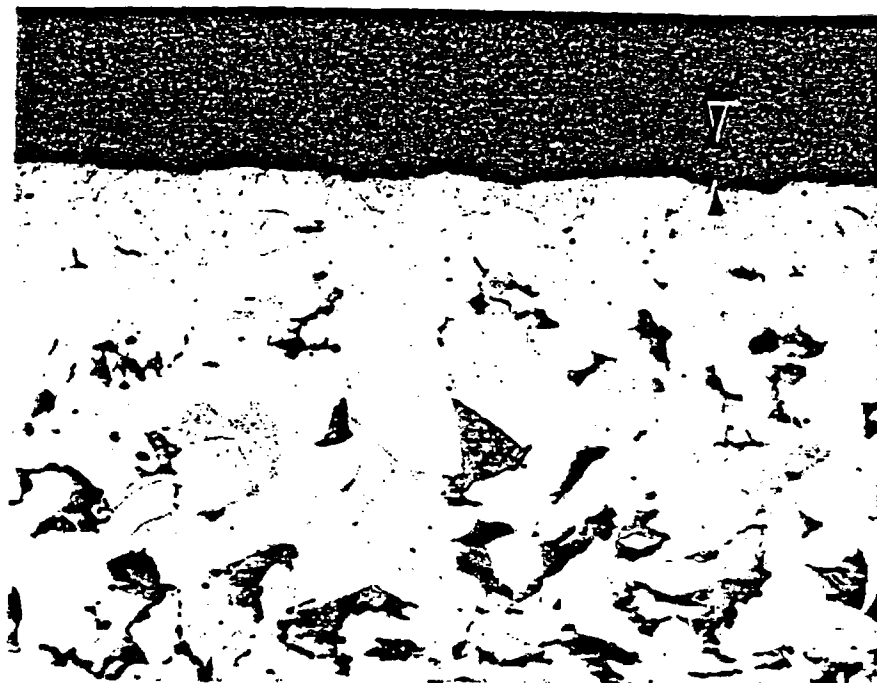


Figure 3.37. Micrograph of outside diameter of carbon steel sleeve subsequent to Phase I test reaction showing metal oxide and thick clay deposition layer between arrows (250X).



Figure 3.38. SEM-EDX micrograph of iron-rich layered material in Phase I test carbon steel surface product (1000X).

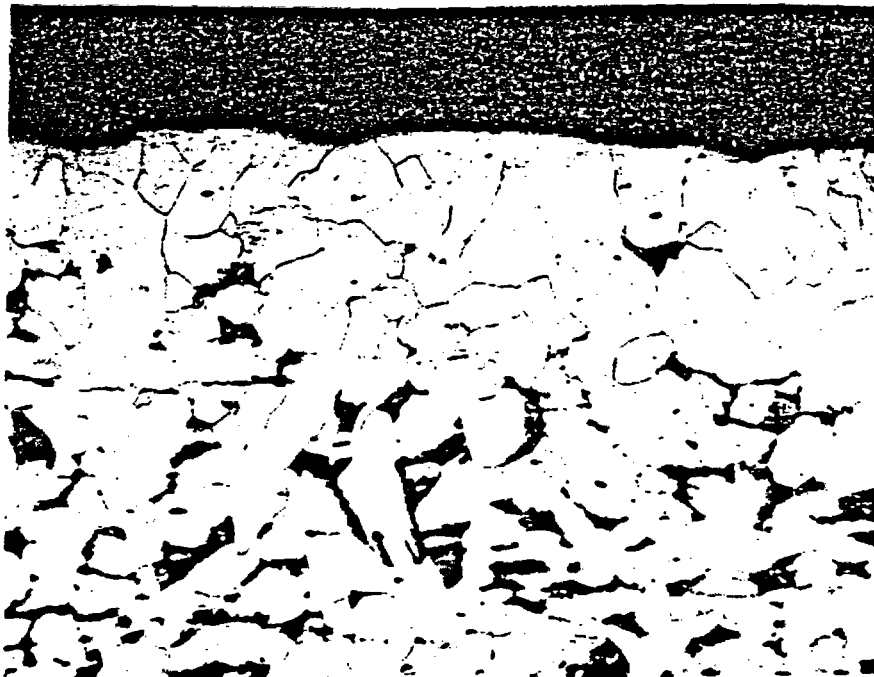


Figure 3.39. Micrograph of outside diameter of carbon steel sleeve prior to Phase I test reaction (250X). (Note the presence of decarburized surface.)

accelerated corrosion at the welded end cap was evident (Figure 3.35). The occurrence of more severe corrosion on the steel exposed to vapor has been reported in another study (PNL-4452, 1983). In that work, cast ductile iron was placed in an autoclave with oxitic basaltic groundwater and crushed basalt at a temperature of 250°C, a pressure of 5.2 MPa (700 psi) and a gamma dose rate of $\approx 2 \times 10^5$ rad/h for periods up to three months with no bentonite present. Between the one- and three-month test periods, the autoclave operated in the vapor phase for several days, apparently because of a slightly elevated temperature. The present observation of accelerated corrosion in the vapor phase could, therefore, be associated with higher oxygen levels or, possibly, with waterline corrosion.

Figure 3.40 shows the appearance of weld metal at the top of the Phase I test steel sleeve. A thin broken oxide layer is just visible. Fusion of the metal has removed the decarburized layer and ferrite-rich grain boundary regions are formed. Again, no pitting or intergranular attack was detected.

3.5.9.2 Metallography of Phase II Test Sleeve

In the Phase II test, prior polishing of the sleeve had removed the decarburized surface layer (Figure 3.41). A very thin, irregular surface oxide is seen above which is a thin clay layer (between arrows). Several hemispherically-shaped pits are present. These are approximately 12 microns in depth after the 60-day reaction period. If one makes the highly conservative assumption that the pit depth increases linearly with time, then the depth after the minimum 300-year radionuclide containment period would be 2.2 cm. This would be insufficient to penetrate any of the carbon steel containers specified by Westinghouse Electric Corporation for conceptual waste package designs (AESD-TME-3142, 1982). For these, the container wall thicknesses vary between 5.3 and 8.7 cm.

The adherent materials on the Phase II test sleeve were studied with SEM-EDX, electron diffraction, and electron energy loss spectroscopy (EELS) in an attempt to identify the orange-brown portion and magnetic green-yellow portion. Micrographs of these materials are shown in Figures 3.42 and 3.43, respectively. The EDX analyses of these samples showed that (1) the orange-brown material contained large amounts of Si, Fe and Al with some Ca, Mg and S in the darker areas, and some Ca, Mg and K in the lighter areas and (2) the green-yellow material contained large amounts of Fe and Si with some Al, Mg and Ca. The samples were shown to be well-defined crystalline materials that contained oxygen by use of EELS. See Figure 3.44 for the two-point plot of the EELS spectrum of the orange-brown material. A similar one was obtained for the green-yellow specimen. Subsequently Debye-Scherrer patterns were obtained (see Figures 45 and 46). The d-spacings were calculated by measuring the patterns, which had been calibrated against a gold standard and are listed in Table 3.12. They did not match any of the spacings reported for common iron-silicate materials. It is believed that these specimens contain hydroxyl groups and/or water molecules because they were degraded by an electron beam. The identify of these materials is not presently known.

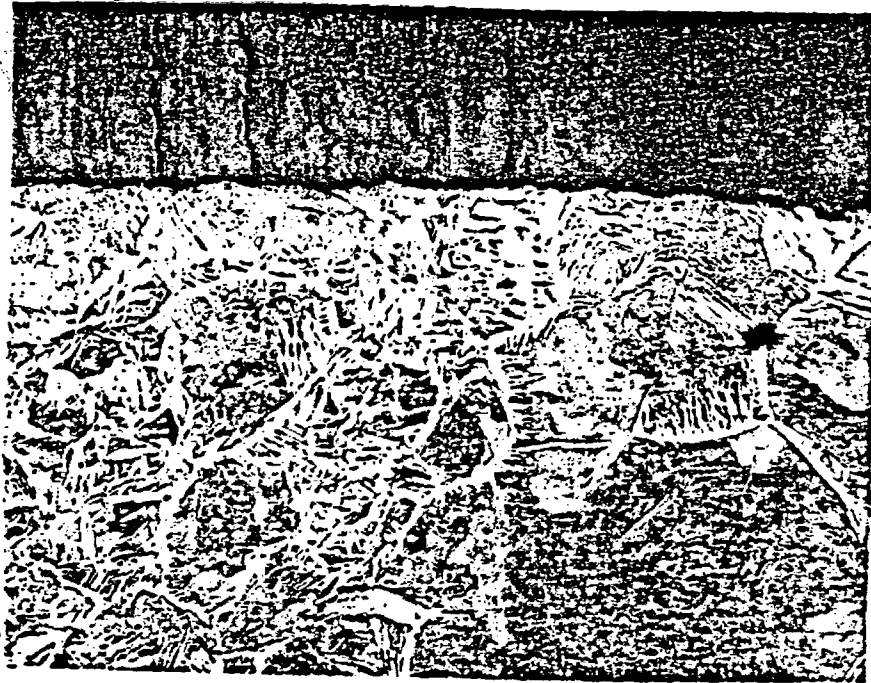


Figure 3.40. Micrograph of weld metal in carbon steel sleeve subsequent to Phase I test reaction (250X).



Figure 3.41. Micrograph of outside diameter of carbon steel sleeve subsequent to Phase II test reaction showing metal oxide and thin clay deposition layer (marked by arrows) (250X).

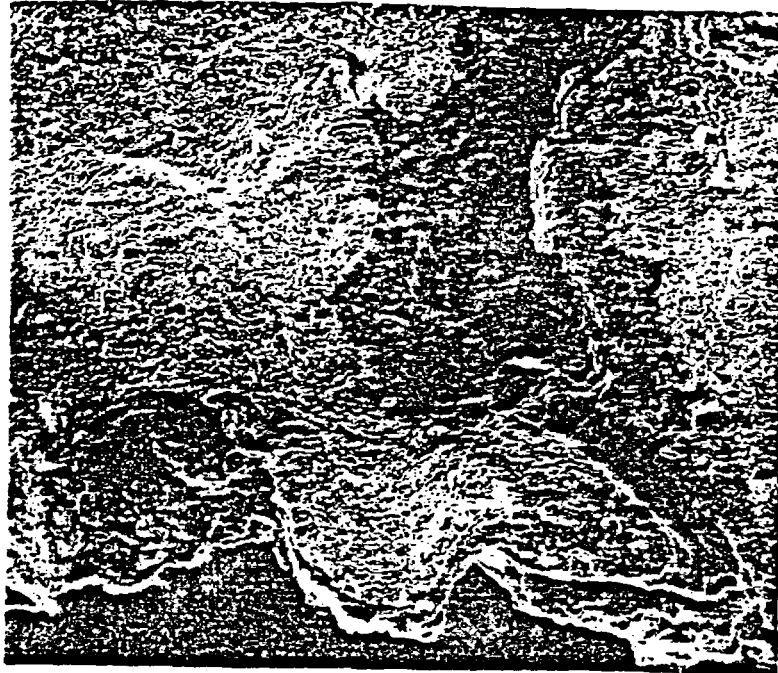


Figure 3.42. Micrograph (SEM) of orange-brown sleeve surface product from Phase II test (100X).



Figure 3.43. Micrograph (SEM) of magnetic green-yellow sleeve surface product from Phase II test (100X).

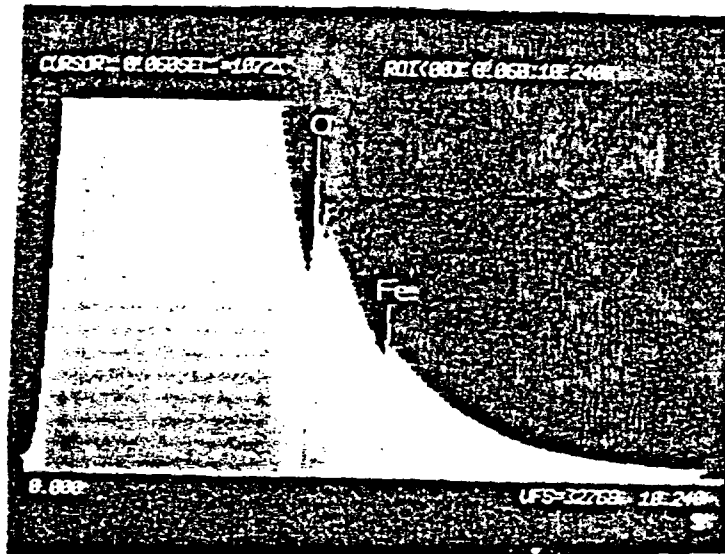


Figure 3.44. Point plot of EELS spectrum of orange-brown sleeve surface product from the Phase II test showing well-defined crystalline material containing iron and oxygen.

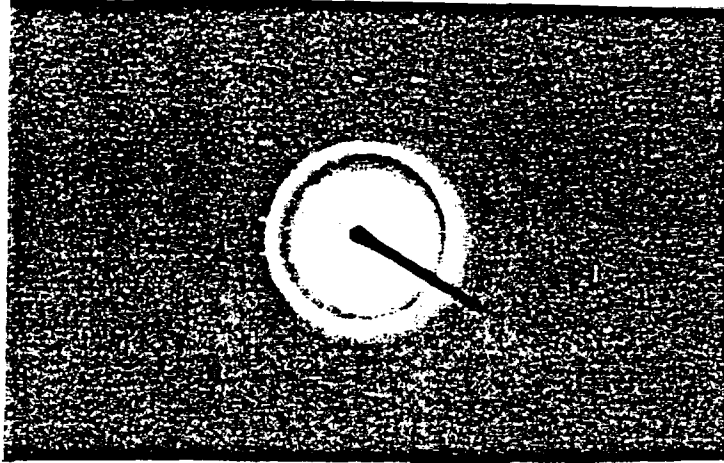


Figure 3.45. Debye-Scherrer powder pattern for orange-brown sleeve surface product from Phase III test.

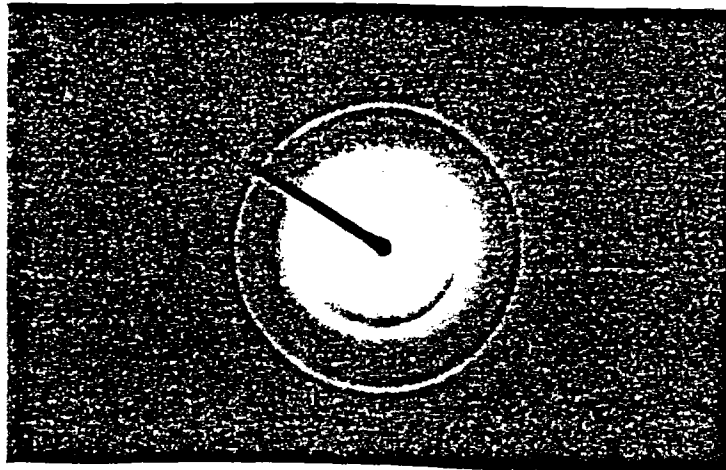


Figure 3.46. Debye-Scherrer powder pattern for green-yellow sleeve surface product from Phase II test.

Table 3.12. Calculated d-spacings of Phase II test sleeve surface product based on measured Debye-Scherrer electron diffraction powder patterns.^a

d (Å) Green Oxide ^b	d (Å) Red (Orange) Oxide ^b
4.69	4.40
2.60	2.49
1.76	1.63
1.55	1.47
1.36	1.26
1.00	

^aSpacings were calculated based on the measured patterns. A gold standard was used for calibration.

^bOxygen was determined to be present by use of EELS (electron energy loss spectroscopy).

3.5.9.3 Metallography of Phase III Sleeve

In the Phase III control test, carried out in a non-irradiation environment, pitting is also observed (see Figure 3.47). The pits in this case are more shallow and more closely spaced than those in the Phase II experiment (Figure 3.41). Based on an assumed linear pit propagation rate, the pit depth after 300 years would be about 1.5 cm. It should be noted that polishing the carbon steel sleeve prior to testing did not completely remove the surface-decarburized layer. Therefore, pit initiation and growth do not seem to be dependent on the presence of carbide phases. Figure 3.47 also shows a thin oxide layer which was detached from the metal substrate. It is approximately seven microns in thickness, which is similar to the oxide thickness for the Phase I test sleeve shown in Figure 3.36. If the oxide is assumed to be magnetite (Fe_3O_4), it may be shown that the 7- μ oxide layer was formed from 3.2 μ of steel during the 60-day test period¹⁵. Again, a highly conservative assumption of a linear rate for uniform corrosion gives a metal loss of 0.6 cm in 300 years. Thus, uniform corrosion will not be a significant failure mode for a carbon steel container in a basalt repository.

The material adhering to the Phase III test carbon steel sleeve was analyzed by SEM-EDX and X-ray diffraction to determine if an identification could be made. One product was green in color. A micrograph and EDX analysis of

¹⁵The amount of O_2 present in this amount of magnetite is estimated to be ≈ 140 mg. There is a maximum of 22 mg of O_2 in the plenum and dissolved in the water. The remaining O_2 probably originates from adsorbed oxygen and/or radiolysis of water.



Figure 3.47. Micrograph of outside diameter of carbon steel sleeve subsequent to Phase III test showing pitting, and a thin detached oxide layer (250X).

this material are shown in Figures 3.48 and 3.49. The other product was orange-brown in color and relevant information is given in Figures 3.50 and 3.51. Both materials contain large amounts of Si and Fe. The green product also has a high Ca content. Some Mg, Al, and Cl are also present in each. The XRD diffraction pattern (scan range $2\theta = 3-68^\circ$) of the orange-brown material yielded five sets of d-spacings: 3.03-3.08 Å, 2.51-2.56 Å, 2.10-2.11 Å, 1.91-1.93 Å and 1.88-1.89 Å. This compound or mixture of compounds was not identifiable.

3.5.9.4 Comparison of Pitting Corrosion For All Tests

The results of the carbon steel corrosion evaluations show that pitting may occur during 60-day tests at 150°C in the presence of basalt/bentonite packing material. Gamma irradiation and surface decarburization of the steel did not have a significant influence on the initiation of pitting. Pits were only found, however, on pre-polished metal surfaces exposed to methane-containing water. It is not clear whether the surface polishing or the methane was responsible for this type of corrosion. Although the pitting rates obtained in this study were found to be too low to penetrate a typical steel container for a basalt repository, it must be realized that the test temperature of 150°C is much lower than the maximum value of about 300°C relevant to actual container conditions.

3.6. Summary

The objective of this program was to determine the chemical environment that will be present within high level nuclear waste packages emplaced in a basalt repository. For this purpose, low carbon 1020 steel (current BWIP reference container material), synthetic basaltic groundwater and a mixture of bentonite and basalt were exposed in an autoclave to a specific repository condition after sealing (150°C, 1500 psi) in a gamma radiation environment with a dose rate of $(3.8 \pm 0.5) \times 10^4$ rad/h. The experiment consisted of three test phases.

The Phase I test involved a two-month irradiation test in an argon environment. The Phase II test is a similar test in a methane environment in the presence of radiation. These two tests were followed by a Phase III control test which is similar to the Phase II study but which was conducted in the absence of radiation.

A summary of findings is given below:

- Over the two-month test periods, the gas pressure in the autoclave ranged from 9.3-9.7 MPa in the Phase I test, from 11.1-13.2 MPa in the Phase II test and from 9.8-11.7 MPa in the Phase III test. There was a trend to decreasing pressures followed by a trend to pressures approaching or slightly exceeding the initial values.
- In all three tests, hydrogen was produced and oxygen was consumed, as determined by gas analyses and dissolved oxygen measurements. More hydrogen was produced in the Phase II test than in the Phase I and III

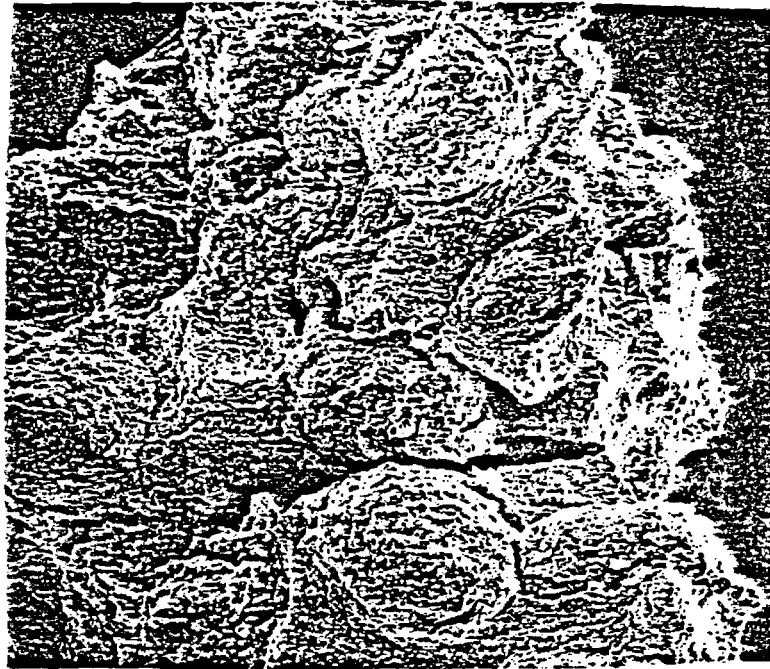


Figure 3.48. Micrograph of Phase III test green carbon steel surface product (100X).



Figure 3.49. EDX of Phase III test green carbon steel surface product.

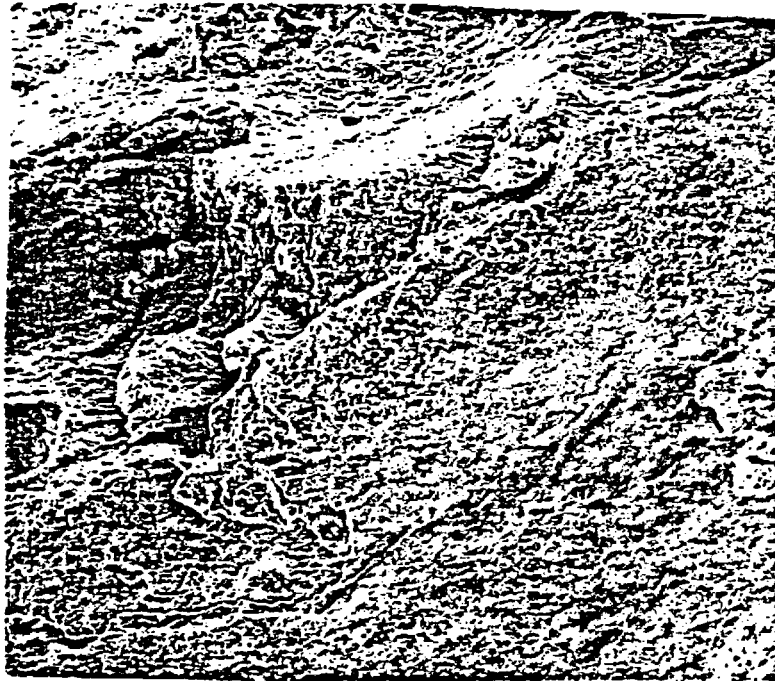


Figure 3.50. Micrograph of Phase III test orange-brown carbon steel surface product (100X).



Figure 3.51. EDX of Phase III test orange-brown carbon steel surface product.

tests due to the radiolysis of methane. Similar amounts of hydrogen were produced in the irradiated Phase I test and in the non-irradiated Phase III test.

- After cooling the autoclave over a period of 25 minutes, the pH of the water in the basalt/bentonite packing material measured at room temperature was nearly neutral. There did not appear to be a significant change in pH across the thermal gradient in the packing material in any of the three tests.
- There did not appear to be a significant change in DO across the thermal gradient of the packing material in any of the three tests.
- The calculated Eh values indicated that an oxidizing environment existed after quenching the contents of the autoclave. Radiolysis of groundwater did not appear to increase the oxidizing potential overall.
- The concentration of Cl^- and SO_4^{2-} measured at room temperature were significantly greater near the cooler end of the thermal gradient in the tests.
- The bulk of the Fe and Si content of the reacted water is present as colloidal material that is filterable. Gamma radiation enhanced colloid formation.
- Hydrothermal conditions cause some change in the bentonite component of the packing material.
- Optical and XRD studies indicate that some changes occur in the mineralogical content of basalt during hydrothermal testing.
- There was no pitting on the carbon steel sleeve or the steel weldment in the Phase I test. There were hemispherically-shaped pits approximately 12μ in depth after 60 days of irradiation in the Phase II test. In the Phase III test, shallower (approximately 8μ in depth) and more closely-spaced pits were formed on the carbon steel sleeve. Based on a highly conservative assumption of linear pitting rates the maximum pit depth after 300 years is about 2.2 cm.
- Adherent surface products removed from the carbon steel sleeve in the Phase I test contained mainly montmorillonite clay. SEM-EDX analysis indicated the presence of other materials containing more Fe than that found in the montmorillonite. Surface products removed from the carbon steel sleeve in the Phase II test were analyzed by SEM-EDX and electron diffraction but were not readily identifiable. (An orange-brown product contained large amounts of Si, Fe, and Al, while the green-yellow product was largely composed of Fe and Si.) Identification was also not possible for the Phase III surface products, which were analyzed by SEM-EDX and XRD. Both Phase III surface products contained large amounts of Si and Fe, with the green phase also containing a large amount of Ca.

3.7. Recommendations for Future Work

The following recommendations are made for additional and confirmatory experiments:

- A number of identical experiments need to be performed to establish statistical variations.
- Longer term experiments should be performed to determine changes in gas composition and pressure buildup.
- The effect of quenching the autoclave on the measured values of pH, DO, Cl^- , SO_4^{2-} and Fe needs to be determined.
- Changes in the clay and basalt during hydrothermal reaction need to be specified and explained to predict long term performance.
- Full characterization of the colloidal material in terms of composition and size distribution needs to be performed.
- Mineralogical changes in the basalt, especially with regard to the glassy phases, need to be fully evaluated. Correlations could be made with predictions generated by use of geochemical codes, such as WATEQ and PHREEQE.
- Long term corrosion studies are needed to determine the extent of localized corrosion in container steels. Hydrogen uptake by steel, and its effect on embrittlement also needs to be established.
- Applicability of the current laboratory data to repository environments needs to be established by in situ experiments. These experiments should simulate hydrothermal conditions and may involve pressurizing a test borehole. Similar tests will need to be developed and conducted for waste package performance experiments. Repository field tests, such as those which have been carried out by WIPP (SAND 83-1516C, 1983), may provide a basis for designing tests relevant to a basalt repository.

3.8. References

AESD-TME-3142, "Waste Package Conceptual Designs for a Nuclear Repository in Basalt," C. R. Bolmgren and others, Westinghouse Electric Corporation, 1982.

ANL-83-19, "Fuel Cycle Programs - Quarterly Progress Report, October-December 1982," J. J. Steindler and others, Argonne National Laboratory, 1983.

Arai, H., S. Nagai, K. Matsuda and M. Hatada, "Effect of Irradiation Temperature on the Radiolysis of Methane," Radiat. Phys. Chem. 17, 151-157, 1981.

- Bonham, L. C., "Solubility of Methane in Water at Elevated Temperatures and Pressures," American Association of Petroleum Geologists Bulletin 62, 2478-2488, 1978.
- Braker, W. and A. L. Mossman, Gas Data Book, Matheson Gas Products, Inc., Secaucus, New Jersey, 1980.
- Brunauer, S., P. H. Emmett and E. Teller, "Adsorption of Gases in Multimolecular Layers," J. Amer. Chem. Soc. 60, 309-319, 1938.
- BWIP/NRC Geochemistry Workshop, January 9-12, 1984, Richland, Washington.
- Carroll, D., Clay Minerals: A Guide to Their X-Ray Identification, Geological Society of America, Boulder, Colorado, 1970.
- Dean, J. A., Lange's Handbook of Chemistry, McGraw-Hill, 1979, p. 10-5.
- Deer, W. A., R. A. Howie and J. Zussman, An Introduction to the Rock-Forming Minerals, London, Longman Group Ltd, 1966.
- DOE/RL 82-3, Vol. II, "Site Characterization Report for the Basalt Waste Isolation Project," November 1982.
- DP-1464, "Radiolytic Gas Production From Concrete Containing Savannah River Plant Waste," N. E. Bibler, Savannah River Laboratory, January 1978.
- DP-MS-76-51, "Radiolytic Gas Production During Long-Term Storage of Nuclear Wastes," N. E. Bibler, Savannah River Laboratory, October 1976.
- Draganic, I. G. and Z. D. Draganic, The Radiation Chemistry of Water, New York, Academic Press, 1971.
- Greenberg, A. E., J. T. Connors and D. Jenkins, Standard Methods for the Examination of Water and Wastewater, American Public Health Association, Washington, D. C., 1981.
- Grimshaw, R. W., The Chemistry and Physics of Clays and Other Ceramic Materials, New York, John Wiley and Sons, 1971.
- Hall, E. E., "Corrosion of Cast Iron and Low Carbon Steel Nuclear Waste Containers in a Basalt Repository," U. S. Nuclear Regulatory Commission, August 1982.
- Himmelblau, D. M., "Solubilities of Inert Gases in Water, 0°C to Near the Critical Point of Water," J. Chem. Eng. Data, Vol. 5, 10-15, 1960.
- Kraus, E. H., W. F. Hunt and L. S. Ramsdell, Mineralogy, New York, McGraw-Hill, 1959.
- Krumhansl, J. L., "Mineralogic Stability of a Bentonite Backfill in a Bedded Salt Repository Environment," Abstract for 1982 Meeting Geological Society of America.

Lerman, A., Geochemical Processes Water and Sediment Environments, New York, Wiley, 1979, p. 389.

Maurin, J., "Etude de la Radiolyse due Methane en Phase Gazeuse, J. Chim. Phys. 59, 15-26, 1962.

Norfolk, D. J. and T. Swan, "Gamma Radiolysis of Methane Adsorbed on Gamma-Alumina - Part I: Development of Sites Active in Energy Transfer," J. Chem. Soc. Faraday Trans. I 73, 1454-1466, 1977.

Norfolk, D. J., R. F. Skinner and W. J. Williams, "Hydrocarbon Chemistry in Irradiated CO₂/CO/CH₄/H₂O/H₂ Mixtures - I," Radiat. Phys. Chem. 21, 307-319, 1983.

NUREG-0960, Vol. 2, "Draft Site Characterization Analysis of the Site Characterization Report for the Basalt Waste Isolation Project," U. S. Nuclear Regulatory Commission, March 1983.

NUREG/CR-2482, Vol. 3, BNL-NUREG-51494, "Review of DOE Waste Package Program: Subtask 1.1 - National Waste Package Program, April 1982-September 1982," P. Soo and others, Brookhaven National Laboratory, March 1983.

NUREG/CR-2482, Vol. 4, BNL-NUREG-51494, "Review of DOE Waste Package Program: Subtask 1.1 - National Waste Package Program, October 1982-March 1983," P. Soo and others, Brookhaven National Laboratory, September 1983.

NUREG/CR-3091, Vol. 1, BNL-NUREG-51630, "Review of Waste Package Verification Tests: Semiannual Report Covering the Period April-September 1982," P. Soo and others, Brookhaven National Laboratory, April 1983.

NUREG/CR-3091, Vol. 2, BNL-NUREG-51630, "Review of Waste Package Verification Tests: Semiannual Report Covering the Period October 1982-March 1983," P. Soo and others, Brookhaven National Laboratory, August 1983.

NUREG/CR-3091, Vol. 3, BNL-NUREG-51630, "Review of Waste Package Verification Tests: Biannual Report," B. Siskind and others, December 1983.

NUREG/CR-3389, "Valence Effects on the Sorption of Nuclides on Rocks and Minerals," R. E. Meyer, W. D. Arnold and F. I. Case, Oak Ridge National Laboratory, February 1984.

PNL-4452, "Nuclear Waste Package Materials Testing Report: Basalt and Tuffaceous Environments," D. J. Bradley and others, Pacific Northwest Laboratory, March 1983.

RHO-BW-SA-219P, "Experimental Investigation of Sodium Bentonite Stability in Hanford Basalt," M. I. Wood, Rockwell Hanford Operations, 1983.

RHO-BW-SA-303P, "Repository and Waste Package Designs for High Level Nuclear Waste Disposal," M. J. Smith and others, Rockwell Hanford, 1983.

RHO-BW-SA-315P, "Gamma Radiolysis Effects on Grande Ronde Basalt Groundwater," W. J. Gray, Pacific Northwest Laboratory, October 1983.

RHO-BW-ST-21P, "Evaluation of Sodium Bentonite and Crushed Basalt as Waste Package Backfill Materials," M. I. Wood, G. D. Aden and D. L. Lane, Rockwell Hanford Operations, October 1982.

RHO-BWI-C-66, "Preliminary Geochemical and Physical Testing of Materials for Plugging Man-Made Accesses to a Repository in Basalt," C. L. Taylor and others, Rockwell Hanford, April 1980.

RHO-BWI-C-105, "The Geochemical Behavior of Supercalcine Waste Form: Its Stability in a Basalt Environment," J. R. Halloway and others, Rockwell Hanford Operations, June 1981.

RHO-RE-SR-5, "Reference Material Chemistry - Synthetic Groundwater Formation," T. E. Jones, Rockwell Hanford Operations, April 1982.

Rose, A. J., Tables permettant le depouillement des diagrammes de rayons X et Abaques de réglage des monochromateurs a lame courbe, Paris, Centre National de la Recherche Scientifique, 1957.

SAND 83-1516C, "The Waste Package Materials Field Test in S. E. New Mexico Salt," M. A. Molecke and T. M. Torres, Sandia National Laboratories, November 1983.

SD-BWI-TP-022, "Barrier Materials Test Plan," Rockwell Hanford Operations, March 1984.

Seyfried, W. E., Jr. and J. L. Bischoff, "Low Temperature Basalt Alteration by Seawater: An Experimental Study at 70°C and 150°C," Geochimica et Cosmochimica Acta 43, 1937-1947, 1979.

Stevens, G. C., R. M. Clarke and E. J. Hart, "Radiolysis of Aqueous Methane Solutions," J. Phys. Chem. 76, 3863-3867, 1972.

Stoessell, R. K. and P. A. Byrne, "Methane Solubilities in Clay Slurries," Clays and Clay Minerals 30, 67-72, 1982.

Van Olphen, H., An Introduction to Clay Colloid Chemistry, New York, Wiley, 1977.

Van Olphen, H. and J. J. Fripiat, Data Handbook for Clay Materials and Other Non-Metallic Minerals, Oxford, England, Pergamon Press, 1979, p. 19.

4. TESTING FOR STRESS CORROSION CRACKING OF HIGH LEVEL WASTE CONTAINER MATERIALS IN TUFF REPOSITORY ENVIRONMENTS

4.1 Introduction

The Nevada Nuclear Waste Storage Investigations (NNWSI) project is developing a waste package for the disposal of high level nuclear waste in a tuff repository. One of the reasons that prompted NNWSI to consider emplacing waste in the tuff unsaturated zone at the Nevada Test Site was the greatly decreased amounts of water that would be present in the vicinity of the waste package. This was considered highly desirable since container corrosion and waste leaching would be reduced.

From a literature survey, Russell and others (1984) assessed the likely performance of 17 candidate canister materials using corrosion resistance, mechanical properties, weldability, and cost as equally-weighted selection criteria. The reference material was stated to be Type 304L stainless steel (SS) with Type 316L SS, Type 321 SS, and Incoloy 825 as alternates. The applicability of the selection criteria used by these authors to a repository situation is questionable since corrosion resistance is much more important with respect to containing the waste than, for example, mechanical strength or cost. There is also evidence in the literature that some of the alloys being considered by NNWSI are susceptible to stress corrosion cracking (SCC) in steam and in water environments very similar to those expected in a tuff repository. Below is given a brief literature survey of stainless steel stress corrosion behavior in environments which are similar or extrapolatable to tuff repository conditions. It shows that there is a very strong potential for stress corrosion cracking and an experimental verification would be highly desirable. On this basis a detailed testing program was initiated at BNL to check the integrity of the NNWSI reference materials.

4.2 Survey of Stress-Corrosion Behavior of Austenitic Stainless Steels in Relatively Pure Steam/Water/Air Environments

Figure 4.1 shows that austenitic stainless steels exposed to the steam phase of alkaline-phosphate treated boiler water, and given intermittent wetting cycles, will fail by stress-corrosion cracking even though the water contains very low Cl^-/O_2 levels (Williams, W. L., 1957). For example, 5 ppm O_2 and 5 ppm Cl^- in the boiler water will cause failure of stainless steels exposed to the steam phase. Tuff repository water will contain about 7.5 ppm Cl^- and this will be saturated with oxygen from the surrounding air (UCRL-89988, 1983). Initial evaporation of groundwater and subsequent dissolution of previously precipitated salt can make the concentration of Cl^- and other ions in the water coming in contact with a waste package much higher than the values currently assumed.

Data in Figure 4.2 show results from bent-beam tests on Type 321 stainless steel. Strained samples were maintained at 200° and 300°C in the steam phase above water containing 5 ppm Cl^- . For strains as low as 10^{-3} failure readily occurs in times of 40-100 hours (Birchon, D., 1964).

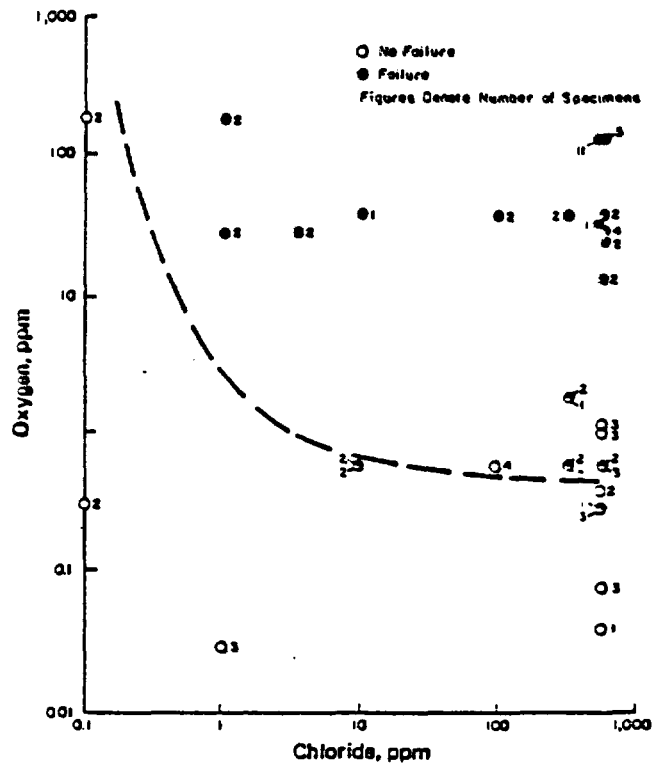


Figure 4.1. Proposed relationship between chloride and oxygen content of alkaline phosphate treated boiler water and susceptibility to stress corrosion cracking of austenitic stainless steel exposed to the steam phase with intermittent wetting (Williams, W. L., 1957).

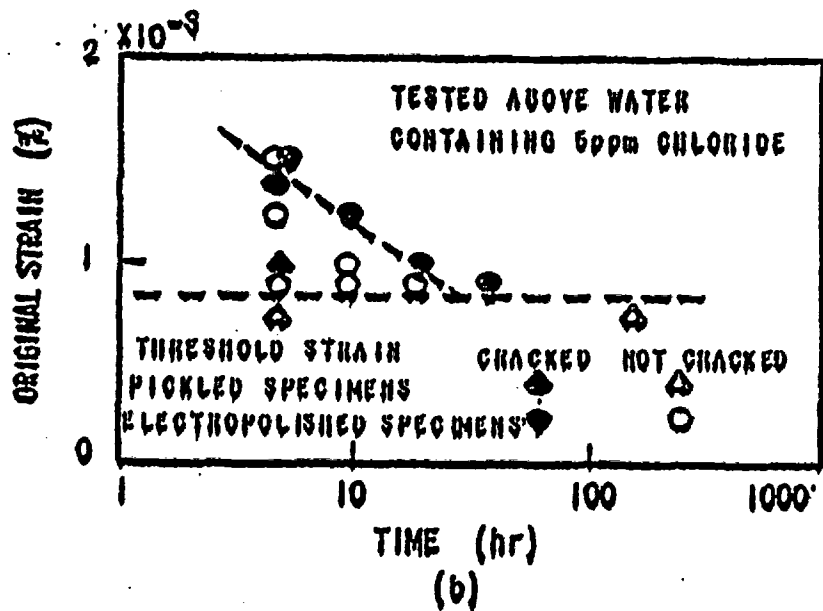
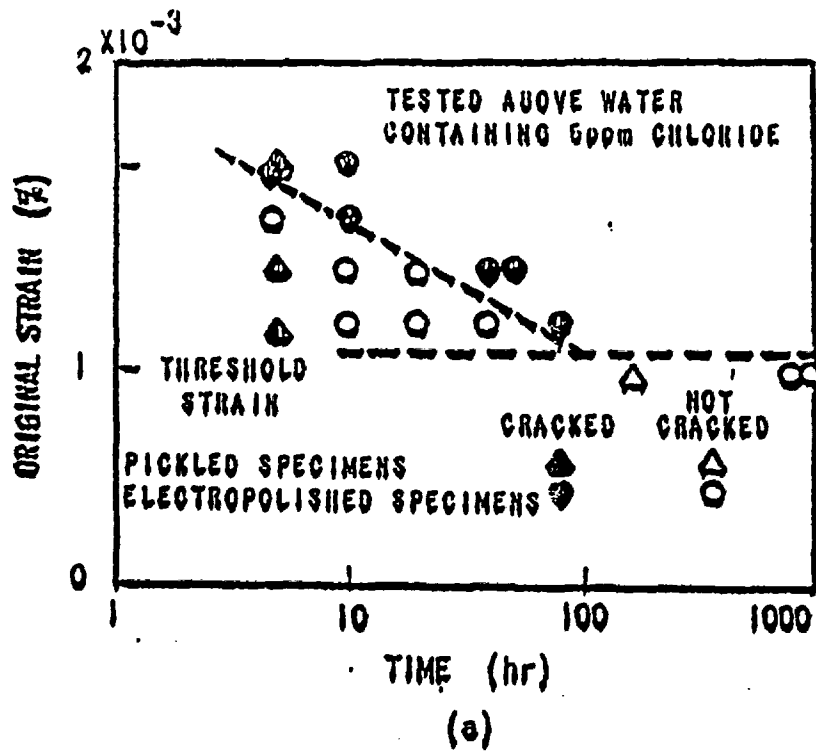


Figure 4.2. The relationship between original strain in bent-beam specimens and time-to-crack for (a) Type 321 stainless steel at 300°C and (b) Type 304 stainless steel at 200°C (Bircon, D., 1964).

There is also much information on the aqueous (as opposed to steam) corrosion of stainless steel. This type of data would be pertinent to the situation where boiling of water around the waste package has ceased and liquid water from the surface of the repository percolates past the container. Figure 4.3 shows that Type 304 SS U-bend samples will fail by stress corrosion cracking in 100°C water containing 10 ppm Cl⁻ (Warren, D., 1960). Failures begin after about one month and all exposed samples failed after about nine months.

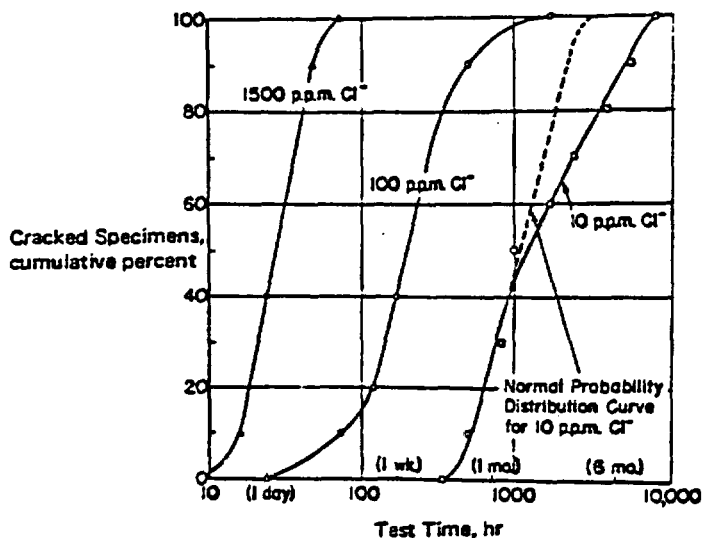


Figure 4.3. Effect of chloride added as NaCl on cracking of Type 304 stainless steel at 100°C. Solution transported by porous material to specimen (Warren, D., 1960).

Other data from Japan (JAERI-M-82-145, 1983) on a range of stainless steels and high nickel alloys in boiling deionized water also show that even these "benign" conditions can cause failure. The test apparatus is shown in Figure 4.4. Double-U-bend samples were used, some containing V notches at the specimen apexes to give stress concentration effects. Table 4.1 shows that Type 304 and Type 304L display stress corrosion cracking behavior without irradiation and also under a gamma dose rate of 1.1×10^5 R/h. Usually, cracking occurs on the inner U-bend specimens, but it also occurs on the outer specimens which have V notches. Irradiated solutions are more damaging than non-irradiated ones.

The observations that cracking is more likely on the inner U-bend samples is probably connected with crevice type conditions in which small volumes of trapped water can alter their composition and Eh/pH conditions more rapidly than those exposed to large amounts of free solution. Crushed tuff packing adjacent to the HLW container will likely give such crevice-like conditions.

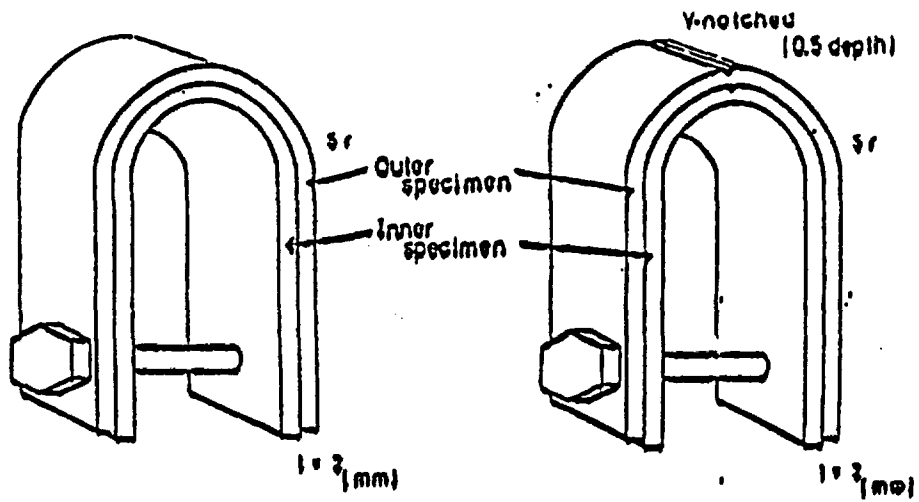


Figure 4.4(a). Schematic diagram of double U-bend type specimen.

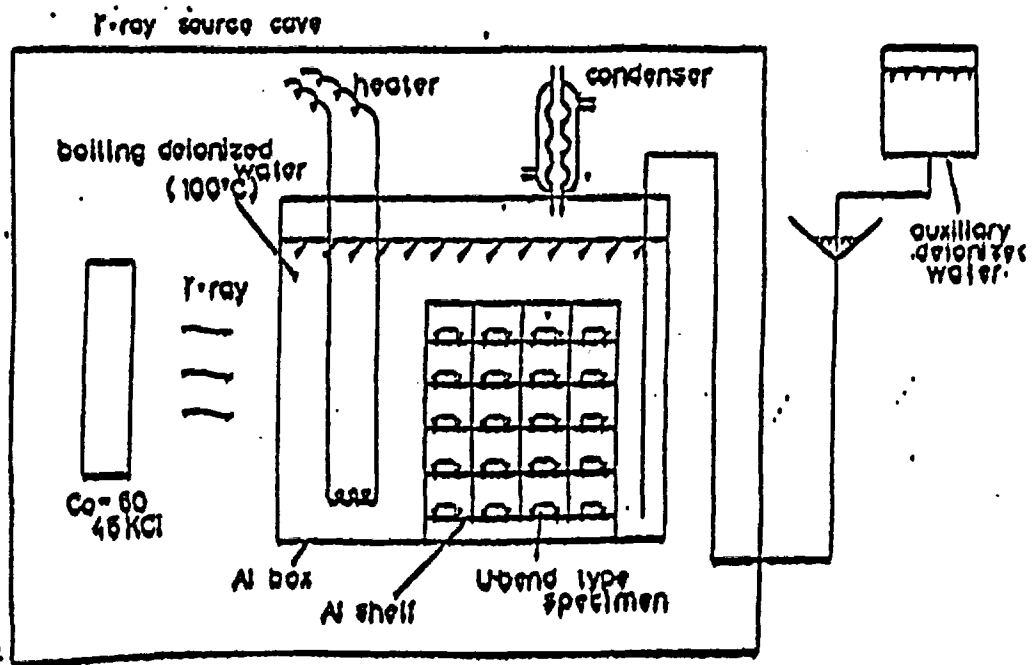


Figure 4.4(b). Schematic diagram of γ -ray irradiation (first test) (JAERI-M-82-145, 1983).

Table 4.1. SCC test in boiling deionized water (first test). (Dose rate: 1.1×10^5 R/h).

(Dose rate ; 1.1×10^5 R/hr
Specimen numbers for each test ; 2)

Alloy	Time (day)	γ-ray irradiation				Non irradiation	
		Total dose (R)	Max. depth of SCC (mm)		Max. depth of SCC (mm)		
			Plain	V-notched	Plain	V-notched	
Type 304 ss	7	2.5×10^7	1.1 ¹ , 0.7 ²	1.5 ¹ , 1.8 ²	1.2 ¹ , 2.2 ²	1.5 ¹ , 1.3 ²	
	14	4.5×10^7	2.0, 2.0	2.0, 2.0	2.0, 2.0	1.5 ¹ , 1.5 ²	
	21	6.5×10^7	2.0, 2.0	2.0, 2.0	2.0, 2.0	2.0, 2.0	
	28	8.5×10^7	2.0, 2.0	2.0, 2.0 ³	2.0, 2.0	2.0, 2.0	
	35	1.1×10^8	2.0, 2.0	2.0 ¹ , 2.0	2.0, 2.0	1.5 ¹ , 1.5 ²	
Type 304L ss	100	1.1×10^8	2.0, 2.0	2.0 ¹ , 2.0 ¹	2.0, 2.0	1.5 ¹ , 1.5 ²	
	150	1.6×10^8	2.0, 2.0	2.0 ¹ , 2.0 ¹	2.0, 2.0	1.5 ¹ , 1.5 ²	
Type 304L ss	7	2.5×10^7	0.0, 0.0	0.0, 0.0	0.0, 0.0	0.0, 0.0	
	14	4.5×10^7	0.0, 0.0	0.0, 0.0	0.0, 0.0	0.0, 0.0	
	21	6.5×10^7	0.0, 0.0	0.0, 0.0	0.0, 0.0	0.0, 0.0	
	28	8.5×10^7	0.0, 0.0	0.0, 0.0	0.0, 0.0	0.0, 0.0	
	35	1.1×10^8	0.0, 0.0	0.0, 0.0	0.0, 0.0	0.0, 0.0	
Type 307S ss	100	1.1×10^8	2.0, 2.0	- , -	2.0, 0.0	- , -	
Incoloy 823	150	1.6×10^8	0.0, 0.0	0.0, 0.0	0.0, 0.0	0.0, 0.0	
Inconel 600	150	1.6×10^8	0.0, 0.0	0.0, 0.0	0.0, 0.0	0.0, 0.0	
Inconel 625	150	1.6×10^8	0.0, 0.0	0.0, 0.0	0.0, 0.0	0.0, 0.0	
SMA 39	150	1.6×10^8	0.0, 0.0 ⁴	- , -	0.0, 0.0 ⁵	- , -	

¹ ; Max. depth of SCC on laser specimen
² ; Max. depth of SCC on dater specimen
³ ; 0.2 : failed from other than V-notched root
⁴ ; 0.3 : failed from V-notched root
⁵ ; Pitting corrosion was observed

Preliminary work at LLNL using slow-strain-rate testing under tuff repository conditions indicates that stress-assisted failure is unlikely (UCRL-89988, 1983). However, these tests are accelerated tests and do not address the very long term exposures which may be needed to initiate cracks. This work also did not include the potentially adverse effects of gamma radiolysis of solutions which would be an added source of O₂ and H₂.

Clearly, the above data from the literature show that stressed Types 304, 304L and 321 stainless steel are very susceptible to failure in steam and liquid water environments containing very low levels of Cl⁻ and O₂. In fact, the tuff repository conditions which are likely to prevail during the steam and liquid water periods appear to be much more aggressive than those cited above. It is important, therefore, to examine the likelihood of failure of NNWSI candidate container materials. In the present BNL testing program the goal is to assess the stress corrosion cracking susceptibility of the four alloys being considered by NNWSI. The tests will last for a period of up to one year in an

environment consisting of simulated J-13 groundwater in equilibrium with crushed tuff at 100°C. Below are given the experimental details of this program along with results obtained to date.

4.3 Test Plan

C-ring stress corrosion cracking testing is planned on as-received and sensitized Types 304L, 316L and 321 stainless steel and Incoloy 825. Testing will be conducted in synthetic J-13 and ten-times concentrated J-13 water in equilibrium with crushed tuff. Specimens will be tested in the steam phase above the two solutions as well as in the solutions. The testing in the steam phase corresponds to the initial period of repository life, and that in the liquid phase corresponds to the later period when the waste package would have cooled down sufficiently to prevent boiling. In the present tests, steam will be present at approximately 100°C, although in a repository the steam temperature could be initially much higher.

Tests will be conducted in parallel for three-, six- and twelve-month durations. Thus, there will be six independent test vessels, three for each solution. To obtain good statistics for the results, triplicate samples will be used for each test condition. A total of 288 specimens will be used in this test plan as described in the test matrix given in Table 4.2.

Table 4.2. Test matrix for stress corrosion of candidate stainless steels and Incoloy-825.^a

Sample Condition	Exposure Medium ^b	Total Exposure Time and Number of Samples		
		3-Month	6-Month	12-Month
Solution Annealed (SA)	J-13 Steam	3	3	3
SA + Sensitized	J-13 Steam	3	3	3
SA	J-13 Water	3	3	3
SA + Sensitized	J-13 Water	3	3	3
SA	(J-13 Steam)X10 ^c	3	3	3
SA + Sensitized	(J-13 Steam)X10	3	3	3
SA	(J-13 Water)X10	3	3	3
SA + Sensitized	(J-13 Water)X10	3	3	3

^aThis test matrix comprising 72 samples constitutes the tests on one of the four candidate materials. An identical matrix will be used for all eight materials and the total number of all specimens tested will be 288.

^bAll tests are conducted in the presence of crushed tuff.

^cThis environment is the steam/air phase above 10X concentrated J-13 well water.

4.4 Materials and Specimens

C-Rings:

Types 304L, 316L and 321 stainless steel and Incoloy 825 are the materials selected for the SCC tests. Seamless 0.75-inch o.d. x 0.125-inch wall tubing of stainless steel and 0.84-inch o.d. x 0.109-inch wall tubing for the Incoloy was purchased from Royce Aerospace Materials Corporation*. Chemical compositions and mechanical properties of these alloys, as supplied by the vendor, are given in Tables 4.3 and 4.4, respectively.

Table 4.3. Vendor supplied chemical analysis of test alloys (weight percent).

Alloy	C	Mn	Si	P	S	Cr	Ni	Mo	Ti	Al	Fe
Type 304L SS	0.016	1.95	0.48	0.038	0.025	18.54	10.55				Balance
Type 316L SS	0.016	1.94	0.37	0.035	0.010	16.66	12.80	2.02			Balance
Type 321 SS	0.028	1.03	0.74	0.026	0.002	17.41	10.75		0.24		Balance
Incoloy 825	0.02	0.44	0.27		0.001	22.34	44.14	2.78	0.84	0.07	27.26

Table 4.4. Mechanical properties of as-received test alloys (vendor supplied data).

Alloy	Ultimate Tensile Strength (MPa)	Ultimate Tensile Strength (ksi)	0.2% Offset Yield Strength (MPa)	0.2% Offset Yield Strength (ksi)	Elongation (%)	Rockwell Hardness (RB)
Type 304L SS	536	77.8	276	40.1	65.3	85.2
Type 316L SS	562	81.5	254	36.9	59.2	69.4
Type 321 SS	558	81.0	225	32.7	65	78
Incoloy 825	799	116.0	475	68.9	36	95

*West Babylon, New York.

C-ring test specimens were fabricated from the as-received (solution annealed) as well as from heat treated (sensitized) tubing for each alloy. During heat treatment the tubing was maintained at 600°C for 100 hours followed by furnace cooling. This treatment is expected to sensitize the specimens because of the formation of chromium-depleted zones adjacent to grain boundary carbides. This can lead to stress corrosion cracking along the grain boundaries. Sensitization of HLW containers can possibly occur during glass pouring or welding operations.

The procedure for testing C-ring samples is given elsewhere (ASTM, 1979). The surfaces of the as-received and heat treated tubing were rough so it was decided to obtain a consistent surface by polishing with 600-grit silicon carbide paper. Notched C-ring specimens were machined from the polished tubing according to the specifications given in Figure 4.5. Before stressing, each specimen was degreased in trichloroethane and then cleaned with Alconox soap, methanol and distilled water.

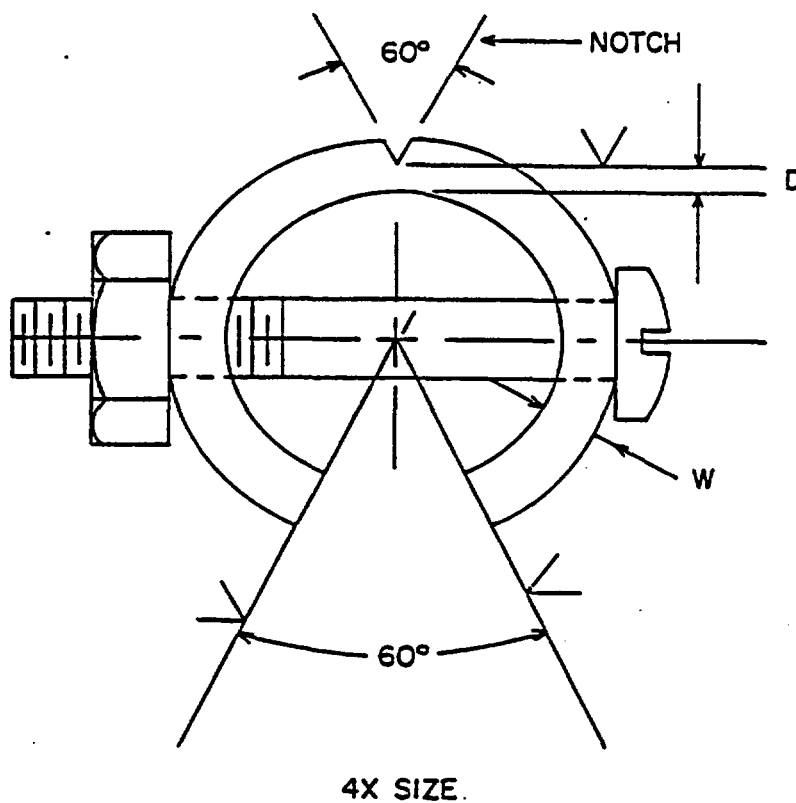


Figure 4.5. C-ring specimen design.

Tuff:

Topopah Spring tuff was supplied by Ward's Natural Science Establishment, Inc. from a surface outcrop of the Paintbrush tuff formation, southern Fran Ridge, between the J-13 well and eastern Yucca Mountain. The approximate geographical location of the site from where specimens were obtained is 116° 25' west and 36° 50' north.

The mineral composition of the rock specimens, as determined by Globo de Plomo Enterprises* using a Kevex energy-dispersive X-ray spectrometer is given in Table 4.5. Aluminum is the lightest element which could be determined quantitatively. The results are normalized to SiO₂ whose absolute concentration was not determined. As was clear from visible observation, the rock specimens had varying appearance and, hence, also varying composition from rock to rock. Results in Table 4.4 represent a typical composition. A brief geochemical description of the tuff given by Globo de Plomo Enterprises is presented below:

"The rock is a welded vitric tuff of rhyolite composition composed of flattened glass fragments kneaded into a streaky fabric. Welding has not been sufficient to blur fragment boundaries. The fragments carry scattered phenocrysts of sanidine with less plagioclase and oxidized biotite. Traces of augite and oxyhornblende were observed in addition to accessory magnetite. Other accessories found near magnetite and mafites include zircon, allanite, and monazite.

"All of the glass domains have just begun to devitrify, producing orthoclase, quartz, and iron oxides. Tridymite lines collapsed voids and has formed in certain frothy glasses instead of quartz. Some larger voids are lined with chalcedony, then tridymite, then iron oxides, and are infilled with caliche-like calcite.

"A polished section reveals that accessory magnetite grains are penetrated and about half replaced by tablets of hematite. Rutile was also observed.

"Phenocrysts comprise about 20% of the rock by volume and a breakdown is: plagioclase 30%, biotite 5%, augite 2%, magnetite 2%, oxyhornblende 1%, sanidine 60%. Matrix components are too fine grained and intimately intergrown to estimate."

The as-supplied tuff specimens were too large to be used in the corrosion tests. Therefore, they were crushed into small pieces which were then sieved to separate them into two sizes, viz. coarse (0.25 in.-0.50 in.) and fine (0.187 in.-0.250 in.). In a preliminary test to estimate the solution chemistry crushed tuff of a finer size (0.0165 in.-0.187 in.) was used.

*P. O. Box 872, Douglas, Arizona.

Table 4.5. Geochemical analysis of Topopah Spring tuff (values in ppm unless percent is specified).

Al ₂ O ₃	13.1%
K ₂ O	4.52%
CaO	2.21%
TiO ₂	0.38%
MnO	0.07%
Fe ₂ O ₃	1.83%
Cu	17
Zn	35
As	22
Th	18
Rb	116
Sr	109
Y	17
Zr	482
Nb	13
Sb	15
Ba	314
La	62
Ce	83

Groundwater:

Although there is no information available on the composition of groundwater which would come in contact with the waste package in tuff, groundwater from the J-13 well (which is located below the repository horizon) has been designated as the reference test solution (UCRL-89988, 1983). A chemical analysis of reference J-13 groundwater as given in Table 4.6 has been specified by DOE subcontractors (UCRL-89988, 1983) but there is no procedure given for its preparation in the laboratory. The J-13 water used by NNWSI is obtained from the actual site rather than prepared artificially. Therefore, a solution preparation procedure was developed at BNL.

Table 4.6. Reference groundwater composition for tuff repositories (based on composition of Jackass Flats Well J-13 at the Nevada Test Site).

	Concentration (mg/liter)
Lithium	0.05
Sodium	51.0
Potassium	4.9
Magnesium	2.1
Calcium	14.0
Strontium	0.05
Barium	0.003
Iron	0.04
Aluminum	0.03
Silica	61.0
Fluoride	2.2
Chloride	7.5
Carbonate	0.0
Bicarbonate	120.0
Sulfate	22.0
Nitrate	5.6
Phosphate	0.12

pH - slightly basic (7.1).

Fourteen reagents were selected such that their solution in water would give ionic concentrations very close to that found in reference J-13 groundwater. The amount of chemical compounds added to distilled water to make 20 liters of synthetic J-13 water is given in Table 4.7. Initially, there was a problem in dissolving the required amount of silicic acid. With some trial and error and considering higher solubility of silica at higher temperature and pH, this problem was resolved by first adding NaHCO_3 to distilled water, heating it to near boiling and then adding silicic acid; other compounds were added subsequently.

Table 4.7. Amount of chemical compounds used in preparing 20 liters of synthetic J-13 water (mg).

1.	NaHCO ₃	3292
2.	KOH	140
3.	SiO ₂ ·XH ₂ O (1.87% H ₂ O)	1243
4.	CaCl ₂	232
5.	CaSO ₄ (460 mg CaCO ₃ + 440 mg H ₂ SO ₄)	624
6.	Ca(NO ₃) ₂	48
7.	Mg(NO ₃) ₂ ·6H ₂ O	256
8.	MgF ₂ (46.6 mg MgO + 96.5 mg HF - 48%)	72
9.	LiNO ₃	10
10.	Sr(NO ₃) ₂	2.4
11.	BaCl ₂ ·2H ₂ O	1.8
12.	Fe(NO ₃) ₃ ·9H ₂ O	7.2
13.	H ₃ PO ₄ (85%)	2.8
14.	Al(NO ₃) ₃ ·9H ₂ O	13.9

As mentioned above, groundwater coming in contact with a HLW canister can have much higher ionic concentrations than in J-13 groundwater. This would happen when salts, precipitated during initial evaporation of groundwater, are redissolved as new cooler groundwater arrives at a later time. Since there are no estimates available for this groundwater concentration effect, we have arbitrarily assumed a concentration factor of ten. However, for a ten-times concentration solution some of the species (e.g. SiO₂, divalent cations) may be already past their saturation limit at room temperature. However, the solubility would be increased at the 100°C test temperature used. The equilibrium composition of ten-times concentrated J-13 water at 100°C is difficult to determine. Therefore, we have added ten times the quantity of salts needed for synthetic J-13 water and let the salts (including those insoluble at room temperature) equilibrate at 100°C. Such a liquid, which is not transparent at room temperature, provides ten times higher ionic concentration of the soluble species and saturation concentration of insoluble species of the corrosion specimen kept at 100°C. In the actual tests to be performed the solution composition will be further modified due to the interaction between water and crushed tuff. Thus, post-test analysis of the solutions were carried out.

4.5 Apparatus

The tests are conducted in six identical test vessels (corresponding to six different test conditions). One is shown in Figure 4.6. In each unit, C-ring specimens along with crushed rock and test solution are stacked in a 4-liter Pyrex vessel. Approximately 6/7 of the vessel height is enclosed within an electrical furnace. The lid of the vessel has space for four connections, two of which are kept closed. A thermometer and a cold water condenser are placed in the other two receptacles. Flowing cold water helps in condensing the steam approaching the condenser to water which drips back into the kettle. The top of the condenser is open to the atmosphere so that some air is present.

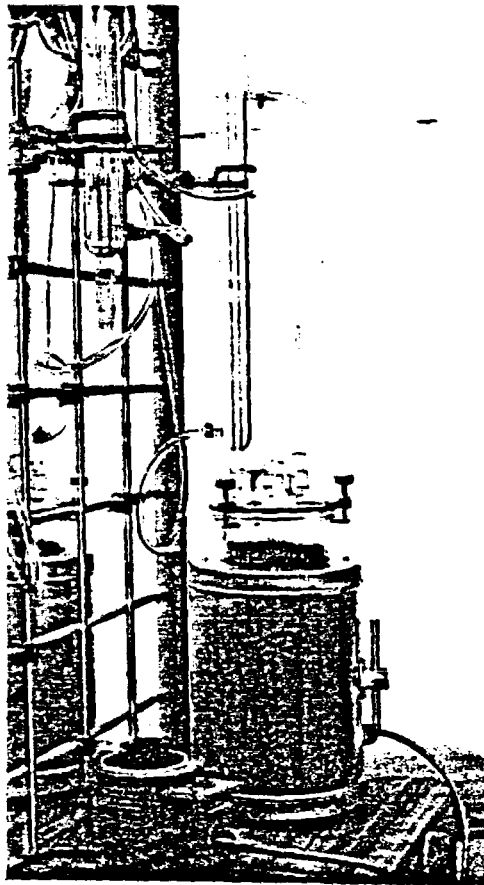


Figure 4.6. C-ring stress corrosion cracking test apparatus.

To measure the in situ pH of the solution during a test it becomes necessary to have easy access to the solution. For this purpose, a 15-mm o.d. quartz tube with many small holes along its length is placed in the center of the vessel. A microcombination pH probe (MI-410, Microelectrodes, Inc.) can be inserted in this tube from the top of the vessel and the solution pH measured with a standard pH meter.

4.6 Test Procedure

According to the test plan, a C-ring specimen is supposed to be stressed such that stress levels at the apex of an unnotched (smooth) specimen would be 90 percent of the elastic limit at room temperature. Therefore, one smooth C-ring specimen for each of the eight alloys (three stainless steels and Incoloy 825 in the as-received and sensitized conditions), identical in dimensions to notched test specimens, was tested in an Instron machine to obtain stress-strain characteristics. A typical load vs deflection curve is shown in Figure 4.7 for as-received Type 304L sensitized stainless steel; the C-ring was stressed in the same orientation as expected from the usual nut and bolt arrangement. The load and deflection at the elastic limit (shown by arrow) obtained from such curves are given in Table 4.8. The notched C-ring test specimens

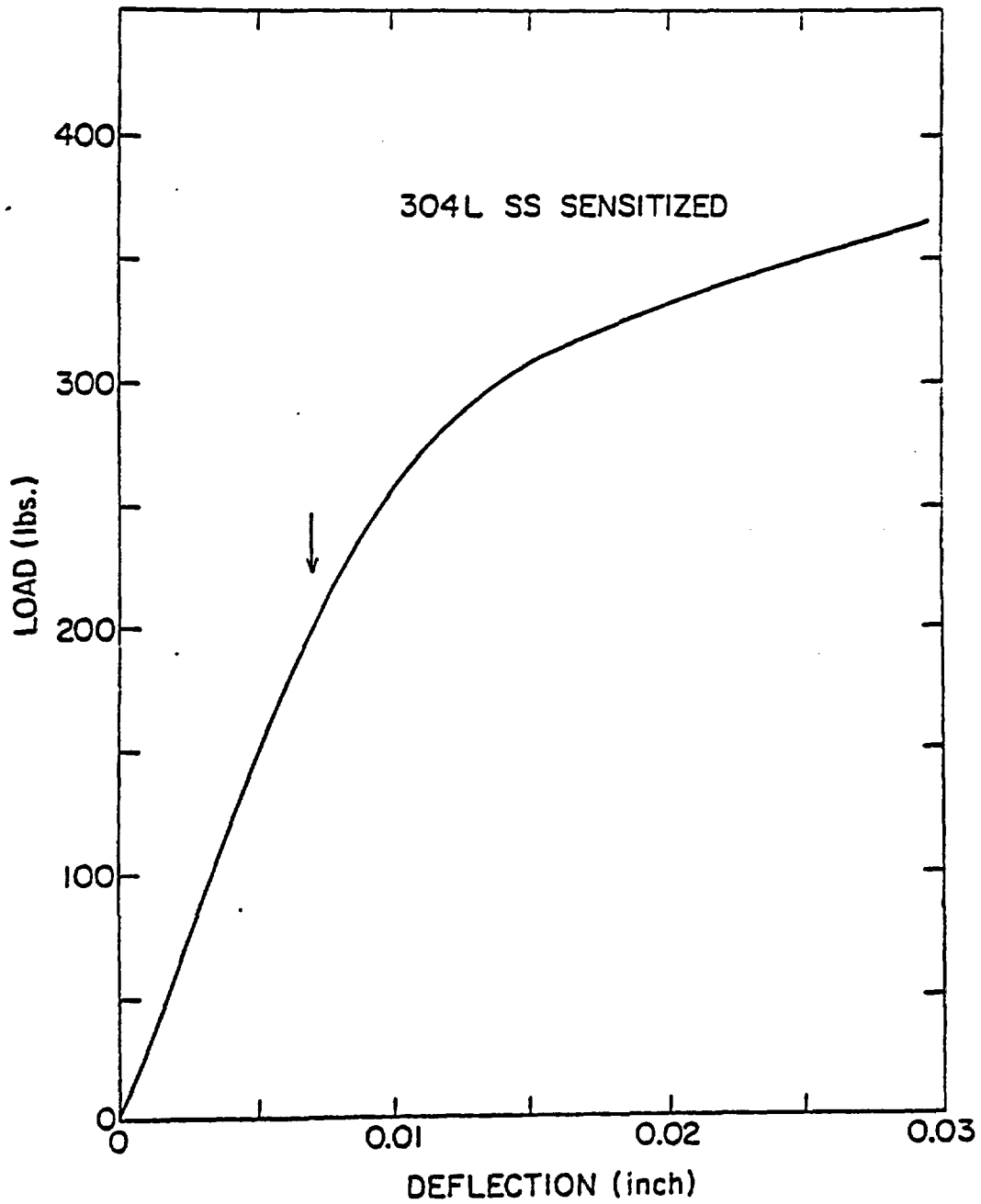


Figure 4.7 Load vs deflection of Type 304L stainless steel sensitized C-ring test specimen under compression.

were stressed with the help of commercial stainless steel nuts and bolts such that the change in o.d. was 90% of the deflection at the elastic limit (Table 4.8).

Table 4.8. Stress-strain properties of eight alloys as obtained from Instron machine tests on smooth C-ring specimens.

Alloy	Load at 100% Elastic Limit (kg)	Deflection at 100% Elastic Limit (cm)	Deflection at 90% Elastic Limit (cm)	Longitudinal Strain at Elastic Limit (10^{-6})
Type 304L SS (as-received)	102.0	0.0254	0.0229	1564
Type 304L SS (sensitized)	90.7	0.0178	0.0160	1339
Type 316L SS (as-received)	124.5	0.0356	0.0320	1730
Type 316L SS (sensitized)	113.4	0.0267	0.0241	1517
Type 321 SS (as-received)	79.4	0.0163	0.0147	1200
Type 321 SS (sensitized)	90.7	0.0178	0.0160	1198
Incoloy 825 (as-received)	170.1	0.0394	0.0356	2770
Incoloy 825 (sensitized)	283.5	0.0610	0.0549	3707

A specific mark was indented on the side of a specimen to identify the alloy. Triplicate samples of each alloy were stacked within the crushed tuff in two layers at two levels in a test vessel (Figure 4.8). The samples at the lower level were submerged in solution whereas those at the upper level were surrounded by crushed tuff, air and steam. Note that the C-ring specimens were surrounded only by fine size crushed tuff. Before filling the vessel with tuff, the pH tube was placed in the center of the vessel. Care was exercised so that no specimens touched.

Crushed rock surrounding the specimens filled nearly to the top and approximately 1100 cc of test solution was added to bring the liquid level to half the depth of the vessel. After some time the liquid became slightly lower

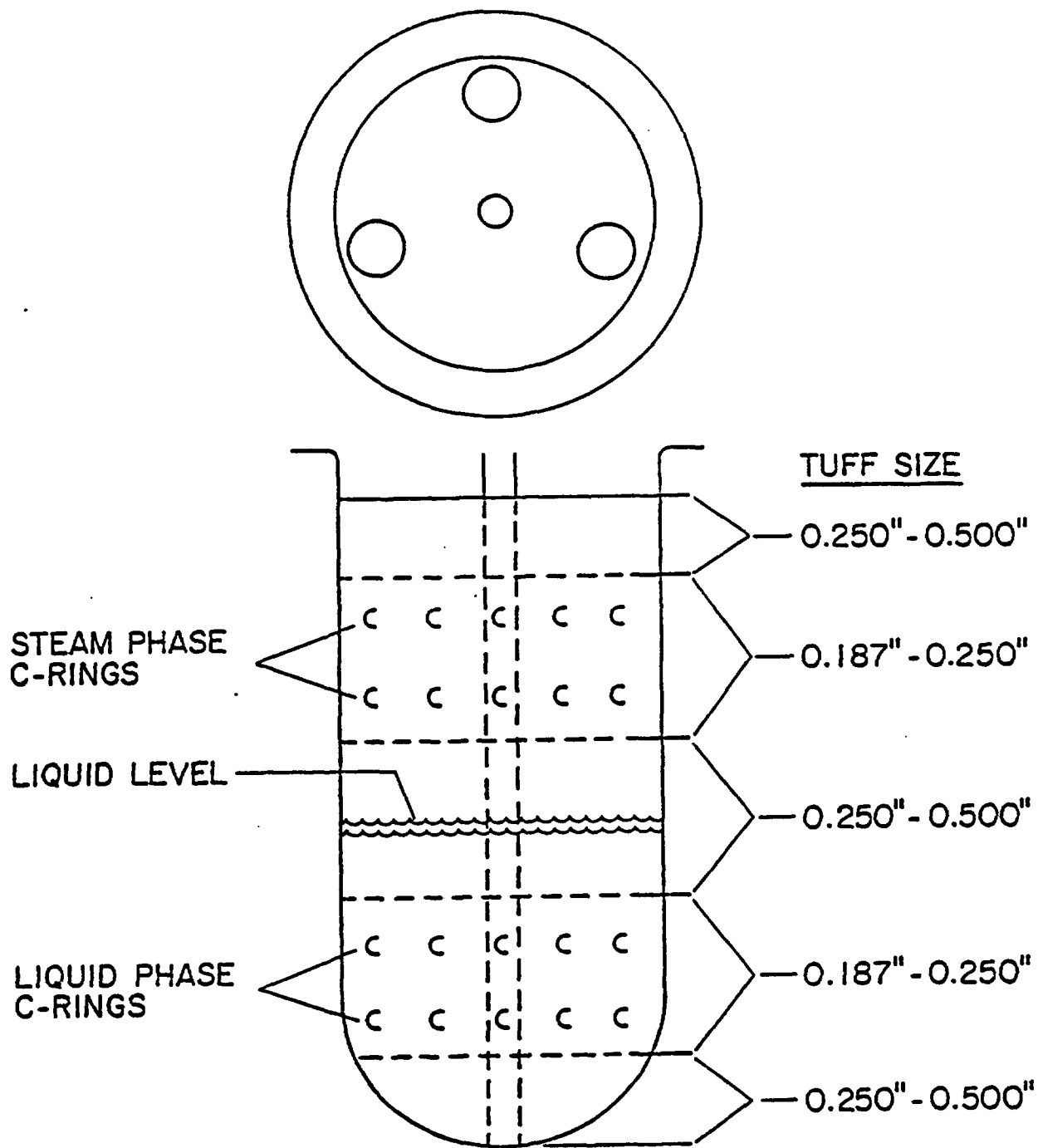


Figure 4.8. Schematic of the specimen arrangement in a test vessel.

presumably due to soaking by the rocks but the lower level specimens were always well submerged in solution as confirmed by checking the water level every week. After putting the lid with thermometer and condenser in place, the vessel was slowly heated to bring the solution to boiling. The furnace power was adjusted so that the water from the condenser dripped at a rate of 5-10 drops per minute.

4.7 Results to Date

The notched C-ring specimens used in the present study were stressed to 90% of the elastic limit measured at the apex of smooth specimens. The notches in the specimens would result in local deformation. This was confirmed by the observation that when the stress on selected specimens was removed, the deflection was only partially recovered. Such stress concentration effects could occur on the surface of a HLW container when, for example, scratches or dents are inadvertently produced during handling.

An attempt was made to determine the strain present on the surface of a smooth C-ring specimen. Three longitudinal and one transverse strain gauges were attached on the outer surface of the specimen which was then compressed in an Instron machine. A typical load vs strain curve from these measurements is shown in Figure 4.9 for as-received Type 316L stainless steel. The average value of three longitudinal strains corresponding to elastic limit is given in Table 4.8.

The metallographic examination of Types 304L, 316L and 321 stainless steel and Incoloy 825 have been completed. A comparison of microstructures for the as-received (annealed) and heat treated condition shows that the heat treatment (100 hours at 600°C, followed by furnace cooling) has sensitized the stainless steels by precipitating carbides at the grain boundaries. Such an observation is much less evident in the case of Incoloy 825, for which the heat treatment has resulted in the precipitation of second-phase particles (probably TiC).

It is interesting to note that sensitization in the stainless steels is stronger near the surfaces of the C-ring specimens. These surfaces are the inner and outer diameters of the tubing from which the samples were fabricated. Figure 4.10 shows this effect for Type 304L stainless steel for which the microstructure near the outer diameter is more heavily etched. This preferential sensitization is most likely due to unavoidable contamination from lubricants, coupled with higher residual stresses at the tubing surfaces during manufacturing processes. The extra surface strain energy enhances carbide nucleation and growth processes. For a HLW stainless steel container, this observation suggests that any stresses introduced on the container surface during its production or handling would enhance its susceptibility to sensitization and, therefore, to stress corrosion cracking.

A few days after starting each test, small white precipitates appeared on some of the tuff pieces near the top of the vessel and also on the inside of the vessel. These are presumably due to vapor phase transport of some compound in solution. We plan to characterize the white compound at the end of each test and hope to evaluate its effect on metal corrosion.

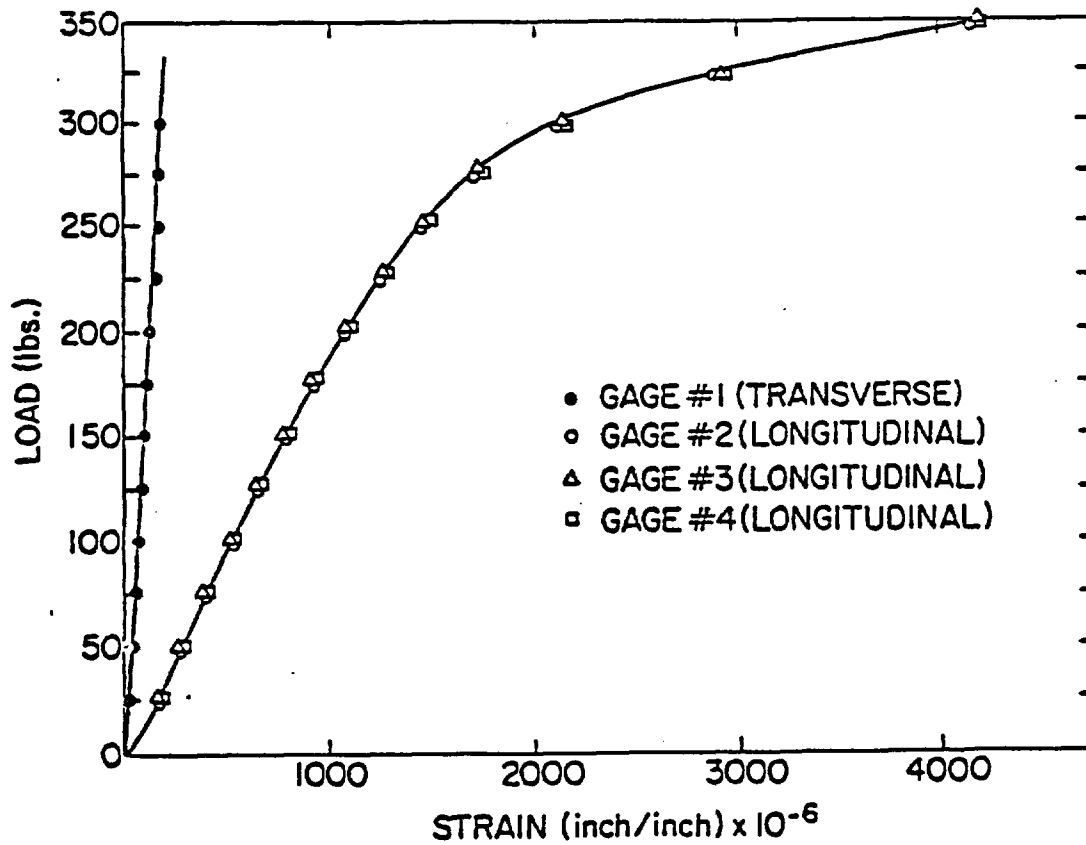
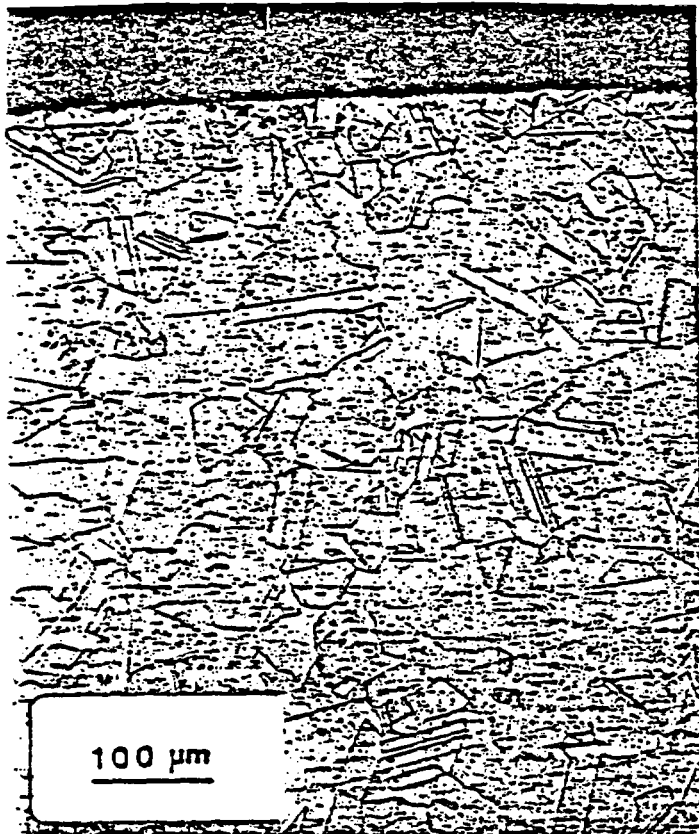
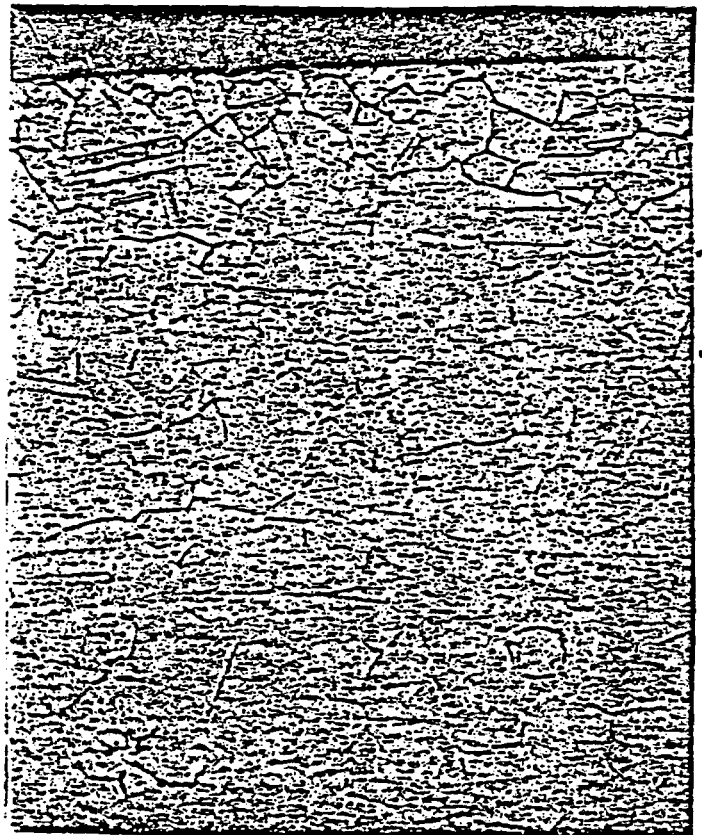


Figure 4.9. Load vs in situ strain at the apex of a Type 316L stainless steel C-ring specimen.



(a)



(b)

Figure 4.10. Microstructure of Type 304L stainless steel.
(a) As-received, etched in glyceric acid.
(b) Sensitized at 600°C for 100 hours, etched in oxalic acid.

The pH of as-prepared J-13 and ten-times concentrated J-13 water at room temperature was determined to be 8.4 and 8.3, respectively. When these solutions were heated to boiling, the pH decreased to 6.9 and 7.9, respectively. Subsequent changes during tests are shown in Figure 4.11. After an initial sharp increase, the solution pH appears to be decreasing slowly with time. However, there is a large amount of scatter from vessel to vessel, and additional long-term results are needed to confirm this trend.

The six- and twelve-month tests are continuing and the three-month test has been just terminated. The pH of the solution at the end of the three-month test has been measured. The value increased with decreasing temperature as shown in Table 4.9. Nearly equal values of pH were measured for both the test solutions suggesting that the crushed tuff may be buffering the water by steam.

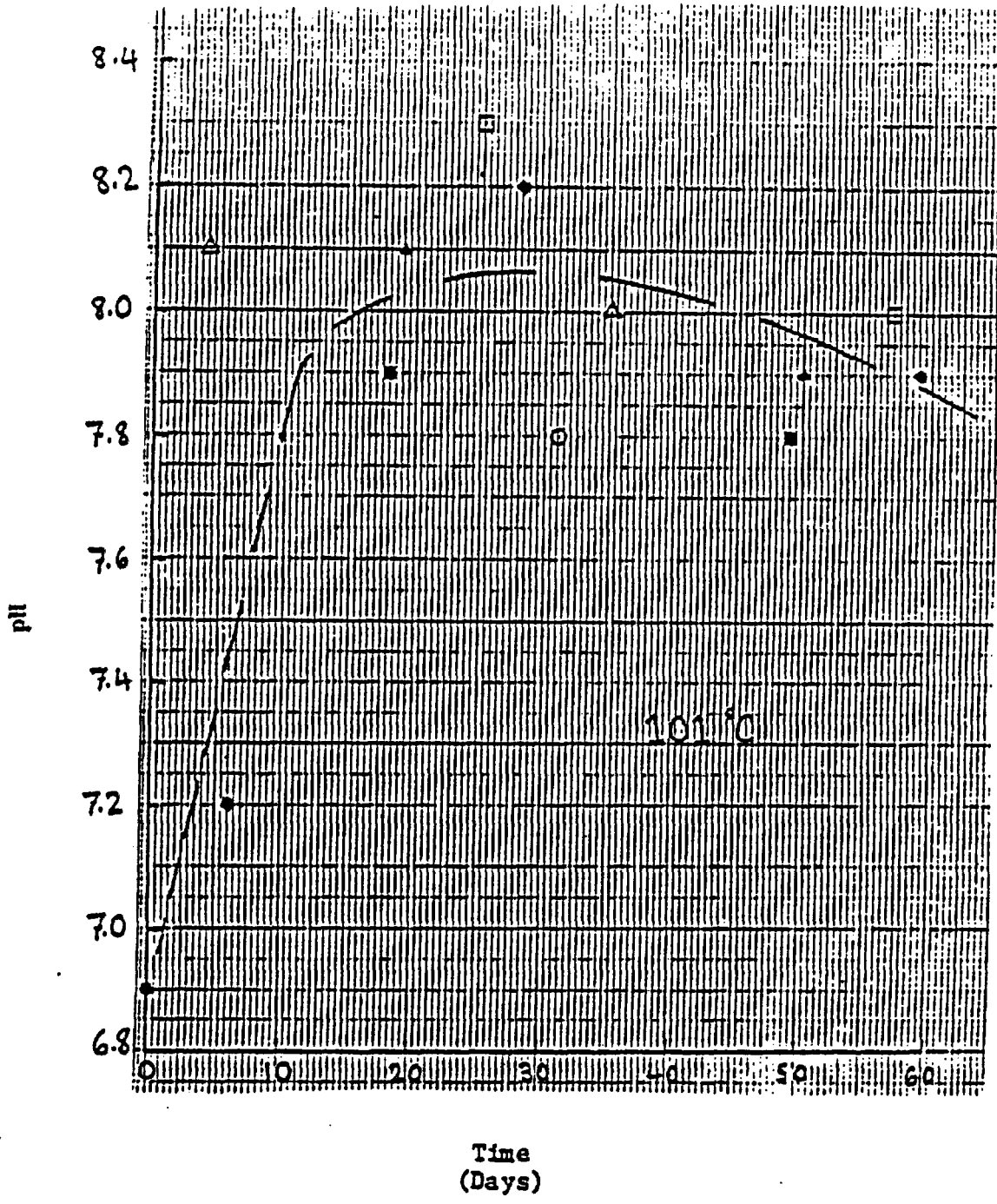


Figure 4.11. pH of the six test solutions at 101°C as a function of time. Each symbol represents the solution in one test vessel.

Table 4.9. pH of test solutions at the end of the three-month tests.

J-13 Solution		Concentrated J-13 Solution	
Temperature (°C)	pH	Temperature (°C)	pH
101.4	7.7	101.7	7.6
68.0	8.1	50.0	8.1
60.0	8.1	44.0	8.2
35.0	8.3	33.0	8.3
27.0	8.4	26.5	8.4

The C-ring specimens from the three-month tests have been only briefly examined. No macroscopic cracks have been found on these samples, but in some cases initiation of pitting is apparent. A complete examination will be conducted in the near future which would show whether or not any microcracks are present. All C-ring specimens placed in solution have a generally uniform coating of salt and corrosion scale, whereas stainless steel specimens in the steam phase show patches of unreacted metal surrounded by a brown, rust-colored scale (Figure 4.12). Incoloy specimens in steam do not show any corrosion scale. It appears that stainless steel specimens did not corrode in the areas touching tuff pieces. Such areas apparently had a film of relatively pure condensed water whereas the rest of the sample was exposed to steam and air.

The chemical analyses of the solution obtained from the central tube at the end of the three-month tests are given in Table 4.10; results for Na^+ , K^+ and NO_3^- will become available in the near future. Note that ionic concentrations are much higher than J-13 groundwater (Table 4.6). Part of the increased ionic concentration may be from dissolution of salts present in the tuff (see below results from preliminary groundwater chemistry test). To estimate solution chemistry at 100°C, 100 mL specimens of the hot test solution were mixed with boiling distilled water and filtered through Whatman 42 paper (specimens No. 6 and No. 9). The dilution was expected to prevent precipitation on cooling. Solution No. 7 and No. 10 were not diluted but filtered as before. To determine the concentration of any particles suspended in solution, Sample No. 7 was also analyzed without filtering (called No. 8). A comparison of the two (Table 4.10) indicates that there is no significant amount of suspended solid material which could be filtered through a Whatman 42 paper. A comparison of results for undiluted and diluted solutions suggests that dilution by a factor of two reduces the concentrations approximately by a factor of two for all species. Therefore, no significant precipitation appears to occur during the cooling of undiluted solution.

To estimate the possible range of solution chemistry a parallel test was conducted in a vessel similar to the ones used in the C-ring tests. It was filled with crushed tuff of relatively fine size (0.165 to 0.187 inch) and distilled water and then equilibrated under boiling water conditions. Crushed tuff was used in the as-received condition. The chemical analysis of the water after a test period of one month (Table 4.11) suggests that major cations and

anions can be present in concentrations much larger than assumed in J-13 reference groundwater. Apparently, large ionic concentrations were found in the as-received tuff equilibrated water due to the dissolution of salts present in tuff outcrop material. To determine the extent of such contributions to the chemical composition of groundwater, the test was continued, first by draining all the existing solution, and then adding 1150 mL of distilled water. The test vessel was heated to and maintained under boiling water conditions for a period of one month just as in the C-ring tests. The chemical analysis of a water sample obtained at the end of this test is given in the last column of Table 4.11. We note that although the ionic concentration in the second test is lower by a factor of two to four than in the first test, it is still much higher than in the reference J-13 groundwater. Thus, high anion concentrations (e.g. Cl^-) in the second water sample suggests that the use of J-13 groundwater composition in container corrosion studies may not correspond to the most severe possible conditions in a tuff repository.

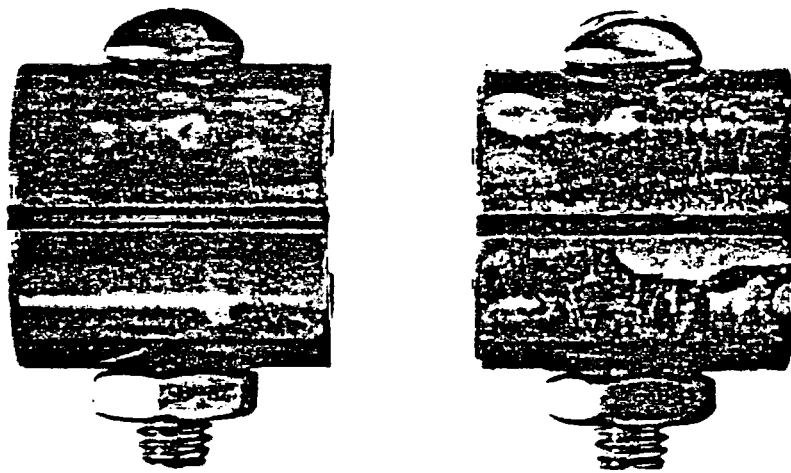


Figure 4.12. C-ring specimens of Type 321 sensitized stainless steel after three-month test in "synthetic J-13 water." The specimen on left was exposed to liquid phase and the one on the right was exposed to steam phase (X2.2).

Table 4.10. Chemical composition of test solutions obtained at the end of three-month tests ($\mu\text{g/mL}$).

	Starting Solution: Synthetic J-13 Water		Starting Solution: Ten-Times Concentrated J-13 Water		
	Sample No. 7 (Undiluted, Filtered)	Sample No. 6 (Diluted, Filtered)	Sample No. 10 (Undiluted, Filtered)	Sample No. 9 (Diluted, Filtered)	Sample No. 11 (Undiluted, Unfiltered)
Mg	<0.05	<0.05	<0.05	<0.05	<0.05
Ca	308	151	301	161	332
Fe	<0.1	<0.1	<0.1	<0.1	<0.1
Ni	<0.1	<0.1	<0.1	<0.1	<0.1
Sr	3.35	1.97	4.38	2.18	4.24
Al	<2.0	<2.0	<2.0	<2.0	<2.0
Cu	<0.1	<0.1	<0.1	<0.1	<0.1
F ⁻	12.1	7.1	14	8.9	15
Cl ⁻	130	72	330	160	330
SO ₄ ²⁻	820	420	1300	660	1300
PO ₄ ³⁻	<1	<1	<1	<1	<1
SiO ₂	414	219	408	205	421

Table 4.11. Room temperature chemical composition of filtered solutions obtained from the reaction of distilled water with crushed tuff. Composition of reference J-13 groundwater is included for the purpose of comparison ($\mu\text{g/mL}$).

	J-13 Groundwater	Test Solution Following One-Month Equilibration of Crushed Tuff With Distilled Water	Test Solution Following the Subsequent One- Month Equili- bration of the Same Crushed Tuff With Fresh Distilled Water
Na ⁺	45	308	190
K ⁺	4.9	50.5	21
Mg ⁺	2.1	Not determined	<0.1
Ca ²⁺	14	930	298
F ⁻	2.2	8.5	<4
Cl ⁻	7.5	160	43.7
HCO ₃ ⁻	120	Not determined	Not determined
SO ₄ ²⁻	22	343	530
NO ₃ ⁻	5.6	460	188
PO ₄ ³⁻	0.12	Not determined	Not detected
Silica	61	95.1	142
pH (at room temperature)	8.5	8.4	8.5 7.6 (at 100°C)

4.8 References

ASTM, Annual Book of Standards, Part 10, Making and Using C-Ring Stress Corrosion Test Specimens, Designation G38-73, 1979.

Birchon, D. and G. G. Boothe, "Stress Corrosion Cracking of Some Austenitic Stainless Steels as Affected by Surface Treatment and Water Composition," in Proceedings of 2nd International Congress on Metallic Corrosion, NACE, 1964, p. 33.

JAERI-M-82-145, "Progress Report on Safety Research of High Level Waste Management for the Period April 1981 to March 1982," S. Ashiro, JAERI, 1982.

Russell, E. W. and others, "Selection of Barrier Metals for a Waste Package in Tuff," in Scientific Basis for Nuclear Waste Management, VII, G. L. McVay, Editor, New York, North Holland, 1984, p. 763.

UCRL-89988, "Selection of Candidate Canister Materials for High Level Nuclear Waste Containment in a Tuff Repository," R. D. McRight and others, University of California Radiation Laboratory, November 1983.

Warren, D., "Chloride-Bearing Cooling Water and the Stress Corrosion Cracking of Iron-Nickel-Chromium Alloys," in Proceedings of the 15th Industrial Waste Conference, 1960, p. 420.

Williams, W. L., "Chloride and Caustic Stress Corrosion of Austenitic Stainless Steel in Hot Water and Steam," Corrosion 13, 539A, 1957.

WORKSHOP ON THE COUPLING OF GEOCHEMICAL AND HYDROLOGIC MODELS

In connection with the ISIRS Project, a workshop was held at the OECD in Paris in June 1984 to discuss the coupling of geochemical and hydrologic models. It was attended by 46 specialists from 13 countries and the Commission of the European Communities. A report on the workshop, available from the NEA Secretariat free upon request, will shortly be available. Some of the principal general conclusions, as endorsed by the ISIRS Technical Committee, were:

- 1) There is a definite need for some coupling between geochemical and hydrologic models in nuclear waste performance assessment. This need arises from the inherently coupled nature of radionuclide migration which is dependent on advection, on dispersion and on chemical processes. There is no, and there need not be, a unique method to perform this coupling. Specific problems and analyses of specific systems require individual approaches.
- 2) Coupling in this context is not limited to mean exclusively the co-execution of geochemical and hydrologic computer codes but is intended to encompass all methods of passing data and of merging geochemical and hydrologic understanding in performance assessment modelling.
- 3) The development of "megacodes" (i.e. very large directly coupled hydrochemical-geologic computer codes capable of performing detailed calculations in both areas for a wide variety of problems and conditions) is practically unrealistic and undesirable. Indirect coupling methods and the coupling of limited submodels should nevertheless provide useful tools for helping to answer a number of specific questions. Since comprehensive megacodes are impractical, an understanding is desirable of where simplifications can be made.
- 4) Coupled models are only one tool among a wide variety which may be used to predict potential radionuclide migration. These models must be used in conjunction with larger thermodynamically-based geochemistry codes, with laboratory work and with observation of nature (natural analogs). Reaction kinetics and colloid formation cannot be neglected.
- 5) Basic to the use of any of these predictive techniques is the understanding of the physical and chemical processes involved. This understanding must be developed in order to maximise confidence in predictions.

WORKSHOP ON EXPERIMENTAL METHODOLOGIES IN RADIONUCLIDE SORPTION STUDIES

The summary document of this workshop, held 6th and 7th June in Paris, has now been published. This report, entitled "Sorpton Modelling and Measurement for Nuclear Waste Disposal Studies", is available at no cost upon request to the NEA Secretariat.

Attachment-5

NUREG/CR-2482
BNL-NUREG-51494
Vol. 8

REVIEW OF DOE WASTE PACKAGE PROGRAM
DRAFT BIENNIAL REPORT

M. S. DAVIS, Editor

CONTRIBUTORS:

C. Brewster
M. S. Davis
E. Gause
H. Jain
C. Pescatore
P. Soo
T. Sullivan
E. Veakis

Manuscript Completed - January 1985

Prepared by the Nuclear Waste Management Division
P. Soo, Head
Department of Nuclear Energy, Brookhaven National Laboratory
Associated Universities, Inc.
Upton, New York 11973

Prepared for the U. S. Nuclear Regulatory Commission
Office of Nuclear Materials Safety and Safeguards
Contract No. DE-AC02-76CH00016
FIN No. A-3164

ABSTRACT

A large number of technical reports on waste package component performance were reviewed over the last year in support of the NRC's review of the Department of Energy's (DOE's) Environmental Assessment reports. The intent was to assess in some detail the quantity and quality of the DOE data and their relevance to the high-level waste repository site selection process. A representative selection of the reviews is presented for the salt, basalt and tuff repository projects. Areas for future research have been outlined.

CONTENTS

	<u>Page</u>
ABSTRACT.	111
ACKNOWLEDGEMENT	vi
EXECUTIVE SUMMARY	1
1. INTRODUCTION	3
2. COMPILATION AND REVIEW OF RELEVANT DOE WASTE PACKAGE DATA	5
2.1 Basalt Repository Project (Appendices 1 and 4).	5
2.1.1 Waste Form Evaluations	5
2.1.2 Container Evaluations.	6
2.1.3 Packing Material Evaluations	7
2.2 Salt Repository Project (Appendices 2 and 4).	8
2.2.1 Waste Form Evaluations	8
2.2.2 Container Evaluations.	8
2.2.3 Packing Material Evaluations	9
2.3 Tuff Repository Project (Appendices 3 and 4).	9
2.3.1 Waste Form Evaluations	9
2.3.2 Container Evaluations.	10
2.3.3 Packing Material Evaluations	10
2.4 Modeling of Waste Package Performance	11
3. ACCURACY, RELIABILITY, AND APPLICABILITY OF WASTE PACKAGE DATA	11
4. WASTE PACKAGE ISSUES RELEVANT TO SITE SELECTION.	13
5. CONCLUSIONS.	13
6. REFERENCES	15
APPENDIX 1 - REVIEW OF WASTE PACKAGE DATA FOR BASALT REPOSITORY PROGRAM.	A1-1
APPENDIX 2 - REVIEW OF WASTE PACKAGE DATA FOR SALT REPOSITORY PROGRAM.	A2-1
APPENDIX 3 - REVIEW OF WASTE PACKAGE DATA FOR TUFF REPOSITORY PROGRAM.	A3-1
APPENDIX 4 - REVIEW OF GENERAL WASTE PACKAGE DATA	A4-1
APPENDIX 5 - DETAILED REVIEWS OF WASTE PACKAGE DATA	A5-1

ACKNOWLEDGMENTS

The authors gratefully acknowledge the assistance of Ms. M. McGrath, Mrs. G. Searles, Ms. S. Bennett and Mrs. A. Spira in the typing and preparation of this report.

EXECUTIVE SUMMARY

As part of the Waste Package Program, BNL has carried out a review of recent DOE waste package research data for the basalt, salt and tuff repository programs. The intent was to assess the quantity and quality of the data with respect to the DOE repository site selection process. The work included:

- a. Compiling a list of recent reports, data and assumptions pertinent to waste package performance for the three host rocks.
- b. Assessing the accuracy, reliability and applicability of DOE data on waste package performance.
- c. Identifying, using the data reviews, those issues which will determine the suitability of a site for further evaluation and development.
- d. Determination of the additional data needed for package performance assessment.

Most of the testing to date has centered on individual package components but there is some information on the effects of component interactions on waste form leaching and container corrosion. Nevertheless, there is a severe lack of whole package testing work either in the form of laboratory tests or in situ evaluations. Because of this, there is very limited information on the effect of waste emplacement on the geochemistry and rock characteristics of basalt, salt and tuff. Since these two geotechnical factors are included as DOE's site selection criteria, a complete rationale for selecting a particular site for further development cannot be made. Thus, one expects that those sites which appear to have the fewest limitations, based on limited available data, will be selected for additional study.

The additional information which would be useful in an evaluation of the interactions of the immediate environment with the waste package includes the following which relate to the geochemistry and rock characteristic site selection guidelines in 10 CFR 960.

- a. Data are needed to quantify how early boiling of groundwater, and associated precipitation of dissolved solids and host rock alteration, will change the composition of water subsequently entering a waste package borehole when boiling ceases. Major changes in repository water composition, pH and redox condition may render invalid much of the current waste package performance data.
- b. A more accurate quantification of the water ingress rate into the repository and the rate of pressurization is required.
- c. Information on the cracking of basalt and tuff host rock arising from repository excavation and the high temperatures caused by waste emplacement is needed.

- d. For basalt and salt it is known that the horizontal component of the lithostatic stress is much larger than the vertical component. The effect of the large horizontal stress on waste package/repository integrity needs to be addressed.
- e. There is a need to outline the most likely scenarios for engineered barrier system failure/degradation so that relevant performance assessment calculations can be conducted. Without such information there will be considerable uncertainty in determining containment failure times, controlled release rates and releases to the accessible environment.
- f. The ease of waste package retrieval will vary for the different host rocks. It seems to be more difficult for a salt site since the high temperatures during the repository operations period may cause the host rock to creep towards the waste package, thereby sealing it in place if a borehole liner is not used. A description is needed of the procedures to be undertaken to ensure ease of retrieval for all candidate sites.
- g. Documentation is required on pre-closure package and repository monitoring procedures that will be needed to confirm that the repository and waste package are performing within established design limits.

At this time, it seems that the site selection process, which is currently centered on Environmental Assessment report analysis, will not be dominated by engineered barrier system factors since, in most cases, limitations in the repository site can be mitigated by changes in the design of the barrier system. Thus, there should be comprehensive research and development to evaluate the interaction of the engineered barrier system and the host geology so that finalized designs can be established.

1. INTRODUCTION

The Nuclear Waste Policy Act of 1982 mandates that in the development of high-level nuclear waste repositories, Environmental Assessment (EA) reports shall be prepared for each candidate repository site. The reports will contain a description and evaluation of each site based on a set of site-selection guidelines specified by DOE in order to determine which sites would be suitable for further development. A list of the proposed guidelines is given in the Code of Federal Regulations (10 CFR 960, February 7, 1983). They include consideration of:

1. Site geometry
2. Geohydrology
3. Geochemistry
4. Rock characteristics
5. Tectonic environment
6. Human intrusion.
7. Surface characteristics
8. Population density and distribution.

Clearly, most of these factors are concerned with natural site characteristics which will not be influenced by waste emplacement. The exceptions are to be found in the guidelines on Geochemistry and Rock Characteristics. Relevant parts of these sections of 10 CFR 960 are reproduced below:

10 CFR 960.5-3 Geochemistry

The site shall have geochemical characteristics compatible with waste containment, isolation, and retrieval. The site shall be such that the chemical interactions among radionuclides, rock, groundwater, and engineered components would not lead to a projection of radionuclide releases greater than those discussed in §960.3-2.

(a) Favorable conditions. (1) The nature and rates of the geochemical processes operating within the geologic setting during the past million years would, if continued in the future, not affect or would favorably affect the ability of the geologic repository to isolate the waste [10 CFR 60.122(b)(1)].

(2) Geochemical conditions that promote the precipitation or sorption of radionuclides; inhibit the formation of particulates, colloids, and inorganic and organic complexes that increase the mobility of radionuclides; or inhibit the transport of radionuclides by particulates, colloids, and complexes [10 CFR 60.122(b)(4)].

(3) Mineral assemblages that, when subjected to the expected thermal loading, will remain unaltered or will be altered to mineral assemblages with equal or increased capability to inhibit radionuclide transport [10 CFR 60.122(b)(5)].

(b) Potentially adverse conditions. (1) Groundwater conditions in the host rock — including chemical composition, high ionic strength, or oxidizing or reducing conditions and pH — that could increase the solubility or chemical reactivity of the engineered barrier systems [10 CFR 60.122(c)(8)].

(2) Geochemical processes that would reduce the sorption of radionuclides, result in the degradation of the rock strength, or adversely affect the performance of the engineered barrier systems [10 CFR 60.122(c)(9)].

(3) For disposal in the saturated zone, groundwater conditions in the host rock that are not chemically reducing [10 CFR 60.122(c)(10)].

10 CFR 960.5-4. Rock Characteristics

The site shall have geologic characteristics compatible with waste containment, isolation, and retrieval.

§ 960.5-4-1 Physical properties.

The site shall provide a geologic system that is capable of accommodating the geomechanical, chemical, thermal, and radiation-induced stresses that are expected to be caused by interactions between the waste and the host rock.

(a) Favorable conditions. None specified.

(b) Potentially adverse conditions. Potential for such phenomena as thermally induced fractures, hydration and dehydration of mineral components, brine migration, or other physical, chemical, or radiological phenomena that could lead to projections of radionuclide releases greater than those discussed in § 960.3-2.

As part of the General Technical Assistance task in the FIN A-3164 Waste Package Program, BNL has carried out a review of recent DOE waste package research data for the basalt, salt, and tuff repository programs. No attempt was made to evaluate all the geotechnical factors listed above, since most of these are being addressed by others. The major aspects of the BNL waste package evaluation work are to:

- a. Compile a list of recent reports, data and assumptions pertinent to waste package performance for the three host rocks.
- b. Assess the accuracy, reliability and applicability of DOE data on waste package performance.
- c. Identify, using the data reviews, those issues which will determine the suitability of a site for further evaluation and development.
- d. Determine what additional data are needed by NRC for its EA report reviews.

Activities in these areas are described below.

2. COMPILATION AND REVIEW OF RELEVANT DOE WASTE PACKAGE DATA

The review process undertaken by BNL proceeded in a step wise fashion from obtaining available documents and data, identifying primary issues and reviewing key documents and data. The final step which involved an in-depth review of key documents, included an assessment of whether the data provided were adequate, whether uncertainties in the data have been identified and whether alternative interpretations are available.

A comprehensive literature search was carried out and DOE reports and technical papers on waste package research and analytical work were procured for review. In order to cover the large volume of literature in the time available, reviews were usually carried out on information published over the last five years. In addition, it was also necessary in most cases to have brief general reviews in order to complete the work. However, certain reports were selected for in-depth comment because of their importance to the waste package program.

The appendices to this report include the reviews carried out to date. They are divided into sections dealing with basalt (Appendix 1), salt (Appendix 2), and tuff (Appendix 3) waste package data, and Appendix 4 is concerned with reports/papers which are generic to all three host rocks. Within each appendix, the reviews are placed in order of the year of publication. Within each year they are listed in alphabetical order, according to the authors name. Reports considered to be key documents were reviewed in detail. These were selected if they contained a detailed data base, described a new important effect with respect to waste package behavior, described an analytical approach that addresses licensing criteria, or contained data on long-term tests that help establish behavioral trends. These reviews appear in Appendix 5. An overview of waste package data relevant to each host rock is given below.

2.1 Basalt Repository Project (Appendices 1 and 4)

2.1.1 Waste Form Evaluations

Early evaluations of waste forms, including glass, spent fuel and ceramics, started five to six years ago (see McCarthy and others, RHO-BWI-C-16, 1978; RHO-BWI-C-35, 1978; RHO-C-12, 1978; RHO-BWI-SA-12A, 1979; all reviewed in Appendix 1). The tests were conducted over a wide range of temperatures in basaltic water and deionized water. Since that time there have been follow-on studies in which emphasis was focused on glass with some effort devoted to spent fuel and SYNROC. The reviews carried out in Appendix 1 show several obvious shortcomings in the waste form work:

- There has been too much emphasis on leaching in deionized water as a test medium. Early tests clearly show that leach rates vary considerably depending on water chemistry (Katayama, 1980; Weed, 1980 - Appendix 4).

- Water chemistries that simulate pristine groundwater are also not likely to be valid since they do not account for changes in ionic strength, pH, redox condition caused by hydrothermal interaction with host rock and packing materials. In addition, groundwater samples may contain lower concentrations of dissolved gases since depressurization effects may release large amounts of gases present under prototypic geologic conditions.
- Most of the work which measures leach rates for radionuclides cannot be used to show compliance with NRC release criterion since, under anticipated slow-water-flow conditions, the solubility of radionuclides and the amounts of colloids containing radionuclides will principally determine the release rates. Leach rates from short-term experiments only indicate the speed at which solubility limits may be reached in the near-field environment.
- Isothermal leaching/solubility tests may not yield conservative values. For example, Fullam's work (1982 - Appendix 4) shows that solubilities of radionuclides, measured after cooling a saturated solution to the test temperature, gave much higher values than those obtained by carrying out isothermal tests. Since a repository is subjected to a cooling trend, values obtained by cooling saturated solutions may be more conservative.
- No leaching/solubility tests have been carried out on waste forms which chemically simulate aged materials. Assuming that the radionuclides are contained for 300 to 1000 years, the fission product inventory will be depleted and the radionuclides of interest are the actinides.
- A few long-term leaching tests have been carried out for spent fuel at 25°C lasting up to 3.3 years (Katayama, 1980 - Appendix 4), and for glass in deionized water for times to one year (Strachen, 1982 - Appendix 4). Generally, however, the test times are less than one year, and these are insufficient to establish long-term behavioral trends. Tests lasting for five to ten years should be carried out.

2.1.2 Container Evaluations

Several screening tests have been carried out on container materials relevant to the basalt program (Pitman, 1980; Westerman, 1982 - Appendix 1; Pitman, 1981 - Appendix 4). Materials include iron/steel, stainless steels, copper-, titanium-, zirconium-, and nickel-based alloys. One might have expected that a firm choice for the container metal would have been made several years ago so that in-depth testing could have been well under way by this time. Instead, the comprehensive testing of low-carbon steel (current reference) appears to be commencing this year with the issuance of the Barrier Materials Test Plan by BWIP. Specific comments on the container evaluation effort are given below:

- Anticipated hydrothermal conditions are being used in testing but the groundwaters being evaluated may not reflect those present in the repository. There are few, if any, tests that incorporate corrosion in the presence of contacting packing materials. This is a serious

shortcoming since the water chemistry and pH in the metal/packing interface is likely to be much different than that when packing is absent. For example, crevice conditions could exist between metal and basalt pieces such that low pH conditions and accelerated local attack could occur. Specimens exposed to large volumes of free water would not experience these aggressive conditions. Work at BNL indicates that major increases in SO_4^{2-} concentrations are also likely in basaltic water at 250°C due to the presence of packing material (NUREG/CR-3091, Vol. 3, 1984, Appendix D).

- Few data are available to evaluate the effects of gamma irradiation on uniform and local corrosion. Possibly, the generation of radiolytic oxidants will prevent reducing conditions from being attained, thus leading to accelerated corrosion rates.
- Hydrogen from radiolysis of groundwater may be absorbed by the container, leading to embrittlement effects. These have yet to be adequately quantified.
- Very-long-term corrosion experiments lasting for five to ten years are needed to assess the potential for corrosion failure modes having long incubation times. These include stress-corrosion cracking and hydrogen embrittlement.
- There are few corrosion data on weldments.

2.1.3 Packing Material Evaluations

It has been stated by BWIP for many years that a 75%/25% basalt/bentonite mixture is the reference packing material. However, there are relatively few experiments that study this composite packing. Most tests carried out by BWIP involve basalt/water and bentonite/water studies. It is felt that most work should be on the basalt/bentonite/ H_2O system to evaluate bentonite swelling capabilities, permeability, sorption/desorption behavior, geochemical alteration, and water chemistry changes since these represent the prototypic condition. Other comments on the packing material data include:

- Sorption/desorption tests carried out at high temperatures for fission products are relevant only for accident scenarios in which the container is prematurely breached. Thus, studies such as those described by Komarneni, 1980; Salter and others, 1981; and Wood, 1982 (Appendix 1) are of little use in addressing the NRC controlled release criterion.
- Only a few studies (Barney, 1982; Salter and Jacobs, 1982 - Appendix 1) appear to address the low-temperature behavior of barrier materials with respect to radionuclide solubility, sorption, and transport. More comprehensive data are needed to adequately address the NRC controlled release criterion and the EPA standard.
- There appear to be no data available to determine whether performed packing has the same integrity as the laboratory packing materials which are being tested.

- The effects of alpha-radiolysis from the actinides on redox conditions, solubility and sorption behavior have not been fully addressed. Since alpha irradiation will prevail for thousands of years, and increase as actinides accumulate in the package components and the near-field, associated effects need to be quantified.

2.2 Salt Repository Project (Appendices 2 and 4)

2.2.1 Waste Form Evaluations

The effort on waste form evaluations for a salt repository are relatively modest, compared to those for basalt. A possible reason lies in the fact that there will be limited amounts of brine available for leaching, and it is also difficult to visualize a scenario in which brine migrating to the hot waste will be able to transport radionuclides to the accessible environment. Much of the data on waste form leaching is for relatively low temperatures (<150°C) in WIPP brines. Such studies appear to be in support of the defense program at WIPP (Kircher and others, 1982 - Appendix 2; Duker and others, 1980 and Wicks and others, 1982 - Appendix 4). Kircher's work, however, describes component interaction effects on leaching of glass. Comments on the waste form program are:

- There is a relatively small data base on the leaching of glass and spent fuel in brine.
- No data are available on leaching/solubility measurements for aged waste or spent fuel.
- No data are apparently available for very-long-term tests on waste form leaching or actinide solubility.

2.2.2 Container Evaluations

A major effort has been under way for several years in support of container assessment for a salt repository. The data are being obtained for both the defense (WIPP) and commercial waste programs. Test temperatures extend to 300°C and test solutions include WIPP brines and seawater. A range of metals and alloys, similar to those given in Section 2.1.2, were evaluated.

A review of many of the available PNL and SNL publications may be found in Appendices 1 and 4.

General conclusions for the salt repository container programs are:

- The WIPP program reference container material is titanium alloy 12, whereas that for the commercial program appears to be carbon steel, with alloy 12 as an alternate.
- For titanium, the most important failure modes include hydrogen embrittlement and crevice corrosion. Stress-corrosion cracking is not likely to occur in brine, based on slow-strain-rate tests.

- Few data are available for welds.
- Few very-long-term tests have been conducted. Tests lasting five to ten years should, therefore, be initiated to determine if failure mechanisms with very long incubation times are likely.

2.2.3 Packing Material Evaluations

In the commercial repository program there will possibly be a crushed salt packing material. Studies carried out on gamma irradiation effects (Levy, 1981 - Appendix 2) and compaction under stress and heat (Shor and others, 1981; Holcomb, 1982 - Appendix 2) address the behavior of crushed salt. Several studies have been performed to evaluate the rate of migration of brine inclusions in the near-field to the hot waste (Krause, 1981; Jenks and Claiborne, 1981; and Biggers, 1982 - Appendix 2) and work on brine radiolysis has been under way for the last few years (Jenks, 1980; Jenks and Walton, 1981; Glass, 1981 - Appendix 2). Owing to the complex chemistry of brine, however, and the effects of its interaction with colloidal sodium in irradiated rock salt (Levy, 1981 - Appendix 2) an accurate determination of the changing waste package environment in salt is likely to be difficult.

Some data are available on the sorption of radionuclides on sedimentary rocks contained in bedded and domed salt (Serne, 1981 - Appendix 4). These are useful in determining the effectiveness of salt minerals in sorbing radionuclides.

2.3 Tuff Repository Project (Appendices 3 and 4)

The decision to locate the tuff repository in the unsaturated zone at Yucca Mountain took place about two years ago. Because of this, waste package evaluations for unsaturated conditions are limited. Some relevant studies are summarized below.

2.3.1 Waste Form Evaluations

Preliminary leaching experiments have been conducted on 76-68 glass in J-13 well water at 90°C in the presence, and in the absence, of crushed tuff and Type 304L stainless steel container material (Oversby, 1983 - Appendix 3). Based on boron concentrations in the water, it was found that the addition of tuff and steel significantly decreased the leach rate. Oversby also gives preliminary data on the solubility of U from irradiated fuel pellets and pellets clad with defective Zircaloy tubing. Compared to bare fuel, the defective cladding reduced the concentration of U in 25°C deionized water by one to two orders of magnitude. Other leaching tests of relevance to the tuff repository water have been conducted at PNL in HCO₃⁻ solutions at temperatures up to 90°C (Weed, 1980; Strachen, 1981 and 1982; Wang, 1981; Wicks, 1982 - Appendix 4). The following are comments on these studies:

- The low-temperature leaching of glass and spent fuel are pertinent to the post-containmentment period when liquid water, rather than steam, will be present in a tuff repository. However, there is no information on

the leaching/solubility of simulated aged waste glass compositions. Thus, the data obtained so far are not strictly relevant for addressing the NRC controlled release criterion.

- There are some data on steam/glass hydration effects (Bates, 1983 - Appendix 4). Although they show the importance of surface alteration effects, they did not address the release of radionuclides by steam/air environments in a tuff repository. Such data will be required since there is a possibility that steam conditions will still be present after a 300-year containment period.

2.3.2 Container Evaluations

Screening evaluations for tuff repository container materials were only recently completed (Russell, 1983 - Appendix 3). The four references include Types 304L, 316L, 321 stainless steel and Incoloy-825. These and other secondary metals, such as carbon steel, were tested in water and steam environments to evaluate corrosion failure modes (McCright, 1983 - Appendix 3). At 100°C in tuff conditioned water several carbon steels suffered crevice attack but T304L and T316L show no crevice or local attack after 1000 hours. Slow strain rate tests in 150°C tuff conditioned water revealed no evidence for embrittlement compared to air tests. Carbon steel corrosion rates appear to be unaffected by γ -irradiation but T304L stainless steel showed an increase. Comments on this work are:

- These data are very preliminary since the test times are very short (1000 h). Since mechanisms such as stress corrosion may take years to appear, the work performed does not significantly reduce the potential for this failure mode in the light of data in the literature which show that the 300 series of stainless steels are susceptible to stress corrosion under conditions similar to those expected in tuff repositories.
- Long-term gamma irradiation may cause nitric acid formation since N_2/O_2 mixtures from the air are present and are known to form nitrogen oxides.
- Long-term tests (five to ten years) are needed to fully evaluate possible corrosion failure modes.

2.3.3 Packing Material Evaluations

Packing materials being considered for a waste package in a tuff repository include crushed tuff with or without a clay binder (Gregg, 1983 - Appendix 3). This will most likely be used for a spent fuel waste package only, since this waste form alone may not meet the NRC controlled release criterion. Significant work has been done on the radionuclide sorption capabilities of tuff (Serne, 1981 - Appendix 4 and Wolfsberg and others, 1981 - Appendix 3). However, work on tuff/clay composite packing does not seem to have been initiated. A major effort will be required to evaluate volatile radionuclide transport through a tuff packing material by steam-air transport mechanisms, if this environment is present after containment fails. Alteration of the packing during the high-temperature steam/air containment period must also be studied, including effects of nitric acid formation during gamma irradiation.

2.4 Modeling of Waste Package Performance

Many modeling efforts are in place within the DOE programs to evaluate waste package and near-field behavior. Some appear to be quite sophisticated and capable of predicting long-term behavior, provided there is sufficient knowledge of the waste package design and near-field characteristics. For example, the HEATING5 code is capable of conducting one-, two-, and three-dimensional calculations on temperature distributions around glass and spent fuel waste packages in a basalt repository (Altenhofen, 1981 - Appendix 1). However, the accuracy of the temperature distributions depends sensitively on factors such as the thermal conductivity of the packing material. Other important input data include inhomogeneities in the far-field geology and the need to couple heat and moisture flow effects.

The BALANCE code was developed to calculate mass transfer for geochemical interactions in groundwater (Parkhurst and others, 1982 - Appendix 4). It is based on quantifying chemical interactions between mineral phases, organic substances and gases with groundwater. It is limited in usefulness, however, since the authors warn that the calculations are not totally constrained by thermodynamic criteria and there is a possibility that reactions which are energetically unlikely will indeed be predicted to occur.

Another important code is EQ3/EQ6, developed to perform calculations on geochemical speciation and reaction paths in rock/water systems pertinent to waste performance assessment (INTERA, 1983 - Appendix 4). It appears to be a flexible and useful code but requires additional review to establish any limitations.

A recent code for evaluating engineered barrier system performance is WAPPA. This has been independently reviewed by BNL staff as part of the FIN A-3167 (NUREG/CR-3091, Draft Report, 1985) program. It is composed of individual submodels including the Thermal Model, the Leach-and-Transport Model, and the Radiation and Attenuation Model. It is felt that there are many shortcomings in WAPPA and much additional work will be needed before it can serve as an effective and defensible performance assessment code.

In general, the importance of code development cannot be overemphasized. It is through calculations that demonstration of compliance with regulatory criteria will be achieved. Comprehensive and reliable barrier system performance data must be obtained together with a knowledge of the dominant system failure modes and failure scenarios. Without such information the accuracy with which a code can predict long-term behavior will be severely limited, even though the code itself might be technically excellent.

3. ACCURACY, RELIABILITY, AND APPLICABILITY OF WASTE PACKAGE DATA

After the general review of DOE data was completed in Appendices 1 through 4, a more detailed assessment was made of the accuracy, reliability and applicability of selected publications. These are given in Appendix 5. Although general procedures for carrying out the tests are given, there is usually limited information on possible errors in measurements. Nor is there a

systematic attempt to measure a particular property using different test techniques to establish the accuracy of the techniques with respect to known standards.

One of the most detailed studies on the precision of leach testing data was conducted by the Materials Characterization Center in which 25 laboratories carried out MCC-1 static leaching tests on standard glass specimens under a well-defined set of test parameters (Johnson, PNL-4249, 1982). It was found that an experienced laboratory could be expected to measure elemental mass losses with a precision of 6-11%. The relative between-laboratory precision was between 25-40%. Thus, under less-controlled test conditions one would clearly expect very large ranges of elemental leach rates because of different glass-surface-area-to-water-volume ratios, sample preparation techniques, water flow rates, solution analyses procedures, etc., even if the same glass composition and leachant were used. There is, therefore, an urgent need to accurately determine the anticipated waste package environment so that meaningful leaching/solubility data can be obtained for the waste form. This will necessarily include the incorporation of appropriate test temperatures, aged waste form compositions, the presence of container and packing components, relevant water chemistries, and extended test times to quantify radionuclide release rates. Similar statements are applicable to container and packing material testing.

Even when tests are conducted according to well-defined procedures to increase accuracy and precision, there could remain significant uncertainties in the data obtained. The detailed reviews given in Appendix 5 show that these include:

- Testing under limited ranges of temperature and limited numbers of temperature, makes extrapolation and interpolation difficult.
- Testing under limited ranges of redox conditions also makes extrapolation and interpolation difficult.
- Too few replicate tests to check precision.
- Limitations in ability to quantify irradiation dose and dose rate effects using short-term laboratory tests.
- Few very long-term tests to determine the validity of extrapolation procedures.
- Little information on the effects of long-term alteration and aging on waste package component properties.
- Few tests to evaluate interaction effects among waste package components and the near-field geochemistry and hydrology.
- No detailed in situ tests to correlate laboratory and field data.

All of these factors must be addressed before the behavior of the waste package and near-field system can be adequately understood and modeled to predict whether compliance with NRC and EPA criteria can be met.

4. WASTE PACKAGE ISSUES RELEVANT TO SITE SELECTION

In addressing the relevance of performance data for the engineered barrier system with respect to the site selection process (i.e. the DOE EA program) two questions need to be addressed:

1. Is the performance of the engineered barrier system sufficiently well known that its impact on the repository site can be accurately predicted?
2. What are the adverse effects that waste emplacement will have in determining whether a particular site is suitable for further characterization?

Clearly, from the literature reviews carried out in Appendices 1 through 5, and the summaries given above in Sections 2 and 3, there is still great uncertainty in the performance of the waste packages. Until waste package designs and materials have been finalized, and appropriate performance data and performance assessment calculations have been made, the effects of waste emplacement on site suitability cannot be adequately quantified. Specifically, those aspects detailed in Section 1, above, on the Geochemistry and Rock Characteristics from the 10 CFR 960.5 site selection criteria can only be addressed peripherally at this time. It must, however, be recognized that in some cases a potential shortcoming in site geochemistry or in rock characteristics that might render a site less suitable for development can be overcome by a modified waste package design. For example, BWIP staff assumes that the environment in a basalt repository will be reducing so that container corrosion effects and radionuclide solubilities will be decreased. If further studies show that this is an incorrect assumption then the effects of the more oxidizing conditions can be minimized by selecting a higher integrity container material and a packing material that would be more effective in sorbing radionuclides. Nevertheless, each of the three repository host rocks have inherent advantages and disadvantages which are currently known. These need to be addressed, as well as possible, using available data before a site can be recommended for continued development. A brief summary of these is given in Table 1, below, together with a very general outline of their impact on the design of the waste package system (a more complete comparison of the three host rocks may be found elsewhere (DOE/EA-0210, 1983)). The table shows that the basalt repository is possibly more difficult to characterize with respect to basic geochemical and hydrological characteristics. After waste emplacement, the nature of waste/rock interactions will probably also be more complex compared to salt and tuff environments. However, as mentioned above, there is no clear indication that Hanford basalt cannot be successfully utilized for waste isolation, although it may require more detailed laboratory and in situ testing to specify an engineered barrier system design that will counter deficiencies in site performance.

5. CONCLUSIONS

A general review has been carried out on reports and technical papers concerned with DOE research and development on engineered barrier systems pertinent to high-level waste repositories in basalt, salt and tuff. Much of the

Table 1. Potential advantages and disadvantages of siting a waste repository in basalt, salt and tuff.

Host Rock	Advantages	Disadvantages	Effects on Waste Package Design
Basalt (Hanford)	<ul style="list-style-type: none"> o Located on federal land associated with nuclear activities o Low population density o Good radionuclide sorption behavior. 	<ul style="list-style-type: none"> o Low thermal conductivity o Basalt flows of limited thickness (but wide lateral extent) o Complex mineralogy and hydrology o Difficult mining. 	Relatively difficult to characterize repository environment. May need sophisticated waste package design to compensate for uncertainties.
Salt (Generic)	<ul style="list-style-type: none"> o Low water content o Low water permeability o Slow radionuclide release to accessible environment o High thermal conductivity o Self sealing by salt creep o Simple mineralogy o Easy mining 	<ul style="list-style-type: none"> o Aggressive corrosion environment o Complex gamma irradiation effects on brine and salt o Potential for thermal release of acidic gases o Bedded salt has limited thickness (but wide lateral extent.) Salt domes show opposite characteristics o Purer salt has poor radionuclide sorption behavior. 	Relatively difficult to characterize brine chemistry. May need high integrity container to prevent early loss of containment. The selection of a site with low brine content and low secondary mineral content will probably limit container/waste form corrosion and minimize gamma irradiation effects on salt and brine.
Tuff (Topopah Spring)	<ul style="list-style-type: none"> o Located on federal land associated with nuclear activities o Low population density o Low lithostatic stress o Low water flow rates and simple hydrology o Probably low radionuclide release to accessible environment o Easy mining. o Good radionuclide sorption behavior. 	<ul style="list-style-type: none"> o Low thermal conductivity o Limited thickness and moderate lateral extent o Potential for HNO₃ formation due to radiolysis of air/steam/water mixtures o Oxidizing conditions will probably increase radionuclide solubilities and container corrosion. 	Oxidizing conditions and potential for HNO ₃ formation may increase container corrosion rate.

earlier work was in the form of screening studies on waste package components with the objective of selecting reference materials. At this time, firm selections for containers and packing materials have yet to be made but the waste forms are likely to be spent fuel and borosilicate glass.

Most of the testing has centered on individual package components but there is some information on the effects of component interactions on waste form leaching and container corrosion. Nevertheless, there is a severe lack of whole package testing work either in the form of laboratory tests or in situ evaluations. Because of this, there is very limited information on the effect of waste emplacement on the geochemistry and rock characteristics of basalt, salt and tuff. Since these two geotechnical factors are included as DOE's site selection criteria in 10 CFR 960, a complete rationale for selecting a particular site for further development cannot be made. Thus, one expects that those sites which appear to have the fewest limitations, based on limited available data, will be selected for additional study.

The additional information which would be useful in an evaluation of the interactions of the immediate environment with the waste package includes the following which relate to the geochemistry and rock characteristic site selection guidelines in 10 CFR 960.

- a. Data are needed to quantify how early boiling of groundwater, and associated precipitation of dissolved solids, and host rock alteration, will change the composition of water subsequently entering a waste package borehole when boiling ceases. Major changes in repository water composition, pH and redox condition may render invalid much of the current waste package performance data.
- b. A more accurate quantification of the water ingress rate into the repository and the rate of pressurization is required.
- c. Information on the cracking of basalt and tuff host rock arising from repository excavation and the high temperatures caused by waste emplacement is needed.
- d. For basalt and salt it is known that the horizontal component of the lithostatic stress is much larger than the vertical component. The effect of the large horizontal stress on waste package/repository integrity needs to be addressed.
- e. Data are needed to assess the consequences of the recent announcement at the Hydrology Workshop in Seattle (reported by M. McNeil, NRC) that the basalt repository horizon is expected to intersect a basalt flow-top. This will lead to a significantly increased rate of water intrusion during repository operation and after closure.
- f. There is a need to outline the most likely scenarios for engineered barrier system failure/degradation so that relevant performance assessment calculations can be conducted. Without such information there will be considerable uncertainty in determining containment failure times, controlled release rates, and releases to the accessible environment.

- g. The ease of waste package retrieval will vary for the different host rocks. It seems to be more difficult for a salt site since the high temperatures during the repository operations period may cause the host rock to creep towards the waste package, thereby sealing it in place if a borehole liner is not used. A description is needed of the procedures to be undertaken to ensure ease of retrieval for all candidate sites.
- h. Documentation is required on pre-closure package and repository monitoring procedures that will be needed to confirm that the repository and waste package are performing within established design limits.

At this time, it seems that the site selection process, which is currently centered on Environmental Assessment report analysis, will not be dominated by engineered barrier system factors since, in most cases, limitations in the repository site can be mitigated by changes in the design of the barrier system. Thus, there should be comprehensive research and development to evaluate the interaction of the engineered barrier system and the host geology so that finalized designs can be established.

6. REFERENCES

DOE/EA-0210 "Draft Environmental Assessment for Characterization of the Hanford Site Pursuant to the Nuclear Waste Policy Act of 1982 (Public Law 97-425)," February 1983.

NUREG/CR-3091, BNL-NUREG 51630, Volume 3, P. Soo, Editor "Review of Waste Package Verification Tests," February, 1984.

NUREG/CR-3091, BNL-NUREG 51630, Volume 6, Draft Report, "Review of Waste Package Verification Tests," January, 1985.

APPENDIX 1

REVIEW OF WASTE PACKAGE DATA FOR BASALT REPOSITORY PROGRAM

DOCUMENT REVIEW FORM

AUTHOR: M. Barnes (Penn State Univ)

TITLE: Hanford and Columbia River Basin Basalts: X-ray Characterization
Before and After Hydrothermal Treatment

REFERENCE: RHO-BWI-C-17, June 1978

AVAILABILITY: NTIS

KEY WORDS: basalt, hydrothermal, x-ray diffraction

DATA SUMMARY:

Property and Form of Data:
X-ray diffractogram

Materials and Specimen Geometry:
Basalt Powder

Test Conditions:
T: 100-400°C
P: 300 Bars
Time: 28-56 days

COMMENTS ON DATA VALIDITY:

There were no major changes in the basalt diffractograms taken before and after hydrothermal treatment. All the principal labradorite, augite, and magnetite-ulvospinel lines remained along with a broad glassy band at $2\theta \sim 28^\circ$ ($\text{CuK}\alpha$). The ratio of ulvospinel to magnetite ratio changed slightly and indicate a change in oxidation state of the system towards reducing conditions (i.e., higher ratio). This could also be an experimental artifact.

DOCUMENT ABSTRACT

The principal minerals of Basalts BCR-1 and DDII-3 are still present after hydrothermal treatment up to 400°C. No new phases have been observed, with the exception of one in the longest run, 300°C for 56 days. There is not enough of this phase present to give positive identification in the bulk powder diffractogram.

The spinel magnetite-ulvöspinel was observed to change oxidation state under some conditions. Because uranium and plutonium are both far more soluble in the +6 state than in the +4 state, the oxidation state of the system basalt + waste + water is important. The basalt is in enormous excess and contains both ferrous and ferric iron in its spinels and in augite. Together they should be the principal influence on the oxidation state of the system.

Several further X-ray measurements would be useful: first, examination of spinels in runs already made with 2 percent water and with 10x by weight water; second, examination of runs made in an all-stainless system; third examination of the Umtanum Basalt from Umtanum Ridge; fourth, search for ilmenite after further magnetic separation; and; fifth, look for possible changes in both spinels in order to follow the oxidation state in basalt + waste + water.

DOCUMENT REVIEW FORM

AUTHOR: McCarthy, G. J., et al.
TITLE: Simulated High-Level Waste-Basalt Interaction Experiments Second Interim Progress Report

REFERENCE: RHO-BWI-C-16, June 1978

AVAILABILITY: Available

KEY WORDS: basalt, HLW, hydrothermal interactions

DATA SUMMARY:

Property and Form of Data:

x-ray diffraction:glass; SEM:glass.
surfaces; description of alteration products

Materials and Specimen Geometry:

76-68 glass; Hanford basalt (ilintunum)

Test Conditions:

1. 300° C; 300 bars; 28 days: basalt Hanford water/waste form
2. 100° C and 300° C; 300 bars: 2-12 months duration

COMMENTS ON DATA VALIDITY:

Provides detailed analysis of the hydrothermal alteration of PNL 76-68 glass including solid phase alteration products and analysis of solutions following hydrothermal treatment.

The usefulness of this document is questionable given the higher than expected temperatures used. The solid phase alteration products observed may, however, be indicative of products that may result over long time periods and under less extreme temperatures. These studies do not take into account radiolysis/radiation effects in the alteration process.

DOCUMENT ABSTRACT

With the completion of the reconnaissance experiments in March 1978, the nature of our overall effort has shifted its emphasis to more detailed individual experiments or sequences of experiments in an attempt to obtain a clearer understanding of the nature and rate of radionuclide release. The hydrothermal alteration of glass, which initially was a leading candidate, has been a major thrust area in the recent past. This work has been completed at a modest temperature (300°C) under repository conditions and has shown that alteration is nearly complete.

To reflect the greater interest in spent unprocessed fuel (SURF), the majority of the current work is being performed on simulated SURF itself or on those phases in SURF that contain potential near-term hazardous radionuclides and uranium.

As this approach to the understanding of radioactive waste-basalt interactions has evolved, it has been increasingly clear that the "closed" system hydrothermal experiments would point the direction to potential interactions. But, if a closer representation of repository ambients under hydrothermal conditions were necessary, then an alternative technique in an "open" system was needed. This open system was available and has been advanced into an operative condition. The next several months should see the implementation of this apparatus, and the results of initial basalt alteration experiments.

DOCUMENT REVIEW FORM

AUTHOR: McCarthy, G. J., et al. (Penn State Univ)

TITLE: Reaction of Water with a Simulated High-Level Nuclear Waste Glass at 300°C, 300 Bars

REFERENCE: RHO-BWI-C-35, 1978

AVAILABILITY: Available

KEY WORDS: waste glass, hydrothermal interactions

DATA SUMMARY:

Property and Form of Data:

Electron microprobe for quantitative elemental analysis; EDX and SEM provided qualitative elemental analysis; X-ray diffraction data on crystalline phases; also atomic emission spec.

Materials and Specimen Geometry:

PNL-76-68 glass; specimens were single shards broken from a layer fragment; wt ~30 mg

Test Conditions:

Pressure: ~30 bars; artificial Hanford water used as well as deionized water; experiments performed in inert gold capsules; duration: 7, 14, 21 and 28 days.

COMMENTS ON DATA VALIDITY:

Temperatures investigated much higher than anticipated temperatures. Elemental composition varied by as much as 10-20% of the base composition for 76-68 glass due to the inclusions present. The experiments used predominantly deionized water and their "closed system" does not take into account the effects of radiolysis on solubilities. Under hydrothermal conditions, alteration is a major variable influencing the enhanced leach rate. Since alteration is accompanied by complications such as stress generation, a delineation of the mechanisms involved in hydrothermal leaching is not easily achieved and was not attempted by this study.

DOCUMENT ABSTRACT

Terminal storage in underground rock formations is presently considered the most feasible method of isolating high-level nuclear power plant wastes from the biosphere. Among the candidates for geologic repositories are the basalt formations underlying the Hanford Site in eastern Washington State. One of the many factors that will need to be considered in repository design and in setting high-level waste form acceptance criteria is the effects of the heat produced by radionuclide decay. Heat would have certain effects on the physical properties of the repository and, especially when combined with water encroachment, heat would promote chemical reactions within the immediate repository (1). Exploring and then carefully defining the effects of hot pressurized groundwaters on simulated waste forms such as spent fuel and high-level waste glass in a basalt repository are the goals of a research project at The Pennsylvania State University (PSU). Research of this type is one of the activities of the Basalt Waste Isolation Program at Rockwell Hanford Operations (2).

An important feature of the PSU research is concern for the products of reactions as well as the reactivity of the waste form. Whether hydrothermal* reactions in a basalt repository would be beneficial or detrimental to waste containment is primarily a question of the long-term stability of the reactions products.

DOCUMENT REVIEW FORM

AUTHOR: McCarthy, G. J. and M. W. Grutzeck

TITLE: Preliminary Evaluation of the Characteristics of Nuclear Wastes
Relevant to Geologic Isolation in Basalt

REFERENCE: RHO-C-12, May 1978

AVAILABILITY: Available

KEY WORDS: waste forms, basalt repository environment

DATA SUMMARY:

Property and Form of Data:

General review: thermodynamic stability, chemical composition,
leachability

Materials and Specimen Geometry:

glass (76-68); spent fuel; supercalcine; specimen geometry not
reported

Test Conditions:

76-68-waste: leachability: distilled water; 25°C and 95°C;
soxhlet; spent fuel: leachability: 25°C; Hanford groundwater and
deionized water; time period not specified

COMMENTS ON DATA VALIDITY:

This document lacks any usefulness with respect to current efforts for the following reasons: (1) The evaluations used results based on distilled or deionized water for the leach tests. Such conditions are not applicable to an evaluation of waste forms under actual repository conditions; (2) The presence of radiation was not taken into account in these evaluations. Radiolysis resulting in an alteration of groundwater composition, including solubility, and the liberation of gases will affect the rates and extent of leaching. The temperature ranges used to evaluate the candidate waste forms do not reflect the range of temperatures likely to be encountered under actual repository conditions. In addition, the lack of information as to specimen geometry and time durations of tests adds to the lack of usefulness of the document.

DOCUMENT ABSTRACT

The physical and chemical characteristics of radioactive waste which have bearing upon the concept of geologic storage in basalt are reviewed and discussed. Each class of waste form (spent unprocessed fuel, calcine, glass, and supercalcine) has its own unique characteristics which may or may not affect the concept of final storage of radioactive waste in basalt. These characteristics form the basis for scientific evaluation of the relative merits of each of the waste/basalt pairs.

DOCUMENT REVIEW FORM

AUTHOR: McCarthy, G. J. et al. (Penn State)

TITLE: Hydrothermal Stability of Spent Fuel and High Level Waste Ceramics in the Geologic Repository and Environment

REFERENCE: RHO-BWI-SA-12 A, April 1979

AVAILABILITY: Abstract only

KEY WORDS: spent fuel, borosilicate glass, hydrothermal conditions, basalt

DATA SUMMARY:

Property and Form of Data:

reactivity; solution composition; alteration properties

Materials and Specimen Geometry:

spent fuel, waste glass, supercalcine ceramic (geometry unspecified)

Test Conditions:

deionized waste; Hanford groundwater (artificial), 100-300° C; 300 bars; time period up to 1 year.

COMMENTS ON DATA VALIDITY:

Data not available for comment; information that supercedes this report indicates that test conditions may be appropriate as part of a screening effort, however, conditions are not realistic and expected conditions are likely to change over time and include radiolysis effects.

This report, as abstracted here, does not appear useful in the overall review effort.

This paper was presented at the American Ceramic Society Symposium Meeting, Cincinnati, Ohio, April 30, 1979.

DOCUMENT ABSTRACT

Terminal storage in underground rock formations is presently considered the most feasible method of isolating high-level nuclear power plant wastes from the biosphere. One of the many factors that will need to be considered in geologic repository design is the effect of the heat produced by radionuclide decay. Heat would have certain effects on the physical properties of the repository rock and, if combined with the encroachment of water pressurized by the rock overburden, heat could promote chemical reactions within the immediate repository.⁽¹⁾ This combination of hot and pressurized water could give rise to hydrothermal* conditions.

The occurrence of such a hydrothermal incident could have various ramifications for nuclear waste isolation. If containment of the wastes is maintained throughout the thermal period, then the solutions would only alter the nearby rock, overpack, and so on. However, if the hydrothermal solutions contact the waste due to breach of containment, alteration of the waste and interaction with the repository environment could take place.⁽²⁾

*The term "hydrothermal" is used here to denote reactions involving superheated water; i.e., reactions at any temperature above 100 degrees centigrade where pressure is sufficient to maintain H₂O in the liquid phase. Note that in strict earth sciences nomenclature, such conditions involving temperatures between 100 and 373 degrees centigrade are "mesothermal."

Both the rate and the products of these interactions are, of course, strongly temperature-dependent, so increases in the volume of the waste (decrease in the concentration of waste fission products in the waste) and/or the repository can be adopted to reduce temperatures. But, as the authors have pointed out,⁽¹⁾ this may not be necessary if the alteration-interaction products are themselves suitable "source terms."

The research described here deals largely with the first stage of comprehensive waste-rock hydrothermal interaction studies, closed system waste-water reactions. Closed system experiments are ideal for exploring the reactivity of solid-liquid systems and establishing the direction of thermodynamic equilibrium. The experiments simulate the case where superheated water is admitted through a breached canister and reacts with the waste in a region where the chemistry of the waste initially dominates the course of the reactions. Determination of the long-term reactions and the ultimate source terms requires experiments incorporating canisters and massive excesses of the repository rock. Initial results from these waste-rock experiments will be described to illustrate the importance of these more complex studies in deriving waste form performance criteria.

Experimental conditions included temperatures from 100 to 300 degrees centigrade at 300 bars pressure. Spent fuel and 2 simulated waste forms, a glass and a supercalcine-ceramic were treated under these conditions with deionized water (DW), an artificial Hanford ground water (HGW), and a brine. It will be shown that, in the upper temperature range, spent fuel and supercalcine were largely unreactive with the DW and HGW, but moderately reactive with the brine. The glass reacted readily with all solutions, but the reaction mechanism differed between the DW/HGW and the brine. Reaction rates, of course, decreased with decreasing temperature.

It will also be shown that when two non-evaporite rocks, basalts, and shales were incorporated into these experiments, the reaction behavior in the two cases was comparable, but, as expected, the resultant source terms were quite different.

This research is supported by the U. S. Department of Energy through the Office of Nuclear Waste Isolation and Rockwell Hanford Operations.

DOCUMENT REVIEW FORM

AUTHOR: Smith, M. J. (Principal Author)

TITLE: Engineered Barrier Development for a Nuclear Waste Repository in Basalt

REFERENCE: RHO-BWI-ST-7, 1980

AVAILABILITY: Published

KEY WORDS: basalt, waste package, corrosion, backfill, glass

DATA SUMMARY:

Property and Form of Data:

Corrosion data of candidate canister material - in/yr, swelling pressure and permeability of backfill MPa vs. ton/m^3 - m/s vs. ton/m^3 .

Materials and Specimen Geometry:

Alloys of steel, titanium, chromium, nickel and zirconium, borosilicate glass, Synroc, supercalcine, bentonite, zeolites.

Test Conditions:

Single and interactive tests in simulated repository conditions.

COMMENTS ON DATA VALIDITY:

This publication is a comprehensive compilation of data, integrated for the purpose of understanding the effects of isolating nuclear waste in the basalts at the Hanford site. It contains a considerable amount of useful data regarding canister corrosion, physical and chemical characteristics of backfill materials, leach data of radionuclide from waste forms in simulated groundwater, and chemical and mineralogical composition of several flows in basalt. This report can serve as a useful reference for evaluating the isolation of nuclear waste in a basalt repository.

DOCUMENT ABSTRACT

None

DOCUMENT REVIEW FORM

AUTHOR: Ames, L. L. and J. E. McGarrah (PNL)

TITLE: High-Temperature Determination of Radionuclide Distribution
Coefficients for Columbia River Basalts

REFERENCE: RHO-BWI-C-111, 1980

AVAILABILITY: NTIS

KEY WORDS: sorption, basalt, hydrothermal, cesium

DATA SUMMARY:

Property and Form of Data:
Kd.

Materials and Specimen Geometry:

Test Conditions:

P: 6.9-27.6 MPa.
T: 150°C and 300°C.

COMMENTS ON DATA VALIDITY:

A Kd represents an empirical result that can be affected by system variables. If all components of the system as it will exist are not included in the testing, the validity of the Kd value is open to question. The Kd values reported for Pu and Am are essentially meaningless, because they are so large, especially at high temperatures. Complete sorption on the Teflon liner occurred even in the absence of basalt. Both radionuclides were probably present at pH 8.0 of the synthetic groundwater as colloidal polymers that tended to further polymerize and sorb on surfaces as a result of increasing temperature and solution ionic strength. This process cannot be properly described by ion-exchange concepts such as Kd.

DOCUMENT ABSTRACT

This report discusses initial results of the high-temperature sorption studies on Columbia River basalts. From the results, the following conclusions were made:

- Cesium Kd temperature effects, used as an example of the high-temperature Kd experiments, showed that the techniques developed for the high-temperature Kd work yielded valid and reproducible Kd results.
- The best techniques included frequent sampling at temperature and pressure of relatively high chloride solutions over a 45- to 60-d period with no agitation of vessel contents and use of a relatively large solution volume, heated externally in a Teflon-lined Inconel 600 pressure vessel. *Inconel was chosen because it is resistant to embrittlement by chloride ions.*
- Initial temperature effects on the cesium Kd with basalts showed a decrease with increasing temperature to 150°C. Above 150° to 300°C, cesium Kd values increase, perhaps due to sorption and removal on growing secondary mineral phases or incorporation into secondary minerals.
- Pressure effects on cesium Kd values were found to be minimal between the 6.9 to 27.6 MPa (1,000 to 4,000 lb/in.²g) pressure range expected in a nuclear waste repository in basalt.

DOCUMENT REVIEW FORM

AUTHOR: Barney, G. S., Wood, B. J.

TITLE: Identification of Key Radionuclides in a Nuclear Waste Repository
in Basalt

REFERENCE: RHO-BWI-ST-9, 1980

AVAILABILITY: Published

KEY WORDS: migration, basalt, commercial waste, spent fuel

DATA SUMMARY:

Property and Form of Data:

Ranking system identifying the degree of radionuclide hazard according to quantity, toxicity, leach rate and transport rate.

Materials and Specimen Geometry:

Input data is based on waste from an LWR or PWR as a borosilicate waste form and spent fuel. Radionuclide quantities were obtained by using the code ORIGEN and their toxicities from the recommended concentration guide.

Test Conditions:

Hazard measure (HM) is obtained from the sums of the individual hazard rankings. Transport data is based on release rate and application of the single dimension transport equation.

COMMENTS ON DATA VALIDITY:

Radionuclides have been ranked in a descending order of their hazard measure. Additional information concerning waste forms, geology of the repository and transport properties could alter the order of the list. The methodology seems appropriate but the procedure in the report raises questions, e.g. the fact that leach rate data are based on the use of deionized water.

DOCUMENT ABSTRACT

RHO-BWI-ST-9

ABSTRACT

Radionuclides were identified which appear to pose the greatest potential hazard to man during long-term storage of nuclear waste in a repository mined in the Columbia Plateau basalt formation. The criteria used to select key radionuclides were as follows:

- o Quantity of radionuclide in stored waste
- o Biological toxicity
- o Leach rate of the wastes into groundwater
- o Transport rate via groundwater flow.

The waste forms were assumed to be either unprocessed spent fuel or borosilicate glass containing reprocessed high-level waste. The nuclear waste composition was assumed to be that from a light water reactor.

Radionuclides were ranked according to quantity, toxicity, and release rate from the repository. These rankings were combined to obtain a single list of key radionuclides. The ten most important radionuclides in order of decreasing hazard are: ^{99}Tc , ^{129}I , ^{237}Np , ^{226}Ra , ^{107}Pd , ^{230}Th , ^{210}Pb , ^{126}Sn , ^{79}Se , and ^{242}Pu . Safety assessment studies and the design of engineered barriers should concentrate on containment of radionuclides in this list.

DOCUMENT REVIEW FORM

AUTHOR: Komarneni, Sridhar, et al. (Rockwell Hanford)

TITLE: Hydrothermal Interactions of Cesium and Strontium Phases from Spent Fuel with Basalt Phases and Basalts

REFERENCE: RHO-BWI-C-70, March 1980

AVAILABILITY: Available

KEY WORDS: spent fuel, basalt, hydrothermal, cesium, strontium

DATA SUMMARY:

Property and Form of Data:

Hydrothermal solubility determined/stability of the phases investigated. Elemental and phase composition results from X-ray diffraction and atomic absorption spectrometry are presented.

Materials and Specimen Geometry:

Natural and synthetic basalt, -200 mesh (<75 μm) reacted with $\text{Cs}_2\text{U}_2\text{O}_7$ and SrZrO_3 (synthesized).

Test Conditions:

Pressure: 300 bars, temperatures: 200°C for 56 days, 300°C for 28 days, reacted in sealed gold capsules.

COMMENTS ON DATA VALIDITY:

Test temperatures are higher than anticipated under actual repository conditions.

Decreasing solubility of Cs with increasing temperatures is questionable.

Elevated oxygen pressure prevalent during the experiments is not likely to be present under actual repository conditions.

Water used in the experiments does not reflect the chemical composition of groundwater exposed to a radiation field such as is likely to be present under actual conditions. Changes due to radiolysis will alter solubility results.

DOCUMENT ABSTRACT

None

DOCUMENT REVIEW FORM

AUTHOR: Kupfer, M. J. and Palmer, R. A.

TITLE: Physical and Chemical Characterization of Borosilicate Glasses
Containing Hanford HLW

REFERENCE: RHO-SA-189, October 1980

AVAILABILITY: Published

KEY WORDS: borosilicate glass, leach resistance, phase separation,
mechanical strength, thermal analyses, Hanford waste

DATA SUMMARY:

Property and Form of Data:

Composition of waste/glass (wgt %), leach resistance (% wgt loss), thermal characteristics (e.g. melt temp.), thermal conductivities (w/mK), crystalline phases, thermal expansion coefficient.

Materials and Specimen Geometry:

1. Leach specimens - crushed glasses; 2. Thermal expansion - 5 cm rods; 3. Conductivity - solid pieces; 4. Phase analysis - samples cooled at rate of 15°C/hr from 1100 to 400°C.

Test Conditions:

1. Leaching - DIW, 1 M HNO₃, 1 M NaOH, soxlet test at 95°C, at 25°C in DIW; 2. Thermal expansion - 5 cm rods, 250°C-350°C; 3. Thermal conductivity - solid pieces, 25°C, 110°C, 300°C.

COMMENTS ON DATA VALIDITY:

For specimens studied, leach resistance found to increase with decreased waste loading. Devitrification studies done isothermally and some glasses show development of crystalline phases. In glasses showing development of crystalline phases, leach rate increases from 1.5 → 5 x. Data serves to compare potential resistance of different glass-waste compositions. Data also indicates changes induced by devitrification. Data not applicable to expected repository conditions. No groundwater/repository water leach data or analyses for components released.

RHO-SA-189
DOCUMENT ABSTRACT

Scouting studies are being performed to develop and evaluate silicate glass forms for immobilization of Hanford high-level wastes. Detailed knowledge of the physical and chemical properties of these glasses is required to assess their suitability for long-term storage or disposal.

Some key properties to be considered in selecting a glass waste form include leach resistance, resistance to radiation, microstructure (includes devitrification behavior or crystallinity), homogeneity, viscosity, electrical resistivity, mechanical ruggedness, thermal expansion, thermal conductivity, density, softening point, annealing point, strain point, glass transformation temperature, and refractive index. Other properties that are important during processing of the glass include volatilization of glass and waste components, and corrosivity of the glass on melter components.

Experimental procedures used to characterize silicate waste glass forms and typical properties of selected glass compositions containing simulated Hanford sludge and residual liquid wastes are presented. A discussion of the significance and use of each measured property is also presented.

DOCUMENT REVIEW FORM

AUTHOR: Pitman, S. G., B. Griggs and R. R. Elmore (PNL)

TITLE: Evaluation of Metallic Materials for Use in Engineering Barrier Systems

REFERENCE: PNL-SA-8939, November 1980

AVAILABILITY: Available

KEY WORDS: HLW, corrosion, metals, alloys, basalt, brines

DATA SUMMARY:

Property and Form of Data:

Chemistry of leach solutions; V-notched specimen tensile, impact and fracture roughness tests; weight change data and extrapolations.

Materials and Specimen Geometry:

Crushed basalt; V-notched and plates used; 304L SS; 316L SS; 321L S/S; 405L S/S; 410L S/S; Inconel 600, 625, 800; Titanium 2, 12, 6AL-4V; Zircaloy, cast iron, copper.

Test Conditions:

Hanford basalt groundwater; NaCl-MgCl₂ brine; autoclave - 5.52 MPa; 250°C/tensile tests - 20-250°C V-notched specimens tested; fatigue-crack-growth rate tests - 90°C; corrosion tests duration - 20-72 days.

COMMENTS ON DATA VALIDITY:

The corrosion data was conducted in simulated Hanford groundwater at 150°C. This type of testing is useful in screening a variety of candidate metal/alloys but does not represent conditions likely to be encountered under actual repository conditions. The contacting solution is likely to undergo several changes in chemistry over to operations and post-emplacement period as a result of radiolysis and alteration product (host rock) formation.

The test results in this report appear too preliminary for useful application in current review efforts.

DOCUMENT ABSTRACT

None

DOCUMENT REVIEW FORM

AUTHOR: Scheetz, B. E., et al. (PSU)

TITLE: Hydrothermal Interaction of Simulated Nuclear Waste Glass in the Presence of Basalts

REFERENCE: Scientific Basis for Nuclear Waste Management, Vol. 2, Plenum Press, N.Y., 1980, pp. 209-214

AVAILABILITY: Published

KEY WORDS: basalt, glass, hydrothermal reaction, reaction products, solution composition, Cs, Sr, Ba, Ca, Na, Si

DATA SUMMARY:

Property and Form of Data:

Glass-basalt hydrothermal reactions. Interaction products identified and quantified and concentrations of Na, Rb, Cs and U in solution were measured.

Materials and Specimen Geometry:

- (a) Intimate mixtures of Umtanum basalt and 76-68 glass powders.
- (b) Large pieces of the same materials.

Test Conditions:

Hydrothermal conditions (300°C, 300 bars) were used. Samples exposed in gold lined capsules for periods up to 4 months.

COMMENTS ON DATA VALIDITY:

The work verified the importance of the Fe^{++}/Fe^{+++} content of basalt in altering the oxidation state, and hence solubility of U. For large glass/basalt surface area ratios Wecksite was formed and the U^{6+} content was not significantly altered. In the presence of abundant basalt, however, the U^{6+} was reduced.

Basalt increases the Cs release rate by a factor of 2-4 but reduces the loss of Sr, Ba, Ca, Na and Si. Thus basalt/glass effects are very important.

These data are extremely valuable since they directly address synergistic effects of waste package components.

DOCUMENT ABSTRACT

Chemical analyses of the solutions indicated that the percentages of Ca released from glass into solution at 100° or 300°C increased by a factor of 2 to 4, while Sr, Ba, Ca, Na and Si seem to have decreased to various extents in the presence of basalt. The principal conclusion which results from these studies is that basalt has a marked influence on the hydrothermal alteration behavior of the glass waste form. Not only does it cause new solid phases to form, but it also modifies the solution chemistry significantly. In particular, it seems to increase the amount of Ca which is taken into solution, a result which requires more careful investigation.

One important result of these experiments is the verification of the oxygen buffering capacity of the ferrous/ferric content of the basalt and its effect on the uranium component of the waste glass. Where the glass was the most reactive material, as in the experiments with solids of low surface area, wecksite was formed, indicating that the U^{6+} content was not effectively reduced. However, where the surface area was large, the U^{6+} component was reduced, preventing the formation of wecksite.

The solid phase characterization has revealed several compounds from the long duration runs that were not observed in products of the shorter runs. New phases such as quartz, orthoclase, pollucite and willemite were found. The presence of these phases may be indicative of a closer approach to equilibrium, or at least an indication of phases which are more stable in the presence of basalt than in its absence.

DOCUMENT REVIEW FORM

AUTHOR: Altenhofen, M. K.

TITLE: Waste Package Heat-Transfer Analysis: Model Development and Temperature Estimates for Waste Packages in a Repository Located in Basalt

REFERENCE: RHO-BWI-ST-18 (October 1981)

AVAILABILITY: National Technical Information Service,
Springfield, VA 22161

KEY WORDS: Thermal, Model, Package, Basalt, Heat

GENERAL COMMENTS: The author presents thermal analyses of vertically emplaced waste packages in Umtanum basalt based on the heat conduction code HEATINGS. The author assumes a quasi-steady-state equilibrium condition in the package and then examines acceptable ways to determine the reference temperature of the edge of the emplacement hole. In order to do that, the author compares the prediction of 3-D, 2-D and 1-D calculations. It turns out that a 3-D model for the far-field is needed during the first 100 years after emplacement. Later on a 2-D model can do. A 1-D model could be used after a few thousand years.

Regardless of whether the analyzed designs and emplacement option are still pursued by DOE for the BWIP site, the report is a good illustration of an acceptable methodology for coupling near- and far-field models without sacrificing accuracy to costs. Also, the conclusions reached by this author are noteworthy, i.e., (1) inhomogeneities of the far-field should be incorporated in future studies, however they do not constitute a priority issue; (2) coupling of heat and moisture flow within the waste package packing and in the very near-field basalt should be a priority issue, as peak waste package temperatures are very sensitive to the thermal conductivity of packing materials.

DOCUMENT ABSTRACT (Abridged)

Heat-transfer analyses were performed for three nuclear waste types which exhibit different characteristics—commercial and defense high-level waste (both immobilized in borosilicate glass) and spent-fuel elements. The waste-isolation system parameters used in these analyses reflect the current conceptual designs for a high-level nuclear waste repository constructed in basalt. Details of the thermal properties of the host rock and waste package relevant to a repository in Columbia River basalt and the relevant properties of the waste forms themselves are presented and discussed.

The physical layout of the nuclear waste repository was modeled using the heat-conduction computer code, HEATING5. This code uses the Crank-Nicolson finite-difference method to evaluate transient temperature behavior. Transient heat-transfer analysis is necessary because the heat generated by nuclear waste varies with the radioactive decay of fission products.

The results of one-, two-, and three-dimensional models were integrated to produce an accurate estimate of waste package/host rock-interface temperatures as a function of time. The more precise three-dimensional model provided the most accurate estimate of temperature behavior very near the waste package. A comparison of the two- and three-dimensional models indicates that the two-dimensional results are equivalent to the three-dimensional results for positions ≥ 2.14 m from the waste package row centerline. Comparison of the one- and two-dimensional model results beyond 500 yr of storage indicates that the one-dimensional results are equivalent to the two-dimensional results for positions ≥ 4.9 m above the waste package. The one- and two-dimensional models always underestimate the temperatures near the waste package; however, at times $>1,000$ yr, the error becomes insignificant. This error is primarily due to the fact that in the simpler model the heat source is distributed over a much larger volume.

In order to use the results of one- and two-dimensional models, far- and near-field-temperature estimates were used to determine hole surface temperatures beyond the time for which the three-dimensional model is used (100 yr). Linkage was provided by extrapolating the short-term transient gradient behavior from the three-dimensional model to the long-term gradient behavior calculated using a quasi-steady-state relationship for a single cylindrical heat source in basalt. At low-heat strength, the transient gradient will approach the quasi-steady-state gradient. The extrapolated transient gradient behavior was used to estimate emplacement hole temperatures from two-dimensional model results. Waste package internal temperatures were then evaluated by applying quasi-steady-state conditions between the emplacement hole surface and the waste package materials.

The results of this analysis indicate that peak temperatures and the times for which they occur at the waste package centerline, canister, and emplacement hole surface are 426°C (2.5 yr), 362°C (3 yr), and 255°C (4.5 yr) for commercial high-level waste; 178°C (22 yr), 172°C (23 yr), and 164°C (26 yr) for defense high-level waste; and 269°C (4 yr), 264°C (4 yr), and 191°C (7 yr) for spent-fuel elements. These results reflect the decay-heat characteristics of each of the waste types and the emplacement configuration of each of the waste packages.

DOCUMENT REVIEW FORM

AUTHOR: Anderson, W. J., PNL

TITLE: Corrosion Tests of Canister and Overpack Materials in Simulated Basalt Groundwater

REFERENCE: RHO-BWI-ST-15, 1981

AVAILABILITY: Published

KEY WORDS: basalt, canister, corrosion, groundwater

DATA SUMMARY:

Property and Form of Data:

Weight change measurements expressed in mg/dm^2 in addition to visual observation of the test specimens for corrosion.

Materials and Specimen Geometry:

Inconel, Hastelloy, Titanium, Ferrallium, Cupronickel and Zircalloy - sheet 3/4"x4".

Test Conditions:

Autoclave, 250°C, 5.8 MPa, simulated groundwater, anoxic environment - separate tests with variable pH for a 60 day period.

COMMENTS ON DATA VALIDITY:

The results indicate that simulated groundwater with varying levels of oxygen is not highly corrosive to the materials tested, with the exception of the cupronickel alloys. These alloys showed significant corrosion at higher oxygen levels during the 60 day test.

The data appears applicable but does not include probable synergistic repository effects.

DOCUMENT ABSTRACT

RHO-BW1-ST-15

ABSTRACT

Corrosion tests of candidate container materials for nuclear waste in a simulated basalt environment are in progress. Test conditions in the first series of autoclave tests were 250°C temperature, 5.8 MPa pressure, with simulated groundwater (oxygen fugacity ca 10^{-50} MPa, pH ca 9.5). Control of oxygen fugacity of the water was obtained by use of an argon/hydrogen mixture in the test chamber and in the solution reservoir. Periodic sampling and analysis of the test solution were used to monitor the efficacy of the control of water chemistry and the products of specimen corrosion. Materials placed under test included titanium, nickel, copper, and iron-based alloys identified as potentially useful for either canister or overpack containers in the engineered barrier system concept. Results regarding control of water composition and material corrosion in the initial phase of testing are presented.

DOCUMENT REVIEW FORM

AUTHOR: Barney, G. S.

TITLE: Radionuclide Reactions with Groundwater and Basalts from Columbia River Basalt Formations

REFERENCE: RHO-SA-217, 1981

AVAILABILITY: NTIS

KEY WORDS: sorption, basalt, Kd values

DATA SUMMARY:

Property and Form of Data:

K_D .

Materials and Specimen Geometry:

Basalt, altered basalt, secondary minerals, crushed.

Test Conditions:

Ambient.

COMMENTS ON DATA VALIDITY:

In general, sorption of each radionuclide increases in the order: basalt < altered basalt < secondary minerals. This document conveys the complexity of mechanisms that are operative in radionuclide sorption reactions. However, the data was obtained under ambient conditions and did not include other materials which will be present in the repository situation.

Several conclusions can be made concerning the mechanisms of radionuclide sorption reactions in Columbia River basalt formations. Cesium sorption on the solids is by ion exchange with possibly some Cs^+ "fixed" in mica-like minerals. Both K^+ and NH_4^+ ions can replace part of the sorbed Cs. Sorption is very extensive for both altered basalt and secondary minerals. A slow diffusion of Cs^+ into secondary mineral sorption sites continues over many weeks after an initially rapid sorption reaction.

Strontium sorption appears to be strictly a simple ion exchange reaction, except when Sr concentrations are high and Sr is precipitated. Sodium and Ca^{2+} ions effectively compete with Sr for sorption sites. In Grande Ronde groundwater Na^+ concentration is much higher than Ca^{2+} and therefore, Na^+ dominates the exchange reactions. Because of slow dissolution of Ca^{2+} and Mg^{2+} from basalt, Sr is slowly desorbed over a period of ≈ 20 weeks.

Under the Eh conditions of Grande Ronde basalt formations, Np should exist as Np(IV). Using a hydrazine Eh buffer, Np(IV) was found to sorb much more strongly than Np(V). Bicarbonate decreases sorption by forming $Np(CO_3)_x^{+(4-2x)}$ complexes. Large differences in Na^+ , K^+ , or Ca^{2+} concentration had no effect on Np sorption indicating that sorption is not by ion exchange. Additional evidence for this conclusion is the fact that Np(IV) sorption on secondary minerals (which had the highest ion exchange capacity) was the weakest of the solids measured. Neptunium(IV) must be chemisorbed on the mineral surfaces.

The oxidation state of Pu in basalt is probably Pu(IV). Plutonium(IV) is much more strongly sorbed than the higher oxidation states. Calcium and sodium salts increase sorption by formation of insoluble Pu compounds. These may be slightly soluble double salts such as $CaPuF_6$ or $NaPuF_5$. As for Np, no evidence for ion exchange of Pu on minerals surfaces was found.

Americium solubility and sorption are strongly influenced by Mg^{2+} . The solubility is lowered and sorption is increased when Mg^{2+} is present. It appears that Am forms an insoluble compound with Mg. Bicarbonate and SO_4^{2-} decrease sorption due to formation of complexes such as $AmCO_3^+$ and $AmSO_4^+$.

Technetium probably exists in the +4 oxidation state under the reducing conditions of a basalt formation. A possible species is TcO^{2+} which is

strongly sorbed on the three solids studied. The only significant parameter found was the Eh buffer, hydrazine, which reduced TcO_4^- to Tc(IV) .

Selenite ion, SeO_3^{2-} , was not reduced to Se^0 by hydrazine as expected from the standard half-cell potentials. Selenium does not sorb by anion exchange, but by chemisorption or precipitation. Calcium increases sorption probably by formation of a CaSe compound. Carbonate decreases sorption by making Ca^{2+} unavailable by forming complexes such as CaHCO_3^+ and CaCO_3^0 .

As might be expected, Ra sorption is similar to that of Sr. Cation exchange is the main sorption mechanism. Sodium ion and K^+ both compete with Ra for sorption sites.

All sorption reactions studied thus far can be accurately described using the Freundlich isotherm, except when precipitation occurs. These isotherms can be used to quantify sorption and to determine at which point precipitation becomes important for various radionuclide-groundwater-solid systems.

Kinetics studies show that most sorption reactions are relatively fast. However, some groundwater-geologic solid reactions are slow and can influence sorption by dissolution of solid components. These are most important for reactions with secondary minerals which are not near equilibrium with Grand Ronde groundwater. Altered basalt, however, comes very close to being in equilibrium with this groundwater.

BLANK PAGE

DOCUMENT REVIEW FORM

AUTHOR: Coons, W. E.

TITLE: Basalt Waste Isolation Project Data Package for Reference
Physicochemical Conditions

REFERENCE: Scientific Basis for Nuclear Waste Management, Vol. 3, 1981

AVAILABILITY: Published

KEY WORDS: basalt, groundwater, temperature

DATA SUMMARY:

Property and Form of Data:

fO_2 , Eh and pH as a function of temperature. Log fO_2 (atm),
pH, Eh(V), temperature ($^{\circ}C$) - hydrostatic and lithostatic pressure
(bars, psi).

Materials and Specimen Geometry:

Field measurements, experimental testing and calculations - no
details given - Ref. RHO-BWI-ST-7.

Test Conditions:

Calculated for repository "period of geologic controls" and
"thermal period."

COMMENTS ON DATA VALIDITY:

Groundwater compositions used in the test are reported to be in agreement with USGS data. The fO_2 , pH and Eh were calculated as functions of temperature and a maximum lithostatic pressure of 300 bars for the operational and containment periods of a basalt repository. The report states that pH will function as the ratio of rock to water changes, i.e. the pH will be lower when groundwater is dominant and will increase when the rock is dominant. The data is more readily applicable to a stagnant system and less predictable where groundwater is freely flowing.

DOCUMENT ABSTRACT

ABSTRACT

This package defines the physicochemical conditions expected to prevail in a closed nuclear waste repository mined from Columbia River Basalt. Estimates have been derived from experimental data, in-situ measurements, or thermodynamic calculations. Equations are provided from estimation of fO_2 , Eh and pH as a function of temperature. Expected conditions are summarized below.

	<u>Temper- ature (°C)</u>	<u>Equili- brium pH</u>	<u>log Oxygen Fugacity (atm)</u>	<u>Eh(V)</u>
Period of Geologic Controls	65	9.4	-64.5 to -67.15	-0.50 to -0.54
Thermal Period	100	8.7	-57.8 to -60.0	-0.49 to -0.53
	150	7.9	-49.6 to -51.8	-0.48 to -0.53
	200	7.2	-43.3 to -45.4	-0.47 to -0.52
	250	6.7	-38.3 to -40.2	-0.48 to -0.52
	300	6.2	-34.1 to -35.9	-0.45 to -0.51

DOCUMENT REVIEW FORM

AUTHOR: Salter, P. F., L. L. Ames, J. E. McGarrah (Rockwell Hanford)

TITLE: The Sorption Behavior of Selected Radionuclides on Columbia River Basalts

REFERENCE: RHO-BWI-LD-48, Informal Report, August 1981

AVAILABILITY: NTIS

KEY WORDS: Umtanum basalt, sorption, Kd, hydrothermal conditions

DATA SUMMARY:

Property and Form of Data:

Sorption, Kd values for I, Se, Tc, Sr, Cs, U, Ra, Pu, Am, Np.

Materials and Specimen Geometry:

Columbia River basalts - 0.30 to 0.85 mm.

Test Conditions:

Effects of temperature, pressure, groundwater composition, and Eh (reducing and oxidizing) ~ -.4V (150°C, 6.9 MPa) and (300°C, 27.6 MPa), 60 day.

COMMENTS ON DATA VALIDITY:

Based on the sorption data presented, it appears that, under the expected ambient repository conditions, the Columbia River basalts are capable of strongly retarding Cs, Sr, Ra, and Np migration and moderately retarding U, Tc, and Pu migration. The basalts are not capable of significantly retarding the migration of I and Se. It should be noted that Kd values are empirical and may vary depending on what environment is occurring. Whole package testing conditions and specific reference basalts should be used.

DOCUMENT ABSTRACT

Radionuclide distribution ratios provide one means of evaluating the ability of a geologic substrate to retard the migration of key radionuclides to the accessible environment from a repository mined in basalt. Due to the empirical nature of the K_d value, it is necessary that radionuclide K_d values be determined under conditions which simulate the expected repository environment as closely as possible. Radionuclide K_d values determined for I, Tc, Np, Se, U, Ra, Pu, Am, Cs, and Sr under oxidizing and, where applicable, reducing conditions for the Columbia River basalts indicate:

- (1) Iodine is present as a simple uncomplexed anion and is poorly sorbed by the basalts.
- (2) Cesium is present as a simple uncomplexed cation and is strongly sorbed by the basalts. Cesium K_d values vary with temperature as a function of changing competing ion concentrations and secondary reactions (new mineral formation).
- (3) Strontium, Ra, and Se (oxidizing conditions) sorption is probably a combination of ion exchange and chemisorption. Strontium and Ra, being cationic, are strongly sorbed by the basalt and Se, being anionic, is poorly sorbed by the basalts. Their K_d values vary with temperature as a function of increasing competing ion concentration and secondary reactions (incorporation into or sorption onto new mineral phases).
- (4) Uranium, Np, and Pu are weakly sorbed by basalt under oxidizing conditions. Under reducing conditions, solubility constraints will keep U concentrations $< 1 \text{ E-}08\text{M}$, Np concentrations $< 1 \text{ E-}10\text{M}$, and Pu concentrations $< 1 \text{ E-}09\text{M}$ in the groundwater. Their sorption is very dependent on temperature, pH, and groundwater composition since these factors strongly influence their speciation (e.g., whether they are dominantly anionic or cationic).
- (5) Americium, under oxidizing conditions, is strongly sorbed by the basalt. Solubility constraints should keep the Am concentration below $1 \text{ E-}10\text{M}$.
- (6) Technetium, under oxidizing conditions, is present as an anion and, therefore, is poorly sorbed by the basalts. Under reducing conditions, Tc concentration is controlled by the solubility of TcO_2 and the aqueous speciation of Tc(IV) .

DOCUMENT REVIEW FORM

AUTHOR: M. J. Smith, P. F. Salter, and G. K. Jacobs

TITLE: Waste Package Performance Requirements for a Repository in Basalt

REFERENCE: RHO-BWI-SA-172, 1981

AVAILABILITY: Published

KEY WORDS: Waste Package, Basalt

GENERAL COMMENTS: This paper provides a summary of a study performed to describe preliminary waste package performance requirements in a basalt repository and establish a relationship between NRC criteria applicable at or near the waste package and EPA total curie release criteria applied at the accessible environment.

This study does not perform a near field analysis. It assumes that the waste is contained for 1000 years after which there is a 1000 year leach time for all nuclides. Given this release rate, the transport to the environment is calculated using a one-dimensional model. This procedure was first used by Wood, RHO-BWI-ST-10.

Two test problems were modeled and evaluations were made by first ignoring and then considering solubility limits of the nuclides. The first problem considered transport through 2.8 km of basalt to the environment with a groundwater velocity of 0.32 m/yr. The second problem assumed that an event occurred that increased the water velocity to 7.9 m/yr.

The results of the studies indicate if solubility limits are not taken into account the waste package must have release rates less than 10^{-3} per year, as assumed, for many of the actinides and some must have release rates less than the NRC limit of 10^{-5} per year in order to meet the EPA standards. This applies for both test problems. When solubility limits are accounted for, all nuclides have cumulative releases less than the EPA limit in the low flow rate case. However, Np-237 and Pu-239 exceed the EPA limit in the high flow rate problem.

This report suffers from a lack of documentation and/or motivation in describing their reasoning behind the selection of key parameters. An example of this is the solubility limits used. There is no reference detailing where they obtained the data or the test conditions. Before accepting the quantitative results of this study a thorough evaluation of the key variables in the model is needed.

DOCUMENT ABSTRACT

None

DOCUMENT REVIEW FORM

AUTHOR: Anderson, W. J., PNL

TITLE: Conceptual Design Requirements for Spent Fuel, High-Level Waste
and Transuranic Waste Packages

REFERENCE: RHO-BW-ST-25P, 1982

AVAILABILITY: Published

KEY WORDS: commercial waste, spent fuel, basalt, waste package

DATA SUMMARY:

Property and Form of Data:

Data form given is mostly "number presently used in design" (NPUD)-
heat generation rates of CHLW, DHLW and SF vs. time-temperature limits
for waste package components °C - physical properties of basalt.

Materials and Specimen Geometry:

See the references and appendices given in the report.

Test Conditions:

Information compiled for the storage of spent fuel, CHLW, DHLW and
TRU waste in a basalt repository.

COMMENTS ON DATA VALIDITY:

This report is a compendium summarizing the available data that is
presently being used for waste package design. It could serve as a useful
reference to the BWIP program, but only up to the publication date.

DOCUMENT ABSTRACT

None

DOCUMENT REVIEW FORM

AUTHOR: Barney, G. S.

TITLE: Radionuclide Sorption and Desorption Mechanisms in Interbed/
Groundwater Systems of the Columbia River Basalt Formation

REFERENCE: RHO-BW-SA-276P, October 1982

AVAILABILITY: NTIS

KEY WORDS: sorption, desorption, basalt, interbed, hysteresis

DATA SUMMARY:

Property and Form of Data:
Sorption, isotherms.

Materials and Specimen Geometry:
Sandstone and tuff interbed materials, crushed.

Test Conditions:
< 85°C.
Reducing and oxidizing.
(-0.8 V).

COMMENTS ON DATA VALIDITY:

Desorption isotherms for Se, Tc, Np, U, and Ra have much smaller slopes than for corresponding sorption isotherms (except for Se and Tc under oxidizing conditions). These nuclides are apparently irreversibly sorbed on the interbed solids. This is applicable only to the waste package in the sense that criteria for containment of the waste in the package can be viewed in terms of the containment provided by the site. Perhaps some of the data on the tuff interbed material would be applicable to a tuff repository.

DOCUMENT ABSTRACT

The sorption and desorption mechanisms of key radionuclides (Tc, Np, Pu, Am, Cs, Sr, and Ra) in groundwater-interbed systems of the Columbia River basalt formation were investigated. Sandstone and tuff interbed materials from selected sedimentary interbeds were used in these experiments. The effects of groundwater composition and Eh on radionuclide sorption and desorption on the selected geologic solid were studied. Sodium, potassium, and calcium in the groundwater decrease sorption of Cs, Sr, and Ra by ion exchange reactions. Groundwater Eh strongly affects sorption of Tc, Np, Pu, and U since chemical species of these elements maintaining the lower oxidation states are more extensively sorbed by chemisorption. Effects of radionuclide complexation by groundwater anions on sorption were not observed except for neptunium carbonate (or bicarbonate) complexes and plutonium sulfate complexes.

Sorption and desorption isotherms were obtained for sorption of key radionuclides under oxidizing and reducing conditions. The Freundlich equation accurately describes most of these isotherms. Most radionuclides are apparently irreversibly sorbed on each of the geologic solids since the slopes of sorption and desorption isotherms for a given radionuclide are different. This hysteresis effect is very large and will cause a significant delay in radionuclide transport. It, therefore, should be included in modeling radionuclide transport to accurately assess the isolation capabilities of a repository in basalt.

DOCUMENT REVIEW FORM

AUTHOR: Barney, G. S.

TITLE: Radionuclide Sorption of Columbia River Basalt Interbed Materials

REFERENCE: RHO-BW-SA-198P, May 1982

AVAILABILITY: NTIS

KEY WORDS: sorption, isotherms, basalt, interbed, K_D

DATA SUMMARY:

Property and Form of Data:

Sorption, isotherms, K_D values.

Materials and Specimen Geometry:

Sandstone, tuff, crushed materials.

Test Conditions:

23°, 60°, 85°C.

Oxidizing, reducing.

COMMENTS ON DATA VALIDITY:

This material is not directly applicable to the package. However, some of the testing techniques are. The use of hydrazine to lower the Eh of the system interfered with the sorption of Cs^+ , Sr^{2+} , and Ra^{2+} because the protonated form of hydrazine, $N_2H_5^+$, competes with Cs^+ , Sr^{2+} , and Ra^{2+} for sorption sites. The use of hydrazine may also interfere with the sorption of Np, Pu, and Tc.

DOCUMENT ABSTRACT

Sorption and precipitation of key radionuclides in the groundwater-rock systems expected in Columbia River interbed zones were investigated. Sorption isotherms were defined for sorption of Cs, Sr, Se, Tc, Ra, U, Np, and Am on an interbed sandstone standard from the Rattlesnake Ridge interbed. In addition, the effect of groundwater composition and redox potential on sorption and precipitation of these radionuclides on interbed sandstone and tuff were studied. Isotherms were measured at 23°, 60°, and 85°C. The Freundlich equation accurately fits the isotherm data when precipitation does not occur. Solubility limits were obtained for Tc and Se using the isotherms. Sorption of Cs, Se, Tc, U, and Am is strongly affected by temperature over the 23° to 85°C range.

The major chemical components of Grande Ronde groundwater (Na^+ , Ca^{2+} , K^+ , Mg^{2+} , Cl^- , F^- , CO_3^{2-} , HCO_3^- , and SO_4^{2-}) were studied for their influence on sorption and precipitation. Statistically designed experiments identified significant groundwater components and measured their effects. The results gave evidence for selecting sorption mechanisms for each radionuclide (ion exchange, chemisorption, redox reactions, complex formation, or precipitation). Strontium, Ra, and Cs are sorbed by ion exchange and compete for exchange sites with ions of similar size. The Np, Pu, and Tc are reduced by hydrazine to their (IV) oxidation states and are sorbed by chemisorption. Selenium is not reduced to the metal by hydrazine, but appears to be precipitated as a calcium compound. The groundwater variables had little effect on Am sorption. A slightly soluble Am compound appears to form which is more soluble at low pH.

DOCUMENT REVIEW FORM

AUTHOR: Early, T. O., Jacobs, A. K., Drewes, D. R.

TITLE: Geochemical Controls on Radionuclides Releases From a Nuclear Waste Repository in Basalt, Estimated Solubilities for Selected Elements

REFERENCE: RHO-BW-SA-282P, 1982

AVAILABILITY: Published

KEY WORDS: solubilities, speciation in groundwater, thermodynamic data, actinides, fission products

DATA SUMMARY:

Property and Form of Data:

Calculated maximum concentration of (m/L) of dissolved radionuclides in equil. with stable solid phase. Reference Grande Ronde water composition, dominant solution species.

Materials and Specimen Geometry:

Basaltic groundwater, Ni, Sc, Np, Zr, Pu, Pd, Sn, Sm, Eu, Pb, Th, U, Am.

Test Conditions:

Data only applicable at 25°C, pH range ~9, Eh = -0.6V → 0V.

COMMENTS ON DATA VALIDITY:

Analyses limited by uncertainties in thermodynamic data base, assumptions used (e.g. reducing conditions, pH, low temperature, no radiolysis effects for very near field). No estimate of data uncertainties on results of the calculation.

DOCUMENT ABSTRACT

Two basalt flows within the Grande Ronde Basalt at the Hanford Site in southeastern Washington are candidates for a high-level nuclear waste repository. In order to determine the anticipated rate of release and migration of key radionuclides from the repository, solubility controls must be determined. Solubilities, solids controlling solubility, and aqueous speciation in groundwater have been determined from available thermodynamic data for a variety of actinides and fission products. Groundwater compositions used include all available analyses from the selected radionuclides include hydroxides and hydrous oxides (Pd, Sb, Sm, Eu, Pb, Am), oxides (Ni, Sn, Th, Np, Pu), elements (Se, Pd, Sb), and silicates (Zr, U). Dominant soluble species include hydroxy complexes (Zr, Pd, Sn, Sb, Sm, Eu, Th, U, Np) and carbonate species (Ni, Sm, Eu, Pb, U, Np, Pu, Am). In addition to limitations in completeness and accuracy of thermodynamic data, solubility estimates of the radionuclides are sensitive to the following: (1) Eh and the degree of redox equilibrium, (2) temperature, (3) formation of metastable solid phases, and (4) coprecipitation. Eh effects have been evaluated for each radionuclide and are significant for Se, Pd, Sn, and possibly U and Np. Solubility estimates also have been calculated at ambient temperature ($\sim 55 \pm 5^\circ\text{C}$) for Grande Ronde basalts for those nuclides for which sufficient data exist. Effects of metastability and coprecipitation cannot be treated quantitatively but their contributions have been estimated in reference to available experimental data.

DOCUMENT REVIEW FORM

AUTHOR: Hodges, F. N., et al. (PNL)

TITLE: Development of a Backfill for Containment of High Level Nuclear Waste

REFERENCE: Scientific Basis for Nuclear Waste Management V, Vol. 11, Elsevier, N.Y., 1982, pp. 641-648

AVAILABILITY: Published

KEY WORDS: bentonite, water migration, swelling, sorption, controlled releases, Rd

DATA SUMMARY:

Property and Form of Data:

Rd values for selected radionuclides, hydraulic conductivities for bentonites and bentonite/sand mixtures, thermal conductivities of bentonites.

Materials and Specimen Geometry:

Na- and Ca-bentonites, sand-bentonite mixtures. Disk samples of bentonite are compacted to a density of 2.1 g/cc for permeability tests.

Test Conditions:

For permeability tests the water pressure used is 2200 psi; tests were at RT for times up to 28 days.

COMMENTS ON DATA VALIDITY:

The paper specifies the attributes of a well designed backfill including retardation of water flow and radionuclide migration, retardation of corrosive species to the container, control of Eh/pH, and provision of mechanical support for the container and waste. Work was focussed on bentonite for non-salt repositories.

Water migration rates through compacted bentonite (2.1 g/cm³ density) show that water will migrate through thin samples quickly but that the rate of migration is slower in terms of breakthrough times for thicker specimens. Slow water diffusion through the swellable clay is postulated to explain this behavior.

It was found that Cs, Sr and Am are strongly sorbed to bentonite and Np and U are moderately sorbed.

These data are of scientific interest but should be used with caution in the design of a waste package. This is especially true for the water permeability studies since in BWIP, for example, the bentonite is blown into the borehole and compacted clay will not be present unless the borehole collapses around the waste package.

DOCUMENT ABSTRACT

Sodium and calcium bentonites, pressed to densities between 1.9 and 2.2 g/cm³, have hydraulic conductivities in the range of 10⁻¹¹ to 10⁻¹³ cm/s. Batch sorption distribution ratios (R_d) indicate that Sr, Cs, and Am are strongly sorbed on bentonites and zeolites, that Np and U are moderately sorbed on bentonites and zeolites, and that Am, Np, U, I, and Tc are strongly sorbed on charcoal. Sorption results with basalt and tuff ground waters are similar; however, iodine in tuff ground water sorbs more strongly on bentonites. Thermal diffusivity measurements for dry, compacted (ρ ~ 2.1 g/cm³) sodium bentonite indicate that the thermal conductivity of a high density bentonite backfill should be roughly similar to that of silicate host rocks (basalt, granite, tuff). These results indicate that a bentonite backfill can significantly delay the first release of many radionuclides into the host rock and that by forming a diffusion barrier a bentonite backfill can significantly decrease the long-term release rate of radionuclides from the waste package.

DOCUMENT REVIEW FORM

AUTHOR: Palmer, R. A., et al.

TITLE: Characterization of Reference Materials for the Barrier Materials Test Program

REFERENCE: RHO-BW-ST-27P, June 1982

AVAILABILITY: NTIS

KEY WORDS: basalt, metals, alloys, clay, waste form, examination, analyses, waste package

DATA SUMMARY:

Property and Form of Data:

Physical and chemical properties characterization.

Materials and Specimen Geometry:

Engineered barrier reference materials as received.

Test Conditions:

Ambient.

COMMENTS ON DATA VALIDITY:

The RUE-1 basalt was found to be a siliceous mass consisting of a glassy mesostasis, plagioclase, pyroxene, titaniferous magnetite and clay. Qualitative SEM/EDS examination of the reference bentonite confirmed the presence of calcium plagioclase, iron oxides, gypsum, and nontronite as well as the primary phase, sodium-montmorillonite. Also present are small amounts of quartz, illite, and possibly calcite. Metal characterization by SEM/EDS of the candidate canister materials are reported. The chemical composition of a variety of waste forms is also detailed.

This report details the procedure for preparing standard sieved basalt from basalt monoliths. It states that all weathered basalt should be removed by hand from the unweathered basalt before final processing because weathered basalt may interfere. It is identified by a yellow exterior surface. Tests should be run with basalt as received.

DOCUMENT ABSTRACT

Reference basalt entablature, colonnade, and flow top specimens have been selected from the Umtanum flow, which is the primary basalt flow under consideration for repository siting. Material from the Mabton Interbed Stratum, Pomona Flow basalt, smectite clay from the Pomona Flow, a potassium clinoptilolite, Beverly sandstone and tuff, and Grande Ronde groundwater are also included in the suite of reference geologic materials. Reference engineered barrier materials include sodium bentonite and canister metals such as carbon steel, cupronickel, Hastelloy and Inconel alloys. Spent fuel, borosilicate glass, and supercalcine ceramic comprise the reference waste forms.

Characterization of these materials has ranged from simple macroscopic examination of the bulk material to sophisticated analyses with analytical electron microscopes. Chemical compositions of the materials were determined by X-ray fluorescence spectroscopy, electron microprobe, and energy dispersive X-ray spectrometry in combination with scanning and analytical scanning transmission electron microscopy (SEM, ANSTEM). Particle morphologies were determined by optical microscopy, SEM, and ANSTEM. Petrographic analyses of thin sections, X-ray powder diffractometry, and electron diffraction in the ANSTEM were all utilized to identify the crystalline phases present in these materials.

Analyses of the elemental and phase chemistries for most of the reference materials have been completed on typical samples. Determinations of material homogeneity are currently being performed. These analyses provide the basis for the interpretation of later experiments designed to define the behavior of host rock components, engineered barriers, and the waste form under conditions expected in a repository in basalt.

The data included in this document reflect the work completed through May of 1982.

DOCUMENT REVIEW FORM

AUTHOR: Salter, P. F., et al. (RHO)

TITLE: Application of Systems Analysis to Develop Engineered System
Performance Requirements for a Hard Rock Nuclear Waste Repository

REFERENCE: RHO-BW-SA-210P, 1982 (?)

AVAILABILITY: Obtained as preprint from author.

KEY WORDS: basalt, engineered barriers, natural barriers, controlled
release, system analysis

DATA SUMMARY:

Property and Form of Data:

System analysis data addressing the performance of BWIP system
with respect to regulatory criteria.

Materials and Specimen Geometry:

As per BWIP.

Test Conditions:

As per BWIP.

COMMENTS ON DATA VALIDITY:

The paper describes a general analysis to evaluate the roles of
engineered and natural barriers in meeting NRC/EPA criteria. Two release
scenarios were postulated for the calculations: Case I - Non-disruptive
phenomena: transport through a basalt flow-top to the accessible environment;
and Case II - Disruptive phenomenon: transport through an interbed to the
accessible environment. If radionuclide release is assumed to be not con-
trolled by solubility effects then, for Case I, ^{14}C , ^{79}Se , ^{99}Tc , ^{237}Np
and U isotopes and their daughters were the only potential problems. For Case
II, additional elements were ^{135}Cs , ^{126}Sn , ^{107}Pd , ^{243}Am , ^{242}Pu and
 ^{237}Pu . If solubilities are estimated from experiments and calculation as-
suming solubility limits then it is found that all radionuclide releases to
the accessible environment are within EPA criteria. Also, releases meet the
NRC controlled release criterion.

The main potential problems with this analysis center on the use of valid
solubility data. There is currently little information on solubilities mea-
sured from the supersaturated solution condition (see Fullam's paper), the
effects of colloidal material transport, irradiation effects which could still
prevent reducing conditions from being present, etc. More representative
analytical data are needed before the findings of this paper can be verified.

DOCUMENT ABSTRACT

The Basalt Waste Isolation Project has developed a systems-analysis approach to establishing performance requirements for the engineered system of a geologic nuclear waste repository. These requirements assure that the engineered system is designed to complement the natural system. This approach results in the optimal design for the engineered system by reducing the functional requirements of that system. While applied only to the basalt system at this time, this approach is applicable to any geologic system. As an example, the systems-analysis approach has been applied to the problem of establishing performance requirements for a waste package in basalt and has resulted in the design of a less-complex, more cost-efficient waste package for a nuclear waste repository in basalt. This paper points out the importance of developing site specific rather than generic waste packages.

DOCUMENT REVIEW FORM

AUTHOR: Salter, P. F. and G. K. Jacobs

TITLE: Evaluation of Radionuclide Transport: Effect of Radionuclide Sorption and Solubility

REFERENCE: Scientific Basis for High-Level Waste Management V, Vol. 11, Elsevier, N.Y., 1982, pp. 801-810

AVAILABILITY: Published

KEY WORDS: BWIP, controlled release, sorption, solubility, groundwater travel times, Eh/pH

DATA SUMMARY:

Property and Form of Data:

Calculated radionuclide release rates at the accessible environment to selected radionuclides.

Materials and Specimen Geometry:

Not specifically given.

Test Conditions:

Specified for the anticipated BWIP repository system: 59-300°C, 1-114 bar, Eh + 0.5 to -0.61V, pH, 6.0-9.6.

COMMENTS ON DATA VALIDITY:

The work is a preliminary assessment of radionuclide release using available data on sorption and solubility of key radionuclides for the BWIP system. Using estimated conditions within BWIP it is concluded that the release of the following radionuclides can be controlled to values within those specified by the EPA at the accessible environment.

One potential problem is that sorption of radionuclides for the reducing conditions anticipated over the long term were estimated in tests in which hydrazine was used to obtain the highly reducing conditions. This procedure has been questioned by NRC in the SCA report. Also it is not clear whether solubility data were selected for the appropriate radionuclide species. Much more work is needed to obtain a more solid data base on sorption/solubility effects before an accurate analysis can be made. The NRC 10^{-5} /y controlled release rate has not been addressed.

DOCUMENT ABSTRACT

None

DOCUMENT REVIEW FORM

AUTHOR: Westerman, R. E., et al. (PNL)

TITLE: Development of Engineered Structural Barriers for Nuclear Waste Packages

REFERENCE: Scientific Basis for Nuclear Waste Management, Vol. 6, North-Holland, N.Y., 1982, pp. 363-370

AVAILABILITY: Published

KEY WORDS: uniform corrosion, crack growth tests, stress-corrosion cracking, basaltic water, gamma radiation, cast iron, cast steel, titanium grade 2, titanium grade 12

DATA SUMMARY:

Property and Form of Data:

Uniform corrosion rates, fast crack propagation rates, slow strain rate tests.

Materials and Specimen Geometry:

Titanium grades 2 and 12, ASTM A536 grade 60-40-18 ductile cast iron and ASTM A217 grades WC6 and WC9 cast steel coupons and tensile specimens.

Test Conditions:

Slow strain rate tests at displacement rate of 2×10^{-7} to 10^{-4} in/sec.; corrosion tests at 250°C in basaltic water, crack growth tests were done at 90°C in Hanford groundwater.

COMMENTS ON DATA VALIDITY:

This study conducts screening tests on Titanium grades 2 and 12, ductile cast iron, and two cast steels in the presence and absence of γ irradiation in basaltic groundwater. Slow strain rate tests on the titanium based metals show some degradation of ductility at 250°C which may be partly due to internal effects not associated with aqueous corrosion. At 90°C there was no environmental effect on fast crack growth rates. General corrosion of the iron/steel samples was conservatively estimated to be about 1"/1000 years at 250°C. No stress-corrosion cracking was detected in U bend specimens. Basaltic water chemistry was not altered by 10^5 rad/h γ -irradiation at 40°C. However, oxygen levels were not apparently measured.

The tests are adequate for preliminary screening purposes to identify corrosion failure modes. However, very long term exposures of several years may be needed to fully determine the likelihood of a particular failure mechanism occurring.

DOCUMENT ABSTRACT

The development of structural barriers for nuclear waste packages involves selection of candidate materials, their screening by mechanical and corrosion testing, rigorous accelerated testing, and evaluation and comparison with other package elements. This document presents results from work conducted on titanium and cast steels.

DOCUMENT REVIEW FORM

AUTHOR: Wood, M. I. (RHO)

TITLE: Evaluation of Sodium Bentonite and Crushed Basalt as Waste Package Backfill Materials

REFERENCE: RHO-BW-ST-21P, 1982

AVAILABILITY: Published

KEY WORDS: bentonite, basalt, groundwater, pH, Eh, ionic strength, hydrothermal tests, sorption, alteration, swelling pressure

DATA SUMMARY:

Property and Form of Data:

Solubilities of selection of ions at 200, 300°C. Swelling pressure of bentonite, pH changes with time for groundwater in presence of packing.

Materials and Specimen Geometry:

Compacted bentonite for swelling tests, 75%/25% by weight of basalt/bentonite for solubility tests.

Test Conditions:

Solubility and pH tests at 200°C/300 bars, 300°C/300 bars.

COMMENTS ON DATA VALIDITY:

The report described results of studies to quantify the aqueous conditions in BWIP waste package packing material and the identification of alteration products in the packing. The data show that at 300°C/300 bars and 200°C/300 bars the basalt glassy phase alters to illite and a smectite clay and quartz; reducing conditions were stated to be present and the pH of the water fell to a stable value of ~6. No significant changes in F^- , Cl^- , SO_4^{-2} were detected.

An issue is raised in this work since similar studies at BNL (NUREG/CR-3091, Vol. 3, Appendix D, 1984) show that the F^- level decreases, Cl^- remains unchanged but SO_4^{-2} concentrations are raised by a factor of about 4. Si and Fe are also greatly increased. The major difference in the RHO and BNL studies was the presence of a gamma field in the BNL work. This increased sulfate may alter the corrosion behavior of the container and should be further studied by RHO.

Data were also given on sorption for various radionuclides.

In the BNL work, CH_4 was found to be present after testing. No such observation was made in the RHO study. More work will be needed to assess CH_4 effects since these have been identified in groundwater samples taken at the BWIP repository horizon.

DOCUMENT ABSTRACT

Hydrothermal experiments in the basalt/groundwater and the bentonite/groundwater systems were conducted as part of an overall program designed to evaluate the suitability of crushed basalt and bentonite as waste package backfill materials in a basalt environment. The major purpose of the experiments was to estimate the chemical (e.g., long term) stability of these materials.

Preliminary hydrothermal experiments were completed at 300°C, 300 bars and 200°C, 300 bars in the basalt/groundwater system to determine the chemical stability of crushed basalt. Analysis of solution data from the 300°C experiments as a function of time and reaction products indicated that the primary reaction was the alteration of the basalt glass phase to illite and/or smectite clays and quartz. The establishment of steady state pH values of ~6, the apparent rapid occurrence of a highly reducing environment in the system, and an insignificant increase in the solution concentration of potentially corrosive aqueous species (fluoride, chloride, and sulfate) were observed. These data indicate that a waste package backfill containing a significant amount of crushed basalt will provide a near-field geochemical environment favorable to the chemical stability of metal canister materials. Also, such an environment will promote the low solubility of actinides.

A preliminary experiment was also completed in the sodium bentonite/groundwater system at 300°C, 300 bars. Analyses of the reacted solutions and solids show that bentonite remains essentially stable with only minor alterations to albite. Sorption data were generated on crushed basalt, secondary minerals in basalt, and sodium bentonite at 60 to 65°C under oxic and anoxic conditions. These data indicate that cesium and strontium will be completely contained in a waste package backfill due to the formation of insoluble secondary minerals, ion exchange, and specific adsorption. Under reducing conditions, neptunium will be retained beyond 1,000 yr and uranium and plutonium will be retained under reducing conditions over 300 yr. An increase in retention time can be expected to occur with an increase in temperature. Theoretically, calculations and a limited data base have been used to propose a reference waste package backfill component which will (1) diffusively control mass transport, (2) exert a swelling pressure less than hydrostatic pressure (~10 MPa), and (3) effectively conduct heat away from the waste package such that maximum allowable waste package temperatures are not exceeded. The reference backfill component consists of 25% sodium bentonite and 75% crushed basalt with an initial density of 2.1 g/cm³ and a thickness of 0.152 m.

DOCUMENT REVIEW FORM

AUTHOR: Smith, M. J., et al. (RHO)

TITLE: Repository and Waste Package Designs for High-Level Nuclear Disposal in Basalt

REFERENCE: RHO-BW-SA-303P, 1983

AVAILABILITY: Available as preprint for paper to be presented at the International Conference on Radioactive Waste Management, Seattle, WA, May 1983.

KEY WORDS: repository design, waste package design, container corrosion, bentonite, thermal conditions, groundwater

DATA SUMMARY:

Property and Form of Data:

General description of waste package and repository designs, including anticipated repository conditions.

Materials and Specimen Geometry:

Varies depending on type of waste package.

Test Conditions:

Not applicable.

COMMENTS ON DATA VALIDITY:

The paper describes in general detail the efforts of BWIP and subcontractors in defining waste package designs for CHLW, DHLW and spent fuels. Included are descriptions of the pristine geology, geochemistry, temperature and pressure at the repository horizon and what changes are anticipated from waste emplacement.

For spent fuel the borehole surface temperature will be a maximum of 235°C after 5-10 years of emplacement. At closure the temperature will fall to 170-200°C. Hydrothermal tests at BWIP show that dissolved oxygen in the groundwater will fall to levels of $<10^{-3}$ mg/L in 600 h at 150°C due to a basalt/H₂O interaction. However, tests at BNL indicate that radiolysis effects may not give these highly reducing conditions. This, then, is an open issue. Nevertheless, BWIP is specifying a 1 cm corrosion allowance on the carbon steel container to give 1000 y containment. BWIP also assumes that pneumatic injection of dry bentonite around a container will be sufficiently dense (>50% theoretical density) to inhibit groundwater travel. No actual tests have been run to confirm this. It seems that long distance pneumatic injection could allow voids to form in the packing which would allow easy access of water to the container.

DOCUMENT ABSTRACT

The Basalt Waste Isolation Project is part of the U.S. Department of Energy's National Waste Terminal Storage Program. An important feature of the Basalt Waste Isolation Project's mission is to develop compatible waste package and repository designs for spent fuel and processed high-level waste disposal in basalt. This paper will report the results of a joint effort among the Basalt Waste Isolation Project, Westinghouse-Waste Technology Services Division, and Raymond Kaiser Engineers Inc./Parsons Brinckerhoff Quade & Douglas, Inc. to develop a repository conceptual design and compatible waste package conceptual designs for basalt. During fiscal year 1982, waste package and repository designs for the permanent disposal of commercial and defense high-level waste and circular bundles of spent fuel rods from three pressurized water reactor assemblies or seven boiling water reactor assemblies were developed on the basis of cost effectiveness. Each of the designs is based on environmental and regulatory performance factors that were used in the development of waste package and repository design criteria. The Basalt Waste Isolation Project reference waste package conceptual design, based on site-specific environmental conditions, consists of a waste form contained by a low-carbon steel canister, which is then surrounded by a backfill mixture of bentonite clay and crushed basalt. The waste package designs have been fully integrated into the remainder of the engineered repository structure.

DOCUMENT REVIEW FORM.

AUTHOR: Smith, M. J., et al. (RHO)

TITLE: Waste Packages for a Repository Located in Basalt

REFERENCE: RHO-BW-SA-330P, 1983

AVAILABILITY: Preprint of paper to be presented in Civilian Radioactive Waste Management Information Meeting, Washington, D.C., December 1983

KEY WORDS: waste package, corrosion, bentonite, stability, gamma irradiation, basalt, design, performance evaluation, hydraulic conductivity, sorption

DATA SUMMARY:

Property and Form of Data:

Variety of corrosion, sorption, hydraulic conductivity and bentonite stability data are given.

Materials and Specimen Geometry:

Carbon steel, bentonite, basalt.

Test Conditions:

High temperature tests up to 370°C for the various package components.

COMMENTS ON DATA VALIDITY:

Paper describes progress towards an advanced waste package conceptual design. Included are general descriptions of procedures for pneumatic injection of package, an ASME code case for structural design and alternate package configurations. In hydrothermal tests at 200°C the solubility of many radionuclides from CHLW are decreased due to establishment of reducing conditions. Sr and Sm, however, have elevated solubilities. Low carbon steel corrosion rates in anoxic groundwater decrease with time and increasing temperature. Corrosion products in the presence of bentonite are either Fe-rich clay or Fe silicates. Corrosion tests at PNL under oxic conditions in the presence of basalt gave pitting with the deepest pit measuring 11.5 mils after exposure at 150°C for >5 months. A linear extrapolation will give a pit depth of 8.3 inches after 300 years. For a corrosion test under a gamma flux of 3×10^5 rad/h for 13 months the uniform corrosion rate increase by a factor of 2-3 compared with non-irradiation conditions. In bentonite rehydration tests it was stated that experiments showed that heating to temperatures up to 370°C did not destroy the clays ability to reswell upon contact with water so that its water retardation behavior would not be compromised.

Issues arising from the paper center on the fact that gamma radiolysis will not allow the establishment of reducing conditions so that accelerated corrosion and pitting are quite possible. More long term irradiation-corrosion tests are required for whole package configurations.

An outline of waste package performance evaluation is also given.

DOCUMENT ABSTRACT

This paper presents the status of the BWIP waste package materials testing, modeling, and design activities and plans for continuing these activities through FY 1984. The first in a series of design activities leading to the final design of waste packages that will reliably meet Federal performance criteria has been completed. These activities have led to the development of waste package conceptual designs for commercial and defense high-level waste (borosilicate glass) and spent fuel rods. Planned engineering studies, together with an improved materials data base, will provide the necessary information for the preparation of waste package advanced conceptual design requirements during FY 1984.

Tests of hydrothermal reactions between basalt and simulated Grande Ronde Basalt groundwater showed that Eh conditions that were initially oxidizing became progressively more reducing as oxygen was consumed by the oxidation of ferrous iron released by the dissolving (glass) mesostasis. The pH of samples periodically withdrawn from the autoclaves decreased rapidly from a value of 9.8 and then rose to stable values of 7.5 and 7.6 at 200°C and 300°C, respectively. Hydrothermal tests show that basalt will reduce radionuclide releases from waste forms under conditions simulating those expected in an NWRB. As an example, in testing of Tc-doped borosilicate glass, steady-state concentrations of Tc in solution were found to be about three orders of magnitude lower when basalt was present. Hot cells have been prepared and hydrothermal testing using fully radioactive waste forms was initiated by the BWIP on November 1, 1983. An extensive program to test waste package components in the presence of radioactive waste forms and to assess the effect of basalt and barrier materials on releases of key radionuclides from waste packages under repository conditions has been developed for the hot-cell facility.

Corrosion testing of the BWIP reference canister material, LCS, and the two backup materials, Fe9Cr1Mo alloy steel, and 90-10 Cupronickel are being conducted to develop a reliable data base for waste package design and modeling activities. Exposure of LCSs with varying carbon content at temperatures from 100°C to 300°C in the presence of the basalt/bentonite backfill showed that, under the conditions of the test, corrosion rate was independent of carbon content. Also, corrosion rates generally decreased with increasing temperature. This feature was attributed to the tenacity and degree of development of an iron-rich clay surface corrosion product that became more protective as the temperature increased. Testing to date also shows that under oxic conditions and at high flow rates (35 mL/hr), the corrosion rates of iron-base materials increased two to three times in the presence of gamma radiation. Preliminary SSR testing of LCS in repository-specific groundwater showed a slight susceptibility to stress-corrosion-cracking, whereas early results of static crack growth testing under equivalent conditions revealed no tendency toward stress-corrosion-cracking.

Studies of the effects of radiation on corrosion and mechanical behavior will continue in FY 1984. Studies to develop pitting kinetics will be initiated. In addition, long-term corrosion tests will be started to improve the corrosion data base for waste package performance modeling.

Irreversible dehydration of the crushed basalt/bentonite reference packing material is not expected to occur at temperatures below 370°C as demonstrated in thermal testing. At 300°C exposure it was found that bentonite reactions were relatively minor and chemical stability was little affected. Thus, the reference packing material (75% crushed basalt/25% bentonite) may remain stable over long periods of time. Measured hydraulic conductivity of packing material was found to be significantly less than that required to maintain diffusional control of radionuclide releases, an expected means of controlling radionuclide mass transport through the packing material. Sorption hysteresis effects observed in recent radionuclide sorption studies are expected to decrease the mobility of radionuclides in the packing material. During FY 1984, hydrothermal long-term (up to 5 yr) packing material stability tests at 150°C will be initiated. The measurement of thermal conductivity of saturated packing materials will be initiated. Measurement of packing material physical properties (swelling, hydraulic conductivity, etc.) will continue.

Models are being developed to allow prediction of waste package reliability, degradation, and radionuclide release. In addition, two engineering test plans have been completed for tests that employ full-scale waste packages to measure the rate of packing material saturation under a thermal gradient and the degradation of waste package canister and packing material using canister heaters to simulate radiogenic heat.

DOCUMENT REVIEW FORM

AUTHOR: M. I. Wood

TITLE: Experimental Investigation of Sodium Bentonite Stability in Hanford Basalt

REFERENCE: RHO-BW-SA-219P, February 1983

AVAILABILITY: NTIS

KEY WORDS: bentonite, basalt, hydrothermal

DATA SUMMARY:

Property and Form of Data:
Ionic concentrations.

Materials and Specimen Geometry:

Umtanum basalt powder (fines washed off), bentonite powder, synthetic groundwater.

Test Conditions:

T = 300°C, P = 300 bars, 616 hrs, 2130 hrs.

COMMENTS ON DATA VALIDITY:

The change in concentration of the following were monitored with time in a system containing basalt and bentonite: Si, Na, Al, K, Ca, Mg, Fe, B, SO_4^{2-} , F^- , Cl^- . Potassium showed an increase followed by a decrease in concentration in the basalt-containing system. Data is shown in document abstract. The sulfate species decreased with time, which is the opposite of what occurred in FIN A-3167, Task 4 Phase I and Phase II experiments (whole package). The data presented in this report do not support the conclusion that bentonite will be hydrothermally stable and will continue to swell to the same degree. Experiments should have subjected mixture to dry heat, to simulate repository condition before water ingress, before testing packing material in the autoclave.

DOCUMENT ABSTRACT

Sodium bentonite is a candidate material for the waste package backfill component in a repository in basalt at the Hanford Site. Preliminary hydrothermal experiments have been conducted under near-field geochemical conditions expected to occur in the reference repository location in the Grande Ronde Basalt. Experiments have been conducted in the basalt/groundwater, bentonite/groundwater, and basalt/bentonite/groundwater systems. The experiments have been conducted at 300°C using a simulated Grande Ronde groundwater, reference Umtanum basalt, and sodium bentonite. Key data generated by the experiments include experimental solution analyses as a function of time and preliminary solids analysis by scanning transmission electron microscopy and X-ray diffraction. Solution trends of the major aqueous species were similar in the three systems and are characterized by: (1) the gradual reduction of the pH value from ~9.75 to a steady-state value of ~6, (2) an initial rapid increase followed by a gradual decrease in silica concentration, and (3) a slight or negligible increase in sodium, sulfate, and chloride concentrations. In the bentonite/groundwater experiment, small amounts (<1%) of an albite reaction product were observed. Conversely, the formation of illite, a common bentonite alteration product, was not observed. These results indicate that sodium bentonite will remain sufficiently stable at 300°C under hydrothermal conditions in basalt to permit its use as a backfill material.

The experimental data discussed above indicate that montmorillonite will remain sufficiently stable at 300°C under hydrothermal conditions to permit its use as a backfill material. Limited experimental data in the literature which might be applicable to the basalt geochemical environment also suggest that sodium montmorillonite is stable at 300°C. Other experiments involving hydrothermally reacted montmorillonites at high temperatures [4] show that saturated montmorillonite did not react to mixed-layer clay in a potassium-free system at 300°C for 1 month. However, noticeable reaction did occur at 400°C in a 17-day run where the reaction products rectorite (mixed-layer paragonite and montmorillonite), albite, kaolinite, and quartz were observed. More experiments and longer run times are required to determine the behavior of sodium bentonite under site-specific geochemical conditions. In particular, the validity of the albite alteration and the degree of alteration must be addressed in future experiments.

Umtanum basalt (RUE-2) + bentonite + synthetic Grande Ronde groundwater, 300°C
300 bars; initial water:solids = 10:1; basalt:bentonite = 1:1; basalt mesh
size = -115+250, 3 months

Concentration (mg/L)	Time (hr)							
	0	1	20	118	334	672	1337	2130
Si	34	333	551	632	661	632	537	479
Na	375	361	314	295	290	302	238	213
Al	<0.08	15.9	11.1	7.4	6.0	4.5	3.6	3.0
K	4.00	27.2	37.4	36.9	29.0	24.9	18.1	14.8
Ca	3.01	2.60	1.59	1.68	1.92	2.35	1.12	0.78
Mg	0.31	<0.10	<0.10	<0.10	<0.10	<0.10	<0.10	<0.1
Fe	<0.006	0.13	0.05	0.04	0.04	0.08	0.03	0.05
B	0.27	1.35	2.49	2.45	2.54	2.89	2.60	2.48
SO ₄ ²⁻	168		150	170	170	180	90	50
F ⁻	30		21.5	16	10	7	6.5	5.5
Cl ⁻	276		320	320	320	350	345	285
pH (25°C)	9.78	6.67	5.94	5.79	5.78	5.42	5.38	5.35

Zero hour solution sample = starting synthetic groundwater

DOCUMENT REVIEW FORM

AUTHOR: Wood, M. I. (RHO)

TITLE: Experimental Investigation of Sodium Bentonite Stability in Hanford Basalt

REFERENCE: Scientific Basis for Nuclear Waste Management VI, Vol. 15, North-Holland, N.Y., 1983, pp. 727-734

AVAILABILITY: Published

KEY WORDS: sodium bentonite, Umtanum basalt, Grande Ronde groundwater, pH, solution chemistry, hydrothermal testing, alteration, stability

DATA SUMMARY:

Property and Form of Data:

Solution pH and chemistry, examination of alteration products.

Materials and Specimen Geometry:

Bentonite powder, and crushed Umtanum basalt (-115 to +250 mesh) from an outcropping, synthetic Grande Ronde water.

Test Conditions:

300°C, 300 bar autoclave tests for up to 2000 h.

COMMENTS ON DATA VALIDITY:

The study evaluated Na-bentonite chemical stability with and without the presence of Umtanum basalt at 300°C and 300 bars. Synthetic Grande Ronde groundwater present in the autoclave was periodically analyzed for changes in dissolved species. The results show that the pH falls from an initial value of ~9.75 to about 6. Si concentration initially increases and then slowly decreases, whereas Na⁺, SO₄²⁻, and Cl⁻ show small or negligible increases. In the presence of bentonite an albite product was detected but illite, a common bentonite alteration product was not found. It was, therefore, concluded that bentonite would be stable enough at 300°C to be useful as a BWIP packing material.

The results presented are useful for determining initial fast changes in groundwater pH and chemistry, and bentonite alteration over a period of 2000 h. However, stability of bentonite can only be assured if much longer hydrothermal tests are conducted.

DOCUMENT ABSTRACT

Sodium bentonite is a candidate material for the waste package backfill component in a repository in basalt at the Hanford Site. Preliminary hydrothermal experiments have been conducted under near-field geochemical conditions expected to occur in the reference repository location in the Grande Ronde Basalt. Experiments have been conducted in the basalt/groundwater, bentonite/groundwater, and basalt/bentonite/groundwater systems. The experiments have been conducted at 300°C using a simulated Grande Ronde groundwater, reference Ustunus basalt, and sodium bentonite. Key data generated by the experiments include experimental solution analyses as a function of time and preliminary solids analysis by scanning transmission electron microscopy and X-ray diffraction. Solution trends of the major aqueous species were similar in the three systems and are characterized by: (1) the gradual reduction of the pH value from ~9.75 to a steady-state value of ~6, (2) an initial rapid increase followed by a gradual decrease in silica concentration, and (3) a slight or negligible increase in sodium, sulfate, and chloride concentrations. In the bentonite/groundwater experiment, small amounts (<1%) of an albite reaction product were observed. Conversely, the formation of illite, a common bentonite alteration product, was not observed. These results indicate that sodium bentonite will remain sufficiently stable at 300°C under hydrothermal conditions in basalt to permit its use as a backfill material.

DOCUMENT REVIEW FORM

AUTHOR: Wood, M. I., et al. (RHO)

TITLE: The Near Field Waste Package Environment in Basalt and Its Effect on Waste Form Releases

REFERENCE: RHO-BW-SA-331P, 1983

AVAILABILITY: Preprint of paper to be published in Civilian Radioactive Waste Management Information Meeting, Washington, D.C., December 1983

KEY WORDS: solubility, hydraulic conductivity, controlled release, modeling, Eh

DATA SUMMARY:

Property and Form of Data:

General data on solubilities, hydraulic conductivities, gives simple ID mass transfer calculation to estimate controlled release.

Materials and Specimen Geometry:

Not usually specified.

Test Conditions:

Generally pertinent to BWIP conditions.

COMMENTS ON DATA VALIDITY:

Wood gives data on the kinetics of dissolved oxygen depletion in Grande Ronde water at 100° and 150°C with and without basalt present. Basalt quickly decreases the oxygen level to a value <1 mg/L at 150°C over a period of only 200 h. A measured Eh value of between 0 to -0.1V was obtained. RHO cite this evidence for reducing conditions as being highly beneficial since it will decrease container corrosion and the solubility of radionuclides in water. However, they have done little if any work to measure dissolved oxygen levels and Eh in the presence of gamma radiolysis effects. Testing at BNL indicates that for a simulated waste package at ~150°C in the presence of gamma radiolysis, oxidizing conditions prevail after 60 days of reaction.

In calculating controlled release values to assess compliance with 10CFR60 and 40CFR191 Wood assumes (a) solubility constraints apply with the low Eh value defining the solubility levels, (b) mass transport through package is diffusion controlled. Assumption (a) is questionable since gamma or alpha radiolysis may still be significant in the post-containment period. Also, solubility levels used in Wood's calculations could be in error if they are estimated from isothermal tests since work at PNL (Fullam, 1982) show solubilities are greatly elevated when approached from the "supersaturated" direction. Also the assumption of diffusion-controlled transport through packing is not adequately supported.

DOCUMENT ABSTRACT

A licensable waste package for a nuclear waste repository in basalt must control long-term radionuclide release to the host rock within approved limits as defined by regulatory criteria. Demonstration of satisfactory long-term performance requires experimental data that characterize radionuclide behavior in the expected geochemical waste package environment. Also, an accepted model is required to predict the long-term release of radionuclides from the waste package into the host rock. Experimental data are summarized that pertain to radionuclide behavior in the nuclear waste repository in basalt waste package (e.g., oxygen consumption, hydrothermal reactions, hydraulic conductivity). A simple, one-dimensional, composite media transport model is described that provides calculations of maximum radionuclide release rates and cumulative releases (over 10,000 yr) at the waste package packing material/host rock interface on a radionuclide-by-radionuclide basis. The model demonstrates that radionuclide release from the waste package is linearly dependent on the solubility values chosen for the radionuclides of interest. The calculated releases are compared with Nuclear Regulatory Commission and Environmental Protection Agency criteria as well as the available experimental data. The experimental data indicate that the maximum release rates and cumulative releases of the radionuclides technetium, neptunium, and plutonium from the waste package should satisfy Environmental Protection Agency and Nuclear Regulatory Commission requirements.

APPENDIX 2

REVIEW OF WASTE PACKAGE DATA FOR SALT REPOSITORY PROGRAM

BLANK PAGE

DOCUMENT REVIEW FORM

AUTHOR: Jenks, G. H.

TITLE: Radiolysis and Hydrolysis in Salt-Mine Brines

REFERENCE: ORNL-TM-3717, March 1972

AVAILABILITY: Published

KEY WORDS: salt, temperature, migration, brine

DATA SUMMARY:

Property and Form of Data:

Radiation levels (rad/hr) and temperature ($^{\circ}\text{C}$) around waste cans as a function of time (yrs)-brine composition (molarity) and G-value of H_2 -reaction for thermal and radiation chemistries.

Materials and Specimen Geometry:

Buried waste can in a salt-mine, high level waste repository.

Test Conditions:

Literature review.

COMMENTS ON DATA VALIDITY:

The information presented is based on data compiled during a test in which a pilot waste container with 10 year old waste was emplaced in crushed salt. Interpretation of the data with respect to brine migration by high temperature fracture of the salt and radiolytic hydrogen generation are discussed. Estimation of hydrogen diffusion through the salt beds with the potential hazard for ignition are considered. Although the work is dated, it is a multi-component test and has data which could be applicable.

DOCUMENT ABSTRACT

Summary

We made a detailed review and analysis of literature information bearing on the radiation and thermal chemistries of the salt and brines within the vicinity of a buried waste can in a salt-mine, high-level, waste repository. The objectives were to identify the final radiolysis- and thermal reaction-products and to estimate the amounts formed and released into the spaces around a can.

Important radiolysis products include H_2 , O_2 and possibly ClO_3^- , and BrO_3^- . Most of the ClO_3^- and BrO_3^- will decompose to halides and O_2 at the high temperatures around a can; $Mg(BrO_3)_2$ if present may give rise to some Br_2 . Nearly all of the H_2 , and the accompanying oxidized species, are formed within the migrating brine inclusions by the radiations absorbed within the brine and by dissolution of the interstitial chlorine and trapped electrons from the irradiated solid salt. The brine is rich in $MgCl_2$ (2.3 to 3M), and hydrolysis of the $MgCl_2$ around a can will produce HCl.

No possibly-serious problems arising from radiolytic or thermal effects in the repository were recognized which couldn't be counteracted by some modification of the design or operation of the repository. However, the possible effects have not been completely evaluated. The repository project is planning or is presently conducting additional work in a number of additional areas including work in brine migration and radiolysis and radiation damage in the salt. The results of this work will help in evaluating the amounts and the effects of radiolysis, hydrolysis and corrosion products.

DOCUMENT REVIEW FORM

AUTHOR: B. W. Davis

TITLE: Preliminary Assessment of the Thermal Effects of An Annular Air Space Surrounding An Emplaced Nuclear Waste Canister

REFERENCE: UCRL 15014

AVAILABILITY: Published, April 1979

KEY WORDS: Thermal, Canister, Salt

GENERAL COMMENTS: This report presents the results of a study of the effect that an annular air space around a horizontally emplaced canister may have on the heat transfer from the spent fuel canister to a surrounding salt environment. Their results showed (1) the air gap could lead to canister surface temperatures significantly lower than would be obtained if a crushed salt backfill was used; (2) radiation heat transfer is more important than convection and; (3) the air gap did not greatly alter the temperature distribution in the far field, defined as distances greater than 5 ft. from the canister.

The analysis is limited in that (1) the calculation was performed for only one set of values for the physical parameters and only one geometry; (2) the possibility of salt creep diminishing and eventually closing the air gap was not considered; and (3) the effects of saturated air or steam on convective and radiative heat transfer was neglected.

DOCUMENT ABSTRACT

Modeling results have previously shown that the presence of a large air space (e.g., a repository room) within a nuclear waste repository is expected to cause a waste canister's temperature to remain cooler than it would otherwise be. Results presented herein show that an annular air space surrounding the waste canisters can have similar cooling effects under certain prescribable conditions; for a 16' x 1' diameter canister containing 650 FWR rods which initially generate a total of 4.61 kw, analysis will show that annular air spaces greater than 11" will permit the canister surface to attain peak temperatures lower than that which would result from a zero-gap/perfect thermal contact.* It was determined that the peak radial temperature gradient in the salt varies in proportion to the inverse of the drill hole radius. Thermal radiation is shown to be the dominant mode of heat transfer across an annular air space during the first two years after emplacement. Finally, a methodology is presented which will allow investigators to easily model radiation and convection heat transfer through air spaces by treating the space as a conduction element that possesses non-linear temperature dependent conductivity.

*Only this one set of power level (4.61 kw) and canister geometry was studied in numerical detail. It should be noted that a different power level and/or a different canister geometry will result in an air space size different from 11" (for the condition yielding temperatures equivalent to perfect thermal contact).

DOCUMENT REVIEW FORM

AUTHOR: Claiborne, H. C., et al.

TITLE: Expected Environments in High-Level Nuclear Waste and Spent Fuel Repositories in Salt

REFERENCE: ORNL/TM-7201, August 1980

AVAILABILITY: Published

KEY WORDS: salt, brine, canister, temperature, spent fuel

DATA SUMMARY:

Property and Form of Data:

Heat generation HLW and SF (relative value vs. years), thermal conductivity of salt ($^{\circ}\text{C}, \text{W}/\text{m}\cdot\text{k}$), density (kg/m^3), heat capacity ($\text{J}/\text{g}\cdot\text{k}$), conductivity ($\text{W}/\text{m}\cdot\text{k}$) for HLW, SF and salt, salt stratigraphy (m), corrosion (mil/year)

Materials and Specimen Geometry:

Steel, zirconium.

Test Conditions:

Literature review.

COMMENTS ON DATA VALIDITY:

The purpose of this report is to describe the expected environments associated with HLW and SF repositories in salt formations. These environments include the thermal, fluid, pressure, brine chemistry and radiation fields predicted for the repository conceptual designs. The authors state that "at this time, design parameters for a HLW or SF repository in salt are sufficiently well defined that it is possible to predict with some confidence many of the conditions that will be encountered in the vicinity of the waste canisters in the repository." Generally, the results are based on calculations using single component tests. Interactive tests would provide more complete data.

DOCUMENT ABSTRACT

1

EXPECTED ENVIRONMENT IN HIGH-LEVEL NUCLEAR WASTE AND
SPENT FUEL REPOSITORIES IN SALT

H. C. Claiborne, L. D. Rickertsen,* and R. F. Graham*

ABSTRACT (ABBREVIATED)

The purpose of this report is to describe the expected environments associated with high-level waste (HLW) and spent fuel (SF) repositories in salt formations. These environments include the thermal, fluid, pressure, brine chemistry, and radiation fields predicted for the repository conceptual designs.

Initial thermal loadings, distributed over the room and pillar areas, are assumed to be 2.16 kW/canister and 150 kW/acre (37.1 W/m²) for HLW and 0.55 kW/canister and 60 kW/acre (14.8 W/m²) for SF in a baseline repository. Thermal environments are calculated in terms of near-field and far-field models. The salt temperature for HLW peaks at 412°F (211°C) ~15 yr after emplacement of 10-yr-old waste. The peak for SF is broader, occurring ~50 yr after emplacement at a temperature of 211°F (99.4°C). At the canister surface, with a 4-in. (10.2-cm) barrier [2 in. (1 cm) of crushed salt and a 2-in. (5.1-cm) air gap], the maximum HLW temperature is 587°F (308°C) and peaks ~10 yr after emplacement. For SF, the maximum canister temperature is 237°F (114°C) and occurs ~25 yr after emplacement. The maximum HLW waste centerline temperature of 670°F (354°C) is reached ~3 yr after emplacement. The maximum temperature of the SF pin assembly is 280°F (138°C), occurring ~5 yr after emplacement.

Sensitivity studies are presented to show the effect of changing the areal heat load, the canister heat load, the barrier material and thickness, ventilation of the storage room, and adding a second row to the emplacement configuration. Decreasing either the areal heat load or the canister heat load reduces the canister surface temperature. For decreasing areal heat load, the effect becomes more pronounced as the years after emplacement increase; however, the effect for a decreasing canister heat load is most dramatic during the early years after emplacement. The effect on canister surface temperature of a change in the barrier is presented in the form of graphs which will permit the designer

The calculated thermal environment is used as input for brine migration calculations. The brine inclusions can be considered in terms of a particle density that obeys the time-dependent continuity equation. A computer code (MIGRAIN) was developed, and predictions compared favorably with experimental data of the Waste Isolation Pilot Plant (WIPP) Salt Block II. The total flow for HLW is ~12 g after 1500 yr, and the corresponding flow for SF is 6 g.

DOCUMENT REVIEW FORM

AUTHOR: Jenks, G.

TITLE: Review of Information on the Radiation Chemistry of Materials
Around Waste Canisters in Salt and Assessment of the Need for
Additional Experimental Information

REFERENCE: ORNL-5607, March 1980

AVAILABILITY: Available

KEY WORDS: brine, radiation, salt repository, radiolysis

DATA SUMMARY:

Property and Form of Data:

Dose rates; temperatures; brine compositions; brine radiolysis;
gas formation.

Materials and Specimen Geometry:

Reference HLW package in salt; generic effects of radiation on
brine and salt.

Test Conditions:

Overview document.

COMMENTS ON DATA VALIDITY:

Useful review monograph on radiation effects in a salt-brine environment, including radiation damage to salt, gas generation and changes in brine chemistry. Work applicable to both spent fuel and HLW. Emphasis is given to the radiolytic formation of oxidants (O_2 or ClO_3^- or both) under certain conditions. The pH conditions likely to be encountered over the period of interest are not addressed. Recent BNL work on irradiation of salt and brine has indicated a wide range of pH conditions are likely to exist at any particular point in time throughout the operational and post-emplacement time period. Changes in brine-salt chemistry over time require experimental verification not offered in this report.

DOCUMENT ABSTRACT

The brines, vapors, and salts precipitated from the brines will be exposed to gamma rays and to elevated temperatures in the regions close to a waste package in the salt. Accordingly, they will be subject to changes in composition brought about by reactions induced by the radiations and heat.

The objectives of the work discussed in this report were to review the status of information on the radiation chemistry of brines, gases, and solids which might be present around a waste package in salt and to assess the need for additional laboratory investigations on the radiation chemistry of these materials.

The basic aspects of the radiation chemistry of water and aqueous solutions, including concentrated salt solutions, were reviewed briefly and found to be substantially unchanged from those presented in Jenks's 1972 review of radiolysis and hydrolysis in salt-mine brines. Some additional information pertaining to the radiolytic yields and reactions in brine solutions has become available since the previous review, and this information will be useful in the eventual, complete elucidation of the radiation chemistry of the salt-mine brines.

DOCUMENT REVIEW FORM

AUTHOR: Lowry, W. E., B. W. Davis and H. Cheung (LLL)

TITLE: The Effects of Annular Air Gaps Surrounding an Emplaced
Nuclear Waste Canister in Deep Geologic Storage

REFERENCE: UCRL-84152, June 1980

AVAILABILITY: Available

KEY WORDS: annular air gaps, waste package, temperature, bedded salt,
basalt, spent fuel

DATA SUMMARY:

Property and Form of Data:

Three-dimensional numeric modeling results: gap sizes;
temperatures.

Materials and Specimen Geometry:

Modeling efforts.

Test Conditions:

Spent fuel (aged 3-10 yrs); canister size: 1' diam x 16' length;
air gaps of 3, 6, 18, and 42 inches used.

COMMENTS ON DATA VALIDITY:

Approach useful in design-configuration aspects of emplacement. The temperature of the waste canister is determined in response to variations in (1) surface properties of the gap, (2) the size of the annular air gap, (3) the presence/absence of a sleeve, and (4) canister and areal initial thermal power levels. As gap size increases from zero gap, the temperature rapidly approaches peak at a critical width; beyond this width gaps produce lower temperatures. Results of such efforts should be investigated in the field.

DOCUMENT ABSTRACT

THE EFFECTS OF ANNULAR AIR GAPS
SURROUNDING AN EMPLACED NUCLEAR
WASTE CANISTER IN DEEP GEOLOGIC STORAGE *

William E. Lowry
University of California, Lawrence Livermore National Laboratory
Livermore, California

Bill W. Davis
Northern Arizona University

Henry Cheung
University of California, Lawrence Livermore National Laboratory
Livermore, California

ABSTRACT

Annular air spaces surrounding an emplaced nuclear waste canister in deep geologic storage will have significant effects on the long-term performance of the waste form. Addressed specifically in this analysis is the influence of a gap on the thermal response of the waste package. Three dimensional numerical modeling predicts temperature effects for a series of parameter variations, including the influence of gap size, surface emissivities, initial thermal power generation rate of the canister, and the presence/absence of a sleeve. Particular emphasis is placed on determining the effects these variables have on the canister surface temperature. We have identified critical gap sizes at which the peak transient temperature occurs when gap widths are varied for a range of power levels. It is also shown that high emissivities for the heat exchanging surfaces are desirable, while that of the canister surface has the greatest influence. Gap effects are more pronounced, and therefore more effort should be devoted to optimal design, in situations where the absolute temperature of the near field medium is high. This occurs for higher power level emplacements and in geomedias with low thermal conductivities. Finally, loosely inserting a sleeve in the borehole effectively creates two gaps and drastically raises the canister peak temperature. It is possible to use these results in the design of an optimum package configuration which will maintain the canister at acceptable temperature levels. A discussion is provided which relates these findings to NRC regulatory considerations.

DOCUMENT REVIEW FORM

AUTHOR: Magnami, N. J., and Braithwaite, J. W. (SNL)

TITLE: Corrosion Resistant Metallic Canisters for Nuclear Waste Isolation

REFERENCE: Scientific Basis for Nuclear Waste Management, Vol. 2,
Plenum Press, N.Y., 1980, pp. 377-384.

AVAILABILITY: Published

KEY WORDS: T304 SS, TiCode 12, WIPP Brine A, seawater, uniform corrosion,
stress-corrosion, slow-strain-rate testing

DATA SUMMARY:

Property and Form of Data:

Uniform corrosion rates in $\mu\text{m}/\text{y}$ and reduction-in-area values from slow-strain-rate tensile tests to evaluate stress-corrosion cracking.

Materials and Specimen Geometry:

TiCode-12 and T304 SS metal coupons for uniform corrosion tests and tensile specimens for stress-corrosion tests.

Test Conditions:

Seawater and Brine A for uniform corrosion at 250°C ; seawater, Brine A, air, dry salt and wet salt for slow-strain-rate tests at 250°C .

COMMENTS ON DATA VALIDITY:

The program is designed to give basic data on corrosion of containers for the WIPP and the subseabed disposal program. The data show that in deoxygenated solutions the uniform corrosion rates for both materials are higher in Brine A. For both solutions the uniform corrosion rate for TiCode-12 is 6 times lower in seawater.

In the slow-strain-rate tests the T304 SS is embrittled in wet salt and Brine A but not in dry salt (0.7% H_2O). TiCode-12 is not embrittled in dry salt or Brine A. Dissolved O_2 is a major factor in susceptibility of T304 SS to embrittlement.

The test temperature is possibly high for commercial waste disposal in salt but is a useful accelerated test to show that stress corrosion is a possible failure mode for stainless steel. No data are given for irradiation corrosion or the effects of adjacent waste package components.

DOCUMENT ABSTRACT

A program with the goal of estimating the potential of a material to survive 300 years as a nuclear waste canister is underway at Sandia Laboratories. The corrosion and stress corrosion cracking behavior of the leading candidate, TiCode-12***, is contrasted to that of a commonly used engineering alloy, 304 stainless steel. Experimental evidence is presented which shows the inadequacy of 304 stainless steel in potential repository environments and shows that TiCode-12 could endure the desired 300 years. Further work required to qualify TiCode-12 is outlined.

DOCUMENT REVIEW FORM

AUTHOR: Rankin, W. N. (SRL)

TITLE: Canister Compatibility with Carlsbad Salt

REFERENCE: Scientific Basis for Nuclear Waste Management, Vol. 2,
Plenum Press, N.Y., 1980, pp. 395-402.

AVAILABILITY: Published

KEY WORDS: rock salt, Cor-Ten carbon steel, T304 SS, uniform corrosion,
container

DATA SUMMARY:

Property and Form of Data:

Uniform corrosion depth in mils. Some characterization of metal oxides formed.

Materials and Specimen Geometry:

Cor-Ten carbon steel and T304L SS cylindrical specimens embedded to crushed rock salt.

Test Conditions:

Sealed capsules exposed for 5000 h at 80 and 225°C and unsealed capsules exposed for 10,000 h at 80, 225 and 600°C.

COMMENTS ON DATA VALIDITY:

The study addresses the corrosion of Cor-Ten carbon steel and T304L SS as candidate materials for HLW containers to be emplaced in bedded salt. For samples heated for 10,000 h the materials exposed at 80°C showed no visible corrosion. At 225°C the T304L SS showed only small patches of attack 1 mil in thickness after 10,000 h. In the same period the carbon steel was attacked and contained corrosion products to a thickness of 0.6 mil. Samples of T304 SS exposed in sealed capsules for 5000 h at 80 and 225°C showed no oxidation. Carbon steel samples, however, were covered with a black oxide. At 600°C the stainless steel was covered with a thin black oxide and the carbon steel showed a much thicker oxide scale.

The data are valid for predicting general oxidation behavior in the presence of rock salt. However, much longer term tests will be needed to determine the uniform corrosion rates which can be used in design, and to ascertain if new corrosion failure modes are likely.

DOCUMENT ABSTRACT

No significant reaction was found when candidate canister alloys were heated with salt from Carlsbad, New Mexico, for up to 5000 hours in sealed capsules and for up to 10,000 hours in unsealed capsules at temperatures (80 to 225°C) that bracket the maximum temperature calculated for reference Savannah River Plant (SRP) waste containers at 20-foot spacings in salt (2). Additional tests were made at 600°C in sealed capsules to characterize reactions that may occur between candidate canister alloys and any component of the salt that is released when decrepitation occurs. Under these extreme conditions there was no significant attack of Type 304L stainless steel. But, there was up to 20-mils attack of the low-carbon steel.

DOCUMENT REVIEW FORM

AUTHOR: Glass, Robert S.

TITLE: Effects of Radiation on the Chemical Environment Surrounding Waste Canisters in Proposed Repository Sites and Possible Effects of the Corrosion Process

REFERENCE: SAND81-1677, December 1981

AVAILABILITY: Published

KEY WORDS: canister, groundwater, corrosion, radiation damage

DATA SUMMARY:

Property and Form of Data:

Tuff groundwater composition mg/L, seawater, Brines A and B ppm, chemical reactions produced in H₂O, seawater and brines by gamma radiation (rads/hr).

Materials and Specimen Geometry:

Titanium alloys, stainless steel, Fe, Cu, Ni.

Test Conditions:

Literature Review.

COMMENTS ON DATA VALIDITY:

This report provides several of the chemical reactions that will occur during irradiation of the environment surrounding the canisters. The corrosion effects caused by this irradiated environment to possible canister materials such as stainless steel and Fe, Cu, Ni and Ti alloys are given. This information is useful for supplementing data taken from other component tests. Irradiated interactive tests that include backfill and host rock are not provided in this report.

DOCUMENT ABSTRACT

SAND81-1677
Unlimited Release

**EFFECTS OF RADIATION ON THE CHEMICAL ENVIRONMENT SURROUNDING
WASTE CANISTERS IN PROPOSED REPOSITORY SITES AND POSSIBLE
EFFECTS ON THE CORROSION PROCESS***

Robert S. Glass
Sandia National Laboratories
Albuquerque, NM 87185

ABSTRACT

This report explores the interaction of ionizing radiation with various environments. In particular, worst case (aqueous) environments for the proposed nuclear waste repository sites are considered. Emphasis is on the fundamental chemical and physical processes involved. The identities of possible radiolysis products (both transient and stable) have been sought through a literature search. The effect of radiation on corrosion processes is discussed.

The radiation-induced chemical environment in the worst case repository sites is not well defined. Attention should therefore be given to fundamental studies exploring the interaction of such environments with components of the nuclear waste package, including the canister materials and backfills. Identification and quantification of radiolysis products would be helpful in this regard.

*This work supported by the U.S. Department of Energy.

DOCUMENT REVIEW FORM

AUTHOR: G. H. Jenks and J. R. Walton

TITLE: Radiation Chemistry of Salt-Mine Brines and Hydrates

REFERENCE: ORNL-5726, July 1981

AVAILABILITY: Available

KEY WORDS: radiation, salt, brines, hydrates

DATA SUMMARY:

Property and Form of Data:

Analysis for ClO_3^- , H_2O_2 , Cl_2 and other gas components (H_2 , O_2 , CH_4 , CO_2 , N_2 , Ar, He).

Materials and Specimen Geometry:

NaCl-saturated MgCl_2 -containing solutions; MgCl_2 hydrates.

Test Conditions:

Temperatures in the range of 30-180°C; aerated and deaerated solutions used; irradiation time, 20-210 minutes; cobalt source used (Shepherd 89-TBq).

COMMENTS ON DATA VALIDITY:

Document useful in documenting experimental work undertaken to establish the values for the yield of $\text{H}_2[\text{G}(\text{H}_2)]$ in the gamma-ray radiolysis of concentrated brines that might occur in waste repositories in salt. However, gas liberation and generation will also take place from the irradiation and heating of the rock salt and contribute to the overall gas production process. The availability of hydrogen formation may contribute to hydrogen-assisted failure of titanium. Brines also tend to be acidic at elevated temperatures and could yield HCl. Also, the interaction of sodium with brine may lead to the formation of sodium hydroxide (NaOH). These factors will contribute to the deterioration of the container and packing material.

Certain aspects of the radiation chemistry of NaCl-saturated MgCl₂ solutions and MgCl₂ hydrates at temperatures in the range of 30 to 180°C were investigated through experiments. A principal objective was to establish the values for the yields of H₂ [$G(H_2)$] and accompanying oxidants in the gamma-ray radiolysis of concentrated brines that might occur in waste repositories in salt.

We concluded that $G(H_2)$ from gamma-irradiated brine solution into a simultaneously irradiated, deaerated atmosphere above the solution is between 0.48 and 0.49 over most of the range 30 to 143°C. The yield is probably somewhat lower at the lower end of this range, averaging 0.44 at 30 to 45°C. Changes in the relative amounts of MgCl₂ and NaCl in the NaCl-saturated solutions have negligible effects on the yield.

The yield of O₂ into the same atmosphere averages 0.13, independent of the temperature and brine composition, showing that only ~50% of the radiolytic oxidant that was formed along with the H₂ was present as O₂. We did not identify the species that compose the remainder of the oxidant.

We concluded that the yield of H₂ from a gamma-irradiated brine solution into a simultaneously irradiated atmosphere containing 5 to 8% air in He may be greater than the yield in deaerated systems by amounts ranging from 0% for temperatures of 73 to 85°C, to about 30 and 40% for temperatures in the ranges 100 to 143°C and 30 to 45°C, respectively. We did not establish the mechanism whereby the air affected the yields of H₂ and O₂.

The values found in this work for $G(H_2)$ in deaerated systems are in approximate agreement with the value of 0.44 for the gamma-irradiation yield of H₂ in pure H₂O at room temperature. They are also in agreement with the values predicted by extrapolation from the findings of previous researchers for the value for $G(H_2)$ in 2 M NaCl solutions at room temperature. They are in poorer agreement with the value of $G(H_2) = 0.42$ for NaCl-saturated solutions in the range 0 to 85°C stated by Spitsyn et al.¹ The higher values for $G(H_2)$ in brine (~2) inferred by Jenks² from results with KCl solutions reported by previous Russian workers are completely discounted.

Our conclusions regarding the effects of 5 to 8% air on the values for $G(H_2)$ apparently do not agree with the stated findings

of Spitsyn et al. that the value for $G(H_2)$ in salt solutions is independent of O₂.

Additionally, we concluded that deaerated solutions containing 10 to 12 M MgCl₂ and irradiated at 150 to 180°C exhibit $G(H_2)$ values greater than those for solutions of lower MgCl₂ concentrations at lower temperatures by factors ranging from 1.0-1.25 at 150-160°C to 1.6-2.0 at 170-180°C. Presumably, the increased hydrolysis of MgCl₂ at higher temperatures and concentrations is responsible for some or all of the increase in $G(H_2)$. Also, we found that radiolytic decomposition of the water of hydration in crystals of MgCl₂·6H₂O takes place, but that the effective values for $G(H_2)$ are much less than those in a liquefied solution with the same ratio of MgCl₂ to H₂O. Most of the H₂ is not released from the crystals until the irradiated material is heated above the liquefaction temperature.

Some suggestions for additional experimental work are presented which would help (1) in the identification of the several oxidized species that are apparently formed in the radiolysis of brine solutions and (2) in the further clarification of radiolysis in the brines.

DOCUMENT REVIEW FORM

AUTHOR: G. H. Jenks, H. C. Claiborne

TITLE: Brine Migration in Salt and Its Implications in the Geologic Disposal of Nuclear Waste

REFERENCE: ORNL-5818, December 1981

AVAILABILITY: Available

KEY WORDS: brine, salt repository, migration, HLW

DATA SUMMARY:

Property and Form of Data:

Theoretical and experimental; brine migration data; thermal gradient-induced brine migration.

Materials and Specimen Geometry:

Bedded salt; various geometries, single crystal and crushed salt.

Test Conditions:

Overview document includes data on migration rates of brine in single crystals at temperatures up to $\sim 250^{\circ}\text{C}$; thermal gradient-induced brine migration at temperatures from $50\text{-}200^{\circ}\text{C}$.

COMMENTS ON DATA VALIDITY:

Useful overview on rock salt characteristics affecting brine migration; theoretical aspects of liquid brine migration within crystals of NaCl; migration rate data for bedded salt; migration of gas-liquid inclusions in NaCl; experimental and theoretical information on migration of fluids within rock salt walls of waste emplacement hole; brine flow estimates based on MIGRAIN code. Such aspects as decrepitation and consolidation not taken into account with regards to enhancing brine inflow rates. Radiation effects, such as weakening of salt structure and lowering temperature at which decrepitation occurs, not considered in this report.

DOCUMENT ABSTRACT

Bedded and domal salt deposits within the United States that are being considered for use in the disposal of spent light-water reactor (LWR) fuel and/or solidified high-level wastes contain a small volume fraction of brine inclusions, which are located within salt crystals and/or at crystal boundaries. These inclusions can migrate through the salt to the waste package when sufficiently large gradients (primarily temperature gradients) exist in the chemical potential of the salt around the inclusions. The fluids could also move hydraulically if sufficiently large microcracks are formed in the salt.

Information concerning the rates and total amounts of brine migrating to a waste package within a salt repository are needed in evaluating the suitability of a given disposal concept. Brine migration in salt has been studied extensively during the past 15 years, and the objective of the present report is to provide a comprehensive review and analysis of this available information for use in the preparation of a licensing topical report (LTR) on brine migration. The objectives of the licensing report are discussed elsewhere.

The topics covered in this report relate to three general areas: (1) the characteristics of salt formations and waste packages germane to considerations of rates, amounts, and effects of brine migration, (2) experimental and theoretical information on brine migrations, and (3) means of designing to minimize any adverse effects of brine migration. Flooding, brine pockets, or other factors will presumably be precluded by appropriate site selection and repository design.

DOCUMENT REVIEW FORM

AUTHOR: Krause, W. B., and P. F. Gnirk

TITLE: Domal Salt Brine Migration Experiments at Avery Island

REFERENCE: The Technology of High-Level Waste Disposals, Technical Information Center, DOE, 1981, pp. 110-135

AVAILABILITY: Published

KEY WORDS: brine migration, thermal gradient, Avery Island, heaters

DATA SUMMARY:

Property and Form of Data:

Moisture collection rates in gms for given thermal gradients in domal salt.

Materials and Specimen Geometry:

Avery Island salt dome.

Test Conditions:

Maximum salt temperatures between 30-53°C, and thermal gradients up to 1.42 °C/cm. Test times up to 325 d.

COMMENTS ON DATA VALIDITY:

The paper reviews prior work on brine migration in salt and gives a detailed account of the Avery Island heater experiments. Measurements were made of brine migration rates in thermal gradients imposed on the salt by the heaters. A model is proposed for the migration mechanism which is in agreement with measured values.

This paper is of value in defining the anticipated influx of brine into a package borehole. It will be useful with respect to quantifying the amount of brine available for container corrosion and glass leaching and also will help to understand the importance of brine migration in assessing the controlled release rates for radionuclides.

DOCUMENT ABSTRACT

Conclusion

The concept of the migration of brine inclusions surrounding a heater borehole can be studied on both a macroscopic and microscopic scale. The macroscopic scale considers the gross influences of thermal conditions (gradient and temperature) on the moisture moving toward the heater borehole. Microscopic studies consider the change in inclusion shape, possible movement of tagged synthetic brine through grain boundaries, and related petrographic examinations.

These brine migration experiments had three primary objectives. The first was to conduct scoping and exploratory experiments in domal salt to examine brine movement. This objective has been achieved. The second objective was to examine techniques for more sophisticated future follow-on experiments. A more sophisticated moisture collection system should include a "closed-loop cold-trap system" and dew-point sensing methods to determine the relative humidity in the heated borehole environment. The third objective was to determine the in situ permeability of salt at different temperatures; it was also achieved. The measurements indicate that permeability changes

significantly during rapid cool down of a heater borehole.

Because of the low moisture content of domal salt and the relatively moderate salt temperatures and thermal gradients in these experiments, we expected only a small inflow of moisture to the heater borehole. The moisture collection rates were indeed quite small, but they were still within a reasonable measurement range for the long-term test. The measured moisture inflow showed reasonable agreement with analytical predictions based on present brine inclusion migration theory.

Although the heater power levels at sites SB and NB were moderate, the heat fluxes produced by the heaters are significantly greater than those of certain types of nuclear fuel. This information was originally discussed by Krause (1979) in the experimental plan for the brine migration experiments at Avery Island. These comparisons are summarized in Table 5.

DOCUMENT REVIEW FORM

AUTHOR: Levy, P. W., et al. (BNL)

TITLE: Radiation Damage Studies on Synthetic and Natural Rock Salt
for Radioactive Waste Disposal Applications

REFERENCE: The Technology of High Level Waste Disposal, Technical
Information Center, DOE, 1981, pp. 136-167

AVAILABILITY: Published

KEY WORDS: natural salt, pure salt, electron irradiation, colloidal
sodium, F-centers, dose rate, hydrogen

DATA SUMMARY:

Property and Form of Data:

F-center and colloidal Na generation rates as a function of
irradiation time, dose rate, and temperature.

Materials and Specimen Geometry:

Salt samples from Asse, Avery Island, WIPP, Lyons, Retsof (NY)
and Saskatchewan; melt-grown NaCl from Harshaw Chemical Co.

Test Conditions:

1.5 MeV electron irradiation between 100-200°C, doses 30-340
Mrads/h, irradiation times up to 1.6×10^4 sec.

COMMENTS ON DATA VALIDITY:

The paper describes a basic study to evaluate damage to synthetic and
natural salt caused by 1.5 MeV electrons at temperatures between 100 and
300°C. Production rates for F-centers and Na colloids were measured by
optical absorption techniques for different dose rates and shown to increase
monotonically. For Na colloid formation the Jain-Lidraid theory was shown to
be capable of predicting much of the observed concentrations.

Results of this work are valuable for defining the amounts of F-center
and colloidal sodium formed during irradiation. This will enable calculations
to be made regarding the anticipated change in pH and alkalinity, and in
hydrogen release caused by brine interaction with colloidal sodium. Waste
form and container corrosion are closely connected with these parameters.

DOCUMENT ABSTRACT

Radiation damage, particularly F-center and sodium metal colloid particle formation, was studied at 100 to 300°C in synthetic melt-grown NaCl crystals and natural rock salt from different geological localities. Optical absorption measurements were made at controlled temperatures during irradiation with 1.5-MeV electrons in a unique facility for making optical absorption and other measurements during irradiation. The electron irradiations produced the same damage as do gamma rays of similar energy. Phenomenologically, damage formation was similar in pristine natural and unstrained synthetic rock salt. At temperatures where colloids are formed readily, F-center concentration vs. dose curves increased monotonically at a decreasing rate to a well-defined plateau. Concomitantly, colloid formation was described by classical nucleation and growth curves, with the onset of rapid growth (i.e., the end of the induction period) occurring at doses of roughly 10^7 rads, where the F-centers reach a plateau. The F-center plateau levels were highest at 100°C, decreased monotonically with increasing temperature, and were negligible at 300°C. In contrast, the colloid formation rate was low or zero near 100°C, increased with increasing temperature to a broad maximum at 150 to 175°C, and decreased to a negligible level at high temperatures (275 to 300°C). The high-dose part of the colloid growth curves was well approximated by (irradiation time)ⁿ or (dose)ⁿ relations. In natural rock salt not strained in the laboratory the average n value for 14 samples was 1.35 ± 0.18 at 150°C and at a dose rate of 1.2×10^8 rads/h. In unstrained synthetic NaCl, n values were in the 4 to 6 region below and in the 2 to 3 region above 190°C. At

all temperatures the n values in both types of salt were reduced to 1.5 to 1.6 by plastic deformation before irradiation. In both natural and synthetic salt, the induction period was altered by straining before irradiation, diminishing as the strain increased to 10% and becoming negligible for larger strains. Preliminary measurements showed that, on a unit dose basis, the colloid formation rate increases as the dose rate decreases. The Jain-Lidiard theory for radiation-induced colloid formation in NaCl accounts for some but not all of the observations. Overall the theory appears to apply better to natural than to synthetic rock salt. The measurements made to date have been confined to total doses of 2 to 4×10^8 rads. Extrapolating the (irradiation time)ⁿ or (dose)ⁿ relations to doses expected at the surface of the waste form in a radioactive waste repository indicated that doses of 10^{10} rads will convert 0.1 to 10% and 2×10^{10} rads will convert 1 to 50% of the adjacent rock salt to sodium metal colloid particles. The salt adjacent to the canisters will reach these doses in 50 to 400 yr. Since this large variation in damage formation results from differences in the radiation-induced colloid formation rates between samples from different locations, radioactive waste repositories are best placed in localities and/or horizons where the damage rates are low. Also, the properties of rock salt subjected to doses of 10^8 to 10^{10} rads differ markedly from those of unirradiated salt. Irradiated salt is brittle and friable, contains chlorine, and reacts with water to form H₂ gas and other products. Thus waste form canisters, which will be subject to heat, radiation, and pressure, must be designed to withstand a variety of physical and chemical interactions with irradiated rock salt.

DOCUMENT REVIEW FORM

AUTHOR: Molecke, M. (Sandia), Bradley, D. J., and Shade, J. W. (PNL)

TITLE: PNL Sandia HLW Package Interactions Test: Phase One

REFERENCE: SAND81-1442C, November 1981

AVAILABILITY: Paper

KEY WORDS: corrosion, backfill, interaction, waste package, salt

DATA SUMMARY:

Property and Form of Data:

Brine composition in ppm before and after test.

Materials and Specimen Geometry:

1.0 mm TiCode-12, PNL 76-68 glass, brine, 304L SS canister
1.3 mm thick.

Test Conditions:

Interactive test in autoclave 13.3 MPa, 250°C, 95 days.

COMMENTS ON DATA VALIDITY:

This test is composed of a 3" dia x 15" HLW form in a SS 304L canister inside a TiCode-12 overpack surrounded by brine saturated 30^w/o bentonite in sand, enveloped in rock salt and placed in an autoclave lined with Inconel-600. The results of this test indicate that the glass leach rate is not linear, e.g. the reaction rate was similar to static leach rates of a shorter duration. Post-test mechanical testing of TiCode-12 did not yield any significant degradation of properties. Extensive general corrosion was observed on the SS 304L canister particularly around the welds. The Inconel-600 liner clearly showed evidence of pitting corrosion. Relative weight percents of Al, Si, and Fe in the backfill were analyzed before and after the test. It was observed that the ratios of Si/Fe and Si/Al had increased during the test. This appears to be a worthwhile interactive test but the effects of radiation are not included.

DOCUMENT ABSTRACT

ABSTRACT

The first phase of a complex high-level waste (HLW) package interactions test in a salt environment has been completed. The test system consisted of PHL 76-68 HLW glass (loaded with inactive fission products and ²³⁸U) surrounded by a stainless steel waste canister, a TiCode-12 overpack, a bentonite/sand backfill, excess brine leachant, and a bedded rock salt container, all held within a 19-liter autoclave. All components were physically compromised in order to force wasteform-barrier-salt interactions to occur during this 95-day, 250°C overtest. Analyses of leachant, wasteform, and all barrier surfaces were performed. Test data included the synergistic effects between barriers and confirmed previous analyses of simpler systems. The glass wasteform exhibited some surface alteration but was not dissolved to any significant degree. The TiCode-12 overpack showed minimal uniform corrosion and no localized attack. Observed mineralogical alteration of the backfill was minimal.

DOCUMENT REVIEW FORM

AUTHOR: Molecke, M. A., et al.

TITLE: Sandia HLW Canister/Overpack Studies Applicable for a Salt Repository

REFERENCE: SAND81-1585, October 1981

AVAILABILITY: Published

KEY WORDS: salt, corrosion, canister, brine, commercial waste

DATA SUMMARY:

Property and Form of Data:

Corrosion rate (mm/yr) for seawater, Brine A, Brine B, Brine A with 600 ppm O₂ - corrosion rate (mm/yr) in test solutions above as a function of gamma radiation (rads/hr).

Materials and Specimen Geometry:

1018 steel, SS-304L, 316L, Nitronic 50, Ebrite, Monel, Inconel, Zr, Ti alloys.

Test Conditions:

Temperature 250°C, 28 days and 90°C, 49-87 days for irradiated tests.

COMMENTS ON DATA VALIDITY:

This report gives corrosion data for approximately 20 HLW candidate alloys under irradiated and non-irradiated conditions. TiCode-12 was shown to be the least corrosive of all the materials tested. Other materials such as Inconel, Incoloy, 1018 steel and some cast irons are still being evaluated as alternates. The data appears significant and could be used in conjunction with other information.

DOCUMENT ABSTRACT

ABSTRACT

An experimental program to develop candidate materials for use as high-level waste (HLW) overpacks or canisters in a salt repository has been in progress at Sandia National Laboratories since 1976. The main objective of this program has been to provide a waste package barrier having a long lifetime in the chemical and physical environment of a repository. This paper summarizes the recent corrosion and metallurgical results for the prime overpack material TiCode-12 in the areas of uniform corrosion (extremely low rate and extent), local attack, e.g. pits and crevices (none found), stress corrosion cracking susceptibility (no significant changes in macroscopic tensile properties detected) and hydrogen sorption/embrittlement effects (testing still in process), effects of gamma irradiation in solution (still in process), and sensitization effects (still in process). Previous candidate screening analyses on other alloys and recent work on alternate overpack alloys are reviewed. All phases of these interrelated laboratory, hot-cell, and field experimental studies are described.

DOCUMENT REVIEW FORM

AUTHOR: Shor, A. J., C. F. Baes, Jr., and C. M. Canonico

TITLE: Consolidation and Permeability of Salt in Brine

REFERENCE: ORNL-5774, July 1981

AVAILABILITY: Available

KEY WORDS: salt repositories, consolidation, permeability, brine

DATA SUMMARY:

Property and Form of Data:

Consolidation: void fraction/time with temperature.

Materials and Specimen Geometry:

Beads of NaCl crystals sized in the ranges of 75-150, 150-177, 177-250, 250-420 μm in Monel tubes (1.27 or 2.54 cm ID used) and stressed by piston-driven ram.

Test Conditions:

Temperatures: 20°C; 50°C; 85°C

Time: 10⁰ to 10⁴ minutes

Stress: to 155 bars (range: 20-155 bars)

COMMENTS ON DATA VALIDITY:

Salt crystals in brine subjected to constant stress consolidated in an approximately linear fashion with the logarithm of time. The rate of consolidation was found to decrease with additions to the brine of MgCl₂ (resulting in decreased NaCl solubility). The approach is useful, however radiolysis effects will alter solubilities and affect consolidation. This type of experimentation should be undertaken to include the presence of a radiation field.

DOCUMENT ABSTRACT

CONSOLIDATION AND PERMEABILITY OF SALT IN BRINE

A. J. Shor, C. F. Baes, Jr., and C. M. Canonico

ABSTRACT

The consolidation and loss of permeability of salt crystal aggregates, important in assessing the effects of water in salt repositories, has been studied as a function of several variables. The kinetic behavior was similar to that often observed in sintering and suggested the following expression for the time dependence of the void fraction:

$$\phi(t) = \phi(0) - (A/B) \ln(1 + Bt/\bar{z}(0)^3),$$

where A and B are rate constants and $\bar{z}(0)$ is initial average particle size. With brine present, A and $\phi(0)$ varied linearly with stress. The initial void fraction was also dependent to some extent on the particle size distribution. The rate of consolidation was most rapid in brine and least rapid in the presence of only air as the fluid. A brine containing 5 m $MgCl_2$ showed an intermediate rate, presumably because of the greatly reduced solubility of $NaCl$. A substantial wall effect was indicated by an observed increase in the void fraction of consolidated columns with distance from the top where the stress was applied and by a dependence of consolidation rate on the column height and radius. The distance through which the stress fell by a factor of e was estimated to change inversely as the fourth power of the column diameter. With increasing temperature (to $85^\circ C$), consolidation proceeded somewhat more rapidly and the wall effect was reduced. The permeability of the columns dropped rapidly with consolidation, decreasing with about the sixth power of the void fraction. In general, extrapolation of the results to repository conditions confirms the self-sealing properties of bedded salt as a storage medium for radioactive waste.

DOCUMENT REVIEW FORM

AUTHOR: Biggers, J. V. and G. O. Dayton (Penn State)

TITLE: Brine Migration in Hot-Pressed Polycrystalline Sodium Chloride

REFERENCE: ONWI-415, December 1982

AVAILABILITY: Available

KEY WORDS: brine migration, salt

DATA SUMMARY:

Property and Form of Data:

Microstructural analysis of hot-pressed samples; brine migration.

Materials and Specimen Geometry:

Polycrystalline NaCl (hot-pressed); pressed into circular cylinders:
4.7 cm in diam., 5 cm long.

Test Conditions:

3 migration cells used: one using thermal gradient of 120°C/cm;
a second using 10-15°C/cm; a third using 4-8°C/cm.

COMMENTS ON DATA VALIDITY:

The attempt was made to provide an assessment of the effects of grain boundaries in polycrystalline salt on the mechanisms and rates of brine migration. Experimental difficulties resulted in the attempt to produce defect-free specimens (i.e. to adequately control microstructure) and in the assembly of experimental equipment capable of maintaining a linear thermal gradient. Microstructural changes occurring in the polycrystalline salt were difficult to observe. There is indirect evidence to suggest that migration rates are enhanced along paths that follow grain boundaries and other similar crystal defects.

Continued efforts in this area are needed and should involve the use of natural salt and radiation-induced damaged salt. Attempts should be made to provide quantitative data on migration velocities.

DOCUMENT ABSTRACT

This report describes experiments designed to provide data on brine migration in polycrystalline salt. Polycrystalline samples of various grain sizes, density, and purity were prepared from several commercial grade salts by hot-pressing. Three distinct experimental set-ups were used to place salt billets in an induced thermal gradient in contact with a brine source. The test designs varied primarily in the way in the thermal gradient was applied and monitored and the way in which brine migration was determined. All migration was in enclosed vessels which precluded visual observation of brine movement through the microstructure.

Migration velocities were estimated either by the timed appearance of brine at the hot face of the sample, or by determination of the penetration distance of migration artifacts in the microstructure after tests of fixed duration. For various reasons both of these methods were subject to a large degree of error. Our results suggest, however, that the migration velocity in dense polycrystalline salt may be at least an order of magnitude greater than that suggested by single crystal experiments.

Microstructural analysis shows that brine prefers to migrate along paths of high crystalline activity such as grain and subgrain boundaries and is dispersed rather quickly in the microstructure. A series of tests were performed using various types of tracers in brine in order to flag migration paths and locate brine in the microstructure more decisively. These attempts failed and it appears that only the aqueous portion of the brine moves through the microstructure with the dissolved ions being lost and replaced rather quickly. This suggests the use of deuterium as a tracer in future work.

DOCUMENT REVIEW FORM

AUTHOR: Griess, J. C. (ORNL)

TITLE: Evaluation of Corrosion Damage to Materials After Three Years
in the Avery Island Salt Mine

REFERENCE: ORNL/TM-8351, August 1982

AVAILABILITY: Available

KEY WORDS: corrosion, salt, metals, alloys, carbon steel, hastelloy
titanium, zircaloy

DATA SUMMARY:

Property and Form of Data:

Corrosion: descaled weight loss (mg/cm^2).

Average corrosion rate ($\mu\text{m}/\text{year}$).

Corrosion with depth (m).

Materials and Specimen Geometry:

Specimens: carbon steel; titanium; E-Brite 26-1; Hastelloy C-276;
304L SS; and Zircaloy-2 coupons (~4 cm long x 1 cm wide) mounted on
sleeves.

Test Conditions:

Electric heaters used to simulate decay heat in mine floor,
152 m below sea level; specimen coupons and thermocouples attached
to sleeves and lowered into borehole; time, ~3 years; temperature
range, ~25-280°C.

COMMENTS ON DATA VALIDITY:

This type of field testing extremely useful in assessing corrosion damage
of candidate materials. No backfill was used for these studies (experiments
with crushed salt backfill underway); the presence of radiation in studies of
this type will more closely resemble actual repository conditions and effects
on corrosion rates will be more realistic and thus more useful.

DOCUMENT ABSTRACT

EVALUATION OF CORROSION DAMAGE TO MATERIALS AFTER
THREE YEARS IN THE AVERY ISLAND SALT MINE

J. C. Griess

ABSTRACT

The corrosion results obtained from two heated steel pipes that had been buried in a salt mine at Avery Island, Louisiana, for about three years are reported. In addition, weight losses of corrosion specimens of several alloys attached to the outer surfaces of the pipes were also obtained, and the maximum depths of penetration were measured. The greatest attack was noted on carbon steel, particularly when the water content of the salt was high. The maximum penetration rate observed was about 1 mm/year. All other materials tested underwent much less attack than did carbon steel; titanium and Hastelloy C-276 were totally unaffected on both pipes. Minimal attack was also noted on Zircaloy-2 and type 304L stainless steel, whereas E-Brite 26-1 experienced pitting, and, at high temperatures, a more general attack on some areas.

DOCUMENT REVIEW FORM

AUTHOR: D. Holcomb and D. Hannum

TITLE: Consolidation of Crushed Salt Backfill Under Conditions
Appropriate to the WIPP Facility

REFERENCE: SAND-82-0630, November 1982

AVAILABILITY: Available

KEY WORDS: salt, backfill, consolidation, WIPP, creep tests

DATA SUMMARY:

Property and Form of Data:

Time-dependent compaction of crushed salt; changes in sample volume due to compaction (quasistatic tests and creep tests conducted).

Materials and Specimen Geometry:

Crushed rock salt ~1 cm particle size.

Test Conditions:

Temperature Range: 21-100°C.

Pressure: 1.72 MPa-21 MPa

Duration: Quasistatic, 8000 sec; Creep, 300,000 sec.

COMMENTS ON DATA VALIDITY:

The tests were conducted assuming dry conditions. The presence of brine will enhance the rate and extent of consolidation and should be included in experiments of this type. The test durations were limited to 3×10^5 seconds and although the creep consolidation rate was seen to decelerate (under dry conditions), it is not known whether the deceleration will continue and at what rate. Also consolidation is known to result in the expulsion of brine; this report does not address whether or not brine was released from the salt during consolidation. Although consolidation under dry conditions was seen not to be very temperature dependent in the range of 21°C to 100°C this situation may differ in the presence of brine.

DOCUMENT ABSTRACT

Mechanical properties of granulated rock salt are of interest to the WIPP project because native salt from the excavations will probably be used as backfill around the waste packages and as void filler in storage rooms, shafts and other openings. Backfill properties will be an important factor in controlling room closure rates and local permeability. To fill the need for data on time dependent compaction of crushed salt, we have done a series of tests to measure the compaction as a function of time, temperature and pressure. Tests were done for a range of temperatures from 21 to 100 °C and pressures from 1.72 MPa to 21 MPa, under quasistatic and creep conditions. All tests were done under pure hydrostatic conditions. A rock crusher was used to produce crushed salt with a maximum particle size of 1 cm. All tests were done under nominally dry conditions which means the only water present was the $\approx .5\%$ water content of the salt. The major conclusions are: (1) Creep consolidation under hydrostatic stresses proceeds at a rate of approximately $t^{-0.5}$, where t is the time in seconds. Total creep consolidation is a function of $\log(t)$ and is very slow. (2) Consolidation is not very temperature dependent in the range 21°C to 100°C. These conclusions are tested only for times up to 3×10^6 seconds. The major question is whether the creep consolidation rate will continue to decelerate rapidly. If rapid deceleration continues, then for the time periods of interest, creep consolidation will be small compared to the consolidation produced by quasistatic pressurization.

DOCUMENT REVIEW FORM

AUTHOR: Magnami, N. J. (SNL)

TITLE: Corrosion Resistant Canisters for Nuclear Waste Isolation

REFERENCE: Scientific Basis for Nuclear Waste Management, VI, Vol. 15,
1983, pp. 669-676

AVAILABILITY: Published

KEY WORDS: Ti, TiCode-12, Inconel 600, Inconel 625, Incoloy 825,
Hastelloy C-276, Cu, Cupronickel 90-10, Monel 400,
uniform corrosion, container, brine, basaltic water, SCC

DATA SUMMARY:

Property and Form of Data:

Uniform corrosion, crevice corrosion, H₂ embrittlement, SCC
data for temperatures between 70-250°C.

Materials and Specimen Geometry:

As above.

Test Conditions:

Varied for different corrosion mechanisms. Temperatures between
70-250°C, dissolved oxygen between 30 ppb to 450 ppm. Brine A and
seawater.

COMMENTS ON DATA VALIDITY:

Brief review of 9 metals and alloys in order to select a reference HLW canister material for the SNL waste container program. At 250°C, tests in Brine A and seawater for a period of 28 d shows that TiCode-12 has a uniform corrosion rate of 3 μm/g in Brine A and 1 μm/g in seawater. This was the lowest of the range of alloys tested. Electrochemical tests show that titanium based materials have a high resistance to passivity breakdown. TiCode-12 shows less corrosion at 250°C in 450 ppm O₂ brine when compared to 30 ppb O₂ brine.

The SNL studies state that no crevice attack has been seen to date and that very acidic conditions will not destroy passivity. Work at BNL refutes both these statements. In the area of SCC in brine and basaltic water SNL believes that it is not a likely problem with TiCode-12 unless it is associated with hydrogen embrittlement. Detailed work on such embrittlement is under way.

Magnami also discusses iron/steel corrosion failure modes. He concludes that pitting and SCC are not likely in basaltic water or brines. Recent unpublished BNL work shows pitting in 150°C basaltic water, however. The data review is preliminary and does not recognize new important corrosion data at BNL.

DOCUMENT ABSTRACT

Corrosion resistant canisters are an important component of the engineered barriers of a nuclear waste disposal system. In addition to providing containment for the waste form during transportation and emplacement, a durable canister can eliminate hydrothermal interactions with the waste form. The selection of a repository site and emplacement technique will affect canister design and could also impact material selection. While there are still many issues to be resolved, there are two different concepts being evaluated to provide durable canisters for waste disposal: (1) canisters fabricated out of extremely corrosion resistant materials such as Ti-base or Ni-base alloys, and (2) canisters fabricated out of less durable materials but designed with a corrosion allowance. Each of these types of canisters could fail to meet the design objectives through a variety of failure processes. The more important of these are discussed.

DOCUMENT REVIEW FORM

AUTHOR: Molecke, M. A., et al. (SNL)

TITLE: Materials for High Level Waste Canister/Overpacks in Salt Formations

REFERENCE: SAND-0429, 1982

AVAILABILITY: Published

KEY WORDS: TiCode-12, iron/steel, corrosion, gamma irradiation, salt, brine, seawater, pH, gamma irradiation

DATA SUMMARY:

Property and Form of Data:

Uniform and localized corrosion data for temperatures up to 300°C.
Slow strain rate tensile tests at 90°C.

Materials and Specimen Geometry:

Mainly TiCode-12 and cast iron.

Test Conditions:

Brine A, Brine B, seawater corrosion data for temperatures up to 300°C.

COMMENTS ON DATA VALIDITY:

The paper is a detailed account of much of the available work in DOE on HLW container material selection and evaluation for salt repositories. After initial screening tests the 2 main materials studied were cast iron and TiCode-12. In some tests, heating of Brine A to 250°C in the presence of bentonite gave a solution pH of 3.4. This was thought to be due to the formation of Mg oxysulfates and HCl.

SNL did not at any time observe crevice corrosion in TiCode-12 in high temperature brine but stated that BNL studies had shown it to be present in 150°C Brine A.

Gamma irradiation tests indicated that radiation accelerated uniform corrosion, possibly by the action of radiolytic H₂ in partially reducing the passive film.

Test data were also given to show that TiCode-12 is susceptible to H₂ embrittlement for H₂ levels \geq 200 wppm. BNL work confirms this.

Other data described were from the PNL/SNL whole package test program, reviewed elsewhere in the current study.

SNL does not address the potential formation of NaOH in brine due to gamma radiation of rock salt. High pH levels could enhance the uniform corrosion of TiCode-12 and increase H₂ pickup rates according to BNL work.

DOCUMENT ABSTRACT

Studies on the corrosion and mechanical behavior of TiCode-12 and other titanium alloys, for use as candidate canister or overpack barriers in a high-level waste repository or test facility in salt, are reported herein. These studies have been in progress at Sandia National Laboratories since 1976. Titanium alloys were selected as the primary materials for detailed testing based on candidate screening analyses (general corrosion and economic assessments) of about 20 different alloys. Recent material results on titanium alloys are described and related to the long-term physical integrity of waste package barriers in salt; results on other candidate alloys are reviewed.

The corrosion behavior of TiCode-12 has been evaluated as a function of: brine composition, temperature, time, pH, oxygen concentration, and gamma radiolysis. Uniform corrosion rates are in the range of 0.1 to 10 $\mu\text{m}/\text{yr}$; pitting or crevice corrosion has not yet been observed. The highly adherent, passivating titanium oxide film that provides the corrosion protection is being evaluated via electro-chemical polarization and surface analytical techniques to enable modeling of the corrosion mechanism(s). An increase in the corrosion rate by a factor of about 2 was observed for sensitized TiCode-12; changes in the alloy microstructure are being analyzed in order to model this phenomenon. Alterations in the chemistry and processing procedure of TiCode-12 are being evaluated to optimize corrosion, mechanical, and mill-productibility properties for high-level waste package applications.

Slow strain rate testing of TiCode-12 revealed no apparent susceptibility to stress corrosion cracking; no significant changes in tensile properties were observed, but alterations in fracture mode were determined to be caused by internal hydrogen content. Hydrogen effects on titanium alloy mechanical properties and crack susceptibility are being studied. Some hydrogen embrittlement occurs at hydrogen concentrations in the range of 200 to 300 ppm by weight, but the strength of TiCode-12 is not affected at concentrations up to 1100 wppm. Further research on slow crack growth threshold stress intensity as a function of H content is required.

Based on the analysis of available corrosion and metallurgical results, we are proposing a TiCode-12 HLW canister-package for use in a repository or test facility in salt. Such a simplified HLW canister could provide long-term containment integrity and significantly minimize total HLW isolation system costs when compared to other waste package design concepts.

DOCUMENT REVIEW FORM

AUTHOR: Molecke, M. (SNL), D. J. Bradley, J. W. Shade (PNL)

TITLE: PNL-Sandia HLW Package Interactions Test, Phase One

REFERENCE: Scientific Basis for Nuclear Waste Management, Vol. 6,
North-Holland, N.Y., 1982, pp. 337-345

AVAILABILITY: Published

KEY WORDS: waste package test, 76-68 glass, T304L SS, TiCode-12, rock salt,
bentonite, Brine A, corrosion, glass leaching

DATA SUMMARY:

Property and Form of Data:

Summary of waste package component interaction tests under hydrothermal brine conditions.

Materials and Specimen Geometry:

76-68 glass, T304L SS, TiCode-12, Inconel 600, rock salt, Brine A.

Test Conditions:

91 d hydrothermal tests on simulated salt waste packages at 250°C.

COMMENTS ON DATA VALIDITY:

Evaluation performed on a borosilicate glass waste form doped with fission products and U, surrounded by a T304L SS/TiCode-12 container/overpack system, a bentonite/sand backfill, excess brine and a salt host rock. The components were all breached prior to test to determine synergistic effects in a 95 d, 250°C test in an autoclave.

The brine pH decreased from 6.8 to 3.8 after test which is stated to be a result of reactions between $MgCl_2$ and SiO_2 and aluminosilicates. It could also be due to release of HCl from the salt during heating. An analysis of the glass surface showed the presence of SiO_2 , MgO_2 , Fe_2O_3 , Na_2O , and ZrO_2 plus small amounts of Zn, U, Nd, Ni and Cr. The TiCode-12 container contained TiH_2 platelets, throughout the thickness, omega phase in the beta phase, and Ti_2Ni on α/β interfaces. The H_2 content increased from 50 to 600-700 ppm. At this level embrittlement effects are likely as shown by other SNL and BNL work. The 304L SS container suffered extensive general corrosion particularly at welds. Brine interaction caused significant changes in the bentonite clay.

These data are of significant value in assessing synergistic interactions between W.P. components and address mainly early waste package failure at high temperature. It has been shown that many of the effects are similar to single component tests and thus helps validate the latter.

DOCUMENT ABSTRACT

The first phase of a complex high-level waste (HLW) package interactions test in a salt environment has been completed. The test system consisted of PNL 76-68 HM glass (loaded with inactive fission products and ²³⁸U) surrounded by a stainless steel waste canister, a TiCode-12 overpack, a bentonite/nann backfill, exsiccant brine leachant, and a bedded rock salt container, all held within a 19-liter autoclave. All components were physically compromised in order to force wasteform-barrier-salt interactions to occur during this 95-day, 250°C overtest. Analysis of leachant, wasteform, and all barrier surfaces were performed. Test data included the synergistic effects between barriers and confirmed previous analyses of simpler systems. The glass wasteform exhibited some surface alteration but was not dissolved to any significant degree. The TiCode-12 overpack showed minimal uniform corrosion and no localized attack. Observed mineralogical alteration of the backfill was minimal.

DOCUMENT REVIEW FORM

AUTHOR: Baes, Jr., C. F., et al. (ORNL)

TITLE: The Effect of Water in Salt Repositories, Final Report

REFERENCE: ORNL-5950, September 1983

AVAILABILITY: Available

KEY WORDS: salt, brine, migration, consolidation, permeability

DATA SUMMARY:

Property and Form of Data:

Permeability as brine flow in g/min through an area of 1 cm² under hydrostatic pressure grad. 1 bar/cm.

Stress (bars): 155

Temperature (range): 20-65°C

Brine expelled from salt, in grams.

Materials and Specimen Geometry:

Columns with diameters of 1.27 and 2.54 cm of monel; cylindrical specimens of salt and brine; hydraulic ram used to apply stress consolidation (void fraction) of 250- to 420 μm salt crystals.

Test Conditions:

Crystal interface permeability measured at 20°C.

COMMENTS ON DATA VALIDITY:

Consolidation results in brine loss or expulsion within stressed salt specimens. No evidence of significant amounts of brine being trapped. Consolidation occurs readily in the presence of brine with fairly predictable kinetics. The effects of radiolysis (changes in solubility; radiation damage) are not considered in this study. Gas formation as a result of radiolysis will also affect pressure gradients and should be included in future efforts of this type.

DOCUMENT ABSTRACT

**THE EFFECT OF WATER IN SALT REPOSITORIES:
FINAL REPORT**

C. F. Baes, Jr., L. O. Gilpatrick, F. G. Kitts,
H. R. Bronstein, and A. J. Shor

ABSTRACT

Additional results confirm that during most of the consolidation of polycrystalline salt in brine, the previously proposed rate expression applies. The final consolidation, however, proceeds at a lower rate than predicted. The presence of clay hastens the consolidation process but does not greatly affect the previously observed relationship between permeability and void fraction. Studies of the migration of brine within polycrystalline salt specimens under stress indicate that the principal effect is the exclusion of brine as a result of consolidation, a process that evidently can proceed to completion. No clear effect of a temperature gradient could be identified. A previously reported linear increase with time of the reciprocal permeability of salt-crystal interfaces to brine was confirmed, though the rate of increase appears more nearly proportional to the product of $\sigma\Delta P$ rather than $\sigma\Delta P^2$ (σ is the uniaxial stress normal to the interface and ΔP is the hydraulic pressure drop). The new results suggest that a limiting permeability may be reached. A model for the permeability of salt-crystal interfaces to brine is developed that is reasonably consistent with the present results and may be used to predict the permeability of bedded salt. More measurements are needed, however, to choose between two limiting forms of the model.

DOCUMENT REVIEW FORM

AUTHOR: Canfield, T. R.

TITLE: Stresses Near Waste Canisters Buried in Salt

REFERENCE: SAND-82-0525, March 1983

AVAILABILITY: Published

KEY WORDS: salt, modeling, canister, temperature

DATA SUMMARY:

Property and Form of Data:

Canister thermal loads °C vs. meters. Canister pressure loads - MPa as a function of time (years) and distance in meters.

Materials and Specimen Geometry:

Codes - COYOTE, SANCHO, MERLIN(3).

Test Conditions:

Based on calculations.

COMMENTS ON DATA VALIDITY:

Borehole closure is dependent on the overburden pressure distribution and relative geometry. The presence of backfill material in place of the air gap would also hasten borehole closure. Radial stress on canisters (without an air gap) reached a maximum after about one year and gradually decreased for a period of up to 80 years and thereafter remained constant. The calculation indicates that the peak pressure would not persist and that pressure driven brine migration is possible.

DOCUMENT ABSTRACT

Conclusion (ABBREVIATED)

Bulk pressure distribution showed a peak near the borehole in the early period of calculation. This peak was also observed in stress calculations for the Salt Block II experiments (9,10). It was hoped that this peak in pressure might persist throughout the 1000 year period of the calculation because it would serve as a barrier to any brine migration that was driven by pressure gradients. This was not the case but the availability of these bulk pressure distributions would make estimates of pressure driven brine migration possible.

The creep mechanism was responsible for the slow inward displacement of material and closure of the borehole in the first calculation. The magnitude of the elastic response is seen to be negligible by observing the initial displacement distributions in figures 13, 15 and 17. Thermoelastic strain was also relatively small. Temperatures reached their maximums in the first few years of calculation while inward motion continued unabated for 60 years.

It was evident that borehole closure was dependent upon both the nature of the overburden pressure distribution and the relative geometry. If the air gap was smaller, hole closure would have occurred sooner and in addition hole closure could occur if the access drift was left open. The presence of backfill material in place of the air gap would also have hastened borehole closure and encapsulation of the canister. The results shown in figure 10 indicate that the rate of hole closure decreases with time and hole closure is nearly complete within 60 years. From curves of this type hole closure times could be predicted. Borehole size could be selected to time encapsulation and achieve retrievability goals.

While a borehole were closing, it would be expected that the radial stress would follow a path similar to that traced by the upper curve in figures 8 and 9. At the time of contact the stress would then increase in magnitude and approach the value of the lower curve. It can be seen that delaying hole closure would reduce the magnitude of contact pressure when contact occurs. This could have a significant effect on canister design.

DOCUMENT REVIEW FORM

AUTHOR: Krause, W. B.

TITLE: Avery Island Brine Migration Tests: Installation, Operation,
Data Collection, and Analysis

REFERENCE: ONWI-190(4), December 1983

AVAILABILITY: Available

KEY WORDS: brine migration, domal salt, Avery Island

DATA SUMMARY:

Property and Form of Data:

Temperature profiles; moisture collection (grams); atomic absorption used to determine Mg concentration in synthetic brine used to monitor brine movement in the salt around the heater borehole.

Materials and Specimen Geometry:

Domal salt; in-situ brine migration tests using heaters emplaced on the floor of the Avery Island Salt Mine at a depth of 169 m.

Test Conditions:

Thermocouples and tagged synthetic brine used to evaluate the movement of brine under elevated temperatures. Maximum salt temperature, ~52°C; Heating period, 325 days after which heating was terminated with a stepped power reduction.

COMMENTS ON DATA VALIDITY:

Temperature lower than anticipated; study useful in that it addresses gross thermal influences and stress conditions effecting moisture movement toward the heater borehole; considers changes in brine inclusion shape and movement of tagged synthetic brine along grain boundaries. An increase in moisture collection and permeability was observed during the cool-down period (i.e., the stepped power reduction period).

DOCUMENT ABSTRACT

Three brine migration tests were performed in domal salt at the Avery Island salt mine. The primary measurements included temperature, moisture collection, and pre- and post-test permeability. This report presents the data for the brine migration tests, an analysis of these data, comparison of the data with a brine migration theory, and related discussion and recommendations for future brine migration experiments.

DOCUMENT REVIEW FORM

AUTHOR: Moody, N., and S. Robinson (SNL)

TITLE: Internal Hydrogen Effects in TiCode-12 Overpack/Canister Material

REFERENCE: Scientific Basis for Nuclear Waste Management VI, Vol. 15,
North Holland, N.Y., 1983, pp. 753-760

AVAILABILITY: Published

KEY WORDS: hydrogen embrittlement, tensile tests, TiCode-12, microstructure,
secondary cracking

DATA SUMMARY:

Property and Form of Data:

Ductility, yield and fracture strengths as a function of hydrogen level.

Materials and Specimen Geometry:

TiCode-12 round bar tensile specimen, 3.2 mm dia. and 15.2 mm gage length.

Test Conditions:

Room temperature tensile tests.

COMMENTS ON DATA VALIDITY:

The tests carried out were on TiCode-12 specimens which were charged in a hydrogen furnace at 750°C to give dissolved H₂ levels of 160-1100 ppm. Tensile tests were carried out at RT to measure reduction-in-cross-sectional area, fracture stress and yield strength.

There was a slight decrease in elongation and reduction-in-area as the hydrogen concentration increased from 16 to 1100 ppm. The fracture strength showed a large decrease, however, as the H₂ level increased to 200 ppm but it remained constant at higher levels. The embrittlement was characterized by the appearance of secondary cracking.

These data are valid for licensing since they quantify an important mechanical failure mode for TiCode-12. More work will be needed to measure H₂ uptake rates as a function of gamma radiolysis of groundwater and uniform corrosion rates since these are an important source of H₂.

DOCUMENT ABSTRACT

The effects of internal hydrogen on the mechanical properties of Ti Code 12 were studied by gas phase charging smooth bar tensile samples. Tensile tests showed no change in yield strength with increasing hydrogen concentration. A slight decrease in ductility and fracture stress at hydrogen concentrations above 200 wppm accompanied by secondary cracking along grain boundaries indicated embrittlement. At hydrogen concentrations near and above 400 wppm, cleavage fracture associated with strain-induced hydrides was also observed.

DOCUMENT REVIEW FORM

AUTHOR: Pfeifle, T. W., et al. (RE/SPEC)

TITLE: Preliminary Constitutive Properties for Salt and Nonsalt Rocks
From Four Potential Repository Sites

REFERENCE: ONWI-450, July 1983

AVAILABILITY: Available

KEY WORDS: HLW, repositories, salt, strength, creep

DATA SUMMARY:

Property and Form of Data:

Creep strain vs. a function of time; elastic parameters; strength; elastic moduli.

Materials and Specimen Geometry:

Salt from various localities; core samples used.

Test Conditions:

Creep experiments: 5 MPa/100°C; 10 MPa/100°C; 5 MPa/200°C;
confining pressure of 15 MPa. Quasi-static experiments: 24°C;
confining pressure of 0, 5, 10, and 15 MPa.

COMMENTS ON DATA VALIDITY:

The usefulness of this report is in illustrating the variations in physical/mechanical behavior that can exist from site to site. Generic data or modeling efforts will require critical evaluation and field validation given the variations that exist in salt formations. In addition, generic data should not be used in assessing waste package behavior since the effects of emplacement on the near-field environment will be a function of site-specific parameters (i.e., site-specific creep behavior).

In other respects, the usefulness of this document is limited to site-selection concerns and not relevant to the waste package.

DOCUMENT ABSTRACT

Results are presented from laboratory strength and creep tests performed on salt and nonsalt specimens from the Richton Dome in Mississippi, the Vacherie Dome in Louisiana, the Permian Basin in Texas, and the Paradox Basin in Utah. The constitutive properties obtained for salt are the elastic moduli and the failure envelope at 24°C and parameter values for the exponential-time creep law. Some additional data are presented to indicate how the elastic moduli and strength change with temperature. The nonsalt constitutive properties reported are the elastic moduli, the unconfined compressive strength and the tensile strength at 24°C. The properties given in this report will be used in subsequent numerical simulations that will provide information to assist in the screening and selection of site locations for a nuclear waste repository and to assist in the repository design at the selected site.

The matrix of tests performed is the minimum effort required to obtain these constitutive properties. The preliminary values obtained will be supplemented by additional testing for sites that are selected for further investigation.

DOCUMENT REVIEW FORM

AUTHOR: Reference Repository Conditions Interface Working Group

TITLE: Results of Repository Conditions Studies for Commercial and
Defense High Level Nuclear Wastes and Spent Fuel Repositories
in Salt

REFERENCE: ONWI-483, July 1983

AVAILABILITY: Published

KEY WORDS: repository conditions, salt repository, CHLW, DHLW and
spent fuel

DATA SUMMARY:

Property and Form of Data:

Temperature, pressure, fluid, chemical radiation environments
anticipated in salt repository. Not site specific.

Materials and Specimen Geometry:

Waste: UO_2 and glass.

Canister: carbon steel (SF), stainless steel for CHLW and DHLW.

Overpack: carbon steel.

Backfill: crushed salt.

Test Conditions:

COMMENTS ON DATA VALIDITY:

Calculations were performed to scope the range of conditions that might be present in a salt repository. The intent of the report is to provide a guide for materials test performance. The authors note that some reference conditions (e.g. brine composition) will be site dependent. In addition, no attempt is made to address the combined effects of heat and radiation on the waste package environment and therefore the package performance.

ONWI-483

DOCUMENT ABSTRACT

This report summarizes activities to determine repository conditions for temperatures, pressure, fluid, chemical, and radiation environments that are expected to exist in commercial and defense high-level nuclear waste and spent fuel repositories in salt. These conditions were generated by the Reference Repository Conditions Interface Working Group (RRC-IWG), an ad hoc IWG established by the National Waste Terminal Storage Program's (NWTSP) Isolation Interface Control Board (I-ICB). These repository conditions are based on the standard room-and-pillar mined repository concept with waste emplaced in vertical holes drilled in the room floor.

Some important results obtained are given below for selected local areal thermal loadings of 25, 25, and 11.5 W/m² for spent fuel (SF), commercial high-level waste (CHLW) and defense high-level waste (DHLW), respectively. In all cases, the results below are given in order for SF, CHLW, and DHLW. Some thermal results are: maximum waste temperature - 190, 320, and 100 C; maximum canister surface temperature - 160, 260, and 90 C; and maximum rock temperature - 150, 160, and 80 C. The length of significant thermal exposure is greater for SF than the other wastes. Thermal histories are given in the report. Vapor phase pressures are not expected to rise significantly above atmospheric pressure until the repository is sealed. After sealing, the pressure will gradually increase to approach lithostatic equilibrium. Estimated volumes of accumulation of brine from thermal migration for 1,000 years are 3 to 4 liters, 8 liters, and 0.5 liter. Reference brine compositions are given, although actual brine compositions are strongly site dependent. The maximum absorbed gamma radiation dose delivered to the salt after 10⁴ year is 1.5 x 10¹⁰ rads, and 9.6 x 10⁸ rads for the CHLW and SF canisters, respectively.

DOCUMENT REVIEW FORM

AUTHOR: Ruppen, J. A., et al. (SNL)

TITLE: Some Effects of Microstructure and Chemistry on Corrosion and Hydrogen Embrittlement of TiCode-12

REFERENCE: Scientific Basis for Nuclear Waste Management VI, Vol. 15, North Holland, N.Y., 1983, pp. 685-693

AVAILABILITY: Published

KEY WORDS: TiCode-12, sensitization, heat treatment, microstructure, hydrogen embrittlement, slow-strain-rate tests, air, Brine A

DATA SUMMARY:

Property and Form of Data:

Uniform corrosion rates and ductility and fractographic measurements.

Materials and Specimen Geometry:

TiCode-12 tensile specimens and corrosion coupons.

Test Conditions:

Room temperature tensile tests and corrosion tests in 70°C and boiling HCl and 200°C Brine A.

COMMENTS ON DATA VALIDITY:

The research described in the paper was undertaken to determine whether annealing effects associated with welding could lead to sensitization and accelerated corrosion and also to assess hydrogen embrittlement effects. It was found that annealing 6 heats of TiCode-12 between 575-675°C for periods between 0.25-128 h gave a maximum increase in uniform corrosion rate in boiling 1N HCl of only 100 percent.

Hydrogen embrittlement as measured by slow strain rate tests showed that for H₂ levels up to 130 ppm no embrittlement was detected. For 220 ppm H₂, and higher, loss in ductility and cleavage effects were noted. It is believed that H₂ embrittlement effects may be avoided if the concentration of hydrogen is kept below 200 ppm, but additional work is needed on the effects of H₂ level on the threshold stress intensity for crack growth.

This work is of importance to licensing since it evaluates failure modes for TiCode-12 and attempts to define procedures for mitigating them.

DOCUMENT ABSTRACT

Effects of microstructure and chemistry on corrosion and hydrogen embrittlement of TiCode-12 have been investigated. Heat treating mill-annealed TiCode-12 in the temperature range 500-750°C results in a sensitization effect, i.e., an increase in the uniform corrosion rate when tested in either boiling 1N HCl or a MgCl₂ brine. This effect is caused by microstructural changes involving the precipitation of Ti₂Ni. Electrochemical studies indicate that sensitization results from galvanic coupling between Ti₂Ni, acting as cathode, and the α -Ti matrix with resultant shifts in corrosion potential. Increasing the Fe content of the alloy promotes the sensitization effect.

Hydrogen embrittlement of TiCode-12 was studied using the slow strain rate technique. Hydrogen concentrations to 130 wppm did not cause embrittlement. However, above 220 wppm hydrogen, degradation was observed as a decrease in mechanical behavior and the appearance of cleavage-like secondary cracks. The embrittlement was dependent on temperature and alloy chemistry but not environment (air or brine).

DOCUMENT REVIEW FORM

AUTHOR: Westinghouse Electric Corporation, Advanced Energy Systems Division

TITLE: Engineered Waste Package Conceptual Design: Defense High-Level Waste (Form 1), Commercial High Level Waste (Form 1), and Spent Fuel (Form 2) Disposal in Salt

REFERENCE: ONWI-438, April 1983

AVAILABILITY: Published

KEY WORDS: waste package, conceptual design, salt repository, spent fuel, CHLW, DHLW

DATA SUMMARY:

Property and Form of Data:

Corrosion data for Ti (Grade 12) and cast steel. Compilation of backfill data and leaching data for spent fuel and glass. Thermal models, brine migration models; cost projections.

Materials and Specimen Geometry:

Test Conditions:

Data presented ranges over the conditions anticipated in the reference designs (e.g., corrosion data up to 250°C, as function of O₂ concentration, in brines and seawater).

COMMENTS ON DATA VALIDITY:

All data reported is taken from published work of other researchers. Data is used to assess potential of certain materials for use in HLW package and to justify choice of reference package design and alternative designs. The authors recognize the need for more testing of these materials under conditions anticipated in a salt repository. Various aspects of the data and assumptions used in this report have been reviewed and commented on by BNL previously.

DOCUMENT ABSTRACT

ABSTRACT

This report provides conceptual waste package designs for use by the Office of Nuclear Waste Isolation (ONWI) in preparing a repository conceptual design in salt. Included are designs for the current reference waste form configurations of Defense High Level Waste, which consists of Savannah River Laboratory wastes immobilized in borosilicate glass, Commercial High Level Waste, which is a borosilicate glass waste form that results from the immobilization of commercial spent fuel reprocessing wastes, and Spent Fuel - Form 2, which consists of consolidated spent fuel rods from PWR or BWR assemblies. Reference designs are presented which are used as a baseline to evaluate design alternatives resulting from variations in the waste form configuration, the design approach, and the design data base. This broad spectrum of conceptual designs for salt has been included to provide ONWI a basis for concept comparison, an indication as to which of several package and repository design approaches are more cost effective, and guidance as to which approaches should be pursued in future design efforts.

Based on available data and the analyses performed, all the concepts in this report offer technically viable approaches to the containment of the waste form for at least 1,000 years and for adequate isolation of radionuclides thereafter. The reference borehole-type design is one which provides containment through the use of a titanium alloy corrosion resistant overpack, backed with a carbon steel structural reinforcing member. An alternate borehole design is one which provides containment with an all-steel overpack which is sufficiently thick to withstand expected crushing loads and to accommodate expected corrosion. The self-shielded package approach provides containment through use of a thick section of moderately corrosion resistant ferrous alloy material.

Development programs are identified that will be required to support designs during licensing.

APPENDIX 3

REVIEW OF WASTE PACKAGE DATA FOR TUFF REPOSITORY PROGRAM

BLANK PAGE

DOCUMENT REVIEW FORM

AUTHOR: RRC/IWG, Raines, G. E., Chairman

TITLE: Interim Reference Repository Conditions for Spent Fuel and
Commercial High Level Nuclear Repositories in Tuff

REFERENCE: DOE/NWTS-12, 1981

AVAILABILITY: Published

KEY WORDS: tuff, commercial waste, spent fuel, canister, groundwater

DATA SUMMARY:

Property and Form of Data:

Waste and canister temperature ($^{\circ}\text{C}$) as a function of time (year),
physical description of waste, canisters m, m^3 , thermal loading KW,
pressure MPa, radiation level (rads/hr), tuff composition wt%.

Materials and Specimen Geometry:

Test Conditions:

Literature review and compilation.

COMMENTS ON DATA VALIDITY:

This report is a summary of conditions expected in a tuff repository. Maximum waste temperatures, canister temperatures, radiation levels, pressure and physical dimensions are given. The data appears significant and should have relevancy.

DOCUMENT ABSTRACT

This report summarizes activities to determine interim reference conditions for temperatures, pressure, fluid, chemical, and radiation environments that are expected to exist in commercial high-level nuclear waste and spent fuel repositories in tuff. Similar reports will be issued for salt, basalt, and granite. These interim conditions are being generated by the Reference Repository Conditions Interface Working Group (RRC-IWG), an ad hoc IWG established by the National Waste Terminal Storage Program's (NWTS) Isolation Interface Control Board (I-ICB).

Present plans call for the completion of generic reference repository conditions for salt, basalt, tuff and granite by December 1981. Shale has been assigned a lower priority and RRC work on that rock type has been discontinued.

Reference repository conditions are based on the standard room-and-pillar mined repository concept with waste emplaced in vertical holes drilled in the room floor.

Some important results obtained are given below for selected reference local areal thermal loadings of 25 W/m^2 for spent fuel (SF) and commercial high-level waste (CHLW) respectively. In all cases, the results below are given first for SF. Some thermal results are: maximum waste temperature - 230 and 295 C; maximum canister surface temperature - 190 and 260 C; and maximum rock temperature - 185 and 225 C. These temperatures are upper bounds based on evaporating water from inside the 100 C isotherm in the tuff. Lower bounds were calculated based on no evaporation of water. The length of significant thermal exposure is greater for SF than the other wastes. Thermal histories are given in the report. Vapor phase pressures are not expected to rise significantly above atmospheric until the repository is sealed. After sealing, the pressure will gradually increase to the regional hydrostatic head. A reference tuff ground-water composition and expected gamma radiation doses are also provided in the report.

CUMENT REVIEW FORM

AUTHOR: Wolfsberg, et al. (LASL)

TITLE: Sorption-Desorption Studies on Tuff. III. A Continuation of Studies With Samples From Jackass Flats and Yucca Mountain, Nevada

REFERENCE: LA-8747-MS, 1981

AVAILABILITY: Published

KEY WORDS: sorption ratio, desorption ratio, tuff, Cs, Sr, Pu, U, Ba, Am, Eu, batch tests, column test

DATA SUMMARY:

Property and Form of Data:

Sorption and desorption ratio for various radionuclides in tuff/water systems.

Materials and Specimen Geometry:

Crushed tuff samples.

Test Conditions:

Tuff samples exposed to static and column type conditions at room temperature.

COMMENTS ON DATA VALIDITY:

The report describes the most recent sorption-desorption work on previously unstudied tuff samples (from Jackass Flats and Yucca Mountain). Differences were found for the two types of material. For example, the sorption ratios for Am and Pu were somewhat higher for tuff from Jackass Flats. Also, sorption and desorption values for U(VI) were small for Yucca Mountain tuff and the desorption values were higher than the sorption values. Sorption ratios were smaller when measured by column techniques compared to batch procedures.

For Sr, Cs, Ba and Eu at concentrations between $\sim 10^{-8}$ to $\sim 10^{-3}M$ the higher concentrations gave the largest deviations from ideal behavior. This may be due to saturation of sorption sites and precipitation.

Anions when compared to cations had poorer sorptive behavior for tuff.

The studies described are very valuable in establishing a data base for sorption-desorption processes in tuff and are necessary for quantifying the behavior of radionuclide migration in tuff systems. The solution-to-solid ratios used (5:1 and 30:1), however, may be too high since the amount of water in the unsaturated zone is expected to be very small.

DOCUMENT ABSTRACT

This report is the third in a series of reports describing studies of sorption and migration of radionuclides in tuff. The investigations were extended to lithologies of tuff not previously studied. Continuing experiments with uranium, plutonium, and americium are described. The dependence of sorption on the concentration of the sorbing element and on the solution-to-solid ratio was investigated for a number of nuclides and two lithologies. A circulating system was designed for measuring sorption ratios. Values obtained from this system, batch measurements, and column elutions are compared. Progress on measuring and controlling Eh is described.

DOCUMENT REVIEW FORM

AUTHOR: Burns, P. J.

TITLE: TACO2D - A Finite Element Heat Transfer Code

REFERENCE: UCID - 17980 Rev. 2 (January 1982)

AVAILABILITY: National Technical Information Service, Springfield, VA 22161

KEY WORDS: Heat, Thermal, Code

GENERAL COMMENTS: TACO2D is a nonlinear, two-dimensional, implicit, finite element code designed for single-phase heat conduction analysis of both transient and steady-state cases in plane and axisymmetric geometry. With appropriate zoning the code can handle a wide variety of nonlinearities including space-, time-, and temperature-dependent materials properties, heat generation rates and boundary conditions.

TACO2D has little mesh generation capability. Only rows of evenly spaced nodes and rows of sequential elements may be generated. For complex zoning TACO2D relies on separate, 2-D mesh generation codes. In particular, in the interior region, TACO2D utilizes a four-node isoparametric element which can be made to degenerate into a three node triangle. The Galerkin principle is then utilized to obtain the element heat capacity and conductivity matrices and the element thermal load vector. The problem is thus reduced to a system of ODE's in terms of the nodal temperatures, through which one can later interpolate with the original element interpolating functions.

TACO2D transient analysis rests on an implicit scheme of user's choice. The user also selects the time step, which does not need to be constant during the calculations. The user, however, is cautioned to make more than one run using different time steps to insure convergence. Overall the document reads well. I did not detect any incongruity, except on page 4, Equation (7), where the same symbol is used for the space- and time-dependent temperature and the nodal temperature.

TACO2D is presently used at LLNL for waste package thermal analysis in a tuff repository.

DOCUMENT ABSTRACT

Unavailable

DOCUMENT REVIEW FORM

AUTHOR: Ballou, L. B. (LLNL)

TITLE: Waste Package for a Repository Located in Tuff

REFERENCE: UCRL-90044, 1983

AVAILABILITY: Available as preprint for Civilian Radioactive Waste Management Information Meeting, Washington, D.C., December 1983

KEY WORDS: tuff, waste package, design, T304L SS, T316L SS, T321 SS, Incoloy-825, 76-68 glass, spent fuel, leaching, uniform corrosion, localized corrosion

DATA SUMMARY:

Property and Form of Data:
None.

Materials and Specimen Geometry:
See above.

Test Conditions:
None specifically given.

COMMENTS ON DATA VALIDITY:

The paper is a general description of the waste package and the environment it will be placed in. Initial tests with Topopah Spring tuff in contact with J-13 well water indicate that water chemistry changes around the package will be small. However, it seems possible that in the unsaturated zone local boiling of water may leave behind salt deposits which when contacted later by cooler groundwater will redissolve to give concentrated water which could affect canister corrosion and waste form leaching. This should be evaluated further.

Very preliminary outlines are given regarding the leaching of 76-68 glass and bare spent fuel and fuel with failed cladding around it.

Screening evaluations were performed on 17 metallic materials using data from the literature. Four metals (T304L, T316L, T321 stainless steels and Incoloy 825) were selected for experimental evaluation for use as container materials. It was noted on the Dublin meeting between NNWSI/NRC that the 300 series of SS are susceptible to stress corrosion cracking in $O_2/Cl^-/\text{gamma}$ irradiation environments and it is stated in the paper that such effects will be investigated.

Details of the package design were outlined.

DOCUMENT ABSTRACT

The development of waste packages for emplacement in a tuff repository has been proceeding during the past year on a broad front. . Experimental work has been focused on determination of important package environment parameters and testing the response of waste forms and package materials to the anticipated environment. Conceptual designs have been selected with alternatives to accommodate present uncertainties in the environment and material performance. Computational capabilities are being adapted to provide analyses of anticipated package performance and plans are being developed for in-situ testing. The waste package activities have been integrated into the overall NNWSI project to assure timely completion consistent with the statutory and regulatory requirements leading to repository site selection around the end of the decade.

DOCUMENT REVIEW FORM

AUTHOR: U.S. Department of Energy

TITLE: Nevada Nuclear Waste Storage Investigations

REFERENCE: NVO-196-33, 1983

AVAILABILITY: NTIS

KEY WORDS: tuff, carbon steel, corrosion, unsaturated

DATA SUMMARY:

Property and Form of Data:
General corrosion, mils/year.

Materials and Specimen Geometry:
AISI 1020.

Test Conditions:
100°C, 1 atm.

COMMENTS ON DATA VALIDITY:

While the data from this experiment show maximum corrosion rates at 70 to 80°C, the repository-relevant condition where irons and steels may attain their highest corrosion rates could be at the boiling point of water where the boiling heat transfer occurring at the metal/environment interface could maximize the concurrent effects of convection, presence of an electrolyte, and oxygen mass transport.

DOCUMENT ABSTRACT

HIGHLIGHTS

- A preliminary evaluation of site characterization data on Yucca Mountain indicated that the Topopah Spring tuff in the unsaturated zone is an appropriate rock unit on which to focus initial detailed site characterization studies.
- Documentation of the unsaturated groundwater flow code SAGUARO was completed and development of a conceptual vapor transport model to be included in SAGUARO was completed.
- An experiment was conducted in the laboratory to measure the corrosion rates of irons and steels in aerated, tuff-conditioned waters in the temperature range of 50 to 100°C at atmospheric pressure. In most cases, the crevice corrosion penetration was greater than the pitting penetration. The data also show that, in a system open to the atmosphere, the general corrosion rate maximum occurs at 70 to 80°C.
- Thermal analyses were begun on the candidate conceptual designs to model the maximum temperatures which would result from waste heat loading for specific waste package dimensions and spacings.
- A file (WAPLIB) has been created on the LLNL Cray computer system to provide users with the most recent version of the WAPPA waste package performance assessment code and its associated data bases.

General Corrosion Rate--The highest average corrosion rate occurred on the mild steel (AISI 1020) at 80°C (20.9 mils/year). The gray cast iron suffered somewhat less corrosion, its maximum average rate (16.7 mpy) occurring at 70°C. Similarly, the 2 1/4 Cr - 1 Mo alloy steel exhibited its highest average corrosion rate (18.5 mpy) at 70°C. The 9 Cr - 1 Mo alloy steel showed much less general corrosion than the other metals with a maximum rate (0.84 mpy) at 70°C. Under aerated ambient pressure conditions in near-neutral waters, irons and steels typically show a corrosion rate maximum at 70-80°C. Dissolved oxygen in the water is the dominant corroding specie so that the corrosion rate of the iron or steel is governed by the accessibility (mass transport) of oxygen to the surface. The mass transport is the product of the concentration of oxygen and the diffusivity of oxygen. Convection effects are also important in determining the accessibility of oxygen to the surface. In this particular experiment, air sparging served to agitate the solutions and was the primary mechanism for oxygen transport to the metal surfaces; thermal convection was also operating in all of the experimental cells (as well as boiling in the 100°C cell). In a system open to the atmosphere, the oxygen solubility decreases as the temperature increases and the diffusivity and chemical reaction rate both increase with temperature; the data indicate that these effects result in a corrosion maximum at 70 to 80°C.

Metal/steam/air (or metal/water vapor/air), which is expected to prevail over an extended period of time for a repository in the vadose zone at Yucca Mountain, will also be addressed in upcoming experiments.

DOCUMENT REVIEW FORM

AUTHOR: Gregg, D. W. and W. C. O'Neal (LLNL)

TITLE: Initial Specifications for Nuclear Waste Package External
Dimensions and Materials

REFERENCE: UCID-19926, September 1983

AVAILABILITY: Available as an informal report with limited external
distribution

KEY WORDS: CHLW, DHLW, spent fuel, waste package, design, materials,
corrosion, weldability, cost effectiveness

DATA SUMMARY:

Property and Form of Data:

Design drawings for waste packages and philosophy of materials
selection.

Materials and Specimen Geometry:

Various, depending on package component.

Test Conditions:

Not applicable.

COMMENTS ON DATA VALIDITY:

The report describes preliminary work to specify designs, dimensions and materials for tuff repository waste packages for DHLW, CHLW, and SF. Current designs include vertical and horizontal emplacement. For the latter, a carbon steel borehole liner will be used to facilitate retrieval. Canister material selection considered literature reviews of 17 different metals and alloys with equal weight being given to corrosion resistance, mechanical properties, weldability, and material and fabrication costs. Four materials selected for full evaluation: T304L SS, T316L SS, T321 SS, Incoloy 825. This reviewer believes that much higher weighting be assigned to corrosion resistance since all other factors can be accommodated by suitable design procedures.

Maximum glass waste form temperatures are based on devitrification effects and for spent fuel the temperature is determined by the rupture probability for the Zircaloy cladding. Based on these assumptions the maximum allowable temperatures are specified to be 350, 400 and 500°C for SF, CHLW and DHLW, respectively. More supporting data are needed to validate these design temperatures. Other aspects of the paper address criticality and retrieval.

The work is a reasonable attempt towards focusing on a final design but much more data will be required before such a design can be specified. This reviewer is concerned about the choice of T304L as the prime container material because of its known susceptibility to stress corrosion cracking.

DOCUMENT ABSTRACT

Initial specifications of external dimensions and materials for waste package conceptual designs are given for Defense High Level Waste (DHLW), Commercial High Level Waste (CHLW) and Spent Fuel (SF). The designs have been developed for use in a high-level waste repository sited in a tuff media in the unsaturated zone. Drawings for reference and alternative package conceptual designs are presented for each waste form for both vertical and horizontal emplacement configurations. Four metal alloys: 304L SS, 321 SS, 316L SS and Incoloy 825 are considered for the canister or overpack; 1020 carbon steel was selected for horizontal borehole liners, and a preliminary packing material selection is either compressed tuff or compressed tuff containing iron bearing smectite clay as a binder.

DOCUMENT REVIEW FORM

AUTHOR: Hockman, J. N. and O'Neal, W. C.

TITLE: Thermal Modeling of Nuclear Waste Package Designs
for Disposal in Tuff

REFERENCE: UCRL-80820/Preprint (September, 1983)

AVAILABILITY: Lawrence Livermore National Laboratory, Livermore, CA 94550

KEY WORDS: Thermal, Model, Package, Tuff, Heat

GENERAL COMMENTS: The document reports results of thermal analyses of various, conceptual waste package designs and emplacement options for a tuff repository. The reference code was TACO2D, a finite-element two-dimensional heat transfer code. In order to adapt a 2-D code to a 3-D problem, the authors had to make several assumptions based on engineering judgement. These should be checked in final calculations.

The document suggests that (1) the use of packing materials may cause thermal limits to be exceeded for the proposed waste forms. The problem is particularly serious for spent fuel with a maximum allowable temperature of 350°C; (2) the use of fins within canisters containing spent fuel pins may lower peak temperatures by up to 70°C for 6 fins and 86°C for 12 fins. A third result, which the report does not document, is that WAPPA's calculations compare favorably with those based on TACO2D.

The paper is important in that it outlines DOE's rationale for proposing to drop the packing materials. Although this paper is preliminary in nature, the results are reasonable.

DOCUMENT ABSTRACT

Lawrence Livermore National Laboratory is involved in the design and testing of high level nuclear waste packages. Many of the aspects of waste package design and testing (e.g., corrosion and leaching) depend in part on the temperature history of the emplaced packages. This paper discusses thermal modeling and analysis of various emplaced waste package conceptual designs including the models used, the assumptions and approximations made, and the results obtained.

DOCUMENT REVIEW FORM

AUTHOR: McCright, R. D., et al. (LLNL)

TITLE: Selection of Candidate Canister Materials for High-Level Nuclear Waste Containment in a Tuff Repository

REFERENCE: UCRL-89988, November 1983

AVAILABILITY: Available as preprint for NACE Annual Meeting, New Orleans, April 1, 1984

KEY WORDS: uniform corrosion, crevice corrosion, stress-corrosion cracking, gamma irradiation, tuffaceous groundwater, T304L, T316L, T321, I-825, carbon steel

DATA SUMMARY:

Property and Form of Data:

Uniform and crevice corrosion data and slow strain rate tests.

Materials and Specimen Geometry:

Mainly T304L, T304, T316L, I-825 corrosion coupons and tensile specimens. Some specimens were sensitized.

Test Conditions:

Uniform and crevice corrosion tests at 100°C for 1000 h; radiation corrosion at 105°C (3×10^5 rad/h) and 150°C (6×10^5 rad/h) for 2 months; slow strain rate tests at strain rates of 2×10^{-7} to 10^{-4} /sec.

COMMENTS ON DATA VALIDITY:

Evaluates the corrosion behavior of T304L, T304, T321 stainless steels and Incoloy 825 in tuff aqueous and steam environments. Other additional materials were also evaluated in support of the 4 main candidate steels. At 100°C in tuff conditioned water several carbon steels suffered crevice attack but T304L and T316L show no crevice or local attack after 1000 h. Slow strain rate tests in 150°C tuff-conditioned water revealed no evidence for embrittlement compared to air tests. Carbon steel corrosion rates appear to be unaffected by γ -irradiation but T304L SS showed an increase.

It is felt that these data are very preliminary since the test times are very short (1000 h). Since mechanisms such as stress-corrosion may take years to appear, the work performed at LLNL does not significantly reduce the potential for this failure mode in the light of data in the literature which shows that the 300 series of stainless steels are susceptible to stress corrosion under conditions similar to those expected in tuff repositories.

DOCUMENT ABSTRACT

A repository located at Yucca Mountain at the Nevada Test Site is a potential site for permanent geological disposal of high level nuclear waste. The repository can be located in a horizon in welded tuff, a volcanic rock, which is above the static water level at this site. The environmental conditions in this unsaturated zone are expected to be air and water vapor dominated for much of the containment period. Type 304L stainless steel is the reference material for fabricating canisters to contain the solid high-level wastes. Alternative stainless alloys are considered because of possible susceptibility of 304L to localized and stress forms of corrosion. For the reprocessed glass wastes, the canisters serve as the recipient for pouring the glass with the result that a sensitized microstructure may develop because of the times at elevated temperatures. Corrosion testing of the reference and alternative materials has begun in tuff-conditioned water and steam environments.

DOCUMENT REVIEW FORM

AUTHOR: Oversby, V. M.

TITLE: Performance Testing of Waste Forms in a Tuff Environment

REFERENCE: UCRL-90045, November 1983

AVAILABILITY: Available

KEY WORDS: HLW, tuff, waste forms, groundwater chemistry, spent fuel,
borosilicate glass

DATA SUMMARY:

Property and Form of Data:

Water chemistry determinations solution analyses; SEM surface analysis studies.

Materials and Specimen Geometry:

Crushed tuff; borosilicate glass; groundwater

Test Conditions:

Hydrothermal experiments: 90°C and 150°C.

Autoclaves; duration ~70 days; longer testing to 4 months at 150°C; MCC-1-76-68 glass with and without crushed tuff in tuff groundwater, duration - ~180 days at 90°C.

COMMENTS ON DATA VALIDITY:

Groundwater used in the experiments was obtained from the saturated zone; current plans will place the repository in the unsaturated zone.

304L corrosion estimates ~0.1 cm per 1000 years by uniform corrosion. Stress corrosion cracking is viewed as most likely mechanism to result in a breached container.

Test conditions appear adequate for initial testing. Additional testing should incorporate radiation effects. The report concludes that emplacement of wastes should cause only small changes in water chemistry, however radiolysis effects were not taken into account.

DOCUMENT ABSTRACT

The Nevada Nuclear Waste Storage Investigations Project (NNWSI) is studying the tuffaceous rock units located at Yucca Mountain on the western boundary of the Nevada Test Site. The objective of these studies is to allow an evaluation to be made of the suitability of the Yucca Mountain tuff units as a potential location for a high level radioactive waste repository. As part of the NNWSI Project, Lawrence Livermore National Laboratory is responsible for the design of the waste package and for determining the expected performance of the waste package in the repository environment.

The reference horizon for a potential repository at Yucca Mountain is the densely welded, devitrified portion of the Topopah Spring Member of the Paintbrush Tuff (Vieth 1982; Dudley and Erdal 1982). The water table at Yucca Mountain is more than 500 m deep beneath the central portion of the mountain; as a result, the Topopah Spring Member lies entirely within the unsaturated zone (Dudley and Erdal 1982). The mineralogy of the reference horizon is an assemblage of very fine grained alkali feldspar, quartz and cristobalite, with minor amounts of smectite clay. Glass and zeolites are generally absent within the densely welded, devitrified portion of the Topopah Spring (Bish et al. 1981; Caporuscio et al. 1982). The matrix porosity of the welded tuff is approximately 13 percent, and the rock has a fracture density of 0.8 to 3.9 fractures per meter (Dudley and Erdal 1982).

DOCUMENT REVIEW FORM

AUTHOR: Russell, E. W., et al. (LLNL)

TITLE: Selection of Barrier Metals for a Waste Package in Tuff

REFERENCE: UCRL-89404 Rev. 1, 1983

AVAILABILITY: Available as preprint for Materials Research Society Meeting,
November 1983, Boston, MA

KEY WORDS: T304L SS, T316L SS, T321 SS, Incoloy 825, materials selection,
container, weldability, cost, corrosion, mechanical properties

DATA SUMMARY:

Property and Form of Data:

General engineering data from the literature.

Materials and Specimen Geometry:

17 metals and alloys considered; the above 4 were selected for
detailed tests.

Test Conditions:

Various.

COMMENTS ON DATA VALIDITY:

General description of the selection of 4 out of 17 candidate materials
for study. Final selection was based on consideration of corrosion resis-
tance, weldability, cost, and mechanical strength. T304L, T316L, T321 stain-
less steels and Incoloy 825 were selected as prospective canister materials
and low carbon steel was selected for borehole liners.

This reviewer believes, as was stated at the NNWSI/NRC meeting in Dublin,
CA, October 1983, that equal weighting of the above 4 selection criteria was
inappropriate. Corrosion resistance is obviously the most important and
should be heavily emphasized. If it were, then in all likelihood most of the
current 4 reference materials would be eliminated.

DOCUMENT ABSTRACT

We have selected a few candidate metals for conceptual design of canisters and overpacks, and for use in corrosion tests under repository conditions. Important materials properties data, reflecting engineering design requirements for potential candidate materials were developed. The metals that were initially considered fall into the following categories: stainless steels--austenitic, ferritic, and duplex; high-nickel alloys, titanium alloys, zirconium alloys, copper-nickel alloys, low-carbon steels, and cast irons. These metals are all commercially available.

Our procedure was to determine and evaluate the engineering properties considered to be important in meeting design requirements cost-effectively--corrosion resistance, tensile strength, weldability, etc. Four general categories were considered:

- General and local corrosion resistance
- Fabrication costs
- Required mechanical properties
- Weldability

From this analysis we selected four metals for canister and overpack materials, and one for hole liners:

1. AISI 304L stainless steel.
2. AISI 321 stainless steel.
3. AISI 316L stainless steel.
4. Incoloy P25 nickel-base alloy.
5. AISI 1020 carbon steel (for horizontal borehole liners).

The reference canister and overpack metal is AISI 304L stainless steel, but alternative metals will also be considered for two reasons: (1) to provide a replacement material until the reference material is confirmed by testing under site specific conditions; (2) to provide comparative data to support the choice of AISI 304L stainless steel as the reference material during the regulatory review.

APPENDIX 4

REVIEW OF GENERAL WASTE PACKAGE DATA

BLANK PAGE

DOCUMENT REVIEW FORM

AUTHOR: Dukes, M. D., et al. (SRL)

TITLE: Multibarrier Storage of Savannah River Plant Waste

REFERENCE: Scientific Basis for Nuclear Waste Management, Vol. 2,
Plenum Press, N.Y., 1980, pp. 231-238

AVAILABILITY: Published

KEY WORDS:

DATA SUMMARY:

Property and Form of Data:

Overview of waste package component functions and anticipated performance.

Materials and Specimen Geometry:

Borosilicate glass, Cor-Ten, T304L SS containers, bentonite packing and salt host rock.

Test Conditions:

General conditions were for a salt repository with a maximum anticipated container temperature of 100°C and the presence of WIPP Brine B.

COMMENTS ON DATA VALIDITY:

The paper is a short overview of barriers which could be used for defense waste emplaced in a salt repository. Glass leach data obtained at 20-25°C, 90°C, and 120°C are presented. The tests were conducted on crushed glass containing a ¹³⁷Cs tracer. The tests up to and including the 90°C temperature were performed under static conditions with periodic water changes, whereas the 120°C were conducted in an autoclave.

After 60 d the leach rate of the glass decreased from 8.4×10^{-6} to 5.6×10^{-8} g/cm²-d at 90°C for WIPP-Brine B. These rates are 3-5 times greater than those at room temperature.

10,000 h tests on container materials in contact with dry salt indicated little reaction.

There is a brief discussion of the use of other barriers such as bentonite to sort radionuclides and retard water migration.

The data given are preliminary but useful. No data on synergistic effects are given and "decayed" glass composition is not addressed.

DOCUMENT ABSTRACT

Borosilicate glass will perform well as part of a multibarrier system for SRP high level waste. Storage temperatures can be kept to $\leq 100^{\circ}\text{C}$ with appropriate spacing of the reference canisters. Under dry conditions, the waste package should remain intact for very long periods of time. Even if the package is breached and water contacts the glass, the radionuclide release rate will be very low.

DOCUMENT REVIEW FORM

AUTHOR: Flynn, K. F., et al. (ANL)

TITLE: Resistance of High-Level Waste Materials to Dissolution in Aqueous Media

REFERENCE: Scientific Basis for Nuclear Waste Management, Vol. 2, Plenum Press, N.Y., 1980

AVAILABILITY: Published

KEY WORDS: glass, leaching, distilled water, Co, Zn, Zr, Ru, Ag, I, Cs, Ba, Ce, U, Eu, Np, neutron activation

DATA SUMMARY:

Property and Form of Data:

Leach rates given in units of g/cm^2-d .

Materials and Specimen Geometry:

76-68 borosilicate glass wafers doped with U, and 76-68 borosilicate glass spheres doped with Pu-Np. Latter samples have S/V ratios between 14 to 1200 m^{-1} .

Test Conditions:

7-day leach tests at 25°, 100°, and 286°C for the U-doped samples and 25°, 100°, and 254°C for the Pu-Np-doped samples. Some sequential leach tests were run. All tests in distilled water.

COMMENTS ON DATA VALIDITY:

Uses neutron activation to produce a variety of radionuclides whose leach rates are then determined under tests conditions. Radionuclides evaluated include ^{60}Co , ^{65}Zn , ^{95}Zr , ^{103}Ru , ^{110m}Ag , ^{131}I , ^{134}Cs , ^{140}Ba , ^{141}Ce , ^{152}Eu , ^{237}U , ^{239}Np . The Eu and Cs leach rates obey an arrhenius relationship. All leach rates decrease with time because of diffusion in the matrix, but were not solubility controlled.

Data are of general interest but not very applicable since the neutron activation process may alter glass conditions. Synergistic effects with other barrier materials not addressed. Nor were the effects of leaching "decayed" glass compositions.

DOCUMENT ABSTRACT

(CONCLUSIONS)

Practical experiments that can help produce answers to specific questions have been invoked in this work. While it is desirable to minimize the surface area subject to potential leaching, it is probably unrealistic to expect to achieve a surface to volume ratio significantly lower than about 100m^{-1} .

Among the variables associated with the leaching of glass matrices, the effect of temperature is, by far, the most severe. Cesium (and iodine) were found to leach, from the glass matrices studied, three orders of magnitude faster than europium at 290°C , whereas the difference in leach rate at 25°C was significantly less than one order of magnitude. Ten other elements studied were found to behave intermediately between these extremes. If the leach rates at the higher temperatures are considered unacceptable, then additional barrier material would be necessary for as long as the temperature remains high.

DOCUMENT REVIEW FORM

AUTHOR: Katayama, Y. B., and Bradley, D. J. (PNL)

TITLE: Long-Term Leaching of Irradiated Spent Fuel

REFERENCE: Scientific Basis for Nuclear Waste Management, Vol. 2,
Plenum Press, N.Y., 1980, pp. 323-374

AVAILABILITY: Published

KEY WORDS: leach, spent fuel, ^{137}Cs , $^{239+240}\text{Pu}$, ^{244}Cm , DIW, WIPP,
Brine B, NaHCO_3 , CaCl_2 , NaCl

DATA SUMMARY:

Property and Form of Data:

Leach rate of irradiated spent fuel in $\text{g/cm}^2\text{-d}$. Radionuclides include ^{137}Cs , $^{239+240}\text{Pu}$ and ^{244}Cm .

Materials and Specimen Geometry:

Unclad fuel fragments of LWR spent fuel with burnups of 9, 28 and 54 Mwd/kgU .

Test Conditions:

Fuel with the 3 different burnups tested at 25°C in DIW in a Paige apparatus. Also, the 28 Mwd/kgU fuel was IAEA leach tested in DIW, 0.03 M NaCl , 0.015 M CaCl_2 , 0.03 M NaHCO_3 , and WIPP Brine B. Test times were up to about 3.3 years.

COMMENTS ON DATA VALIDITY:

The fuel leach rate was essentially independent of burnup. DIW gave the largest release rate and 0.015 M CaCl_2 the lowest. Usually, the spent fuel has a leach rate which is 2-3 times as large as that for borosilicate glass, except for NaHCO_3 some where the rates are similar. There was found to be a period of accelerated leaching after about 600 days which necessitates very long term testing to observe and characterize.

The data give some information on the corrosiveness of 5 relevant groundwater formulations but serve only to give data of general scientific interest. The 25°C test temperature and fresh spent fuel composition are not relevant to addressing the controlled release rate.

DOCUMENT ABSTRACT

Spent light-water reactor (LWR) fuel with burnups of 9, 28 and 54 MWd/kgU were leach tested at 25°C in deionized water in a Paige apparatus. No discernible differences in long term leach rates were observed relative to burnup. An accelerated leaching period was observed during the Paige leach test of the 54 MWd/kgU spent fuel. Additionally, the 28 MWd/kgU fuel was IAEA leach-tested in five different leach solutions. Deionized water gave the highest leach rates, and calcium chloride solution gave the lowest.

Comparisons between spent fuel and borosilicate waste glass leach rates are made. In sodium bicarbonate solution, the leach rates are nearly equal and the glass becomes increasingly more resistant in calcium chloride solution, followed in order by sodium chloride solution, WIPP "B" brine and deionized water--in which the glass is two to three orders of magnitude more leach-resistant than in spent fuel.

DOCUMENT REVIEW FORM

AUTHOR: Weed, H. C., et al. (LLL, PNL)

TITLE: Leaching Characteristics of Actinides From Simulated Reactor Waste

REFERENCE: Scientific Basis for Nuclear Waste Management, Vol. 2,
Plenum Press, N.Y., 1980, pp. 167-173

AVAILABILITY: Published

KEY WORDS: glass, ^{237}Np , ^{239}Pu , flow rate, leaching, WIPP brine,
distilled water, bicarbonate water

DATA SUMMARY:

Property and Form of Data:

Leach rates for ^{137}Np and ^{239}Pu given in units of $\text{g}/\text{cm}^2\text{-d}$.

Materials and Specimen Geometry:

8 mm diameter glass beads with the 76-68 composition doped with
 ^{237}Np and ^{239}Pu .

Test Conditions:

Single-pass leaching at 25 and 75°C using WIPP brine, NaHCO_3 -rich
water, and distilled water. Some modified IAEA leach tests run for
comparison. Water flow rates were 10, 43, 300 cm^3/d with leaching
times to 420 d.

COMMENTS ON DATA VALIDITY:

The leach rates vary from 2×10^{-4} to $2 \times 10^{-7} \text{g}/\text{cm}^2\text{-d}$ for ^{237}Np and
from 2×10^{-5} to $2 \times 10^{-9} \text{g}/\text{cm}^2\text{-d}$ for Pu. At 75°C the Np release rates
are essentially independent of time but the rates for Pu show a decrease.
All leach rates increase as the water flow rate increases. For the various
solutions there are no large differences in the leach rates. Temperature
increases enhance leaching.

The data are not very relevant to licensing since the temperatures are
too low, the release rates are for fresh glass compositions, and synergistic
effects with adjacent components are not addressed.

DOCUMENT ABSTRACT

(CONCLUSIONS)

The following general trends can be seen in the results:

1. Leach rates increase with flow rate at high temperature but are approximately independent of it at room temperature.
2. Agreement between the results from the one-pass method and those from the LAEA method is fair in the case of WIPP brine solution and good in the case of the others.
3. The ^{237}Np leach rates increase with temperature, but the ^{239}Pu leach rates either decrease with temperature or do not change.

DOCUMENT REVIEW FORM

AUTHOR: Merz, M. D., et al.

TITLE: Materials Characterization Center Workshop on Corrosion of
Engineered Barriers

REFERENCE: PNL-3720, March 1981

AVAILABILITY: Published

KEY WORDS: corrosion, canister, waste package

DATA SUMMARY:

Property and Form of Data:
Not applicable.

Materials and Specimen Geometry:
Not applicable.

Test Conditions:

COMMENTS ON DATA VALIDITY:

This publication presents the findings of a workshop held for the purpose of determining corrosion tests of the engineered barriers. The types of corrosion mechanisms are described along with hydrogen effects and proposed MCC test procedures. Emphasis is placed on the need for techniques for accelerated corrosion testing. The report ranks the types of tests that should be undertaken with the most important being a system test, incorporating as many features of the near-field storage environment as is practicable, including contact by proposed filler and buffer materials and full-scale duplication of the component array for a single emplacement hole.

DOCUMENT ABSTRACT

MATERIALS CHARACTERIZATION CENTER WORKSHOP ON CORROSION OF ENGINEERED BARRIERS

1.0 SUMMARY

A workshop on corrosion test procedures for materials to be used as barriers in nuclear waste repositories was conducted August 19 and 20, 1980, at the Battelle Seattle Research Center. The purpose of the meeting was to obtain guidance for the Materials Characterization Center (MCC) in preparing test procedures to be approved by the Materials Review Board. The workshop identified test procedures that address failure modes of uniform corrosion, pitting and crevice corrosion, stress corrosion, and hydrogen effects that can cause delayed failures. The principal areas that will require further consideration beyond current engineering practices involve the analyses of pitting, crevice corrosion, and stress corrosion, especially with respect to quantitative predictions of the lifetime of barriers. Special techniques involving accelerated corrosion testing for uniform attack will require development.

DOCUMENT REVIEW FORM

AUTHOR: McVay, G. L., et al. (PNL, ONWI)

TITLE: Elemental Release From Glass and Spent Fuel

REFERENCE: The Technology of High Level Nuclear Waste Disposal, Technical Information Center, DOE, 1981, pp. 171-202

AVAILABILITY: Published

KEY WORDS: 76-68 glass, spent fuel, leaching, DIW, radiation, pH/Eh

DATA SUMMARY:

Property and Form of Data:

Mainly leaching data for 76-68 glass and spent fuel at 25-90°C.

Materials and Specimen Geometry:

76-68 glass and spent fuel.

Test Conditions:

25-90°C leach tests in DIW.

COMMENTS ON DATA VALIDITY:

The paper represents a short review of the test methodologies which may be used to characterize the performance of engineered barriers. Reviews of static and dynamic glass and spent fuel leach tests are described and critiqued. Some leach data for glass are given for distilled water at 90°C and effects of pH/Eh outlined. For spent fuel, the release of ¹³⁷Cs is given for temperatures of 25 and 70°C under oxidizing and reducing conditions. The dissolution mechanism for UO₂ is discussed. Tests at 25°C in demineralized water show that actinide release in spent fuel is about 2 orders of magnitude higher than that for 76-68 glass. The general conclusion by the authors is that available tests for leaching are not adequate to quantify long-term behavior and that more detailed testing using site specific groundwater and evaluation of effects of adjacent barrier components will be needed.

The paper clearly outlines shortcomings in available leach tests and suggests reasonable modifications.

DOCUMENT ABSTRACT

In the past several years, emphasis on interactions between waste forms and aqueous solutions has shifted from data gathering to understanding, and numerous mechanistic investigations have been initiated. These rely heavily on surface analytical techniques and control of many of the variables. Out of these efforts has come new insight into interactions between waste forms and water. This paper concentrates on glass and spent-fuel waste forms.

Because of the fundamental differences in the interactions of simple silicate and complex borosilicate waste glasses with aqueous solutions, predictive models and/or results derived from simple silicate glasses generally cannot be used to predict the behavior of complex borosilicate glasses. In addition, it has been shown that realistic flow rates and groundwater differences do not alter elemental release from glass or spent fuel by amounts greater than one order of magnitude.

The solubility limits for actinides contained in glasses have been shown to be identical to those observed for crystalline actinide oxide states themselves. Therefore thermodynamic arguments can be used to predict the upper limits of actinide isotopes in solution.

Radiolysis effects in the absence of air have been shown to be important at lower temperatures but not significant at the elevated tempera-

tures expected in a repository. If air (or perhaps just nitrogen) is present, however, nitric acid is generated as a radiolysis product; this greatly enhances elemental removal at all temperatures.

Leaching of spent fuel is less sensitive to temperature change than is leaching of glass and, in some cases, shows a negative temperature dependence. As the oxygen content of the leachate decreases, actinide removal from both glass and spent fuel also decreases.

In general, existing release models for glass and spent fuel are not adequate to predict long-term behavior in a meaningful and believable manner. Enough understanding has been and is being generated, however, that the next version of predictive equations should be capable of defensible predictions. More detailed testing with site-specific groundwaters and package components under expected repository conditions are under way.

DOCUMENT REVIEW FORM

AUTHOR: Ogard, Allen, et al.

TITLE: Are Solubility Limits Important to Leaching?

REFERENCE: Scientific Basis for Nuclear Waste Management, Vol. 3,
pp. 331-337

AVAILABILITY: Published, Plenum Press, N.Y., 1981

KEY WORDS: leaching, actinides, temperature

DATA SUMMARY:

Property and Form of Data:

Leach data in moles/liter as a function of temperature °C.
Leach ratios of U to fission products and actinides at °C.

Materials and Specimen Geometry:

Spent fuel - U, Eu, Ce, Am, Pu, Cs, Sr, Sb

Test Conditions:

Leach studies of spent fuel at 25°C and 70°C with oxidizing
and reducing atmospheres.

COMMENTS ON DATA VALIDITY:

The source for this study is based on the fact that fission products and actinides have remained at the reactor site of the Oklu Natural Fission Reactor for two billion years. An explanation for this occurrence is believed to be the extreme reducing environments in a deep geologic formation. This test provided for leach studies of spent fuel in oxidizing and reducing conditions at temperatures of 25 and 70°C. At 25°C uranium was uniformly leached for a 60 day period regardless of redox conditions. After the temperature was increased to 70°C uranium developed a negative temperature coefficient of solubility in a reducing environment. This occurred for ⁹⁰Sr, ¹²⁵Sb and to a lesser degree for ¹³⁷Cs. The leachant used for this study was deionized water and therefore the data presented may not be significant to an interactive repository environment.

DOCUMENT ABSTRACT

Conclusions

The solubilities of some radionuclides, especially rare earths and actinides, may be an important and controlling factor in leaching of waste forms. These solubilities should be measured accurately as a function of pH and not as a part of a multicomponent system.

Although the amount of data is small it is interesting to postulate that a negative temperature coefficient of solubility is being exhibited by the actinides and rare earths in Figs. 1 and 2. Individual solubilities should be measured as a function of temperature to determine if a kinetic effect is being observed in the data. A negative temperature coefficient of solubility for actinides and rare earths in water would have important consequences for nuclear reactor safety and for the management of nuclear wastes.

DOCUMENT REVIEW FORM

AUTHOR: Pitman, S. G., et al.

TITLE: Evaluation of Metallic Materials for Use in Engineered Barrier Systems

REFERENCE: Scientific Basis for Nuclear Waste Management, Vol. 3, 1981

AVAILABILITY: Published

KEY WORDS: corrosion, basalt, groundwater, brine

DATA SUMMARY:

Property and Form of Data:

Weight change in 2-3 month intervals, in mg/dm^2 for basalt groundwater, 20 to 72 day tests in brine expressed as weight change mg/dm^2 - mechanical tests of Ti Grade 2 and 12.

Materials and Specimen Geometry:

Plate and sheet material. Round tensile specimens. Charpy V-notch specimens. 300-400 S.S., Incolloys, titanium alloys, cast iron, Zircaloy, Cu-Ni.

Test Conditions:

Autoclave, flowing and static, simulated Hanford groundwater, brine.

COMMENTS ON DATA VALIDITY:

The results of these tests indicate that Inconel-600 and 625, Incoloy 800, Hastelloy C-276 and Grade 2 and 12 Titanium have excellent corrosion resistance in a postulated repository environment. Weight change data for cast irons appears high. An extrapolation of this data to 1000 years would indicate a loss of 2.5 cm if corrosion were uniform. Pitting corrosion indicates higher rates of penetration. The data presented in this paper is the result of interactive components of radiation, ground water, basalt, temperature, pressure and static and flowing conditions and could serve to supplement other data.

DOCUMENT ABSTRACT

None

DOCUMENT REVIEW FORM

AUTHOR: Serne, R. J., and J. F. Relyea (PNL)

TITLE: The Status of Radionuclide Sorption-Desorption Studies Performed
by the WRIT Program

REFERENCE: The Technology of High-Level Nuclear Waste Disposal, Technical
Information Center, DOE, 1981, pp. 203-254

AVAILABILITY: Published

KEY WORDS: sorption, Tc, Pu, Np, U, clay, zeolites

DATA SUMMARY:

Property and Form of Data:

Kd, Rd, D, actinides, mechanisms, sorption, desorption, far-field.

Materials and Specimen Geometry:

Eleana argillite, tuff, granite.

Test Conditions:

Far-field environments, static (batch) and flow-through tests.

COMMENTS ON DATA VALIDITY:

The paper is an excellent and detailed review of the quantification of sorption-desorption process for water-rock systems. Definitions of Kd, Rd, and D and their usefulness in quantifying the sorption-desorption behavior of radionuclide species in the far-field environment are given. The batch and flow-through procedures for determining these parameters are reviewed and stated to be complementary. Mechanisms for sorption-desorption are also discussed and nuclides of concern to HLW management specified. The most important are stated to be Tc, Pu, Np, I, U, Cs, Ra, Sr and C. The second most important class includes Am, Sm, Ni, Se and Cm; and the least important are thought to be Zr, Mo, Eu, Pd, Th, Pb, Pa and Nb.

The results and arguments presented are convincing and should serve as a basis for future DOE work in this important area.

DOCUMENT ABSTRACT

This paper focuses on interactions between dissolved radionuclides in groundwater and rocks and sediments away from the near-field repository. Two approaches were used to study the primary mechanism, adsorption-desorption. Empirical studies rely on distribution coefficient measurements, and mechanism studies strive to identify, differentiate, and quantify the processes that control nuclide retardation.

The empirical approach quantifies adsorption by use of a distribution coefficient (R_d), which is the ratio of the mass of a radionuclide present on the rock to the mass present in solution. Studies to standardize laboratory methods for measuring R_d are described. No one laboratory method best simulates all possible rock-groundwater-nuclide combinations, but two methods, batch and one-through-flow column, appear to complement each other and are recommended for further standardization. Their strengths and weaknesses are discussed. Results of generic empirical R_d work are summarized in tables of nuclide R_d values for five potential repository rock types. These data are ranked, and future improvements in the treatment of nuclide retardation in

existing computer safety assessment codes are suggested.

The status of sorption mechanism studies is discussed, with emphasis on delineating the usefulness of ideal ion-exchange, site-binding electrical double-layer, and redox-controlled sorption constructs. Since studies to date show greater potential for site-binding electrical double-layer models, future efforts will concentrate on this construct.

Laboratory studies are discussed which corroborate the importance of redox reactions in causing nuclide retardation for multivalent elements, such as Tc, Np, Pu, and U. Results suggest that both solution-mediated reduction, such as the Fe(II)-Fe(III) couple, and solid-solution heterogeneous reduction reactions, such as reduction of solution Pu(VI) at the mineral surface by structural Fe(II), occur.

Coupled microscopy, microprobe, and autoradiography studies have determined actual sorption sites for radionuclides on polymineralic rocks. The studies show that it is possible for minor phases to completely dominate the mass of radionuclides adsorbed. The most active minerals are typically alteration products (clays and zeolites).

Several exercises are discussed which rank radionuclides according to their potential dose hazards. In each of the analyses discussed, the top four radionuclides are I, Tc, Np, and Ra. Other elements that rank high in potential hazards are Pu, U, Am, Th, Pb, Sn, Pd, and Se.

A brief review of field nuclide migration and laboratory R_d comparisons shows general agreement between field observation and laboratory predictions of nuclide migration. The interplay between laboratory observations, field nuclide migration, and natural analog studies is discussed.

DOCUMENT REVIEW FORM

AUTHOR: Strachan, D. M., et al.

TITLE: Standard Leach Tests for Nuclear Waste Materials

REFERENCE: Scientific Basis for Nuclear Waste Management, Vol. 3,
pp. 347-354

AVAILABILITY: Published - Plenum Press, NY., 1981

KEY WORDS: leaching, glass, temperature

DATA SUMMARY:

Property and Form of Data:

Mass weight loss g/m^2 , concentration of solutions mg/L ,
temperature $^{\circ}\text{C}$.

Materials and Specimen Geometry:

PNL-76-68 glass - monolithic and powdered.

Test Conditions:

Based on Materials Characterization Center standard leach tests.

COMMENTS ON DATA VALIDITY:

This paper summarizes five leach tests performed in accordance with methods proposed by the MCC. Three of the tests were at static conditions, one under flowing conditions and the last used a soxhlet apparatus. All tests were for a 28 day period. Tests 1-3 were performed at 90°C and 250°C using either a glass monolith or powder in ranges of <100, <200 and <325 mesh. Measurements were made for mass loss and solution concentration. All tests were performed with water as the leachate and are not representative of repository conditions.

DOCUMENT ABSTRACT

None

DOCUMENT REVIEW FORM

AUTHOR: Wang, Rong

TITLE: Probable Leaching Mechanisms for UO_2 and Spent Fuel

REFERENCE: Scientific Basis for Nuclear Waste Management, Vol. 3,
pp. 379-386

AVAILABILITY: Published - Plenum Press, N.Y., 1981

KEY WORDS: leaching, spent fuel, mechanism

DATA SUMMARY:

Property and Form of Data:

Leach data measured as a function potential V (SCE) vs. current density.

Materials and Specimen Geometry:

Single crystals of UO_2 , deionized H_2O , $NaHCO_3$ and WIPP "B" Brine.

Test Conditions:

Autoclave - electrochemical dissolution at 25° and $75^\circ C$.

COMMENTS ON DATA VALIDITY:

Electrochemical method for determining surface conditions, dissolution rate and accelerated dissolution behavior for UO_2 and spent fuel. The author believes this method can be used in-situ during the progress of the leaching process. It seems that more effort is required to establish a correlation between this method and actual repository conditions.

DOCUMENT ABSTRACT

CONCLUSIONS

The oxidation and dissolution mechanisms for UO_2 and spent fuel will be quite similar based on this preliminary work with electrochemical leaching of UO_2 and spent fuel. In solutions containing oxygen or other oxidizing species, the UO_2 surface will be rapidly oxidized and dissolved following the transformation of uranium from U(IV) to U(VI). The hydrolysis of dissolved uranyl ions forms solid UO_3 hydrates or related complex compounds deposited onto the UO_2 surface, or other surfaces, as thin or thick coatings. Depending on the pH, temperature and time, the various kinds of porosity and the mechanical properties of the hydrate coatings will control the dissolution rates. The effects of radiation, in terms of generation of H_2O_2 will enhance the dissolution kinetics.

Electrochemical methods may be useful for determining the surface conditions, dissolution rate and accelerated dissolution behavior for UO_2 and spent fuel. Electrochemical methods can rapidly generate much information in terms of dissolution rate and surface film properties such as thickness, porosity and oxidation state, in-situ during the progress of the leaching process.

DOCUMENT REVIEW FORM

AUTHOR: Fullam, H. T. (PNL)

TITLE: Solubility Effects in Waste Glass/Demineralized Water Systems

REFERENCE: Scientific Basis for Nuclear Waste Management, Vol. 6,
North-Holland, N.Y., 1982, pp. 173-180

AVAILABILITY: Published

KEY WORDS:

DATA SUMMARY:

Property and Form of Data:

Solubility measurements determined from the undersaturated and supersaturated water conditions.

Materials and Specimen Geometry:

Crushed 76-68 glass.

Test Conditions:

Temperatures between 35-150°C, for S/V ratios between 0.075 to 310 cm⁻¹. Test times were up to 7650 h.

COMMENTS ON DATA VALIDITY:

Solubility experiments were carried out on crushed glass/water systems using 2 types of tests: (i) long term tests at constant temperature followed by solution analysis and pH determination, and (ii) high temperature interaction followed by chemical analysis and pH determination at a lower temperature to obtain solubilities which have been approached from the supersaturation condition. It was found that the latter type of test gave solubilities which were 1-2 orders of magnitude higher than the isothermal tests and that the pH values were substantially higher. It was postulated that differences in the two tests could be connected with differences in diffusion rates through the glass surface layer and the nature of the surface layers. Precipitation effects could give different solid species in the supersaturation tests which will give a higher solubility. It seems, therefore, that supersaturation tests may be more valid and more conservative since actual waste will be at higher temperatures initially so that solubilities, indeed, are approached from the supersaturated condition.

DOCUMENT ABSTRACT

A study was carried out to determine the solubility limits of various elements found in waste glasses in demineralized water as a function of temperature. The work was sponsored by the Office of Nuclear Waste Isolation under contract to the Department of Energy. Solubility measurements were carried out at 35°, 65°, 95°, and 150°C using three nonradioactive waste glass compositions. Subsaturation and supersaturation methods were used to determine the solubility limits. The two methods gave markedly different values for most glass components. The results obtained indicate that it is difficult to assign solubility limits to most glass components without thoroughly describing the glass-water system. This includes not only defining the glass type, and system temperature, but also the glass surface area-to-water volume (S/V) ratio of the system and its thermal history.

DOCUMENT REVIEW FORM

AUTHOR: Grambow, B. (PNL)

TITLE: The Role of Metal Ion Solubility in the Leaching of Nuclear Waste Glasses

REFERENCE: Scientific Basis for Nuclear Waste Management, Vol. 11, Elsevier, N.Y., 1982, pp. 93-102

AVAILABILITY: Published

KEY WORDS: solution concentration, static leaching, alteration layer, long term prediction, 76-68 glass

DATA SUMMARY:

Property and Form of Data:

Calculated equilibrium concentrations for 76-68 based on the identification of surface alteration products.

Materials and Specimen Geometry:

76-68 glass.

Test Conditions:

Static and dynamic tests per MCC-1 and MCC-5 at 90°C.

COMMENTS ON DATA VALIDITY:

This is an important study since it attempts to develop a calculational approach to the determination of equilibrium concentrations of species in glass leaching solutions. It shows that alteration products formed on a leached surface may control the equilibrium solubilities rather than the glass itself. If such an approach can be developed further it will possibly simplify the prediction of radionuclide concentrations in reporting groundwaters and their transport to the accessible environment.

The major shortcoming in this work is that it does not address "aged" glass compositions relevant to the post-300 year containment period. It is possible that alteration layers on the glass will be strongly influenced by the glass composition and, therefore, will give different concentrations of dissolved species than the one obtained for "fresh" waste.

DOCUMENT ABSTRACT

(CONCLUSIONS)

From the results of a variety of experiments it can be concluded that reaction of the matrix is the fundamental process that occurs in the leaching of PNL 76-68 glass. This reaction has two aspects. Without solubility restrictions, congruent leaching behavior occurs at all pH values and leachant compositions. When this reaction raises solution concentrations of certain elements to the level at which new solid phases form, these phases will regulate the solution concentration. These solid phases are dominant constituents of the leached layer. For the leaching of PNL 76-68 glass, the solubilities of these reaction products regulate the solution concentration as if the solution is in equilibrium with pure $\text{Fe}(\text{OH})_3$ (amorphous), $\text{Zn}(\text{OH})_2$ (amorphous), $\text{Nd}(\text{OH})_3$, SrCO_3 or CaCO_3 . The experimental conditions, in particular the pH value, that govern the formation of solid reaction products and control of the solution concentrations can be identified.

DOCUMENT REVIEW FORM

AUTHOR: Parkhurst, D. L.; Plummer, L. N.; Thorstenson, D. C.

TITLE: BALANCE - A Computer Program for Calculating Mass Transfer for Geochemical Reactions in Groundwater

REFERENCE: USGS/WRD/WRI/82-060 (February 1982)
NTIS Accession No. PB82-255902

AVAILABILITY: National Technical Information Service,
Springfield, VA 22161

KEY WORDS: Geochemical, Code, Mass, Transfer

GENERAL COMMENTS: BALANCE is a Fortran computer program designed to help quantify chemical reactions between aqueous systems and other extraneous phases such as minerals, organic substances and gases. Ideally, given two aqueous compositions and a selected set of extra phases, BALANCE calculates the amounts of these phases which have been produced or used in order for the aqueous system to evolve from its initial to final states.

The models implemented in the code are linear. BALANCE users are warned that these models are not constrained by any thermodynamic criteria and may imply reactions which are thermodynamically impossible. This shortcoming of the code, along with the fact that initial and final aqueous states as well as extraneous phases are supposed to be known beforehand, makes BALANCE unsuitable for use as a predictive code.

The better known geochemical code PHREEQE was produced by the same authors.

DOCUMENT ABSTRACT

BALANCE is a Fortran computer program designed to define and quantify chemical reactions between groundwater and minerals. Using (1) the chemical compositions of water samples from two points along a flow path and (2) a set of mineral phases hypothesized to be the reactive constituents in the system, the program calculates the mass transfer (amounts of the phases entering or leaving the aqueous phase) necessary to account for the observed changes in composition between the two water samples. Additional constraints can be included in the problem formulation to account for mixing of two end-member waters, redox reactions, and, in a simplified form, isotopic composition. The computer code and a description of the input necessary to run the program are presented. Three examples typical of groundwater systems are described.

DOCUMENT REVIEW FORM

AUTHOR: Strachen, D. M. (PNL)

TITLE: Results From a One-Year Leach Test: Long Term Use of MCC-1

REFERENCE: Scientific Basis for Nuclear Waste Management V, Vol. 11,
Elsevier, N.Y., 1982, pp. 182-191

AVAILABILITY: Published

KEY WORDS: 76-68 glass, MCC-1 leach test, long term leaching, DIW,
brine, silicate water, leachant analysis, surface layers

DATA SUMMARY:

Property and Form of Data:

Elemental mass loss in $g \cdot m^{-2}$, pH changes in leachant.

Materials and Specimen Geometry:

Monolithic samples per MCC-1.

Test Conditions:

40°, 90°C static tests for 1 year in DIW, silicic acid/sodium
bicarbonate solution, and a K, Mg, Na chloride brine.

COMMENTS ON DATA VALIDITY:

Tests were performed in DIW, silicate water and brine. Concentrations of Ca, Si, Cs and Sr were measured. At 90°C DIW and silicate water gave similar leach rates for these elements. The Eh after 1 year was 0.2 V indicating an air saturated condition. Ca and Sr concentrations decreased over a 28 day period and remained constant thereafter, indicating that the solubility was controlled by $SrCO_3$ and $CaCO_3$. A surface gel layer was found and shown to be rich in Fe, Nd, La, Ti, etc. and depleted in B.

At 40°C the loss of Cs and Si and other elements was lower than that at 90°C.

In brine at 90°C the leach rate for Cs was not suppressed compared to DIW as other work suggests. However, this was thought to be caused by a magnesium rich surface layer which is not found in DIW and silicate water. In the latter leachants a Zn silicate layer is present.

The paper is of general scientific interest but it does not address the "decayed" chemical composition of glass which will be present during the post-containment period.

DOCUMENT ABSTRACT

(CONCLUSIONS)

The results of the 1-year leach test led to the following conclusions:

- The MCC-1P Static Leach Test Method has been demonstrated to be useful for studies up to 1 year at temperatures up to 90°C.
- Accurate measurements of leachant volume at the start and the end of the test are important.
- PNL 76-68 glass appears to continue to alter, albeit at a significantly reduced rate, even though the solution concentrations of many elements are saturated or supersaturated with respect to alteration phases.
- The original surface of the glass was still present after 1 year, evidence that the gel layer will slowly get thicker but dissolution will not occur, or will occur at extremely slow rates.
- At 40°C, more than 1 year is required to reach saturation of some important elements. Even at 90°C, testing beyond 1 year is needed to define alteration rates and details of the leaching mechanisms.

DOCUMENT REVIEW FORM

AUTHOR: Strickert, R. G., and D. Rai (PNL)

TITLE: Predicting Pu Concentrations in Solutions Contacting Geologic Materials

REFERENCE: Scientific Basis for Nuclear Waste Management, Vol. 6, North-Holland, N.Y., 1982, pp. 215-221

AVAILABILITY: Published

KEY WORDS: PuO_2 , Pu(OH)_4 , solubility, pH, pe, oxidation state

DATA SUMMARY:

Property and Form of Data:

Equilibrium solubilities of Pu in low ionic strength solutions.

Materials and Specimen Geometry:

Crystalline PuO_2 , amorphous Pu(OH)_4 powders, Pu-doped borosilicate glass, and Pu-contaminated sediments.

Test Conditions:

Room temperature equilibration of Pu-containing solids in 0.0015 M CaCl_2 .

COMMENTS ON DATA VALIDITY:

The paper specifically evaluates the Pu species which control the solubility of plutonium in low ionic strength water. The procedure utilized crystalline PuO_2 and amorphous Pu(OH)_4 which were equilibrated for 130 days at room temperature. Analysis showed that the oxidation state was essentially Pu(V). For Pu contaminated sediments equilibrated in the water the measured concentration of Pu fell close to those obtained for crystalline PuO_2 . Equilibration of borosilicate glass beads containing Pu in water also showed that Pu solubility was controlled by a PuO_2 phase even though there was little evidence to show that a PuO_2 phase exists in the glass. When Pu(OH)_4 suspensions were aged the solubility of Pu decreased to values close to those controlled by the presence of PuO_2 .

This paper is a good attempt to determine equilibrium phases of Pu in solution and should help in determining equilibrium concentrations in groundwater for waste package performance assessment.

DOCUMENT ABSTRACT

Knowledge of Pu solid phases present in nuclear wastes is important for predicting the geochemical behavior of Pu. Thermodynamic data and experimental measurements using discrete Pu compounds, Pu-doped borosilicate glasses (simulating a high-level waste form), and Pu contaminated sediments suggest that $\text{PuO}_2(\text{c})$ is very stable and is expected to be present in the repository. The solubility of the stable phase, such as $\text{PuO}_2(\text{c})$, can be used to predict the maximum Pu concentration in solutions for long-term safety assessment of nuclear waste repositories.

DOCUMENT REVIEW FORM

AUTHOR: Treher, E. N., and N. A. Raybold

TITLE: The Elution of Radionuclides Through Columns of Crushed Rock From the Nevada Test Site

REFERENCE: LA-9329-MS, 1982

AVAILABILITY: Published

KEY WORDS: elution, column tests, batch tests, ^{85}Sr , ^{137}Cs , ^{133}Ba , ^{141}Ce , ^{152}Eu , $^{95\text{m}}\text{Tc}$, tuff, granite, argillite

DATA SUMMARY:

Property and Form of Data:

Elution data for various radionuclides for tuff, granite and argillite.

Materials and Specimen Geometry:

Crushed rock.

Test Conditions:

Room temperature tests using flowing (column) and batch tests.

COMMENTS ON DATA VALIDITY:

This work is a comprehensive study of the elution behavior of selected radionuclides on crushed tuff, granite and argillite using column and batch procedures. In the column experiments the elution behavior was measured in 3 ways, (a) passing a continuous stream of radionuclide-containing solution through a column and measuring the concentrations of radionuclides in the exiting solution, (b) passing a solution through the column containing a spiked increment and measuring the concentrations of radionuclides versus the volume of water passed, (c) measuring the activities of the radionuclides in the solution collected after an incremental spiked solution has been passed into the column. From solution analyses and measurements on disassembled columns the elution characteristics of the radionuclides were determined.

There was good agreement between column experiments and batch samples which had been used to determine elution behavior.

These data are of value in determining general data on sorption-desorption phenomena and provide a data base for repository/site performance assessments. For near-field evaluation, higher temperature tests will be needed.

DOCUMENT ABSTRACT

Results from the elution of radionuclides through columns of crushed tuff, granite, and argillite are presented. Good agreement between column and batch measurements on washed samples is generally observed for all three rock types. This is encouraging, since the results of batch measurements are often of value to show relative sorption under a variety of conditions, and their relevance to the migration of radionuclides under flowing conditions has been questioned.

Column elution behavior depended upon sample mineralogy. For example, ^{85}Sr gave fairly sharp, symmetric peaks on granite, argillite, and devitrified tuffs; however, on a vitrophyre, the peak was 10 to 100 times broader. For ^{137}Cs , the most unusual behavior was found on granites, where for columns run at ~ 20 m/year, most of the cesium was retained at the load point. For all the radionuclides studied, except $^{95\text{m}}\text{Tc}$, zeolite-containing tuffs had to be run at flow rates of 10^3 to 10^4 m/year to obtain elutions, while samples composed primarily of alkali feldspar and SiO_2 gave elutions of ^{85}Sr , ^{137}Cs , and ^{133}Ba at flow rates of 10 to 100 m/year. Knowledge of the mineralogic compositions of tuffs and their ability to retard the migration of radionuclides is important--not only to identify the optimum horizon for a nuclear waste repository in Yucca Mountain, but also to estimate how well the repository will perform.

DOCUMENT REVIEW FORM

AUTHOR: Wicks, G. G., et al. (SRL)

TITLE: Chemical Durability of Glass Containing SRP Waste-Leachability Characteristics, Protective Layer Formation, and Repository System Interactions

REFERENCE: Scientific Basis for Nuclear Waste Management V, Vol. 11, Elsevier, N.Y., 1982, pp. 15-24

AVAILABILITY: Published

KEY WORDS: MCC-1, leaching, static tests, dynamic tests, synergistic effects, brine, basalt, tuff, granite, shale, surface layer, SRL-131 glass

DATA SUMMARY:

Property and Form of Data:

Concentrations of Si, Cs, Sr, Fe, Mn in solution after 7 day tests.

Materials and Specimen Geometry:

Per MCC-1.

Test Conditions:

MCC-1 static and also dynamic flow tests in brine, basaltic, tuffaceous, granitic and shale groundwater at 90°C for 7 days.

COMMENTS ON DATA VALIDITY:

Carried out MCC-1 type static leach tests at 90°C for 7 day periods in DIW, simulated brine, and basaltic, shale, tuff and granite groundwater compositions. DIW was usually most aggressive with respect to leaching. An adherent gel layer forms made up mainly of non-waste elements which lowers the rate of release with time. As expected, a reduction in the amount of leachant also decreases the leach rate.

Static tests in the presence of T304L SS, TiCode-12, bentonite/sand packing and charcoal. These materials can have beneficial, marginal and possibly detrimental effects on leaching. Some tests in the presence of Pb showed lower release rates because of the formation of a Pb-rich layer on the glass surface.

In dynamic 'repository' tests used for acceleration purposes the studies gave only small increases in leach rate even for fast water flow rates of 100 and 200 mL/min. Fe was found in the surface layers.

These data are of scientific interest but do not reflect the waste form chemistry anticipated during the controlled release period since most fission products will have decayed.

DOCUMENT ABSTRACT

- Leach rates calculated from solution data (Table 2) show that leach rates decrease as the SA/V ratios increase for all samples based on mass loss and extraction of nine different elements. This effect has been observed before⁴ and can be beneficial for long term repository storage because of the relatively small quantities of water that are anticipated.
- "Effective leachability" generally decreases but only slightly for leaching by deionized water in the presence of rocks (salt, basalt, shale, granite and tuff).
- Leach rates can vary significantly for different elements.
- At a given SA/V ratio, leachate concentration and subsequent leachability generally correlate well with final pH of the solution. This suggests a non-destructive means for monitoring leachability.
- Leaching in the presence of salt reduces leachability most appreciably, especially at high SA/V ratios. The salt dissolves more readily than any other rock and forms brine which is a less aggressive leachant than deionized water.
- There is no significant difference in the leachability of waste glass when leached in the presence of Carlsbad salt compared to Avery Island salt.
- Key elements such as Fe, Mn, and Mg show very low leach rates for all systems and SA/V ratios studied. Previous studies¹ have shown that the low leach rates correspond to retention of these species within the leached surface layers and generally result in a reduction of glass leachability. Therefore, glass leachability in a repository environment would also be expected to decrease with time.
- Glass leached in simulated groundwater generally results in a lower leachability than glass leached in deionized water. (This observation is based on silicon extraction after correcting for the initial silicon concentration in the leachant.) Hence, product performance involving groundwaters in a repository should be better than the results from most laboratory tests using deionized water as leachant.
- For leaching of glass using simulated groundwaters in the presence of host rock, the leachability is generally reduced further, although only slightly in most cases.
- The largest reductions in leachability were for brine solutions. The largest source of experimental error was also for salt systems due to the dissolving host rock.
- The simulated shale groundwater was only slightly more aggressive than the actual groundwater and the rock-equilibrated groundwater was the most aggressive leachate used except for deionized water.
- Leachabilities of glass using MCC groundwaters, which incorporate only major elements of the groundwaters, are similar to more complete simulated groundwater compositions. However, this comparison becomes less clear for leaching in the presence of rocks, perhaps due to inherent variations in rock compositions.
- In system tests involving waste glass, canister material, overpack metal, backfill, and five different rock types, the backfill constituent most strongly influenced the release rate of species of interest.
- Backfill can be beneficial, marginal, or perhaps detrimental to the release rate of species of interest depending on the choice of material.
- Waste glass release rates are significantly lowered in the presence of lead due to the formation of a lead enriched surface layer.

DOCUMENT REVIEW FORM

AUTHOR: Bates, J. K., et al. (ANL)

TITLE: Extended Leach Studies of Actinide-Doped SRL-131 Glass

REFERENCE: Scientific Basis for Nuclear Waste Management VI, Vol. 15.
North-Holland, N.Y., 1983, pp. 183-190

AVAILABILITY: Published

KEY WORDS: SRL-131 glass, leachate analysis, surface products, Pu, Am,
Np, U

DATA SUMMARY:

Property and Form of Data:

Elemental losses in g/m^2 as a function of time.

Materials and Specimen Geometry:

Per MCC-1.

Test Conditions:

MCC-1 static leach tests at 90°C in DIW. Test times approach
400 d.

COMMENTS ON DATA VALIDITY:

Bates' work involves the characterization of leach rates and surface products for SRL-131 glass under static conditions at 90°C. The work is of general scientific interest since it may determine the more important radionuclides which should be considered for system analysis. However, the data do not represent controlled released scenarios for the post-containment period since they pertain to fresh glass compositions. They are of use in addressing early container failure scenarios but they still do not address the effects of adjacent container and packing materials.

It is shown that for the conditions used Pu and Am have slow release rates whereas Np and U accumulate continuously in solution.

DOCUMENT ABSTRACT

The effects on the leachability of SRL 131 glass as a result of slight changes in the glass composition were monitored by leachate and surface analyses. The compositional changes had marked effects on solution and layer composition and on the precipitated alteration products that formed after 546 days of static leaching. The leaching behavior of long-lived actinide elements were measured, with Pu and Am showing little tendency to become solubilized and Np and U continuously accumulating in solution.

DOCUMENT REVIEW FORM

AUTHOR: Harper, W. V.

TITLE: Sensitivity/Uncertainty Analysis Techniques for Non-stochastic Computer Codes

REFERENCE: ONWI-444 (May 1983)

AVAILABILITY: National Technical Information Service
Springfield, VA 22161

KEY WORDS: Uncertainty, Sensitivity, Reliability

GENERAL COMMENTS: The document indicates that ONWI will model most of the aspects of underground waste storage through the use of deterministic codes. Two levels of coding will be pursued: (a) system or subsystem codes which describe pertinent phenomena to a first degree of approximation and (b) detailed, individual process codes. Uncertainty analysis will be an integral part of performance assessment. Uncertainty analysis will be preceded by sensitivity analysis, i.e., first the key parameters which cause maximum performance function variability are identified, and then key parameter uncertainty is propagated to judge the overall effect on the output performance function. In particular, the document analyzes merits and faults of adjoint and statistical methods in performing a sensitivity/uncertainty analysis. The author seems to be partial to adjoint methods for performing sensitivity analysis. To the enthusiasm of this author, one must contrast the more cautious approach of ONWI-488 (July 1983) which indicates that sensitivity coefficients calculated by adjoint methods "depend on the assumed parameter field," whereas "sensitivities calculated by sampling are not so limited." This document also claims substantial computer savings of adjoint methods versus sampling methods. However, problems are known to exist in the applicability of adjoint methods to non-linear equations and to systems of equations.

The statistical methods examined by this author for uncertainty analysis fall in two categories: (a) experimental design methods and (b) sampling methods. Among the two methods the latter is considered superior.

This document does indicate ONWI's proposition to produce a sensitivity/uncertainty analysis of nuclear waste isolation systems. The contents of the report were effective as of May 1982.

DOCUMENT ABSTRACT

ONWI's approach to sensitivity/uncertainty analysis for deterministic continuum process computer codes is based on in-depth sensitivity analyses. ONWI will use both the adjoint and statistical methods for the sensitivity analyses of these codes. Statistical methods are well suited to codes with a limited number of parameters, whereas the adjoint method is most useful for a large number of parameters. Regardless of the sensitivity analysis method chosen, statistical methods will be used to determine input uncertainty that will be used to quantify the output uncertainty. This report gives the advantages/disadvantages of alternative approaches to sensitivity/uncertainty analysis for deterministic computer codes.

DOCUMENT REVIEW FORM

AUTHOR: INTERA Environmental Consultants, Inc.

TITLE: Workshop on Uncertainty Analysis of Postclosure Nuclear Waste Isolation System Performance

REFERENCE: ONWI-419 (April 1983)

AVAILABILITY: National Technical Information Service
Springfield, VA 22161

KEY WORDS: Uncertainty, Reliability, Sensitivity

GENERAL COMMENTS: This is probably the oldest document on uncertainties in the performance of nuclear waste isolation systems.

In October 1980, INTERA organized a "Workshop on Uncertainty Analysis of Post-Closure Nuclear Waste Isolation System Performance." Twelve professionals who had been invited to a pre-workshop planning session contributed three papers which were later distributed to the workshop participants. Although effective as of September 1982, this document is essentially the same as that handed out to the workshop participants two years before.

The three contributed papers are on (1) uncertainties in (discrete) event modeling, (2) uncertainties in (continuum) process modeling, and (3) uncertainties in systems modeling. Event modeling refers to phenomena which change the repository system practically instantaneously with respect to the repository lifetime. Magmatic intrusion and faulting, or drilling for mineral resources can be modeled as events. Continuum processes are those which take place slowly on time frames comparable to the repository lifetime. Systems uncertainties are related to the overall uncertainty that a series of process and event models has in representing the real world. In general, however, two types of uncertainties are identified as most important: (a) uncertainty in data applicability and (b) uncertainty in data gathering.

Overall this is an interesting document where all sorts of uncertainties are touched upon. It constitutes good reading in order to better comprehend ONWI-488 "A Proposed Approach to Uncertainty Analysis," of which this report constitutes the basis.

DOCUMENT ABSTRACT

A "Workshop on Uncertainty Analysis of Post-Closure Nuclear Waste Isolation System Performance" was held on October 2-3, 1980 in Galveston, Texas. The Workshop was organized by INIERA Environmental Consultants, Inc., under contract to the Office of Nuclear Waste Isolation. About seventy-five persons attended the workshop.

Twelve participants, representing a range of disciplines, were invited to a pre-Workshop Planning Session on September 29 - October 1, 1980. During this session they prepared a survey of various aspects and approaches to uncertainty analysis for nuclear waste applications. This survey provided a focus for discussion in the Workshop itself. On October 2, presentations were made by the members of this planning group, followed by questions and discussions with the Workshop attendees. On October 3, an invited panel gave their reactions to the draft document and discussions of the previous day. There was also audience interaction with these panelists.

This document presents a summary, but not a consensus, of the various views expressed by the participants in the pre-workshop planning session and in the workshop sessions. The document does not necessarily represent the opinions of INIERA or ONWI. The information presented in this document has formed part of the basis for defining the approach to uncertainty analysis under the SCEPTER project.

DOCUMENT REVIEW FORM

AUTHOR: INTERA

TITLE: DOT: A Nonlinear Heat-Transfer Code for Analysis of Two-Dimensional Planar and Axisymmetric Representations of Structures

REFERENCE: ONWI-420, April 1983

AVAILABILITY: Published

KEY WORDS: Heat Transfer, Code

GENERAL COMMENTS: The DOT code is an important part of the SCEPTER program. It has been used to supply time-dependent temperatures to thermomechanical codes and waste package performance codes such as WAPPA.

DOT is a finite element code that solves the space-time heat conduction problem through estimation of the spatial derivatives by interpolation functions. This reduces the governing equation to a system of time-dependent ordinary differential equations. The details of this transformation are not found in the manual. To further increase solution speed coupling between the time rate-of-change of temperature at adjacent nodes is removed by a lumped parameter technique. The accuracy of the technique depends on the shape of the element and the number of nodes. Again, the exact details are not presented in the manual.

DOT has been verified against analytical solutions on a number of test problems. DOT has also received limited validation in modeling heat transfer in underground heating experiments conducted in granite at Stupa, Sweden.

Dot has the following limitations:

- (a) DOT can not directly model convective or radiative heat transfer in the interior of the body. Convection becomes more important as the permeability increases. Thus, it may be important near a major fracture. Radiative heat transfer can be important in salt repositories and when a waste package is separated from the host rock by an air gap. For this reason, DOT is not recommended for thermal analysis of the waste package. Dot can model a salt repository by introducing an equivalent thermal conductivity.
- (b) DOT can not model two phase heat transfer phenomena which would arise if the groundwater began to boil.
- (c) Numerically, DOT uses a first order integration scheme with constant time steps. There is no provision to estimate the error in the calculation. The code user must judge if the solution is numerically accurate.

DOCUMENT ABSTRACT

One of the key issues related to location and design of a nuclear waste repository is the dissipation of the heat generated by the isolated waste. The Determination of Temperature (DOT) code is a general purpose finite element heat transfer code developed by Polivka and Wilson in 1976 at the University of California, Berkeley, that is appropriate for predicting thermal environments. The code deals with linear and nonlinear transient or steady-state heat conduction in two-dimensional planar or axisymmetric representations of structures. Capabilities are provided for modeling anisotropic heterogeneous materials with temperature-dependent thermal properties and time-dependent temperature, heat flux, convection and radiation boundary conditions, together with time-dependent internal heat generation.

This documentation describes the mathematical model, solution techniques and computer code design. It also contains a detailed user manual. The use of DOT as an integrated part of the SCEPTER technology package has been emphasized throughout the report. Links with the thermomechanical codes MATLOC, VISCOT, and UTAH2 have been identified and described in detail, as have "stand-alone" applications of DOT and its use with the waste package performance assessment code WAPPA. Output from DOT consists of a steady-state temperature distribution or a set of nodal temperatures at various times for a transient problem.

Strengths of the DOT code include its flexibility, wide range of possible boundary conditions, nonlinear material properties, and its efficient equation solution algorithm. Limitations include the lack of a three-dimensional analysis capability, no radiative or convective internal heat transfer, and the need to maintain a constant time step in each program execution.

In the Section 1.5 of this document the code custodianship and control is described along with the status of verification, validation and peer review of this report.

DOCUMENT REVIEW FORM

AUTHOR: INTERA Environmental Consultants, Inc.
TITLE: GEOTHER: A Two-Phase Fluid Flow and Heat Transport Code
REFERENCE: ONWI-434 (April 1983)
AVAILABILITY: National Technical Information Service
Springfield, VA 22161
KEY WORDS: Thermal, Code, Heat, Two-Phase, Porous Medium

GENERAL COMMENTS: The document is well written and the attached Abstract is a good representation of the document contents.

In the body of the document the authors clearly state the assumptions made in the modeling parts and point out the limitations of the code. The modeling assumptions are justified with reference to the state-of-the-art in the field. The limitations of the code are indicated to be as follows:

1. The model cannot treat systems that vary greatly from pure water. GEOTHER would need modifications to treat brine fluids or any fluids which contain large amounts of dissolved species, e.g. CO₂.
 2. GEOTHER cannot be used for fractured media which do not approximate porous media behavior.
 3. The model has no thermomechanical capability
 4. The model is limited by the thermodynamic ranges of the regression equations.
- A further limitation of the code which I found is that
5. GEOTHER has no solute transport and deposition modeling capability.

Item 1 is the most limiting as it bars the use of GEOTHER for salt repositories, and may limit its use to tuff and basalt waters. Item 5 may also prove limiting unless it is shown that deposition of soluble salts out of the water vapor phase into the rock channels will not influence significantly the thermal properties of the system. Item 3 is also important, as small differences in thermodynamic approximation resulted in notable differences between models in a code-to-code validation effort.

DOCUMENT ABSTRACT

GEOETHER is a three-dimensional geothermal reservoir simulation code. The model describes heat transport and flow of a single component, two-phase fluid in porous media. It is based on the continuity equations for steam and water, which are reduced to two nonlinear partial differential equations in which the dependent variables are fluid pressure and enthalpy. These equations, describing three-dimensional effects, are approximated using finite-difference techniques and are solved using an iterative technique. The nonlinear coefficients are calculated using Newton-Raphson iteration, and an option is provided for using either upstream or midpoint weighting on the mobility terms.

GEOETHER can be used to simulate the fluid-thermal interaction in rock that can be approximated by a porous media representation. It can simulate heat transport and the flow of compressed water, two-phase mixtures, and superheated steam in porous media over a temperature range of 10 C to 300 C. In addition, it can treat the conversion from single- to two-phase flow, and vice versa. It can be used for evaluation of a near repository spatial scale and a time scale of a few years to thousands of years. The model can be used to investigate temperature and fluid pressure changes in response to thermal loading by waste materials.

In Section 1.5 of this document the code custodianship and control is described along with the status of verification, validation and peer review of this report.

DOCUMENT REVIEW FORM

AUTHOR: INTERA

TITLE: EQ3/EQ6: A Geochemical Speciation and Reaction Path Code Package Suitable for Nuclear Waste Performance Assessment

REFERENCE: ONWI-472 , 1983

AVAILABILITY: Published

KEY WORDS: Geochemical, Code

GENERAL COMMENTS: The EQ3/EQ6 codes have been selected (ONWI-473) as part of the SCEPTER program to perform geochemical calculations for both near and far field applications. Given data regarding the mass of each element, EQ3 calculates the equilibrium distribution of species within the system. EQ6 contains a reaction path model that follows the compositional evolution from one equilibrium state to the next in a closed or open (flow through) system. The reaction path may be described by changes in temperature or irreversible rock/water interactions. By following the reaction path, the appearance and disappearance of secondary mineral phases is possible.

Although the EQ3/EQ6 package is one of the best geochemical codes available, caution must be used when operating the code and interpreting the results. First, any geochemical code is only as good as its data base. The EQ3/EQ6 data base is limited to temperatures between 0 and 350°C at a pressure of 500 bars or atmospheric pressure until 100°C and then follows the vapor/liquid equilibrium curve for water. Also, thermodynamic data for many species may not be accurately known. Comparisons between the geochemical code PHREEQE and EQ3/EQ6 have shown substantial differences in the calculated amount of a species because of the use of different data. This problem is particularly important for minor species. Also, because of the correlations used to obtain activity coefficients do not apply if the molality exceeds 1, EQ3/EQ6 cannot be used for brine solutions.

Use of any geochemical code borders on being an art form and requires experience and insight. To run EQ3/EQ6 the user must have a priori knowledge of all the significant mineral phases that are expected to appear as the reaction proceeds. Furthermore, convergence of the numerical solution is dependent on the ordering of the different phases within the computational procedure. Failure to include the proper species or improper ordering can lead to erroneous results or non-convergence of the solution. EQ3/EQ6 does have automated procedures to reorder the equations when convergence is a problem. These procedures do reduce the burden to the user but they are not infallible.

EQ6 is a reaction path model. It begins the calculation by taking the distribution of species as provided by EQ3 and making adjustments for effects like supersaturation. It then proceeds by incrementing the reaction path variable and calculating a new equilibrium based on the updated value of this variable. For example, in modeling glass dissolution the reaction path variable could be chosen as the amount of silicon in solution. This procedure is repeated until the end of the calculation as determined by the reaction path variable reaching equilibrium or some other criterion.

There are a few problems with the reaction path approach to modeling chemical reactions. First, it treats a dynamic system through a series of equilibrium calculations. There is an implicit assumption that there is enough time to allow all chemical reactions to reach completion. Therefore, EQ6 provides no information concerning the timing of the problem and is likely to miss any metastable phases that form. Second, there is no guarantee that the reaction path is unique. Third, the user can select only one reaction path variable. In a repository, the groundwater will interact with the host rock, backfill if present, waste canister, and waste form. There is no single reaction path variable that can describe all of these processes. Furthermore, in a complicated problem like this, it may not be obvious which reaction path should be followed. Finally, if the temperature is not the reaction path variable, it must either be constant or specified as a polynomial function of the reaction path variable. It is unlikely that a priori knowledge of the temperature as a function of reaction path variable is available. Because of these problems, it is not clear how useful EQ3/EQ6 will be in modeling groundwater flow through a nuclear waste repository.

In general, before EQ3/EQ6 or any geochemical code is to be trusted an in depth analysis and review of the code is necessary.

DOCUMENT ABSTRACT

Geochemical processes influence the performance of nuclear waste repositories. The EQ3 and EQ6 codes were selected to describe these processes. EQ3 simulates a distribution of species and the resulting fluid is used in EQ6 to model a reaction path. Together, they can be applied to far-field and near-field performance assessment, to evaluate data acquisition needs, and to assist in data interpretation.

Chemical processes such as adsorption can be modeled using EQ3/EQ6. The resulting distribution coefficients can then be input to a far-field transport code. In the near-field, EQ3/EQ6 can be used to derive solubility limits on radionuclides. These constraints can then be used as input to evaluate the leaching process in waste package performance assessment.

The codes described embody the ion-association conceptual model of solution behavior and simulate geochemical reactions. The codes require thermodynamic data for each solid, gaseous or dissolved chemical species being modeled. The data bases accompanying the codes are for testing purposes only and should not be applied to real problems without first being carefully examined for applicability on a case-by-case basis. Two test problems have been described to illustrate code applications. One sample problem verifies the codes' ability to follow abrupt redox changes in a reaction path simulation, while the other tests the temperature changing capability of the codes.

Routines to manipulate thermodynamic data were written to make the thermodynamic data bases interchangeable between EQ3/EQ6 and another geochemical code, PHREEQE. The EQTL and PQLT data preprocessor codes are documented in an appendix.

In Section 1.5 of this document the code custodianship and control is described along with the status of verification, validation and peer review of this report.

BLANK PAGE

DOCUMENT REVIEW FORM

AUTHOR: INTERA Environmental Consultants

TITLE: Geochemical Models Suitable for Performance Assessment of Nuclear Waste Storage: Comparison of PHREEQE and EQ3/EQ6

REFERENCE: ONWI-473 (June 1983)

AVAILABILITY: National Technical Information Service, Springfield, VA 22161

KEY WORDS: Geochemical, Code, Model

GENERAL COMMENTS: The document presents the authors' rationale for narrowing down to EQ3/EQ6 and PHREEQE the choice of computer codes to be used by the SCEPTER Program for future near- and far-field analysis. The document further reports a comparison of the two codes on a set of five test problems.

EQ3/EQ6 and PHREEQE were selected among all the other codes because they incorporate all the aqueous speciation modeling functions of the WATEQ/SOLMNEQ group of codes while still providing reaction modeling capabilities. As a Mass Transfer Model, PHREEQE solves directly for the final equilibrium state of a system given its initial state and the predicted reaction path. As a Reaction Path Model, given the system initial conditions, EQ6 figures out the reaction path and computes intermediate states of the system up to the final state.

When compared against each other, the two codes give essentially identical answers provided the same thermodynamic data base is used. On one hand this provides code-to-code verification. On the other hand the discrepancies which arise when different data bases are used indicate that data accuracy is of paramount importance for using these codes.

It is to be noted that, as both codes are based on thermodynamic principles, they do not address evolution of the system with time. Furthermore, the aqueous solution models implemented by these codes break down for solutions such as brines which have salt contents higher than a few molal.

This is an important document in that it outlines the geochemical modeling strategy of the SCEPTER Program. The document is well written and interesting.

DOCUMENT ABSTRACT

Geochemical processes will significantly influence the performance of nuclear waste repositories. The computer codes EQ3/EQ6 and PHREEQE, can be used to describe these processes. They can be applied to far-field and near-field performance assessment, and to evaluate data acquisition needs and test data. Both codes embody the ion- association conceptual model of solution behavior and can simulate geochemical reactions. The codes require thermodynamic data for each solid, gaseous or dissolved chemical species being modeled. The data bases accompanying the codes are for testing purposes only and should not be applied to real problems without first being carefully examined. Five test problems have been run for code verification and demonstration. Routines to manipulate thermodynamic data were written so that each code could run with both data sets. Two problems of aqueous speciation in sea water verified the codes by comparison of results with hand calculations and illustrated the extent of the test data bases supplied. The third problem simulated the dissolution of microcline and verified both codes' ability to locate phase boundaries and simulate non-redox reaction paths. The fourth problem verified the codes' ability to follow abrupt redox changes in a reaction path simulation, while the fifth tested the temperature changing capacity of the codes. When run with the same thermodynamic data, each code gave virtually identical results in all problems.

DOCUMENT REVIEW FORM

AUTHOR: INTERA Environmental Consultants, Inc.
TITLE: A Proposed Approach to Uncertainty Analysis
REFERENCE: ONWI-488 (July 1983)
AVAILABILITY: National Technical Information Service
Springfield, VA 22161
KEY WORDS: Uncertainty, Reliability, Sensitivity

GENERAL COMMENTS: This is a rather complex document on uncertainty analysis.

Two fundamental types of uncertainty are identified as fit for consideration: (a) uncertainty in models applicability and (b) uncertainty in data gathering and adequacy. The document does not offer a suggestion on how to quantify uncertainty in model applicability. It talks rather of model "validation" to be accomplished through comparison of numerical tests with actual data, comparison with natural analogs, comparison with known limiting behaviors, use of peer review, and model-to-model comparison. "Validated" models will be considered to be exact. Uncertainty in data gathering and adequacy is to be quantified in terms of a probability distribution function (PDF). Once a PDF has been established, it will be assumed to contain no further uncertainty.

Based on the above quantification of original uncertainty, uncertainty analysis will predict the output uncertainty of models. It is proposed that several levels of uncertainty analysis be performed according to the application for which the analysis is intended: R & D, integrated characterization, test design and data interpretation. Thus different levels of model complexity should be used.

Methods of uncertainty analysis to be used are identified as (1) simulation sampling methods, and (2) first-order second moment stochastic methods. The former ones are fit for system modeling. The latter ones for individual models.

The document is important in that it outlines the uncertainty analysis approach proposed to become an integral part of the SCEPTER Program. Overall the approach is consistent with the suggested NRC guidelines to DOE. The contents of the document were effective as of October 1982. It should be interesting to find out whether ONWI is pursuing this proposed approach.

DOCUMENT ABSTRACT

A variety of methods are described that deal with the uncertainties inherent in the performance assessment of the geologic disposal of nuclear waste. Utilizing these methods, an approach to uncertainty analysis for the SCEPTER (Systematic Comprehensive Evaluation of Performance and Total Effectiveness of Repositories) Program is proposed. The approach recognizes two fundamental types of uncertainty: (1) uncertainty in the adequacy of performance assessment models; and (2) data uncertainties. The first type of uncertainty will be addressed through model verification and validation. The second type will be accounted for by using either a simulation sampling method, or first order-second moment stochastic methods. Among the former methods are Monte Carlo simulation, and Latin hypercube sampling. Among the latter methods are adjoint sensitivity and other first order numerical methods. The selection of an appropriate method depends on the data available and the application.

A list of input and output variables, and a suggested level of sophistication for the uncertainty analysis, of each SCEPTER sub-system model is given. The relationship of performance assessment and uncertainty analysis between process, sub-system and system models is described.

DOCUMENT REVIEW FORM

AUTHOR: Kuhn, W. L., and R. D. Peters

TITLE: Leach Models for a Commercial Nuclear Waste Glass

REFERENCE: Scientific Basis for Nuclear Waste Management VI, Vol. 15,
North-Holland, N.Y., 1983, pp. 107-174

AVAILABILITY: Published

KEY WORDS: 76-68 glass, leaching, modeling, diffusion, solubility

DATA SUMMARY:

Property and Form of Data:

Applies theory to the leaching of 76-68 glass taking into consideration the effects of surface layers and the solubilities of glass constituents.

Materials and Specimen Geometry:

76-68 glass.

Test Conditions:

Leach tests under static conditions at 50, 75, 90, 100 and 150°C.

COMMENTS ON DATA VALIDITY:

The work describes a reanalysis of the leaching behavior of 76-68 glass taking into consideration the diffusion of glass constituents. It is claimed that simple early models are inadequate since there is an accumulation of insoluble surface products on the glass and that solubility of glass constituents is ignored. Using data from static leach tests they show that the new model is able to more accurately predict measured behavior. They discuss the use of the model to predict glass leaching under repository conditions.

There are insufficient data to assess the validity of the model for the ranges of conditions in a repository. Also, synergistic effects with containers, packing and host rock are not addressed. However, it is a more sophisticated model than those available to date and should be pursued.

DOCUMENT ABSTRACT

A review of the leaching behavior of 76-68 glass shows that it cannot be explained in terms of diffusion in the glass, which has been the basis for several leach models. Instead, we present two models based on a dissolution rate impeded by surface processes: the accumulation of a protective layer of insoluble reaction products, and adsorption of reaction products on the surface. The resulting predicted time dependences are identical and predict a change from linear to parabolic rate laws for soluble species, which is found to agree with the data over a range of temperatures. Incongruent release is attributed primarily to solubility effects. The relative merits of the models are discussed on the basis of the effect of surface area-to-volume ratio in static leach tests. Their relevance to modeling repository behavior is discussed.

DOCUMENT REVIEW FORM

AUTHOR: R. A. McCann

TITLE: HYDRA-I: A Three-Dimensional Finite Difference Code for Calculating the Thermohydraulic Performance of a Fuel Assembly Contained within a Canister

REFERENCE: PNL-3367 , 1983

AVAILABILITY: Published

KEY WORDS: Computer Code, Thermohydraulic, Fuel Assembly, Canister

GENERAL COMMENTS: HYDRA-I uses conservation of mass, momentum, and energy to simulate steady state thermal conditions in fuel rod array/ canister configurations. Several test problems are posed and the results obtained from HYDRA-I are presented.

This document is poorly written and often confusing. In the development transforming the conservation equations to a form usable for numerical implementation there is not enough detail to fully evaluate the modeling. For example, it is never made clear that the solution procedure involves obtaining the steady state solution through a time dependent calculation which has converged to the steady state. The lack of clarity in the document may hinder the use of HYDRA-I.

The HYDRA-I solution procedure solves the simultaneous process of heat transfer and fluid flow sequentially. This can lead to numerical instabilities depending on the size of the time step. Although recommended values of the parameters used in selecting the time step are provided, the author states that these may not work for all problems. There is no discussion of the logic used to select the time step parameters and the code user is left to trial and error if the recommended values fail to lead to a converged solution.

The geometric modeling of the fuel assemblies is limited to assemblies with an odd number of rods and a 45° line of symmetry. Modeling rod bundles with a circular cross section or chopped rods is not possible.

HYDRA-I was used to predict the temperature distribution within the fuel assembly/canister system for several cases. The effects of fuel age, filler material, and canister temperature were investigated and the important modes of heat transfer identified. Although agreement of the results with experimental data was favorable for the one case presented, the author stresses the need for more data to fully validate the model

DOCUMENT ABSTRACT

A finite difference computer code, named HYDRA-I, has been developed to simulate the three-dimensional performance of a spent fuel assembly contained within a cylindrical canister. The code accounts for the coupled heat transfer modes of conduction, convection, and radiation and permits spatially varying boundary conditions, thermophysical properties, and power generation rates.

This document is intended as a manual for potential users of HYDRA-I. A brief discussion of the governing equations, the solution technique, and a detailed description of how to set up and execute a problem is presented. HYDRA-I is designed for operation on a CDC 7600 computer.

An appendix is included that summarizes approximately two dozen different cases that have been examined. The cases encompass variations in fuel assembly and canister configurations, power generation rates, filler materials, and gases. The results presented show maximum and various local temperatures and heat fluxes illustrating the changing importance of the three heat transfer modes. Finally, the need for comparison with experimental data is emphasized as an aid in code verification although the limited data available indicate excellent agreement.

DOCUMENT REVIEW FORM

AUTHOR: Mendel, J. (PNL)

TITLE: The Scientific Basis for Long-Term Prediction of Waste-Form Performance Under Repository Conditions

REFERENCE: Scientific Basis for Nuclear Waste Management VI, Vol. 15, North-Holland, N.Y., 1983, pp. 1-7

AVAILABILITY: Published

KEY WORDS: test methodology, basalt, salt, tuff, geochemistry, hydrology, waste aging, solution chemistry

DATA SUMMARY:

Property and Form of Data:
No specific data given.

Materials and Specimen Geometry:
Not applicable.

Test Conditions:
Not applicable.

COMMENTS ON DATA VALIDITY:

This overview paper does not present data on the performance of engineered or natural barriers to radionuclide release, per se, but it outlines a technical approach for assessing performance. Mendel addresses the important repository conditions for basalt, salt and tuff including geochemistry, hydrology, groundwater chemistry and Eh/pH conditions. The effects of emplaced waste in altering undisturbed conditions is outlined also. One very important factor which is mentioned is the need to consider the leaching behavior of aged waste since water should not cause leaching until the containment period has ended. Thus the release of actinides becomes important. Mendel cites work which indicates that the release of Pu and Np is controlled by their solubility in groundwater so that simple waste-form/water tests may be valid for predicting the release rate. From data on radionuclide decay rates and their sorption on rocks he states that the most important species are ^{237}Np , ^{226}Ra , ^{99}Tc , ^{210}Pb , ^{79}Se , ^{93}Zr , ^{126}Sr and ^{135}Cs . The importance of multicomponent tests to evaluate interaction effects is emphasized.

This paper outlines a sensible philosophy for quantifying system performance and should be considered in all DOE programs for HLW system tests.

DOCUMENT ABSTRACT

None

DOCUMENT REVIEW FORM

AUTHOR: Rai, D. and others (PNL)

TITLE: Actinide Solubility Controls in Performance Assessment of Nuclear Waste Repositories

REFERENCE: Waste Management '83, March 1983

AVAILABILITY: Published

KEY WORDS: solubility, groundwater chemistry, radionuclides

DATA SUMMARY:

Property and Form of Data:

Log of the concentration in solution as pH and time. Calculated and experimental data.

Materials and Specimen Geometry:

Np/Np-doped glass; Np/Np-doped glass w/ $\text{NpO}_2 \cdot \text{Am}(\text{OH})_3$.

Test Conditions:

DIW, room temperature, pH = 6 to 10 for Am.

COMMENTS ON DATA VALIDITY:

Data valid only under conditions sited and in the absence of heat, radiation and actual groundwater chemistries. Note that solubility of Am increases ~8 orders of magnitude as the pH changes from ~9 to 6. Note is made of changes caused by changing the oxidizing/reducing nature of the medium and the effect of counterions. Value of data for predicting source term is limited by these factors and the exclusion of heat and radiation. Authors do indicate need to determine solubilities under more realistic (anticipated) conditions.

DOCUMENT ABSTRACT

The importance of solubility control of radionuclide concentrations in repository groundwaters is discussed. Such control allows readily defensible estimation of the maximum concentrations of some actinide radionuclides in groundwaters. Estimates from currently available data indicate a number of cases where such maximum concentrations will be near or below the concentrations that are permissible, without the benefit of other processes that will lower the concentrations even more. Available information is briefly summarized and further research needs, which are not overly extensive, are discussed.

DOCUMENT REVIEW FORM

AUTHOR: Sutcliffe, W. G.
TITLE: Uncertainty Analysis: An Illustration from Nuclear Waste Package Development
REFERENCE: UCRL-90042/Preprint (October 1983)

AVAILABILITY: Lawrence Livermore National Laboratory, Livermore, CA 94550

KEY WORDS: Uncertainty, Reliability, Sensitivity, Package

GENERAL COMMENTS: The aim of this report is to propose a technique for uncertainty/reliability analysis. Like with random sampling methods, e.g., Monte Carlo calculations, the technique does refer to deterministic models and does make use of probability distributions for the model parameters. However, unlike random sampling methods, the technique separates probability calculations from performance measure calculations. The technique is illustrated with an application to canister corrosion and it is claimed superior to random sampling in that (1) it is simpler and more easily understood and (2) it allows a greater amount of insight resulting in fewer calculations. I find this last claim dubious. However a more detailed review is in order to check these claims.

Regardless of the proposed calculational technique, the document is noteworthy in that it references the NRC position on waste package reliability. The author finds that "uncertainty analysis also has a role in establishing reliability and reasonable assurance of waste package performance in the licensing process" and that "it is evident from NRC publications that an uncertainty analysis is necessary to demonstrate that these (the NRC's) criteria can be met." As previously suggested by the NRC to the DOE, the author indicates that uncertainty analysis "should be used as a guide in directing R & D, in particular in determining the quality and quantity of data needed to support design and licensing." Quite uncommittally the author also sustains the NRC position that "there is usually an uncertainty in the applicability of a model" and that this uncertainty should be "a data or input uncertainty." Information elicited from experts is also seen as a viable procedure to determine probability distributions.

This document is an indirect endorsement of the NRC position on waste package reliability.

DOCUMENT ABSTRACT

A method of uncertainty analysis is illustrated by analyzing canister corrosion in a nuclear waste package. The application of the method for satisfying the NRC regulation, 10CFR60, governing the disposal of nuclear waste is discussed. In this method uncertainty is represented by a probability distribution in the form of a histogram. This facilitates the separation of the probability calculations from the evaluations of the performance measure. This simplicity results in a great amount of insight, and often less calculation than a Monte Carlo approach. The method is easy to understand and applicable to a wide variety of problems.

DOCUMENT REVIEW FORM

AUTHOR: Svalstad, D. K.

TITLE: User's manual for SPECTROM-41: A Finite-Element Heat Transfer Program

REFERENCE: ONWI-326 (June 1983)

AVAILABILITY: National Technical Information Service, Springfield, VA 22161

KEY WORDS: Thermal, Heat, Model, Code

GENERAL COMMENTS: The contents of this report are limited to a generalized description of the code's computer program. Presentation of the theoretical formulation of the heat conduction program using the finite element method is not included.

SPECTROM-41 is the updated version of TRANCO. The code is designed to solve heat conduction problems in two-dimensional plane and axisymmetric geometry. The code can handle composite systems, a variety of boundary conditions, anisotropic and temperature-dependent thermal conductivity, and time-dependent heat generation rates.

SPECTROM-41 uses eight-noded isoparametric quadrilateral elements. The resulting system of ODE's in terms of nodal temperatures is solved by Gaussian elimination for steady state analyses. Gaussian elimination is coupled to a two-point recurrence scheme for transient analyses. The code uses dynamic dimensioning to limit computer core requirements. Program limits because of array dimensioning are reported in the document.

The authors reference the ORNL/TM-7112 report of 1979 to indicate that SPECTROM-41 calculations (formally TRANCO) agree within 5% with 2-D calculations from a set of 5 other computer codes. The authors also reference the ONWI-137 report of December 1980 to indicate that SPECTROM-41 showed excellent agreement, on one sample problem, with the commercial finite element code MARC-CDC.

The contents of this document were effective as of June 1981. ONI-5 of May 1983, Table 5-1, reports SPECTROM-41 as being used by ONWI and NNSWI, and as its being extended to 3-D.

DOCUMENT ABSTRACT

This User's Manual addresses SPECTROM-41: A Finite Element Heat Transfer Computer Program. The user is introduced to the program's capabilities and operation, with required user input outlined in detail. Example problems are included to illustrate the use of the various program features, and analytical solutions are presented for four of the examples to provide a measure of program accuracy. Past and ongoing comparative benchmark analyses are highlighted to provide the user with an indication of how SPECTROM-41 predictions compare with other available heat transfer programs.

DOCUMENT REVIEW FORM

AUTHOR: Thomas J. Wolery

TITLE: EQ3NR A Computer Program for Geochemical Aqueous Speciation - Solubility Calculations: Users Guide and Documentation.

REFERENCE: UCRL - 53414

AVAILABILITY: Published

KEY WORDS: Geochemical, Computer Code

GENERAL COMMENTS: This document provides the geochemical theory, numerical and computational methods, and input manual for EQ3NR a geochemical aqueous speciation - solubility program. It also supplies a brief review of other geochemical computer codes.

EQ3NR is the improved version of EQ3 and calculates the distribution of species based on thermodynamic considerations. EQ3NR provides the initial condition for its companion program EQ6 which calculates reaction progress due to rock/water interactions, and changes in temperature and pressure.

Two important limitations of EQ3NR are: (1) it is not applicable to solutions where the molality is greater than unity which is the case for brines and (2) the thermodynamic data base requires the pressure be 1 atmosphere for temperature between 0 and 100°C and follow the vapor/liquid equilibrium curve for water when the temperature is less than 300°C. Work is proceeding to remove the first limitation, and a report should be out soon.

The EQ3NR/6 package is important because DOE used these codes to predict water chemistry at the BWIP site.

DOCUMENT ABSTRACT

EQ3NR is a geochemical aqueous speciation-solubility FORTRAN program developed for application with the EQ3/6 software package. The program models the thermodynamic state of an aqueous solution by using a modified Newton-Raphson algorithm to calculate the distribution of aqueous species such as simple ions, ion-pairs, and aqueous complexes. Input to EQ3NR primarily consists of data derived from total analytical concentrations of dissolved components and can also include pH, alkalinity, electrical balance, phase equilibrium (solubility) constraints, and a default value for either Eh, pe, or the logarithm of oxygen fugacity.

The program evaluates the degree of disequilibrium for various reactions and computes either the saturation index ($SI = \log Q/K$) or thermodynamic affinity ($A = -2.303 RT \log Q/K$) for minerals. Individual values of Eh, pe, equilibrium oxygen fugacity, and Ah (redox affinity, a new parameter) are computed for aqueous redox couples. Differences in these values define the degree of aqueous redox disequilibrium. EQ3NR can be used alone. It must be used to initialize a reaction-path calculation by EQ6, its companion program.

EQ3NR reads a secondary data file, DATA1, created from a primary data file, DATA0, by the data base preprocessor, EQTL. The temperature range for the thermodynamic data in the file is 0-300°C. Addition or deletion of species or changes in associated thermodynamic data are made by changing only the file. Changes are not made to either EQ3NR or EQTL. Modification or substitution of equilibrium constant values can be selected on the EQ3NR INPUT file by the user at run time. EQ3NR and EQTL were developed for the FTN and CFT FORTRAN languages on the CDC 7600 and Cray-1 computers. Special FORTRAN conventions have been implemented for ease of portability to IBM, UNIVAC, and VAX computers.

DOCUMENT REVIEW FORM

AUTHOR: Wolery, T. J.

TITLE: Chemical Modeling of Irreversible Reactions in Nuclear Waste-Water-Rock Systems

REFERENCE: UCRL-85582 (February, 1981)

AVAILABILITY: Lawrence Livermore National Laboratory,
Livermore, CA 94550

KEY WORDS: Geochemical, Model, Code, Uranium

GENERAL COMMENTS: The document offers a perspective on geochemical modeling along with an update of work done on EQ6 to improve convergence. Also provided are a few data on uranium compounds.

The document isolates EQ6 from other codes in that EQ6 is a Reaction Path Model, i.e., it attempts to predict the irreversible evolution of a reacting aqueous geochemical system. EQ6 implements the concept of partial equilibrium whereby only a few reactions in a system proceed irreversibly; all the others adjust themselves reversibly striving to maintain equilibrium. Problems with this approach, as implemented by Helgeson first and Wolery later (EQ6), relate to (1) the determination of which reactions are approximately equilibrium reactions, and (2) the relationship of this model with the time variable.

With reference to item (1) many codes assume global redox equilibrium in solution. This is presented here as a questionable assumption. EQ3 and WATEQ improve on it by checking the redox potential of each major redox couple in the system, so that one can determine whether or not these couples equilibrate with respect to one another. With reference to item (2) since the model is based on thermodynamics, the relationship of EQ3/EQ6 with time is arbitrary. To change this, kinetics concepts should be used.

The document further reports about fixing convergence problems in EQ6. Since EQ3/EQ6 is being proposed as basically the reference geochemical package for salt, tuff and basalt, it should be checked thoroughly for (1) scientific soundness, (2) relevance of the data base, (3) accuracy of the modeling and its coding, (4) time-dependence handling capability.

DOCUMENT ABSTRACT

Chemical models of aqueous geochemical systems are usually built on the concept of thermodynamic equilibrium. Though many elementary reactions in a geochemical system may be close to equilibrium, others may not be. Chemical models of aqueous fluids should take into account that many aqueous redox reactions are among the latter. The behavior of redox reactions may critically affect migration of certain radionuclides, especially the actinides. In addition, the progress of reaction in geochemical systems requires thermodynamic driving forces associated with elementary reactions not at equilibrium, which are termed irreversible reactions. Both static chemical models of fluids and dynamic models of reacting systems have been applied to a wide spectrum of problems in water-rock interactions. Potential applications in nuclear waste disposal range from problems in geochemical aspects of site evaluation to those of waste-water-rock interactions. However, much further work in the laboratory and the field will be required to develop and verify such applications of chemical modeling.

APPENDIX 5

DETAILED REVIEWS OF WASTE PACKAGE DATA

BLANK PAGE

WASTE PACKAGE DATA REVIEW FORM

TYPE OF DATA

Schematic designs, characteristics and inventory of PWR and BWR spent fuel assemblies. Reference compositions for defense and commercial high level borosilicate glass waste forms. Description of reference packing material for use around a spent fuel waste package, including the results of its thermal conductivity measurements.

MATERIAL

Crushed Topopah Spring tuff for packing; iron-smectite clays and silica gel as additives. Glasses made to incorporate DHLW from the Savannah River plant and CHLW from West Valley (PNL 76-68 and MCC 76-68).

TEST CONDITIONS

- (a) For sample preparation: -60 or -100 mesh size crushed tuff powder; 10 to 30 ksi isostatic compaction pressure.
- (b) For thermal conductivity measurements on compacted packing:
test temperature: room temperature, 60, 100, 130, 165, and 200°C.

METHODS OF ANALYSIS

- (a) Thermal conductivity was determined by heating a specimen in the center and measuring the temperature with thermocouples which were placed at the surface and the center of the specimen. Duplicate measurements were made at room temperature and 100°C.
- (b) The method for determining the density is not described.
- (c) The nominal composition of the glass (supplied by SRL) was determined using electron microprobe at 10 spots on a sample, and then averaged over five samples.

AMOUNT OF DATA

Original Data

- (a) Composition of DHLW glass (simulated waste).
- (b) Density of compacted packing. -60 mesh crushed powder: density after compaction pressures of 15 and 25 ksi; -100 mesh crushed powder: density after compaction pressures of 10, 15, 20, 25, 30, and 35 ksi; -18 mesh crushed powder: unsuccessful compaction.

- (c) Thermal conductivity of crushed tuff: 12 data points for six temperatures. Qualitative mention of thermal conductivity of one sample containing 95% crushed tuff plus 5% bentonite clay.

Data Quoted From Other Sources

- (a) Burnup and time of discharge of commercial SF in inventory.
- (b) Physical characteristics of LWR assemblies.
- (c) Estimate of percent failure of fuel rods.
- (d) Inventory of dominant fission products and activation products in SF.
- (e) Radioactivity and temperature decay profile for spent fuel assembly.
- (f) Fission gas release as a function of burnup time from LWR fuel rods.
- (g) Plutonium, cesium, tellurium and iodine concentration profile in a fuel pellet.
- (h) Dimensions of a canister, and composition of the glasses developed at Savannah River Plant.
- (i) Chemical and radionuclide composition of the defense sludge-supernate glass. Its heat and radioactivity decay profiles.
- (j) Composition of a DHLW glass used in NNWSI testing.
- (k) Estimated composition and radioactivity of wastes at West Valley. Specifications for the waste form and canisters to be used for this waste.
- (l) Chemical composition of PNL 76-68 and MCC 76-68 glasses.

UNCERTAINTIES IN THE DATA

The uncertainty in the density measurements on compacted crushed tuff specimens has been listed 1.7-3.5%. Duplicate measurements for thermal conductivity are made at each temperature. Although a numerical value for experimental error is not mentioned, the data in the figure show a reproducibility of approximately 8% or better. However, it is not clear if the data obtained on specimens prepared from tuff rocks from different locations will also have thermal conductivity within the reported range.

The uncertainty estimates for the composition of DHLW glass are based on the standard deviation of the average of results on five samples. These values range from 4% to 30% depending on the element analyzed and include uncertainty in measurements as well as inhomogeneity in the samples.

The uncertainty in data quoted from other sources has not been mentioned although, for example, the data for fission gas release shows very large scatter.

DEFICIENCIES IN THE DATA BASE

Topopah Spring tuff crushed to pass 100-mesh screen and compressed isostatically at 20 ksi has been identified in this report as the reference packing material with the possible additions of small amounts of clay or silica gel. The -100 and -60 mesh but not the -18 mesh powder could be compacted into a specimen suitable for thermal conductivity measurements. However, it is not clear if a full size packing component can be fabricated under the reference conditions and if it would be mechanically strong enough for normal handling.

The thermal conductivity data are shown for one specimen prepared under one set of conditions. There are no data on the effect of processing parameters such as compaction pressure, particle size, etc. on thermal conductivity. It would be useful to establish if there is a simple correlation between packing density, particle size, or composition with the thermal conductivity. The beneficial or detrimental effects of the proposed additives on packing performance remain to be determined.

APPLICATION OF DATA TO LICENSING

[Key Data (X), Supporting Data ()].

GENERAL COMMENTS

This report describes composition and other data for reference waste forms and packing for a tuff repository. However, the original data are given only for the thermal conductivity and density of crushed tuff packing which is very limited and based on preliminary experiments. The purpose of a packing material is to impede the ingress of groundwater into and release of radionuclides from the waste package. The information on thermal conductivity of packing is essential in designing the waste package, determining the waste loading, etc. However, the usefulness of the packing needs to be determined in terms of its sorption and water migration properties under appropriate repository conditions of temperature, radiation, pressure, humidity, thermal gradient, etc.

ORGANIZATION PRODUCING DATA

Lawrence Livermore National Laboratory (NNWSI).

AUTHORS/REFERENCE

Oversby, V. M., "Reference Waste Forms and Packing Material for the Nevada Nuclear Waste Storage Investigations Project," UCRL-53531, March 1984.

AVAILABILITY

NTIS

KEY WORDS

Topopah Spring tuff, reference compositions, waste forms, packing, thermal conductivity, spent fuel, DHLW, CHLW.

DATE REVIEWED

October 1984.

gfs
11/19/84

ABSTRACT

The Lawrence Livermore National Laboratory (LLNL), Livermore, Calif., has been given the task of designing and verifying the performance of waste packages for the Nevada Nuclear Waste Storage Investigations (NNWSI) Project. NNWSI is studying the suitability of the tuffaceous rocks at Yucca Mountain, Nevada Test Site, for the potential construction of a high-level nuclear waste repository. This report gives a summary description of the three waste forms for which LLNL is designing waste packages: spent fuel, either as intact assemblies or as consolidated fuel pins, reprocessed commercial high-level waste in the form of borosilicate glass, and reprocessed defense high-level waste from the Defense Waste Processing Facility in Aiken, S.C. Reference packing material for use with the alternative waste package design for spent fuel is also described.

BLANK PAGE

WASTE PACKAGE DATA REVIEW FORM

TYPE OF DATA

Permeability of tuff blocks in a temperature gradient for tuffaceous groundwater. Chemical composition of the test solution after permeating through the test rock.

MATERIAL

Tuff from the Paintbrush section of the Topopah Spring Member (densely welded, devitrified and nonzeolitized); J-13 groundwater.

TEST CONDITIONS

The groundwater was forced to flow from high temperature borehole at the center of a cylindrical specimen to its outer surface (jacket) at a lower temperature. Three experiments were conducted under the following conditions:

Experiment No.	1	2	3
Borehole temperature (°C)	150	90	250
Jacket temperature (°C)	50	36	83
Differential pressure (MPa)	0.15	0.15	---
Test duration (days)	20	17	21
Average flow rate (ml/sec)	1.15×10^{-3}	1.45×10^{-3}	2×10^{-4}
Confining pressure (MPa)	30	30	30

In one of the experiments the flow of groundwater was stopped intermittently, and in another case the flow rate was varied from 2×10^{-5} to 2×10^{-2} ml/sec.

METHODS OF ANALYSIS

Permeability for a particular set of test conditions as a function of time is calculated from the mass flow rate under a constant pore pressure differential and Darcy's law for radial flow. The methods employed in the chemical analysis of fluids have not been described.

AMOUNT OF DATA

- (a) Only three specimens were tested, one of which could not sustain a pressure differential due to a large continuous void across the thickness.
- (b) Permeability data are shown as a function of time for two specimens (1 and 2) on a graph for a period of 20 days.

- (c) pH (at room temperature) and chemical analyses of 8 to 10 fluid specimens collected during each test are given for Na^+ , K^+ , Mg^{2+} , Ca^{2+} , HCO_3^- , SO_4^{2-} , NO_2^- , NO_3^- , PO_4^{3-} , F^- and Cl^- ions, and SiO_2 . The results include the analyses for solutions collected at the room as well as the test temperatures.
- (d) In Experiment No. 2, fluid samples were collected after 25, 50, and 100 hours of no-flow condition. In Experiment No. 3, four flow rates in the range of 2×10^{-2} to 2×10^{-5} ml/sec were included.

UNCERTAINTIES IN THE DATA

The authors have not given any value for the uncertainty or error in experimental data, and since only one experiment has been conducted for a given set of conditions, it is difficult to estimate the uncertainty in data. Perhaps the largest source of uncertainty in the present data is due to the lack of information about the specimen itself. For example, the room temperature permeability for two specimens had the values of 3 and 65 μ darcsies under very similar conditions. Such a large variation in permeability reflects the difference in cracks, voids, fractures, etc. present in different specimens. However, for a particular specimen some estimate of uncertainty can be obtained from the scatter in time dependence of permeability.

DEFICIENCIES IN THE DATA BASE

- (a) A difference by a factor of 20 in the permeability of two specimens suggests that there can be a big range in the properties of tuff such as mineral composition, density and distribution of voids, cracks, etc. The present data are very limited in describing the complete range of permeability values, and a much larger number of specimens need to be tested. Similarly, a range of pore pressure differential needs to be included in these tests.
- (b) Because of non-uniform distribution of cracks and voids, it is possible that the results may depend on the size of specimen.
- (c) The permeability of the J-13 groundwater did not show very large changes within the test period. However, it is possible that if concentrated groundwater (due to initial evaporation and then subsequent dissolution of the precipitated salts) passes through the same specimen, the permeability may decrease due to enhanced mineral growth.
- (d) In these tests the water flow direction is from central borehole at high temperature to the outside surface at lower temperature. However, in the initial stages the groundwater will migrate from cold surroundings to hot waste package. The mineral growth and, therefore, the changes in permeability could be very different under such reversed thermal gradient.

APPLICATION OF DATA TO LICENSING

[Key Data (X), Supporting Data ()].

GENERAL COMMENTS

- (a) Although the results given in this paper are important in evaluating the water flow conditions in a tuff repository, the data are extremely limited. Considering the possibility of large variations in the properties of tuff, it is difficult to draw general conclusions.
- (b) The Bullfrog tuff which is believed to be representative of a much deeper level in the saturated zone shows much larger effects on fluid chemistry and temperature dependence of permeability. On the contrary, the Topopah Spring tuff does not show such large effects. But the reason for this difference and whether it is a general observation are not clear.
- (c) The maximum duration of testing (20 days) may be too short to show the effects of slow mineral growth and alteration which may affect the groundwater permeability on a repository time scale.
- (d) The high permeability of Topopah Spring tuff as found in the present tests has been considered beneficial for the waste package because the groundwater would not stay around it to cause corrosion. However, if the waste package is breached by some mechanism, because of high permeability the radionuclides would escape the repository more easily.

ORGANIZATION PRODUCING DATA

U. S. Geological Survey, Menlo Park, California.

AUTHORS/REFERENCE

Morrow, C. A., D. E. Moore and J. D. Byerlee, "Permeability and Pore-Fluid Chemistry of the Topopah Spring Member of the Paintbrush Tuff, Nevada Test Site, in a Temperature Gradient - Application to Nuclear Waste Storage," in Scientific Basis for Nuclear Waste Management VII, G. L. McVay, Editor, New York, Elsevier, 1984, p. 883.

AVAILABILITY

Elsevier Science Publishing Co., Inc.

KEY WORDS

Topopah Spring tuff, permeability, temperature gradient, J-13 groundwater, pore fluid chemistry.

DATE REVIEWED

October 1984.

gfs, 11/16/84

ABSTRACT

The Topopah Spring Member of the Paintbrush Tuff from the Nevada Test Site is being investigated by the Nevada Nuclear Waste Storage Investigations project (NNWSI) as a possible nuclear waste repository host rock. Changes with time of the permeability and fluid chemistry of the Topopah Spring Member have been measured in samples subjected to a temperature gradient. Maximum temperatures of the imposed gradients ranged from 90° to 250°C; minimum temperatures were 36° to 83°C. Confining and pore pressures simulated a depth of about 1.2 km, which is greater than the proposed repository depth, but chosen for comparison with previous studies at these pressures. Pore fluid used in the experiments was groundwater from the Nevada Test Site; the direction of pore-fluid flow was from the high- to the low-temperature side of the tuffs.

Initial permeabilities of the tuff samples ranged from 1 to 65 μ darcys, the wide range in values resulting from differences in the void and fracture geometries of the samples. Heating the tuffs produced no change in permeability in the lowest temperature experiment and only small changes at higher temperatures. The fluids discharged from the tuffs were dilute waters of near-neutral pH that differed only slightly from the original groundwater composition.

Since proposed burial in the Topopah Spring Member would be in the unsaturated zone, the high initial permeability and the absence of permeability change with heating may be desirable, because downward-percolating waters would be able to drain into deeper formations and not collect at the repository level. In addition, any fluids that may come in contact with waste canisters will not have acquired any potentially corrosive characteristics through interaction with the tuff.

WASTE PACKAGE DATA REVIEW FORM

TYPE OF DATA

Quantitative analyses of minerals in Bullfrog Member tuff core wafers in as-received condition and after reacting with J-13 groundwater; the analysis is given for various oxides, fluorine and chlorine. Ordinary histograms for anorthite and orthoclase. Scanning electron micrographs of reacted wafers. Changes in the weight of wafers and pH of solution.

MATERIAL

Bullfrog Member tuff taken from a 20-ft interval in the Lathrop Wells section; J-13 groundwater.

TEST CONDITIONS

- (a) Polished tuff wafers were reacted with J-13 groundwater in Teflon-lined autoclaves at 150°C.
- (b) Surface/volume ratio: 1100-2200 cm⁻¹.
- (c) Reaction times: 1, 2, 3, 4, 6, and 8 weeks.

METHODS OF ANALYSIS

- (a) Surface examination using a scanning electron microscope.
- (b) Qualitative energy dispersive spectrometry and quantitative wavelength dispersive analysis using an electron microprobe. Elemental concentrations were obtained by comparing the data with appropriate silicate standards.
- (c) The bulk chemistry of the rock has been determined by neutron activation analysis and X-ray diffraction, but these are not discussed in any detail.

AMOUNT OF DATA

The oxide composition is determined for SiO₂, Al₂O₃, K₂O, Na₂O, CaO, MgO, TiO₂, FeO, BaO, MnO and ZrO₂. For a rock specimen the analysis of plagioclase, sanidine, biotite, hornblende, magnetite, pumice, zircon, ilmenite, fracture filling and matrix are given separately. Sanidine and plagioclase have been analyzed at the largest number of points (20's), but pumice, zircon, ilmenite and magnetite have been analyzed at very few points. In a histogram for anorthite the maximum number of samples ranged from three to six, but for orthoclase it ranged from two to eight.

UNCERTAINTIES IN THE DATA

- (a) The estimate of error in experimental measurements is not given. However, a limit on such uncertainties can be assessed where analysis has been obtained for numerous points on a given wafer.
- (b) The J-13 groundwater has been obtained by directly pumping from the well. The reproducibility of composition, Eh and pH of this water collected on different occasions is not described.
- (c) The alkali elements are known to evaporate easily when heated under an electron beam. Therefore, these elements were analyzed first, but there still remains larger uncertainty in the concentration of these elements.
- (d) Use of Teflon vessels has been shown to affect the solution pH by absorbing CO₂. It is not clear what effects this change in pH could have on present results.
- (e) The as-collected tuff specimens were cut and then washed to remove weathering or alteration products. It is not clear if any such treatments would have also removed some minerals which are an intrinsic part of tuff.

DEFICIENCIES IN THE DATA BASE

The data are reported for a very limited number of wafers taken from a specific location in the Bullfrog Member. Since a large variability is known to exist in the composition and distribution of minerals in a tuff deposit of the size of a repository, no general conclusions may be drawn from the present data and only specific information is available.

Although a wafer had a polished surface in the beginning of test, its reaction with solution would have introduced some surface roughness which, in turn, can introduce an error in composition determination. Whereas this factor has been discussed in the report, it has not been corrected.

A temperature gradient or radiation was not present in the tests but in a repository these factors can influence the growth of alteration products, etc.

APPLICATION OF DATA TO LICENSING

[Key Data (), Supporting Data (X)].

GENERAL COMMENTS

The tuff samples studied in this work were taken from the Lathrop Wells section of the Bullfrog Member of the Crater Flat tuff. These specimens are representative of the deposits below the water table beneath Yucca Mountain. Since the start of this work, the repository horizon has been decided to be in

an unsaturated zone above the water table. Therefore, the present results are not directly relevant to characterize the near-field conditions in the proposed repository. As the author points out, however, the results may be useful in the development of a geochemical modeling code.

In contradiction to the title of the report, analyses of the aqueous phase are not included.

ORGANIZATION PRODUCING DATA

Lawrence Livermore National Laboratory.

AUTHORS/REFERENCE

K. G. Knauss, "Hydrothermal Interaction Studies of Bullfrog Member Tuff Core Wafers in J-13 Water at 150°C: Quantitative Analyses of Aqueous and Solid Phases," UCRL-53521, February 1984.

AVAILABILITY

Available as a formal report.

KEY WORDS

Bullfrog Member tuff, mineral composition, alteration, J-13 groundwater.

DATE REVIEWED

September 1984.

gfs
11/15/84

ABSTRACT

This paper describes the experimental work conducted to understand the water chemistry in the near-field surrounding a nuclear waste repository in the Bullfrog Member of the Crater Flat Tuff, Nev., and to study any changes in the rock itself due to hydrothermal alteration. The work is part of the Nevada Nuclear Waste Storage Investigations (NNWSI) Project to determine the suitability of the volcanic units at Yucca Mountain for storing high-level nuclear waste.

Static hydrothermal experiments with polished core wafers were run for 60 d; all faces of the core wafers were exposed to solution. Quantitative solution analyses indicate that the solution chemistry for both crushed tuff and solid core wafers is in good agreement. Analyses of the solid phases suggest that the extent of reaction, at least over the 60-d period, is relatively minor, even though solution effects were observed. These experiments show that conditions in a repository located in the Bullfrog Member would be relatively benign with respect to waste form and waste package survival.

WASTE PACKAGE DATA REVIEW FORM

TYPE OF DATA

Permeability of tuff tested under a temperature gradient for deionized and J-13 water as a function of time. Chemical analyses and pH (at room temperature) of the solution collected after migrating through the test rock. Some data for the room temperature permeability.

MATERIAL

Tuff from the Bullfrog Member of the Crater Flat, Yucca Mountain, deionized water and J-13 groundwater. The tuff specimens were devitrified, non-zeolitized and moderately welded, containing deformed elongated pumice fragments and voids.

TEST CONDITIONS

The water was forced to flow from a high temperature borehole at the center of the specimen to the circumference (jacket) at lower temperatures. The following range of conditions was used:

Borehole temperature	150-250°C
Jacket temperature	48-73°C
Differential pore pressure	1.4-2.5 bar
Average daily flow rate	14.5-100 ml
Confining pressure	300 bar
Specimen dimensions	Cylinder of 7.62 cm diameter and 8.89 cm length

METHODS OF ANALYSIS

- (a) Permeability was calculated from mass flow rate under a constant pore pressure differential and assuming Darcy's law for radial flow.
- (b) SiO₂ in the fluid was determined by digesting the solution in NaOH and then using the molybdate blue method.
- (c) Sodium, potassium, calcium and magnesium in the solution were analyzed using atomic absorption techniques.
- (d) The concentrations of Cl⁻, F⁻, SO₄²⁻, NO₃⁻, NO₂⁻ and PO₄³⁻ were determined using ion chromatography.
- (e) The total dissolved inorganic carbon content was determined with a carbon analyzer.
- (f) To estimate ionization of silica and the CO₃²⁻/HCO₃⁻ ratio, the SOLMNEQ computer program was used for the data of 25°C.

AMOUNT OF DATA

- (a) Only three tuff specimens, two at a borehole temperature of 250°C and one of 150°C are tested.
- (b) Permeability data are shown on a graph for a period of 22 days.
- (c) pH and chemical analyses are given for 18-21 fluid samples collected at different time intervals spanning through the duration of test (14 to 37 days).
- (d) A few of the data points include results obtained at room temperature before heating the core.

UNCERTAINTIES IN THE DATA

There is only one experiment conducted for a given set of conditions which makes it difficult to estimate the uncertainty in or reproducibility of the data. The experimental uncertainties in permeability or chemical composition are not given, but these are probably small compared to the uncertainty in the characteristics of a test specimen. Some estimate of uncertainty in the data can be obtained from the scatter observed as a function of time.

There is a significant unbalance between the total cationic and anionic concentrations, thus emphasizing the uncertainty in reported numbers; error in pH measurements has been cited as a major cause of this discrepancy.

DEFICIENCIES IN THE DATA BASE

- (a) Considering that there can be a big range of the properties of tuff such as mineral composition, density and distribution of voids and cracks, etc., a much larger number of rock specimens need to be tested to arrive at a general conclusion. The range of pore pressure difference and temperature has also been very limited in the present tests.
- (b) During the initial heating of a tuff specimen, the permeability showed a sudden increase which gradually returned to close to pre-heating value. Some of the transient increase in permeability was attributed to the production and subsequent healing of thermal cracks. Therefore, there is a possibility of mineral growth and subsequent change in permeability in tuff rocks also. The authors have discussed this possibility but concluded that void size is rather large to change the overall permeability. Further experiments are needed to verify this conclusion for tuff from other sources.
- (c) In the present tests the water flows under a pressure gradient from high temperature borehole to low temperature jacket at the outer surface of the sample. Incorporation of pressure as well as temperature gradient in these tests is relevant to a repository situation. However, in the initial stages, the groundwater will be traveling from cold surroundings to

a hot waste package. The nature of mineral growth and, therefore, the changes in permeability could be very different under such conditions. Therefore, parallel testing is needed to assess the permeability of tuff rock in the early stages of water intrusion.

APPLICATION OF DATA TO LICENSING

[Key Data (), Supporting Data (X)].

GENERAL COMMENTS

This paper reports permeability testing of tuff under the conditions of temperature and pressure gradients which are likely to be present in a HLW repository. However, the data are extremely limited and considering large variations in the properties of tuff, it is difficult to draw general conclusions.

The maximum test duration has been only a few weeks which is much too short to observe the effect of mineral growth in large voids present in test specimens. On a repository time scale the mineral growth can be sufficient to change the permeability values. Some accelerated testing in conjunction with the present tests will be useful to understand the water flow to and from a waste package.

The ionic concentration in the solution is found to be much larger in the initial stages of the test, presumably due to the presence of some soluble salts. If this is true for the entire tuff rock encountered by the water percolating to a waste package, ionic concentration approaching the solubility limit may be reached. The concentration effects are also possible due to initial evaporation and subsequent dissolution of the precipitated salts. Therefore, testing with more concentrated ionic solution will be needed.

Rather high pH (10.6) values were observed for some fluid samples. A cause of this observation and an upper limit on the pH value should be established as this may be a very important factor in the waste package performance. Finally, the present results are only indirectly useful because Bullfrog tuff may not be the best representation of that at the proposed repository horizon in the unsaturated zone.

ORGANIZATION PRODUCING DATA

U. S. Department of the Interior, Geological Survey.

AUTHORS/REFERENCE

Byerlee, J., C. Morrow and D. Moore, "Permeability and Pore-Fluid Chemistry of the Bullfrog Tuff in a Temperature Gradient: Summary of Results," Open-File Report 83-475.

AVAILABILITY

Preliminary report.

KEY WORDS

Bullfrog tuff, permeability, temperature gradient, groundwater chemistry.

DATE REVIEWED

September 1984.

gfs
10/9/84

ABSTRACT

The permeability and fluid chemistry of a Nevada Test Site tuff is being studied under conditions simulating a nuclear waste repository environment. The purpose of this project is to investigate the changes that take place with time when groundwater comes in contact with heated rock, and to determine the ease with which potential radionuclide-bearing groundwater could be carried into the environment.

BLANK PAGE

WASTE PACKAGE DATA REVIEW FORM

TYPE OF DATA

Anion and cation concentrations in J-13 groundwater which is equilibrated with crushed or core wafer samples of Topopah Spring tuff. Change in pH and alkalinity of groundwater after reacting with tuff. Weight loss of core wafers as a result of reaction with the groundwater. Qualitative information from electron microprobe and SEM studies.

MATERIAL

J-13 groundwater, tuff rocks taken from a surface outcrop at Fran Ridge, east of Yucca Mountain.

TEST CONDITIONS

- (a) For 100-mesh crushed tuff: 0.2, 0.4 and 0.8 g of rock were equilibrated with 12 ml of J-13 groundwater at 150°C for 1, 2, 4, 8, 16, 31 and 48 days. For tests at 90°C, 0.4, 0.8, 1.6 and 3.2 g of rock were equilibrated with 48 ml of groundwater for 1, 3, 6, 12, 24, 36, 48, 60 and 72 days. Teflon reaction vessels or gold rocking autoclaves were used as test containers. All specimens were washed in J-13 water for two minutes and then equilibrated overnight as part of a pretreatment.
- (b) For core wafers of tuff: Polished specimens were equilibrated with groundwater or water saturated air at 150°C for a period of up to four months.

METHODS OF ANALYSIS

- (a) Anion and cation concentrations in and alkalinity of groundwater are determined presumably using analytical techniques; specific procedures are not described.
- (b) Changes in rock properties are determined by weight loss measurements, and observations under an electron microprobe or scanning electron microscope.

AMOUNT OF DATA

- (a) Crushed tuff experiments: F^- , Cl^- , NO_3^- , SO_4^{2-} and carbonate alkalinity have been measured but the data are given only for Cl^- , NO_3^- and SO_4^{2-} anions. Among cations, the concentrations of Na^+ , K^+ , Ca^{2+} , and Al^{3+} have been measured but the time dependence of the data are shown only for the last two which show major change. A concentration of silicon has also been determined but its chemical nature in the solution is not

established. Results for a 64-day test at 150°C with tuff selected from three vertical drill holes and one horizontal air-drilled hole are also given.

- (b) Core wafer experiments: Concentrations of Al, Si, Ca, K, Mg and Na in and pH of the solution after reacting with core wafers at 150°C. Loss in the weight of core wafers.

UNCERTAINTIES IN THE DATA

- (a) Apparently all the results are based on single tests for a given set of conditions. There is no indication of the magnitude of uncertainty in or reproducibility of the anion and cation concentrations determined from chemical analyses.
- (b) The authors have found that the use of Teflon containers may have affected the solution pH and alkalinity. This renders some of their data less useful. The details of reaction of CO₂ with Teflon are not established. This information may be relevant to other kinds of experiments where Teflon containers are used.
- (c) The basis for drawing curves through experimental data points is not mentioned.

DEFICIENCIES IN THE DATA BASE

All the data appear to be from single tests under a given set of conditions. In some cases, the solution composition did not reach a plateau, thus suggesting that equilibrium was not achieved and tests for longer duration would be desirable.

Although under one set of test conditions tuff specimens from four different drill holes were reacted with J-13 groundwater, these may not represent the complete range of rock compositions which the groundwater may encounter in the repository.

APPLICATION OF DATA TO LICENSING

[Key Data (), Supporting Data (X)].

GENERAL COMMENTS

The authors have used a pretreatment in which the rock specimens are washed to remove readily soluble salts. These salts are assumed to be present only at the surface of the repository site. At present, the composition of water reaching the repository horizon in the unsaturated zone has not been established. It is possible that the rainwater dissolves surface salts and

then approaches the repository horizon, thus may have higher solute concentration than suggested at present. A much higher solute concentration is also expected due to initial evaporation of groundwater and then subsequent dissolution of the precipitated salts.

The presence of colloids and the effect of radiation on the chemistry of the groundwater may influence some of the present conclusions.

ORGANIZATION PRODUCING DATA

Department of Earth Sciences, Lawrence Livermore National Laboratory.

AUTHORS/REFERENCE

Knauss, K. G., V. M. Oversby and T. J. Wolery, "Post Emplacement Environment of Waste Packages," in The Scientific Basis for Nuclear Waste Management, VII, G. L. McVay, Editor, New York, Elsevier Publishing, 1984, p. 301.

AVAILABILITY

Published.

KEY WORDS

Tuff, groundwater chemistry, Teflon container, rock-water interaction.

DATE REVIEWED

September 1984.

gfs
10/12/84

ABSTRACT

Experiments have been conducted as part of the Nevada Nuclear Waste Storage Investigations Project to determine the changes in water chemistry due to reaction of the Topopah Spring tuff with natural groundwater at temperatures up to 150°C. The reaction extent has been investigated as a function of rock-to-water ratio, temperature, reaction time, physical state of the samples, and geographic location of the samples within the tuff unit. Results of these experiments will be used to provide information on the water chemistry to be expected if a high level waste repository were to be constructed in the Topopah Spring tuff.

WASTE PACKAGE DATA REVIEW FORM

TYPE OF DATA

Mineral composition of an exploration block in the vicinity of the repository horizon at Yucca Mountain. Some estimates of composition variations along vertical as well as horizontal directions. Cation, anion and dissolved oxygen concentrations in and pH of groundwater taken from 11 wells in the vicinity of Yucca Mountain.

MATERIAL

Yucca Mountain tuff and groundwater.

TEST CONDITIONS

X-ray diffraction, optical petrography and electron microprobe techniques have been employed to determine mineral compositions; the details are referred elsewhere. Groundwater samples were obtained by pumping it to the surface from below the static water table. The test conditions and experimental procedures for chemical analyses are not given in this paper.

METHODS OF ANALYSIS

Not specified.

AMOUNT OF DATA

- (a) Map of the exploration block and the locations of drill holes in the Yucca Mountain.
- (b) North-south cross-sectional diagram to show vertical distribution of tridymite, cristobalite, quartz and alkali feldspar at various depths above and below the repository horizon. The location of static water table and zeolitized minerals above it are also shown in a west-east cross-section.
- (c) Mineralogy of various zones along the transport pathways below the repository. This includes the thickness and composition range in zeolite Interval I, basalt vitrophyre, vitric zone, zeolite Interval II, Central Prow Pass member, zeolite Interval III, Central Bullfrog member, zeolite Interval IV and deeper petrologic zones. The presence of zeolites which have good sorption properties is particularly emphasized.
- (d) Elemental concentrations of Ca, Mg, Na, K, Li, Fe, Mn, Al and Si in groundwater from 11 locations. Well J-13 is ≈6 km southwest of the repository block. Six wells are within or at the edge of the repository block. One well is drilled deep down to the paleozoic rocks below the tuffs.

- (e) Eh, pH and the concentrations of F^- , Cl^- , SO_4^{2-} , HCO_3^- , NO_3^- and dissolved oxygen in all the groundwater samples.
- (f) Total organic content of the groundwater from two wells. High molecular weight organics are a major constituent among organic constituents but specific compounds are not determined.
- (g) One sample of groundwater from the deep zone, which was isolated with packers and pumped up to avoid mixing with overlying waters.

UNCERTAINTIES IN THE DATA

This paper primarily describes the results without giving experimental details or uncertainties. However, a range of composition for a particular mineral in a given horizon is given presumably based on data taken from different locations. In the case of groundwater chemistry, it is not clear how the chemical analyses varied for samples taken at different times, except for the groundwater from the deep well. The chemical analysis for cations gives total elemental concentrations without mentioning ionic state which can give information about the oxidation potential of the solution.

DEFICIENCIES IN THE DATA BASE

The process of drilling the holes and collecting samples is likely to have affected some of the results, particularly those of groundwater chemistry. For example, the oxidation potential of in situ groundwater might be affected when it comes in contact with drilling liquids or atmospheric oxygen. This is possibly one of the reasons for the significant difference in the analyses of groundwater samples taken 26 days apart from the same well; for example, Eh changed from -40 mV (non-oxidizing) to 156 mV (oxidizing).

APPLICATION OF DATA TO LICENSING

[Key Data (X), Supporting Data ()].

GENERAL COMMENTS

The data given in this paper are based on a limited number of drill holes at the edge of the exploration block. To characterize the complete repository area and its vicinity more extensive data will be needed. This comment is supported by the authors' conclusion that mineralogic homogeneity of the repository horizon throughout most of the exploration block is not a general feature outside the exploration block. To obtain limits of variability in composition, more samples from lateral holes need to be characterized.

All the groundwater samples analyzed in this study were taken from the static water table which lies under the proposed unsaturated repository horizon. From this information it is difficult to determine the composition

of water that would come in contact with a waste package. Depending on the rate of rainfall and available soluble salts on its path to the repository, the rainwater can be of significantly different composition than given in this paper.

ORGANIZATION PRODUCING DATA

Los Alamos National Laboratory and U. S. Geological Survey, Denver.

AUTHORS/REFERENCE

Bish, David L., Allen E. Ogard and David T. Vaniman, "Mineralogy-Petrology and Groundwater Geochemistry of Yucca Mountain Tuffs," in The Scientific Basis for Nuclear Waste Management, VII, G. L. McVay, Editor, New York, Elsevier Publishing, 1984, p. 283.

AVAILABILITY

Published.

KEY WORDS

Mineralogy, Yucca Mountain, tuff, groundwater chemistry, zeolites.

DATE REVIEWED

September 1984.

gfs
10/12

ABSTRACT

From these results, several preliminary conclusions can be drawn. (1) These are quite dilute waters and, other than oxygen in the waters, there are no major constituents that can rapidly attack waste-package container materials. (2) Bicarbonate and hydroxyl anions are the major actinide complexing ligands in the waters. (3) Although the bicarbonate concentration in the Paleozoic rock water is high, its effect will be minimal because this water must come into contact with solid waste, wherever it may occur, before the solubility of any waste element increases as a result of complex formation. Once a waste element is in solution, additional complexing ligands will not increase the concentration. (4) Many of the waste elements exhibit minimum solubilities in the pH range of Yucca Mountain water. (5) At best, deeper reducing waters will reduce neptunium and plutonium ions to their more insoluble +IV oxidation state but will not reduce UO_2^{+2} or TcO_4^- . (6) Finally, it appears that water composition may be useful in the definition of flowpath.

WASTE PACKAGE DATA REVIEW FORM

TYPE OF DATA

Chemistry of groundwater which has been equilibrated with crushed powder and wafers of tuff rock at 90°C and 150°C. Solution analyses for Ca, Al and Si as a function of reaction time. Final values of pH, alkalinity (related to the concentration of HCO_3^-) and concentrations of Mg, K for rocks taken from different locations (within Topopah Spring).

Boron leach data for borosilicate glass compositions based on PNL 76-68 glass. Effect of adding tuff and 304L on this leach rate. Leaching of uranium from defected Zircaloy-clad UO_2 in deionized water at room temperature.

MATERIAL

J-13 groundwater. Tuff (crushed or wafers) from Topopah Spring Member outcrop or drilled cores. PNL 76-68 borosilicate glass. Zircaloy-clad spent fuel elements.

TEST CONDITIONS

(a) Groundwater Chemistry:

Temperature 90°C and 150°C. Crushed tuff reacted with J-13 water in Teflon vessels; tuff wafers reacted with J-13 water in Teflon vessels; and crushed tuff reacted with J-13 water in Dickson-type gold autoclaves. Test duration up to 70 days.

(b) Wasteform Leaching:

PNL 76-68 glass in J-13 water at 90°C with a glass surface area-to-solution volume ratio (SA/V) of 0.1 cm^{-1} (which is consistent with the MCC-1 procedure) and 1.0. Tests also included monolithic tuff, 304L stainless steel, and/or crushed tuff. Five-inch-long PWR fuel pieces fitted with water-tight end caps in deionized water at room temperature. The specimens had undefected cladding, one or two 200-micron diameter holes, or a slit 150-microns wide and 2.5-cm long. Solution analyzed after 1, 5, 15, 30, and 60 days.

METHODS OF ANALYSIS

- (a) Groundwater composition is determined presumably using analytical chemistry methods; specific details are not mentioned.
- (b) Scanning electron microscope and electron microprobe are used to determine any changes on the surface of polished wafers due to hydrothermal reaction.

- (c) Boron and uranium concentrations are measured in groundwater to determine leaching characteristics of borosilicate glass and Zircaloy-clad spent fuel, respectively, but the method of analysis is not described.

AMOUNT OF DATA

(a) Groundwater Chemistry:

1. Concentration of Al, Ca and Si are given as a function of reaction time up to 70 days.
2. Higher pH of the test solutions equilibrated in Teflon autoclaves is attributed to the loss of CO₂ to the container walls. Gold bag autoclave eliminates this problem.
3. Concentrations of K and Mg are also mentioned but for a fixed test duration.
4. Anion concentrations are described, but mostly qualitatively.
5. It is shown qualitatively that as a result of hydrothermal reaction magnesium calcite precipitates and cristobalite dissolves.

(b) Wasteform Leaching:

1. Boron leach data for reaction time up to six months at 90°C. SA/V = 0.1 and 1.0 cm⁻¹.
2. Effect of adding tuff and/or 304L stainless steel to J-13 groundwater on the leaching behavior.
3. Uranium leach data in deionized water at room temperature for a period up to two months. Results obtained on defected and undefected cladding are compared.

UNCERTAINTIES IN THE DATA

- (a) Cation Concentration: No indication is given of the uncertainty or reproducibility of the results.
- (b) Anion Concentration: Described qualitatively as a few ppm without mentioning the detectability limits of the techniques used.
- (c) pH: Uncertainty or reproducibility is not mentioned.
- (d) The variation in composition and characteristics of the rock specimens are not mentioned, although rocks from different locations are used.
- (e) No estimate of uncertainty or reproducibility of leach data for glass or Zircaloy-clad spent fuel is given.
- (f) The basis for drawing curves through experimental data points is not specified.

DEFICIENCIES IN THE DATA BASE

All the experimental results are presented in the form of diagrams without giving any numerical values. Since no error bars are assigned to the actual data points, it would be difficult to quantitatively use these results in any modeling work. All the information appears to be based on single tests; replicate testing is needed to establish the uncertainty limits. At present the spent fuel leach data is obtained only for ambient conditions whereas repository conditions are likely to be much more aggressive. Also, no radiation field was present in any of the tests.

APPLICATION OF DATA TO LICENSING

[Key Data (), Supporting Data (X)].

GENERAL COMMENTS

This paper describes the results which are obtained in the initial stages of the research program. Therefore, a large fraction of the paper is devoted to the future plans rather than to the results already obtained. Some assumptions are made in calculating the amount of groundwater that will reach the waste package, which are either design specific or based on limited supporting data. Therefore, a wide range of SA/V ratio and wasteform compositions should be included in the future testing.

The conclusions regarding improved leach resistance of borosilicate glass due to the addition of crushed tuff is based on the solution analysis for boron under very limited conditions. It needs to be substantiated by a more comprehensive study.

The nature of defects in Zircaloy cladding on the spent fuel rods is highly uncertain. Therefore, a wider range of anticipated defects should be incorporated in future testing.

In determining the groundwater chemistry much less information is presented for the anions which are likely to be a major factor in determining the container corrosion. No consideration is given to the solution concentration or radiation effects. Finally, a useful information is mentioned in that the use of Teflon containers in a test can absorb CO₂ and alter solution pH; the use of a gold bag autoclave eliminates this problem.

ORGANIZATION PRODUCING THE DATA

Lawrence Livermore National Laboratory.

AUTHORS/REFERENCE

Oversby, V. M., "Performance Testing of Waste Forms in a Tuff Environment," UCRL-90045, November 1983.

AVAILABILITY

Available as a preprint.

KEY WORDS

Groundwater chemistry, tuff, spent fuel, borosilicate glass, leaching.

DATE REVIEWED

September 1984.

gfs
11/16/84

ABSTRACT

Experiments conducted using Topopah Spring tuff and J-13 well water have been conducted to provide an estimate of the post-emplacment environment for waste packages in a repository at Yucca Mountain. The results show that emplacement of waste packages should cause only small changes in the water chemistry and rock mineralogy. The changes in environment should not have any detrimental effects on the performance of metal barriers or waste forms.

The NNWSI waste form testing program has provided preliminary results related to the release rate of radionuclides from the waste package. Those results indicate that release rates from both spent fuel and borosilicate glass should be below 1 part in 10^5 per year. Future testing will be directed toward making release rate testing more closely relevant to site specific conditions.

BLANK PAGE

WASTE PACKAGE DATA REVIEW FORM

TYPE OF DATA

Uniform corrosion rates from coupon immersion tests in steam and boiling groundwater; effect of radiation on uniform corrosion of carbon, alloy and stainless steels; qualitative observation of crevice and other localized attack; slow-strain-rate test results; electrochemical measurements for corrosion potential, protection potential and uniform corrosion rates. Reference compositions of welded tuff and tuffaceous groundwater.

MATERIAL

C1020, C1025, A36 and A366 carbon steels; 2.25Cr-1Mo alloy steel; 409, 416, 304L, 316L, 317L, 321, and 347 stainless steels; Incoloy 825. Only a few of these alloys were used in all the tests; 304L was tested in solution annealed as well as sensitized conditions. J-13 groundwater. Topopah Spring tuff.

TEST CONDITIONS

(a) Uniform Corrosion Without Radiation:

Environment: 100°C saturated steam at atmospheric pressure and 100°C J-13 water conditioned with crushed tuff rock.
Duration: 1000 h.

(b) Uniform Corrosion in the Presence of Radiation:

Environment: J-13 water (untreated and treated with tuff) at 105°C with 3×10^5 rads/h radiation dose, and at 150°C with 6×10^5 rads/h radiation dose.
Duration: Two months.

(c) Stress Corrosion:

Environment: air and tuff conditioned J-13 groundwater at 150°C.
Strain Rate: 10^{-4} and 2×10^{-7} /sec.

(d) Electrochemical Measurements:

Corrosion potential and potentiodynamic measurements were made on exposed sample area of 1 cm^2 in J-13 groundwater at 50 to 100°C. Scan rate was 1 mV/sec.

METHODS OF ANALYSIS

- (a) Uniform corrosion rates were determined from weight loss measurements on coupons using ASTM G-1 test procedure. The corrosion rates were also determined using linear polarization resistance and Tafel slope extrapolation methods.
- (b) Susceptibility to stress corrosion cracking was determined using slow-strain-rate tests with air as the control atmosphere. Fracture surfaces were examined to determine the nature of failure.
- (c) Susceptibility to pitting and crevice corrosion was determined from the surface examination of coupons and the measurements of corrosion and protection potentials. The measurement of hysteresis of the forward and backward scan in cyclic anodic polarization has been mentioned to evaluate the susceptibility to localized corrosion, but no data are given.

AMOUNT OF DATA

- (a) 1000-hour coupon tests for uniform corrosion and surface examination: Data are given for C1020, A36, A366, 2.25Cr-1Mo, 9Cr-1Mo, 409, 416, 304L, 316L, and 317L alloys in 100°C saturated steam and 100°C J-13 tuff conditioned groundwater.
- (b) Two-month coupon tests for uniform corrosion in the presence of radiation: Data are given for C1025, 9Cr-1Mo, solution annealed and sensitized 304L alloys in J-13 water with and without crushed tuff at 105 and 150°C.
- (c) Slow-strain-rate test results are given for solution annealed and sensitized 304L stainless steel in 150°C tuff-conditioned J-13 groundwater at a strain rate of 10^{-4} /sec. The sensitized specimens were also tested in air at a strain rate of 10^{-4} /sec, and in J-13 water at 2×10^{-7} /sec.
- (d) Corrosion penetration rate data from linear polarization resistance and Tafel methods are given for 304L, 316L, 317L, 321, 347 alloys in J-13 water at 100°C. The coupons were tested freshly exposed and also after an exposure of 500 hours.
- (e) Corrosion and protection potential values are given for 304L, 316L, 321, and 825 alloys in tuff-conditioned J-13 groundwater at 50, 70, 80, 90, and 100°C.
- (f) The following information is given on the anticipated test conditions:
 - 1. Range of bulk composition for reference welded tuff.
 - 2. Reference composition of J-13 groundwater.
 - 3. Dimensions and power load outputs for reference waste packages.
 - 4. Expected composition of J-13 groundwater after reacting with Topopah Spring tuff at 90°C and 150°C.

UNCERTAINTIES IN THE DATA

The coupon tests in the absence of radiation were conducted on triplicate specimens. In the presence of radiation one to seven specimens were tested for a given condition. In slow-strain-rate tests replicate specimens were used. Therefore, there is reasonably good information available on the reproducibility of data in these tests. However, most of the electrochemical data are based on single tests. In some of the cases where duplicate experiments were conducted, the scatter in data is sufficiently large that it is difficult to draw definite conclusions.

DEFICIENCIES IN THE DATA BASE

This report, according to the authors, describes the data which are obtained in the early stages of a long-term research program and, therefore, some of the deficiencies would be corrected from the tests of longer durations. However, in its present form the uniform, pitting or crevice corrosion information is based on tests of too short durations. For example, the incubation period for the initiation of pitting or crevice corrosion of some of the alloys may be too long to be observed under present test conditions. Once these forms of corrosion start, the rate of corrosion propagation is usually much higher. In the cases where localized attack has been qualitatively confirmed, a quantitative data base is needed for long-term predictions. The coupon tests for different durations would be necessary to establish the form of corrosion rate equation.

The slow-strain-rate tests (SSRT) are useful in establishing the relative susceptibility of different alloys to stress corrosion cracking. However, in the present form the data are very limited in terms of strain rate, temperature and test environment, whereas it is known that an alloy can be susceptible to SSRT in a limited range of these parameters.

All the tests were conducted in J-13 or tuff conditioned J-13 groundwater. However, due to initial evaporation of groundwater and subsequent dissolution of previously precipitated salts, the solute concentration in the water coming in contact with a waste package can be much higher. Therefore, tests in concentrated J-13 water should also be included in the test matrix.

The radiation has been included only in coupon immersion tests. It should be included in other kinds of tests also.

APPLICATION OF DATA TO LICENSING

[Key Data (), Supporting Data (X)].

GENERAL COMMENTS

A major part of this report is devoted to the description of anticipated repository environment, the waste forms, reference and alternative materials for canisters, overpacks, etc. Next, the reasons for the selection of reference (304L stainless steel) and alternate alloys for the canister are discussed with specific reference to sensitization and welding considerations. The experimental data are limited at this stage, but more extensive work is proposed for the future.

In some cases where tests have been repeated under a given set of conditions, the reproducibility of data appears to be rather poor. For example, in radiation corrosion test at 150°C the corrosion rate of C1025 carbon steel ranged from 20 to 126 $\mu\text{m}/\text{yr}$. In such cases the highest number, not the average, should be considered in predicting the conservative value of canister lifetime. It will also be useful to understand the reasons such as surface conditions, heat treatment, etc. which give such a large range of results.

ORGANIZATION PRODUCING DATA

Lawrence Livermore National Laboratory.

AUTHORS/REFERENCE

McCright, R. D., H. Weiss, M. C. Juhas and R. W. Logan, "Selection of Candidate Canister Materials for High-Level Nuclear Waste Containment in a Tuff Repository," UCRL-89988, November 1983.

AVAILABILITY

Available as a preprint.

KEY WORDS

Canister materials, tuff, uniform corrosion, pitting, crevice corrosion, J-13 groundwater, radiation, stress corrosion, sensitization, welding, reference conditions.

DATE REVIEWED

October 1984.

gfs
11/19/84

ABSTRACT

A repository located at Yucca Mountain at the Nevada Test Site is a potential site for permanent geological disposal of high level nuclear waste. The repository can be located in a horizon in welded tuff, a volcanic rock, which is above the static water level at this site. The environmental conditions in this unsaturated zone are expected to be air and water vapor dominated for much of the containment period. Type 304L stainless steel is the reference material for fabricating canisters to contain the solid high-level wastes. Alternative stainless alloys are considered because of possible susceptibility of 304L to localized and stress forms of corrosion. For the reprocessed glass wastes, the canisters serve as the recipient for pouring the glass with the result that a sensitized microstructure may develop because of the times at elevated temperatures. Corrosion testing of the reference and alternative materials has begun in tuff-conditioned water and steam environments.

BLANK PAGE

WASTE PACKAGE DATA REVIEW FORM

TYPE OF DATA

Screening criteria for a metal for HLW canisters and overpacks; reference corrosion conditions; estimates of corrosion rates, weldability, mechanical properties and costs of 17 candidate metals; underground environment in Topopah Spring tuff and Chino silt loam. Selection is made of four metals for canisters and one metal for borehole liners based on this information.

MATERIAL

AISI 1020 and A537 steels; 409 Ti stabilized, 26Cr-1Mo, 304L, 321, 316L, 317L, Nitronic 33, JS 700, and Ferralium 255 stainless steels; Incoloy 825 and 625; Ti Grades 2 and 12; Zr 702; CDA 715 (copper/nickel 70/30).

TEST CONDITIONS

Varying test conditions which are not specified in detail — data taken from various sources. Many test conditions are significantly different from those expected in a repository.

METHODS OF ANALYSIS

Each of the 17 alloys is graded for corrosion resistance, mechanical properties, weldability and cost on a three-point ("2" for superior, "1" for suitable and "0" for some advantages) system. The four selected metals scored seven points. Quantitative screening criteria are used for corrosion resistance, mechanical properties and the cost. Weldability of an alloy is evaluated qualitatively in terms of the following attributes: preheat, special interpass temperature, post-heat treatment, special atmosphere, low weld HAZ toughness, non-standard process, non-standard NDE, non-economical relative to AISI 304 stainless steel and special fit-up. The grading for weldability of an alloy is determined by comparing these properties relative to 304 stainless steel.

AMOUNT OF DATA

Reference waste package designs for DHLW, CHLW and spent fuel emplaced in a vertical borehole. Estimated relative maximum corrosion rates and probability for the 17 candidate metals for general, pitting, crevice, intergranular and transgranular stress corrosion and hydrogen embrittlement in the presence of a continuous air/water film. Near-field conditions in a Topopah Spring tuff repository. Estimate of raw material and manufacturing cost for 1/2-inch wall welded pipe. Tensile strength, yield strength (at 800°C), minimum static elongation, nil ductility temperature and fracture toughness of the

candidate alloys. Presence or absence of various problems (mentioned above under Test Conditions) during welding. Ranking of various candidate alloys on a scale of 1 to 3. One of the appendices gives a temperature-time-sensitization diagram and susceptibility of 304 stainless steel to localized corrosion as a function of temperature and chloride ion concentration.

UNCERTAINTIES IN THE DATA

The experimental uncertainties in the data are not presented. However, considering that the present data are used only for relative evaluation of various alloys, the final conclusions would not change if the uncertainties are nearly the same for all cases. On the other hand, there is much larger uncertainty due to the fact that the repository conditions may be very different than those for which the data are available. The corrosion data are presented with the explicit intent of comparing different alloys rather than estimating the corrosion life of a particular alloy. However, some of the conclusions may be seriously affected when data obtained under more repository representative conditions become available. The assessment of weldability of an alloy is described as "good" or "no good" which is too qualitative and does not indicate the extent of the problem. Actual cost of an alloy will vary depending on the current market prices.

DEFICIENCIES IN THE DATA BASE

The major deficiency in the data is the lack of confidence in its relevance to repository conditions. The data are presented without giving enough justification for the applicability to the performance of a HLW container. Localized corrosion (pitting, crevice or SCC) has been expressed in terms of corrosion rate and probability, but how can these be transformed in comparing the life of a container is not explained. The assumptions made in arriving at the estimated values given in various tables need to be clearly expressed.

There is virtually no information available on the effect of radiation on corrosion of different alloys. In some cases, the nitric acid generated by the radiolysis of moist air may be most detrimental to the corrosion life whereas in others hydrogen generated by radiolysis may be the cause of embrittlement. Therefore, the selection of alloys based on the presently available limited information may need a re-evaluation as more data become available.

APPLICATION OF DATA TO LICENSING

[Key Data (), Supporting Data (X)].

GENERAL COMMENTS

This paper describes the selection procedure for containment barrier metals based on available information from the literature which, as mentioned above, is not complete to represent various aspects of a HLW repository.

Nevertheless, the ranking procedure assumes the same weight for corrosion resistance, mechanical properties, weldability and cost. This basis of selection is questionable because these four factors may not be considered equally important. For example, if the mechanical properties of one alloy are significantly better than another alloy, the present procedure would rank the two differently even if both the alloys have better than minimum required strength. Also, corrosion is perhaps the most likely failure mode for a HLW container and, therefore, should have a higher weighting factor.

For horizontal borehole liners only one alloy (AISI 1020 carbon steel which has the lowest ranking) has been selected for further testing. It will be useful to have one or two more backup alloys if this alloy is found to be unfit for some reason.

ORGANIZATION PRODUCING DATA

Lawrence Livermore National Laboratory.

AUTHORS/REFERENCE

Russell, E. W., R. D. McCright and W. C. O'Neal, "Containment Barrier Metals for High Level Waste Packages in a Tuff Repository," UCRL-53449, October 1983.

AVAILABILITY

NTIS

KEY WORDS

HLW container alloys, corrosion, weldability, cost, tuff.

DATE REVIEWED

September 1984.

gfs
10/9/84

ABSTRACT

The Nevada Nuclear Waste Storage Investigations (NNWSI) Waste Package project is part of the U.S. Department of Energy's Civilian Radioactive Waste Management (CRWM) Program. The NNWSI project is working towards the development of multibarriered packages for the disposal of spent fuel and high-level waste in tuff in the unsaturated zone at Yucca Mountain at the Nevada Test Site (NTS). The final engineered barrier system design may be composed of a waste form, canister, overpack, borehole liner, packing, and the near field host rock, or some combination thereof. Lawrence Livermore National Laboratory's (LLNL) role is to design, model, and test the waste package subsystem for the tuff repository.

At the present stage of development of the nuclear waste management program at LLNL, the detailed requirements for the waste package design are not yet firmly established. In spite of these uncertainties as to the detailed package requirements, we have begun the conceptual design stage. By conceptual design, we mean design based on our best assessment of present and future regulatory requirements. We anticipate that changes will occur as the detailed requirements for waste package design are finalized.

WASTE PACKAGE DATA REVIEW FORM

TYPE OF DATA

Sorption ratio of americium, cesium, neptunium, plutonium, radium, strontium, technetium and barium on tuff as a function of composition. Solubility and speciation of various species are calculated from thermodynamic data.

MATERIAL

Tuff from Yucca Mountain area.

TEST CONDITIONS

Data from three kinds of tests are used. These are (1) batch sorption test, (2) crushed rock column test and (3) a circulating system batch sorption test. Experiments have been conducted to include the effects of contact time, temperature, atmosphere and particle size, but the details are not described in this paper.

METHODS OF ANALYSIS

Not described.

AMOUNT OF DATA

Quantitative sorption data are not described. However, a qualitative summary based on numerical data has been included. The effect of zeolite abundance in tuff on sorption properties for various species is discussed. Sorption and desorption data are compared to determine the reversibility of a process. Qualitative results from the calculations of solubility and speciation as a function of composition, pH, Eh, and temperature of the groundwater and the oxidation state of a given ion are described. The calculations are performed for strontium, uranium, plutonium, cesium and carbon in water that is characteristic of Yucca Mountain.

UNCERTAINTIES IN THE DATA

Uncertainty in the data for sorption or desorption is not mentioned. In the case of solubility calculations, several uncertainties due to the lack of thermodynamic or chemical information are discussed.

DEFICIENCIES IN THE DATA BASE

The present paper is a qualitative discussion based on data taken from

other sources and the details of original data have not been included. Therefore, it is difficult to judge the deficiencies present.

Zeolite is shown to be one of the most important constituents of the host rock. However, it is not clear if groundwater will always have to pass through the zeolitized zone or the radionuclides may not at all come in contact with such a highly sorbing component.

APPLICATION OF DATA TO LICENSING

[Key Data (), Supporting Data (X)].

GENERAL COMMENTS

Sorption/desorption or solubility of various ionic species discussed in this paper may strongly depend on their ionic states which are likely to be affected by the ionizing radiation. Therefore, testing in the presence of radiation is very important in assessing the sorption efficiency of tuff. The thermodynamic approach of calculating solubility and speciation may be a good starting point, but metastable equilibria, kinetically very slow reactions and the presence of colloid make the predictions undependable. Therefore, the results obtained from thermodynamic calculations need to be verified experimentally for the complete range of repository conditions.

ORGANIZATION PRODUCING DATA

Los Alamos National Laboratory.

AUTHORS/REFERENCE

Ogard, A. E. and others, "Retardation of Radionuclides by Rock Units Along the Path to the Accessible Environment," in The Scientific Basis for Nuclear Waste Management, VII, G. L. McVay, Editor, New York, Elsevier Publishing, 1984, p. 329.

AVAILABILITY

Published.

KEY WORDS

Sorption, desorption, tuff, groundwater, solubility, zeolite.

DATE REVIEWED

September 1984.

ABSTRACT

Until further information is obtained on flow paths, fracture versus porous flow, diffusion rates, speciation, and solubility, it can be stated that the most important retardation mechanism in the tuffs of Yucca Mountain is sorption. Based on information from the mineralogy-petrology presentation earlier in this session there is a 100-m-thick zeolitized zone in the unsaturated Calico Hills and Prow Pass units below the repository horizon in the Topopah Spring Member. These tuffs are ~60% zeolitized and exist under the entire 8×10^6 m² of the repository. If an average cation-exchange capacity of the zeolites of 2.5 meq/g is assumed, the unsaturated zeolitized tuff volumes are capable of sorbing by ion exchange $>5 \times 10^5$ metric tons of waste elements if the relatively unfractured rock of these zeolitized tuffs all comes into contact with the waste elements. A presentation by Travis of Los Alamos in a different session of this meeting will discuss calculations on travel times of waste elements to the accessible environment in the tuffs of Yucca Mountain.

gfs
10/12/84

BLANK PAGE

WASTE PACKAGE DATA REVIEW FORM

TYPE OF DATA

Uniform corrosion rates obtained with and without gamma radiation from weight loss measurements in coupon immersion tests. Qualitative information on crevices formed between the test alloys and Teflon. Total elongation and fracture failure mode examination in slow strain rate tests. Breakdown and protection potentials obtained from anodic potentiodynamic scans.

MATERIAL

304L, 316L and 317L stainless steels, J-13 groundwater, and crushed tuff. Most of the data are for 304L stainless steel solution annealed (1050°C, 15 minutes, water quenched) or sensitized (600°C, 10 hours, air cooled).

TEST CONDITIONS

- (a) Uniform corrosion: ASTM G-1 test procedure adopted.
 - 1. Test environment in the absence of radiation: 100°C saturated steam at atmospheric pressure or 100°C J-13 water conditioned with crushed tuff rock (average particle size 2 mm). Exposure time 1000 hours.
 - 2. Test environment with radiation: Air sparged J-13 flowing water at 105°C (10^5 rads/h) or 150°C (6×10^5 rads/h). Crushed tuff rocks were present at the bottom of the vessel. Exposure time two months.
- (b) Stress corrosion: Test environment air or air-sparged tuff-conditioned J-13 water. Samples pulled at a strain rate of 10^{-4} or 2×10^{-7} /sec.
- (c) Electrochemical polarization: Test environment J-13 water in the 50-100°C temperature range, potential sweep rate or other details are not mentioned.

METHODS OF ANALYSIS

- (a) Uniform Corrosion: Weight loss measurements on triplicate coupons for each test condition. Surface condition examined for localized or crevice attack.
- (b) Stress Corrosion: Total elongation at failure for replicate tests.
- (c) Electrochemical Data: Corrosion and protection potential data are given in a figure without further details.

AMOUNT OF DATA

- (a) Uniform Corrosion: For 304L, 316L and 317L stainless steel in 100°C steam and J-13 groundwater.
- (b) Uniform Corrosion in Radiation Environment: For 304L sensitized and solution annealed stainless steel specimens in J-13 water with and without tuff at 105° and 150°C.
- (c) Stress Corrosion: Total elongation and yield stress for solution annealed and sensitized 304L stainless steel specimens in J-13 water at a strain rate of 10^{-4} /sec. Only one sensitized specimen tested in air for comparison. One set of duplicate sensitized specimens also tested in J-13 water at a strain rate of 2×10^{-7} /sec.
- (d) Electrochemical Measurements: Corrosion and protection potentials for 304L stainless steel in J-13 water at 50, 70, 80, 90, and 100°C.

UNCERTAINTIES IN THE DATA

Some information on the uncertainty in uniform corrosion data is available as triplicate (or duplicate in the case of radiation) coupons have been used. A weight loss detection limit corresponding to 0.13 $\mu\text{m}/\text{yr}$ corrosion rate has been estimated. Because the test duration has been short, the amount of corrosion is small and the uncertainty in data very large.

From duplicate specimens, the reproducibility of total elongation in slow strain rate tests is within 5%, but the details of microstructure, degree of sensitization or other metallurgical information are not given.

In potentiodynamic study, except at 100°C, single measurements of potentials are made. The set of three measurements at 100°C shows that there is a considerable scatter in the data, but its reason is not clear.

DEFICIENCIES IN THE DATA BASE

This paper presents very preliminary data and, therefore, some of the deficiencies mentioned here will probably be corrected by the future data. The uniform corrosion data are given from a very short-term test. The corrosion rates are too small to be accurately and reproducibly measured from such short duration tests. At present the data are given only for a single test duration. To be able to extrapolate the data on a repository time scale, time dependence of the corrosion rates needs to be determined from the data taken at different intervals.

Slow strain rate tests have been conducted for very limited conditions of strain rate and temperature, whereas it is known that there may be only a narrow range of these parameters for which stress corrosion mechanisms may operate. Also, the slow strain technique may not show the development of a crack if its initiation time is very long. In fact, stainless steels under similar conditions are known to be susceptible to stress corrosion cracking.

The electrochemical measurements are generally useful as a guideline in material selection and actual corrosion testing is required under relevant conditions to determine the possible extent of corrosion by different mechanisms.

APPLICATION OF DATA TO LICENSING

[Key Data (), Supporting Data (X)].

GENERAL COMMENTS

At present, there is no information available on the groundwater which will be present in the unsaturated zone. All the tests have been conducted in J-13 water or J-13 water treated with crushed tuff. However, evaporation of groundwater and subsequent dissolution of the deposited salts could increase the solute concentration in groundwater coming in contact with the waste package considerably. Therefore, parallel tests need to be conducted in a concentrated solution of J-13 groundwater.

The radiation field which has been used only in uniform corrosion tests shows enhanced corrosion rates. Its effect through radiolysis products on other kinds of corrosion also needs to be determined.

ORGANIZATION PRODUCING DATA

Lawrence Livermore Laboratory.

AUTHORS/REFERENCE

McCright, R. D., R. A. Van Konynenburg and L. B. Ballou, "Corrosion Test Plan to Guide Canister Material Selection and Design for a Tuff Repository," in The Scientific Basis for Nuclear Waste Management, VII, Vol. 26, G. L. McVay, Editor, New York, Elsevier Publishing, 1984, p. 309.

AVAILABILITY

Published proceedings.

KEY WORDS

Stainless steel, uniform corrosion, stress corrosion, tuffaceous groundwater, corrosion and protection potentials, gamma radiation.

DATE REVIEWED

September 1984.

ABSTRACT

Corrosion rates and the mode of corrosion attack form a most important basis for selection of canister materials and design of a nuclear waste package. Type 304L stainless steel was selected as the reference material for canister fabrication because of its generally excellent corrosion resistance in water, steam and air. However, 304L may be susceptible to localized and stress-assisted forms of corrosion under certain conditions. Alternative alloys are also investigated; these alloys were chosen because of their improved resistance to these forms of corrosion. The fabrication and welding processes, as well as the glass pouring operation for defense and commercial high-level wastes, may influence the susceptibility of the canister to localized and stress forms of corrosion.

gfs
10/9/84

WASTE PACKAGE DATA REVIEW FORM

TYPE OF DATA

Leaching of radionuclides from spent PWR fuel elements with artificially induced cladding defects. Results on unclad fuel specimens also included for comparison.

MATERIAL

PWR 15 x 15 spent fuel, deionized water.

TEST CONDITIONS

- (a) Specimens: 1. Rod segments with undefected cladding. 2. Rod segments with two laser drilled holes $\approx 200 \mu\text{m}$ in diameter. This is equivalent to the defect size $\approx 10^6 \mu\text{m}^2/\text{kg}$ of the fuel. 3. Rod segments with a machined slit $\approx 2\text{-cm}$ long and $150\text{-}\mu\text{m}$ wide. This is equivalent to the defect size $10^8 \mu\text{m}^2/\text{kg}$ of the fuel. 4. Bare fuel.
- (b) Leaching Environment: Deionized water under air at 22 to 28°C. Static leaching conditions.
- (c) Test Duration: Up to 180 days.

METHODS OF ANALYSIS

The radionuclides were leached from fuel elements into the solution. A few quartz rods were included in the tests to determine the concentration of radionuclides plated on their surfaces. The concentration of the leached elements was determined using radiochemical analysis by alpha and gamma spectrographic methods. Uranium concentration was determined by the laser excited fluorescence method.

AMOUNT OF DATA

- (a) Concentration of U, $^{239+240}\text{Pu}$, and ^{137}Cs in solution taken after 1, 5, 15, 30, 60, 90, 120, 150, and 180 days of leaching.
- (b) Concentration of U, $^{239+240}\text{Pu}$, and ^{137}Cs plated on glass rods kept in leaching solution for 5, 30, 60, 120, and 180 days.
- (c) Concentration of ^{244}Cm , $^{239+240}\text{Pu}$, ^{154}Eu , ^{137}Cs , ^{125}Sb , ^{60}Co and U in a bare fuel leach solution after 202 days. The solution was analyzed in unfiltered and filtered (through $0.4\text{-}\mu\text{m}$ and 18A filters) conditions to determine the extent of colloid formation by these species.

UNCERTAINTIES IN THE DATA

There are no estimates given for the uncertainties or reproducibility of the dimensions of hole and slit made in the cladding, and the leaching data for various radionuclides. Some estimate of the uncertainty in leaching data can be obtained from the scatter in concentration vs leach time diagrams.

DEFICIENCIES IN THE DATA BASE

This paper reports very preliminary data which is useful in scoping the problem of leaching from spent fuel HLW. The corrosion conditions in a repository are expected to be much different than deionized water at room temperature, which is used in the present tests. In other words, future leach testing is needed under appropriate conditions of temperature and pressure in a solution representative of each HLW repository. It may be necessary to form a test matrix which includes the range of various test parameters.

The data show lower leaching rates from cladded specimens with two kinds of defects than from bare specimens. The two defects differed in area/kg of fuel by two orders of magnitude, yet the leach rates were not always very different. Therefore, the significance of the parameter area/kg is not very clear with respect to leaching phenomenon. In this regard, we note that the anticipated range of size and distribution of defects in spent fuel elements is not established, although it is an important information for modeling of leaching from an assembly of fuel elements.

APPLICATION OF DATA TO LICENSING

[Key Data (), Supporting Data (X)].

GENERAL COMMENTS

- (a) The data consisting of nine observations for each radionuclide during a period of six months indicate the trend of leaching behavior, but are not sufficient to give an accurate extrapolation equation valid for repository time scale.
- (b) Future tests should include the composition and temperature of test solution which is representative of repository conditions.
- (c) The mechanisms proposed to explain the leaching behavior of different radionuclides and uranium are based on very limited information and, therefore, need further supporting evidence from experiments other than chemical analysis of the solution.
- (d) If leaching rates are shown to be limited by a solubility limit, the rate of flow of groundwater/brine in a repository will become an important parameter in determining the release rate of radionuclides.

- (e) In one test, some of the radionuclides are shown to be present as colloids which could increase the concentration of radionuclides in solution above the thermodynamic solubility limit. Further experiments are needed to evaluate the role of colloid formation in determining the release rates.

ORGANIZATION PRODUCING DATA

Lawrence Livermore National Laboratory and Westinghouse Hanford Company.

AUTHORS/REFERENCE

Wilson, C. N. and V. M. Oversby, "Spent Fuel Containment Credit Tests," UCRL-89869, February 1984.

AVAILABILITY

Available as a preprint of the paper presented at the Waste Management '84 Conference, Tucson, Arizona.

KEY WORDS

PWR spent fuel, leaching, deionized water, cladding defects.

DATE REVIEWED

October 1984.

gfs
11/19/84

ABSTRACT

Preliminary tests are being conducted to evaluate the effectiveness of defected cladding as a barrier to radionuclide release from spent fuel rods stored in a geological repository. The tests are being conducted at the Hanford Engineering Development Laboratory for the Lawrence Livermore National Laboratory Waste Package Task of the Nevada Nuclear Waste Storage Investigations (NNWSI) tuff repository project. In these tests, spent PWR fuel rod specimens with various artificially induced cladding defects are leach tested in a test matrix which also includes both bare fuel specimens (unclad) and undefected spent fuel rod specimens. Artificial cladding defects are made by laser drilling and sawing to give defect areas in the 10^4 to 10^6 μm^2 range. Periodic samples are taken of the leach solution and fused quartz rods contained in the test vessels. Results for the first 180 days of testing are presented.

WASTE PACKAGE DATA REVIEW FORM

TYPE OF DATA

Thermodynamic data for aqueous species and solid species of americium, equilibrium constants, data for reactions of americium with other aqueous species.

MATERIAL

Available literature information on americium (thermodynamic information as well as measured solubilities).

TEST CONDITIONS

Not applicable.

METHODS OF ANALYSIS

Not applicable.

AMOUNT OF DATA

This report contains a compilation in graphical form of some of the available literature data on the speciation and solubility of americium. These data include a plot of $\log K$ vs ligand number for $\text{Am}(\text{OH})_n^{(3-n)}$ (9 points), a plot of \log (molarity) of Am vs pH (9 discrete points, 3 predicted curves), percent aqueous species of Am present in CO_3^{2-} solutions, pH 6 to 12, two independent studies. Predicted solubility (\log molarity) of Am as a function of pH at 25°C in J-13 well water, predicted speciation (% in solution) of Am as a function of pH in J-13 well water. The appendices in the report contain the following data: Thermodynamic data, where available, for 29 forms of Am in solution (reference to source of data is also given), thermodynamic data, where available, for 4 solid forms of Am (references to data source given), listing of chemical reactions (25 reactions) of Am in solution, \log_{10} of equilibrium constants for those reactions with a judgement of the quality of the input data. Equilibrium constants are calculated for 0, 25, 60, 100, 150, 200, 250, and 300°C.

UNCERTAINTIES IN THE DATA

Uncertainty exists in the available thermodynamic data base, the measured solubilities and speciation data, selection of average data in the calculation as opposed to range of values for measured data, and potential calculational errors. In addition, the assumption that the solubility of Am and the speciation in repository waters can be predicted from single specie data introduces further uncertainty. Data available are also only at 25°C.

DEFICIENCIES IN THE DATA BASE

There are two separate areas where deficiencies exist. The first is in the available data base. In all instances, available data are for 25°C, simple systems. The second lies in the arbitrary selection of a data set in those instances where conflicting information is available. In addition, averages are often employed and no attempt has been made to calculate changes in the equilibrium constants or in the anticipated solubilities or specie concentration with ranges of input data.

APPLICATION OF DATA TO LICENSING

[Key Data (), Supporting Data (X)].

GENERAL COMMENTS

The predicted equilibrium constants, speciation curves and solubilities may contain large uncertainties. However, this is an attempt to formulate as complete as is possible a data base on americium and to identify those areas which are speculative and uncertain.

ORGANIZATION PRODUCING DATA

DOE/Los Alamos National Laboratory.

AUTHORS/REFERENCE

Kerrisk, J. F., "Americium Thermodynamic Data for EQ3/6 Database," LA-10040-MS, July 1984.

AVAILABILITY

Published.

KEY WORDS

Americium, thermodynamic data, EQ3/6 Database, tuff groundwaters.

DATE REVIEWED

October 1984.

gfs
10/9/84

ABSTRACT

Existing thermodynamic data for aqueous and solid species of americium have been reviewed and collected in a form that can be used with the EQ3/6 database. Data that are important in solubility calculations for americium at a proposed Yucca Mountain nuclear waste repository were emphasized. Conflicting data exist for americium complexes with carbonates. Essentially no data are available for americium solids or complexes at temperatures greater than 25°C.

BLANK PAGE

WASTE PACKAGE DATA REVIEW FORM

TYPE OF DATA

MCC-1 (static) leach tests on actual SRP-type borosilicate glass in DIW, MCC brine and silicate water, at 40°C. Data gave normalized mass losses for ^{137}Cs , ^{90}Sr , and ^{238}Pu together with pH changes of solution with time.

MATERIAL

Glass made from 30 weight percent SRP waste for Tank 11 and 70 weight percent SRP Frit 131.

TEST CONDITIONS

Test conditions follow those specified for MCC-1 tests. Test temperature was 40°C, the leaching times in DIW extended to 300 d and for MCC brine and MCC silicate water they were up to 200 d.

The leaching containers were polypropylene rather than Teflon since the latter has poor radiation stability. Platinum baskets were used to support the specimens in the brine tests instead of stainless steel since this may stress-corrosion crack. Prior to testing, the test vessels were soaked for 16 h at room temperature, followed by rinsing in DIW, followed by two soakings at 90°C for 16 h in DIW. Samples were obtained by fracturing larger samples and estimating the surface areas. Errors in estimating the surface area were cited to be <20 percent.

METHODS OF ANALYSIS

The normalized mass loss of the glass (g of glass lost/unit area) was calculated from

$$(\text{NL})_{i,t} = \frac{V_1 \cdot C_{i,e}}{\text{SA} \cdot C_{i,g}}$$

where $(\text{NL})_{i,t}$ is the grams of glass leached per unit surface area (SA) in total time t for specie i . V_1 is the volume of leachant, $C_{i,g}$ is the concentration of species i in the glass (mCi/g glass) and $C_{i,e}$ is the concentration of i in the leachant (mCi/ml).

After test, the glass is removed from the test vessel and the leachant is acidified and allowed to stand for one day before determination of ^{137}Cs , ^{90}Sr , and ^{238}Pu activities using standard counting techniques. The vessel was then rinsed with 4 M HNO_3 to determine amount of radioactivity sorbed. About 10-25 percent of the ^{238}Pu activity was found to be on the wall, but there was little ^{137}Cs or ^{90}Sr detected.

AMOUNT OF DATA

(a) DIW Leaching Tests

Eleven data points each for ^{238}Pu , ^{137}Cs , and ^{90}Sr . Data points for test times to 28 d were from MCC-1 test methodology and, thereafter, periodic renewal of leachant was undertaken.

(b) MCC Silicate Water Leaching Tests

Eleven data points for each radionuclide as for DIW, above.

(c) MCC Brine Leaching Tests

Eleven data points for each radionuclide as for DIW, above.

(d) pH Changes in Long-Term Tests

pH measured as a function of time as the leachant was irradiated by α and β particles from the glass. Dose to the leachant was $\approx 10^6$ rad.

DIW and silicate waste show pH increases, whereas brine shows a decrease.

UNCERTAINTIES IN THE DATA

(a) Based on duplicate tests the general level of reproducibility is about ± 20 percent.

(b) The data may not be strictly appropriate for modeling a waste package system since container, packing and host rock components were not included. Each of these components may significantly alter the chemistry Eh/pH conditions and thereby change the rate of leaching.

(c) ^{137}Cs and ^{90}Sr will not be leached in significant quantities if the package contains radionuclides for 300 to 1000 years.

DEFICIENCIES IN THE DATA BASE

(a) Leach rates for other radionuclides are not given.

(b) The test temperature (40°C) does not cover the range that would be expected for DHLW. Temperatures up to about 100°C would be more appropriate since they would cover premature container failure, for which higher-temperature leaching would occur.

APPLICATION OF DATA TO LICENSING

[Key Data (), Supporting Data (X)].

GENERAL COMMENTS

Quality and objectives of the study are good. Follow-up studies should be planned to expand the data base and increase the value of the work for the performance assessment program.

ORGANIZATION PRODUCING DATA

DOE/SRL

AUTHORS/REFERENCE

Bibler, N. E., "Characterization of Borosilicate Glass - Containing Savannah River Plant Radioactive Waste," in Geochemical Behavior of Disposed Radioactive Waste, G. S. Barney, Editor, ACS Symposium 246, 1984, pp. 359-372.

AVAILABILITY

Published.

KEY WORDS

Borosilicate glass, leaching, DIW, brine, silicate water, solubility.

DATE REVIEWED

September 1984.

gfs
9/26/84

ABSTRACT

Results are presented from static leach tests on borosilicate glass containing high-level radioactive nuclear waste from the Savannah River Plant. Tests were performed in shielded facilities closely following MCC-1 procedures. Leachants were deionized water, MCC brine, or silicate water, all at 40°C. Normalized mass losses (g/m^2) based on ^{137}Cs , ^{90}Sr , and ^{238}Pu were calculated. Results of leach times of 3, 7, 14, 28, and 300 days are reported for deionized water. Results for 28 and 200 days are reported for silicate water and brine. Normalized mass losses and pH changes indicate that glass containing radioactive waste leaches similarly to glass containing nonradioactive, simulated waste. Release rates in the two simulated groundwaters were slightly less than in deionized water. Also, radiolysis of the leachant by alpha, beta, and gamma rays from the glass did not significantly affect the normalized mass losses or the pH changes due to leaching. Results of the long-term tests suggest that equilibrium concentrations of radionuclides will be achieved. Based on tests with different ratios of glass surface area to leachant volume, these concentrations are controlled more by solubility and surface layer effects than by the surface area of the glass.

WASTE PACKAGE DATA REVIEW FORM

TYPE OF DATA

Leaching of spent fuel elements in water at 25°C and 70°C under reducing and oxidizing conditions yielded values for the concentrations of U, ²⁴¹Am, ¹⁴⁴Ce, ¹³⁷Cs, ²³⁹Pu, ¹²⁵Sb, ⁹⁰Sr, and ¹⁵⁴Eu in the leachate at various times. These values are tabulated and given in plots to show the difference between the oxidizing and the reducing environments.

MATERIAL

Slices of spent fuel elements in water.

TEST CONDITIONS

Leaching (dissolution) was carried out in water at 25°C and ambient pressure under oxidizing and reducing atmospheres for 65 days in the absence of radiation. The temperature was then raised to 70°C and the dissolution was continued for an additional 125 days. Periodically, new leachant was added. At various times, leachant was removed through a glass fritted disk and analyzed for radioactive elements. The atmospheres were achieved by bubbling air (CO₂-free) or 94% Ar-6% H₂ through the leachants. Platinum gauze was also present in the reducing atmosphere experiments.

METHODS OF ANALYSIS

Not stated.

AMOUNT OF DATA

<u>Element</u>	<u>Concentration Units</u>
U	g/5 ml
²⁴¹ Am	d/m
¹⁴⁴ Ce	d/m
¹³⁷ Cs	d/m
²³⁹ Pu	g/5 ml
¹²⁵ Sb	d/m
⁹⁰ Sr	cpm
¹⁵⁴ Eu	d/m

Less than 15 measurements in each of the following categories: oxidizing 25°C, reducing 25°C, oxidizing 70°C, reducing 70°C.

UNCERTAINTIES IN THE DATA

Statistical information and limits of detection were not provided.

DEFICIENCIES IN THE DATA BASE

- The conditions under which the leaching was performed are not representative of repository environments after emplacement of the waste package.
- The reducing environment was not defined in terms of DO content.
- The longest leach time is ≈40 days. Much longer leach times are needed.
- Amounts of radionuclides precipitated are not specified.

APPLICATION OF DATA TO LICENSING

[Key Data (), Supporting Data (X)].

GENERAL COMMENTS

Ogard estimates that at pH 4 the solubility of uranium in deionized water may vary 10 orders of magnitude depending on whether conditions are oxidizing or reducing. It had been estimated from available thermodynamic data that the concentration of uranium in equilibrium with UO_2 in pH 7 water that is free of dissolved oxygen is $\approx 10^{-11}$ M. Ogard's estimates of solubility are based on the results of spent fuel element leaching experiments in oxidizing and reducing media at 25°C and 70°C, in which it was difficult to readily duplicate the reducing conditions anticipated in deep geologic burial. It must be emphasized that these arguments are based on studies conducted in pure water, at low temperatures. The data at 70°C indicate concentrations lower for most of the elements studied when compared to the concentrations at 25°C, thus suggesting that some of these elements may possess retrograde solubility under the stated conditions.

ORGANIZATION PRODUCING DATA

Los Alamos Scientific Laboratory.

AUTHORS/REFERENCE

Ogard, A. and others, "Are Solubility Limits of Importance in Leaching?" in Scientific Basis for Nuclear Waste Management III, J. G. Moore, Editor, New York, Plenum Press, 1981, pp. 331-337.

AVAILABILITY

Published proceedings.

KEY WORDS

Solubility, uranium, water, leaching spent fuel.

DATE REVIEWED

October 1984.

gfs
10/30/84

ABSTRACT

The solubilities of some radionuclides, especially rare earths and actinides, may be an important and controlling factor in leaching of waste forms. These solubilities should be measured accurately as a function of pH and not as a part of a multicomponent system.

Although the amount of data is small it is interesting to postulate that a negative temperature coefficient of solubility is being exhibited by the actinides and rare earths in Figs. 1 and 2. Individual solubilities should be measured as a function of temperature to determine if a kinetic effect is being observed in the data. A negative temperature coefficient of solubility for actinides and rare earths in water would have important consequences for nuclear reactor safety and for the management of nuclear wastes.

WASTE PACKAGE DATA REVIEW FORM

TYPE OF DATA

Synthetic and actual groundwater compositions. pH of both vs temperature.

MATERIAL

Synthetic basalt groundwater composition, basalt groundwater from Borehole DC-6 (below the Umtanum flow).

TEST CONDITIONS

Eh of natural water measured with Pt electrode, reported vs. H₂ electrode. pH vs temperature (25°C, 45°C, 65°C) for natural and synthetic water.

METHOD OF DATA COLLECTION/ANALYSIS

Two stock solutions with estimated shelf life of one year mixed, pH adjusted, and diluted. Resulting solution stable for ~2 weeks and must be protected from exposure to air. Atomic absorption, atomic emission, wet bench chemical methods are used for analysis. Procedures for stock solutions and dilutions are given in an appendix.

AMOUNT/Form OF DATA

Chemical composition at 25°C for major cations and anions in actual and synthetic basalt water. Ions include Na⁺, K⁺, Ca⁺², Mg⁺², F⁻, Cl⁻, SO₄²⁻. Alkalinity reported as mol/L inorganic carbon and mg/L silica. Weight (grams) of chemicals required to make the two stock solutions.

UNCERTAINTIES IN DATA

The major uncertainty lies in the representativeness of the natural groundwater and therefore in the synthetic analogue. Author notes that natural groundwater is unstable and "considerable vertical and horizontal variation in the chemistry of groundwater samples collected from test horizons" has been determined. No range in this variation was given. A single composition was selected, not an average or a range. No attempt to simulate trace organics or trace metal ions or dissolved gases. No redox measurement reported for synthetic groundwater. The second source of error lies in the stability of the solutions and the usefulness for testing barrier materials. It is noted that the synthetic water has a shelf life of ~2 weeks but no indication is given to indicate how the composition changes. No data are given on effects of temperature or radiation on either the natural or synthetic water other than pH change over a limited temperature region.

DEFICIENCIES IN THE DATA BASE

These experiments, while simulating major constituents of a single groundwater, are incomplete. Since a large variability is known to exist in the groundwater, the range in chemical composition should be given and perhaps several reference waters studied. As a minimum, changes in groundwater composition with time, temperature and radiation need to be established and ranges and uncertainties in composition determined.

APPLICABILITY OF DATA TO LICENSING [KEY DATA (), SUPPORTING DATA (X)]

Relationship to WP Performance Issues Already Identified:

The data generally addresses an issue in the SCA report (NUREG-0960, Vol. 1, 1983). See Issue Number 1.1.6, Table C-2.

General Comments:

Data are given for Umtanum basalt only, and a standard procedure for simulating the water is given. The data for the natural water may serve to establish the range in the groundwater composition, both vertically and horizontally, in a given area. However, no indication is given of the variability of these data (e.g. sample to sample variation) and the number of components listed is limited to major constituents only.

The outlining of a standard procedure will be useful to insure the uniformity of test conditions. However, some criteria for determining when the solutions should no longer be used should be incorporated in the future and a "range" in repository waters specified.

ORGANIZATION PRODUCING DATA

DOE/BWIP.

AUTHORS/REFERENCE

Jones, T. E., "Reference Material Chemistry ---
Synthetic Groundwater Formulation," RHO-BW-ST-37P, April 1982.

AVAILABILITY

Published.

KEY WORDS

Basalt groundwater composition, Umtanum flow, Borehole DC-6, reference synthetic groundwater composition.

DATE REVIEWED

April, 1984.

Abstract (Summary) From Reference:

A recipe has been developed for the preparation of a synthetic Grande Ronde Basalt groundwater. The recipe is based on water samples collected from the test horizon just below the Umtanum flow (3,242 to 3,529 ft). The recipe presented establishes two stable concentrated stock solutions. Forty liters of synthetic groundwater can be prepared from 1 L of each stock solution. Limitations of the synthetic groundwater recipe are discussed. It was perceived that water from this test horizon would be the most likely to migrate into either of the two candidate repository horizons within the Grande Ronde Basalt (i.e., the Umtanum and middle Sentinel Bluffs flows).

BLANK PAGE

WASTE PACKAGE DATA REVIEW FORM

TYPE OF DATA

Uniform corrosion rates, fast crack propagation rates, slow strain rate tests data, solution analysis of solutions used.

MATERIAL

ASTM A536 Grade 60-40-18 ductile cast iron
ASTM A217 Grades WC6 and WC9 cast steel coupons and tensile specimens
Ti Grades 2 and 12.

TEST CONDITIONS

- (a) Tensile specimens from sheet metal for slow strain rate tests at 250°C, simulated basalt groundwater and crushed basalt, 6 ppm O₂ content.
- (b) Fatigue Crack Growth Tests: Ti Grade-2 and Grade-12, Hanford basalt water, F⁻-enhanced basalt water (220 ppm), high purity water, 90°C, solution exposed to air, pre-cracked specimens (crack perpendicular to primary rolling direction or crack parallel), frequencies of 1.0 to 0.1 Hz, sinusoidal wave form.
- (c) Corrosion of Ductile and Cast Steels: 150°C and 250°C, U-bend, coupon samples and galvanic couples with Ti, simulated groundwater + crushed basalt at a flow rate of 35 ml/h through basalt, initial O₂ at 6 ppm, outlet O₂ ≈ 1 ppm, 3-month tests, 1-month tests, O₂ concentrations: 50 ppb, 1 ppm, 6 ppm.
- (d) Water Chemistry Tests: Basalt water, crushed basalt, flow rate over crushed basalt of 35 ml/h, values given for SRR test water compositions (inlet and outlet), corrosion screening tests (250°C) and radiation tests (40°C).

METHODS OF ANALYSIS

No details given.

AMOUNT OF DATA

- (a) Slow Strain Rate Tests: Three graphical presentations for reduction of area and elongation (%) vs displacement rate (in./sec) for three samples (Ti Grade-12 LT at 250°C, Ti-Grade-12 TL at 250°C and Ti Grade-2 LT at 250°C), % reduction of area given for samples in groundwater and in air, % elongation given in groundwater and in air.

- (b) FCGR Tests: Only qualitative information on Ti Grades 2 and 12.
- (c) Corrosion of Fe-base Alloys: Tables of corrosion penetration estimates (depth of penetration in 1000 years), test durations of 3 months and 1 month.
- (d) Water Chemistry Tests: Concentration in ppm of 13 cations, 3 anions, as well as pH for inlet and outlet samples. Data are for SSR test solutions (250°C) with titanium samples, general corrosion samples at 250°C and radiation studies at 40°C (10^6 rad/h).

UNCERTAINTIES IN THE DATA

- (a) Slow Strain Rate Tests:
 - 1. Ti Grade-12, LT, data in air and in groundwater, % reduction in area. Only one to three points are given depending on displacement rate, when given largest scatter appears to be $\pm 10\%$, % elongation in water and air, largest scatter appears to be $\pm 10\%$.
 - 2. Ti Grade-12 and Grade-2, TL and LT samples, respectively. Only single points given.
- (b) FCGR: No numerical data or uncertainties given.
- (c) Corrosion Screening of Fe-base Alloys: No corrosion data (weight loss or range in weight loss for given metal under a single set of conditions) are given. Based on penetration rates in 1000 years, penetration is approximately a factor of 3 less at 150°C than at 250°C after a 1-month test.
- (d) Water Chemistry Tests: No range or uncertainties given. Major changes in SSR data appear to be in concentrations of Ca, Mg, Si. Major changes in corrosion screening tests appear to be associated with Al, B, Ca, K, Si and Cl ion concentrations. No major changes in ion concentrations appear to occur in the radiation screening tests.

DEFICIENCIES IN THE DATA BASE

All corrosion data presented are for a single temperature, no radiation present, and there is no indication of number of samples tested or range in measured parameter. Corrosion screening tests represent only 1-month or 3-month data. Tests appear to be flow-through tests. There is no justification for flow rates given and no indication of when outlet water samples were taken and analyzed. There are no interactive (e.g. backfill/metal corrosion screening) or weldment tests reported.

APPLICATION OF DATA TO LICENSING

[Key Data (), Supporting Data (X)].

GENERAL COMMENTS

The tests are adequate for preliminary screening purposes to identify corrosion failure modes. However, very long-term exposures of several years and a range of conditions may be needed to fully determine the likelihood of a particular failure mechanism occurring and to quantify the rates and uncertainties in the major failure modes.

ORGANIZATION PRODUCING DATA

DOE/Battelle Pacific Northwest Laboratory.

AUTHORS/REFERENCE

Westerman, R. E. and others, "Development of Engineered Structural Barriers for Nuclear Waste Packages," in Scientific Basis for Nuclear Waste Management, Vol. 6, S. V. Topp, Editor, New York, Elsevier, 1982, pp. 363-370.

AVAILABILITY

Published.

KEY WORDS

Uniform corrosion, crack growth tests, stress-corrosion cracking, basaltic water, gamma radiation, cast iron, cast steel, titanium Grade-2, titanium Grade-12.

DATE REVIEWED

September 1984.

gfs
9/27/84

ABSTRACT

The development of structural barriers for nuclear waste packages involves selection of candidate materials, their screening by mechanical and corrosion testing, rigorous accelerated testing, and evaluation and comparison with other package elements. This document presents results from work conducted on titanium and cast steels.

WASTE PACKAGE DATA REVIEW FORM

TYPE OF DATA

Steady state concentration of radionuclides (mg/l) for waste form + water ± basalt tests, short-term corrosion data for Fe alloys + packing material + basalt water; corrosion rates for Fe alloys + anoxic basalt water; corrosion data for Fe-base alloys + oxidic basalt water + irradiation; pit depths when applicable, hydraulic conductivity of packing material, thermal conductivity of backfill, solubilities for Ra and Am in packing materials.

MATERIAL

- (a) Waste form + basalt water ± basalt: Simulated SF and HLW (borosilicate glass with tracer levels of isotopes), simulated basalt water, basalt.
- (b) Basalt-groundwater: Details not given.
- (c) Canister materials corrosion: Low carbon steel, 90-10 cupronickel, Fe9-Cr1-Mo alloy, cast ductile iron, Fe2-1/2-Cr1-Mo steel, 75% crushed basalt/25% bentonite, basalt waters.
- (d) Packing material testing: Bentonite, basalt, combination 75/25 weight percent basalt/bentonite, basalt/groundwater, bentonite/groundwater, U, Pu, Np, Am, Ra.

TEST CONDITIONS

- (a) Waste Form + Water ± Basalt: Gold bag sampling autoclave at T = 90°C to 300°C, 30 MPa, periodic sampling of solution.
- (b) Basalt/Water Interactions: Hydrothermal, no values given.
- (c) Canister Material Corrosion:
 - 1. AISI 1020, 1006, 1025 and Fe9-Cr1-Mo Backfill Tests: Temperatures of 250, 200, 150 and 100°C, static conditions, synthetic Grande Ronde basalt water, pH 9.75, anoxic conditions.
 - 2. Fe9-Cr1-Mo, AISI 1020 (Wrought and Cast), Cupronickel Basalt Water Tests: pH 9.75, 50 ppm O₂, 200°C, 5 months, flow rate 0.02 ml/min, titanium lined autoclave.
 - 3. Fe-based Alloys + Basalt Water, Oxidic Conditions Tests: Temperatures of 250°C and 150°C, exposure time 1 to 17 months (5 months for wrought and cast steel), with and without radiation at 3x10⁵ rad/h for up to 13 months.

(d) Packing Material Stability and Physical Tests:

1. Chemical Stability: Dry Na bentonite at 370°C, ≈1 yr, bentonite/groundwater and bentonite/basalt/groundwater at 300°C.
2. Hydraulic Conductivity: 75/25 weight percent basalt/bentonite, up to T = 90°C.
3. Thermal Conductivity: Dry mixtures of basalt/bentonite variables were percent bentonite by weight, particle size of crushed basalt, temperature and density.
4. Sorption of Radionuclides: Ra, Am, Pu, U, Np on packing material solids (not specified), under reducing conditions (not specified), Tc, Se on packing materials (not specified), under anoxic conditions (not specified).
5. Solubilities: Am and Ra, packing material (not specified), 60°C.

METHODS OF ANALYSIS

- (a) Waste Form + Water ± Basalt: Analysis methods not given.
- (b) Basalt/Water Interactions: Not specified.
- (c) Canister Material Corrosion: Uniform rates measured by weight loss.
- (d) Packing Materials Testing: Not given.

AMOUNT OF DATA

- (a) Waste Form + Water ± Basalt: Table of steady state concentrations of 7 nuclides, temperature at 200°C only. Data are for SF + water, SF + water + basalt, CHLW + water, CHLW + water + basalt.
- (b) Basalt/Water Interactions: pH values initial (9.8) and at 200°C and 300°C after steady state is reached (7.5 and 7.6, respectively).
- (c) Canister Material Corrosion:
 1. Short term tests for Fe alloys/basalt groundwater/packing/anoxic.
 - AISI 1020: 2-week test: 7 points at 250°C, 2 points at 200°C, 4 points at 150°C.
 - 4-week test: 21 points at 250°C, 3 points at 100°C
 - 6-week test: 3 points at 250°C.
 - AISI 1006: 2-week test: 3 points at 250°C, 3 points at 150°C.
 - AISI 1025: 2-week test: 3 points at 250°C, 3 points at 150°C.
 - Fe9-Cr1-Mo: 4-week test: 3 points at 250°C, 3 points at 100°C.

2. Five-month test of Fe base alloys/basalt water/200°C/anoxic.
Numbers of samples for each material not specified, rate given with mean and standard deviation. No pitting observed.
3. Fe-base alloy corrosion/groundwater/oxic conditions.
- 1020 (Wrought): 2-month test: 3 points and deepest pit depth at 150°C.
3-month test: 2 points at 250°C, 3 points and deepest pit depth at 150°C.
5-month test: 4 points at 250°C, 3 points and deepest pit depth at 150°C.
- 1025 (Cast Steel): 3-month test: 2 points at 250°C, 2 points at 150°C.
5-month test: 2 points at 250°C, 2 points at 150°C.
- Cast Ductile Iron: 1-month test: 2 points at 250°C, 2 points at 150°C.
3-month test: 2 points at 250°C, 2 points at 150°C and notation of "significant pitting."
6-month test: 2 points at 250°C, 2 points at 150°C.
12-month test: 3 points at 250°C, 3 points at 150°C.
17-month test: 2 points at 250°C, 2 points at 150°C.
- 2 1/2% Cr, 1% Mo
Cast Steel: 1-month test: 2 points at 250°C, 1 point at 150°C.
3-month test: 2 points at 250°C, 2 points at 150°C.
6-month test: 2 points at 250°C, 2 points at 150°C.
12-month test: 3 points at 250°C, 3 points at 150°C.
17-month test: 2 points at 250°C and notation of significant pitting, 2 points at 150°C and notation of significant pitting.
- 1 1/4% Cr, 1/2% Mo
Cast Steel: 1-month test: 2 points at 250°C and deepest pit depth, 2 points at 150°C.
3-month test: 2 points at 250°C, 2 points at 150°C.
6-month test: 2 points at 250°C, 2 points at 150°C.
12-month test: 3 points at 250°C, 4 points at 150°C with notation of significant pitting.
17-month test: 2 points at 250°C, 2 points at 150°C.
4. Irradiation/corrosion data of Fe base alloys/basalt water/oxic.
T = 250°C.
- Cast Ductile Iron: 2 points each for test samples taken at 1, 3, 5 and 6 months, 1 point for samples at 10, 11, and 13 months.
- 2 1/2% Cr, 1% Mo
Cast Steel: 2 points each for samples taken at 1, 3, 5, and 6 months, 1 point for samples taken at 10, 11, 12, and 13 months.

1025 Cast Steel: Single data points for 6-month and 8-month tests.

1020 Wrought Steel: 5 points for 2-month test.

(d) Packing Material:

1. Hydraulic conductivity value for 75/25 packing material.
2. Thermal conductivity - range in values.
3. Range in solubility for Ra and Am at 60°C in packing material.

UNCERTAINTIES IN THE DATA

- (a) Waste Form + Basalt Water ± Basalt: Single values are given with no indication of range in data or uncertainties. In many instances specific radionuclides were not analyzed for so that intercomparison cannot be made between situations with and without basalt.
- (b) Basalt/Groundwater: No range or uncertainties in pH given.
- (c) Canister Material Corrosion: Data for short-term corrosion tests under anoxic conditions give individual rates and the mean and standard deviation. Five-month corrosion data (anoxic conditions, no packing material) are given with mean and standard deviation. Corrosion data for iron base alloys, oxic conditions give only individual points for each test condition but an estimate of mean and standard deviation for all test data at times >5 months. Irradiation corrosion data contain individual points with no estimate of uncertainties for each sampling time. However, an overall mean and standard deviation is given for test data at times >5 months.

DEFICIENCIES IN THE DATA BASE

This paper summarizes results from the BWIP program on selected areas of research on waste package materials performance. As such, it is limited in scope and cannot perhaps present all available data. However, the reference to prime sources of the data is lacking. Several values for various properties are given with no indication of range. It is not clear whether corrosion data (rates) presented in one table are based on single sample determination or an average of several. Pit depths, when pitting is observed, are not always quantified. Flow rates for different tests are different. Intercomparisons, based on information presented is, at best, difficult.

APPLICATION OF DATA TO LICENSING

[Key data (), Supporting data (X)].

GENERAL COMMENTS

One of the primary shortcomings of this paper is the lack of adequate references to the original work summarized. The original reports may prove to be more valuable to licensing than this summary paper.

Several pertinent issues are, however, raised by this report. Some of these are summarized below:

- Waste form testing did not include realistic conditions (e.g., corrosion products).
- Measured concentrations of several nuclides were "orders of magnitude higher than solubilities calculated from thermodynamic data."
- Basalt/groundwater studies do not appear to include radiation effects.
- Radiation appears to increase uniform corrosion by factors of two to three.
- Pitting has been observed in some LCS at temperatures lower than 250°C.
- Solubilities have not been determined for conditions anticipated at failure.

ORGANIZATION PRODUCING DATA

DOE/Basalt Waste Isolation Project.

AUTHORS/REFERENCE

Smith, M. J. and others, "Waste Packages for a Repository Located in Basalt," RHO-BW-SA-330P, 1983.

AVAILABILITY

Paper presented in Civilian Radioactive Waste Management Information Meeting, Washington, D. C., December 1983.

KEY WORDS

Waste package, corrosion, bentonite, stability, gamma irradiation, basalt, design, performance evaluation, hydraulic conductivity, sorption.

DATE REVIEWED

September 1984.

gfs
9/27/84

ABSTRACT

This paper presents the status of the BWIP waste package materials testing, modeling, and design activities and plans for continuing these activities through FY 1984. The first in a series of design activities leading to the final design of waste packages that will reliably meet Federal performance criteria has been completed. These activities have led to the development of waste package conceptual designs for commercial and defense high-level waste (borosilicate glass) and spent fuel rods. Planned engineering studies, together with an improved materials data base, will provide the necessary information for the preparation of waste package advanced conceptual design requirements during FY 1984.

Tests of hydrothermal reactions between basalt and simulated Grande Ronde Basalt groundwater showed that Eh conditions that were initially oxidizing became progressively more reducing as oxygen was consumed by the oxidation of ferrous iron released by the dissolving (glass) mesostasis. The pH of samples periodically withdrawn from the autoclaves decreased rapidly from a value of 9.8 and then rose to stable values of 7.5 and 7.6 at 200°C and 300°C, respectively. Hydrothermal tests show that basalt will reduce radionuclide releases from waste forms under conditions simulating those expected in an NWRB. As an example, in testing of Tc-doped borosilicate glass, steady-state concentrations of Tc in solution were found to be about three orders of magnitude lower when basalt was present. Hot cells have been prepared and hydrothermal testing using fully radioactive waste forms was initiated by the BWIP on November 1, 1983. An extensive program to test waste package components in the presence of radioactive waste forms and to assess the effect of basalt and barrier materials on releases of key radionuclides from waste packages under repository conditions has been developed for the hot-cell facility.

Corrosion testing of the BWIP reference canister material, LCS, and the two backup materials, FeCrMo alloy steel, and 90-10 Cupronickel are being conducted to develop a reliable data base for waste package design and modeling activities. Exposure of LCSs with varying carbon content at temperatures from 100°C to 300°C in the presence of the basalt/bentonite backfill showed that, under the conditions of the test, corrosion rate was independent of carbon content. Also, corrosion rates generally decreased with increasing temperature. This feature was attributed to the tenacity and degree of development of an iron-rich clay surface corrosion product that became more protective as the temperature increased. Testing to date also shows that under oxic conditions and at high flow rates (35 mL/hr), the corrosion rates of iron-base materials increased two to three times in the presence of gamma radiation. Preliminary SSR testing of LCS in repository-specific groundwater showed a slight susceptibility to stress-corrosion-cracking, whereas early results of static crack growth testing under equivalent conditions revealed no tendency toward stress-corrosion-cracking.

Studies of the effects of radiation on corrosion and mechanical behavior will continue in FY 1984. Studies to develop pitting kinetics will be initiated. In addition, long-term corrosion tests will be started to improve the corrosion data base for waste package performance modeling.

Irreversible dehydration of the crushed basalt/bentonite reference packing material is not expected to occur at temperatures below 370°C as demonstrated in thermal testing. At 300°C exposure it was found that bentonite reactions were relatively minor and chemical stability was little affected. Thus, the reference packing material (75% crushed basalt/25% bentonite) may remain stable over long periods of time. Measured hydraulic conductivity of packing material was found to be significantly less than that required to maintain diffusional control of radionuclide releases, an expected means of controlling radionuclide mass transport through the packing material. Sorption hysteresis effects observed in recent radionuclide sorption studies are expected to decrease the mobility of radionuclides in the packing material. During FY 1984, hydrothermal long-term (up to 5 yr) packing material stability tests at 150°C will be initiated. The measurement of thermal conductivity of saturated packing materials will be initiated. Measurement of packing material physical properties (swelling, hydraulic conductivity, etc.) will continue.

Models are being developed to allow prediction of waste package reliability, degradation, and radionuclide release. In addition, two engineering test plans have been completed for tests that employ full-scale waste packages to measure the rate of packing material saturation under a thermal gradient and the degradation of waste package canister and packing material using canister heaters to simulate radiogenic heat.

WASTE PACKAGE DATA REVIEW FORM

TYPE OF DATA

Hydraulic conductivity, thermal diffusivity, density, clay expansion, uniform corrosion, SSR test results, release rates from glass, pH.

MATERIAL

Natural untreated bentonite (CS-50), calcium bentonite, ductile cast iron, 1 1/4% Cr-1/2% Mo cast steel, 2 1/2% Cr, 1% Mo cast steel, Ti Grade-2 and Grade-12, PNL-76-68 glass, reference basalt and tuff groundwaters, basalt and tuff rocks.

TEST CONDITIONS

(a) Backfill Materials:

1. Water migration: Na-bentonite compacted to 2.1 g/cm³, cylinders 3 to 5 cm long, 15 MPa water pressure, times of 4 hours to 42 days, ambient temperature.
2. Hydraulic conductivity: Na and Ca bentonite, tuff and basalt groundwater, different densities (≈ 1.7 to 2.3 g/cm³), ambient temperature, confining force <100 lbs.
3. Radionuclide migration: Reference basalt and tuff groundwater, 25°C, ⁸⁵Sr, ⁹⁹Tc, ¹²⁵I, ¹³⁷Cs, ²³³U, ²³⁷Np and ²⁴¹Am, several backfill materials, oxid.
4. Thermal conductivity: Dry compacted Na-bentonite (2.1 g/cm³), air saturated (5 weight % H₂O) bentonite, permeability cell.
5. Compaction studies: Na and Ca bentonite, 50/50 and 75/25 mix of Na-bentonite and quartz sand, water content "0" to $\approx 14\%$, compaction pressures 55 to 276 MPa held for 1 min, zero order water is for clay sample held at 110°C for 16 hours.
6. Materials stability: Na and Ca bentonite, heated in air to 100, 200 and 300°C for up to 1 year, bentonite irradiated to total dose 9.5×10^9 rad.

(b) Corrosion Studies: Cast Fe materials with minimum dimension of 5 inches, surfaces were ground, Ti alloys used as-received, basalt rock from Umtanum surface outcrop, tuff rock from Bullfrog horizon.

1. General Corrosion: Flowing autoclave (35 ml/h), 800 to 1000 psi at 250°C, 6 to 8 ppm O₂. Test in basalt run at 150 and 250°C for 6 months. Tuff tests and DIW tests done at 250°C for 1 month and 3 months, respectively.

2. Irradiation Corrosion: Fe alloys and titanium alloys in flowing autoclaves (35 ml/h), dose rate of $\approx 2 \times 10^6$ rad/h, 700 psi at 250°C, oxic basalt groundwater for maximum time of 3 months. Ti alloy tests included general corrosion coupons, U-bend, V-notch and tension fracture toughness specimens bolt loaded to 20 KSi $\sqrt{\text{in.}}$. Dose rate varied from 10^6 to 10^4 rad/h over geometry of autoclave.
3. Slow Strain Rate, Fatigue Crack Growth Rate Test: Crushed basalt, basalt water, flowing system, strain rates of 10^{-4} to 2×10^{-7} in./in.-sec, temperature $\approx 250^\circ\text{C}$. For FCG studies, preflawed specimens, simulated groundwater, water enriched in F^- and high purity water, loading frequency from 0.01 to 5 Hz, atmosphere pressure and 90°C, refreshed water.

(c) Waste Form Release:

1. Groundwater Effects: 90°C, static leach test in DIW, and reference basalt and tuff groundwaters, SA/V = m^{-1} , total 32 days.
2. SA/V Effects: 90°C, DIW, SA/V = 1, 10, 100 and 1600 m^{-1} .
3. Radiation Effects: SA/V = 20 m^{-1} , DIW and reference basalt water, capsules degassed and backfilled with He, temperatures of 50°, 70° and 90°C.

(d) Component Compatibility:

1. Solution/Rock Tests: Rocking autoclave with gold sample bag, 300°C, 2112 hours, 300 bars, sampled at 200, 336, 840 and 2112 hours.
2. Waste Form/Clay: Powdered mixture of 76-68 glass and either kaolin, bentonite, quartz or tuff, 90°, 150° and 250°C for 3 weeks.
3. Thermal Gradient Effects: Waste form powder, powdered rock, "simplified groundwater," 15°C/cm thermal gradient for 60 days.
4. Single Pass Continuous Flow Leaching/Sorption: Doped (Np,Pu) 76-68 glass or UO_2 , basalt groundwater, basalt rock column, 75° and 25°C, 1 1/4 years, 3 flow rates (1 ml/d, 10 ml/d, 300 ml/d).
5. Sensitivity Tests: 150°C, 30 to 60 days, solution/solid weight ratio = 10/1, 8 tests each for basalt and tuff with varying weight % of Fe powder and/or bentonite.
6. Interaction Tests: Fe and glass coupons with SA/V = 10 m^{-1} , T = 90°C, basalt water, tuff water and DIW, 28 days.
7. Systems Tests: U-doped PNL-76-68 glass, minicanister (2 cm diameter x 7.5 cm long), flat open surface at one end to which is pressed a rock pellet (quartz monozite, basalt, bedded salt), 4 to 6 weeks, 150° or 250°C, 600 to 2000 psig, solution-to-package ratio of 0.5 or 3.0.

METHODS OF ANALYSIS

- (a) Backfill Materials: X-ray diffraction to characterize material. Other procedures not given. Thermal diffusivity measured using a transient laser thermal pulse technique.
- (b) Corrosion:
 - 1. General Corrosion: Visual examination, oxide stripping by inhibited HCl and abrasion, weight measurement. Corrosion layer on specimen of ductile iron (250°C, 6 months, basalt water) analyzed by X-ray diffraction. Waterline specimen from tuff study examined by X-ray diffraction.
 - 2. Irradiation Corrosion: Corrosion films analyzed by X-ray analysis.
 - 3. Slow Strain Rate, Fatigue Crack Growth: Schematic of apparatus given. Crack extension monitored by a traveling microscope.
- (c) Waste Form Release Studies:
 - 1. Groundwater Effects: Methods not given.
 - 2. SA/V Effects: All methods not given, reaction layer thickness determined by secondary ion mass spectroscopy.
- (d) Component Compatibility:
 - 1. Solution/Rock: HCO_3^- and CO_3^{2-} determined in quenched samples by titration, Eh measured with Pt electrode in inert atmosphere.
 - 2. Waste Form/Clay: Details not given.
 - 3. Thermal Gradient Effects: Polished solid samples examined by EDX.
 - 4. Single Pass Continuous Flow Leaching/Sorption: Details not given.
 - 5. Sensitivity Tests: Details not given.
 - 6. Interaction Tests: Solution analysis and surface analysis by EDAX and SIMS.
 - 7. System Test: Examine glass surface by SEM.

AMOUNT OF DATA

- (a) Backfill Materials:
 - 1. Water Migration: Graphical data of percent water in clay vs depth, family of curves for 9 different times.

2. Hydraulic Conditions: Graphical presentation of conductivity vs compacted density for Na and Ca bentonite, graphical data of hydraulic conductivity of sand-Na-bentonite mixtures vs compacted density.
 3. Radionuclide Migration: (28-day tests) list of R_d for 18 backfill materials, including 5 American Clays Institute source clays, basalt water. R_d for Na- and Ca-bentonite and charcoal using tuff groundwater.
 4. Thermal Conductivity: Graphical information on thermal diffusivity of dry Na-bentonite as a function of temperature (15 points), table of thermal conductivities for air saturated Na- and Ca-bentonite (conductivity, density, pressing force).
 5. Compaction Properties: Four graphical presentations of density vs water content. Each contains a family of curves for different compaction pressures.
 6. Stability Studies: Two graphical presentations of Na-bentonite expansion vs time. One is for clay heated at 100°, 200° and 300°C, the other for clay irradiated to a total of 9.5×10^9 rads. Table of hydraulic conductivities for untreated, heated and irradiated clay (4 points).
- (b) Corrosion Studies: Tabular summary of nominal composition of Ti alloys and Fe-base alloys. Tabular summary of room temperature mechanical properties. Table of composition of tuff and basalt rocks used in the study.
1. General Corrosion: For Fe alloys, 2 graphs of corrosion rate vs exposure time at 250° and 150°C (duplicates of each point given), 2 graphs of weight loss vs time at 250° and 150°C. Graphical presentation of corrosion rate in tuff water with time, only a single time point at 250°C. Corrosion rate of Fe alloys in DIW at 250°C, 2 data points for each alloy, at 2 times.
 2. Irradiation Corrosion: Corrosion rates vs exposure time for Fe alloys. Duplicate sample points for each alloy at 1 month and 3 months. Ductile iron exhibits pits over 2/3 of surface. Observations reported for Ti alloys, no SCC, no crack extension, weight change did vary with position of coupon in autoclave (radiation field). Weight changes in Ti alloys are presented graphically as a function of sample position (18 points for each alloy).
 3. SSR and FCG Studies: Graphical presentation of SSR tests on Ti Grade-2 and Grade-12 at 250°C as a function of displacement rate. Data are for percent reduction in area and percent elongation in air and basalt water at 250°C, LT and TL orientations. Graphical data on effect of temperature on ductility at constant strain (% elongation and % reduction in areas), duplicate samples, Ti Grade-2 LT orientation, total of 8 points for each (i.e., % elongation or % area reduction). Crack growth rates vs stress intensity for Ti Grade-2, 19 points at 0.1 Hz high F^- water, 4 points at 1 Hz normal basalt water.

Crack growth rate vs stress intensity for T1 Grade-12, 21 points at 0.1 Hz high F⁻ basalt water and 6 points at 1 Hz for normal basalt water.

(c) Waste Form Release: Table summarizing composition of PNL-76-68 waste glass:

1. Groundwater Effects: Normalized release of Cs and B vs time in 3 waters, 3 to 4 points for each ion in each water.
2. SA/V Effects: Log of normalized release vs log SA/V for Na, B, Si, Cs and Ca, 4 points for each element. Graph also includes results of previous work. Si, Na and Ca releases as a function of leach time. Concentration (atm %) of B, Na, Si, Cs in depletion layer as function of SA/V.
3. Radiation Effects: Table of Si release rates vs temperature for irradiated and unirradiated samples (3 values each) in DIW, dose rate dependence for release of Si, B, Cs and Fe (5 points for each, dose rates up to 2 R/h). Log Si and Log B removal vs 1/T at 3 temperatures, irradiated and unirradiated. Graph of ppm B and Cs vs time in unirradiated and irradiated DIW and basalt water at 50°C. Effects of radiation on CO₃⁻² waters; pH and concentration of oxalate.

(d) Component Compatibility Tests:

1. Solution/Rock: Tabular comparison of BWIP data with PNL data for 9 solution species and pH, graphical comparison of BWIP and PNL data for Na and Si.
2. Waste Form/Clay: pH vs temperature for various mixtures, log moles in solution for Mo, Cs, Na and Si in the glass-Kaolin system g/glass vs 1/T.
3. Thermal Gradient Effects: Graphical presentation of relative distribution of Nd, Mo and Cs, after migration in basalt under a thermal gradient (6 to 22 points each).
4. Single Pass Continuous Flow Leaching/Sorption: No data.
5. Sensitivity Tests: No data given.
6. Interaction Tests: PNL-76-68 glass release data for B and Cs with and without ductile iron coupon, 3-4 data points for each, reaction depth layers for glass in 3 waters with and without Fe coupon. Changes in Si and Ca concentration in basalt and tuff water when Fe coupon present (no glass), 5 points each with and without filtration to remove colloids. Reaction layer thickness for basalt water + clay + glass, DIW + clay + glass vs time, 5 points each over ≈35 days.

7. System Tests: For salt tests, report lowering of solution pH to 3.0. In basalt and granite, report reduced concentrations of soluble Cs relative to salt tests and glass-water tests under hydrothermal conditions. U not found in rock surfaces contacting liquid, only in surfaces contacting vapor. U not observed at concentrations >15 ppb. Changes in solution composition with time given for Cs, Mo, B, Na, Si and K. Weight % of Si, Na, Fe, U, Zn, Mo and Zr in glass reaction layers vs depth.

UNCERTAINTIES IN THE DATA

(a) Backfill Materials:

1. Water Migration: Water content as a function of position in the sample is given for several times. No error bars are associated with the individual points. Hydraulic conductivity values are given for Na- and Ca-bentonite as a function of compacted density. No error bars are given and only a single value is reported for tuff groundwaters.
2. Radionuclide Migration: Batch R_d s are reported with no indication of range anticipated from replicate measurements. Only a narrow range of conditions have been used (25°C, oxic, 28 days).
3. Thermal Conductivity: The thermal diffusivity is given with a standard deviation. However, the thermal conductivity for dry compacted Na-bentonite is calculated with an assumed heat capacity. The results give a range in conductivities that are reported to be "considerably" higher than the values used in design studies." The thermal conductivities of Na- and Ca-bentonite (air saturated) have been determined as a function of compacted density for various composition pressures. Ranges within a given measurement are not reported. Potential changes with temperature are not addressed.
4. Composition Studies: A limited number of points is given for each pressure and weight percent water with no indication of reproducibility.
5. Materials Stability Studies: Expansion data do not give an indication of scatter or uncertainty to tell whether there are significant differences as a function of temperature. Clays tested were heated under dry conditions. In some instances only two points are given. A single dose rate was used for the radiation studies, only five points are given with no information on scatter or uncertainties from replicate determinations. Samples irradiated were heat treated so that no data are available on range of expansion and permeability with water content, etc.

(b) Corrosion Studies:

1. General Corrosion Studies: General corrosion data at 150° and 250°C consist of three points for each metal/water system and an indication that at least replicate determinations were made. Data for cast iron

alloys in tuff water at 250°C consist of single time points (replicates) experiments. In DIW at 250°C there are only 2 time points (replicate samples). A different behavior is noted between weight loss of Fe alloys in basalt water at 150°C and that at 250°C. Almost no change with time at 250°C vs an almost linear increase with time at 150°C.

2. Irradiation Corrosion: For ductile Fe and 2 1/2 Cr, 1% Mo, only 2 time periods were samples (1 month and 3 months). Replicate samples are given. In both cases the sample-to-sample values of the corrosion rate increases with the time of exposure and is greater than the rates observed in basalt water with no irradiation. Titanium Grade-2 coupons show sensitivity to dose rate at 250°C. No indication is given, however, in spread of each data point presented.
3. Environmental-Mechanical Tests: Data presented have no indication of the scatter or uncertainty in each point. There is a limited number of data points presented and only one temperature is used.

(c) Waste Form Release:

1. Groundwater Effects: There are no error bars associated with each data point or statement of the degree of reproducibility. Only a single temperature (90°C) is considered.
2. SA/V Effects: Data presented include a comparison where possible of previously obtained values. This may give some indication of reproducibilities. In work done by PNL and reported in this report, no indication is given of range in each data point.
3. Gamma Radiolysis Effects: Replicate data points are given in some instances (unirradiated). Radiolysis effects alter release of some elements by as much as a factor of 10. Replicate values for irradiated samples not given.

- (d) Component Compatibility: With few exceptions, no indication is given of the spread or uncertainty in the data presented. Data do, however, indicate the presence of other barrier materials can affect the behavior of glass or Fe alloys or bentonite in a manner different from that anticipated based on single component studies.

DEFICIENCIES IN THE DATA BASE

(a) Backfill Materials:

1. Water Migration Studies: These studies concentrated on the water migration in Na- and Ca-bentonite. No work was reported for the reference backfill mixture basalt/bentonite in the form to be used in a repository in basalt, nor is there any work reported on the changes in migration rates with temperature. Hydraulic conductivities are not reported for the reference backfill material (basalt/bentonite) under conditions anticipated in the repository.

2. Radionuclide Migration: Retardation properties of the reference backfill material, basalt/bentonite, have not been reported for comparison. Temperatures at which they have been determined are less than ambient temperature in the horizon and do not consider possible range in temperatures from time of breach (i.e. at 300 years as a maximum temperature).
 3. Thermal Conductivity Studies: Data presented do not include data on reference backfill material. No data are reported for changes in thermal conductivity with water content.
 4. Compaction Studies: No information is given for the reference backfill.
 5. Material Stability Study: No information is given on the reference backfill material. For data presented, no combined study of temperature and radiation effects under various weight percent water content.
- (b) Corrosion Studies:
1. General Corrosion Studies: A single flow was used with no justification of its applicability. Temperatures were limited, test times were short and it appears that only replicate samples were studied. For tuff groundwaters only a single time was samples (\approx 1 month).
 2. Irradiation Corrosion: Studies were short-term and data indicate larger sample-to-sample uncertainty for longer exposures. Only a single temperature was utilized and data on basalt/water interactions at 90°C indicate decreased pH and increased oxalate concentration. These tests do not take into account the environment of the corrosion barrier (backfill material, varying temperature, etc.).
 3. Environmental-Mechanical Tests: Testing was performed in typical groundwaters but did not include irradiation and tests were reported only for 250°C (SCGR) and 90°C (FCG).
- (c) Waste Form Release: There is a good indication of range or uncertainties in some of the data. Effects of temperature and changes in waste form characteristics are not addressed. Much of the work reported is centered on Cs, Sr, Si, etc. release. At 300 years, the minimum containment time, Cs and Sr should not be the main concern. In general, the information has very little to do with what the repository will be like at 300 years and beyond, and how the immediate environment will affect releases of long-lived nuclides from the waste form.
- (d) Component Compatibility: These tests indicate the importance of defining a range of scenarios for studying multicomponent behavior. In all instances, the presence of other components (e.g. glass + Fe coupons) alters the behavior of the single component. However, these tests as reported do not include the interplay of heat and radiation, or necessarily include all pertinent components. While multicomponent tests may not yield highly quantitative data, reproducibility of data would be an indication of potential long-term performance.

APPLICATION OF DATA TO LICENSING

[Key Data (), Supporting Data (X)].

GENERAL COMMENTS

This document summarizes PNL's current data on single component, bicomponent and some systems tests. From the current status of these tests recommendations have been made for further test programs. While much of the information can be used as supportive data for narrowing test ranges or test programs, and for looking at potential ranges in package component behavior, much of the information does not apply to anticipated repository conditions. Data on tuff is scarce, testing times are short and in most instances do not consider the interplay of radiation and temperature. Some materials tested are not directly related to current package designs (e.g. the backfill data).

ORGANIZATION PRODUCING DATA

DOE/Pacific Northwest Laboratory.

AUTHORS/REFERENCE

Bradley, D. J. and others, "Nuclear Waste Package Materials Testing Report: Basaltic and Tuffaceous Environments," PNL-4452, March 1983.

AVAILABILITY

Published.

KEYWORDS

Backfill, bentonite, corrosion, iron alloys, tuff, basalt, glass, whole package tests.

DATE REVIEWED

September 1984.

gfs
9/28/84

ABSTRACT

The disposal of high-level nuclear wastes in underground repositories in the continental United States requires the development of a waste package that will contain radionuclides for a time period commensurate with performance criteria, which may be up to 1000 years. This report addresses materials testing in support of a waste package for a basalt (Hanford, Washington) or a tuff (Nevada Test Site) repository.

The materials investigated in this testing effort were:

- sodium and calcium bentonites and mixtures with sand or basalt as a backfill
- iron and titanium-based alloys as structural barriers
- borosilicate waste glass PNL 76-68 as a waste form.

The testing also incorporated site-specific rock media and ground waters: Reference Uranium Entablature-1 basalt and reference basalt ground water, Bullfrog tuff and NTS J-13 well water.

The results of the testing are discussed in four major categories:

- Backfill Materials: emphasizing water migration, radionuclide migration, physical property and long-term stability studies.
- Structural Barriers: emphasizing uniform corrosion, irradiation-corrosion, and environmental-mechanical testing.
- Waste Form Release Characteristics: emphasizing ground water, sample surface area/solution volume ratio, and gamma radiolysis effects.
- Component Compatibility: emphasizing solution/rock, glass/rock, glass/structural carrier, and glass/backfill interaction tests. This area also includes sensitivity testing to determine primary parameters to be studied, and the results of "systems" tests where more than two waste package components were combined during a single test.

The objective of the first two categories is the selection of candidate materials and development of baseline property information to evaluate material or function lifetimes. The waste form research centers on understanding the basic processes involved with waste form/solution interactions so that a release model can be derived for predicting the radioactive "source-term" arising from waste form/solution contact.

The last area, component compatibility testing, is aimed at learning how waste package materials interact with each other under repository conditions. Information gained from the first three areas is being used to understand the systems interactions revealed by testing in the fourth area. Another purpose of component compatibility testing is, as the name implies, to spot potential problems among materials as early as possible. Data from all four areas are being used to develop a model describing the behavior of the waste package as a whole, under both expected and off-normal conditions.

WASTE PACKAGE DATA REVIEW FORM

TYPE OF DATA

Composition of Umtanum basalt, bentonite/groundwater, basalt/groundwater, backfill/groundwater, basalt/bentonite and silica and aluminum concentrations of major repository constituents. pH changes vs time of backfill/groundwater.

MATERIAL

Umtanum basalt sized to -115 to +250 mesh and ultrasonically washed to minimize surface conditions of the outcrop. Wyoming bentonite -400 mesh, as-received. Synthetic groundwater.

TEST CONDITIONS

Individual and multicomponent tests were performed in a gold bag placed in a rocking autoclave. Temperature and pressure were increased to 300°C and 300 bars, respectively and test ratios of water-to-solids were at 10:1 and 15:1. Test durations spanned from three days to three months. Periodic solution samples were collected and analyzed.

METHODS OF ANALYSIS

During the tests small quantities of solution were periodically drawn and analyzed for cations by inductively coupled plasma spectrometry. Anions were characterized by ion chromatography. Post-experimental analyses of solids were determined by scanning electron microscopy, scanning transmission electron microscopy and X-ray diffraction.

AMOUNT OF DATA

Two sets of 10 data points for basalt composition at repository elevation and as an outcrop are reported as weight percent. Three data sets, two with seven data points, the other with eight data points are given in mg/l. The conditions for which these data sets are reported, are groundwater contacted with either bentonite, basalt and bentonite, and basalt at 300°C and 300 bars.

UNCERTAINTIES IN THE DATA

The changes in concentration vs time of the backfill (basalt, bentonite, groundwater) indicate that a reaction is occurring. This is evidenced by silica increasing to a maximum concentration at 334 hours and then gradually decreasing, whereas sodium continually decreased until the test was terminated. The pH also continued to decrease from an initial value of 9.78 to 5.35. No discussion of the environment, whether it was reactive or inert, in which the

test was performed, is given. Also, the data presented do not include the effects of radiolysis nor are there repetitive tests to establish a range of values for data points.

DEFICIENCIES IN THE DATA BASE

Additional experiments in a controlled environment with waste container materials present would be useful to substantiate the data given. Also, longer test times, beyond three months could help to resolve the changing ionic composition and perhaps achieve a near steady state. Tests performed in the presence of radiation could alter the rate of change in the reported data.

APPLICATION OF DATA TO LICENSING

[Key Data (), Supporting Data (X)].

GENERAL COMMENTS

This appears to be a suitable scoping experiment and could provide a base for developing further tests. Additional tests where the pressure and particularly the temperature, would be controlled variables, could provide insight for changes in ionic composition of the backfill and lead to more clearly describing any reactions occurring.

ORGANIZATION PRODUCING DATA

DOE/BWIP

AUTHORS/REFERENCE

Wood, M. I., "Experimental Investigation of Sodium Bentonite Stability in Hanford Basalt," RHO-BW-SA-219P, February 1983.

AVAILABILITY

Published.

KEY WORDS

Basalt, bentonite, backfill, groundwater, hydrothermal interaction.

DATE REVIEWED

September 1984.

gfs, 10/2/84

ABSTRACT

Sodium bentonite is a candidate material for the waste package backfill component in a repository in basalt at the Hanford Site. Preliminary hydrothermal experiments have been conducted under near-field geochemical conditions expected to occur in the reference repository location in the Grande Ronde Basalt. Experiments have been conducted in the basalt/groundwater, bentonite/groundwater, and basalt/bentonite/groundwater systems. The experiments have been conducted at 300°C using a simulated Grande Ronde groundwater, reference Umtanum basalt, and sodium bentonite. Key data generated by the experiments include experimental solution analyses as a function of time and preliminary solids analysis by scanning transmission electron microscopy and X-ray diffraction. Solution trends of the major aqueous species were similar in the three systems and are characterized by: (1) the gradual reduction of the pH value from ~9.75 to a steady-state value of ~6, (2) an initial rapid increase followed by a gradual decrease in silica concentration, and (3) a slight or negligible increase in sodium, sulfate, and chloride concentrations. In the bentonite/groundwater experiment, small amounts (<1%) of an albite reaction product were observed. Conversely, the formation of illite, a common bentonite alteration product, was not observed. These results indicate that sodium bentonite will remain sufficiently stable at 300°C under hydrothermal conditions in basalt to permit its use as a backfill material.

BLANK PAGE

WASTE PACKAGE DATA REVIEW FORM

TYPE OF DATA

Solution pH vs time; concentration of F^- , SO_4^{2-} , Si, Al, K, vs time for various combinations of basalt/basalt water, Na bentonite/basalt water, breakthrough time as a function of K_d , hydraulic conductivity, swelling pressure, solution data for basalt + synthetic groundwater, radionuclide sorption on basalt and basalt secondary mineralization, radionuclide sorption on treated bentonite, chemical analyses of Umtanum basalt.

MATERIALS

1. Basalt/Groundwater Interaction: Crushed basalt from Umtanum flow, simulated groundwaters, rocking autoclave.
2. Bentonite/Groundwater Interaction: Baroid National Western Bentonite (-400 mesh), synthetic basalt groundwater, rocking autoclave, DIW.
3. Sorption Studies: Crushed basalt, Baroid Bentonite, synthetic groundwater, hydrazine to impose reducing conditions.
4. Physical Properties of Crushed Basalt/Bentonite: No data actually generated - authors cite other publications.

TEST CONDITIONS

1. Basalt/Synthetic Water Interactions: Basalt powder/synthetic water (1:10) 300°C, 300 bars and 200°C, 300 bars. Time of test varied from 616 hours to 1,004 hours at 300°C, and 1,004 hours at 200°C. Two separate laboratories conducted the tests.
2. Bentonite/Groundwater Interactions: Water to bentonite ratio (10:1) temperature of 300°C, 300 bars, 616 hours. Second experiment at 300°C, 300 bars, water:rock ratio of 15:1 for 72 hours. Third experiment at 300°C, 300 bars, 10:1 water to rock ratio, DIW and 72 hours.
3. Sorption Studies:
 - (a) Basalt/Groundwater: 60°C, oxic and anoxic conditions; 60 days.
 - (b) Basalt Secondary Minerals/Groundwater: Temperature unspecified, oxic conditions, 50 days (Eh -0.3 to -0.4 V reducing and +0.4 to +0.5 V oxidizing).
 - (c) Bentonite/Groundwater: Bentonite heat treated to 450°C prior to use, test at 65°C, oxic and anoxic conditions, total time six days.
4. Physical Properties of Crushed Basalt/Bentonite: No data actually generated - authors cite other publications.

METHOD OF DATA COLLECTION/ANALYSIS

1. Characterization of Umtanum Basalt Synthetic Water Interaction: Solids by XRD, EDS, SEM, STEM, solutions by ICP, ion-exchange chromatography, room temperature pH, atomic adsorption, gravimetric, colorimetric and fluorometric techniques.
2. Bentonite/Groundwater: Solids analyzed by STEM and SEM.
3. Sorption Studies: Batch equilibrium technique, solutions analyzed by α , β and γ counting techniques.
4. Physical Properties of Crushed Basalt/Bentonite: No data generated.

AMOUNT OF DATA

1. Basalt/Groundwater Interaction:
 - (a) Chemical Analysis of Basalt: 10 oxides no ranges in composition given.
 - (b) Solution Data for Basalt + Synthetic Water:
 - (1) At 300°C-300 bars: 7 points for 11 ions and pH over 616 hours (concentration in mg/L).
 - (2) At 300°C-300 bars: 7 points for 11 ions and the pH over 356 hours (concentration in mg/L) - meant to be a duplicate run.
 - (3) At 300°C-300 bars: 9 points for 13 ions and the pH over 1,004 hours.
 - (4) At 200°C-300 bars: 8 points for 13 ions and the pH over 718 hours.
2. Bentonite/Groundwater Interaction:
 - (a) X-ray analysis and bulk chemical analysis of bentonite, no range in composition given, 10 oxides quantified.
 - (b) Solution data:
 - (1) At 300°C-300 bars: 7 points for 12 ions and the pH over 616 hours, same ions as in basalt/groundwater interaction plus boron.
3. Sorption Studies:
 - (a) Basalt/Groundwater: Batch K_d 's (mL/g) for 8 nuclides under oxidizing conditions and for 4 of these (U, Se, Ra, Np) under reducing conditions. K_d given with error ($\pm 1\sigma$).

- (b) Basalt Secondary Minerals/Groundwater: Batch Kd (mL/g) for 10 radionuclides under oxidizing conditions. Kd reported with error ($\pm 1\sigma$).
- (c) Bentonite/Groundwater:
- (1) Batch Kd with time for U and Np under oxic and anoxic conditions. Kd values reported with error ($\pm 1\sigma$), time: six days.
 - (2) Batch Kd for U under oxic and anoxic conditions, total contact time 30 days, initial concentration in solution varied over ~3 orders of magnitude. Kd given with error ($\pm 1\sigma$).
 - (3) Batch Kd including error ($\pm 1\sigma$) for Cs and Sr, total contact time seven days, initial concentration in solution varied over six orders of magnitude. No error reported for anoxic data.
4. Physical Properties of Crushed Basalt/Bentonite: No data on basalt/bentonite. Summary given of available published data (graphical) on bentonite/sand.

UNCERTAINTIES FOR THE DATA

1. Basalt/Groundwater Interaction:
 - (a) Initial groundwater composition. The groundwater compositions for the two independent sets of experiments differed substantially in Si, K, Ca, SO_4^{2-} and Cl^- content. No indication is given for the spread in concentrations of all species as a function of time. While the overall values for each ion follow a general trend the absolute values are not directly comparable without some indication of range of uncertainty. Differences in solution concentrations and pH exist between 200°C and 300°C. The differences are large enough in the case of several species to indicate real difference and not experimental errors. However, no ranges are indicated to assess the magnitude of these differences.
2. Bentonite/Groundwater Interaction: There is no indication of spread in data for a given measurement and no indication of results from a replicate test. For those ions characterized there is the same overall trend for bentonite/groundwater as basalt/groundwater at 300°C. No information was given on behavior at other temperatures. Bentonite was noted to undergo alteration.
3. Sorption Studies: Uncertainty exists in the use of batch Kd to determine retarding capabilities of basalt or bentonite. Further uncertainty exists in the use of a chemical (hydrazine) to produce reducing conditions. The batch Kd's are reported with an estimated error. Data reported for

basalt at 65°C and 60 days cannot be directly compared with the Kd reported for secondary minerals under oxic conditions since the temperature for the second data set is not indicated. However, it should be noted that the absolute difference in the two values for U under oxic conditions is ~3 orders of magnitude. For the bentonite sorption studies, the bentonite was first pre-treated to remove organics thus resulting in a non-typical bentonite. In the data reported, some uncertainty exists as to whether equilibrium was truly reached. The data are however reported with estimated errors.

4. Physical Properties of Basalt/Bentonite Packing Material: No data on the system basalt/bentonite are reported. Data reviewed give only an indication of potential behavior. The data are not applicable to BWIP backfill material or the conditions it will experience.

DEFICIENCIES OR LIMITATIONS IN THE DATA BASE

1. Basalt/Groundwater - Bentonite/Groundwater: In both cases, there is no way to directly judge the uncertainties due to experimental errors and those associated with the test system. In addition, these tests do not cover a temperature range or include the effects of radiation and the presence of a container. The largest uncertainty and deficiency of the data for evaluating the performance of a basalt-bentonite backfill is that tests were not conducted with a mixture (basalt/bentonite) that is being proposed for use in the repository.
2. Sorption Studies: The largest uncertainties in the data are due to the fact that the mix of backfill material (bentonite and basalt) was not tested, the range of conditions under which the Kd's were measured was very narrow and does not encompass the range of anticipated conditions so that a sensitivity of the sorption properties could be obtained.
3. Physical Properties of Backfill Material: The greatest deficiency is in the fact that there are no data on the basalt/bentonite physical properties.

APPLICABILITY OF DATA TO LICENSING [KEY DATA (), SUPPORTING DATA (X)]

Relationship to WP Performance Issues Already Identified:

The data generally address Issue Number 2.2 in the S.C.A. (NUREG-0960, Vol. 1, 1983).

General Comments:

No data are presented for the system basalt/bentonite. The data presented do, however, give some baseline information on the potential interaction of basalt or bentonite with groundwater. No uncertainty analysis is given and only a limited number of experiments are reported. The Kd measurements may serve as supporting information and do indicate potential ranges of Kd's under oxic and "anoxic conditions" although the means of obtaining anoxic conditions and the overall usefulness of Kd's is suspect.

ORGANIZATION PRODUCING DATA

DOE/BWIP.

AUTHORS/REFERENCE

Wood, M. I., Aden, G. A., Lane, D. L., "Evaluation of Sodium Bentonite and Crushed Basalt as Waste Package Backfill Materials," RHO-BW-ST-21P. October 1982.

AVAILABILITY

Published.

KEY WORDS

Basalt/groundwater, bentonite/groundwater, Kd.

DATE REVIEWED

April, 1984.

Abstract (Summary) From Reference:

Hydrothermal experiments in the basalt/groundwater and the bentonite/groundwater systems were conducted as part of an overall program designed to evaluate the suitability of crushed basalt and bentonite as waste package backfill materials in a basalt environment. The major purpose of the experiments was to estimate the chemical (e.g., long term) stability of these materials.

Preliminary hydrothermal experiments were completed at 300°C, 300 bars and 200°C, 300 bars in the basalt/groundwater system to determine the chemical stability of crushed basalt. Analysis of solution data from the 300°C experiments as a function of time and reaction products indicated that the primary reaction was the alteration of the basalt glass phase to illite and/or smectite clays and quartz. The establishment of steady state pH values of ~6, the apparent rapid occurrence of a highly reducing environment in the system, and an insignificant increase in the solution concentration of potentially corrosive aqueous species (fluoride, chloride, and sulfate) were observed. These data indicate that a waste package backfill containing a significant amount of crushed basalt will provide a near-field geochemical environment favorable to the chemical stability of metal canister materials. Also, such an environment will promote the low solubility of actinides.

A preliminary experiment was also completed in the sodium bentonite/groundwater system at 300°C, 300 bars. Analyses of the reacted solutions and solids show that bentonite remains essentially stable with only minor alterations to albite. Sorption data were generated on crushed basalt, secondary minerals in basalt, and sodium bentonite at 60 to 65°C under oxic and anoxic conditions. These data indicate that cesium and strontium will be completely contained in a waste package backfill due to the formation of insoluble secondary minerals, ion exchange, and specific adsorption. Under reducing conditions, neptunium will be retained beyond 1,000 yr and uranium and plutonium will be retained under reducing conditions over 300 yr. An increase in retention time can be expected to occur with an increase in temperature. Theoretically, calculations and a limited data base have been used to propose a reference waste package backfill component which will (1) diffusively control mass transport, (2) exert a swelling pressure less than hydrostatic pressure (~10 MPa), and (3) effectively conduct heat away from the waste package such that maximum allowable waste package temperatures are not exceeded. The reference backfill component consists of 25% sodium bentonite and 75% crushed basalt with an initial density of 2.1 g/cm³ and a thickness of 0.152 m.

WASTE PACKAGE DATA REVIEW FORM

TYPE OF DATA

Dehydrated Wyoming bentonite was analyzed by X-ray diffractometry (XRD), thermo-gravimetric analysis (TGA), and differential scanning calorimetry (DSC). Solution samples from the hydrothermal tests were analyzed by inductively-coupled plasma-atomic emission spectrometry (ICP-AES) and ion-chromatography (IC). Hydrothermal reaction products were studied by XRD, scanning electron microscopy (SEM), transmission electron microscopy (TEM), and energy-dispersive spectrometry (EDS).

MATERIAL

Materials reacted were:

- (a) Wyoming bentonite, as-received, smaller than 400 mesh
- (b) Umtanum basalt, crushed, hand-picked to remove altered material, sized to -120 to +230 mesh by sieving, and washed with ultrapure water to remove adhering fine particles
- (c) Synthetic Umtanum groundwater.

TEST CONDITIONS

Bentonite dehydration tests were run in furnaces at atmospheric pressure and fixed temperatures from 250° to 550°C to determine the thermal stability of bentonite in a dry environment. Experiment durations ranged from 1 to 365 days. Hydrothermal tests (30 MPa pressure) to determine packing material bentonite/basalt stability in a saturated environment utilized either Dickson-type rocking autoclaves or cold-seal devices. The Dickson-type autoclaves allowed sampling of the water several times during each test, without disturbing experimental temperatures and pressures. Experiments were run at temperatures as high as 300°C to bring the reactions to a steady state on a laboratory time scale (60-379 days).

METHODS OF ANALYSIS

See Type of Data.

AMOUNT OF DATA

For the dehydration of bentonite study, the following observations were made:

- (a) Differential scanning calorimetry thermograms (5) for Wyoming bentonite at ambient pressure: as-received, 250°C/340 d, 370°C/340 d, 440°C/365 d, 550°C/270 d. The structural water peak near 500°C in the unreacted samples disappeared with increasing temperature.

- (b) TGA data indicate that structural water was lost after heating bentonite at 440°C for 1 yr, but remained at heating temperatures below 370°C. Those samples dehydrated at <370°C and were able to reabsorb water.

For the hydrothermal experiment with an equal mixture of basalt/bentonite/water, reacted in synthetic groundwater at 150°C for 120 days, the following observations were made:

- (a) Significant quantities of Si, Al, K, Ca, Na, and SO_4^{2-} entered the solution from the solids.
- (b) Bulk XRD spectra for the reacted samples were virtually identical to that of the unreacted sample.

For the hydrothermal experiment performed at 300°C:

- (a) The concentrations of Si, Al, and K in the water peaked within 60 days.
- (b) There was evidence of the presence of alteration products, iron smectite, quartz, cristobalite, feldspar, and zeolite.

UNCERTAINTIES IN THE DATA

Statistical information and detection limits of instrumentation were not given.

DEFICIENCIES IN THE DATA BASE

- Basalt was finely crushed and washed, which is not representative of basalt to be used in packing material.
- Radiation effects were not studied.
- Loss of structural water at high temperature as shown by thermal analyses is discussed but not loss of sorbed water with increase in temperature.
- These are relatively short-term studies.

APPLICATION OF DATA TO LICENSING

[Key Data (), Supporting Data (X)].

GENERAL COMMENTS

The interpretation of the various results that is given seems to confuse sorbed water and structural water in bentonite. No XRD scans are shown, so it is not possible to tell whether the peak position attributable to the montmorillonite, i.e. "swelling" portion of the clay, was altered by the heating process.

ORGANIZATION PRODUCING DATA

Rockwell Hanford Operations.

AUTHORS/REFERENCE

Allen, C. C., D. L. Lane, R. A. Palmer and R. G. Johnston, "Experimental Studies of Packing Material Stability," in The Scientific Basis for Nuclear Waste Management, VII, Vol. 26, G. L. McVay, Editor, New York, Elsevier Publishing, 1984, pp. 105-112.

AVAILABILITY

Published proceedings.

KEY WORDS

Bentonite, basalt, packing material.

DATE REVIEWED

October 1984.

gfs
10/9/84

ABSTRACT

The Basalt Waste Isolation Project is conducting experiments to assess the stability of bentonite (sodium montmorillonite) and crushed basalt as waste package packing materials in a nuclear waste repository in basalt. The experiments are designed to identify changes in physical, chemical, and mineralogical properties that these materials could undergo in the repository environment. A series of bentonite dehydration experiments showed that after 1 year at 370°C the clay's structural and swelling properties were preserved and only reversible dehydration occurred. At 440°C, however, irreversible dehydration, collapse of the clay structure, and loss of swelling ability took place. Hydrothermal tests using bentonite, or an equal mixture of bentonite and basalt, along with synthetic groundwater, were also conducted. A bentonite + water experiment showed negligible structural alteration at 200°C, although some iron enrichment of the clay occurred. At 300°C, partial conversion of the montmorillonite to an iron- and potassium-rich smectite occurred, along with the formation of secondary quartz and albite. An experiment in the basalt + bentonite + water system at 150°C resulted in partial etching of the basalt grains, but no detectable change in rock or clay mineralogy. At 300°C, the basalt was strongly etched. Furthermore, iron- and potassium-rich smectite apparently replaced montmorillonite as the dominant clay, and secondary silica, zeolites, and minor feldspar were formed. These mineral assemblages are thought to be metastable at 300°C, based on natural analogs. The kinetics and reaction paths of further transformations of packing materials are important areas for continued study.

WASTE PACKAGE DATA REVIEW FORM

TYPE OF DATA

O₂ content in basalt/synthetic groundwater system, concentration of Tc in synthetic basalt groundwater/borosilicate glass with and without crushed basalt, concentration of Np and Pu in synthetic basalt groundwater/borosilicate glass system, hydraulic conductivity of packing material as a function of density and temperature.

MATERIAL

Borosilicate glass, synthetic groundwater, crushed basalt, basalt-bentonite packing material.

TEST CONDITIONS

1. Basalt/Groundwater Interaction: Crushed Grande Ronde basalt and simulated basalt groundwater at 100°C and 150°C for 3000 hrs. Groundwater saturated with air (~8 mg/L). De-oxygenated, deionized groundwater and crushed basalt at 70°C and crushed basalt/groundwater (Eh measurements).
2. Radionuclide Releases:
 - (a) Tc-doped borosilicate glass/synthetic groundwater + crushed basalt at 200°C/30 MPa, SA/V = 10³ m⁻¹, water/solid = 10/1. Test duration 400 to 2800 hours.
 - (b) Pu, Np in borosilicate glass/synthetic groundwater, at 200°C/30 MPa, SA/V = 10³ m⁻¹, water/solid = 10/1. Test duration ~1200 hours.
3. Hydraulic Conductivity of Packing Material: 75% crushed basalt/25% sodium bentonite, bulk density from ~1.6 g/cm³ to 2.0 g/cm³, temperatures of 25°C, 60°C and 90°C.

METHODS OF DATA ANALYSIS

Not specifically given.

AMOUNT OF DATA

Graphical Presentation:

- (a) Dissolved O₂ data: 16 total points with error bars.
- (b) Radionuclide concentrations: Tc - 22 data points, some with error bars.
239Pu: 5 data points - no error bars.
237Np: 4 data points - no error bars.

- (c) Hydraulic Conductivity: 18 data points - no error bars, three test temperatures.
- (d) Modeling of Release Rate: graphical presentation of calculated release vs time for four water velocities.

UNCERTAINTIES FOR THE DATA

1. Basalt/Groundwater Interaction: For the data presented it is not clear whether the error bars represent errors in replicate measurements and/or detection limit error. Data only representative of conditions for fresh basalt surfaces, no radiation, and no other package components present (e.g. canister). Data reported on Eh achieved with crushed basalt, DIW at 70°C are not applicable to the waste package environment. In conjunction with some information on simulated groundwater/basalt, the data indicate more oxidizing conditions. Presence of radiolysis and other materials may result in conditions different from those reported.
2. Radionuclide Releases From Glass: Data suggest a four orders of magnitude decrease in the steady state concentration of Tc when basalt is present. It is not clear, however, what the error bars on the data represent (e.g. replicate measurement or detection limits). For Pu and Np, the indication is that the steady state concentrations are lower than Tc. No indication is given of range of concentrations or uncertainties. In general, the data are not applicable to repository conditions. No information was given on the speciation of Pu and Np or the variations in steady state concentrations with temperature, presence of corrosion products or other changes (pH, Eh) in groundwater properties.
3. Hydraulic Conductivity of Packing Materials: These data show an enormous amount of scatter (e.g. at 25°C and a bulk density of $\sim 1.7 \text{ g/cm}^3$ the hydraulic conductivity appears to range over ~ 2 orders of magnitude). There are no data on the effect of higher temperatures ($>90^\circ\text{C}$) which the packing may experience and which over time may also cause alteration in the bentonite.
4. Model of Diffusive Radionuclide Release: Many uncertainties are present in the assumptions made in modeling the release, e.g. the assumption that reducing conditions are present so that the concentration in solution is solubility limited for the lower redox state of the radionuclide, and that mass transport is dominated by diffusion (i.e. no fracture flow, colloidal transport etc.). No sensitivity analysis was done to indicate the overall impact of uncertainties in key parameters on the results from the model.

DEFICIENCIES IN DATA

Only a very narrow range of conditions is considered. Radiolysis, presence of other package components are not included. No data are given on changes in the steady state concentration of the radionuclides as a function of temperature or changes in water chemistry, or the effect of other package components. Information on backfill material is over a limited temperature

range with no consideration of changes in groundwater chemistry, radiolysis or periodic wetting and drying. In the model calculations there is no sensitivity analysis to indicate impact of uncertainties in key parameters on the results of the calculation.

APPLICABILITY OF DATA LICENSING [KEY DATA (), SUPPORTING DATA (X)]

Relationship to WP Issues Already Identified:

The data generally addresses issues in the SCA (NUREG-0960, Vol. 1, 1983). See Issue Numbers 2.1, 2.2, 2.13.

General Comments:

The report summarizes recent work by BWIP, and as such the data contained in the report are of limited value. It does outline potential behavior of radionuclides, and packing materials. However, the test conditions reported do not simulate the range of conditions that may exist in a repository. The release calculations are one-dimensional, and severely limited by the assumptions made and the lack of any estimate of the impact of uncertainties in the data on the results of the calculation.

ORGANIZATION PRODUCING THE DATA

DOE/BWIP.

AUTHORS/REFERENCE

Wood, M. I., Relyea, J. F., Myers, J. and Apted, M. J., "The Near Field Waste Package Environment in Basalt and Its Effect on Waste Form Releases," RHO-BW-SA-331P, December 1983.

AVAILABILITY

Preprint for Civilian Radioactive Waste Management Information Meeting, December 1983.

KEY WORDS

Basalt water, solubility of radionuclides, hydraulic conductivity, basalt-bentonite backfill, one-dimensional release model.

DATE REVIEWED

April, 1984.

Abstract (Summary) From Reference:

A licensable waste package for a nuclear waste repository in basalt must control long-term radionuclide release to the host rock within approved limits as defined by regulatory criteria. Demonstration of satisfactory long-term performance requires experimental data that characterize radionuclide behavior in the expected geochemical waste package environment. Also, an accepted model is required to predict the long-term release of radionuclides from the waste package into the host rock. Experimental data are summarized that pertain to radionuclide behavior in the nuclear waste repository in basalt waste package (e.g., oxygen consumption, hydrothermal reactions, hydraulic conductivity). A simple, one-dimensional, composite media transport model is described that provides calculations of maximum radionuclide release rates and cumulative releases (over 10,000 yr) at the waste package packing material/host rock interface on a radionuclide-by-radionuclide basis. The model demonstrates that radionuclide release from the waste package is linearly dependent on the solubility values chosen for the radionuclides of interest. The calculated releases are compared with Nuclear Regulatory Commission and Environmental Protection Agency criteria as well as the available experimental data. The experimental data indicate that the maximum release rates and cumulative releases of the radionuclides technetium, neptunium, and plutonium from the waste package should satisfy Environmental Protection Agency and Nuclear Regulatory Commission requirements.

WASTE PACKAGE DATA REVIEW FORM

TYPE OF DATA

Calculated radionuclide solubilities in a basaltic water environment.

MATERIAL

Ni, Se, Zr, Pd, Sn, Sb, Sm, Eu, Pb, Th, U, Np, Pu, Am; reference basalt groundwater (Jones, 1982, RHO-BW-ST-37P).

CONDITIONS

Reactions and log K_{eq} values taken from compilation of Rai and Serne, Benson and Teague, and Phillips. Experimental data from Rai et al. (1982) and Nair et al. (1982).

Temperature 25°C; pH ~ 9.5, Eh from -0.6V to 0.0V (calculation for the nuclides Ni, Se, Sn, U, Np, Pu), presence of S^{-2} and HS^{-} at low Eh, or only SO_4^{2-} at all Eh for a single groundwater composition (Jones, 1982), solubility in chemical compositions of 29 natural Grande Ronde groundwaters.

METHODS OF ANALYSIS

Using ΔG_f° (298°K) for individual solids and aqueous species and with log K_{eq} for chemical equilibria, calculated most stable dissolved species under a set of environmental conditions.

AMOUNT OF DATA

Six graphical summaries of Log of concentration in mol/L vs Eh at 25°C. A table is given listing the solid controlling solubility, dominant solution species, range of computed solubilities in Grande Ronde waters (mol/L), solubility in the reference Grande Ronde groundwater (mol/L), compared to experimental solubilities for Ni, Se, Pb, Th, U, Np, Am (all at Eh = -0.3V).

UNCERTAINTIES IN THE DATA

Uncertainties are present because of the assumptions made (no radiolysis effects, single solubilities, single pH, low temperature). This makes these calculations of limited value. The second major source of uncertainty is in the thermodynamic data base used, i.e. the completeness and accuracy of the thermodynamic data. The authors also note that uncertainties will result if kinetics are slow or colloidal particles form.

The calculated results in general indicate the largest range in solubility as a function of Eh for Ni, Se, and Sn (15 to 20 orders of magnitude). The range in data over the 29 groundwaters is generally two to four orders of magnitude at Eh = -0.3V and increases as the Eh increases. Changes in the

dominant species in solution for Pu could result in 8 orders of magnitude in the solubility. For U, changes in the dominant specie in solution appear to result in a range of solubilities that differ by 12 orders of magnitude. Where experimental data are available for comparison, the agreement when it exists is usually within one to two orders of magnitude. In those cases where the calculated solubilities do not agree with experimental data, the difference is about 5 to 6 orders of magnitude.

DEFICIENCIES IN THE DATA BASE

Since the paper does not present the detailed calculations, no assessment of the adequacy of the assumed equilibria can be made. One major limitation, acknowledged by the authors, is in the completeness and accuracy of the thermodynamic data base. A second limitation is the assumption of constant pH and, for very near field, and the influence of soluble species from other barrier materials (e.g. corrosion products). Changes in repository water characteristics due to irradiation and temperature are not considered. As such, the data are of limited value for estimating or predicting the concentration of radionuclides in the water near the package.

APPLICABILITY OF DATA TO LICENSING [KEY DATA (), SUPPORTING DATA (X)]

Relationship to WP Performance Issues Already Identified:

The data addresses Issue Number 2.13 in the S.C.A. (NUREG-0960, Vol. 1, 1983).

General Comments:

These calculations indicate a wide variability in solubilities as a function of redox conditions, groundwater chemistry and speciation. As such, they show the need for experimental determination of solubilities under conditions more pertinent to a waste package. The data indicate the range in solubilities that might have to be considered for modeling and serve as a data base for comparing experimental with predicted data.

ORGANIZATION PRODUCING DATA

DOE/BWIP.

AUTHORS/REFERENCE

Early, T. O., Jacobs, G. K., Drewes, D. R., "Geochemical Controls on Radionuclide Releases from a Nuclear Waste Repository in Basalt, Estimated Solubilities for Selected Elements," RHO-BW-SA-282P, 1982

AVAILABILITY

Published.

KEY WORDS

Solubilities, basalt groundwaters, actinides, Eh, speciation.

DATE REVIEWED

April, 1984.

Abstract (Summary) From Reference:

Two basalt flows within the Grande Ronde Basalt at the Hanford Site in southeastern Washington are candidates for a high-level nuclear waste repository. In order to determine the anticipated rate of release and migration of key radionuclides from the repository, solubility controls must be determined. Solubilities, solids controlling solubility, and aqueous speciation in groundwater have been determined from available thermodynamic data for a variety of actinides and fission products. Groundwater compositions used include all available analyses from the selected radionuclides include hydroxides and hydrous oxides (Pd, Sb, Sm, Eu, Pb, Am), oxides (Ni, Sn, Th, Np, Pu), elements (Se, Pd, Sb), and silicates (Zr, U). Dominant soluble species include hydroxy complexes (Zr, Pd, Sn, Sb, Sm, Eu, Th, U, Np) and carbonate species (Ni, Sm, Eu, Pb, U, Np, Pu, Am). In addition to limitations in completeness and accuracy of thermodynamic data, solubility estimates of the radionuclides are sensitive to the following: (1) Eh and the degree of redox equilibrium, (2) temperature, (3) formation of metastable solid phases, and (4) coprecipitation. Eh effects have been evaluated for each radionuclide and are significant for Se, Pd, Sn, and possibly U and Np. Solubility estimates also have been calculated at ambient temperature ($\sim 55 \pm 5^\circ\text{C}$) for Grande Ronde basalts for those nuclides for which sufficient data exist. Effects of metastability and coprecipitation cannot be treated quantitatively but their contributions have been estimated in reference to available experimental data.

WASTE PACKAGE DATA REVIEW FORM

TYPE OF DATA

Graphs of the solubility of SrCl_2 ; $\text{SrCl}_2 \cdot \text{H}_2\text{O}$; $\text{SrCl}_2 \cdot 2\text{H}_2\text{O}$; $\text{SrCl}_2 \cdot 6\text{H}_2\text{O}$ (in weight percent) as a function of temperature for different systems: $\text{SrCl}_2 \cdot \text{H}_2\text{O}$; $\text{SrCl}_2 \cdot \text{NaCl} \cdot \text{H}_2\text{O}$; $\text{SrCl}_2 \cdot \text{KCl} \cdot \text{H}_2\text{O}$; $\text{SrCl}_2 \cdot \text{NaCl} \cdot \text{KCl} \cdot \text{H}_2\text{O}$. Most of the data presented was obtained by G. O. Assarsson (1953-1955). Original data is that gathered for the $\text{SrCl}_2 \cdot \text{NaCl} \cdot \text{H}_2\text{O}$ system.

MATERIAL

Salts: $\text{SrCl}_2 \cdot 6\text{H}_2\text{O}$, $\text{SrCl}_2 \cdot 2\text{H}_2\text{O}$, and NaCl .

TEST CONDITIONS

Original data were generated from determinations of the solubility of NaCl , $\text{SrCl}_2 \cdot 6\text{H}_2\text{O}$ and $\text{SrCl}_2 \cdot \text{H}_2\text{O}$ from 18°C to 115°C , using the technique of R. W. Potter and M. A. Clyne (1978) for measuring the solubility of highly soluble salts in aqueous media. The NaCl content was fixed at 0, 5, 10, 15 and 20 weight percent.

METHODS OF ANALYSIS

Data were fitted with equations using polynomial regression techniques. No statistical information was provided.

AMOUNT OF DATA

Number of data points is not specified. The presence of NaCl in solution reduces the SrCl_2 solubility by an amount dependent on the NaCl concentration and the amount of total dissolved solids is higher. Similar effects were reported by Assarsson for $\text{SrCl}_2 \cdot \text{KCl} \cdot \text{H}_2\text{O}$ and $\text{SrCl}_2 \cdot \text{NaCl} \cdot \text{KCl} \cdot \text{H}_2\text{O}$ systems.

UNCERTAINTIES IN THE DATA

Error bars on plots were not shown.

DEFICIENCIES IN THE DATA BASE

Solubilities of SrCl_2 in complex systems at temperatures higher than 100°C have not been measured.

APPLICATION OF DATA TO LICENSING

[Key Data (), Supporting Data (X)].

GENERAL COMMENTS

A significant portion (>30%) of the Sr contained in spent fuel and borosilicate silicate is predicted to be released to brine and bittern. This paper examines the behavior of Sr as SrCl_2 in the salt environment. Most of the data presented is compiled from other publications.

ORGANIZATION PRODUCING DATA

U. S. Geological Survey.

AUTHORS/REFERENCE

M. A. Clyne, I-Ming Chou and J. L. Haas, Jr., "SrCl₂ Solubility in Complex Brines," in Scientific Basis for Nuclear Waste Management III, J. G. Moore, Editor, New York, Plenum Press, 1981, pp. 499-506.

AVAILABILITY

Published proceedings.

KEY WORDS

Solubility, Strontium, brine, bittern, salt.

DATE REVIEWED

October 1984.

No abstract or summary was given.

gfs
11/6/84

WASTE PACKAGE DATA REVIEW FORM

TYPE OF DATA

- (a) General corrosion - penetration rate $\mu\text{m}/\text{yr}$
- (b) Load-elongation plot
- (c) Elongation and reduction of area versus strain rate

MATERIAL

- (a) 2 1/2% Cr, 1 1/2% Mo Fe-base alloy
- (b) 1 1/4% Cr, 1/2% Mo Fe-base alloy
- (c) Ductile cast iron (ASTM A536-77, Grade 60-40-18)
- (d) Cast mild steel (ASTM A27, Grade 60-30, AISI 1025 equivalent)
- (e) Wrought steel sheet AISI 1025
- (f) High purity iron
- (g) Permian Basin No. 2 brine.

TEST CONDITIONS

150°C maximum, up to seven months duration:

General corrosion:

- (a) Without radiation and with gamma radiation (1×10^5 rad/h and 2×10^3 rad/h)
- (b) Oxidic (1.5 ppm DO) and anoxic (0.5 ppm DO)
- (c) Flow-through autoclave 35 ml/h, pressure not specified.

Slow-strain-rate (SSR) tests for stress-corrosion cracking:

- (a) Oxidic Permian 2 brine
- (b) Control - in air
- (c) Strained to failure at rates of $10^{-4}/\text{s}$ and $2 \times 10^{-7}/\text{s}$.

METHODS OF ANALYSIS

No statistics given. Plots of data show a significant amount of scatter. A corrosion model is presented:

$$P = e^{(7.377 - \frac{3120}{T})} (15.5 + 1 + \frac{178}{1.2 \times 10^{-10} F + \frac{177A}{VR}})$$

where

P is the uniform penetration rate of carbon steel in $\mu\text{m}/\text{yr}$
T is in Kelvin
F is flow rate in ℓ/sec
V is volume in ℓ
A is area in cm^2
R is radiation dose rate in rad/h .

AMOUNT OF DATA

37 data points general corrosion (oxic and anoxic) - without irradiation.
21 data points general corrosion - with gamma irradiation.
6-8 data points for each of two strain rates.

UNCERTAINTIES IN THE DATA

Not stated.

DEFICIENCIES IN THE DATA BASE

- (a) Use of flow-through Permian Brine 2 is not justified.
- (b) Data for pitting corrosion was not provided.
- (c) Effect of alpha radiolysis on brine and corrosion was not considered.
- (d) These are short-term data.
- (e) Specimens were polished prior to testing.
- (f) Corrosion under equilibrium conditions was not studied - for example, salt rock should be present as part of the near-field chemical environment.

APPLICATION OF DATA TO LICENSING

[Key Data (X), Supporting Data ()].

GENERAL COMMENTS

This paper describes ongoing studies at PNL. Preliminary conclusions were given concerning the effect of radiation on the corrosion of carbon steel in flowing Permian Basin Brine 2 at temperatures ranging from 110-150°C. It appears that dose rates of $\approx 10^5$ rad/h enhanced corrosion by a factor of ≈ 6 and that dose rates of $\approx 2 \times 10^3$ rad/h showed little or no enhancement over the duration of the test. The iron alloys tested behaved similarly. The data presented will have to be supplemented by further testing in systems that better simulate the repository environment.

ORGANIZATION PRODUCING DATA

Pacific Northwest Laboratory.

AUTHORS/REFERENCE

Westerman, R. E. and others, "Evaluation of Iron-Based Materials," in The Scientific Basis for Nuclear Waste Management, VII, G. L. McVay, Editor, New York, Elsevier Publishing, 1984, pp. 427-436.

AVAILABILITY

Published Proceedings.

KEY WORDS

Corrosion, low-carbon steel, brine, stability, modeling, package.

DATE REVIEWED

September 1984.

gfs
10/1/84

ABSTRACT

Design studies for high-level nuclear waste packages for salt repositories have identified low-carbon steel as a candidate material for containers. Among the requirements are strength, corrosion resistance, and fabricability. The studies of the corrosion resistance and structural stability of iron-base materials (particularly low-carbon steel) are treated in this paper. The materials have been exposed in brines that are characteristic of the potential sites for salt repositories. The effects of temperature, radiation level, oxygen level and other parameters are under investigation. The initial development of corrosion models for these environments is presented with discussion of the key mechanisms under consideration.

WASTE PACKAGE DATA REVIEW FORM

TYPE OF DATA

Reference brine solution compositions, uniform corrosion rates (mm/yr) of 18 metals in four water compositions, pH vs temperature of three salt (brine) compositions corrosion rate w/r/t dissolved O₂ content (three Ti alloys), temperature effect on uniform corrosion rate of three Ti-alloys; effect of γ irradiation on corrosion rates of the four metals; corrosion rate Ti-50A vs time.

MATERIAL

Brine A and B, seawater, mild steel (1018), Corten A steel, Cr-Mo steel, Pb, Cu, cupronickel, 304-LSS, 316-LSS, Nitron-50 SS, Ebrite 26-1 SS, Monel 400, Incoloy 825, Inconel 600, Inconel 625, Hastelloy C-276, Zircaloy-2, Ti-50A, TiCode-12.

CONDITIONS

- (a) Initial screening tests: 29 days to six months accelerated tests at 25°C. Seawater, Brine B, Brine A, Brine A with 600 ppm O₂.
- (b) General Corrosion:
 - 1) Ti-50A: 30 days;
 - 2) Ti-50A: Brine A, temperatures \approx 225°C to \approx 50°C;
 - 3) Ti Alloys: 250°C, 30 days, Brine A and seawater; O₂ conc of 30 ppb or 450-500 ppm; second work in Brine A, 30 ppb O₂, T = 70°C, 150°C, 250°C, 30 days.
- (c) Corrosion Mechanisms:
 - 1) TiCode-12: pH = 1 concentrated NaCl; 200°C, three weeks.
 - 2) TiCode-12: 400 to 600°C in air.
- (d) Radiation Studies: 10⁵ to 10⁷ rad/h, seawater, T = 90°C, 49 or 87 days.
- (e) Environmental Cracking and Embrittlement (TiCode-12)
Tensile Tests: constant strain rate 10⁻⁴ to 10⁻⁷ sec⁻¹, 30 to 250°C, air, Brine A, Brine B or flowing oxygenated solution, prior γ irradiation in brine, heat treatment, weldments.
- (f) Physical/Mechanical Metallurgy:
Sensitized vs unsensitized (mill-annealed) TiCode-12, corrosion rates vs pH, HCl acid medium. Temperature not given.

METHODS OF ANALYSIS

- (a) Initial Screening Tests: weight change for general corrosion rates. Observation for leaching attack.

- (b) General Corrosion:
 - 1) Ti-50A: 30-day test at single temperature - weight loss.
 - 2) Ti-50A: Temperature dependence of corrosion rate; weight change.
 - 3) Ti-alloys: O₂ dependence and temperature dependence; weight change.
- (c) Corrosion Mechanisms: Electrochemical polarization techniques: Auger, ESCA, Raman:
 - 1) TiCode-12: 200°C, pH = 1, three weeks: Auger spectrum.
 - 2) TiCode-12: 400 to 600°C in air: Raman spectrum.
- (d) Radiation Studies: weight change
- (e) Physical and Mechanical Metallurgy: weight change.

AMOUNT OF DATA

- (a) Initial Screening Tests: Table of general corrosion rates in mm/yr; notation of observations on localized attack. Table of pH change vs temperature (25 to 270°C) for Brine A, Brine B and seawater.
- (b) Uniform Corrosion:
 - 1) Graphical presentation of corrosion rate (mm/yr) of Ti-50A vs time, four points, 30 days.
 - 2) Ti-50A: corrosion Brine A vs temperature - graphical presentation, with four points.
 - 3) Ti alloys (Ti-50A, TiCode-12, Ti-0.2% Pd); 12 data points (seven each for two types of water) for effect of two O₂ concentrations. Nine data points for three temperatures in Brine A at 30 ppb O₂.
- (c) Corrosion Mechanisms:
 - 1) TiCode-12; pH = 1 concentrated brine; 200°C; three weeks; graphical presentation; Auger spectrum
 - 2) TiCode-12; 400-600°C in air; Raman spectrum of surface oxide.
- (d) Radiation Studies: Four metals (Ti Code 12, 304L, 1018 steel and Inconel 625), 14 corrosion rates (mm/yr) in various waters, dose rates (either 10⁵ or 10⁷ rads/h) and time.
- (e) Environmental Cracking and Embrittlement.
 - 1) Graphical presentation of reduction of area, ultimate tensile strength and elongation vs strain rate (ratio of properties in Brine B and air).
- (f) Physical and Mechanical Metallurgy: Graphical presentation of corrosion rates (mm/yr) vs pH for sensitized and unsensitized TiCode-12, four points for each material. HCl concentration varies from ±1.6 M to 0.4 M.

UNCERTAINTIES IN THE DATA

- (a) Initial Screening Tests: No indications given of spread in corrosion rates under identical conditions. Where pitting etc., observed, no indication of the magnitude. Most data at a single temperature, pressure and time (28 days). No indication of spread in pH values at given temperature for each solution. The spread in pH values with composition of solution at given temperature can be as much as 2 to 3 pH units.
- (b) Uniform Corrosion:
- 1) Ti-50A general corrosion rate - no point scatter; scatter in measured rate from $t = 1$ day to 30 days. May be as much as $\approx 3 \times 10^{-3}$ mm/yr based on differences at $t = 15$ days and $t = 20$
 - 2) Ti-50A: uniform corrosion vs temperature: no scatter associated with individual points. Rate change (mm/yr $\times 10^3$). Two orders of magnitude change over temperature range studied.
 - 3) Ti-50A, Ti-12, Ti-0.2% Pd: corrosion rate as function of O_2 concentration in Brine A and seawater at $250^\circ C$ and with temperature in Brine A at 30 ppb O_2 : No indication of variability of each data point; only two, extreme O_2 concentrations studied. For temperature studies only one O_2 (≈ 30 ppb) studied at three temperatures.
- (c) Corrosion Mechanisms:
- 1) TiCode; pH = 1 NaCl solution; $200^\circ C$: three weeks: represents analysis of changes under limited set of conditions.
 - 2) TiCode-12; $400-600^\circ C$ (in air): Single spectrum - work done primarily to investigate usefulness of technique for studying corrosion mechanisms.
- (d) Radiation Studies: No individual point scatter indicated. Order of magnitude increase for TiCode-12 in corrosion rate in Brine A with factor of ≈ 2 increase in total dose. Very little increase in seawater corrosion with total dose. Order of magnitude difference in rates at highest total dose between Brine A and seawater (seawater $<$ Brine A rate). For 304L Stainless Steel in Brine A a factor of 200 increase in the corrosion rate for factor ≈ 2 increase in total dose. Only one temperature studied; increase in H_2 levels noted.
- (e) Environmental Cracking and Embrittlement:
- 1) Changes in mechanical properties vs strain rate: data are only "representative" of large data set - no errors or uncertainties indicated from sample to sample etc. Ratio in brine/air > 1 , but scatter not indicated to show what the uncertainty may be.
 - 2) Physical and Mechanical Metallurgy: Corrosion rates are given in highly acidic medium; temperature is not indicated (boiling?). Data very atypical of anticipated repository conditions. Data do, however, indicate an almost factor of two increase in general corrosion rate between sensitized and unsensitized material.

DEFICIENCIES IN THE DATA BASE

No indication is given of replicate reproducibility, i.e. point scatter. The data represent single component tests under a limited range of conditions some of which are not representative of anticipated conditions. Radiation studies are limited and while a fairly large temperature range is investigated, normally only three or four discrete temperatures are studied.

ORGANIZATION PRODUCING DATA

DOE/Sandia National Laboratory.

AUTHORS/REFERENCE

Molecke, M. A. and others, "Sandia HLW Canister/Overpack Studies Applicable for a Salt Repository," SAND81-1585, October 1981.

AVAILABILITY

Published.

KEY WORDS

Salt, corrosion, canister, brine, commercial wastes.

DATE REVIEWED

May 1984.

ABSTRACT

An experimental program to develop candidate materials for use as high-level waste (HLW) overpacks or canisters in a salt repository has been in progress at Sandia National Laboratories since 1976. The main objective of this program has been to provide a waste package barrier having a long lifetime in the chemical and physical environment of a repository. This paper summarizes the recent corrosion and metallurgical results for the prime overpack material TiCode-12 in the areas of uniform corrosion (extremely low rate and extent), local attack, e.g. pits and crevices (none found), stress corrosion cracking susceptibility (no significant changes in macroscopic tensile properties detected) and hydrogen sorption/embrittlement effects (testing still in process), effects of gamma irradiation in solution (still in process), and sensitization effects (still in process). Previous candidate screening analyses on other alloys and recent work on alternate overpack alloys are reviewed. All phases of these interrelated laboratory, hot-cell, and field experimental studies are described.

BLANK PAGE

WASTE PACKAGE DATA REVIEW FORM

TYPE OF DATA

Initial and final brine composition following a "multicomponent" test, analysis and depth of glass surface alteration product, pre- and post-test analysis of TiCode-12, mechanical test results on TiCode-12.

MATERIAL

PNL-76-68 glass (w/3.5% ^{238}U ; S/V = 0.3 cm^{-1}); 304L stainless steel canister (1.3-mm thick), TiCode-12 (1-mm thick) with welds; 30% by weight bentonite-clay/70% sand; saturated brine; rock salt "container," Inconel 600 autoclave liner.

CONDITIONS

PNL-76-68 glass encased in 304L stainless steel canister; overpacked with TiCode-12 canister. Simulated waste package partially immersed in brine and partially immersed in sand-bentonite; entire system placed in a "machined rock salt container"; system flushed with He and pressurized to 13 MPa. Autoclave heated to 250°C for total of 95 days.

METHODS OF ANALYSIS

- (a) Brine leachate: Inductively coupled plasmon spectroscopy and ion chromatography.
- (b) Glass waste form: optical and electron microprobe analysis.
- (c) TiCode-12 overpack: weight loss, SEM, Auger, X-ray diffraction tensile strength.
- (d) 304L stainless steel: EDAX analysis, SEM analysis and optical microscopy.
- (e) Autoclave liner (Inconel 600): SEM
- (f) Bentonite/sand backfill: X-ray diffraction; electron diffraction/transmission microscopy, X-ray fluorescence.

AMOUNT OF DATA

1. Brine leachant: Initial brine leachant composition, composition following mixing with backfill at room temperature; composition following 95 days of testing (13 cations; 4 anions; pH and concentrations of U-238 in mg/L) no indication of replicate uncertainties, no data on replicate tests.

2. Glass waste form: Primarily qualitative surface alteration depth after 95 days (0.8-0.1 mm) observation of surface spalling, partial analysis of major oxides in alteration layer (MgO_2 , SiO_2 , Fe_2O_3 , Na_2O and ZrO_2); observation of fractures parallel to glass, 304-L canister surface; corrosion at glass-metal interface.
3. TiCode-12: Two uniform corrosion rates (mm/yr) for abraded and unabraded samples: SEM analysis showed no localized corrosion of base metal and weld; surface film (1.2 μm) showed presence of 10 species including Cl and ^{238}U ; no Ti; X-ray diffraction of film and surrounding area indicate precipitate of uranium oxide and magnesium silicate; presence of titanium hydride throughout specimen; post-test H_2 levels of $\approx 600-700$ ppm: percent change as measured in percent elongation at 20°C and 175°C and yield strength at 20°C and 175°C.
4. 304L stainless steel: Qualitative observations of surface film and general corrosion around canister; particularly at welds; observation of cracking in both base and weld metal.
5. Autoclave liner: Qualitative observations: 70% of surface covered with colored films; evidence of pitting.
6. Backfill material: No numerical data - qualitative observation.
 - a) Unglycolated samples: formation of a non-interlayered second clay form
 - b) Glycolated samples: formation of a second smectite clay observed.

UNCERTAINTIES IN THE DATA

1. Brine leachant: No indication is given of uncertainties in a single measurement for a set of conditions. Replicate tests were not run. Largest changes are observed for Na^+ , Mg^{+2} , B^{+2} , Zn^{+2} , Mn^{+2} , SO_4^{-2} and pH between pre-test and post-test brines.
2. Glass waste form: No indication of variation in surface film composition given or a comparison with surface film formed during "single" component tests. Data qualitative in nature.
3. TiCode overpack: No indication of uncertainties in estimates of uniform corrosion rates. Factor of 12 increase in H_2 content between pre- and post-tested samples; 13% increase in elongation ongoing from 20° to 175°C. Spread in decrease of yield strength (13-34%) at either temperature (factor ≈ 3).
4. 304-L stainless steel: Only qualitative data.
5. Backfill: Identification of major specie changes - no quantitative data.

DEFICIENCIES IN THE DATA

The data and qualitative information reported in this report represent information on a single "package" test. Replicate testing would help establish the uncertainties in the data. In addition, this work was conducted in the absence of radiation. To further reduce or define uncertainties and the changes occurring in whole package interaction tests, replicate tests run as a function of time and in a radiation field would be advantageous. Temperature is yet another variable that should be included in most component tests.

APPLICATION OF DATA TO LICENSING [KEY DATA (), SUPPORTING DATA (X)]

General Comments:

Evaluation performed on a borosilicate glass waste form doped with fission products and U, surrounded by a T304L stainless steel/TiCode-12 container/overpack system, a bentonite/sand backfill, excess brine and a salt host rock. The components were all breached prior to test to determine synergistic effects in a 95-day, 250°C test in an autoclave.

The brine pH decreased from 6.8 to 3.8 after test which is stated to be a result of reactions between $MgCl_2$ and SiO_2 and aluminosilicates. It could also be due to release of HCl from the salt during heating. An analysis of the glass surface showed the presence of SiO_2 , MgO_2 , Fe_2O_3 , Na_2O , and ZrO_2 plus small amounts of Zn, U, Nd, Ni and Cr. The TiCode-12 container contained TiH_2 platelets throughout the thickness, omega phase in the beta phase, and Ti_2Ni on α/β interfaces. The H_2 content increased from 50 to 600-700 ppm. At this level, embrittlement effects are likely, as shown by other SNL and BNL work. The 304L stainless steel container suffered extensive general corrosion, particularly at welds. Brine interaction caused significant changes in the bentonite clay.

These data are of significant value in assessing synergistic interactions between waste package components and address mainly early waste package failure at high temperature. It has been shown that many of the effects are similar to single component tests and thus help validate the latter.

ORGANIZATION PRODUCING THE DATA

DOE/Sandia National Laboratory and Battelle Pacific Northwest Laboratory.

AUTHORS/REFERENCE

Molecke, M. A. and others "PNL-Sandia HLW Package Interaction Tests: Phase One," Scientific Basis for Radioactive Waste Management, Materials Research Society, Volume 6, North-Holland, NY, 1982, pp. 337-45.

AVAILABILITY

Published.

KEY WORDS

Waste package tests, component interactions, hydrothermal conditions,
brine, salt repository.

DATE REVIEWED

May 1984.

ABSTRACT

The first phase of a complex high-level waste (HLW) package interactions test in a salt environment has been completed. The test system consisted of PNL 76-60 HLW glass (loaded with inactive fission products and ^{238}U) surrounded by a stainless steel waste canister, a TICOD-12 overpack, a bentonite/sand backfill, excess brine leachant, and a bedded rock salt container, all held within a 19-liter autoclave. All components were physically compromised in order to force wasteform-barrier-salt interactions to occur during this 95-day, 250°C overtest. Analyses of leachant, wasteform, and all barrier surfaces were performed. Test data included the synergistic effects between barriers and confirmed previous analyses of simpler systems. The glass wasteform exhibited some surface etching but was not dissolved to any significant degree. The TICOD-12 overpack showed minimal uniform corrosion and no localized attack. Observed mineralogical alteration of the backfill was minimal.

BLANK PAGE

WASTE PACKAGE DATA REVIEW FORM

TYPE OF DATA

- (a) Compositions of saturated salt brines at 25°C in ppm for Na⁺, K⁺, Ca²⁺, Mg²⁺, Sr²⁺, Zn²⁺, Cl⁻, SO₄²⁻, HCO₃⁻, Br⁻, BO₃³⁻, and S²⁻ for Permian Basin Cycles 4 and 5 and Paradox Basin Cycle 6.
- (b) pH values versus accumulated gamma dose (in rads) and versus annealing temperature for Harshaw NaCl and Permian Basin Cycle 4 rock and brine.
- (c) pH values and gas composition of Cycle 4 synthetic Permian brine doped with ²⁴⁴Cm to study alpha radiolysis effects.

MATERIAL

Permian Basin Cycle 4 and 5 rock and brine. Paradox Basin brine.
Harshaw NaCl crystals.

TEST CONDITIONS

The temperatures at which the experiments were carried out is not specified. The composition of the brines is given for 25°C. Gamma irradiations between 10⁸ and 10¹⁰ rad were performed on solutions of 0.1 g salt in 1.0 ml deionized water. Annealing temperature of rock salt prior to further studies had a maximum of 400°C.

METHODS OF ANALYSIS

Not stated. No statistical information given.

AMOUNT OF DATA

- (a) 25 data points for pH versus accumulated gamma dose ranging from 10⁸ to 10¹⁰ rad.
- (b) 12 data points for pH versus annealing temperature.
- (c) Composition of six cations and six anions in brine.
- (d) Four data points each for alpha radiolysis studies:
 - 1. pH
 - 2. gas composition (%): H₂, H₂O, N₂, O₂
 - 3. Nitrate, mg N/l

UNCERTAINTIES IN THE DATA

Statistics not given. Temperatures not stated.

DEFICIENCIES IN THE DATA BASE

See General Comments.

APPLICATION OF DATA TO LICENSING

[Key Data (), Supporting Data (X)].

GENERAL COMMENTS

This is a review of some studies dealing with the alteration of brines by radiolysis. The statement is made that if Cl₂ does not escape the system, then the solution pH will be nearly neutral. Graphs showing pH versus total gamma dose only consider the range of pH =7-14. The presence of gases such as N₂ and the formation of nitric acid are not discussed in regard to effect on the pH of the solution. An evaluation needs to be performed to determine the identity and contact of significant radiolysis products and what the significant dissociation reactions are that control pH over the range of anticipated temperatures.

ORGANIZATION PRODUCING DATA

Pacific Northwest Laboratory.

AUTHORS/REFERENCE

Pederson, L. R. and others, "The Expected Environment for Waste Packages in a Salt Repository," in The Scientific Basis for Nuclear Waste Management, VII, Vol. 26, G. L. McVay, Editor, New York, Elsevier Publishing, 1984, pp. 417-426.

AVAILABILITY

Published Proceedings.

KEY WORDS

Near-field, salt, brine, pH, radiolysis, gamma, alpha.

DATE REVIEWED

September, 1984.

ABSTRACT

This paper discusses results of recent efforts to define the very near-field (within approximately 2m) environmental conditions to which waste packages will be exposed in a salt repository. These conditions must be considered in the experimental design for waste package materials testing, which includes corrosion of barrier materials and leaching of waste forms. Site-specific brine compositions have been determined, and "standard" brine compositions have been selected for testing purposes. Actual brine compositions will vary depending on origin, temperature, irradiation history, and contact with irradiated rock salt. Results of irradiating rock salt, synthetic brines, rock salt/brine mixtures, and reactions of irradiated rock salt with brine solutions are reported.

gfs
10/1/84

BLANK PAGE

WASTE PACKAGE DATA REVIEW FORM

TYPE OF DATA

Estimates for total mass, in kg, of radiation-induced Na-metal colloid that would be produced in natural rock salt from the WIPP site by gamma-ray irradiation for four packages at various times after emplacement.

MATERIAL

Packages in WIPP salt are: CHLW-2.16 kW, CHLW-9.5 kW, SF-0.55 kW, SF-3.3 kW.

TEST CONDITIONS

Experimental irradiation data previously reported for WIPP salt were used to estimate amount of Na-metal colloid formation. See AMOUNT OF DATA Section for details of irradiation conditions.

METHODS OF ANALYSIS

Not specified. No statistical information was given.

AMOUNT OF DATA

Radiation-induced colloid growth curves previously developed for WIPP salt at accumulated doses ranging from 10^6 to $1-2 \times 10^8$ rad at various dose rates of 3×10^7 rad/h, 6×10^7 rad/h, and 1.2×10^8 rad/h were used to generate estimates of quantities of colloidal sodium (in kg) produced as a function of distance (1-15 cm) from the following packages: CHLW-2.16 kW, CHLW-9.5 kW, SF-0.55 kW, SF-3.3 kW as a function of time (10, 25, 50, 100, 200, 300, 400, 500 years).

UNCERTAINTIES IN THE DATA

Author states that information needed to make reliable estimates of radiation damage in rock salt surrounding radioactive waste canisters does not exist at this time. The data used in the estimates were obtained at dose rates orders of magnitude higher than those anticipated in a repository and at accumulated doses orders of magnitude smaller than those anticipated in a repository.

DEFICIENCIES IN THE DATA BASE

These preliminary data were obtained for one type of salt. Measurements of colloid levels on a statistically reliable number of different salt samples from each potential repository site need to be made. The effects of high accumulated dose to $1-2 \times 10^{10}$ rad, low dose rate, and straining of salt before and during irradiation, need to be assessed. The amount and effects of alpha and beta radiation at a salt-waste interface over long periods of time must also be determined.

APPLICATION OF DATA TO LICENSING

[Key Data (), Supporting Data (X)].

GENERAL COMMENTS

These estimates for production of colloidal sodium are based on severely-limited data from WIPP salt. The amount of colloidal sodium produced is very dependent on specific salt characteristics, e.g. impurities and voids.

The radiation induced F-center and colloid growth rates and induction period properties are strong functions of irradiation temperature, gamma dose rate, the strain state of the salt and other factors. For WIPP salt, at a single dose rate, the F-center plateau is highest at 90°C and decreases monotonically as the irradiation temperature increases. The F-center growth rate increases with crystal strain. The colloid growth rate is low at 90°C, increases with increasing temperature to a maximum at 150-175°C and, decreases to negligible level at 250-300°C. The induction period is $>10^4$ sec at 100°C, decreases to a minimum <3000 sec at 150°C and is 10^4 sec at 250°C. The colloid formation dose rate dependence is unusual. As the dose rate diminishes, the colloid growth rate increases and the induction period decreases. In other words low gamma dose rates are more effective in producing colloidal Na than high dose rates. For the estimates described below, the data used were obtained at dose rates 10^3 to 10^4 times larger than those expected from canisters ($1-2 \times 10^4$ rad/h).

Strain effects are likely to control the total colloid produced in a repository. Repository salt will be subject to non-isotropic strain, starting with mining and coring operations and continuing until isotropic equilibrium is established. Straining salt prior to irradiation increases the colloid formation rate and decreases the induction period, for strains up to roughly 10 percent. Apparently studies on strains applied during irradiation have not been attempted. Presumably, straining NaCl during irradiation will cause large increases in the F-center and colloid formation rates.

ORGANIZATION PRODUCING DATA

Brookhaven National Laboratory.

AUTHORS/REFERENCE

Levy, P. W. and J. A. Kierstead, "Very Rough Preliminary Estimates of the Colloidal Sodium Induced in Rock Salt by Radioactive Waste Canister Radiation," in The Scientific Basis for Nuclear Waste Management, VII, Vol. 26, G. L. McVay, Editor, New York, Elsevier Publishing, 1984, pp. 727-734.

AVAILABILITY

Published proceedings.

KEY WORDS

Salt, colloidal sodium, radiolysis, gamma radiation.

DATE REVIEWED

September, 1984.

gfs
10/4/84

ABSTRACT

Very rough estimates have been made of the total amount, the formation rate and spatial distribution of the Na metal colloid particles induced in rock salt adjacent to four types of radioactive waste canisters. A number of extrapolations were required. Salt immediately adjacent to a lightly shielded, 2.16 kW, high level waste canister could be converted entirely to colloidal Na (and presumably chlorine gas) in 200-400 years. The total Na metal formed will be 250-300 kg. A heavily shielded, 3.3 kW, spent fuel canister will convert roughly 0.3 percent of the salt at the canister surface to colloidal Na and the total sodium metal will be roughly 0.5 kg. Even at the lowest colloid levels the Na metal formed should greatly influence interactions between canisters and the surrounding salt, particularly if brine enters.

WASTE PACKAGE DATA REVIEW FORM

TYPE OF DATA

No original data is provided. This report comments on the validity of the conclusions reached by Jenks and Claiborne as a result of these calculations of expected brine in-flow to a nuclear waste repository in salt by discussing uncertainties and errors in input.

MATERIAL

Domal and bedded salt formations.

TEST CONDITIONS

Not applicable.

METHODS OF ANALYSIS

Not applicable.

AMOUNT OF DATA

Not applicable.

UNCERTAINTIES IN THE DATA

According to Roedder and Chou, the conclusions reached by Jenks and Claiborne as a result of calculations of expected brine in-flow to a nuclear waste repository in rock salt are not truly conservative when the observational and theoretical bases are considered. A truly valid calculation is not possible at this time, as there are too many uncertainties, but Roedder and Chou suggest that the in-flow calculations of Jenks and Claiborne are low, perhaps by several orders of magnitude, as a result of a combination of the following:

1. Assumption of a value of 0.19 wt.% H₂O for bedded salt, whereas the true in situ value is almost certainly much higher, perhaps by a factor of 10 or more.

2. Assumption of a Soret coefficient ($-\sigma$) of 0.0004 to 0.005°C⁻¹ between 50° and 200°C, whereas the true value is almost certainly much higher, perhaps even greater than 0.01°C⁻¹.

3. Assumptions about the existence, and magnitude, of a threshold value for the thermal gradient, below which migration is assumed to cease.

4. Assumption that rock salt formations of repository size can be considered to be isotropic and uniformly extremely low in permeability.

5. Assumption that the original location of the water is as intracrystalline inclusions, whereas some and possibly much of the water in any given salt bed is more likely to be already on halite grain boundaries, as intercrystalline fluid inclusions and hydrous mineral impurity grains.

6. Assumption that fluid migration through a polycrystalline, polymineralic rock salt mass can be modelled mathematically as though it were a large single crystal of salt.

DEFICIENCIES IN THE DATA BASE

See uncertainties.

APPLICABILITY OF DATA TO LICENSING

[Key Data (X), Supporting Data ()].

GENERAL COMMENTS

The amount of water reaching a waste package in a salt repository is a critical factor to consider during the breach of containment period. It appears that much uncertainty exists concerning this amount. During the controlled release period, the amount of water reaching the package may not be as critical if it can be shown that the water will not be able to migrate to the accessible environment in 10,000 years.

ORGANIZATION PRODUCING DATA

U. S. Geological Survey

AUTHORS/REFERENCE

USGS-OFR-82-1131, "A Critique of 'Brine Migration in Salt and Its Implications in the Geologic Disposal of Nuclear Waste,' Oak Ridge National Laboratory Report 5818, by G. H. Jenks and H. C. Claiborne, "E. Roedder and J-Ming Chou, U. S. Geological Survey.

AVAILABILITY

NTIS

KEY WORDS

Brine, salt, waste package, migration, accumulation.

DATE REVIEWED

October 1984

as
1/21/85

A critique of "Brine migration in salt and its implications in the geologic disposal of nuclear waste," Oak Ridge National Laboratory Report 5818, by G.H. Jenks and H.C. Claiborne

by Edwin Roedder and I-Ming Chou
U.S. Geological Survey, 959 National Center, Reston, VA 22092

ABSTRACT

Jenks and Claiborne in 1981 published a 164 page "...comprehensive review and analysis of available information relating to brine migration in salt surrounding radioactive waste in a salt repository." Calculations are presented in that publication, that are called "reasonably conservative," to show that the rates and total volumes of brine expected to migrate into a given emplacement hole in bedded salt over the first 100 years are sufficiently low (e.g., <250 ml/year) that they are of relatively minor concern in the engineering design of a nuclear waste repository. We believe that because the values used for the major input parameters are either nonconservative, selected numbers, or are based on inadequate data, the results of these calculations are invalid. Neither we nor others are able to make a truly valid calculation at this time as there are too many uncertainties, but we show that conservative estimates should be larger, and perhaps two orders of magnitude larger, than those made by Jenks and Claiborne.

INTRODUCTION

One of the factors in establishing the safety, cost, and engineering complexity of any proposed nuclear waste repository in salt centers on the possible migration of brine from the salt into the immediate vicinity of the waste package. Jenks and Claiborne (1981; hereafter abbreviated J-C) have presented a "comprehensive review and analysis of available information relating to brine migration in salt surrounding radioactive waste in a salt repository." The major conclusion of this report, for most potential users, lies in the very low (and hence readily manageable) values that they calculate for the possible rate of inflow of water into a canister chamber (<250 ml/yr.). Although some caveats are mentioned in their report, this value (stated to be "reasonably conservative"), will obviously be used in discussions of the feasibility of such repositories.

This low value is based, however, on a series of assumptions and choices of data from the literature, many of which we show are invalid to some degree, and which taken together have the net effect of greatly reducing the calculated rate of inflow, thus making the result far from "conservative." The most important of these assumptions and choices pertain to: 1) the water content to be used in the calculations; 2) the rate of migration of fluid inclusions through single salt crystals; and 3) the behavior of migrating fluid inclusions when they intersect a grain boundary. Although we take similar issue with numerous other points made by J-C, and have so informed them in the past, the following critique centers on the nature and validity of the assumptions in these three key areas.

It is not now possible to calculate the expected rate of inflow with any confidence, as there are far too many uncertainties and unknowns.

WASTE PACKAGE DATA REVIEW FORM

TYPE OF DATA

For the determination of the composition of the rock beds, gamma-ray scattering to locate differences in rock density and neutron scattering to locate hydrogen nuclei in the rock were used. Chemical analyses data for Ca^{2+} , Mg^{2+} , Na^+ , K^+ , SO_4^{2-} , and Cl^- were tabulated for Palo Duro brine/inclusions and WIPP Brines A and B and inclusions.

MATERIAL

Palo Duro salt beds and brine/inclusions.

TEST CONDITIONS

Not stated.

METHODS OF ANALYSIS

Not stated.

AMOUNT OF DATA

- (a) Percentages of anhydrite, clay, and halite for one salt bed in depositional Cycle 4, Lower Andres Formation, Palo Duro Basin, Texas, J. Friemel No. 1 drill hole.
- (b) Composition of fluid inclusion from above salt in ppm for six ions was determined.

UNCERTAINTIES IN THE DATA

Not stated.

DEFICIENCIES IN THE DATA BASE

- (a) No statistical information is provided.
- (b) Composition of brine/inclusions are initial.
- (c) The radiation alteration of the environment is not considered in the alteration of the brine contacting the package.
- (d) CaSO_4 will change to gypsum $\text{CaSO}_4 \cdot 2\text{H}_2\text{O}$. This is soluble in acidic media. The effect of the change in environment on solubility is not considered.

APPLICATION OF DATA TO LICENSING

[Key Data (), Supporting Data (X)].

GENERAL COMMENTS

It is stated that the chemical conditions around the waste package may be significantly altered by the anhydrite in Palo Duro salt. It is proposed that anhydrite will form a protective coating on the canister. CaSO_4 can be corrosive to carbon steel. Anhydrite when it becomes hydrated will form gypsum. Gypsum is soluble in acids. Any change in pH that produces acidic conditions will cause the dissolution of gypsum. The solubility behavior of CaSO_4 in a groundwater system may be significantly different than solubility in a pure water system. It must also be noted that there can be mutual interference effects on solubility. If NaCl and CaSO_4 are dissolved in water together, the solubility of CaSO_4 becomes independent of temperature and is dependent on the NaCl concentration (H. J. Neumann, B. Paczynska-Lahme and D. Severin, Composition and Properties of Petroleum, New York, Halsted Press, 1981). This leads to the general observation that one must consider the effect of the altered environment on the package. The definition of initial conditions is of importance, but behavior of the package will depend on the change in conditions arising from the presence of the package in the environment.

ORGANIZATION PRODUCING DATA

Battelle Memorial Institute.

AUTHORS/REFERENCE

Hubbard, N., D. Livingston and L. Fukui, "The Composition and Stratigraphic Distribution of Materials in the Lower San Andres Salt Unit 4," in The Scientific Basis for Nuclear Waste Management, VII, G. L. McVay, Editor, New York, Elsevier, pp. 405-415.

AVAILABILITY

Published Proceedings.

KEY WORDS

Brine, bedded salt, Deaf Smith, anhydrite.

DATE REVIEWED

September 1984.

gfs
10/1/84

ABSTRACT

The salt bed in depositional cycle 4 of the Permian Lower San Andres Formation, Palo Duro Basin, Deaf Smith County, Texas consists of massive salt interlayered with discrete bands and beds of anhydrite and claystone. The massive salt consists of about 90% halite, with 7% anhydrite and 3% clays disseminated in and among the halite crystals.

The halite in this salt bed contains fluid inclusions filled with a (Na, K, Mg)Cl brine, with an average Mg concentration of about 50,000 mg/liter. The anhydrite in the salt will saturate the brines in CaSO_4 , which in turn may coat the waste package with anhydrite because of the retrograde solubility of CaSO_4 . This may increase waste package lifetime to failure by corrosion.

BLANK PAGE

WASTE PACKAGE DATA REVIEW FORM

TYPE OF DATA

No test data are provided. The results of WAPPA for the following are presented in graph form: temperatures at salt-overpack interface, stress boundary conditions, dose rates from centerline CHLW and SF packages, brine migration inflow rates per canister, penetration rate, failure thickness, accumulated brine.

MATERIAL

Not applicable.

TEST CONDITIONS

Not applicable.

METHODS OF ANALYSIS

Not applicable.

AMOUNT OF DATA

WAPPA results for CHLW and SF PWR waste packages in Palo Duro (PD) bedded salt, Gibson Dome (GD), and Richton Dome (RD) are presented in graphical form.

Boundary Temperatures: Peak temperatures are reached within one to 20 years after burial. They are higher in domal salt than bedded salt. The highest temperature for a SF PWR package is 170°C; for a CHLW package is 270°C.

Boundary Stresses: Assumed normal stress boundary conditions (vertical and radial) at CHLW waste package midplane within 20 years of burial range from 13 MPa to 36 MPa.

Radiation Fields: A SF PWR package at burial generates a radiation dose rate of 3-4 rad/h at the salt-overpack interface in a non-corroded overpack. Initially the intact overpack shields the canister metal-brine interface from two orders of magnitude higher radiation fields. A CHLW package at 100 years generates a radiation dose rate of <3 rad/h at the salt-overpack interface in a non-corroded overpack.

Brine Migration Rate: The brine migration inflow rates per canister are the greatest immediately after burial and range from ≈ 2 l/yr to ≈ 95 l/yr. At 100 years after burial, the rates range from ≈ 0.13 l/yr to ≈ 1.3 l/yr.

Accumulated Brine Volumes: The maximum accumulated volume of brine at a SF PWR waste package in Richton Dome is ≈100 l before corrosion. The maximum accumulated volume of brine at a CHLW package in Palo Duro Basin is ≈900 l before corrosion. But it is proposed that all of the brine reaching the package is immediately used up by reaction with the overpack.

Corrosion and Failure of the Waste Package: The wall thickness at which the CHLW package in Palo Duro Basin would be crushed (i.e. failure thickness) is ≈10 cm. Graphs are presented to show loss of thickness due to corrosion in comparison to failure thickness.

The waste package is not expected to fail from corrosion for thousands of years in the Richton Dome with low Mg thermally-migrating brine. In any of the salt formations, the low Mg dissolution brines used in intrusion scenarios are not expected to cause the waste package to fail unless pitting and stress corrosion cracking cause much greater penetration of the overpack than uniform corrosion.

In the bedded salt formations, with high Mg thermally-migrating brines it is necessary to take credit for the ability of the overpack to react with and use up the water in the brine to prevent package failure within 1,000 years after burial. If the brine is uniformly distributed over the package surface, the brine will be used up before corrosion proceeds to package failure. However, more detailed modeling of the emplacement procedure and early package history will be necessary to determine whether the brine will actually be unevenly distributed. For example, 2.5 times the even-distribution corrosion could fail the package within 300 years. These constraints are based on preliminary corrosion data and on conservative stress analyses in ONWI-438.

UNCERTAINTIES IN THE DATA

Results of the WAPPA code will depend on assumptions made in the code and input. Uncertainties in results were not provided.

DEFICIENCIES IN THE DATA BASE

See GENERAL COMMENTS. Identification of deficiencies would require evaluation of the WAPPA code and details of input into the code. These results for package failure were based on preliminary data for uniform corrosion. The effects of alpha and beta radiation dose rates were not discussed.

APPLICATION OF DATA TO LICENSING

[Key Data (), Supporting Data (X)].

GENERAL COMMENTS

The near-field conditions predicted by the WAPPA code are based on unsubstantiated assumptions and conceptual waste packages. Graphs are presented with little explanation of the significance of the results. Undefined terminology and different time periods considered in the presentation of the information make it very difficult to assimilate and assess the results.

ORGANIZATION PRODUCING DATA

Office of Nuclear Waste Isolation.

AUTHORS/REFERENCE

Jansen, G., "Performance Analysis of Conceptual Waste Package Designs in Salt Repositories," in The Scientific Basis for Nuclear Waste Management, VII, Vol. 26, G. L. McVay, Editor, New York, Elsevier Publishing, 1984, pp. 445-454.

AVAILABILITY

Published Proceedings.

KEY WORDS

Salt, Palo Duro Basin, corrosion, brine, magnesium, WAPPA, waste package, failure analysis.

DATE REVIEWED

September 1984.

gfs
10/1/84

ABSTRACT

A performance analysis of commercial high-level waste and spent fuel conceptual package designs in reference repositories in three salt formations was conducted with the WAPPA waste package code. Expected conditions for temperature, stress, brine composition, radiation level, and brine flow rate were used as boundary conditions to compute expected corrosion of a thick-walled overpack of 1025 wrought steel. In all salt formations corrosion by low Mg salt-dissolution brines typical of intrusion scenarios was too slow to cause the package to fail for thousands of years after burial. In high Mg brines judged typical of thermally migrating brines in bedded salt formations, corrosion rates which would otherwise have caused the packages to fail within a few hundred years were limited by brine availability. All of the brine reaching the package was consumed by reaction with the iron in the overpack, thus preventing further corrosion. Uniform brine distribution over the package surface was an important factor in predicting long package lifetimes for the high Mg brines.

WASTE PACKAGE DATA REVIEW FORM

TYPE OF DATA

Shielding calculations (DOT-IV and FALSTF codes) for a 10-year old PWR fuel assembly which result in the prediction of gamma dose rates as a function of position relative to the assembly (i.e. two-dimensional) for a bare PWR fuel assembly.

MATERIAL

The PWR assembly considered in this report contains 264 stainless steel-clad fuel rods with a burnup of 33,000 MWd/MTU.

TEST CONDITIONS

Two-dimensional rates are presented for two cases:

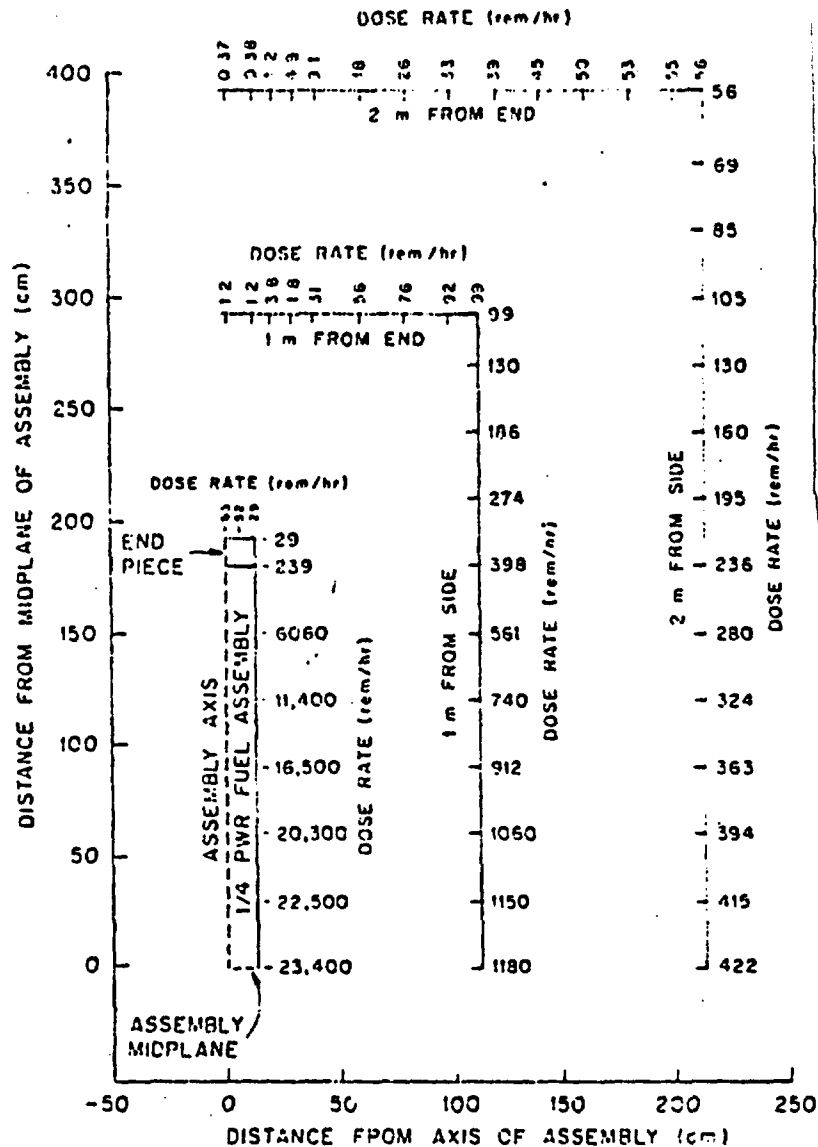
- (a) The radiation source is non-uniformly distributed fission products (i.e. a nonsymmetrical burnup distribution is assumed) or
- (b) the radiation source is a uniformly distributed spike (^{60}Co).

METHODS OF ANALYSIS

Codes used to calculate absolute dose rates were DOT-IV and FALSTF, with input to the codes based on ORIGEN fission product inventory.

AMOUNT OF DATA

The dose rates were calculated for six areas: on the sides and the end surfaces of the fuel assembly, on spatial surfaces 1 m from the side and the end of the fuel assembly, and on spatial surfaces 2 m from the side and the end of the fuel assembly. Data is depicted in the figure below for the fission product (non-uniform burnup) dose rate from a 10-yr old PWR fuel. A similar set of data was generated for a uniform source distribution within the assembly (i.e. 30 ppm of ^{60}Co).



UNCERTAINTIES IN THE DATA

This was not stated. This depends on assumptions implicit in the code and assumptions made for data input.

DEFICIENCIES IN THE DATA BASE

It was considered necessary to simplify the square PWR assembly design in order to make input for the shielding calculation feasible. The assembly was assumed to have the symmetry of a right circular cylinder and to be of homogeneous nature within the assembly volume. Due to the assumed symmetry, only one-fourth of the assembly was considered in the calculations, i.e. upper right quadrant. Since no cross-section data were readily available for Zircaloy, stainless steel was substituted for the Zircaloy in the fuel assembly.

APPLICATION OF DATA TO LICENSING

[Key Data (), Supporting Data (X)].

GENERAL COMMENTS

This report is not directly related to the waste package but it highlights types of dose rate calculations that should be performed on the package. Most dose-rate calculations treat the fuel assembly as an infinitely long source of radiation emitting a specified number of gamma rays per unit length. The dose rate is then calculated as a function of one dimension, the distance from the line source. This approach ignores the decrease in dose that results from the finite length of the assembly and the lower burnup at the ends of the fuel assembly. A one-dimensional calculation cannot predict the dose rates near the corners and on the end of the fuel assembly.

ORGANIZATION PRODUCING DATA

Oak Ridge National Laboratory.

AUTHORS/REFERENCE

ORNL/TM-6754, "Calculated, Two-Dimensional Dose Rates From a (Bare) PWR Fuel Assembly," A. G. Croff, O. W. Hermann, and C. W. Alexander, Oak Ridge National Laboratory, March 1979.

AVAILABILITY

NTIS

KEY WORDS

Spent fuel, PWR, dose rate, gamma radiation.

DATE REVIEWED

September 1984.

gfs
10/8/84

ABSTRACT

This report first describes the physical characteristics of a PWR fuel assembly. A model of the assembly is then defined, and a two-dimensional gamma-ray shielding code is applied to the model to calculate the dose rate from a bare fuel assembly. The results of the calculations are the dose rates from the assembly at points on the surface of the assembly, on spatial surfaces 1 m from a side and the end piece of the assembly, and on spatial surfaces 2 m from a side and the end piece of the assembly. Dose rates are calculated for as-generated mixed fission products and for a uniformly distributed ^{60}Co spike. Factors are given to account for the effect of decay on the dose rates.

WASTE PACKAGE DATA REVIEW FORM

TYPE OF DATA

Qualitative and quantitative analysis of gases (1) produced by radiolysis (gamma) of rock salt at 60°C to an accumulated dose of 1.5×10^8 rad (rate = 2.3×10^6 rad/h) and (2) released by irradiated salt upon heating to 320°C. Reported in % (by volume) for (1) and in ppm for (2). Analysis by mass spectrometry.

MATERIAL

Halite from the Asse salt mine, anhydritic rock salt, gypsum, kieserite with 2 weight percent halite and trace minerals. The water content ranged from 0.3 to 21 weight percent.

TEST CONDITIONS

For radiolysis studies, 500 g ground salt were irradiated at 60°C for 65 h at a dose rate of 2.3×10^6 rad/h gamma in glass ampoules (O.D. 55 mm and length 650 mm). Only half of the volume in the ampoule was filled with salt. Ampoules were purged with nitrogen and sealed. After completion of irradiation, ampoules were opened. The irradiated salt was heated up in a vacuum ($<10^{-4}$ mbar) of a mass spectrometer to 320°C.

METHODS OF ANALYSIS

No information on statistics was provided. It is not stated that replicate samples were studied.

AMOUNT OF DATA

Qualitative and quantitative gas analyses (seven gases) for five salt samples with varying water content.

UNCERTAINTIES IN THE DATA

Not provided in the document. Detection limits were not specified.

DEFICIENCIES IN THE DATA BASE

- (a) Replicates need to be studied and statistical information provided.
- (b) Tests were performed in a nitrogen environment. They should also be performed for a more realistic repository environment, which would include some oxygen and carbon dioxide.

- (3) Tests should be performed to determine if there is a dose rate effect and if there is an equilibrium established in gas production at some dose and time.

APPLICATION OF DATA TO LICENSING

[Key Data (), Supporting Data (X)].

GENERAL COMMENTS

This study identified gases that were produced when Asse salt mine rock was gamma-irradiated at 60°C in a nitrogen atmosphere. This data may or may not be relevant to the environment that a waste package will experience in a repository. The effect of these gases on brine chemistry should be investigated.

ORGANIZATION PRODUCING DATA

Gesellschaft fuer Strahlen - und Umweltforschung mbH Muenchen Institut fuer Tieflagerung, Federal Republic of Germany.

AUTHORS/REFERENCE

Jockwer, N., "Laboratory Investigations on Radiolysis Effects on Rock Salt With Regard to the Disposal of High-Level Radioactive Wastes," in The Scientific Basis for Nuclear Waste Management, VII, G. L. McVay, Editor, New York, Elsevier Publishing, 1984, pp. 17-23.

AVAILABILITY

Published Proceedings.

KEY WORDS

Salt, gamma radiation, gases, radiolysis.

DATE REVIEWED

September 1984.

gfs
10/1/84

ABSTRACT

As a result of the heat producing high-level radioactive waste, volatile components which are in the host rock will be liberated and further gases will be generated by thermal cracking and radiolysis.